Université de Montréal

La formation de biofilm des *Escherichia coli* producteurs de Shiga-toxines :

Caractérisation et rôle du régulon Pho

par Philippe Vogeleer

Département de pathologie et microbiologie
Faculté de médecine vétérinaire

Thèse présentée à la Faculté de médecine vétérinaire
en vue de l'obtention du grade de *Philosophiae Doctor* (Ph.D.)
en sciences vétérinaires option microbiologie

Mars 2019

Université de Montréal

Département de pathologie et microbiologie, Faculté de médecine vétérinaire

Cette thèse intitulée

La formation de biofilm des *Escherichia coli* producteurs de Shiga-toxines :
Caractérisation et rôle du régulon Pho

Présentée par

Philippe Vogeleer

A été évaluée par un jury composé des personnes suivantes

France Daigle
Président-rapporteur

Josée Harel
Directeur de recherche

Mario Jacques
Codirecteur

Christopher Fernandez Prada
Membre du jury

Charles Dozois
Examinateur externe

Résumé

Les *Escherichia coli* producteurs de Shiga-toxines (STEC) sont des bactéries pathogènes d'origine alimentaire responsables de diarrhées, de colites hémorragiques et du syndrome hémolytique et urémique, pouvant entraîner la mort. Une des priorités de l'industrie agro-alimentaire est d'éviter la présence des STEC dans l'environnement et dans les chaînes de production. Dans ce secteur, les bactéries sous forme de biofilm représentent un réel problème car en plus de contaminer les installations des chaînes de production, elles sont plus résistantes aux protocoles de nettoyage et de désinfection. Il est donc nécessaire de mieux caractériser les biofilms formés par les STEC et d'identifier les facteurs qui contribuent à leur développement.

Les objectifs de la première partie de cette thèse étaient de caractériser le potentiel de formation de biofilms de différents sérotypes STEC. Pour cela nous avons montré que la capacité de formation de biofilms des STEC est très variable. Nous avons identifié que les protéines jouent un rôle important dans l'intégrité des biofilms des STEC. De plus, les isolats du séropathotype A (O157:H7 et O157:NM), avaient un meilleur potentiel de formation de biofilm que les isolats du séropathotype B et C. Nous avons aussi montré que le traitement des biofilms STEC avec des désinfectants réduisait la viabilité mais n'éliminait pas complètement la matrice de biofilm. Nos données indiquent que la formation de biofilms dans l'environnement pourrait contribuer à la persistance des STEC et plus précisément des souches du séropathotype A dans l'environnement.

Dans une deuxième partie nous avons étudier comment la carence en phosphate (Pi) affectait la formation de biofilm de la souche O157:H7 EDL933. Les souches *E. coli* O157:H7 peuvent survivre pendant de longues périodes de temps dans un environnement pauvre en nutriments. Les biofilms pourraient contribuer à surmonter les stress rencontrés dans l'environnement. Lorsqu'*E. coli* est cultivée en conditions pauvres en Pi, le régulon Pho est induit par PhoB. Le système de transport spécifique au Pi (Pst) est le transporteur de haute affinité du Pi. Dans le mutant Δ*pst*, PhoB est activée de manière constitutive. Nous avons montré que l'activation de PhoB conduisait à l'augmentation de la formation de biofilm chez la souche O157:H7 EDL933. En réponse à la carence en Pi, l'activation de PhoB stimulait directement l'expression des gènes *waaH* et $ycgV_{EDL933}$, codant respectivement pour une glycosyltransférase et pour un autotransporteur, tous deux impliqués dans l'augmentation du biofilm. Nous avons

également identifié que, dans le mutant Δ*pst*, les lipopolysaccharides (LPS) étaient modifiés et que cela pourrait influencer la composition du biofilm.

Pris ensemble, nos résultats montrent que la formation de biofilms contribue à la persistance des STEC dans l'environnement et que les isolats de séropathotype A ont démontré une capacité accrue à former des biofilms. En réponse au stress environnemental tel que la carence en Pi, les STEC adaptent leur mode de vie et passent d'un état libre à un état sessile. Les connaissances acquises au cours de cette thèse pourrait permettrent l'exploration de deux nouvelles applications pour lutter contre la formation de biofilms des STEC, incluant l'utilisation de protéase pour dégrader le biofilm et l'utilisation de surface recouverte d'ions phosphate pour prévenir la formation de biofilm.

Mots-clés: Biofilm, STEC, Phosphate, LPS, Régulon Pho

Abstract

Shiga-toxin producing *Escherichia coli* (STEC) are food-borne pathogens that cause diarrhea, hemorrhagic colitis, and hemolytic-uremic syndrome, which may result in death. A major priority for the food industry is to avoid the presence of STEC in the environment and the food production chain. In the latter sector, biofilm formed by bacteria represents a real problem because in addition to contaminating the facilities, they are more resistant to traditional cleaning and disinfection protocols. Therefore, it is necessary to better characterize the biofilms formed by STEC and to identify the factors that contribute to their development.

The objective of the first part of this thesis was to evaluate the biofilm formation of human STEC isolates representing the most pathogenic seropathotypes, to characterize the matrix composition of the strongest STEC biofilms and to evaluate their tolerance to sanitizers. The results showed that biofilm formation by STEC strains was highly variable. We also identified that proteins were important for the biofilm integrity. Moreover, seropathotype A isolates (O157:H7 and O157:NM), which are associated to the highest relative incidence of human infection, had a greater ability to form biofilms than seropathotype B and C isolates. Treatment with sanitizers reduced the viability of STEC but did not completely remove the biofilm matrix. Overall, our data indicate that biofilm formation in the environment could contribute to the persistence of STEC and specifically seropathotype A isolates in the environment.

In the second part of this thesis, we studied how the stress of phosphate (Pi) depletion affected the biofilm formation of O157:H7 EDL933. *E. coli* O157:H7 can survive for prolonged periods under nutrient-deprived environmental conditions. Biofilms are thought to participate in this environmental lifestyle. When O157:H7 strain EDL933 was grown under Pi starvation conditions, its Pho regulon was induced by the regulator PhoB. The Pi-specific transport (Pst) system is the high-affinity Pi transporter. In its isogenic Δ*pst* mutant, PhoB was constitutively activated. We identified that PhoB activation lead to the increase of O157:H7 biofilm formation. We have shown that when it was activated, the regulator PhoB was directly controlling the expression of two genes, *waaH* and $ycgV_{EDL933}$, encoding respectively a glycosyltransferase and an autotransporter. These two genes were both shown to be involved in the biofilm increase in response to Pi-starvation. We also identified that in the Δ*pst* mutant, lipopolysaccharides (LPS)

were modified and that this could influence the biofilm composition.

Taken together our results show that biofilm formation contributes to the persistence of STEC in the environment and that seropathotype A isolates have an increased ability to form biofilm. In response to environmental stress such as Pi deficiency, STEC adapt and transit from a free state to a sessile state. The acquired knowledge during this thesis could allow the exploration of two new applications to fight against the biofilm formation of STEC, including the use of protease to degrade the biofilm and the use of surface covered with phosphate ions to prevent biofilm formation.

Keywords: Biofilm, STEC, Phosphate, LPS, Pho regulon

Table des matières

Liste des tableaux

Section II – Revue de littérature

Section III - Caractérisation des biofilms formés par les STEC

Article de recherche 1

Section IV – Etude du régulon Pho dans la formation de biofilm de *Escherichia coli* O157:H7.

Article de recherche 2

Article de recherche 3

Liste des figures

Section II – Revue de littérature

Section III - Caractérisation des biofilms formés par les STEC

Article de recherche 1

Section IV – Etude du régulon Pho dans la formation de biofilm de *Escherichia coli* O157:H7.

Article de recherche 2

Section V - Discussion général

Abréviations

ABC : ATP Binding Cassette

ADN : Acide désoxyribonucléique

AIEC : *Escherichia coli* adhérente et invasive

CT : Toxine cholérique

DGC : Diguanylate cyclase

di-GMP-c : di-guanosine monophosphate cyclique

ECA : « Enterobacterial common antigen »

EHEC : *Escherichia coli* entérohémorragique

EPEC : *Escherichia coli* entéropathogène

ExPEC : *Escherichia. coli* pathogènes extraintestinaux

Gb3 : Récepteur globotriaosylceramide

InPEC : *Escherichia. coli* pathogènes de l'intestin

LEE : Locus d'effacement de l'enterocyte

LPS : Lipopolysaccharide

mM : Milimolaire

MOPS : "3-Nmorpholino propanesulfonic acid"

NAG : N-acétylglucosamine

NM : Non-motiles

OI : O-island

PDE : Phosphodiesterase

PGA : Poly-N-acétylglucosamine

Pi : Phosphate inorganique

polyPi : Polyphosphate

PPi : Pyrophosphate

Pst : « Phosphate specific transport »

PTT : Purpura thrombotique thrombocytopénique

SAAT : Autotransporteurs auto-associés

SHU : Syndrome hémolytique et urémique

SNP : « Single nucleotide polymorphisme »

SST3 : Système de sécrétion de type III

STEC : *Escherichia coli* producteurs de Shiga-toxines

Stx : Shiga-toxine

TCP : Pili corégulé par la toxine

UPEC : *Escherichia coli* uropathogène

WGA : agglutinine de germe de blé

Remerciements

Je souhaite remercier sincèrement Dre Josée Harel, ma directrice de thèse. Merci de m'avoir accueilli dans votre laboratoire. Je vous suis reconnaissant pour votre patience, votre écoute et vos nombreux conseils qui ont permis de faire avancer mon projet.

Je tiens également à remercier Dr Mario Jacques d'avoir accepté la codirection de mon projet de thèse et un grand merci pour sa disponibilité, ainsi que ses conseils et directives.

Je remercie Dr Charles Dozois d'avoir accepté d'être examinateur externe de cette thèse et pour ses précieux commentaires lors de mes comités conseils.

Je remercie également Dr Christopher Fernandez-Prada et Dre France Daigle d'avoir accepté d'évaluer cette thèse en tant que respectivement membre du jury et président-rapporteur.

Je remercie aussi Dr Yannick Tremblay pour son aide inestimable et sa patience dans le début de mon projet. Cela a été un grand plaisir de travailler avec toi.

Je remercie mes collègues Rémi Lavoie, Guillaume LeBihan, Philippe Garneau, Simo Chekabab, Flor Ramirez, Jean-Félix Sicard, et Yaindrys Rodriguez Olivera pour leur esprit d'équipe, leur sympathie et leur bonne humeur.

Je tiens également à remercier particulièrement Josée Labrie, Frédéric Berthiaume et Claudia Duquette pour leurs compétences, leurs écoutes, leurs disponibilités et leurs nombreux conseils.

Merci à l'ensemble des membres du GREMIP, du CRIPA et à tous ceux qui contribuent à la dynamique de groupe, au bien-être et à la réussite des étudiants.

Je remercie aussi les organismes subventionnaires FQRNT et CRSNG pour leur soutien financier.

Un grand merci à mes parents pour tout votre soutien. Merci aussi de m'avoir donné la possibilité de partir étudier à l'étranger (en Suède puis au Canada). Vous m'avez encouragé tout au long de mes études sans jamais douter de mes capacités. Merci encore.

Et pour finir, un milliard de mercis à Alix ! Ton aide est inestimable. Tu as été présente à mes côtés depuis le début de cette thèse. Jour après jour, tu as su m'écouter, me remonter le moral, me faire rire et me conseiller. Je te remercie d'avoir été si forte et si patiente. Tu m'as énormément aidé. Et j'aimerais bien un jour que tu m'expliques comment tu as fait pour supporter mon caractère de cochon. Encore merci. Et pour finir, tu sais c'est quoi le plus imp'?

I. Section I – Introduction

Les *Escherichia coli* producteurs de Shiga-toxines (STEC) et parmi ceux-ci les *E. coli* entérohémorragiques (EHEC) O157:H7, sont des bactéries pathogènes entériques humaines régulièrement responsables de toxi-infections alimentaires collectives graves. Les bovins représentent le réservoir le plus important de STEC et sont les principaux agents de dissémination de ces bactéries pathogènes. C'est par introduction d'aliments souillés dans les chaînes de production suivie d'une consommation de ces aliments que l'humain se contamine. Un cas d'infection par une souche STEC se caractérise par l'apparition de crampes abdominales et de diarrhée, souvent sanglante. Dans quelques cas, des complications post-infectieuses, telles que le syndrome hémolytique et urémique (SHU), peuvent survenir et provoquer la mort des individus infectés (Croxen and Finlay, 2010). Les STEC possèdent de nombreux facteurs de virulence leur permettant de causer la maladie chez l'humain. Le facteur de virulence majeur et commun à tous les STEC est la Shiga-toxine codée par les gènes *stx1* ou *stx2*. Le sérotype de STEC le plus souvent associé à des cas d'épidémie est O157:H7. Cependant 6 sérogroupes non-O157, appelés le « Big six », regroupant *E. coli* les sérogroupes O26, O45, O103, O111, O121 et O145 sont aussi fréquemment impliqués dans des cas d'infections. Le regroupement des sérotypes STEC en fonction de leur incidence, de leur fréquence d'implication dans des épidémies et de la sévérité de la maladie causée a mené à un classement des STEC en 5 séropathotypes (A à E) (Karmali *et al.*, 2003).

Le séropathotype A regroupe les sérotypes O157:H7 et O157:NM et le séropathotype B regroupe les sérotypes du « Big six ». Les autres séropathotypes (C, D et E) regroupent des sérotypes peu ou pas impliqués dans des cas d'épidémies chez l'humain. En plus de produire des Shiga-toxines, les STEC peuvent produire d'autres facteurs de virulence qui participent à la sévérité de la maladie (Paton and Paton, 1998). Ces facteurs sont pour la plupart portés par des îlots de pathogénicité tels que le locus d'effacement de l'entérocyte (LEE) qui code pour le système de sécrétion de type III (SST3), l'intimine (*eae*) et des effecteurs qui seront sécrétés dans la cellule hôte. D'autres facteurs de virulence tels que des fimbriae ou des autotransporteurs, participent également à la virulence des souches STEC (Etcheverria and Padola, 2013). Chez certaines souches STEC, plus particulièrement chez les O157:H7, de tels facteurs d'adhésion, ainsi que la production de polysaccharides (cellulose, poly-β-1,6-N-acetyl-D-glucosamine (PGA)) ont déjà été reliés à la formation de biofilm. Cependant il existe dans la

littérature un manque de connaissances sur le potentiel de formation de biofilm et les facteurs associés des souches STEC de sérotype non-O157.

La formation de biofilm est très souvent associée à une augmentation de la persistance des bactéries pathogènes dans l'environnement et dans les chaînes de transformation alimentaire. Cette persistance est due notamment à une tolérance accrue aux désinfectants (Wang et al., 2012a), entraînant un contrôle difficile de la contamination. La persistance dans l'environnement est également due à la capacité d'une bactérie à s'adapter aux stress environnementaux pour réguler l'expression de ses gènes. Par exemple, dans l'environnement le phosphate inorganique (Pi) est un élément limitant et *E. coli* O157:H7 est capable de survivre et de s'adapter à la carence en Pi.

En faible concentration en Pi, le système à deux composantes PhoBR est activé et PhoB régule ainsi une quarantaine de gènes appartenant au régulon Pho (Yoshida *et al.*, 2012), permettant d'augmenter la survie des bactéries pathogènes telles que *E. coli* O157:H7 dans l'environnement (Chekabab *et al.*, 2012). Par ailleurs, plusieurs études chez d'autres espèces ont déjà montré que l'activation de PhoB pouvait avoir un impact sur la formation de biofilm (Danhorn *et al.*, 2004; Pratt *et al.*, 2009; Xu *et al.*, 2012). Cependant le rôle de PhoB dans la formation de biofilm des souches *E. coli* O157:H7 n'est pas connu.

Cette thèse de doctorat traite de la formation de biofilm des souches STEC comme moyen de persistance environnementale. Ce travail apporte de nouvelles connaissances à la fois sur la persistance des STEC dans l'environnement et sur les mécanismes permettant la transition du mode de vie planctonique à la formation de biofilm. Les perspectives sont d'améliorer la prévention et le contrôle de la formation de biofilms dans l'environnement et dans l'industrie afin de diminuer le risque de contamination des aliments.

Dans la prochaine section, une recension de la littérature détaillée des connaissances actuelles sur les STEC est d'abord décrite. Ensuite l'importance de la formation de biofilm dans la persistance de STEC dans l'environnement est présentée principalement sous forme d'une revue qui a été publiée dans le journal « Frontiers in Microbiology » section « microbial physiology and metabolism » (Vogeleer *et al.*, 2014). Enfin dans une troisième partie,

l’importance de la carence en Pi, du régulon Pho et des mécanismes mis en place par les bactéries pour surmonter ce stress est présentée.

II. Section II – Revue de littérature

II.1 Les *Escherichia coli* producteurs de Shiga-toxines

E. coli est une bactérie à Gram négatif qui colonise le tube digestif de l'humain et des animaux à sang chaud. C'est l'espèce prédominante de la flore aérobie-anaérobie facultative de l'intestin. Il existe beaucoup de souches différentes de *E. coli* et les façons de les classifier sont très nombreuses. Le plus souvent, on distingue deux groupes : les *E. coli* commensaux et les *E. coli* pathogènes.

Les *E. coli* commensaux permettent de prévenir l'établissement d'espèces bactériennes plus néfastes pour l'équilibre intestinal de l'hôte. Ejectés par la matière fécale dans l'environnement, les *E. coli* commensaux se trouvent également dans l'eau et dans les sols. Dans de rares cas, les souches commensales de *E. coli* peuvent être impliquées dans des infections intestinales de patients immunodéprimés ou en cas de rupture de la barrière gastro-intestinale.

Les *E. coli* pathogènes se distinguent des *E. coli* commensaux car ils disposent, en plus des gènes essentiels communs à l'ensemble des *E. coli*, des gènes codant pour des facteurs de virulence et d'adaptation qui contribuent à l'établissement de la maladie chez l'hôte. L'ADN chromosomique des *E. coli* pathogènes subit de nombreux réarrangements. Les gènes codant pour les facteurs de virulence acquis par transfert horizontal sont le plus souvent inclus dans des éléments génétiques (îlots de pathogénicité, transposons, intégrons, phages ou plasmides) qui peuvent être mobilisés dans d'autres souches pour créer de nouvelles combinaisons de facteurs de virulence. Les facteurs de virulence codent pour des adhésines, systèmes de sécrétion et des toxines qui permettent à la bactérie de coloniser un plus grand nombre d'environnements.

Les *E. coli* pathogènes peuvent être responsables de maladie très diverses incluant des maladies intestinales telles que la diarrhée ou la gastro-entérite mais aussi des maladies extra-intestinales telles que des infections urinaires, des septicémies et des méningites. Les *E. coli* pathogènes peuvent être classés selon leurs pathotypes (Finlay et al 2010). Un pathotype est un groupe de souches provenant d'une seule espèce causant une même maladie en utilisant un ensemble commun de facteurs de virulence (Kaper et al 2004).

Parmi les pathotypes d'*E. coli* se trouve le pathotype des *E. coli* producteurs de Shiga-

toxines (STEC). Ces bactéries ont la particularité de produire au moins une version d'une toxine appelée la Shiga-toxine (Stx). Le nom Shiga-toxines est dérivé de la cytotoxine produite par *Shigella dysenteriae* de sérotype 1 (O'Brien *et al.*, 1982). Les STEC peuvent aussi être appelés *E. coli* producteurs de vérocytotoxine (VTEC) car il a été montré que la toxine Stx a des effets cytotoxiques irréversibles sur la lignée cellulaire Véro (Konowalchuk *et al.*, 1977).

II.1.1 STEC ou EHEC ?

Les STEC peuvent être responsables de troubles intestinaux variés allant de la diarrhée aqueuse bénigne à la colite hémorragique. Dans de rare cas, la maladie peut évoluer vers un SHU (Gyles, 2007). Les STEC capables de causer la colite hémorragique sont appelés EHEC dont certaines, sont aussi capables de causer des lésions d'attachement/effacement (Nataro and Kaper, 1998). Les lésions d'attachement et d'effacement sont produites lors de l'attachement étroit de la bactérie à la cellule épithéliale. Cette particularité est également retrouvée chez les souches *E. coli* entéropathogène (EPEC). Lors de cet attachement, la cellule hôte perd ses microvillosités (effacement) car l'actine de la cellule hôte est réarrangée pour former un piédestal sur lequel repose la bactérie (Figure 1).

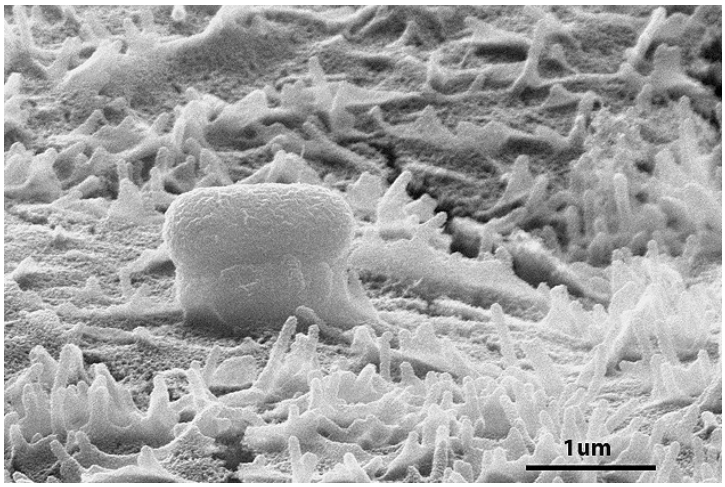

Figure 1. Image montrant le piédestal formé par les EHEC lors des lésions d'attachement et d'effacement dans le gros intestin humain. Ce piédestal est caractéristique des infections causées par les EHEC et les EPEC. Ces structures surélevent la bactérie par rapport à la cellule épithéliale. (Photo provenant du site internet https://today.uconn.edu/2012/07/how-e-coli-cells-work-in-the-human-gut/#).

Les protéines impliquées dans la formation de lésion d'attachement/effacement et du piédestal sont codées par une région contenue dans le génome de certains EHEC et est appelée le LEE (présenté dans la section II.2.3.1). De manière générale, les EHEC regroupent toutes les souches STEC capables de causer la maladie et incluent donc une connotation clinique. Depuis le début des années 80, les EHEC ont causé de nombreuses épidémies. Dans cette thèse lorsque le terme EHEC est employé, cela désigne que la souche a clairement été isolée de cas cliniques. Aussi le terme STEC est employé pour désigner toutes les souches qu'elles aient été ou non associées à la maladie.

II.1.2 Transmission

Les STEC sont des agents zoonotiques. Leur propagation dans l'environnement est donc en lien, direct ou indirect, avec l'animal (Figure. 2). Les STEC sont capables de coloniser et de survivre dans le tractus intestinal des bovins, et spécifiquement dans la partie terminale du rectum (Naylor *et al.*, 2005) sans pour autant causer la maladie. La plupart du temps les bovins sont donc des porteurs sains des souches STEC. Leur intestin en est d'ailleurs le réservoir principal. En plus de coloniser l'intestin des bovins, les STEC sont également retrouvés dans l'intestin d'autres animaux, tels que le porc, le mouton, le cerf, le sanglier, le lapin ou les oiseaux (Ferens and Hovde, 2011).

Une fois ingérée par le bovin (1), la bactérie contenue dans la matière fécale est excrétée dans l'environnement (2) et contamine la nourriture et l'eau potable (3). L'ingestion d'aliments crus ou peu cuits contaminés par les STEC est la voie la plus commune de transmission des STEC. Parmi les aliments à risques, la viande de bœuf hachée mal cuite (hamburger) est souvent incriminée dans les cas d'infections aux EHEC. Le plus souvent la viande est souillée lors de l'abattage de l'animal. En effet des erreurs de manipulation lors de l'éviscération peuvent mettre en contact la viande et la matière fécale. Aussi des négligences de nettoyage des chaînes de production peuvent mener à une contamination du matériel de découpe et contaminer la viande. Dans la majorité des cas, les éclosions sont causées par la consommation d'aliments transformés. La consommation de produits laitiers non pasteurisés, tels que le lait et les fromages, est une aussi cause importante d'infection. En effet le lait peut être contaminé par des mamelles de vaches porteuses de STEC mal nettoyées avant la traite. Les légumes et les fruits

sont également souvent incriminés dans les cas d'infection. La contamination de ces derniers peut se faire via l'épandage de fumier ou bien l'arrosage avec de l'eau souillée par de la matière fécale bovine. (Strachan *et al.*, 2005). Des cas d'infections par contact direct entre l'animal et l'humain ont été rapportés (Renwick *et al.*, 1993; Shukla *et al.*, 1995) (4). Un bref contact physique suffit à transmettre la bactérie, et le lavage des mains après contact est l'unique procédure efficace pour prévenir la transmission directe (National Association of State Public Health Veterinarians *et al.*, 2007). La transmission de la bactérie entre personne est également possible et se produit la plupart du temps par manque d'hygiène (5). Dans ce cas il a été remarqué que le nombre de bactéries suffisant pour causer la maladie est extrêmement faible (10 à 100 cellules) (Strachan *et al.*, 2005; Teunis *et al.*, 2004).

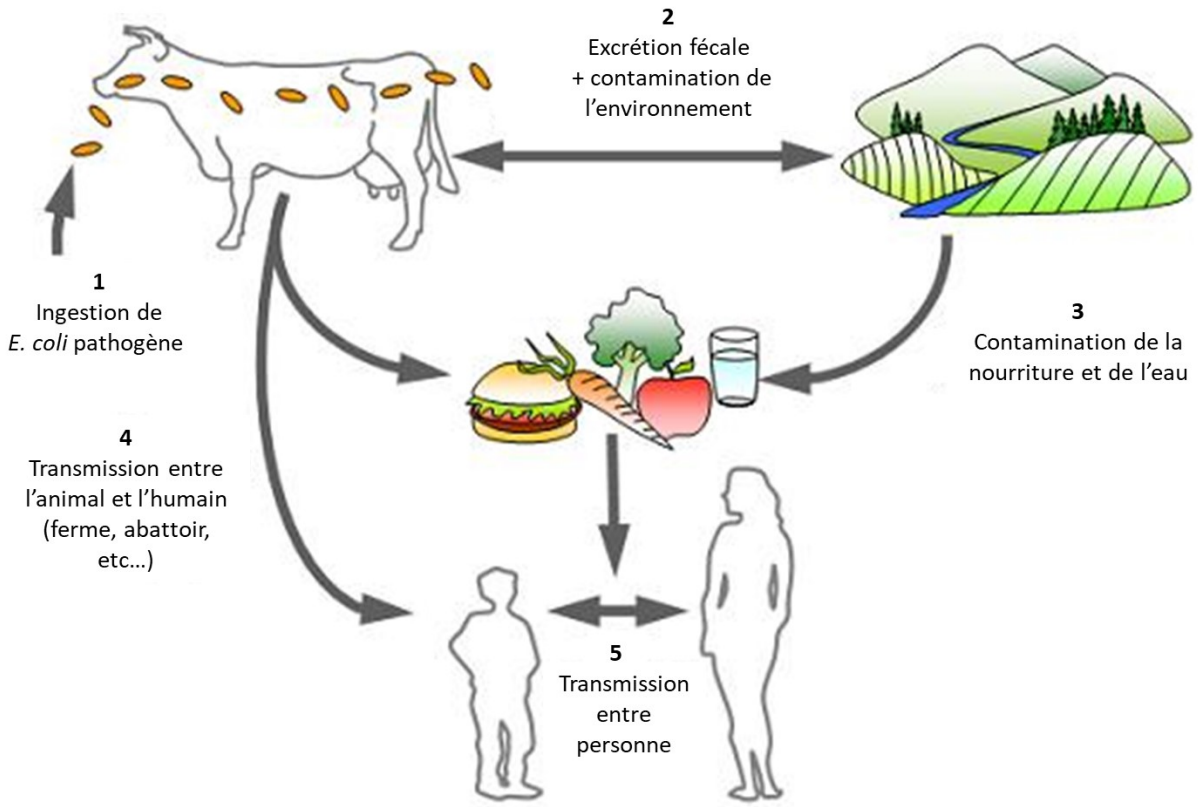

Figure 2. Schéma des différents mécanismes de transmission des souches STEC : du bovin à l'humain. Les STEC ont pour réservoir principal l'intestin des bovins (1). C'est par l'éjection de la matière fécale que l'environnement est contaminé (2). Les STEC peuvent être transmises par les aliments et l'eau (3), le contact animal humain (4) et le contact de personne à personne (5) (tirée de site web EcL: http://www.ecl-lab.ca/en/ecoli/pathogenesis.asp).

II.1.3 Effets cliniques

À la suite de la consommation de nourriture contaminée par les STEC, les premiers symptômes tels que les crampes abdominales, les vomissements et la diarrhée aqueuse apparaissent généralement suite à une période d'incubation de deux ou trois jours. Dans plus de 80 % des cas d'infections aux EHEC O157:H7, la diarrhée devient sanglante (Figure 3) (Tarr, 2005). Chez les personnes les moins sensibles, une infection par EHEC se résout normalement en quelques jours. Cependant dans certains cas le SHU peut se développer entre 5 à 13 jours après l'apparition des premières diarrhées. Le SHU implique une insuffisance rénale aiguë, une thrombocytopénie (diminution du nombre de plaquettes sanguines) et une anémie hémolytique (diminution du nombre de globules rouges) (Tarr, 2005). Aux États-Unis, il a été montré que le SHU se développe en moyenne dans 4 % des cas d'infection par EHEC O157:H7 (Rangel *et al.*, 2005).

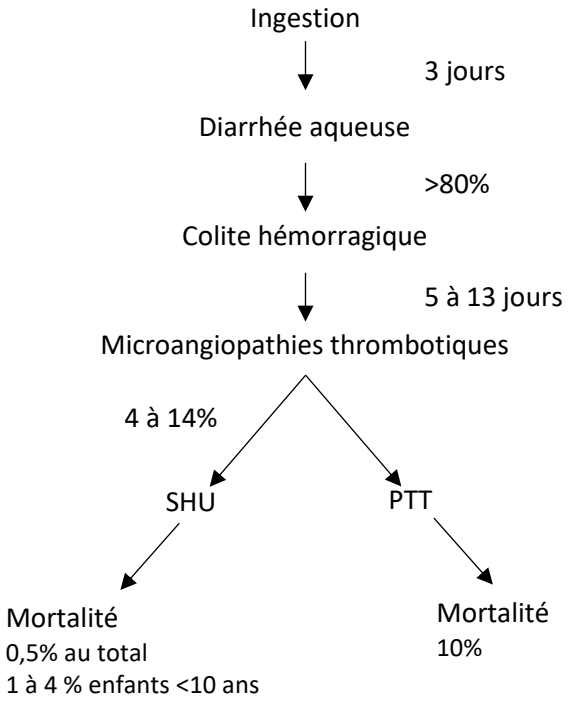

Figure 3. Symptomatologie d'une infection à EHEC O157:H7. Le temps moyen d'incubation est de 3 jours et les premiers symptômes sont les crampes abdominales et la diarrhée. Cette dernière devient sanglante dans 80 % des cas en moyenne. Le SHU se développe dans 4 % des cas et est mortel dans 1 à 4 % des cas chez l'enfant. Le PTT affecte davantage les personnes âgées et est mortel dans 10 % des cas en moyenne. SHU : syndrome hémolytique et urémique ; PTT : purpura thrombotique thrombocytopénique.

Alors que le SHU affecte surtout les reins, d'autres organes vitaux tels que le système nerveux central, les poumons, le pancréas et le cœur, peuvent aussi être touchés. Le SHU crée des séquelles parfois irréversibles et peut entraîner la mort de l'individu infecté. Les enfants de moins de 5 ans et les personnes âgées sont les plus sévèrement touchées (Gyles, 2007). En plus du SHU, le purpura thrombotique thrombocytopénique (PTT) est aussi associé à une infection à EHEC. Au niveau physiopathologique, le PTT est similaire au SHU à la seule différence qu'il s'accompagne de fièvres intenses et affecte plus particulièrement le système nerveux. Le PTT touche principalement les personnes âgées et est mortel dans 10% des cas (Figure 3).

II.1.4 Classification des STEC

Les STEC peuvent être classés en fonction de leur sérotype. Le sérotypage est une méthode de classification basée sur 3 éléments bactériens pouvant déclencher une réponse immunitaire chez l'hôte. Ses éléments sont l'antigène O du lipopolysaccharide (LPS), l'antigène H de la flagelline et l'antigène K de la capsule. Étant donné que peu de laboratoires ont la capacité de typer l'antigène K, le sérotypage basé sur les antigènes O et H est devenu le standard en matière de typage de *E. coli*. Pour l'instant 186 antigènes O et 53 antigènes H ont été décrits pour les *E. coli* (Kaper et al., 2004). Le sérotypage est une base importante pour différencier les souches STEC et est souvent le point de départ de la caractérisation des STEC. Notons qu'un pourcentage élevé de sérotypes STEC sont non-motiles (NM). En raison de l'importance du sérotype O157:H7 dans les maladies humaines, les sérotypes STEC sont divisés en 2 grandes catégories, les O157 et les non-O157.

II.1.4.1 Les souches O157

Le sérotype O157:H7 est le premier sérotype STEC identifié comme responsable d'une épidémie causée par la consommation de bœuf haché en 1982 (O'Brien *et al.*, 1993). Par rapport à la plupart des *E. coli*, les souches de sérotype O157:H7 se distinguent par leur incapacité à fermenter le sorbitol et par l'absence de l'activité β-glucuronidase (activité enzymatique responsable de la dégradation des glucides). Le gène *uidA* qui code pour la β-glucuronidase est bien présent dans le génome de O157:H7 mais deux nucléotides diffèrent du gène *uidA* de K-12 et le rendent non-fonctionnel. En 1998, Feng *et al.* ont proposé un modèle dans lequel les

souches EHEC de sérotype O157:H7 et les souches EPEC de sérotype O55:H7 (positif pour la β-glucuronidase et fermentant le sorbitol) partageraient un ancêtre commun (Figure 4). Trente mille ans plus tôt, ces deux lignées auraient émergé d'un ancêtre commun qui disposait du LEE. Selon ce modèle, la première étape dans la séparation des deux lignées serait l'acquisition du gène *stx2*, probablement par transduction avec le phage, entraînant l'émergence d'une souche O55:H7 positive pour le gène *stx2*, qui a ensuite acquis la région de *rfb* (requis pour la synthèse de l'antigène O157) remplaçant le LPS O55 par O157, un plasmide codant pour l'hémolysine, et plus récemment l'acquisition d'un gène *stx1* codant pour la Shiga-toxine 1. Ce clone a également perdu la capacité de fermenter le sorbitol (SOR) et de produire une activité β-glucuronidase (GUD) fonctionnelle conduisant à l'émergence du clone O157:H7 "sorbitol -" (Figure 4) (Feng *et al.*, 1998).

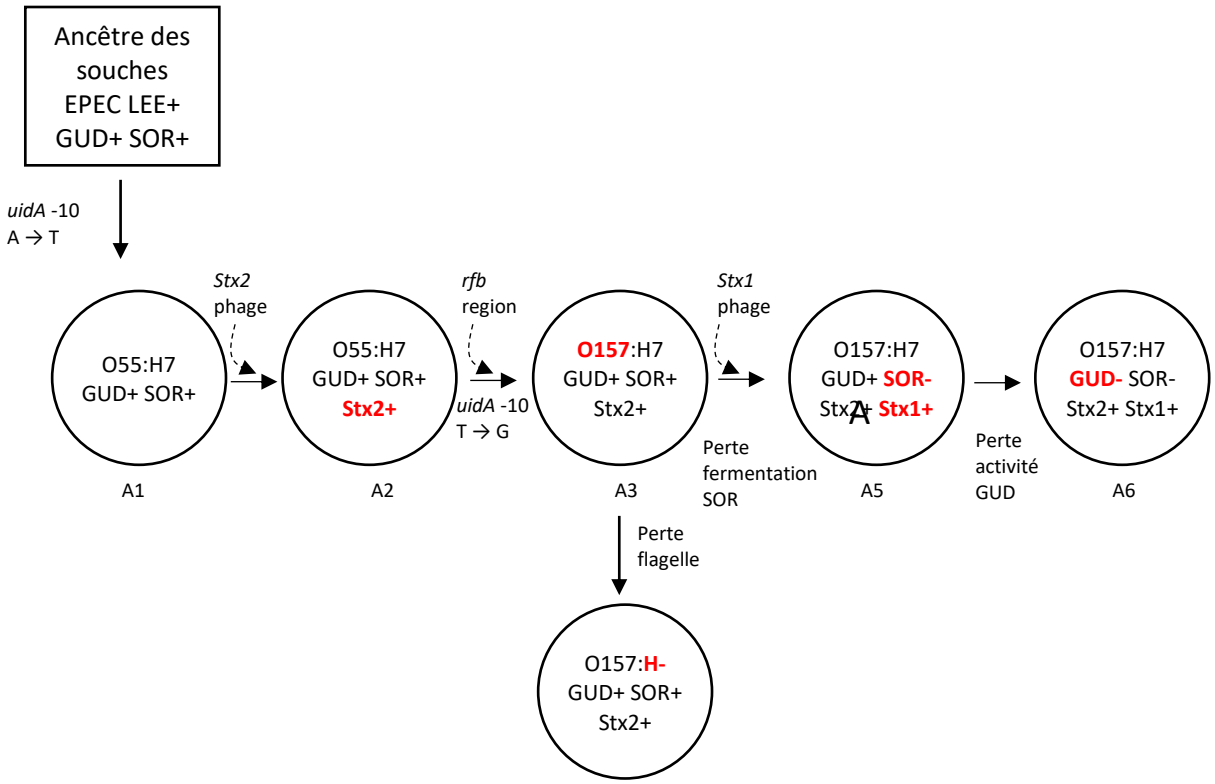

Figure 4. Modèle expliquant l'émergence du sérotype O157:H7. Ce modèle est basé sur les mutations dans *uidA*, la production de Stx et les phénotypes sorbitol (SOR) et β-glucuronidase (GUD). Les phénotypes des ancêtres A1 à A6 sont présentés et les changements sont marqués en gras. Les isolats correspondants sont indiqués sous chaque type. L'ancêtre A3 n'a pas été découvert. Figure adaptée de l'article de Feng (Feng *et al.*, 1998).

En 2008, une phylogénie des souches O157 basée sur le polymorphisme nucléotidique (SNP) de 96 loci a permis de classer les O157 en 9 clades (Figure 5) (Manning *et al.*, 2008). Selon cette classification, EDL933, la première souche O157:H7 américaine responsable d'une épidémie associée à la consommation de viande de hamburger, appartient au clade 3. Typiquement les souches de clade 3 codent pour *stx1* et *stx2*. La souche O157:H7 qui a causé la plus grande épidémie à ce jour avec plus de 5 000 cas d'infections recensés, est la souche d'origine japonaise Sakai (Michino *et al.*, 1999). Sakai appartient au clade 1. La souche TW14359 O157:H7 qui a causé une éclosion liée à la consommation d'épinards en 2006 appartient au clade 8. Le clade 8 contient des souches qui codent pour deux copies de la toxine

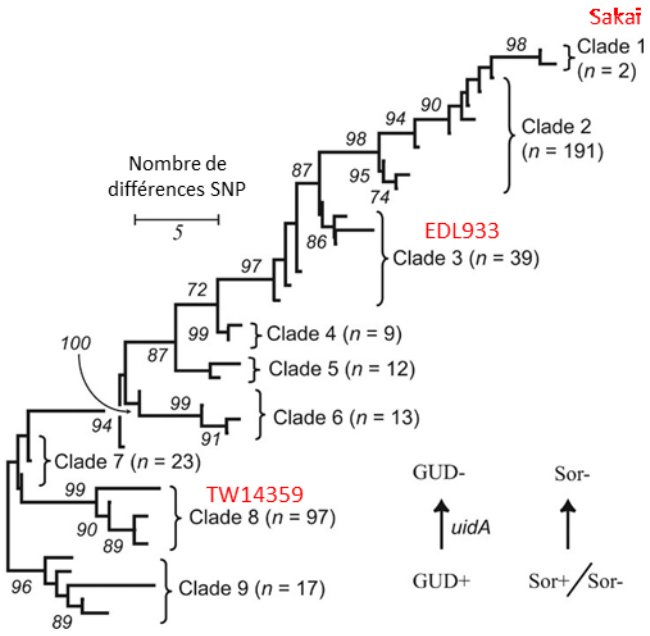

Figure 5. Arbre phylogénétique des différents clades de *E. coli* O157:H7 basée sur le polymorphisme nucléotidique (SNP) de 96 loci. Cet arbre est construit en utilisant l'algorithme d'évolution minimum basé sur la matrice de distance des différences par paires entre les génotypes SNP. L'arbre est présenté avec les pourcentages aux nœuds des valeurs de confiance > 70% et basées sur 1 000 réplicats. Les GUD + et Sor +, qui apparaissent dans le clade 9, sont négatives dans les clades dérivés 1-8 (GUD - et Sor -). En rouge sont présentés le nom des souches représentative des clades 1, 3 et 8. Figure adaptée de Manning 2008 (Manning *et al.*, 2008).

Stx (Stx2 et Stx2c). Alors que l'épidémie de Sakai était associée à un taux d'hospitalisation relativement faible (environ 3%), les victimes de l'épidémie d'épinards de 2006 et d'autres

épidémies associées au clade 8 ont eu un taux élevé d'hospitalisations et de SHU (plus de 50%) (Manning *et al.*, 2008). Donc au sein du sérotype O157:H7, les souches se distinguent notamment par leur capacité à se propager dans l'environnement et par la sévérité de la maladie (Figure 5).

II.1.4.2 Les souches non-O157

En Amérique du Nord, au Japon et dans plusieurs pays de l'Europe, les éclosions STEC ont pendant longtemps été principalement associées au sérotype O157:H7. Il a été estimé que chaque année aux États-Unis, les souches de sérotype O157:H7 sont responsables de plus de 73 000 cas de maladies (Bono *et al.*, 2007). Cependant, depuis sa première description en 1982, les études se sont concentrées sur le sérotype O157:H7, alors que de nombreuses éclosions associées aux sérotypes non-O157 se sont également produites dans les pays développés. Selon un rapport du « center for diseases control » (CDC), le nombre d'infections confirmées en laboratoire par des non-O157 augmente depuis 2000 et dépasse même le nombre d'infections à O157 depuis 2010. Malgré l'augmentation des isolats de STEC non-O157 provenant d'épidémies, l'impact de ces agents pathogènes sur la santé publique est moins bien documenté que celui des O157 en raison d'un diagnostic et d'une surveillance inadéquats. Malgré le nombre important de sérotype STEC, la majorité des infections STEC de sérotype non-O157 sont reliées à l'un des 6 sérogroupes suivant : O26, O45, O103, O111, O121 et O145. Ce groupe de 6 sérogroupes est appelé le « Big six » (Wang et al., 2012a).

II.1.4.3 Séropathotype

Que ce soit les souches de sérotype O157 ou non-O157, de nombreux sérotypes de STEC sont associés à des cas d'infections. Cependant comme décrit dans la section ci-dessus, certains sérotypes se démarquent (O157:H7, le « Big six ») car ils sont plus souvent impliqués dans des cas d'éclosions et/ou associés à des symptômes plus sévères que d'autres sérotypes de STEC. Il existe donc des différences de virulence entre les sérotypes de STEC. Ceci a permis à Karmali *et al.* de proposer une classification des STEC en cinq séropathotypes (de A à E) (Karmali *et al.*, 2003) (Tableau 1).

Tableau 1. Classification des STEC en séropathotypes. Adapté de Karmali *et al.* (Karmali *et al.*, 2003). Le séropathotype est une classification en fonction de l'incidence de la maladie, de la fréquence d'implication dans des épidémies, de la sévérité de la maladie et du sérotype.

Séropathotype	Incidence relative	Fréquence d'implication dans des épidémies	Association avec des maladies graves	Exemple de sérotype
A	Élevée	Fréquent	Oui	O157:H7, O157:NM
B	Modérée	Peu fréquent	Oui	O26:H11, O45:H2, O103:H2, O111:NM, O121:H19, O145:NM
C	Faible	Rare	Oui	O157:H26, O145:H25, O113:H21
D	Faible	Rare	Non	O113:H4
E	Aucune chez l'humain	NA	NA	O103:H14

Le séropathotype A regroupe les souches de sérotypes O157:H7 et O157:NM communément impliqués dans les épidémies et responsables des symptômes les plus graves de la maladie. Le séropathotype B regroupe les sérotypes associés aux éclosions et au SHU mais de manière moins fréquente que le sérotype O157:H7. Le séropathotype B comprend notamment les souches de sérotype retrouvé dans le « Big six » (O26:H11, O45:H2, O103:H2, O111:NM, O121:H19 et O145:NM). Le séropathotype C contient des souches de sérotypes rarement isolées de cas cliniques mais pour lesquels des symptômes graves étaient associés tel que O91:H21 et O113:H21. Le séropathotype D comprend des souches de sérotypes associés à des diarrhées qui n'ont pas été reliées à des épidémies et qui ne sont pas associées à des SHU. Enfin le séropathotype E comprend des souches STEC animales de sérotypes non impliqués dans les maladies humaines. En utilisant la méthode de classification par séropathotype, Karmali *et al.* ont pu montrer que la présence de l'îlot génomique OI-122 dans les génomes de différents sérotypes, était reliée à la fréquence d'implication dans les épidémies et/ou dans le développement de maladies graves. Le concept de séropathotypes est utile pour étudier les facteurs bactériens qui contribuent à maladie et à la transmissibilité des sérotypes STEC (Karmali *et al.*, 2003).

II.1.5 Épidémiologie

Depuis sa première description en 1982, le sérotype O157:H7 est le sérotype STEC le plus commun causant de multiples infections d'origine alimentaire en Amérique du Nord, en Europe et en Asie. Ce sérotype reste d'ailleurs aujourd'hui le sérotype le plus communément associé aux infections EHEC puisqu'au cours de l'année 2016, 2/3 (474/708) des cas d'infections aux EHEC reportées au Canada étaient dus au sérotype O157:H7. Ce sérotype a également été incriminé dans trois épisodes d'épidémies à la suite de la consommation de laitues romaines en 2017 et en 2018 à la fois au Canada et aux États-Unis. Cependant les autres sérotypes ne doivent pas être négligés puisqu'ils sont aussi impliqués dans des épidémies. De plus, selon un rapport du CDC, le nombre d'infections aux EHEC de sérotype non-O157 est en augmentation aux États-Unis. D'ailleurs dans une autre étude effectuée par le CDC, il a été montré que près de 70 % des infections causées par des souches non-O157 entre 1983 et 2002 avaient été causées par le « Big six » (Wang et al., 2012a). D'autres sérotypes, tels que O113:H21 ou O91:H21, ne causent généralement pas d'épidémie mais peuvent être associés à des épisodes sporadiques de SHU (Karmali *et al.*, 2003). Cependant bien qu'étant une maladie à déclaration obligatoire, les infections aux STEC restent le plus souvent au stade de diarrhées ne nécessitant pas d'hospitalisation. Il est donc évident que le nombre de cas rapportés ne reflète pas le nombre réel d'infections. Si on se fie à certaines estimations qui prennent en compte le nombre de maladie non déclarée, le nombre d'infections aux STEC non-O157 par an serait plus élevé que celui des souches O157 (Chui et al., 2018). Au niveau mondial, il a été estimé que les STEC causeraient plus de 2,8 millions de cas de maladies aiguës, 3 890 cas de SHU, 270 cas de maladie rénale permanente et 230 décès par an (Majowicz *et al.*, 2014). Parmi les infections d'origine alimentaire les STEC causent beaucoup moins de cas que la fièvre typhoïde (21.7 millions de cas) ou que les autres salmonelloses (93.8 millions de cas par et 155 000 décès). Cependant, malgré moins de cas et de décès, les STEC entraînent de graves complications et sont responsables de pertes humaines et économiques importantes. Une étude a estimé qu'en 2003, le coût des infections causées par les souches uniquement de sérotype O157:H7 s'élevait à 405 millions de dollars US (Frenzen *et al.*, 2005). Les STEC sont donc des bactéries qui doivent être prises en compte lors de la mise en place de luttes contre les agents pathogènes d'origine alimentaire. De plus, lors de l'épidémie qui a lieu en 2011 en Allemagne

un nouveau type de souche émergente de STEC a pu être identifié (Frank *et al.*, 2011). Cette souche appartenant au sérotype O104:H4, avait un fond génétique de souche de *E. coli* enteroaggrégative (EAEC) typique multirésistante aux antibiotiques mais disposait en plus dans son génome du bactériophage encodant la toxine Stx2 des STEC (Scheutz *et al.*, 2011).

II.1.6 Éléments génétiques mobiles chez les STEC

Comme discuter plus haut, les sérotypes STEC sont très nombreux et les souches STEC proviennent de différentes lignées génétiques. Dans les années 2000, grâce au séquençage du génome, il a pu être mis en évidence que les souches STEC se distinguaient des autres *E. coli* par la taille de leur génome (O'Reilly *et al.*, 2010). En effet le génome des STEC est criblé d'éléments génétiques mobiles tels que des transposons, des prophages et des plasmides. Ces éléments génétiques mobiles codent entre autres pour des facteurs de virulence ou pour des gènes du métabolisme (enzymes) et sont contenus dans des îlots de pathogénicité appelés « O-Island ». L'information génétique contenue dans les éléments génétiques mobiles peut être échangée entre différentes souches de la même espèce ou non, permettant l'émergence de nouveaux variants (Schmidt and Hensel, 2004). Il a d'ailleurs été montré que la différence de virulence qui existe entre les souches pathogènes et non pathogènes d'une même espèce bactérienne pouvait être attribuée en partie aux gènes de virulence contenue sur les îlots de pathogénicité (Ju *et al.*, 2013; Karmali *et al.*, 2003).

II.1.6.1 Le locus d'effacement de l'entérocyte (LEE)

L'élément génétique le plus souvent associé à la pathogenèse des STEC (autres que les prophages qui encodent le gène *stx*) est le LEE. Le LEE est un grand îlot de pathogénicité (environ 42 kb) qui est aussi retrouvé chez les EPEC. Le LEE code pour des facteurs de virulence comme l'intimine, le récepteur de l'intimine, Tir, un système de sécrétion de type III (SST3), et 4 effecteurs (en plus de Tir) qui sont sécrétés par le SST3 directement à l'intérieur de la cellule hôte. L'expression des protéines du LEE et d'autres effecteurs est régulée de manière très complexe. Cependant la présence du LEE n'est pas toujours requise pour que la bactérie soit capable de causer la maladie. En effet certains sérotypes STEC positifs pour le LEE retrouvés chez les bovins n'ont jamais été associés à une maladie humaine (Wilson *et al.*, 1998).

De plus, les sérotypes EHEC négatifs pour le LEE peuvent aussi être associés à des maladies humaines graves (Montero *et al.*, 2017; Nataro and Kaper, 1998). Ces observations suggèrent que des facteurs, autres que le LEE, favorisent l'émergence et augmentent le potentiel de virulence des souches EHEC (Karmali *et al.*, 2003; Montero *et al.*, 2017).

II.1.6.2 Îlots de pathogénicité « O-Island »

Parmi les candidats qui permettent d'augmenter le potentiel de virulence des souches STEC, on retrouve les îlots de pathogénicité (PAI). Plusieurs PAI sont présents dans le génome des EHEC telles que EDL933 et Sakai et sont nommés « O-Island » (OI). Les OI sont absents du génome de *E. coli* K-12 (Hayashi *et al.*, 2001; Perna *et al.*, 2001). Les OI représentent une grande partie du génome des STEC (20 % du génome de EDL933 (Poirier *et al.*, 2008)) et contribue à la pathogénicité des O157 et non-O157 (Cadona *et al.*, 2018; Coombes *et al.*, 2008; Konczy *et al.*, 2008). Cependant, la contribution des OI dans la pathogénicité des STEC reste peu documentée. Certains d'entre eux codent pour des effecteurs (appelé « non-LEE-encoding effector » (nle), ou des adhésines ou pour des protéines similaires à des facteurs de virulence retrouvés chez d'autres bactéries pathogènes (Perna *et al.*, 2001). Par exemple, le OI-122 présent dans la plupart des souches de séropathotype A et B, code pour un homologue du gène *pagC* (impliqué dans la survie de *Salmonella* dans le macrophage (Miller *et al.*, 1989)) ainsi que pour *efa1* (EHEC factor for adherence (Efa-1) aussi connu sous le nom de *lifA* (lymphostatine (LifA)) (Karmali *et al.*, 2003). Il a été montré que l'expression de PagC ainsi que celle de plusieurs autres gènes du OI-122 étaient augmentées lorsque EDL933 se répliquait à l'intérieur de macrophage *in vitro* (Poirier *et al.*, 2008). De plus il a récemment été découvert qu'un îlot de pathogénicité, appelé locus d'adhésion et d'auto-agrégation (LAA) était retrouvé dans un sous-ensemble de souches EHEC LEE négatives associées à des cas de colite hémorragique et de SHU (Colello *et al.*, 2018; Montero *et al.*, 2017). Ainsi les OI permettent aux STEC d'évoluer et contribuent à l'émergence de nouveaux types de STEC.

II.1.6.3 Prophages

Le génome des STEC contient un nombre important de prophages, la plupart d'entre eux sont des phages lambda (Asadulghani *et al.*, 2009; Hayashi *et al.*, 2001). Cependant parmi les

STEC, la taille des prophages et leur site d'insertion varient. Ceci augmente d'autant plus la diversité des souches STEC. Les prophages peuvent coder pour des gènes impliqués dans la virulence, dans la survie de la bactérie ou dans la régulation génétique (Hayashi *et al.*, 2001). Par exemple, chez Sakai les chercheurs ont découvert que 18 prophages (noté Sp1 à Sp18) étaient insérés dans le génome et appartenaient à différentes classes de phage P2, P4, Mu et lambda (Brussow et al., 2004). Parmi les 18 prophages seulement deux (Sp5 and Sp15) codent pour des facteurs de virulence avérés (Stx1 et Stx2). Cependant de nombreux autres prophages codent pour des facteurs de virulence potentiels, comme le Sp4 qui code pour *sodC*; et le Sp6 qui code pour une cytotoxine potentielle (Ohnishi *et al.*, 2001). En analysant la structure du génome de 8 souches O157, Ohnishi et ses collaborateurs ont pu montrer que la composition des génomes variait beaucoup au niveau du contenu en prophages que ce soit au niveau de leur séquence ou de leur site d'insertion. En conclusion les prophages, grâce à leur grande mobilité génétique, participent grandement à la diversité des STEC (Brussow et al., 2004).

II.1.6.4 Plasmides

Le génome des STEC est aussi constitué de plasmides qui varient en nombre et en taille. Ces plasmides, souvent très larges, ne sont pas des éléments génétiques uniformes, mais hétérogènes dans leur composition et dans leur arrangement (Brunder *et al.*, 1999). Par exemple il a été trouvé que ces plasmides (noté pO157, pO26, pO111, pO113 en fonction du sérotype) peuvent coder pour des marqueurs de virulence tels qu'un système de sécrétion de type II, une entérohémolysine (EhxA), un autotransporteur (Saa), une catalase-peroxydase (KatP), une sérine protéase extracellulaire (EspP), une zinc métalloprotéase (StcE) et une subtilase cytotoxine (SubAB). La présence de ces facteurs sur le plasmide varie en fonction du sérotype. Le plasmide des souches O157 (92kb) est un plasmide non-conjugatif qui contient plusieurs éléments génétiques mobiles (Lim *et al.*, 2010b). Le plasmide pO157 code aussi pour l'opéron *ecf* qui code pour plusieurs enzymes qui peuvent modifier les polysaccharides ou les composants du lipopolysaccharides (LPS) et pour une protéine de la membrane externe (Lim *et al.*, 2010b). Le rôle du plasmide pO157 dans la formation de biofilm a été démontré en utilisant une souche *E. coli* O157:H7 qui a perdu son plasmide pO157 (Lim *et al.*, 2010a). Une autre étude a révélé que deux protéines, EhxD (translocateur de l'entérohémolysine EhxA) et EspP (sérine protéase

autotransporteur de type V), étaient directement impliquées dans la formation de biofilm (Puttamreddy, 2010). De plus, certaines études suggèrent que les souches de STEC contenant le pO157 étaient plus souvent associées à des épidémies et au développement de SHU que celles sans pO157 (Abu-Ali *et al.*, 2010; Karmali *et al.*, 2003). Les grands plasmides des souches de sérotype O26:H11, O111:NM, O113:H21 présentent une similarité de séquence avec les plasmides de O157:H7 (Fratamico *et al.*, 2011).

II.1.7 Facteurs de virulence des STEC

Comme nous venons de le décrire dans la section précédente, le génome des STEC est plus grand que le génome des autres *E. coli* (O'Reilly *et al.*, 2010) et contient beaucoup d'ADN supplémentaire parmi lequel on retrouve de nombreux facteurs de virulence. Grâce à l'acquisition de cet ADN supplémentaire, les STEC ont émergé et sont maintenant responsables d'épidémies de maladies gastro-intestinales. Dans cette section nous nous attarderons à la description de la toxine Stx, facteur commun à toutes les STEC. Les facteurs de virulence n'étant pas le propos principal de cette thèse, les autres principaux facteurs de virulence sont résumés sous forme de tableau afin de souligner la grande diversité des STEC et le réservoir de facteurs de virulence qu'ils représentent (Tableau 2).

II.1.7.1 Shiga-toxines

Le principal facteur de virulence des STEC est la production de Shiga-toxines. Chez *E. coli*, il existe deux types de Shiga-toxines, Stx1 et Stx2 (respectivement 99 % et 56 % d'homologie avec la toxine Stx de *Shigella dysenteriae*). Stx1 et Stx2 ont le même mode d'action mais sont immunologiquement distinctes (Melton-Celsa, 2014; O'Brien *et al.*, 1982). Lorsque ces toxines atteignent la circulation sanguine, elles inhibent la synthèse protéique de l'endothélium néphritique ayant pour conséquence le développement de SHU.

Selon les données épidémiologiques, Stx2 est plus souvent associée au développement de SHU que Stx1 (Boerlin *et al.*, 1999). En effet, des études antérieures ont montré que les cellules endothéliales de l'intestin sont 10 fois plus sensibles à Stx2 que Stx1 et que les cellules glomérulaires endothéliales étaient 1 000 fois plus sensibles à Stx2 qu'à Stx1 (Griffin and

Tauxe, 1991; Jacewicz *et al.*, 1999).

Les toxines Stx1 et Stx2 sont codées respectivement par les gènes *stx1AB* et *stx2AB* portés sur des prophages intégrés dans le chromosome des STEC. Leur expression est donc dépendante des mécanismes de régulation des phages. Les bactériophages lambda ont un cycle lysogénique au cours duquel le phage intégré au génome reste silencieux, et un cycle lytique au cours duquel l'ensemble des gènes phagiques sont exprimés, permettant la production et l'assemblage des phages. Le cycle lytique est induit lorsque la bactérie induit la réponse SOS après avoir subi un stress tel qu'un changement de pH, irradiation aux UV ou bien la présence d'antibiotique affectant l'ADN (mitomycine C ou les quinolones). Donc le déclenchement de la réponse SOS va entraîner la surexpression des gènes phagiques incluant celle des toxines Stx. Sachant que la production de Stx1 ou de Stx2 conduit au développement du SHU, c'est pour les mêmes raisons que l'utilisation d'antibiotique est déconseillée pour traiter une infection aux STEC. Plusieurs études ont également montré que l'expression des gènes *stx* serait dépendante de leur propre promoteur (Sung *et al.*, 1990). Même si les facteurs menant à l'expression des gènes *stx in vivo* ne sont pas encore identifiés, la production de H_2O_2 par les neutrophiles semble jouer un rôle sur la production de Stx2 (Wagner *et al.*, 2001).

Les Shiga-toxines (aussi connues sous le nom de Vero toxines) sont des toxines de type AB5, c'est-à-dire qu'elles sont composées d'une sous-unité enzymatique active A (codée par *stx1A* ou *stx2A*) entourée de 5 sous-unités B (codées par *stx1B* ou *stx2B*) responsables de la liaison de la toxine au récepteur. Lorsqu'elles sont produites, les Shiga-toxines traversent l'épithélium intestinal pour atteindre la circulation sanguine. Une fois dans le sang, le pentamère de sous-unités B reconnaît les récepteurs globotriosylcéramide (Gb3) présents à la surface des cellules endothéliales incluant les cellules glomérulaires rénales et de l'endothélium vasculaire. Le Gb3 est un récepteur glycolipidique dont la fonction reste inconnue. Après avoir fixé son récepteur, Stx est internalisée par endocytose, atteint l'appareil de Golgi et voyage par voie rétrograde jusqu'au réticulum endoplasmique. Puis une protéolyse partielle clive la sous-unité A en deux parties par réduction du pont disulfure. Il en résulte une libération intracellulaire de N-glycosidase active (A1), capable d'hydrolyser l'ARN ribosomal 28S, constituant de la sous-unité ribosomale 60S. Cette modification inhibe alors la fonction d'élongation du ribosome,

bloque la synthèse protéique et conduit par conséquent à la mort cellulaire (Figure 6) (Melton-Celsa, 2014).

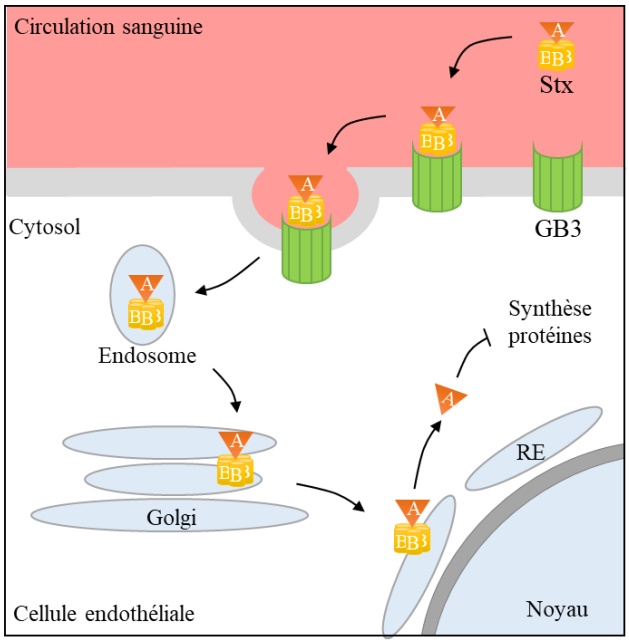

Figure 6. Mode d'action de la Shiga-toxine. La Shiga-toxine (Stx) présente dans la circulation sanguine se lie au récepteur Gb3, est internalisée dans les endosomes, transite par voie rétrograde dans l'appareil de Golgi et atteint le réticulum endoplasmique (RE). La sous-unité A est alors clivée dans le cytosol et inactive la synthèse protéique en inhibant l'activité des ribosomes.

Même si le mécanisme d'action des toxines Stx est bien connu, le mécanisme de translocation des toxines Stx à travers la barrière épithéliale reste cependant un mystère. En effet, chez l'humain, le récepteur Gb3 semble être absent des cellules épithéliales du tractus intestinal (Holgersson *et al.*, 1991). De manière intéressante, il a été montré que Stx1 et Stx2 sont capables de traverser une monocouche de cellules T84 polarisée sans perturber ou inhiber la synthèse protéique (Philpott *et al.*, 1997; Schuller *et al.*, 2004). Pour expliquer la translocation de la toxine à travers des cellules Gb3 négatives, plusieurs hypothèses telles que la macropinocytose, ont été avancées (Malyukova *et al.*, 2009; Schuller *et al.*, 2004). Cependant il a aussi été suggéré que le récepteur Gb3 puisse être présent à la surface des cellules intestinales mais sa détection serait difficile puisqu'insérer dans le cholestérol (Mahfoud *et al.*, 2010;

Melton-Celsa, 2014). De plus, il a aussi été montré que la présence de butyrate (métabolite retrouvé dans l'intestin) rendait les cellules intestinales plus sensibles à la toxine Stx et augmentait le niveau d'expression de l'ARNm Gb3 (Zumbrun *et al.*, 2010; Zumbrun *et al.*, 2013). Ces découvertes suggèrent que les mesures antérieures des taux de Gb3 sur les tissus intestinaux pourraient être sous-estimées.

Chez les bovins, la présence de STEC dans le tractus intestinal est asymptomatique. Une des raisons principales est l'absence de récepteur Gb3 à la surface de l'endothélium (Pruimboom-Brees *et al.*, 2000). Cependant, les cellules épithéliales intestinales bovines expriment aussi des récepteurs Stx fonctionnels (Hoey *et al.*, 2002; Menge *et al.*, 2004a; Stamm *et al.*, 2002). En fait chez le bovin, Stx1 et Stx2 agiraient comme des suppresseurs de la réponse immunitaire. Il a été montré *in vitro* que Stx1 bloque l'activation et la prolifération des lymphocytes et monocytes et altère l'expression des cytokines (Menge *et al.*, 2004b; Menge *et al.*, 1999; Moussay *et al.*, 2006). Stx2 est reliée à l'inhibition de la réponse immunitaire en phase précoce (Hoffman *et al.*, 2006). Stx2 a également été associé à une meilleure colonisation intestinale causée par *E. coli* O157:H7 chez la souris (Robinson *et al.*, 2006). La production de toxines Stx mène donc à une diminution de la réponse immunitaire permettant d'allonger le temps de portage et d'excrétion de la bactérie dans l'intestin du bovin.

II.1.7.2 Autres facteurs de virulence

En plus des toxines Stx, les STEC disposent d'une multitude de facteurs de virulence incluant des effecteurs, des adhésines, des toxines, ainsi que d'autres facteurs importants dans la colonisation (chez l'animal ou chez l'humain) ou toutes autres étapes du processus infectieux. La présence de ces facteurs varie en fonction du sérotype mais aussi en fonction de la souche STEC. Le tableau 2 répertorie une partie des facteurs de virulence connus des STEC et permet de mettre en évidence la grande diversité de fonction de ces facteurs.

Tableau 2. Les facteurs de virulence des EHEC. Adapté de (Elder and Nightingale, 2013).

Nom	Gène	Location	Fonction possible	Références
Intimine	*Eae*	LEE	Adhérence (LEE positive)	(McKee *et al.*, 1995)
"Translocated intimin receptor"	*Tir*	LEE	Adhérence (LEE positive)	(Frankel *et al.*, 2001)
"Tir-cytoskeleton coupling protein"	*tccP/espF*$_u$	Prophage CP-933U (O157:H7)	Polymériation de l'actine (LEE positive)	(Campellone *et al.*, 2004) (Garmendia *et al.*, 2004)
*"*STEC auto-agglutinating adhesin"	*saa*	pO113	Adhérence (LEE negative)	(Paton *et al.*, 2001)
"Sorbitol fermenting EHEC O157 fimbriae"	*sfp*	pSFO157	Adhérence (O157:NM)	(Brunder *et al.*, 2001)
"IrgA homologue adhesion"	*iha*	OI-43, OI-48, pO113	Adhérence (non-O157 STEC)	(Tarr *et al.*, 2000)
"EHEC factor for adherence ou lymphostatine"	*efa-1/lifA*	OI-122	Adhérence (LEE positive)	(Nicholls *et al.*, 2000)
"E. coli common pilus"	*ecpA*	Chromosome	Adhérence (all *E. coli*)	(Rendon *et al.*, 2007)
"Long polar fimbriae"	*lpfA*	OI-141, OI-154	Adhérence (all seropathotypes)	(Doughty *et al.*, 2002; Toma *et al.*, 2004; Torres *et al.*, 2002)
"Hemorrhagic coli pilus"	*hcpA*	Chromosome	Adhérence	(Xicohtencatl-Cortes *et al.*, 2007)
"Non-LEE encoded effectors"	*nleA/espI*	OI-71	Perturbation de la barrière intestinale de l'hôte	(Gruenheid *et al.*, 2004) (Thanabalasuriar *et al.*, 2010)
	nleB	OI-122	Anti-inflammatoire	(Newton *et al.*, 2010)
	nleC	OI-36	Anti-inflammatoire	(Baruch *et al.*, 2011; Pearson *et al.*, 2011)
	nleD	OI-36	Anti-inflammatoire	(Baruch *et al.*, 2011)
	nleE	OI-122	Anti-inflammatoire	(Nadler *et al.*, 2010)*et al.*, 2010; Newton *et al.*, 2010; (Newton *et al.*, 2010; Vossenkamper *et al.*, 2010)

	nleF	OI-71	Inconnue	(Echtenkamp *et al.*, 2008)
	nleG	OI-57, OI-71	Module l'ubiquinintion de la cellule hôte	(Wu *et al.*, 2010)
	nleH	OI-36, OI-71	Inhibition de l'exfoliation des entérocytes	(Hemrajani *et al.*, 2010)
	nleL/espX7	Prophage SP6	Régule la formation du piédestal	(Piscatelli *et al.*, 2011)
"*E. coli* secreted proteins"	*espA*	LEE	Composant du SST3	(Knutton *et al.*, 1998)
	espF	LEE	Apoptose et Perturbation de la barrière intestinale de l'hôte	(Crane *et al.*, 2001; McNamara *et al.*, 2001)
	espJ	Prophage CP933U	Inhibe la phagocytose	(Dahan *et al.*, 2005; Marches *et al.*, 2008)
	espK	Prophage CP933N	Inconnue	(Vlisidou *et al.*, 2006)
	espO	Prophage	Inhibition de l'exfoliation des entérocytes	(Kim *et al.*, 2009)
"Serine protease"	*espP*	pO157	Adhérence	(Brunder *et al.*, 1997)
	espZ	LEE	Inhibition de l'exfoliation des entérocytes	(Shames *et al.*, 2010)
"Cycle inhibiting factor"	*cif*	Prophage	Inhibition de l'exfoliation des entérocytes	(Marches *et al.*, 2003)
"Subtilase cytotoxin"	*subAB*	pO113	Cytotoxine, inconnue	(Paton *et al.*, 2004)
	toxB	pO157	Adhérence et inhibe réponse immunitaire	(Klapproth *et al.*, 2000) (Stevens *et al.*, 2004) (Tatsuno *et al.*, 2001)
"Enterohemolysin"	*ehx*	pO157, pO113, pO26	Cytotoxine, inconnue	(Schmidt *et al.*, 1994)
"Catalase-peroxidase"	*katP*	pO157	Protection contre les dommages oxydatifs dus à l'immunité innée.	(Brunder *et al.*, 1996)
"STEC autotransporter mediating biofilm formation"	*sab*	pO113	Formation de biofilm	(Herold *et al.*, 2009)
"Autotransporter protein"	*epeA*	pO113	Protéolyse et destruction du mucus	(Leyton *et al.*, 2003)

II.1.8 Prévention, traitement et vaccins

À ce jour, il n'existe pas de traitement efficace permettant d'éradiquer la maladie lorsqu'un patient est infecté par une souche EHEC. Les antibiotiques sont contre-indiqués car ils sont associés à un risque accru de SHU. La principale prise en charge recommandée lors d'une infection à EHEC repose principalement sur un suivi et une hydratation du patient (Qadri and Kayali, 1998; Shane *et al.*, 2017). C'est d'ailleurs l'absence de traitement qui représente une menace majeure pour la santé des patients infectés par une souche EHEC. Cependant il existe des possibilités de traitements et de préventions qui sont l'utilisation i) de composés dirigés contre la bactérie mais qui n'induisent pas un relargage de la toxine ; de molécules qui mime le récepteur Gb3 ou altère le trafic de la toxine; (iii) d'anticorps dirigé contre Stx; ou (iv) des thérapies pour prévenir ou traiter le SHU.

II.1.8.1 Les agents antimicrobiens

Lors d'une infection à EHEC, l'usage d'antimicrobien est considéré comme dangereux car il augmente la libération des toxines et donc le risque de SHU. Les antibiotiques agissent de plusieurs manières sur la libération de la toxine. Premièrement l'usage de certains antibiotiques (i.e. ciprofloxacine) à des doses sublétales augmente la production de Stx en induisant le phage lysogène qui code pour la toxine. Par exemple, il a été montré *in vitro* que l'utilisation de certains antibiotiques, tels que les quinolones, le triméthoprime et la furazolidone, induisent une réponse SOS. La réponse SOS a pour fonction de réparer les cassures double-brin de l'ADN et conduit à l'activation du cycle lytique des bactériophages, augmentant ainsi la production de Stx. Deuxièmement, un traitement antibiotique utilisé à des doses létales peut provoquer un éclatement de la bactérie et donc une libération massive de la toxine. Par exemple on sait que l'usage d'antibiotique qui mènent à la lyse cellulaire va induire un relargage massif de Stx1 qui est stockée dans l'espace périplasmique des cellules EHEC (Donohue-Rolfe and Keusch, 1983; Shimizu *et al.*, 2009; Strockbine *et al.*, 1986). Cependant, l'induction ou la libération de Stx pourraient être dépendantes du sérotype (voire de l'isolat) ou de l'agent antimicrobien ainsi que de la dose administrée (Corogeanu *et al.*, 2012; Fadlallah *et al.*, 2015; Grif *et al.*, 1998; Nassar *et al.*, 2013). Par exemple, une étude sur des patient humain a montré qu'un antibiotique tel que la fosfomycine pourrait être utilisée sans danger (Ichinohe *et al.*, 2009). De plus de nombreuse

personnes ont été traitées à la fosfomycine au Japon lors de l'épidémie de la souche O157:H7 Sakai sans augmentation apparente du SHU (Ikeda *et al.*, 1999). Cependant, le faible taux de développement de SHU durant cette épidémie diminue l'impact des conclusions (Fukushima *et al.*, 1999). En 2011, lors de l'éclosion d'infection à *E. coli* O104:H4 en Allemagne, des antibiotiques ont été utilisés chez de nombreux patients (Menne *et al.*, 2012). Alors que l'utilisation d'antibiotiques semblait fonctionner dans certains cas (i.e. ciprofloxacine) (Geerdes-Fenge *et al.*, 2013), il est difficile de tirer des conclusions sur l'efficacité de tels traitements à cause de la non-uniformité des protocoles. De plus, chez plusieurs patients touchés par cette épidémie de *E. coli* O104:H4, le SHU s'est déclaré après le traitement par la ciprofloxacine ou le métronidazole (Binks *et al.*, 2012). Enfin, l'un des aspects uniques de l'épidémie en Allemagne était l'utilisation de l'azithromycine pour réduire l'excrétion de O104:H4 chez les patients qui semblaient être des porteurs à long terme (Nitschke *et al.*, 2012). La possibilité d'utilisation d'antibiotiques doit encore être étudiée car le risque de développement de SHU reste trop élevé (Rahal *et al.*, 2015). En effet chez certaines souches EHEC, un traitement antibiotique peut ne pas altérer l'expression de Stx car les gènes *stx* peuvent être associés à des bactériophages défectueux (Melton-Celsa and O'Brien, 2014). De plus, les antibiotiques sont le plus souvent utilisés chez les patients les plus malades, ce qui peut fausser le risque apparent de développement du SHU. Enfin, les études publiées sur le risque de SHU associé à un traitement antibiotique ont utilisé différents traitements administrés à différents stades du processus pathologique. Le débat sur le traitement par antibiotique des infections EHEC se poursuit.

II.1.8.2 Traitements en développement : la thérapie anti-virulente

Les traitements actuellement utilisés sont destinés à atténuer les symptômes ressentis par le patient. Lors d'une étude clinique, il a été observé que l'augmentation du volume d'eau et de sodium par voie intraveineuse chez les enfants infectés par O157:H7 mais n'ayant pas encore développé de SHU, diminuait le risque de problème rénal par rapport aux enfants qui n'avaient pas subi ce traitement (Ake *et al.*, 2005). Un bon moyen pour traiter les patients infectés par les EHEC serait de cibler le mécanisme d'action des toxines Stx. L'une des stratégies qui pourrait être employée serait d'administrer au patient des bactéries recombinantes ou des dendrimères

exprimant ou mimant le récepteur Gb3 (récepteur des toxines Stx). Ceci permettrait de réduire les effets néfastes liés à la toxine Stx. Un certain nombre d'analogues de récepteurs de toxines ont été mis au point dans l'espoir de neutraliser la toxine dans l'intestin. Pour l'instant, il a été montré *in vitro* et chez des modèles murins que ces agents permettent d'inhiber les effets de Stx en réduisant le nombre de toxines qui vont atteindre les cellules cibles (Rahal *et al.*, 2015). Pinyon et ses collaborateurs ont mis au point une souche *E. coli* K-12 qui exprime à sa surface une protéine qui mime le récepteur Gb3 de la toxine. Une fois ingérée par le patient infecté, cette bactérie permettrait de réduire le nombre de Stx dans l'intestin (Pinyon *et al.*, 2004). Une autre possibilité, également à l'étude, serait d'interférer sur le transport de la toxine directement à l'intérieur de la cellule hôte grâce à l'utilisation de molécules spécifiques qui peuvent pénétrer à l'intérieur de la cellule hôte et cibler spécifiquement Stx lors de son transfert à travers les compartiments cellulaires (Rahal *et al.*, 2015). Il a également été montré que l'utilisation d'anticorps dirigés contre Stx permettait de neutraliser les effets toxiques de Stx après l'infection. En effet l'administration d'anticorps anti-Stx1, anti-Stx2 ou anti-Stx1/2 protégeaient les animaux infectés (Bitzan *et al.*, 2009; Melton-Celsa *et al.*, 2015). Alors qu'il a été montré que tous ces composés protégeaient les cellules ou les animaux contre la toxine Stx purifiée ou les effets toxiques d'une infection par STEC, la plupart de ces composés n'ont pas été testés chez l'humain et doivent donc être soigneusement évalués avant de pouvoir être utilisé en clinique. On ne sait pas dans quelle mesure on pourra trouver des composés sans danger pour l'humain. Néanmoins, l'utilisation d'une thérapie anti-virulente est un réel espoir dans le traitement des infections à STEC car il remplace l'utilisation de l'antibiotique. De plus, contrairement à l'antibiothérapie, l'utilisation d'une thérapie anti-virulente n'affecte pas la croissance et donc il y a moins de chance de développer une résistance (Lee, 2011a). Enfin pour tenter de traiter un patient qui présente déjà un SHU, l'utilisation d'éculizumab (un anticorps monoclonale dirigé contre la protéine de complément C5 utilisée pour traiter le SHU atypique, une maladie pouvant survenir en raison d'une dysrégulation du complément) permettrait de diminuer les symptômes de SHU dans certains cas. Par exemple, l'éculizumab a été utilisé en 2011 pour traiter trois enfants infectés à STEC et atteints de SHU. Malgré une diminution des symptômes, la véritable efficacité du traitement n'a pu être vérifier car d'autres traitements ont également été utilisés. De plus, le nombre de patient (n=3) était très faible et ne permet pas de tirer de conclusions (Lapeyraque *et al.*, 2011). L'éculizumab a également été utilisé pour traiter de nombreux

patients atteints de SHU lors de l'épidémie de O104:H4 en Allemagne en 2011. Malheureusement l'efficacité du traitement du SHU par l'éculizumab n'a pas pu être démontrée chez l'humain car les patients ont tous reçu d'autres traitements, incluant des échanges plasmatiques, une antibiothérapie et des dialyses (Kielstein *et al.*, 2012; Ullrich *et al.*, 2013). De plus, de nombreux patients atteints de SHU ayant reçu de l'éculizumab étaient très malades et présentaient des complications neurologiques. Néanmoins dans certains cas, l'éculizumab semble fonctionner. Par exemple en 2015, un homme de 18 ans qui a développé un SHU grave en raison d'une infection à STEC O121 et qui ne répondait pas aux thérapies traditionnelles a été traité avec succès par l'éculizumab (Dinh *et al.*, 2015). Par conséquent, un essai contrôlé de l'éculizumab est nécessaire pour tester son efficacité dans le traitement du SHU associé à Stx.

II.1.8.3 Traitements préventifs

II.1.8.3.1 Chez l'humain

Aucune stratégie de vaccination chez l'humain n'a été poursuivie à grande échelle. Le candidat vaccinal le plus prometteur pour l'humain est un vaccin conjugué à base d'antigène O157 (O157-rEPA). En phase I ce vaccin a été démontré sans danger et immunogène chez l'adulte (Konadu *et al.*, 1998). Un essai de phase II a permis de montrer qu'il l'était aussi chez les jeunes enfants (2 à 5 ans) (Ahmed et al., 2006a). La phase III a été planifiée et devrait bientôt être initiée (O'Ryan *et al.*, 2015).

II.1.8.3.2 Chez l'animal

Un bon moyen pour prévenir les infections aux STEC serait de réduire ou d'éliminer ces agents pathogènes des chaînes de production alimentaire et donc de l'intestin des bovins d'élevage. La vaccination de l'animal permettrait de réduire le portage et donc la propagation des STEC dans l'environnement. En prévenant la colonisation des STEC dans l'intestin des bovins, un vaccin dirigé contre les STEC réduirait considérablement le nombre d'infections STEC associé aux bétails. Les vaccins développés ou en cours de développement ciblent les protéines associées au phénomène de lésion attachantes et effaçantes sécrétées par le LEE (comme la protéine Tir ou l'intimine), l'antigène O du LPS (O157, O111) ou encore les récepteurs de sidérophores (Butler *et al.*, 2012; Martorelli *et al.*, 2018; Santos *et al.*, 2010;

Schmidt *et al.*, 2018). Récemment il a été suggéré que les vésicules de la membrane externe (OMV) dérivées des STEC présentaient un potentiel pour la formulation de vaccins à la fois humains et vétérinaires (Fingermann *et al.*, 2018). À ce jour, deux vaccins sont commercialement disponibles. L'un d'entre eux, Econiche® (Bioniche Life Sciences INC., Belleville, Ontario, Canada) est un vaccin constitué de composants du système de sécrétion de type III et une étude a montré que 90 % des bovins vaccinés étaient moins susceptibles d'être colonisés par O157 que les animaux non vaccinés pendant une période de 3 mois (Smith *et al.*, 2009). Le principal inconvénient de ce vaccin est qu'il est composé de constituant du SST3 et donc qu'il ne cible pas les STEC qui en sont dépourvus. Le second vaccin, Epitopix® (Epitopix LLC, Willmar Poultry Company (WPC), Minnesota, USA) est un vaccin à base de récepteur de sidérophore et de porines présent à la surface de la bactérie O157 (Thomson *et al.*, 2009). En inhibant la capture du fer par O157, ce vaccin induit un désavantage à O157:H7 par rapport aux autres bactéries de l'intestin. Plusieurs essais sur le terrain avec des bovins immunisés avec le Epitopix® ont montré que les animaux vaccinés excrétaient moins de O157 que les animaux non traités et pendant moins longtemps. Cependant, même si ces études sont prometteuses, aucune d'entre elles ne permet de réduire complètement l'excrétion de O157:H7. De plus on ne sait pas si ces vaccins offrent une protection croisée contre d'autres sérogroupes STEC, notamment ceux appartenant au « Big six » (O'Ryan *et al.*, 2015).

Un autre moyen pour réduire la colonisation des STEC chez les bovins pourrait être de changer le régime alimentaire des bovins afin de modifier leur microbiote permettant de réduire l'implantation des STEC dans l'intestin (Berry and Wells, 2010; Berry et al., 2017; Wells et al., 2009a). L'ajout d'antibiotique, de probiotique ou de bactériophage est également envisagé comme stratégie pour réduire le portage de STEC dans l'intestin des bovins (Sargeant *et al.*, 2007). Des solutions pour le lavage de la peau et d'autres moyens de manipulation des carcasses pour réduire la contamination lors de l'abattage ont également été proposées (Berry and Wells, 2010; Canada, 2015; Centers for Disease Control and Prevention A, 2014; USDA, 2017) et la mise en place de leur application semble être efficace (Karmali, 2017).

II.2 La formation de biofilm des STEC

II.2.1 Introduction

L'essentiel des connaissances acquises en physiologie bactérienne repose sur l'observation du mode de vie planctonique des bactéries, c'est-à-dire à partir d'études réalisées en milieu liquide. Pourtant les bactéries disposent d'un second mode de vie dit « sessile ». À l'état sessile, les bactéries se développent associées aux surfaces et forment des communautés fixées et entourées d'une matrice extra-cellulaire autoproduite appelées biofilms (Stoodley *et al.*, 2002). Les biofilms sont retrouvés dans la plupart des environnements. Leur capacité à se développer dans différents milieux et sur n'importe quel type de surface (biotique ou abiotique) causent de nombreux problèmes dans le milieu industriel mais aussi dans le monde médical. Aujourd'hui les biofilms sont un problème de santé majeur car la matrice extra-cellulaire réduit grandement l'efficacité des antibiotiques et des désinfectants. De plus, la capacité à former des biofilms est reconnu par plusieurs microbiologistes comme une caractéristique universelle des micro-organismes (Lemon *et al.*, 2008). Environ 80 % de la biomasse microbienne mondiale réside sous forme biofilm. Aux États-Unis, le « National Institutes of Health » (« NIH ») a même estimé que plus de 75 % des infections humaines sont causées par la formation et la persistance des biofilms (Jacques *et al.*, 2010; Richards and Melander, 2009). Qu'ils soient formés par des bactéries pathogènes ou non, les biofilms sont souvent considérés comme néfastes pour la santé humaine (dispositifs médicaux), pour l'industrie (contamination des chaînes de production) et pour les environnements aquatiques (tuyaux, coques de bateaux). Cependant, les biofilms peuvent être utiles pour des processus tels que le traitement de l'eau potable, les eaux usées et la détoxification des déchets dangereux (Flemming and Wingender, 2010). Comprendre et contrôler les mécanismes qui régissent la formation de biofilm est devenu un enjeu majeur aussi bien au niveau de la santé publique qu'au niveau économique.

II.2.2 Découverte des biofilms

Antonie Van Leeuwenhoeck (1632-1723) considérée comme « le premier microbiologiste » peut aussi être reconnu comme le découvreur du biofilm puisque les premiers micro-organismes qu'il a observés au microscope résultaient du grattage de la surface de ses

dents. Ce n'est que beaucoup plus tard, en 1943, que Zobell a constaté qu'en milieu marin, la quantité de bactéries fixées à une surface était beaucoup plus importante que la quantité de bactéries en phase liquide (Zobell, 1943). En 1969, Jones et ses collègues ont confirmé la présence d'une matrice polysaccharidique et que les agrégats formés pouvaient être mono ou multi-espèces (Jones *et al.*, 1969). La résistance accrue des bactéries sous forme de biofilm a été décrite en 1973 par Characklis, qui a démontré que les dépôts microbiens dans les systèmes de canalisation d'eau semblaient plus résistants aux désinfectants (Characklis, 1973). En 1978, Costerton et ses collaborateurs ont proposé le concept de biofilm. Leur travail décrit les mécanismes par lesquels les micro-organismes peuvent adhérer à des surfaces biotiques ou abiotiques et les avantages procurés par cette niche écologique (Costerton *et al.*, 1978). Principalement motivée par la nécessité de traiter les problèmes de colonisation de surface (biotique ou abiotique), l'intensité de la recherche sur les biofilms ne cesse d'augmenter en intensité depuis 40 ans. De plus de nombreux outils spécifiques à l'étude des biofilms, tels que les techniques de culture microbiologique (bioréacteur, microfluidique), la microscopie (SEM, confocale) et la biologie moléculaire ont été développées, ce qui permet de stimuler et d'enrichir nos connaissances dans le domaine.

II.2.3 Biofilms dans l'environnement

Dans l'environnement, les bactéries existent principalement sous forme de biofilm (Richards and Melander, 2009). Les biofilms peuvent être trouvés dans des endroits très divers tels les sols, l'eau, les sédiments et aussi dans diverses parties du corps humain (Tremblay *et al.*, 2014). Des biofilms peuvent également être trouvés sur les surfaces des structures artificielles en contact avec des fluides, telles que les pipelines, les coques de navires, les conduits de climatisation et les réservoirs de rétention d'eau.

En termes de morphologie, de structure, de micro-environnement ainsi que d'état physiologique et métabolique, un biofilm est hétérogène. Un nettoyage incorrect des surfaces en contact avec les aliments favorise la formation de biofilms microbiens et peut contribuer aux maladies d'origine alimentaire (Fouladkhah *et al.*, 2013). De plus, il a aussi été décrit qu'au sein d'un biofilm les bactéries communiquent entre elles et adopteraient ainsi un comportement multicellulaire coordonné. La coordination cellulaire entre les bactéries semble être favorisée

par des conditions de croissance non optimales ou même par des stress cellulaires, et confère une meilleure adaptation aux environnements hostiles et une meilleure protection contre ceux-ci (Tremblay *et al.*, 2014).

En raison de l'implication des STEC dans de nombreuses épidémies d'origine alimentaire depuis les années quatre-vingt, il a été suggéré que le potentiel de formation de biofilm des STEC pourrait contribuer à leur persistance dans les chaînes de production alimentaire et dans l'environnement (Wang et al., 2012a). Les connaissances actuelles sur la capacité de formation de biofilm des STEC dans l'environnement sont discutées dans l'article de revue 1.

II.2.4 Article de revue 1 : La vie de l'extérieur : le rôle des biofilms dans la persistance environnementale des *Escherichia coli* producteurs de Shiga-toxines

Philippe Vogeleer, Yannick D.N. Tremblay, Mafu Akier Assanta, Mario Jacques and Josée Harel

Objectif de la revue : Dans cette revue nous avons rassemblé les connaissances sur la formation de biofilm des STEC et évalué la possible contribution de ces biofilms dans la survie des STEC dans l'environnement.

Contribution de l'étudiant : En tant que premier auteur, j'ai rédigé la majeure partie de cette revue. Grâce à l'aide de Yannick D.N. Tremblay, j'ai coordonné et assemblé les corrections de mes directeurs et collaborateur. J'ai aussi proposé la structure du texte et élaboré les figures. Cette revue a été publiée dans le journal Frontiers in Microbiology.

Revue publiée dans le journal Frontiers in Microbiology, juillet 2014

Life on the outside: role of biofilms in environmental persistence of Shiga-toxin producing *Escherichia coli*

Running title: Environmental persistence of STEC

Philippe Vogeleer[1], Yannick D.N. Tremblay[1], Mafu Akier Assanta[2], Mario Jacques[1] and Josée Harel[1]*

[1] Groupe de Recherche sur les Maladies Infectieuses du Porc, Centre de Recherche d'Infectiologie Porcine et Avicole, Département de pathologie et microbiologie, Faculté de médecine vétérinaire, Université de Montréal, C. P. 5000, St-Hyacinthe, Québec, Canada J2S 7C6

[2] Food Research and Development Centre, Agriculture and Agri-Food Canada, 3600, Casavant BLV, St-Hyacinthe, Québec, Canada, J2S 8E3

*Corresponding author:

Josée Harel,

Université de Montréal,

Faculté de médecine vétérinaire,

3200 Sicotte,

St-Hyacinthe, QC, J2S 7C6, Canada.

josee.harel@umontreal.ca

II.2.4.1 Abstract

Escherichia coli is a heterogeneous species that can be part of the normal flora of humans but also includes strains of medical importance. Among pathogenic members, Shiga-toxin producing *E. coli* (STEC) are some of the more prominent pathogenic *E. coli* within the public sphere. STEC disease outbreaks are typically associated with contaminated beef, contaminated drinking water, and contaminated fresh produce. These water- and food-borne pathogens usually colonize cattle asymptomatically; cows will shed STEC in their feces and the subsequent fecal contamination of the environment and processing plants is a major concern for food and public safety. This is especially important because STEC can survive for prolonged periods of time outside its host in environments such as water, produce, and farm soil. Biofilms are hypothesized to be important for survival in the environment especially on produce, in rivers, and in processing plants. Several factors involved in biofilm formation such as curli, cellulose, poly-N-acetylglucosamine, and colanic acid are involved in plant colonization and adherence to different surfaces often found in meat processing plants. In food processing plants, contamination of beef carcasses occurs at different stages of processing and this is often caused by the formation of STEC biofilms on the surface of several pieces of equipment associated with slaughtering and processing. Biofilms protect bacteria against several challenges, including biocides used in industrial processes. STEC biofilms are less sensitive than planktonic cells to several chemical sanitizers such as quaternary ammonium compounds, peroxyacetic acid, and chlorine compounds. Increased resistance to sanitizers by STEC growing in a biofilm is likely to be a source of contamination in the processing plant. This review focuses on the role of biofilm formation by STEC as a means of persistence outside their animal host and factors associated with biofilm formation.

Keywords: STEC, biofilm, sanitizers, processing plant, environment

II.2.4.2 Introduction

Escherichia coli is a diverse species of bacterium that includes members of the normal commensal flora of humans and animals but also pathogenic strains of veterinary and medical

importance. Pathogenic members are usually classified in two major groups: intestinal *E. coli* (InPEC) and extraintestinal *E. coli* (ExPEC). The latter group is typically responsible for urinary tract infections [uropathogenic *E. coli* (UPEC)], neonatal sepsis, and meningitis in humans and various infectious diseases in animals including mastitis (Kaper *et al.*, 2004; Clements *et al.*, 2012). InPEC are classically divided in 8 sub-groups based on the diseases they cause, their virulence factors, and phylogeny. These 8 pathotypes are: adherent-invasive *E. coli* (AIEC) associated with Crohn's disease, diffusely adherent *E. coli* (DAEC), enteroaggregative *E. coli* (EAEC), enterotoxigenic *E. coli* (ETEC), enteropathogenic *E. coli* (EPEC), Shiga-toxin producing *E. coli* (STEC) that includes enterohemorrhagic *E. coli* (EHEC), and enteroinvasive *E. coli* (including *Shigella*) (EIEC) (Kaper *et al.*, 2004; Clements *et al.*, 2012). The characteristics of each pathotype have been described in several reviews (Kaper *et al.*, 2004; Croxen and Finlay, 2010; Clements *et al.*, 2012).

STEC are worldwide water- and food-borne pathogens and are some of the more prominent pathogenic *E. coli* within the public sphere (Etcheverria and Padola, 2013). Cattle are an important animal reservoir of STEC and this colonization is typically asymptomatic (Ferens and Hovde, 2011). STEC can also be shed in the feces of sheep, goats, turkeys, and pigs (Heuvelink *et al.*, 1999; Booher *et al.*, 2002; Cornick and Helgerson, 2004; Vu-Khac and Cornick, 2008; Best *et al.*, 2009; La Ragione *et al.*, 2009). STEC disease outbreaks are typically associated with contaminated beef; however unpasteurized milk, contaminated drinking water, contaminated fresh produce, and unpasteurized apple cider have also been implicated (Ferens and Hovde, 2011). In addition to living within animal reservoirs, STEC can persist for prolonged periods of time in the environment, such as in water and farm soil. For example, EHEC can survive for periods greater than 8 months in water contaminated with bovine feces (Ferens and Hovde, 2011).

STEC are also a major concern in food-processing plants and contamination of beef carcasses with STEC may occur during different stages of processing such as slaughtering, dressing, chilling or cutting (Bacon *et al.*, 2003; Koutsoumanis and Sofos, 2004). Therefore, populations of contaminating STEC are likely present on the surface of several pieces of equipment associated with slaughtering and processing. These pieces of equipment may potentially

contaminate unadulterated carcasses and fresh meat products (Gill and McGinnis, 2000; Barkocy-Gallagher *et al.*, 2001; Gill *et al.*, 2001; Tutenel *et al.*, 2003). The presence of STEC in beef and food processing plants has been well documented and it has been suggested that the ability to form biofilms on different surfaces is responsible for the distribution and persistence of STEC in meat processing plants (Carpentier and Cerf, 1993; Dewanti and Wong, 1995; Aslam *et al.*, 2004; Rivera-Betancourt *et al.*, 2004). In this review, we will explore the role of biofilm formation by STEC as a means of persistence outside their animal hosts and factors associated with biofilm formation.

II.2.4.3 Genetic diversity of STEC

The predominant STEC serotype associated with outbreaks is O157:H7. Since it was one of the first serotypes identified as causing hemolytic uremic syndrome (HUS) and the most severe illness, EHEC O157:H7 is the most commonly reported STEC serotype in the media (Etcheverria and Padola, 2013). However, other clinically relevant serotypes have been identified and are commonly called the ‘‘the Big six’’, these include serogroups O26, O45, O103, O111, O121, and O145 (Wang *et al.*, 2012). Other serotypes (e.g., O113:H21 and O91:H21) generally do not cause outbreaks but have been associated with sporadic cases of HUS (Karmali *et al.*, 2003). Additionally, a new type of emerging STEC strain was identified after the large HUS outbreak in Germany in 2011 (Frank *et al.*, 2011). This strain belongs to the serotype O104:H4 and combines the chromosomal backbone of a typical EAEC strain with the bacteriophage encoding Stx2 from STEC (Scheutz *et al.*, 2011). The *stx2* gene was presumably acquired via horizontal gene transfer. This atypical Shiga-toxin producing enteroaggregative *E. coli* (STEAEC) strain will not be covered in this review because it does not fit within the classic STEC pathotype.

In addition to serotype diversity within the STEC pathotype, genetic diversity in the O157:H7 serotype is gaining ground as a source of variation in virulence between strains (Bono *et al.*, 2007; Manning *et al.*, 2008; Zhang *et al.*, 2010; Shringi *et al.*, 2012). This phenomenon is observed with different *E. coli* O157 strains, where there is a significant association between clades and the severity and duration of disease (Fukushima *et al.*, 1999; Grant *et al.*, 2008; Manning *et al.*, 2008). Furthermore, geographical distribution also appears to influence the

phylogeny of *E. coli* O157 populations and recent findings suggest divergent evolution of EHEC O157 in Australia and the United States (Mellor *et al.*, 2013). Despite this diversity, most studies on STEC biofilm formation are performed with the sequenced reference strain EDL933 that was isolated from meat associated with a USA hemorrhagic colitis outbreak in 1982 (Perna *et al.*, 2001; Manning *et al.*, 2008). Therefore, some of the conclusions may only reflect North American strains rather than strains isolated from other continents.

II.2.4.4 Biofilm formation by STEC

Generally, bacteria do not live freely in suspension (planktonic cells), but in complex communities called biofilms. Biofilms are aggregates of microorganisms (bacteria, fungi, algae, or protozoa) enclosed in a self-produced extracellular polymeric matrix that are attached to a biotic or abiotic surface (Costerton *et al.*, 1999; Hall-Stoodley and Stoodley, 2009; Jacques *et al.*, 2010). Biofilms protect bacteria from several challenges including desiccation, bacteriophages, amoebae, and biocides used in industrial processes (Costerton *et al.*, 1999). With respect to *E. coli* biofilm formation, studies have mostly been performed with K-12 strains and have been reviewed in several publications (Beloin *et al.*, 2008; Wood, 2009). EDL933 and MG1655 share a core set of genes, including some genes involved in biofilm formation; as a result, data obtained using K-12 strains are often used to infer function for STEC strains. However, such inferences are not always appropriate because there are key differences between the genomes of K-12 and EDL933 including the presence of O-islands, lack of type 1 fimbriae production, and the presence of single nucleotide polymorphisms (SNP) (Perna *et al.*, 2001; Roe *et al.*, 2001; Welch *et al.*, 2002; Zhang *et al.*, 2006; Chen *et al.*, 2013). Additionally, the expression and activity of several factors that must act at specific times and at various locations in the biofilm are required for proper biofilm formation (Beloin *et al.*, 2008; Wood, 2009).

II.2.4.5 Differences between STEC and *E. coli* K-12 that may influence biofilm formation

As stated above, there are key differences between K-12 and STEC strains that may have major influences on biofilm formation. For example, the EDL933 genome possesses 177 O-islands (OI), several of which encode fimbrial adhesins (Perna *et al.*, 2001). However, the presence of a gene in a genome does not guarantee its expression. As an example, type 1 fimbriae are

associated with biofilm formation in K-12 strains, but a deletion in the *fim* regulatory region abolished type 1 fimbriae expression in *E. coli* O157:H7 (Roe *et al.*, 2001; Beloin *et al.*, 2004). Therefore, type 1 fimbriae do not play a role in biofilm formation by *E. coli* O157:H7. These data highlight the fact that findings for K-12 do not always represent biological processes for all *E. coli* subtypes. Furthermore, many groups have demonstrated that STEC biofilm formation is more dependent on the strain than the serotype. This could be explained by the presence of SNP that result in premature stop codons in genes encoding adhesins or RpoS, the stationary phase sigma factor that is important for biofilm formation and regulation (Zhang *et al.*, 2006).

In addition to differences at the genomic level, there are key differences in the transcript profiles of K-12 and EHEC strains for biological processes involved in the interactions with lettuce leaves (Fink *et al.*, 2012) including genes that may be involved in biofilm formation. Differences in the transcriptomes of K-12 and STEC strains could be explained by the presence of additional regulators encoded within genomic islands and changes in promoter regions. For example, the genomic island OI-47 of *E. coli* O157:H7 contains a gene, *vmpA*, coding for a c-di-GMP phosphodiesterase that is specific for EHEC O157:H7 and VmpA was shown to influence the regulation of biofilm formation (Branchu *et al.*, 2013). Furthermore, recent findings have highlighted differences in EHEC and EPEC promoter regions that result in the differential regulation of an outer-membrane protease (Thomassin *et al.*, 2012). Taken together, these differences indicate that biofilm data obtained with K-12 strains or other pathotypes are not always directly relevant to STEC strains. Therefore, it is important that biofilm formation be studied in STEC.

II.2.4.6 Steps in biofilm formation

Biofilm formation requires specific steps and is typically described as a four-step process: initial contact, attachment, maturation, and dispersion (Figure 1)

II.2.4.6.1 Initial contact

The first step in biofilm formation is reversible attachment to a surface; this is dependent on a balance of attractive and repulsive forces between the bacteria and the surface. Both environmental and bacterial factors are important for this interaction. Attachment is influenced

by environmental conditions such as temperature, pH, ionic force of the medium, and the rugosity of the surface, in addition to bacterial properties such as hydrophobicity and motility (Fletcher, 1988; Pratt and Kolter, 1998; Danese *et al.*, 2000). Furthermore, flagella-driven motility is considered to be an important factor during the initial step of biofilm formation by *E. coli* because K-12 strains lacking flagella do not produce biofilms. Additionally, Chen and collaborators recently suggested that flagella-driven motility is also involved in biofilm formation of non-O157:H7 STEC (Chen *et al.*, 2013).

II.2.4.6.2 Attachment

The second step in biofilm formation is irreversible attachment, which is often influenced by the presence of surface structures such as fimbrial adhesins (Beloin *et al.*, 2004). Many classes of fimbriae have been implicated in the attachment of STEC to surfaces, including type 1 fimbriae, curli, type 4 pili, long polar fimbriae, and F9 fimbriae (Farfan and Torres, 2012).

II.2.4.6.3 Maturation

The third step in biofilm formation is maturation. During biofilm maturation, bacteria continue to multiply and produce extracellular matrix. At this stage, the biofilm adopts a three-dimensional structure. This growth is mostly due to bacterium–bacterium interactions; several surface proteins and extracellular matrix components are involved in bacterial adhesion and biofilm architecture (Beloin *et al.*, 2008). Two important factors for this step have been identified in *E. coli*: autotransporters for cell-cell interactions and exopolysaccharides (EPS) for the matrix architecture (Beloin *et al.*, 2008).

Important factors for biofilm maturation: autotransporters

Autotransporter adhesins, which are members of the type V secretion system, have been associated with autoaggregation and biofilm formation. Screens in STEC strains have identified 9 autotransporter genes: chromosome encoded *agn43*, *cah*, *ehaA*, *ehaB*, *ehaD*, *ehaG*, *saa*, and *sab* and plasmid-encoded *espP* (Torres *et al.*, 2002; Wells *et al.*, 2008; Herold *et al.*, 2009; Wells *et al.*, 2009; Puttamreddy *et al.*, 2010). The protein products of each of these genes have been associated with biofilm formation (Torres *et al.*, 2002; Wells *et al.*, 2008; Herold *et al.*, 2009;

Wells *et al.*, 2009; Puttamreddy *et al.*, 2010). A comparative study of three autotransporter genes (*agn43*, *cah*, and *ehaA*) among 51 STEC strains found that the presence of autotransporter genes within the genome was variable among STEC serotypes (Biscola *et al.*, 2011). Specifically, *agn43* was present at a higher frequency in non-O157 strains than O157 strains while the frequency of *cah* is higher in O157 strains compared to non-O157 strains (Biscola *et al.*, 2011).

In addition to the autotransporter *espP*, the pO157 plasmid encodes the enterohemolysin translocator *ehxD*, whose protein product was identified as a mediator of biofilm formation, indicating that pO157 is essential for biofilm formation (Puttamreddy *et al.*, 2010). Large plasmids similar to pO157, encoding *espP* and *ehxD* can also be found in most non-O157 EHEC strains (Brunder *et al.*, 1999; Caprioli *et al.*, 2005; Verstraete *et al.*, 2013).

Important factors for biofilm maturation: EPS

The *E. coli* biofilm matrix can be composed of three different EPSs: poly-N-acetylglucosamine (PGA), colanic acid, and/or cellulose. The genes encoding proteins that are involved in the synthesis of these polysaccharides are present in the genomes of STEC strains EDL933 and Sakai (Hayashi *et al.*, 2001; Perna *et al.*, 2001). However, their role in biofilm formation has not been directly established in these strains. In addition, O157:H7 mutants lacking genes encoding proteins needed to make PGA, cellulose, or colanic acid were unable to adhere to alfalfa sprouts (Matthysse *et al.*, 2008). Furthermore, cellulose production was correlated with biofilm formation in O157 strains (Biscola *et al.*, 2011; Lee *et al.*, 2011). Cellulose production is, however, variable and dependent on both the bacterial strain and environmental conditions (Beloin *et al.*, 2008). Colanic acid is produced by *E. coli* O157:H7, but there is limited data for other STEC serotypes (Beloin *et al.*, 2008). The production of colanic acid protects *E. coli* O157:H7 against osmotic and oxidative stress, suggesting that colanic acid may be implicated in STEC biofilm formation, however, this remains to be tested directly (Yeh and Chen, 2004).

Important factors for biofilm maturation: other factors

Lipopolysaccharides (LPS) and capsules, which are surface structures, have been implicated in biofilm formation by *E. coli*. Mutations affecting LPS synthesis affect the ability

of *E. coli* K-12 strains to adhere to surfaces and form biofilms (Genevaux *et al.*, 1999; Beloin *et al.*, 2008). Similar observations were noted for *E. coli* O157:H7 strain EDL933, where O-antigen transposon mutants could not form biofilms (Puttamreddy *et al.*, 2010).

Capsules are known to mask bacterial surface adhesins and often have an indirect effect on biofilm formation (Schembri *et al.*, 2004). According to Whitfield, capsule polysaccharides produced by some EHEC strains belong to the *E. coli* group 4 capsule, which is composed of the same sugar repeats as the LPS O-antigen and acetamido sugars in their repeat-unit structures (Whitfield, 2006). The impact of this capsule-type on biofilm formation by STEC has yet to be investigated. If the group 4 capsule has an impact on biofilm formation, its effect might be serotype specific given the diversity of O-antigen structures among STEC. Furthermore, the capsule is only expressed and present under specific laboratory conditions in EDL933 (Shifrin *et al.*, 2008; Thomassin *et al.*, 2013). Therefore, the role of the capsule in *in vivo* biofilm formation might be difficult to evaluate in an *in vitro* setting given that biofilm formation is also highly dependent on growth conditions.

Curli fimbriae are structures that aggregate on the surface of cells, promote adhesion of *E. coli* to different human cells and biofilm formation on abiotic surfaces (Olsen *et al.*, 1989; Ben Nasr *et al.*, 1996; Vidal *et al.*, 1998; Cookson *et al.*, 2002; Uhlich *et al.*, 2006). Curli expression in some STEC strains has been associated with biofilm formation on polystyrene and stainless-steel surfaces (Cookson *et al.*, 2002; Ryu *et al.*, 2004b; Uhlich *et al.*, 2006). However, curli expression, which is strain dependent and serotype independent, is not essential for biofilm formation (Wang *et al.*, 2012). Additionally, curli can interact with cellulose to create networks resulting in the formation of a hydrophobic extracellular matrix (Zogaj *et al.*, 2001; Gualdi *et al.*, 2008). Curli are thought to facilitate initial cell–surface interactions and, subsequent cell–cell interactions (Cookson *et al.*, 2002; Uhlich *et al.*, 2006). Curli are encoded in two divergently transcribed operons: the *csgBA* operon encodes the structural components and the *csgDEFG* operon encodes the regulator (*csgD*) and the export machinery (*csgE-G*) (Hammar *et al.*, 1995). Both operons are found in the EHEC O157:H7 EDL933 and Sakai reference strains (Hayashi *et al.*, 2001; Perna *et al.*, 2001). Curli production is tightly controlled and complex; several transcriptional regulators (EnvZ/OmpR, CpxR, RcsCDB, RpoS, H-NS, IHF, Crl, and MlrA) and

conditions (temperature, osmolarity, pH, and oxygenation) control curli expression, which involves a network of interactions (Dorel *et al.*, 1999; Prigent-Combaret *et al.*, 2001; Brombacher *et al.*, 2003; Gerstel *et al.*, 2003; Jubelin *et al.*, 2005; Vianney *et al.*, 2005). The complex regulatory network of curli expression is thought to be fine-tuned to allow for the colonization of specific niches by *E. coli* (Prigent-Combaret *et al.*, 2001; Kikuchi *et al.*, 2005).

Important factors for biofilm maturation: Quorum sensing

During the different steps of biofilm formation the bacterial cell population density fluctuates and gene expression varies. To coordinate gene expression, bacteria communicate using quorum sensing (QS) systems (Walters and Sperandio, 2006). QS systems are based on the secretion and/or recognition of signal molecules called autoinducers (AIs). Three types of AIs have been identified: AI-1, AI-2, and AI-3. Both AI-2 and AI-3 are produced, secreted, and recognized by *E. coli* strains including STEC (Walters and Sperandio, 2006). *E. coli* strains including STEC do not produce AI-1; however their genome encodes *sdiA*, the AI-1 sensor, which is a *luxR* homolog. This enables *E. coli* strains including STEC to recognize acyl-homoserine lactone (AHL), the signal molecule for AI-1, secreted by others bacterial species. In Sharma *et al.* (2010) demonstrated that SdiA acts as a repressor of curli and flagellar gene expression. Indeed an O157:H7 Δ*sdiA* strain had increased curli fimbriae and biofilm production, suggesting that the AI-1 system has a negative impact on biofilm formation (Sharma *et al.*, 2010). LuxS, a metabolic enzyme also found in STEC strains, is primarily involved in the conversion of ribosyl-homocysteine into homocysteine and 4,5-dihydroxy-2,3-pentanedione, which is the precursor for AI-2 (Schauder *et al.*, 2001). Biofilm formation was enhanced when AI-2-like molecules were added to an O157:H7 *luxS* deletion strain (Lu *et al.*, 2005; Bansal *et al.*, 2008; Vikram *et al.*, 2010). Furthermore, AI-3 and host-produced epinephrine/norepinephrine are recognized by the QseBC two component system (Walters and Sperandio, 2006). The addition of epinephrine and norepinephrine increase EHEC motility and biofilm formation, while the addition of indole attenuates these phenotypes (Bansal *et al.*, 2007). Moreover, motility and biofilm formation by a *qseC* deletion strain was reduced by half when compared to the wild type strain (Yang *et al.*, 2014).

II.2.4.6.4 Dipsersion

The final step in biofilm formation is the detachment of bacteria from the biofilm and their dispersal, which contributes to the transmission of bacteria. Dispersal is a complex process that involves several environmental signals and effectors and no single dispersal mechanism is used by all bacterial species. As described above, bacteria generally switch from a planktonic to a biofilm lifestyle by sensing environmental changes. Biofilm dispersal has recently been reviewed in detail (Kaplan, 2010). Dispersal is the least understood step in biofilm formation for all bacterial species and has not been investigated for STEC (Figure 1). In *E. coli* other than STEC, modulation of crucial surface structures, such as type IV bundle-forming pili (BFP) in EPEC and aggregative adherence fimbriae (AAFs) in EAEC, results in the detachment of bacteria from the biofilm and surface (Knutton *et al.*, 1999; Sheikh *et al.*, 2002; Velarde *et al.*, 2007). For example in EAEC, positively charged AAFs extend away from the surface of the bacterial cell to mediate surface-adherence when dispersin is produced, because dispersin binds to and neutralizes LPS charge (Sheikh *et al.*, 2002; Velarde *et al.*, 2007). When dispersin is down-regulated, the positively charged AAFs collapse on the bacterial surface due to their interaction with negatively charged LPS. As a consequence of this collapse, AAFs no longer adhere to surfaces and the biofilm disperses (Sheikh *et al.*, 2002; Velarde *et al.*, 2007). Mechanisms involved in biofilm detachment are of increased interest, because the understanding of these mechanisms could lead to the development of clinical or industrial tools to remove biofilms.

II.2.4.7 Survival in the environment: is it biofilm mediated?

STEC contamination of the environment and food-processing plant can occur several different ways (Figure 2). STEC are typically shed in the feces of cattle and this will contaminate the hide and farm environment (Elder *et al.*, 2000; Aslam *et al.*, 2003). STEC that are present in feces can contaminate manure and, consequently, soils either through manure runoff or manure applied to fields (Gagliardi and Karns, 2000; Solomon *et al.*, 2002; van Elsas *et al.*, 2011). At this stage, STEC may persist and grow on fresh produce such as lettuce and can be internalized and survive within plant tissue via a mechanism that is not fully understood (Seo and Frank, 1999; Jeter and Matthysse, 2005; Tyler and Triplett, 2008). Furthermore, manure applied to

fields often ends up in ground or surface water through runoff; this water is often used to irrigate fields and water crops (Ribeiro *et al.*, 2012). As a consequence, fields and crops that were not treated with manure can become contaminated with STEC. All of these contribute to the contamination and spread of STEC in the environment. STEC can survive in soil, on fresh produce, manure, and river water, which is hypothesized to be associated with the ability of STEC to form biofilms.

Soil and manure

Survival of *E. coli* O157:H7 in soil and manure is greatly influenced by microbial diversity; EHEC survival is at its highest when diversity is low (Vidovic *et al.*, 2007; van Overbeek *et al.*, 2010; Ibekwe *et al.*, 2011; van Elsas *et al.*, 2011). On one hand, survival of STEC within soil and manure is also hypothesized to be associated with the absence of various protozoa that graze on STEC (Ravva *et al.*, 2010). On the other hand certain protozoa are proposed to act as a transmission vehicle for EHEC (Chekabab *et al.*, 2012). Taken together these results strongly suggest that STEC survival is influenced by the environmental microcosm. There is, however, little evidence to indicate that STEC are able to form or integrate into biofilms within manure, soil, or in the farm environment. Therefore, there is a need for studies that investigate the role of biofilms in promoting STEC survival within these environments.

Water

Biofilms containing STEC have been detected in freshwater streams that drain or are connected to agricultural land (Cooper *et al.*, 2007; Maal-Bared *et al.*, 2013). It is unknown if STEC can act as the pioneer bacteria in environmental biofilms, but this possibility is unlikely because periphytic *E. coli* isolates appear to form biofilms more readily than human and/or bovine isolates (Moreira *et al.*, 2012). The presence of STEC in environmental biofilms may be explained by the finding that biofilm-negative *E. coli* O157:H7 strains are able to integrate into pre-established biofilms formed by other *E. coli* strains (Uhlich *et al.*, 2010). Therefore, it is likely that STEC can integrate into pre-existing biofilms.

Mixed-species biofilms formed in rivers and river sediments are also of particular interest because they provide ample opportunity for genetic exchange between bacteria (Maal-Bared *et*

al., 2013). Furthermore, the environment within the biofilm is suitable for the transduction of *stx*-encoding phages carried by STEC (Solheim *et al.*, 2013). The transfer of these phages is responsible for the spread of *stx* genes among *E. coli* species. Such genetic exchanges could contribute to the emergence of new pathogenic *E. coli* and give rise to the next outbreak strain.

Fresh produce

Several genes and/or structures associated with biofilm formation have been identified as important factors for plant colonization by STEC. For example, PGA, cellulose, and colanic acid play a role in *E. coli* O157 binding to sprouts and tomato root segments (Matthysse *et al.*, 2008). Furthermore, PGA is essential for binding to sprouts and cellulose and colanic acid increase the efficiency of this attachment (Matthysse *et al.*, 2008). These findings provide evidence that the biofilm matrix associated polysaccharides are crucial for attachment to plants. In addition, these EPSs are expressed under environmental conditions [i.e. room temperature [23–25°C)], in low-ionic-strength medium, and during nutrient limitation by several *E. coli* strains (Gottesman and Stout, 1991; Matthysse *et al.*, 2008). The expression of matrix polysaccharides in environments similar to those encountered in the presence of fresh produce further supports the likelihood that biofilm formation plays a role in STEC survival on produce.

Curli fimbriae improve the adherence of *E. coli* O157:H7 to spinach leaves, and interestingly, the improved adherence was found to be independent of cellulose production (Macarisin *et al.*, 2012). Biofilm modulation genes (*ycfR* and *ybiM*) are also significantly up-regulated when *E. coli* O157:H7 interacts with lettuce roots (Hou *et al.*, 2013). Furthermore, a Δ*ycfR* strain was unable to attach to or colonize lettuce roots (Hou *et al.*, 2013). Taken together these studies suggest that certain factors involved in biofilm formation improve the environmental fitness of STEC, especially in the context of plant colonization.

Biofilms and protozoa

Protozoans living in soil, manure, and rivers probably prey on STEC living in the environment (Ravva *et al.*, 2010). Recent studies have shown that EDL933 can survive in *Acanthamoeba castellanii* and replicate within *Acanthamoeba polyphaga*, protozoa commonly found in soil, water, and fecal slurry (Barker *et al.*, 1999; Chekabab *et al.*, 2012). It was suggested that such

protozoa could also serve as a transmission vehicle for EHEC (Chekabab *et al.*, 2012). In support, the presence of the Stx-encoding prophage increases the survival of STEC isolates in the presence of *Tetrahymena pyriformis* or *Tetrahymena thermophila* (Steinberg and Levin, 2007; Mauro *et al.*, 2013). Protozoa are known to graze on biofilms, and ciliates and flagellates differently influence biofilm communities (Wey *et al.*, 2012). For example, *Glaucoma* and *Tetrahymena* species (ciliates) expel vesicles containing viable *E. coli* O157:H7, whereas *Colpoda steinii* and *Acanthamoeba palestinensis* (flagellates) do not (Gourabathini *et al.*, 2008). Furthermore, protozoans graze less on biofilm communities than on their planktonic cells, suggesting that biofilms may offer some protection from protozoan predation (Wey *et al.*, 2012).

II.2.4.8 STEC biofilms in processing plants, a potential source of meat and produce contamination

In addition to forming biofilms under environmental conditions and on plants, STEC are able to form biofilms on different surfaces often found in meat processing plants, such as stainless steel, polystyrene, glass, polyurethane, and high-density polyethylene (Dewanti and Wong, 1995; Dourou *et al.*, 2011; Nesse *et al.*, 2013). The introduction of contaminated food into processing plants results in the spread of STEC and contamination. As an example, it was estimated that the prevalence of *E. coli* O157 on cattle entering the slaughter floor may range from 10 to > 70% (Woerner *et al.*, 2006). In the meat industry, contamination of surfaces with STEC can be traced to the entry of contaminated hides. Fecal contamination of hides occurs both directly and indirectly during cattle production and transit. Currently, disinfection protocols are used to try to limit the entry of STEC into slaughterhouses and processing plants. Despite the common use of disinfection protocols, STEC contamination of food still occurs, which according to the Center for Disease Control and Prevention (CDC) and Public Health Agency of Canada (PHAC) shows that disinfections protocols do not always prevent contamination (http://www.cdc.gov/ecoli/ and http://www.phac-aspc.gc.ca/fs-sa/fs-fi/ecoli-eng.php). The persistence of STEC in the presence of disinfectants gives rise to the probability that STEC survive and grow within a biofilm in processing plants (Stopforth *et al.*, 2003; Ryu *et al.*, 2004a; Uhlich *et al.*, 2006; Fouladkhah *et al.*, 2013). In this section we will focus on STEC biofilm formation and associated factors in processing plants.

In the processing plant environment, temperatures are normally controlled and maintained between 4 and 15°C. Many studies have shown that STEC are able to grow in a biofilm within this temperature range (Dourou *et al.*, 2011; Fouladkhah *et al.*, 2013; Nesse *et al.*, 2013). For example, *E. coli* O157:H7 is able to colonize surfaces in contact with beef at 15°C (non-production hours temperature) and 4°C (production hours temperature) (Dourou *et al.*, 2011; Fouladkhah *et al.*, 2013). Interestingly, *E. coli* O157:H7 attachment increased at 4°C over time in the presence of a fat-lean tissue homogenate (Dourou *et al.*, 2011). Futhermore, *E. coli* O157:H7 EDL933 is able to adhere and produce a dense biofilm on surfaces that are not favorable for its attachment when collagen I is present, which is a muscle fibrous extracellular matrix protein (Chagnot *et al.*, 2013). In addition to forming biofilms in meat homogenates, *E. coli* O157:H7 is also able to form biofilms on stainless steel when grown in spinach leaf lysates (Carter *et al.*, 2012). Environmental conditions such as temperature and culture broths containing meat or vegetable residues can affect the expression of genes controlled by QS. For example, it was shown that *E. coli* O157:H7 biofilms produce large amounts of AI-2 when cultured in pork, beef or spinach broth (Silagyi *et al.*, 2009). Based on this evidence, it is possible that QS drives biofilm formation in meat processing plants.

Fouladkhah *et al.* showed that the use of quaternary ammonium compound-based and peroxyacetic-based chemical sanitizers on biofilms that had matured for one week were more effective at 4°C than 25°C. However, these commercial sanitizers used at concentrations recommended to kill planktonic STEC were not able to kill and remove STEC biofilm from stainless steel surfaces (Fouladkhah *et al.*, 2013). Furthermore, curli fimbriae, due to their amyloid properties, can protect bacteria from antibacterial agents like chlorine or quaternary ammonium sanitizers (Uhlich *et al.*, 2006; Wang *et al.*, 2012). It has been shown that tolerance of sanitizers by STEC in biofilms does not depend on serotype but on strain (Wang *et al.*, 2012). It was also shown that at 100% relative humidity (RH), *E. coli* O157:H7 biofilms were more resistant to sanitizers than at lower RH (Bae *et al.*, 2012). Furthermore, large biofilms were more resistant to cleaning and disinfection protocols and repeated treatment could result in the presence of viable but nonculturable *E. coli* O157:H7 that were able to regrow as a biofilm on polyurethane (Marouani-Gadri *et al.*, 2010). Taken together, these data indicate that sanitizer efficacy may be limited against STEC growing within a biofilm community.

Interestingly, non-pathogenic bacteria isolated from processing plants, such as *Comamonas testosterone, Acinetobacter calcoaceticus, Burkholderia caryphylli,* and *Ralstonia insidiosa,* can initiate biofilm formation and may allow *E. coli* O157:H7 to integrate within a pre-formed biofilm, resulting in a mixed biofilm (Marouani-Gadri *et al.*, 2009a; Habimana *et al.*, 2010; Liu *et al.*, 2014). For example, *C. testosteroni* can enhance the ability of *E. coli* O157:H7 to form biofilms (Marouani-Gadri *et al.*, 2009a). The presence of *C. testosteroni* within the biofilm did, however, decrease the number of colony-forming units of *E. coli* O157:H7 following chemical treatment when compared to chemical treatment of a single species *E. coli* O157:H7 biofilm (Marouani-Gadri *et al.*, 2010). These data suggest that the presence of non-pathogenic bacterial species has a large influence on the ability of STEC to persist within the processing plant; due to the potential impact of these data, these findings merit further investigation.

The ability to secrete EPS is related to biofilm formation on stainless steel surfaces, but it was shown that overproduction of the EPS inhibits the initial attachment of *E. coli* O157:H7 (Ryu *et al.*, 2004a). EPS production may also protect *E. coli* O157:H7 from sanitizer treatments (Ryu *et al.*, 2004a; Ryu and Beuchat, 2005). As with curli, EPS production may not be essential for biofilm formation on stainless steel by bacterial pathogens, including STEC. In addition, it has been shown that bacteria producing little or no EPS, including *E. coli* O157:H7 could colonize a mature biofilm formed by EPS-producing bacteria (Castonguay *et al.*, 2006; Klayman *et al.*, 2009; Dourou *et al.*, 2011). Although sanitizers are able to reduce or totally kill STEC within biofilms, it is possible that recolonization by STEC or other bacteria will be easier if cleaning protocols do not completely remove the biofilm matrix.

In addition to the protection offered by the biofilm matrix against sanitizers, it is well established that for *E. coli* in general, slow-growing and dormant subpopulations are highly tolerant to antibacterial treatments (Lewis, 2010). Cells from this subpopulation are called multidrug tolerant persister cells and are dormant variants that emerged from regular cells (Lewis, 2010). The emergence of persister cells occurs at a higher frequency within biofilm populations than planktonic populations (Lewis, 2010). This non-heritable variation could permit STEC to survive the sanitation process and these individual cells could remain encased in the biofilm matrix. These cells could then contribute to the reestablishment of a STEC biofilm or population

within the processing plant.

II.2.4.9 Can STEC biofilms be removed?

It is known that STEC biofilms are more resistant to sanitizers than their planktonic counterparts (Wang *et al.*, 2012). In recent years, many studies have focused on cleaning and disinfection procedures using physical and chemical methods. Three primary chemical compounds are used as sanitizers in the food service industry: chlorine-based cleaners, quaternary ammonium, and iodine sanitizers. Because of the toxicity of sanitizer residues and/or increased bacterial resistance to these decontamination reagents (Stopforth *et al.*, 2003; Houari and Di Martino, 2007; Marouani-Gadri *et al.*, 2009b; Hou *et al.*, 2010; Wang *et al.*, 2012), alternative molecules that are preferentially natural with low human and animal toxicity are being tested for their effect on biofilms.

Many essential oils have been shown to have good antibiofilm activity against food-borne pathogens (Giaouris *et al.*, 2013). Perez-Conesa *et al.* have shown that surfactant micelles loaded with eugenol or carvacrol, two essential oils isolated from clove and thyme, are able to kill *E. coli* O157:H7 inside a biofilm. However, the biofilm matrix remains attached to the surface (Perez-Conesa *et al.*, 2006; Perez-Conesa *et al.*, 2011), making reformation of a biofilm a dangerous possibility. While essential oils target cell viability, the best way to remove and prevent reformation of a biofilm on a surface is to degrade the EPS surrounding the bacteria by enzymatic treatment (Gibson *et al.*, 1999; Lequette *et al.*, 2010). A combination of an antimicrobial agent to kill cells within the biofilm with an agent able to remove the entire biofilm matrix could be a solution to reduce and potentially remove *E. coli* O157:H7 biofilms from processing plants. Others strategies such as bacteriophage treatments of *E. coli* O157:H7 biofilms have also been investigated. The KH1 bacteriophage reduces the population of O157:H7 cells attached to stainless steel, but not those incased within a biofilm matrix (Sharma *et al.*, 2005). The effect of combined techniques such as steam and lactic acid (Ban *et al.*, 2012), aerosolized sanitizers (Park *et al.*, 2012), UV and dry heat (Bae and Lee, 2012) were also studied and have the potential to control STEC O157:H7 biofilms found on surfaces present in the food industry. The best approach for controlling STEC biofilm should kill *E. coli* O157:H7 within the biofilm and remove the biofilm matrix from the contaminated surface. For example, a

combination of steam and lactic acid were able to kill *E. coli* O157:H7 and remove the biofilm matrix from stainless steel surfaces (Ban *et al.*, 2012). Further studies should investigate the effect of antibiofilm molecules on the dispersal of biofilms and also focus on mixed biofilms containing both non-pathogenic and STEC bacteria.

II.2.4.10 Conclusion

Contamination of the environment and processing plants with cow feces containing STEC is a major concern for food and public safety, especially since STEC can survive for prolonged periods of time outside its host. Biofilm formation appears to contribute significantly to STEC survival on produce, in rivers, and in processing plants. Several factors involved in biofilm formation such as curli, cellulose, PGA, and colanic acid are involved in plant colonization and attachment to different surfaces often found in meat processing plants. However, the factors involved in STEC survival within biofilms in rivers remain unknown. Furthermore, STEC biofilm formation on farms, in manure, and in soil has not been thoroughly explored despite the presence and persistence of STEC in these environments. The Stx toxin, which is a key factor in human host pathology, also appears to be an important factor for STEC survival against protozoan predation. In the food industry, resistance to sanitizers improves the ability of STEC to persist in the processing plant. Despite the development of new strategies to eradicate biofilms formed by food-borne pathogens, no effective solutions to remove STEC biofilms from surfaces have been identified. Therefore, future research should focus on the identification of factors promoting STEC survival, especially non-O157 STEC, and the persistence of STEC in environmental biofilms on the farm.

II.2.4.11 Conflict of interest statement

The authors declare that the research was conducted in the absence of any commercial or financial relationships that could be construed as a potential conflict of interest.

II.2.4.12 Acknowledgements

We would like to thank Jenny-Lee Thomassin for proofreading and critical reading of the manuscript. We thank the Natural Sciences and Engineering Research Council of Canada

(RGPIN SD-25120-09) to J. H. and Fonds de la recherche du Québec en nature et technologies to J.H. and M.J. (FRQNT PT165375) and a studentship to P.V. from Fonds CRIPA (FRQNT Regroupements stratégiques 111946).

II.2.4.13 References

Aslam, M., Greer, G.G., Nattress, F.M., Gill, C.O., and McMullen, L.M. (2004). Genotypic analysis of *Escherichia coli* recovered from product and equipment at a beef-packing plant. J Appl Microbiol 97(1), 78-86. doi: 10.1111/j.1365-2672.2004.02277.x.

Aslam, M., Nattress, F., Greer, G., Yost, C., Gill, C., and McMullen, L. (2003). Origin of contamination and genetic diversity of *Escherichia coli* in beef cattle. Appl Environ Microbiol 69(5), 2794-2799.

Bacon, R.T., Sofos, J.N., Kendall, P.A., Belk, K.E., and Smith, G.C. (2003). Comparative analysis of acid resistance between susceptible and multi-antimicrobial-resistant *Salmonella* strains cultured under stationary-phase acid tolerance-inducing and noninducing conditions. J Food Prot 66(5), 732-740.

Bae, Y.M., Baek, S.Y., and Lee, S.Y. (2012). Resistance of pathogenic bacteria on the surface of stainless steel depending on attachment form and efficacy of chemical sanitizers. Int J Food Microbiol 153(3), 465-473. doi: 10.1016/j.ijfoodmicro.2011.12.017.

Bae, Y.M., and Lee, S.Y. (2012). Inhibitory effects of UV treatment and a combination of UV and dry heat against pathogens on stainless steel and polypropylene surfaces. J Food Sci 77(1), M61-64. doi: 10.1111/j.1750-3841.2011.02476.x.

Ban, G.H., Park, S.H., Kim, S.O., Ryu, S., and Kang, D.H. (2012). Synergistic effect of steam and lactic acid against *Escherichia coli* O157:H7, *Salmonella* Typhimurium, and *Listeria monocytogenes* biofilms on polyvinyl chloride and stainless steel. Int J Food Microbiol 157(2), 218-223. doi: 10.1016/j.ijfoodmicro.2012.05.006.

Bansal, T., Englert, D., Lee, J., Hegde, M., Wood, T.K., and Jayaraman, A. (2007). Differential effects of epinephrine, norepinephrine, and indole on *Escherichia coli* O157:H7 chemotaxis,

colonization, and gene expression. Infect Immun 75(9), 4597-4607. doi: 10.1128/IAI.00630-07.

Bansal, T., Jesudhasan, P., Pillai, S., Wood, T.K., and Jayaraman, A. (2008). Temporal regulation of enterohemorrhagic *Escherichia coli* virulence mediated by autoinducer-2. Appl Microbiol Biotechnol 78(5), 811-819. doi: 10.1007/s00253-008-1359-8.

Barker, J., Humphrey, T.J., and Brown, M.W. (1999). Survival of *Escherichia coli* O157 in a soil protozoan: implications for disease. FEMS Microbiol Lett 173(2), 291-295.

Barkocy-Gallagher, G.A., Arthur, T.M., Siragusa, G.R., Keen, J.E., Elder, R.O., Laegreid, W.W., *et al.* (2001). Genotypic analyses of *Escherichia coli* O157:H7 and O157 nonmotile isolates recovered from beef cattle and carcasses at processing plants in the Midwestern states of the United States. Appl Environ Microbiol 67(9), 3810-3818.

Beloin, C., Roux, A., and Ghigo, J.M. (2008). *Escherichia coli* biofilms. Curr Top Microbiol Immunol 322, 249-289.

Beloin, C., Valle, J., Latour-Lambert, P., Faure, P., Kzreminski, M., Balestrino, D., *et al.* (2004). Global impact of mature biofilm lifestyle on *Escherichia coli* K-12 gene expression. Mol Microbiol 51(3), 659-674.

Ben Nasr, A., Olsen, A., Sjobring, U., Muller-Esterl, W., and Bjorck, L. (1996). Assembly of human contact phase proteins and release of bradykinin at the surface of curli-expressing *Escherichia coli*. Mol Microbiol 20(5), 927-935.

Best, A., Clifford, D., Crudgington, B., Cooley, W.A., Nunez, A., Carter, B., *et al.* (2009). Intermittent *Escherichia coli* O157:H7 colonisation at the terminal rectum mucosa of conventionally-reared lambs. Vet Res 40(1), 9-9.

Biscola, F.T., Abe, C.M., and Guth, B.E. (2011). Determination of adhesin gene sequences in, and biofilm formation by, O157 and non-O157 Shiga toxin-producing *Escherichia coli* strains isolated from different sources. Appl Environ Microbiol 77(7), 2201-2208. doi: 10.1128/AEM.01920-10.

Bono, J.L., Keen, J.E., Clawson, M.L., Durso, L.M., Heaton, M.P., and Laegreid, W.W. (2007). Association of *Escherichia coli* O157:H7 tir polymorphisms with human infection. BMC Infect Dis 7, 98-98.

Booher, S.L., Cornick, N.A., and Moon, H.W. (2002). Persistence of *Escherichia coli* O157:H7 in experimentally infected swine. Vet Microbiol 89(1), 69-81.

Branchu, P., Hindre, T., Fang, X., Thomas, R., Gomelsky, M., Claret, L., *et al.* (2013). The c-di-GMP phosphodiesterase VmpA absent in *Escherichia coli* K12 strains affects motility and biofilm formation in the enterohemorrhagic O157:H7 serotype. Vet Immunol Immunopathol 152(1-2), 132-140. doi: 10.1016/j.vetimm.2012.09.029.

Brombacher, E., Dorel, C., Zehnder, A.J., and Landini, P. (2003). The curli biosynthesis regulator CsgD co-ordinates the expression of both positive and negative determinants for biofilm formation in *Escherichia coli*. Microbiology 149(Pt 10), 2847-2857.

Brunder, W., Schmidt, H., Frosch, M., and Karch, H. (1999). The large plasmids of Shiga-toxin-producing *Escherichia coli* (STEC) are highly variable genetic elements. Microbiology 145 (Pt 5), 1005-1014.

Caprioli, A., Morabito, S., Brugere, H., and Oswald, E. (2005). Enterohaemorrhagic *Escherichia coli*: emerging issues on virulence and modes of transmission. Vet Res 36(3), 289-311. doi: 10.1051/vetres:2005002.

Carpentier, B., and Cerf, O. (1993). Biofilms and their consequences, with particular reference to hygiene in the food industry. J Appl Bacteriol 75(6), 499-511.

Carter, M.Q., Xue, K., Brandl, M.T., Liu, F., Wu, L., Louie, J.W., *et al.* (2012). Functional metagenomics of *Escherichia coli* O157:H7 interactions with spinach indigenous microorganisms during biofilm formation. PLoS One 7(9), e44186. doi: 10.1371/journal.pone.0044186.

Castonguay, M.H., van der Schaaf, S., Koester, W., Krooneman, J., van der Meer, W., Harmsen, H., *et al.* (2006). Biofilm formation by *Escherichia coli* is stimulated by synergistic interactions

and co-adhesion mechanisms with adherence-proficient bacteria. Res Microbiol 157(5), 471-478. doi: 10.1016/j.resmic.2005.10.003.

Chagnot, C., Agus, A., Renier, S., Peyrin, F., Talon, R., Astruc, T., *et al.* (2013). In vitro colonization of the muscle extracellular matrix components by *Escherichia coli* O157:H7: the influence of growth medium, temperature and pH on initial adhesion and induction of biofilm formation by collagens I and III. PLoS One 8(3), e59386. doi: 10.1371/journal.pone.0059386.

Chekabab, S.M., Daigle, F., Charette, S.J., Dozois, C.M., and Harel, J. (2012). Survival of enterohemorrhagic *Escherichia coli* in the presence of Acanthamoeba castellanii and its dependence on Pho regulon. Microbiologyopen 1(4), 427-437. doi: 10.1002/mbo3.40.

Chen, C.Y., Hofmann, C.S., Cottrell, B.J., Strobaugh, T.P., Jr., Paoli, G.C., Nguyen, L.H., *et al.* (2013). Phenotypic and Genotypic Characterization of Biofilm Forming Capabilities in Non-O157 Shiga Toxin-Producing *Escherichia coli* Strains. PLoS One 8(12), e84863. doi: 10.1371/journal.pone.0084863.

Clements, A., Young, J.C., Constantinou, N., and Frankel, G. (2012). Infection strategies of enteric pathogenic *Escherichia coli*. Gut Microbes 3(2), 71-87. doi: 10.4161/gmic.19182.

Cookson, A.L., Cooley, W.A., and Woodward, M.J. (2002). The role of type 1 and curli fimbriae of Shiga toxin-producing *Escherichia coli* in adherence to abiotic surfaces. Int J Med Microbiol 292(3-4), 195-205. doi: 10.1078/1438-4221-00203.

Cooper, I.R., Taylor, H.D., and Hanlon, G.W. (2007). Virulence traits associated with verocytotoxigenic *Escherichia coli* O157 recovered from freshwater biofilms. J Appl Microbiol 102(5), 1293-1299. doi: 10.1111/j.1365-2672.2006.03178.x.

Cornick, N.A., and Helgerson, A.F. (2004). Transmission and infectious dose of *Escherichia coli* O157:H7 in swine. Appl Environ Microbiol 70(9), 5331-5335. doi: 10.1128/AEM.70.9.5331-5335.2004.

Costerton, J.W., Stewart, P.S., and Greenberg, E.P. (1999). Bacterial biofilms: a common cause of persistent infections. Science 284(5418), 1318-1322.

Croxen, M.A., and Finlay, B.B. (2010). Molecular mechanisms of *Escherichia coli* pathogenicity. Nat Rev Microbiol 8(1), 26-38. doi: 10.1038/nrmicro2265.

Danese, P.N., Pratt, L.A., Dove, S.L., and Kolter, R. (2000). The outer membrane protein, antigen 43, mediates cell-to-cell interactions within *Escherichia coli* biofilms. Mol Microbiol 37(2), 424-432.

Dewanti, R., and Wong, A.C. (1995). Influence of culture conditions on biofilm formation by *Escherichia coli* O157:H7. Int J Food Microbiol 26(2), 147-164.

Dorel, C., Vidal, O., Prigent-Combaret, C., Vallet, I., and Lejeune, P. (1999). Involvement of the Cpx signal transduction pathway of *E. coli* in biofilm formation. FEMS Microbiol Lett 178(1), 169-175.

Dourou, D., Beauchamp, C.S., Yoon, Y., Geornaras, I., Belk, K.E., Smith, G.C., *et al.* (2011). Attachment and biofilm formation by *Escherichia coli* O157:H7 at different temperatures, on various food-contact surfaces encountered in beef processing. Int J Food Microbiol 149(3), 262-268. doi: 10.1016/j.ijfoodmicro.2011.07.004.

Elder, R.O., Keen, J.E., Siragusa, G.R., Barkocy-Gallagher, G.A., Koohmaraie, M., and Laegreid, W.W. (2000). Correlation of enterohemorrhagic *Escherichia coli* O157 prevalence in feces, hides, and carcasses of beef cattle during processing. Proc Natl Acad Sci U S A 97(7), 2999-3003. doi: 10.1073/pnas.060024897.

Etcheverria, A.I., and Padola, N.L. (2013). Shiga toxin-producing *Escherichia coli*: factors involved in virulence and cattle colonization. Virulence 4(5), 366-372. doi: 10.4161/viru.24642.

Farfan, M.J., and Torres, A.G. (2012). Molecular mechanisms that mediate colonization of Shiga toxin-producing *Escherichia coli* strains. Infect Immun 80(3), 903-913. doi: 10.1128/IAI.05907-11.

Ferens, W.A., and Hovde, C.J. (2011). *Escherichia coli* O157:H7: animal reservoir and sources of human infection. Foodborne Pathog Dis 8(4), 465-487. doi: 10.1089/fpd.2010.0673.

Fink, R.C., Black, E.P., Hou, Z., Sugawara, M., Sadowsky, M.J., and Diez-Gonzalez, F. (2012). Transcriptional responses of *Escherichia coli* K-12 and O157:H7 associated with lettuce leaves. Appl Environ Microbiol 78(6), 1752-1764. doi: 10.1128/aem.07454-11.

Fletcher, M. (1988). Attachment of Pseudomonas fluorescens to glass and influence of electrolytes on bacterium-substratum separation distance. J Bacteriol 170(5), 2027-2030.

Fouladkhah, A., Geornaras, I., and Sofos, J.N. (2013). Biofilm Formation of O157 and Non-O157 Shiga Toxin-Producing *Escherichia coli* and Multidrug-Resistant and Susceptible Salmonella Typhimurium and Newport and Their Inactivation by Sanitizers. J Food Sci. doi: 10.1111/1750-3841.12123.

Frank, C., Werber, D., Cramer, J.P., Askar, M., Faber, M., an der Heiden, M., *et al.* (2011). Epidemic profile of Shiga-toxin-producing *Escherichia coli* O104:H4 outbreak in Germany. N Engl J Med 365(19), 1771-1780. doi: 10.1056/NEJMoa1106483.

Fukushima, H., Hashizume, T., Morita, Y., Tanaka, J., Azuma, K., Mizumoto, Y., *et al.* (1999). Clinical experiences in Sakai City Hospital during the massive outbreak of enterohemorrhagic *Escherichia coli* O157 infections in Sakai City, 1996. Pediatr Int 41(2), 213-217.

Gagliardi, J.V., and Karns, J.S. (2000). Leaching of *Escherichia coli* O157:H7 in diverse soils under various agricultural management practices. Appl Environ Microbiol 66(3), 877-883.

Genevaux, P., Bauda, P., DuBow, M.S., and Oudega, B. (1999). Identification of Tn*10* insertions in the *rfaG*, *rfaP*, and *galU* genes involved in lipopolysaccharide core biosynthesis that affect *Escherichia coli* adhesion. Arch Microbiol 172(1), 1-8.

Gerstel, U., Park, C., and Romling, U. (2003). Complex regulation of *csgD* promoter activity by global regulatory proteins. Mol Microbiol 49(3), 639-654.

Giaouris, E., Heir, E., Hebraud, M., Chorianopoulos, N., Langsrud, S., Moretro, T., *et al.* (2013). Attachment and biofilm formation by foodborne bacteria in meat processing environments: Causes, implications, role of bacterial interactions and control by alternative novel methods. Meat Sci. doi: 10.1016/j.meatsci.2013.05.023.

Gibson, H., Taylor, J.H., Hall, K.E., and Holah, J.T. (1999). Effectiveness of cleaning techniques used in the food industry in terms of the removal of bacterial biofilms. J Appl Microbiol 87(1), 41-48.

Gill, C.O., and McGinnis, J.C. (2000). Contamination of beef trimmings with *Escherichia coli* during a carcass breaking process. Food Research International 33(2), 125-130. http://dx.doi.org/10.1016/S0963-9969(00)00026-0.

Gill, C.O., McGinnis, J.C., and Bryant, J. (2001). Contamination of beef chucks with *Escherichia coli* during carcass breaking. J Food Prot 64(11), 1824-1827.

Gottesman, S., and Stout, V. (1991). Regulation of capsular polysaccharide synthesis in *Escherichia coli* K12. Mol Microbiol 5(7), 1599-1606.

Gourabathini, P., Brandl, M.T., Redding, K.S., Gunderson, J.H., and Berk, S.G. (2008). Interactions between food-borne pathogens and protozoa isolated from lettuce and spinach. Appl Environ Microbiol 74(8), 2518-2525.

Grant, J., Wendelboe, A.M., Wendel, A., Jepson, B., Torres, P., Smelser, C., *et al.* (2008). Spinach-associated *Escherichia coli* O157:H7 outbreak, Utah and New Mexico, 2006. Emerg Infect Dis 14(10), 1633-1636.

Gualdi, L., Tagliabue, L., Bertagnoli, S., Ierano, T., De Castro, C., and Landini, P. (2008). Cellulose modulates biofilm formation by counteracting curli-mediated colonization of solid surfaces in *Escherichia coli*. Microbiology 154 (Pt 7), 2017-2024. doi: 10.1099/mic.0.2008/018093-0.

Habimana, O., Heir, E., Langsrud, S., Asli, A.W., and Moretro, T. (2010). Enhanced surface colonization by *Escherichia coli* O157:H7 in biofilms formed by an Acinetobacter calcoaceticus isolate from meat-processing environments. Appl Environ Microbiol 76(13), 4557-4559. doi: 10.1128/AEM.02707-09.

Hall-Stoodley, L., and Stoodley, P. (2009). Evolving concepts in biofilm infections. Cell Microbiol 11(7), 1034-1043. doi: 10.1111/j.1462-5822.2009.01323.x.

Hammar, M.R., Arnqvist, A., Bian, Z., Olsen, A., and Normark, S. (1995). Expression of two csg operons is required for production of fibronectin- and Congo red-binding curli polymers in *Escherichia coli* K-12. Mol Microbiol 18(4), 661-670. doi: 10.1111/j.1365-2958.1995.mmi_18040661.x.

Hayashi, T., Makino, K., Ohnishi, M., Kurokawa, K., Ishii, K., Yokoyama, K., *et al.* (2001). Complete genome sequence of enterohemorrhagic *Escherichia coli* O157:H7 and genomic comparison with a laboratory strain K-12. DNA Res 8(1), 11-22.

Herold, S., Paton, J.C., and Paton, A.W. (2009). Sab, a novel autotransporter of locus of enterocyte effacement-negative shiga-toxigenic *Escherichia coli* O113:H21, contributes to adherence and biofilm formation. Infect Immun 77(8), 3234-3243. doi: 10.1128/IAI.00031-09.

Heuvelink, A.E., Zwartkruis-Nahuis, J.T., van den Biggelaar, F.L., van Leeuwen, W.J., and de Boer, E. (1999). Isolation and characterization of verocytotoxin-producing *Escherichia coli* O157 from slaughter pigs and poultry. Int J Food Microbiol 52(1-2), 67-75.

Hou, S., Liu, Z., Young, A.W., Mark, S.L., Kallenbach, N.R., and Ren, D. (2010). Effects of Trp- and Arg-containing antimicrobial-peptide structure on inhibition of *Escherichia coli* planktonic growth and biofilm formation. Appl Environ Microbiol 76(6), 1967-1974. doi: 10.1128/AEM.02321-09.

Hou, Z., Fink, R.C., Sugawara, M., Diez-Gonzalez, F., and Sadowsky, M.J. (2013). Transcriptional and functional responses of *Escherichia coli* O157:H7 growing in the lettuce rhizoplane. Food Microbiol 35(2), 136-142. doi: 10.1016/j.fm.2013.03.002.

Houari, A., and Di Martino, P. (2007). Effect of chlorhexidine and benzalkonium chloride on bacterial biofilm formation. Lett Appl Microbiol 45(6), 652-656. doi: 10.1111/j.1472-765X.2007.02249.x.

Ibekwe, A.M., Papiernik, S.K., Grieve, C.M., and Yang, C.H. (2011). Quantification of Persistence of *Escherichia coli* O157:H7 in Contrasting Soils. Int J Microbiol 2011. doi: 10.1155/2011/421379.

Jacques, M., Aragon, V., and Tremblay, Y.D. (2010). Biofilm formation in bacterial pathogens of veterinary importance. Anim Health Res Rev 11(2), 97-121. doi: 10.1017/S1466252310000149.

Jeter, C., and Matthysse, A.G. (2005). Characterization of the binding of diarrheagenic strains of *E. coli* to plant surfaces and the role of curli in the interaction of the bacteria with alfalfa sprouts. Mol Plant Microbe Interact 18(11), 1235-1242.

Jubelin, G., Vianney, A., Beloin, C., Ghigo, J.M., Lazzaroni, J.C., Lejeune, P., *et al.* (2005). CpxR/OmpR interplay regulates curli gene expression in response to osmolarity in *Escherichia coli*. J Bacteriol 187(6), 2038-2049. doi: 10.1128/JB.187.6.2038-2049.2005.

Kaper, J.B., Nataro, J.P., and Mobley, H.L. (2004). Pathogenic *Escherichia coli*. Nat Rev Microbiol 2(2), 123-140. doi: 10.1038/nrmicro818.

Kaplan, J.B. (2010). Biofilm dispersal: mechanisms, clinical implications, and potential therapeutic uses. J Dent Res 89(3), 205-218. doi: 10.1177/0022034509359403.

Karmali, M.A., Mascarenhas, M., Shen, S., Ziebell, K., Johnson, S., Reid-Smith, R., *et al.* (2003). Association of genomic O-island 122 of *Escherichia coli* EDL 933 with verocytotoxin-producing *Escherichia coli* seropathotypes that are linked to epidemic and/or serious disease. J Clin Microbiol 41(11), 4930-4940.

Kikuchi, T., Mizunoe, Y., Takade, A., Naito, S., and Yoshida, S. (2005). Curli fibers are required for development of biofilm architecture in *Escherichia coli* K-12 and enhance bacterial adherence to human uroepithelial cells. Microbiol Immunol 49(9), 875-884.

Klayman, B.J., Volden, P.A., Stewart, P.S., and Camper, A.K. (2009). *Escherichia coli* O157:H7 requires colonizing partner to adhere and persist in a capillary flow cell. Environ Sci Technol 43(6), 2105-2111.

Knutton, S., Shaw, R.K., Anantha, R.P., Donnenberg, M.S., and Zorgani, A.A. (1999). The type IV bundle-forming pilus of enteropathogenic *Escherichia coli* undergoes dramatic alterations in structure associated with bacterial adherence, aggregation and dispersal. Mol Microbiol 33(3),

499-509.

Koutsoumanis, K.P., and Sofos, J.N. (2004). Comparative acid stress response of Listeria monocytogenes, *Escherichia coli* O157:H7 and *Salmonella* Typhimurium after habituation at different pH conditions. Lett Appl Microbiol 38(4), 321-326.

La Ragione, R.M., Best, A., Woodward, M.J., and Wales, A.D. (2009). *Escherichia coli* O157:H7 colonization in small domestic ruminants. FEMS Microbiol Rev 33(2), 394-410.

Lee, J.H., Kim, Y.G., Cho, M.H., Wood, T.K., and Lee, J. (2011). Transcriptomic analysis for genetic mechanisms of the factors related to biofilm formation in *Escherichia coli* O157:H7. Curr Microbiol 62(4), 1321-1330. doi: 10.1007/s00284-010-9862-4.

Lequette, Y., Boels, G., Clarisse, M., and Faille, C. (2010). Using enzymes to remove biofilms of bacterial isolates sampled in the food-industry. Biofouling 26(4), 421-431. doi: 10.1080/08927011003699535.

Lewis, K. (2010). Persister cells. Annu Rev Microbiol 64, 357-372. doi: 10.1146/annurev.micro.112408.134306.

Liu, N.T., Nou, X., Lefcourt, A.M., Shelton, D.R., and Lo, Y.M. (2014). Dual-species biofilm formation by *Escherichia coli* O157:H7 and environmental bacteria isolated from fresh-cut processing facilities. Int J Food Microbiol 171, 15-20. doi: 10.1016/j.ijfoodmicro.2013.11.007.

Lu, L., Hume, M.E., and Pillai, S.D. (2005). Autoinducer-2-like activity on vegetable produce and its potential involvement in bacterial biofilm formation on tomatoes. Foodborne Pathog Dis 2(3), 242-249. doi: 10.1089/fpd.2005.2.242.

Maal-Bared, R., Bartlett, K.H., Bowie, W.R., and Hall, E.R. (2013). Phenotypic antibiotic resistance of *Escherichia coli* and *E. coli* O157 isolated from water, sediment and biofilms in an agricultural watershed in British Columbia. Sci Total Environ 443, 315-323. doi: 10.1016/j.scitotenv.2012.10.106.

Macarisin, D., Patel, J., Bauchan, G., Giron, J.A., and Sharma, V.K. (2012). Role of curli and

cellulose expression in adherence of *Escherichia coli* O157:H7 to spinach leaves. Foodborne Pathog Dis 9(2), 160-167.

Manning, S.D., Motiwala, A.S., Springman, A.C., Qi, W., Lacher, D.W., Ouellette, L.M., *et al.* (2008). Variation in virulence among clades of *Escherichia coli* O157:H7 associated with disease outbreaks. Proc Natl Acad Sci U S A 105(12), 4868-4873.

Marouani-Gadri, N., Augier, G., and Carpentier, B. (2009a). Characterization of bacterial strains isolated from a beef-processing plant following cleaning and disinfection - Influence of isolated strains on biofilm formation by Sakai and EDL 933 *E. coli* O157:H7.

Marouani-Gadri, N., Chassaing, D., and Carpentier, B. (2009b). Comparative evaluation of biofilm formation and tolerance to a chemical shock of pathogenic and nonpathogenic *Escherichia coli* O157:H7 strains. J Food Prot 72(1), 157-164.

Marouani-Gadri, N., Firmesse, O., Chassaing, D., Sandris-Nielsen, D., Arneborg, N., and Carpentier, B. (2010). Potential of *Escherichia coli* O157:H7 to persist and form viable but non-culturable cells on a food-contact surface subjected to cycles of soiling and chemical treatment. Int J Food Microbiol 144(1), 96-9103.

Matthysse, A.G., Deora, R., Mishra, M., and Torres, A.G. (2008). Polysaccharides cellulose, poly-beta-1,6-n-acetyl-D-glucosamine, and colanic acid are required for optimal binding of *Escherichia coli* O157:H7 strains to alfalfa sprouts and K-12 strains to plastic but not for binding to epithelial cells. Appl Environ Microbiol 74(8), 2384-2390.

Mauro, S.A., Opalko, H., Lindsay, K., Colon, M.P., and Koudelka, G.B. (2013). The microcosm mediates the persistence of shiga toxin-producing *Escherichia coli* in freshwater ecosystems. Appl Environ Microbiol 79(16), 4821-4828.

Mellor, G.E., Besser, T.E., Davis, M.A., Beavis, B., Jung, W., Smith, H.V., *et al.* (2013). Multilocus genotype analysis of *Escherichia coli* O157 isolates from Australia and the United States provides evidence of geographic divergence. Appl Environ Microbiol 79(16), 5050-5058.

Moreira, S., Brown, A., Ha, R., Iserhoff, K., Yim, M., Yang, J., *et al.* (2012). Persistence of

Escherichia coli in freshwater periphyton: biofilm-forming capacity as a selective advantage. FEMS Microbiol Ecol 79(3), 608-618.

Nesse, L.L., Sekse, C., Berg, K., Johannesen, K.C., Solheim, H., Vestby, L.K., *et al.* (2013). Potentially pathogenic *E. coli* can produce biofilm under conditions relevant for the food production chain. Appl Environ Microbiol. doi: 10.1128/AEM.03331-13.

Olsen, A., Jonsson, A., and Normark, S. (1989). Fibronectin binding mediated by a novel class of surface organelles on *Escherichia coli*. Nature 338(6217), 652-655. doi: 10.1038/338652a0.

Park, S.H., Cheon, H.L., Park, K.H., Chung, M.S., Choi, S.H., Ryu, S., *et al.* (2012). Inactivation of biofilm cells of foodborne pathogen by aerosolized sanitizers. Int J Food Microbiol 154(3), 130-134. doi: 10.1016/j.ijfoodmicro.2011.12.018.

Perez-Conesa, D., Cao, J., Chen, L., McLandsborough, L., and Weiss, J. (2011). Inactivation of Listeria monocytogenes and *Escherichia coli* O157:H7 biofilms by micelle-encapsulated eugenol and carvacrol. J Food Prot 74(1), 55-62. doi: 10.4315/0362-028X.JFP-08-403.

Perez-Conesa, D., McLandsborough, L., and Weiss, J. (2006). Inhibition and inactivation of Listeria monocytogenes and *Escherichia coli* O157:H7 colony biofilms by micellar-encapsulated eugenol and carvacrol. J Food Prot 69(12), 2947-2954.

Perna, N.T., Plunkett, G., 3rd, Burland, V., Mau, B., Glasner, J.D., Rose, D.J., *et al.* (2001). Genome sequence of enterohaemorrhagic *Escherichia coli* O157:H7. Nature 409(6819), 529-533. doi: 10.1038/35054089.

Pratt, L.A., and Kolter, R. (1998). Genetic analysis of *Escherichia coli* biofilm formation: roles of flagella, motility, chemotaxis and type I pili. Mol Microbiol 30(2), 285-293.

Prigent-Combaret, C., Brombacher, E., Vidal, O., Ambert, A., Lejeune, P., Landini, P., *et al.* (2001). Complex regulatory network controls initial adhesion and biofilm formation in *Escherichia coli* via regulation of the *csgD* gene. J Bacteriol 183(24), 7213-7223. doi: 10.1128/JB.183.24.7213-7223.2001.

Puttamreddy, S., Cornick, N.A., and Minion, F.C. (2010). Genome-wide transposon mutagenesis reveals a role for pO157 genes in biofilm development in *Escherichia coli* O157:H7 EDL933. Infect Immun 78(6), 2377-2384. doi: 10.1128/IAI.00156-10.

Ravva, S.V., Sarreal, C.Z., and Mandrell, R.E. (2010). Identification of protozoa in dairy lagoon wastewater that consume *Escherichia coli* O157:H7 preferentially. PLoS One 5(12), e15671. doi: 10.1371/journal.pone.0015671.

Ribeiro, A.F., Laroche, E., Hanin, G., Fournier, M., Quillet, L., Dupont, J.P., *et al.* (2012). Antibiotic-resistant *Escherichia coli* in karstic systems: a biological indicator of the origin of fecal contamination? FEMS Microbiol Ecol 81(1), 267-280. doi: 10.1111/j.1574-6941.2012.01382.x.

Rivera-Betancourt, M., Shackelford, S.D., Arthur, T.M., Westmoreland, K.E., Bellinger, G., Rossman, M., *et al.* (2004). Prevalence of *Escherichia coli* O157:H7, *Listeria monocytogenes*, and *Salmonella* in two geographically distant commercial beef processing plants in the United States. J Food Prot 67(2), 295-302.

Roe, A.J., Currie, C., Smith, D.G., and Gally, D.L. (2001). Analysis of type 1 fimbriae expression in verotoxigenic *Escherichia coli*: a comparison between serotypes O157 and O26. Microbiology 147(Pt 1), 145-152.

Ryu, J.H., and Beuchat, L.R. (2005). Biofilm formation by *Escherichia coli* O157:H7 on stainless steel: effect of exopolysaccharide and Curli production on its resistance to chlorine. Appl Environ Microbiol 71(1), 247-254. doi: 10.1128/AEM.71.1.247-254.2005.

Ryu, J.H., Kim, H., and Beuchat, L.R. (2004a). Attachment and biofilm formation by *Escherichia coli* O157:H7 on stainless steel as influenced by exopolysaccharide production, nutrient availability, and temperature. J Food Prot 67(10), 2123-2131.

Ryu, J.H., Kim, H., Frank, J.F., and Beuchat, L.R. (2004b). Attachment and biofilm formation on stainless steel by *Escherichia coli* O157:H7 as affected by curli production. Lett Appl Microbiol 39(4), 359-362. doi: 10.1111/j.1472-765X.2004.01591.x.

Schauder, S., Shokat, K., Surette, M.G., and Bassler, B.L. (2001). The LuxS family of bacterial autoinducers: biosynthesis of a novel quorum-sensing signal molecule. Mol Microbiol 41(2), 463-476.

Schembri, M.A., Dalsgaard, D., and Klemm, P. (2004). Capsule shields the function of short bacterial adhesins. J Bacteriol 186(5), 1249-1257.

Scheutz, F., Nielsen, E.M., Frimodt-Moller, J., Boisen, N., Morabito, S., Tozzoli, R., *et al.* (2011). Characteristics of the enteroaggregative Shiga toxin/verotoxin-producing *Escherichia coli* O104:H4 strain causing the outbreak of haemolytic uraemic syndrome in Germany, May to June 2011. Euro Surveill 16(24).

Seo, K.H., and Frank, J.F. (1999). Attachment of *Escherichia coli* O157:H7 to lettuce leaf surface and bacterial viability in response to chlorine treatment as demonstrated by using confocal scanning laser microscopy. J Food Prot 62(1), 3-9.

Sharma, M., Ryu, J.H., and Beuchat, L.R. (2005). Inactivation of *Escherichia coli* O157:H7 in biofilm on stainless steel by treatment with an alkaline cleaner and a bacteriophage. J Appl Microbiol 99(3), 449-459. doi: 10.1111/j.1365-2672.2005.02659.x.

Sharma, V.K., Bearson, S.M., and Bearson, B.L. (2010). Evaluation of the effects of sdiA, a luxR homologue, on adherence and motility of *Escherichia coli* O157:H7. Microbiology 156(Pt 5), 1303-1312. doi: 10.1099/mic.0.034330-0.

Sheikh, J., Czeczulin, J.R., Harrington, S., Hicks, S., Henderson, I.R., Le Bouguenec, C., *et al.* (2002). A novel dispersin protein in enteroaggregative *Escherichia coli*. J Clin Invest 110(9), 1329-1337. doi: 10.1172/JCI16172.

Shifrin, Y., Peleg, A., Ilan, O., Nadler, C., Kobi, S., Baruch, K., *et al.* (2008). Transient shielding of intimin and the type III secretion system of enterohemorrhagic and enteropathogenic *Escherichia coli* by a group 4 capsule. J Bacteriol 190(14), 5063-5074. doi: 10.1128/JB.00440-08.

Shringi, S., Garcia, A., Lahmers, K.K., Potter, K.A., Muthupalani, S., Swennes, A.G., *et al.*

(2012). Differential virulence of clinical and bovine-biased enterohemorrhagic *Escherichia coli* O157:H7 genotypes in piglet and Dutch belted rabbit models. Infect Immun 80(1), 369-380.

Silagyi, K., Kim, S.H., Lo, Y.M., and Wei, C.I. (2009). Production of biofilm and quorum sensing by *Escherichia coli* O157:H7 and its transfer from contact surfaces to meat, poultry, ready-to-eat deli, and produce products. Food Microbiol 26(5), 514-519. doi: 10.1016/j.fm.2009.03.004.

Solheim, H.T., Sekse, C., Urdahl, A.M., Wasteson, Y., and Nesse, L.L. (2013). Biofilm as an environment for dissemination of stx genes by transduction. Appl Environ Microbiol 79(3), 896-900. doi: 10.1128/AEM.03512-12.

Solomon, E.B., Yaron, S., and Matthews, K.R. (2002). Transmission of *Escherichia coli* O157:H7 from contaminated manure and irrigation water to lettuce plant tissue and its subsequent internalization. Appl Environ Microbiol 68(1), 397-400.

Steinberg, K.M., and Levin, B.R. (2007). Grazing protozoa and the evolution of the *Escherichia coli* O157:H7 Shiga toxin-encoding prophage. Proc Biol Sci 274(1621), 1921-1929. doi: 10.1098/rspb.2007.0245.

Stopforth, J.D., Samelis, J., Sofos, J.N., Kendall, P.A., and Smith, G.C. (2003). Influence of extended acid stressing in fresh beef decontamination runoff fluids on sanitizer resistance of acid-adapted *Escherichia coli* O157:H7 in biofilms. J Food Prot 66(12), 2258-2266.

Thomassin, J.L., Brannon, J.R., Gibbs, B.F., Gruenheid, S., and Le Moual, H. (2012). OmpT outer membrane proteases of enterohemorrhagic and enteropathogenic *Escherichia coli* contribute differently to the degradation of human LL-37. Infect Immun 80(2), 483-492. doi: 10.1128/IAI.05674-11.

Thomassin, J.L., Lee, M.J., Brannon, J.R., Sheppard, D.C., Gruenheid, S., and Le Moual, H. (2013). Both group 4 capsule and lipopolysaccharide O-antigen contribute to enteropathogenic *Escherichia coli* resistance to human alpha-defensin 5. PLoS One 8(12), e82475. doi: 10.1371/journal.pone.0082475.

Torres, A.G., Perna, N.T., Burland, V., Ruknudin, A., Blattner, F.R., and Kaper, J.B. (2002). Characterization of Cah, a calcium-binding and heat-extractable autotransporter protein of enterohaemorrhagic *Escherichia coli*. Mol Microbiol 45(4), 951-966.

Tutenel, A.V., Pierard, D., Van Hoof, J., Cornelis, M., and De Zutter, L. (2003). Isolation and molecular characterization of *Escherichia coli* O157 isolated from cattle, pigs and chickens at slaughter. Int J Food Microbiol 84(1), 63-69.

Tyler, H.L., and Triplett, E.W. (2008). Plants as a habitat for beneficial and/or human pathogenic bacteria. Annu Rev Phytopathol 46, 53-73.

Uhlich, G.A., Cooke, P.H., and Solomon, E.B. (2006). Analyses of the red-dry-rough phenotype of an *Escherichia coli* O157:H7 strain and its role in biofilm formation and resistance to antibacterial agents. Appl Environ Microbiol 72(4), 2564-2572. doi: 10.1128/AEM.72.4.2564-2572.2006.

Uhlich, G.A., Rogers, D.P., and Mosier, D.A. (2010). *Escherichia coli* serotype O157:H7 retention on solid surfaces and peroxide resistance is enhanced by dual-strain biofilm formation. Foodborne Pathog Dis 7(8), 935-943. doi: 10.1089/fpd.2009.0503.

van Elsas, J.D., Semenov, A.V., Costa, R., and Trevors, J.T. (2011). Survival of *Escherichia coli* in the environment: fundamental and public health aspects. ISME J 5(2), 173-183.

van Overbeek, L.S., Franz, E., Semenov, A.V., de Vos, O.J., and van Bruggen, A.H. (2010). The effect of the native bacterial community structure on the predictability of *E. coli* O157:H7 survival in manure-amended soil. Lett Appl Microbiol 50(4), 425-430. doi: 10.1111/j.1472-765X.2010.02817.x.

Velarde, J.J., Varney, K.M., Inman, K.G., Farfan, M., Dudley, E., Fletcher, J., *et al.* (2007). Solution structure of the novel dispersin protein of enteroaggregative *Escherichia coli*. Mol Microbiol 66(5), 1123-1135. doi: 10.1111/j.1365-2958.2007.05985.x.

Verstraete, K., K, D.E.R., S, V.A.N.W., Pierard, D., L, D.E.Z., Herman, L., *et al.* (2013). Genetic characteristics of Shiga toxin-producing *E. coli* O157, O26, O103, O111 and O145

isolates from humans, food, and cattle in Belgium. Epidemiol Infect 141(12), 2503-2515. doi: 10.1017/S0950268813000307.

Vianney, A., Jubelin, G., Renault, S., Dorel, C., Lejeune, P., and Lazzaroni, J.C. (2005). *Escherichia coli* tol and *rcs* genes participate in the complex network affecting curli synthesis. Microbiology 151(Pt 7), 2487-2497. doi: 10.1099/mic.0.27913-0.

Vidal, O., Longin, R., Prigent-Combaret, C., Dorel, C., Hooreman, M., and Lejeune, P. (1998). Isolation of an *Escherichia coli* K-12 mutant strain able to form biofilms on inert surfaces: involvement of a new *ompR* allele that increases curli expression. J Bacteriol 180(9), 2442-2449.

Vidovic, S., Block, H.C., and Korber, D.R. (2007). Effect of soil composition, temperature, indigenous microflora, and environmental conditions on the survival of *Escherichia coli* O157:H7. Can J Microbiol 53(7), 822-829. doi: 10.1139/W07-041.

Vikram, A., Jayaprakasha, G.K., Jesudhasan, P.R., Pillai, S.D., and Patil, B.S. (2010). Suppression of bacterial cell-cell signalling, biofilm formation and type III secretion system by citrus flavonoids. J Appl Microbiol 109(2), 515-527. doi: 10.1111/j.1365-2672.2010.04677.x.

Vu-Khac, H., and Cornick, N.A. (2008). Prevalence and genetic profiles of Shiga toxin-producing *Escherichia coli* strains isolated from buffaloes, cattle, and goats in central Vietnam. Vet Microbiol 126(4), 356-363.

Walters, M., and Sperandio, V. (2006). Quorum sensing in *Escherichia coli* and *Salmonella*. Int J Med Microbiol 296(2-3), 125-131. doi: 10.1016/j.ijmm.2006.01.041.

Wang, R., Bono, J.L., Kalchayanand, N., Shackelford, S., and Harhay, D.M. (2012). Biofilm Formation by Shiga Toxin-Producing *Escherichia coli* O157:H7 and Non-O157 Strains and Their Tolerance to Sanitizers Commonly Used in the Food Processing Environment. J Food Prot 75(8), 1418-1428. doi: 10.4315/0362-028X.JFP-11-427 [doi].

Welch, R.A., Burland, V., Plunkett, G., Redford, P., Roesch, P., Rasko, D., *et al.* (2002). Extensive mosaic structure revealed by the complete genome sequence of uropathogenic

Escherichia coli. Proc Natl Acad Sci U S A 99(26), 17020-17024.

Wells, T.J., McNeilly, T.N., Totsika, M., Mahajan, A., Gally, D.L., and Schembri, M.A. (2009). The *Escherichia coli* O157:H7 EhaB autotransporter protein binds to laminin and collagen I and induces a serum IgA response in O157:H7 challenged cattle. Environ Microbiol 11(7), 1803-1814. doi: 10.1111/j.1462-2920.2009.01905.x.

Wells, T.J., Sherlock, O., Rivas, L., Mahajan, A., Beatson, S.A., Torpdahl, M., *et al.* (2008). EhaA is a novel autotransporter protein of enterohemorrhagic *Escherichia coli* O157:H7 that contributes to adhesion and biofilm formation. Environ Microbiol 10(3), 589-604. doi: 10.1111/j.1462-2920.2007.01479.x.

Wey, J.K., Jurgens, K., and Weitere, M. (2012). Seasonal and successional influences on bacterial community composition exceed that of protozoan grazing in river biofilms. Appl Environ Microbiol 78(6), 2013-2024. doi: 10.1128/AEM.06517-11.

Whitfield, C. (2006). Biosynthesis and assembly of capsular polysaccharides in *Escherichia coli*. Annu Rev Biochem 75, 39-68. doi: 10.1146/annurev.biochem.75.103004.142545.

Woerner, D.R., Ransom, J.R., Sofos, J.N., Dewell, G.A., Smith, G.C., Salman, M.D., *et al.* (2006). Determining the prevalence of *Escherichia coli* O157 in cattle and beef from the feedlot to the cooler. J Food Prot 69(12), 2824-2827.

Wood, T.K. (2009). Insights on *Escherichia coli* biofilm formation and inhibition from whole-transcriptome profiling. Environ Microbiol 11(1), 1-15. doi: 10.1111/j.1462-2920.2008.01768.x.

Yang, K., Meng, J., Huang, Y.C., Ye, L.H., Li, G.J., Huang, J., *et al.* (2014). The Role of the QseC Quorum-Sensing Sensor Kinase in Epinephrine-Enhanced Motility and Biofilm Formation by *Escherichia coli*. Cell Biochem Biophys. doi: 10.1007/s12013-014-9924-5.

Yeh, J.Y., and Chen, J. (2004). Production of slime polysaccharide by EHEC and STEC as well as the influence of culture conditions on slime production in *Escherichia coli* O157:H7. Lett Appl Microbiol 38(6), 488-492. doi: 10.1111/j.1472-765X.2004.01523.x.

Zhang, W., Qi, W., Albert, T.J., Motiwala, A.S., Alland, D., Hyytia-Trees, E.K., *et al.* (2006). Probing genomic diversity and evolution of *Escherichia coli* O157 by single nucleotide polymorphisms. Genome Res 16(6), 757-767.

Zhang, Y., Laing, C., Zhang, Z., Hallewell, J., You, C., Ziebell, K., *et al.* (2010). Lineage and host source are both correlated with levels of Shiga toxin 2 production by *Escherichia coli* O157:H7 strains. Appl Environ Microbiol 76(2), 474-482.

Zogaj, X., Nimtz, M., Rohde, M., Bokranz, W., and Romling, U. (2001). The multicellular morphotypes of Salmonella typhimurium and *Escherichia coli* produce cellulose as the second component of the extracellular matrix. Mol Microbiol 39(6), 1452-1463.

II.2.4.14 Figures

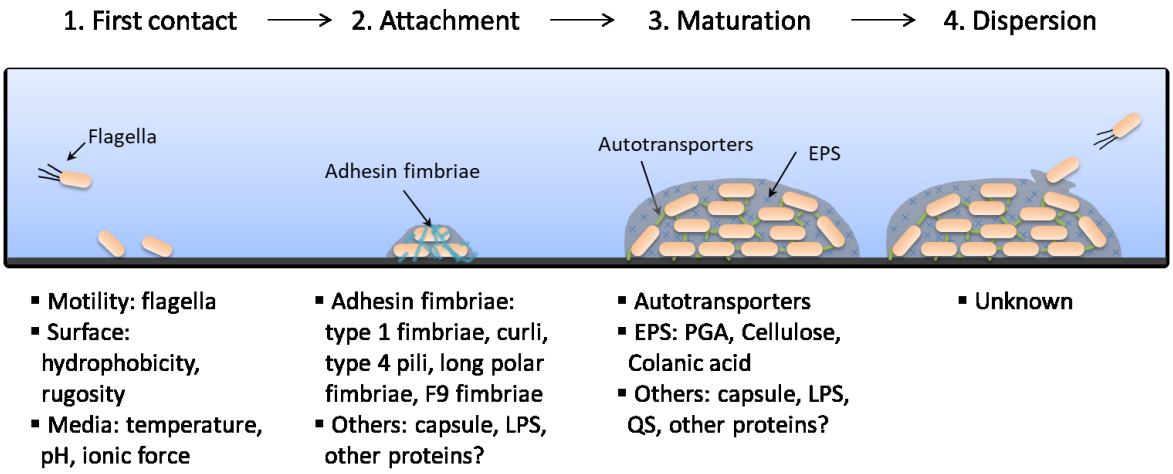

Figure 1. Schematic representation of biofilm formation and STEC factors associated with each step. Biofilm formation is a dynamic and complex process influenced by several bacterial and/or environmental factors. Biofilm formation occurs in four steps: first contact, attachment, maturation, and dispersion. Factors that are known to play a role in STEC biofilm formation are listed below the corresponding step. It should be noted that biofilm formation in STEC is strain dependent and factors presented in this figure are not necessarily representative of all STEC biofilms. PGA: poly-N-acetyl glucosamine, EPS: extracellular polymeric substances, LPS: lipopolysaccharides; QS: quorum sensing.

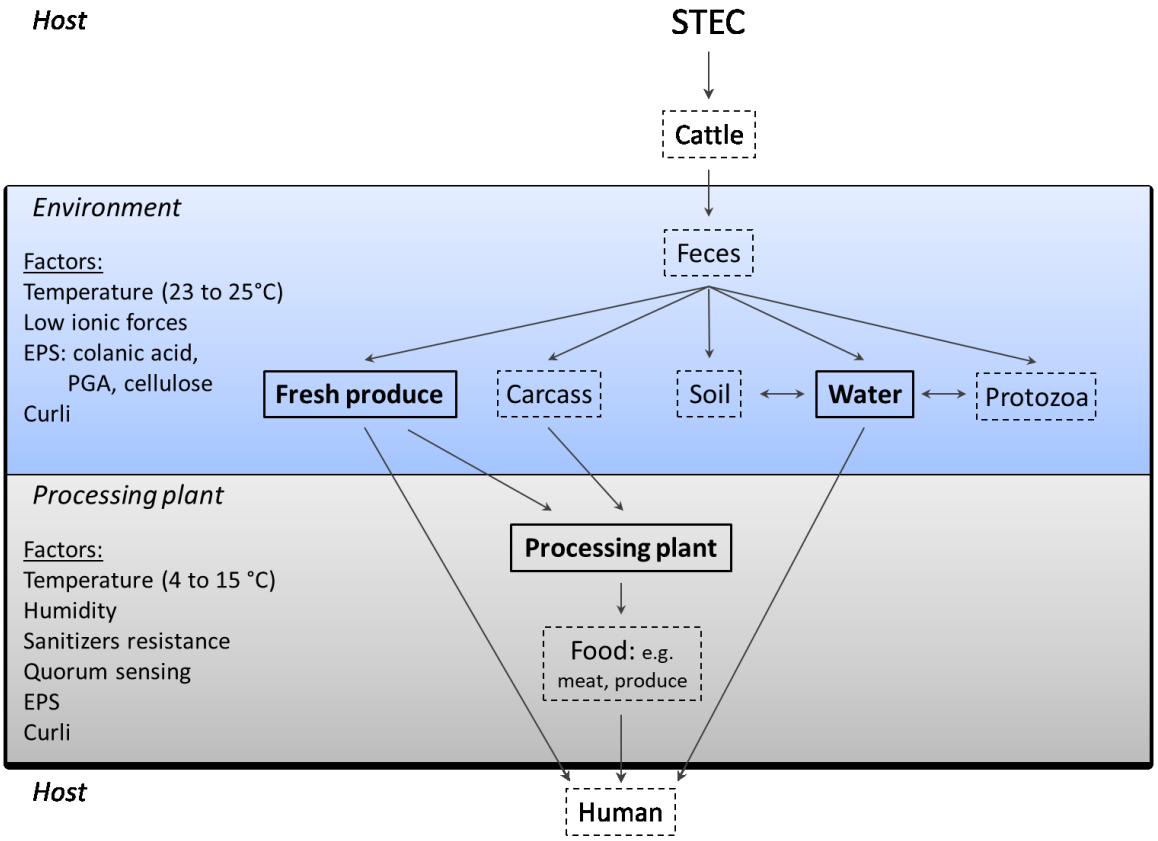

Figure 2. Role of biofilm formation in the transmission and persistence of STEC outside of an animal host. Several studies demonstrated that STEC can persist as a biofilm on fresh produce, in water, and in processing plants. In some cases, factors contributing to biofilm formation have been identified. Texts in bold and framed by solid lines indicate environments where STEC biofilms are identified and participate in the persistence of STEC; dashed lines indicate environments where STEC biofilms are hypothesized to be present. It is currently unknown if STEC biofilm formation plays a role in the colonization of cattle and humans or in STEC survival in feces, soil, protozoans, carcasses, and processed food. PGA: poly-N-acetyl glucosamine, EPS: extracellular polymeric substances, LPS: lipopolysaccharides; QS: quorum sensing.

II.3 Le phosphate et le régulon Pho chez *E. coli*

Le phosphate est un composant cellulaire essentiel. Le phosphate se retrouve dans la composition d'un grand nombre de molécules. Il est impliqué dans le métabolisme énergétique et dans la signalisation cellulaire. De plus, le phosphate est impliqué dans plusieurs réactions biochimiques. Chez *E. coli* l'homéostasie du phosphate est assurée par des systèmes de transport/acquisition, d'un système de régulation et de plusieurs protéines nécessaires au métabolisme de différentes sources de phosphate.

II.3.1 Le phosphate

En chimie, le phosphate est un ion ayant pour formule PO_4^{3-}. Dans sa forme anionique il est composé d'un atome de phosphore (P) entouré par 4 atomes d'oxygène (O) et dispose de 3 charges négatives. Le PO_4^{3-} est la base conjuguée du phosphate inorganique (Pi) ayant pour formule HPO_4^{2-}. À son tour le Pi est la base conjuguée de l'ion dihydrogénophosphate ($H_2PO_4^-$) qui est lui-même la base conjuguée de l'acide phosphorique (H_3PO_4). En polymérisant, l'ion phosphate peut former des polymères tels que le pyrophosphate (PPi) ($P_2O_7^{4-}$), le triphosphate ($P_3O_{10}^{5-}$), voire des molécules beaucoup plus complexes comme les structures linéaires de polyphosphate (polyPi).

En agriculture, les phosphates sont utilisés comme engrais pour fournir aux plantes la source de phosphore nécessaire à leur croissance. Autrefois, le phosphate entrait aussi dans la composition des lessives car en formant des complexes avec le calcium, ils empêchaient la formation de dépôt calcaire sur le linge ou la vaisselle. Lorsque le phosphate se retrouve dans les eaux usées, il sert alors d'engrais pour les algues qui détruisent alors toute autre forme de vie par étouffement dans un processus appelé l'eutrophisation. L'utilisation de phosphate dans les lessives a donc été interdite.

En biologie, le phosphate est retrouvé soit sous forme d'ion phosphate libre soit sous forme d'organophosphate (ester de phosphate). Sous forme d'ion libre, le phosphate est appelé phosphate inorganique et est noté Pi. Le Pi en biologie consiste en une mixture d'ions HPO_4^{2-} et $H_2PO_4^-$. Les organophosphates sont des composés organiques constitués de phosphate. Le Pi

peut être obtenu par hydrolyse des organophosphates tels que l'ADP, de l'ATP, ainsi que du PPi ou des polyPi. Lors de l'hydrolyse, les liens phosphoanhydres présents dans les molécules d'ADP, d'ATP ou de polyPi une énorme quantité d'énergie est relâchée, ce qui donne au phosphate un rôle vital dans tous les organismes vivants. L'ajout et le retrait de phosphate d'une molécule constituent donc un élément clé dans la vie d'une cellule et jouent un rôle important dans les processus métaboliques. Les enzymes permettant la phosphorylation et la déphosphorylation d'un composé sont appelées kinases et phosphatases respectivement.

En bactériologie, le phosphate est un élément essentiel. Il est le cinquième élément le plus présent dans la bactérie après le carbone, l'oxygène, l'azote et l'hydrogène. Il représente 3 % du poids sec d'une cellule bactérienne (Figure 7) (Kjell Magne Fagerbakke, 1966).

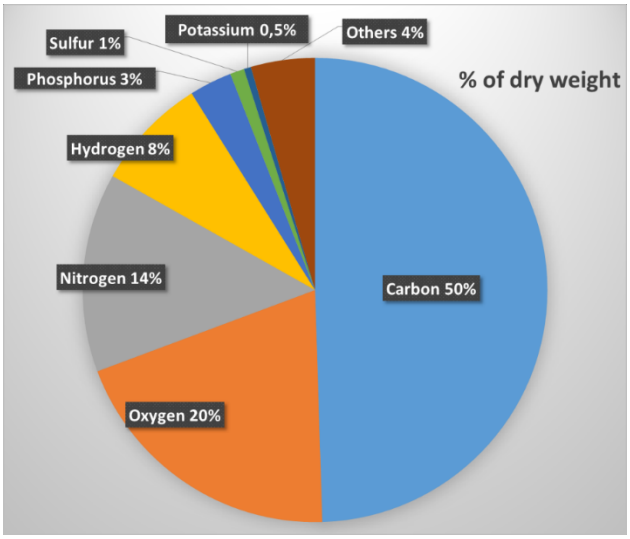

Figure 7. Représentation des principaux éléments composants des cellules bactériennes classés en fonction de leur poids sec. (Adapté de Fagerbakke *et al.*, 1996).

Chez les bactéries, le phosphate se retrouve dans la composition de diverses molécules telles que les lipides membranaires (phospholipides), les acides nucléiques (ADN et ARN) et les sucres complexes comme les LPS. Ajouter lors de modifications post-traductionnelles, le phosphate entre aussi dans la composition des protéines. De plus, toute la production d'énergie de la cellule est basée sur l'hydrolyse de sa liaison avec l'ATP ou avec d'autres nucléotides. Le phosphate participe aussi aux activités biochimiques des protéines et aux cascades signalétiques de nombreuses voies métaboliques en phosphorylant des acides aminés spécifiques tels que

l'histidine, l'aspartate, la sérine, la thréonine et la tyrosine.

II.3.1.1 Les différentes sources de phosphates

Pour ajuster le Pi intracellulaire, *E. coli* puise dans les ressources environnementales et peut utiliser trois sources de phosphate : le Pi, les organophosphates (esters de phosphate) et les phosphonates. Les phosphonates font partie de la famille des organophosphates et ont la particularité d'avoir un lien direct carbone-phosphate au lieu du lien carbone-oxygène-phosphate retrouvés chez les organophosphates.

Quelle que soit la source de phosphate (Pi, organophosphate, phosphonate), le phosphate doit premièrement entrer dans la cellule. Une fois à l'intérieur de la cellule, le phosphate non directement métabolisable est alors converti en Pi. Une fois sous forme de Pi, le phosphate est alors ajouté à une molécule d'ADP en passant par une voie du métabolisme central pour être stocker sous forme d'ATP. C'est sous forme d'ATP que le Pi sera alors ajouté aux molécules.

II.3.1.1.1 Le phosphate inorganique

Le Pi est la plus importante source externe de phosphate car il est directement métabolisable et ne nécessite pas d'activité enzymatique pour être extrait. Une fois dans le périplasme, le Pi est transporté par trois types de transporteurs à travers la membrane interne, le système Pst et les transporteurs PitA et PitB. Dans le cytoplasme, la concentration de Pi se situe aux alentours de 10 mM (Rao *et al.*, 1993; Shulman *et al.*, 1979). Au niveau cellulaire, le Pi peut se trouver sous trois formes : beaucoup sous forme de phosphate inorganique (Pi) (10 mM), moins sous forme de pyrophosphate (PPi) (0.5 mM) et une quantité variable sous forme de polyphosphate (polyPi) (entre 0.1 à 50 mM). Il a été montré que les concentrations intracellulaires de Pi variaient très peu au cours de la vie de la cellule bactérienne (Wanner, 1996). En effet, une certaine concentration en Pi doit être maintenue en permanence dans la bactérie et une trop forte concentration en phosphate est toxique pour la cellule (Rice *et al.*, 2009). Les variations les plus importantes de la concentration en Pi dépendent de la glycolyse et lorsque le Pi extra-cellulaire est faible. Lors de la glycolyse, la concentration en Pi intracellulaire diminue. Ceci serait dû au besoin très rapide en Pi pour la fabrication des molécules d'ATP. Chez *E. coli* lorsque la concentration extra-cellulaire en Pi est faible, la

concentration intracellulaire en Pi augmente (Maloney, 1983; Mason *et al.*, 1981; Xavier *et al.*, 1995). Donc la concentration intracellulaire de Pi est contrôlée en permanence pour assurer une concentration en Pi optimale.

II.3.1.1.2 Les organophosphates et les phosphonates

Le Pi métabolisable peut aussi provenir de la dégradation des organophosphates contenus dans l'environnement. La plupart des organophosphates ne disposent pas de système de transport spécifique mais peuvent tout de même servir de source de Pi car après avoir pénétré l'espace périplasmique à l'aide de porines, les ions Pi sont libérés par différentes phosphatases [dont la plus connue est la phosphatase alcaline (PhoA ou Bap)]. L'expression du gène *phoA* est fortement augmentée lors de conditions de carence en phosphate (jusqu'à 1 000 fois) (272). PhoA est une phosphatase très importante pour la cellule puisqu'elle rend disponible le Pi dont la cellule a besoin pour survivre dans des environnements où le phosphate est rare. La découverte de l'augmentation de la synthèse de PhoA lors de carence en phosphate a d'ailleurs lancé les études sur le régulon Pho dans les années 60 (Torriani, 1960; Wanner, 1996). Cependant, certains organophosphates tels que le glycérol-3-phosphate (G3P) ou l'hexose-6-phosphate (H6P) ainsi que les phosphonates sont pris en charge par la cellule car ils disposent de systèmes de transport spécifique inductibles (Wanner, 1996). Pour pouvoir être utilisée comme source de phosphate, le lien carbone-phosphate des phosphonates doit être clivé par des enzymes spécifiques (phosphonatase ou C-P lyase) dont les gènes sont surexprimés en condition de carence en phosphate.

II.3.1.2 Le transport du phosphate

II.3.1.2.1 L'importation du phosphate

II.3.1.2.1.1 Transport à travers la membrane externe

Pour être internalisés dans la cellule, les phosphates sont le plus souvent transportés par une porine de la membrane externe appelée PhoE. PhoE est surexprimée dans des conditions de carence en phosphate. Cette porine permet la diffusion passive dans le périplasme de petites molécules hydrophiles (jusqu'à 600 Da) comme le Pi et les organophosphates (Eppens *et al.*, 1997).

II.3.1.2.1.2 Transport du Pi à travers la membrane interne

Pour internaliser le Pi dans la cellule, *E. coli* dispose de plusieurs transporteurs. Trois d'entre eux, PitA, PitB et PstSCAB, sont essentiels à la croissance lorsque le Pi est la seule source de phosphore (Harris *et al.*, 2001). PitA et PitB (Pi Transporter A et B) sont des transporteurs de faible affinité alors que *pstSCAB* (phosphate system transport) code pour un transporteur de haute affinité qui transporte le Pi extracellulaire lorsque les concentrations sont faibles. Les transporteurs d'organophosphate et du phosphonate, GlpT, UhpT et PhnCDE sont des transporteurs de faible affinité de Pi mais ne sont pas suffisants pour permettre la croissance lorsque le Pi est la seule source de phosphate (Wanner, 1996).

PitA et PitB : les transporteurs de Pi de faible affinité

PitA et PitB sont des transporteurs de Pi de faible affinité. Ils utilisent la force proton-motrice pour permettre l'entrée de complexes métal-Pi neutre dans la cellule (Harris *et al.*, 2001; Hoffer *et al.*, 2001; van Veen *et al.*, 1994). PitA et PitB sont des protéines transmembranaires. Ces protéines homologues sont composées de 499 acides aminés chacune partageant respectivement 80.8 % d'identité et 89.8 % de similarité de séquence (McCleary, 2017). L'expression de *pitA* est positivement régulée par la présence de Zn(II) et lorsque le Pi est limitant, alors que l'expression de *pitB* est réprimée lorsque les cellules sont cultivées dans des conditions de carence en phosphate (Hoffer *et al.*, 2001). PitB pourrait donc jouer un rôle lorsque le Pi est abondant. Parmi les différentes classes de transporteurs, PitA et PitB font partie de la famille des transporteurs de Pi, PiT (Saier *et al.*, 2016). Cette famille de transporteur est aussi bien retrouvée chez les bactéries, chez les archées et chez les eucaryotes. Ceci montre que ces transporteurs de Pi se sont développés tôt dans l'évolution et qu'ils continuent à jouer un rôle important dans tous les domaines du vivant. Une séquence signature commune à tous ces transporteurs a d'ailleurs été identifiée en N-terminal et en C-terminal (McCleary, 2017). Chez l'humain, cette séquence signature est retrouvée dans les protéines PiT1 et PiT2 qui ont des fonctions métaboliques conservées. Cette séquence est aussi retrouvée dans les protéines Pho-4 et Pho89 respectivement chez *Neurospora crassa* et *Saccharomyces cerevisiae* (Bottger and Pedersen, 2005; Dick *et al.*, 2014). Cette famille de protéines comprend à la fois des symporteurs Pi dépendants du Na^+ et H^+. Alors que PiT1, PiT2, Pho-4 et Pho89 sont des transporteurs

dépendants du Na^+, les protéines PitA, PitB et Pht2_1 d'*Arabidopsis thaliana* sont des symporteurs Pi dépendants de H^+ (Daram *et al.*, 1999). Des mutations dans la séquence signature de la protéine PiT2 empêchent le transport de Pi (Bottger and Pedersen, 2011).
De manière surprenante, il a été suggéré que ni PitA, ni PitB ne jouaient de rôle principal dans le transport de Pi mais fonctionneraient plutôt comme transporteur d'ions métalliques (Hsieh and Wanner, 2010). Cependant, compte tenu des homologies entre PitA et PitB et les transporteurs de Pi présents chez d'autres organismes, il semble peu probable qu'ils aient été conservés dans le génome uniquement en tant que transporteurs de cations de métaux divalents, qui ont également leurs propres transporteurs primaires (Patzer and Hantke, 1998). Il est clair que des travaux supplémentaires sont nécessaires pour mieux comprendre les rôles PitA et PitB dans l'homéostasie Pi.

Le système PstSCAB — le transporteur de Pi de haute affinité

Le système PstSCAB est le transporteur de Pi de haute affinité. Il a un K_m^{app} de 0.2 µM Pi et une Vmax de 16 nmol/min (Willsky and Malamy, 1980). En comparaison PitA et PitB ont des K_m^{app} de 1.9 µM et 6 µM Pi avec des Vmax de 58 nmol/min et 67 nmol/min (Harris *et al.*, 2001). Le complexe PstSCAB, aussi appelé Pst, fait partie de la superfamille des transporteurs « ATP binding cassette » (ABC). Cette famille de protéines, retrouvée dans tous les domaines du vivant, regroupe les transporteurs qui hydrolysent l'ATP pour importer ou exporter toute une variété de substrat à travers la membrane interne (Davidson *et al.*, 2008).

PstSCAB est composé d'une protéine périplasmique PstS qui lie le Pi (HPO_4^{2-} et $H_2PO_4^-$), et le présente aux protéines transmembranaire PstC et PstA qui forment un canal (Cox *et al.*, 1988; Cox *et al.*, 1989). La protéine PstB qui agit en dimère, contient le domaine de liaison de l'ATP qui sera hydrolysé, puis relâché fournissant l'énergie nécessaire pour le transport de Pi. Par similarité avec les autres transporteurs ABC, PstSCAB utiliserait un mécanisme de transport qui alterne entre des états de liaison du substrat (le complexe est tourné vers l'extérieur de la cellule) et des états de libération du substrat (le complexe est tourné vers l'intérieur de la cellule) (voir figure 8) (Beis, 2015). Ces changements de conformation sont gouvernés par l'hydrolyse de l'ATP, la libération de l'ADP et la liaison d'une autre molécule d'ATP. Un modèle propose

que lors de la liaison de l'ATP dans PstB, le complexe adopterait une structure orientée vers l'extérieur permettant la libération de Pi par la protéine PstS. Cet événement déclencherait une hydrolyse de l'ATP qui ferait pivoter les composants transmembranaires vers l'intérieur de la cellule, ouvrant ainsi la porte et permettant à Pi d'accéder au cytoplasme. La libération de l'ADP et la reprise d'une nouvelle molécule d'ATP par PstB perpétuerait ainsi le cycle permettant d'augmenter la concentration intracellulaire de Pi (Beis, 2015; Wilkens, 2015).

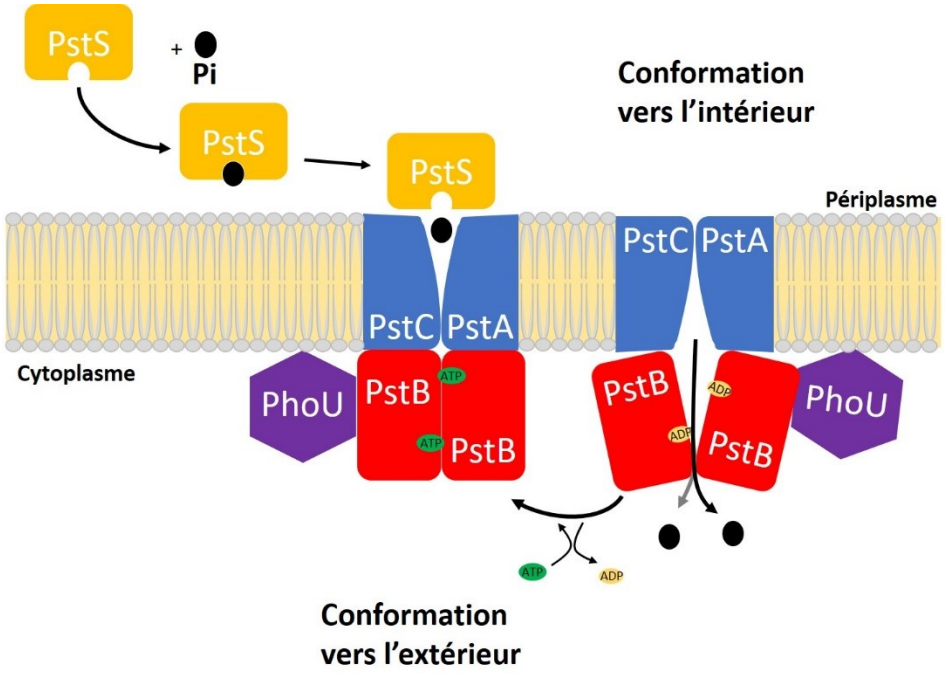

Figure 8. Modèle du mécanisme d'importation du Pi via le transporteur PstSCAB. Selon Mc Cleary *et al.*, (McCleary, 2017). Dans l'espace périplasmique le Pi est fixé à PstS. PstS+Pi est alors recrutée au niveau de la membrane interne par les protéines PstC et PstA. Lorsqu'une molécule d'ATP est liée à la protéine PstB, le complexe PstA et PstC adoptent une conformation orientée vers l'extérieur. En présence de Pi, l'hydrolyse de l'ATP à lieu et provoque un changement de conformation de PstSCAB qui adopte alors une conformation orientée vers l'intérieur. Le Pi transporté est ensuite libéré dans le cytoplasme, ainsi que le Pi provenant de l'hydrolyse de l'ATP. Le transporteur PstSCAB retrouve une conformation orientée vers l'extérieur lorsque PstB lie à nouveau l'ATP. La protéine PhoU intéragit avec la protéine PstB et ralentit le transport lorsque les concentrations de Pi cytoplasmique sont élevées.

L'expression des gènes *pstSCAB* est sous le contrôle du système à deux composants PhoBR décrit ci-dessous. Le promoteur primaire de cet opéron est régulé par la concentration en Pi, et

se trouve en amont du gène *pstS* (Kimura *et al.*, 1989). D'autres promoteurs internes à l'opéron ont été identifiés en amont des gènes *pstC*, *pstB* et *phoU* mais sont plutôt faibles. Cependant ils peuvent jouer un rôle dans le maintien d'un niveau basal de transporteur PstSCAB lorsque le Pi est abondant (Spira *et al.*, 2010).

Les transporteurs spécifiques d'organophosphate et de phosphonate

Le G3P est transporté dans la cellule par 2 transporteurs. GlpT qui est responsable principalement du transport de G3P comme source de carbone. Le système Ugp transporte le G3P comme source de Pi. L'expression de l'opéron *ugpBAECQ* qui code pour un transporteur ABC de G3P et pour une phosphodiesterase, est activé lors de carence en phosphate. Le H6P est transporté par le transporteur UphT. Les phosphonates sont transportés dans la cellule par le transporteur PhnCDE. L'opéron *phnCDEFGHIJKLMNOP* code pour un transporteur de phosphonate et pour un complexe enzymatique, la C-P lyase, permettant de produire un produit phosphoribosyl à partir du phosphonate importé. Tout comme l'opéron *ugpBAECQ,* l'opéron *phnCDEFGHIJKLMNOP* est activé lors de la carence en phosphate.

II.3.1.2.2 Stockage du phosphate

Lorsque le Pi est en excès, le phosphate peut être stocké sous forme de polyphosphate (polyP). Le polyP est une chaine linéaire de Pi de taille variable qui est lié par des liens phosphoanhydrides. La capacité de synthétiser le polyPi par les bactéries est utilisée comme alternative des traitements chimiques pour réduire la concentration en phosphate des eaux usées (Shen and Zhou, 2016). La polymérisation et la dépolymérisation des molécules de polyPi régulent la quantité de Pi intracellulaire disponible. La synthèse de polyPi est effectuée à partir d'ATP par la polyPi kinase qui est codée par le gène *ppk* (Rao *et al.*, 1998). Le polyPi est dégradé par une exopolyphosphatase, codée par le gène *ppx*. Il faut savoir que ce processus est complétement réversible et le polyPi peut servir de source d'énergie pour la cellule puisque sa dégradation libère de l'ATP. En plus de jouer un rôle dans le stockage de Pi et d'énergie, le polyPi participe à de nombreuses autres fonctions, telles que la détoxification des métaux, la signalisation cellulaire, l'expression des gènes de la chaîne respiratoire, la persistance bactérienne et dans les réseaux de réponse au stress (Albi and Serrano, 2016). Il a aussi été

montré récemment que lorsque le Pi extra-cellulaire est très élevé, le polyPi peut même activer *phoB* pendant la phase stationnaire. Une fois activé, le régulateur PhoB inhiberait alors la synthèse de c-di-GMP bloquant ainsi l'expression d'autoinducer-2 (AI-2), menant à l'inhibition de la formation de biofilm (Grillo-Puertas *et al.*, 2016).

II.3.1.2.3 L'exportation du phosphate

En plus d'être impliquées dans l'importation du Pi, les protéines PitA et PitB sont aussi impliquées dans l'exportation du Pi à l'extérieur de la cellule. Trois autres exportateurs de Pi ont été décrits : l'antiport GlpT qui transporte le G3P à l'intérieur de la cellule en expulsant un Pi (Elvin *et al.*, 1985), l'antiport UhpT permettant l'entrée d'H6P en échange de l'export de Pi (Ambudkar *et al.*, 1990) et éventuellement YjbB qui a aussi été montré dans une étude comme potentiel exportateur de Pi (Motomura *et al.*, 2011).

Les mécanismes qui permettent de contrôler les niveaux de Pi intracellulaires sont constitués de multiples protéines de transport qui assurent l'entrée, le métabolisme et la sortie du Pi (Hsieh and Wanner, 2010). Comme mentionné plus haut, l'expression de la plupart de ces systèmes est augmentée en condition de carence en phosphate car ils appartiennent au régulon Pho.

II.3.2 Le régulon Pho

II.3.2.1 Le mécanisme de régulation du régulon Pho

Afin de percevoir et de répondre aux changements environnementaux, les bactéries disposent d'au moins trois mécanismes différents : les mécanismes de senseur de quorum (QS ; « quorum sensing »), des systèmes à un composant et des systèmes à deux composants. Alors que le QS est un processus de communication de cellule à cellule qui dépend de la densité de la population bactérienne, les systèmes à un ou deux composants dépendent du transfert d'un groupement phosphate entre différentes protéines en réponse à un stimulus. Les systèmes à deux composants constituent les voies de signalisation les plus courantes chez les bactéries et régulent de nombreux processus cellulaires importants allant du développement cellulaire à la virulence, en passant par la motilité et le métabolisme. La plupart des espèces possèdent entre 10 et 20

systèmes à deux composants différents (Capra and Laub, 2012; Stock *et al.*, 2000). Le plus souvent, ils sont composés d'un senseur inséré dans la membrane interne et d'un régulateur de réponse situé dans le cytoplasme (Gao and Stock, 2009). Une réaction de phospho-transfert permet de transmettre le signal entre le senseur et le régulateur. Les régulateurs de réponse sont le plus souvent des facteurs de transcription qui interagissent avec l'ADN pour le recrutement de l'ARN polymérase (Galperin, 2010).

Chez *E. coli*, en réponse à la réduction de la concentration en Pi, l'expression des gènes du régulon Pho est contrôlée par le système à deux composants, PhoB et PhoR. PhoR est le senseur et PhoB est le régulateur de réponse.

II.3.2.1.1 Généralité

Par définition un régulon est un groupe de gènes soumis au même mécanisme de régulation. Donc le régulon Pho rassemble les gènes nécessaires au métabolisme du phosphate. En réponse à la diminution du Pi extra-cellulaire, le système de transduction du signal PhoBR s'active pour contrôler l'expression des gènes du régulon Pho. PhoBR est un système à deux composants constitué de l'histidine kinase PhoR et du régulateur transcriptionnel PhoB (Hsieh and Wanner, 2010; Santos-Beneit, 2015). L'activation de ce système repose sur le transfert d'un groupement phosphoryle de la protéine PhoR au régulateur PhoB, ce qui entraîne l'activation de PhoB qui peut alors se lier à l'ADN et moduler l'expression de gènes nécessaires pour augmenter le niveau d'affinité pour le Pi (ex : augmentation de l'expression du transporteur de Pi de haute affinité PstSCAB) et pour utiliser d'autres sources de phosphate (Bachhawat *et al.*, 2005; Makino *et al.*, 1993; Makino *et al.*, 1986; McCleary, 1996). À ce jour 31 gènes ont été décrits comme étant positivement régulés par PhoB. Ces gènes sont appelés le régulon Pho et incluent notamment *phoA*, *pstSCAB*, *phoB* et *phoR* (Hsieh and Wanner, 2010). Les membres du régulon Pho impliqués dans l'utilisation de sources alternatives de phosphate sont l'*ugpBAECQ* et le *phnCDEFGHIJKLMNOP*. L'expression de ces gènes est réprimée lorsque le Pi est en concentration non limitante dans l'environnement. De plus certains gènes sans rapport direct avec le métabolisme du phosphate ont été identifiés.

Lorsque la concentration extracellulaire en Pi est limitante, l'activation du système

PhoBR permet donc de maintenir une concentration intracellulaire en Pi suffisante pour assurer le bon fonctionnement de la cellule et sa survie. La concentration seuil de Pi causant l'activation du régulon Pho est estimée à 4 µM (Wanner, 1996). À cette concentration, c'est le système Pst qui assure le transport Pi dans la cellule. Lorsque la concentration en Pi est suffisante, un mécanisme de rétrocontrôle du système permet de réprimer en permanence le régulon Pho. Une trop forte concentration intracellulaire de Pi est toxique pour la cellule. En effet des mutations dans le gène *phoU*, cinquième gène de l'opéron *pstSCAB-phoU* dont la fonction est de contrôler l'activité du transporteur PstSCAB (Steed and Wanner, 1993; Surin *et al.*, 1985), provoquent un grave défaut de croissance. Ce défaut de croissance serait dû à une accumulation toxique de Pi dans la cellule (Haldimann *et al.*, 1998; Rice *et al.*, 2009; Steed and Wanner, 1993). Conjointement avec PstSCAB-PhoU, PhoBR veille donc à ce que la concentration de Pi intracellulaire soit toujours constante.

II.3.2.1.2 L'histidine kinase PhoR

PhoR est une protéine bifonctionnelle avec une activité histidine kinase et une activité phosphatase. Lorsque le Pi devient limitant dans l'environnement, PhoR s'autophosphoryle sur un résidu histidine avant de le transférer sur le régulateur de réponse PhoB. En revanche dans des conditions riches en Pi, PhoR déphosphoryle PhoB (Carmany *et al.*, 2003; Makino *et al.*, 1989). PhoR est une protéine membranaire homodimérique constituée d'une région membranaire, d'une région cytoplasmique positivement chargée et d'une petite région périplasmique. La partie cytoplasmique est constituée notamment d'un domaine Per-ARNt-Sim (PAS), d'un domaine de dimérisation/histidine phosphorylation appelé DHp, d'un domaine de liaison et de catalyse de l'ATP, noté CA en C-terminal (Figure 9) (Carmany *et al.*, 2003; Etzkorn *et al.*, 2008). Le domaine CA permet de transférer le groupe phosphoryle de l'ATP au résidu histidine du domaine DHp. Les domaines PAS sont des domaines permettant de percevoir le signal. Cependant, PhoR ne contient pas de domaine sensoriel périplasmique car sa partie périplasmique serait trop courte. Il est donc supposé que le domaine PAS cytoplasmique soit capable de détecter un signal inconnu dans le cytoplasme qui refléterait les concentrations de Pi extracellulaire.

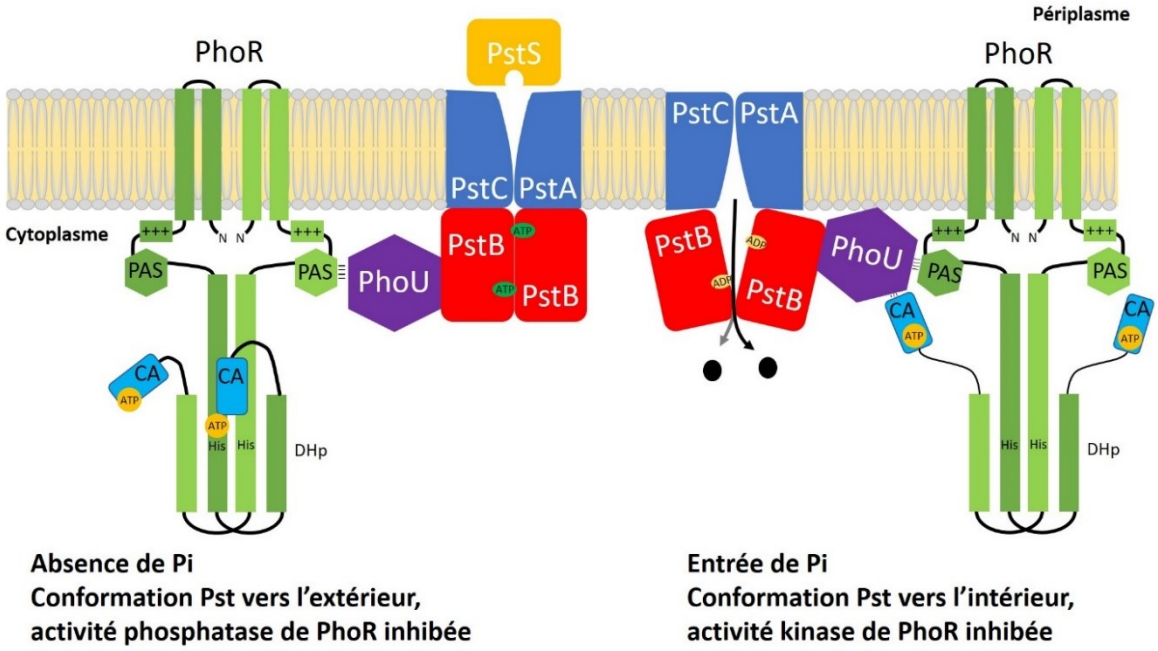

Figure 9. Modèle d'activation de la protéine PhoR et son interaction avec PhoU. Comme montré plus haut, dans le modèle de McCleary, l'interaction entre le transporteur Pst et la protéine change d'orientation lors du transport du Pi. Cette interaction serait médiée par la protéine PhoU. Lorsque le complexe Pst est orienté vers l'extérieur, l'interaction entre PhoU et PhoR, favorise l'activité kinase de PhoR, ce qui permet au domaine CA de se lier à l'ATP et d'autophosphoryler son domaine DHp. Lorsque Pst est tourné vers l'intérieur, PhoU interagit avec PhoR favorisant l'activité phosphatase [Selon Mc Cleary *et al.*, (McCleary, 2017)].

II.3.2.1.3 Le régulateur de réponse PhoB

PhoB est constitué d'un domaine récepteur en N-terminal et d'un domaine de liaison à l'ADN en C-terminal. Le domaine récepteur contient le site de phosphorylation (Asp53) qui permet d'initier l'activation de PhoB. Le domaine récepteur contient aussi les résidus catalytiques nécessaires pour le transfert du groupement phosphoryle de PhoR (McCleary, 1996). En C-terminal, le domaine de liaison à l'ADN a une structure en hélice ailée permettant la fixation de PhoB à l'ADN (Blanco *et al.*, 2002). Lorsque PhoB devient phosphorylé, il forme un dimère qui se lie aux séquences d'ADN, lesquelles appelées boîtes Pho (Blanco *et al.*, 2012; Blanco *et al.*, 2002; Makino *et al.*, 1988; McCleary, 1996). Ces courtes séquences sont situées en amont des gènes du régulon Pho afin de recruter l'ARN polymérase et d'initier la transcription (Blanco *et al.*, 2012; Canals *et al.*, 2012). Cette séquence remplace la région -35 du promoteur et se termine 10 paires de bases (pb) en amont de la région -10 du promoteur. Chez *E. coli* la

séquence consensus de la boîte est constituée de deux séquences répétées de 11 pb séparées par une région AT-riche de 4 pb (Blanco *et al.*, 2002). Chaque région de 11 pb étant reconnue par une sous-unité du dimère de PhoB activé. Ainsi une ou plusieurs boîtes Pho peuvent être retrouvées en amont des gènes du Pho régulon. La présence de plusieurs boîtes Pho en amont d'un gène permettrait d'augmenter l'affinité de PhoB par rapport aux gènes avec des boîtes Pho moins conservées (Blanco *et al.*, 2012; Blanco *et al.*, 2002).

En plus de son rôle d'activateur, PhoB peut jouer le rôle de répresseur. Il a été montré que la présence de boîtes Pho de faible affinité permettrait la fixation de PhoB lorsque celui-ci est en abondance, rendant le promoteur de forte affinité moins accessible. Ce mécanisme permet d'expliquer la répression des gènes par *phoB*.

II.3.2.1.4 Le transducteur de signal Pst

En plus de jouer un rôle dans le transport du Pi, le transporteur Pst joue aussi un rôle dans la transduction du signal. Il a été supposé que Pst jouerait le rôle de senseur pour détecter le Pi extra-cellulaire compensant l'absence de domaine senseur de la protéine PhoR. En effet en absence de Pst, les gènes du régulon Pho sont surexprimés (Wanner, 1996). L'activité biochimique par défaut de PhoR est une autokinase et le rôle de Pst est de réguler négativement cette activité et de stimuler son activité phosphatase de PhoB. Le mécanisme par lequel Pst participe à la transduction du signal est inconnu mais il est suggéré que PhoR pourrait détecter l'activité de transport de Pst (Peterson *et al.*, 2005). Dans ce cas, ce n'est pas la concentration intracellulaire en Pi qui est détectée, mais l'activité du transporteur.

II.3.2.1.4 Le rôle médiateur de la protéine PhoU

La protéine PhoU participe aussi à la transduction de signal du Pi (Peterson *et al.*, 2005). En effet, la délétion ou une mutation de PhoU activent constitutivement l'activité autokinase de PhoR, menant à la surexpression des gènes du régulon Pho. Les mutants *phoU* présentent une faible croissance et accumulent très souvent des mutations compensatoires dans les gènes *phoR*, *phoB* ou *pstSCAB* (Haldimann *et al.*, 1998; Peterson *et al.*, 2005; Rice *et al.*, 2009). PhoU est une protéine membranaire périphérique qui module le transport de Pi par le complexe PstSCAB. Lorsque le Pi est abondant, PhoU agit comme un frein pour empêcher une trop grande

importation de Pi (Rice *et al.*, 2009).

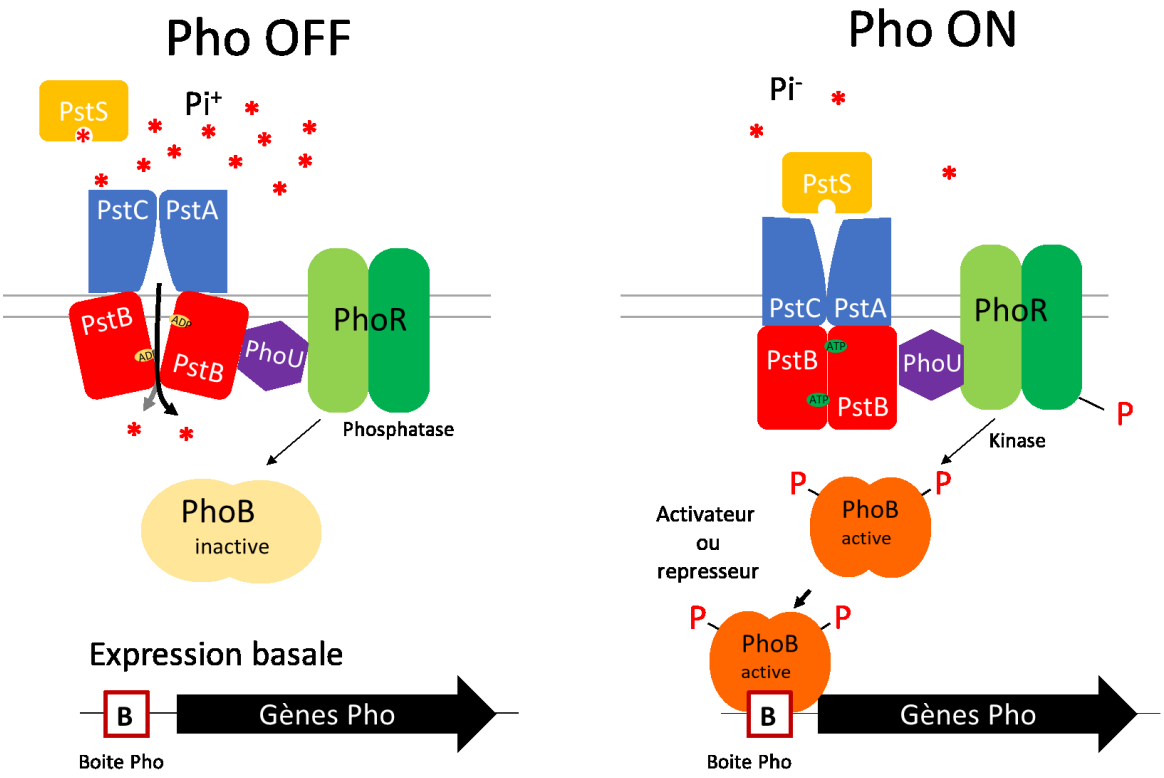

Figure 10. Activation des gènes du régulon Pho. Quand la concentration extracellulaire en Pi est > 4 µM, le régulateur PhoB est inactif. Lorsque la concentration de Pi extracellulaire décroit (<4 µM), l'histidine kinase de PhoR s'autophosphoryle et phosphoryle PhoB. Une fois activé, PhoB se lie aux boîtes Pho situées en amont des gènes du régulon Pho et module leur expression. PhoB ou PhoR peuvent aussi agir de manière indirecte sur l'expression des gènes en jouant sur d'autres régulateurs. Une mutation des gènes du transporteur Pst mène à une expression constitutive des gènes du régulon Pho, de manière indépendante de la disponibilité en Pi de l'environnement. (Abréviations : Pi, phosphate inorganique; P, phosphorylé).

Deux modèles ont été proposés pour expliquer la participation de PhoU dans la voie de transduction du signal. Soit PhoU joue le rôle de médiateur dans le complexe entre le transporteur PstSCAB et PhoR (Wanner, 1996), soit il produit un messager soluble reconnu par les domaines PAS cytoplasmiques de PhoR (Hoffer and Tommassen, 2001; Rao *et al.*, 1986). De nouveaux éléments semblent supporter le modèle proposé par Wanner. En effet, il a été montré que PhoU interagit à la fois avec PstB et avec PhoR (Gardner *et al.*, 2014). Il a aussi été montré que la protéine PhoU interagit avec les domaines PAS et CA de la protéine PhoR. Ainsi,

en fonction de la concentration en Pi, le changement de conformation du complexe PstSCAB (tourné vers l'intérieur ou vers l'extérieur comme montré dans la figure 8) modifierait l'interaction de la protéine PhoU avec les domaines PAS et CA de la protéine PhoR modulant son activité kinase et phosphatase. Dans ce modèle, lorsque la concentration en Pi est faible, le transporteur Pst n'importe plus de Pi de manière active et est bloqué dans sa conformation vers l'extérieur. Dans cette conformation, PhoU est recrutée par le complexe PstSCAB, libérant les domaines PAS et CA de PhoR qui s'autophosphoryle et active PhoB (Figure 10). Lorsque le Pi est abondant, Pst prend sa conformation orientée vers l'intérieur, changeant son interaction avec PhoU de telle manière que le domaine CA de PhoR est encombré, stimulant l'activité phosphatase de PhoR (Vuppada *et al.*, 2018) (Figure 10).

II.3.2.2 Le régulon Pho et la virulence

En plus des gènes déjà identifiés comme étant directement contrôlés par PhoB (Baek and Lee, 2006; Hsieh and Wanner, 2010), plusieurs études utilisant des gels de polyacrylamide 2D ou des méthodes de bio-informatique ont suggéré que près de 400 protéines pourraient être contrôlées directement ou indirectement par PhoB (VanBogelen *et al.*, 1996; Yuan *et al.*, 2006). Parmi ces gènes régulés à la fois positivement et négativement, on retrouve des gènes codant pour des facteurs de virulence de différentes bactéries pathogènes incluant *Vibrio cholerae, Agrobacterium tumefaciens*, *Bacillus anthracis, Pseudomonas aeruginosa* et différents pathotypes de *E. coli.*

Chez *V. cholerae*, il a été identifié qu'en condition de carence en phosphate, l'activation de PhoB mène à une diminution de la production de deux facteurs de virulence : la toxine cholérique (CT) et le pili corégulé par la toxine (TCP). Cette diminution est reliée à la fixation de PhoB sur un régulateur de la cascade d'activation de CT et du TCP. De plus, l'activation constitutive de PhoB entraîne une diminution de la capacité de *V. cholerae* à coloniser l'intestin de souris infectées par un mutant Δ*pst*. Toutefois, dans les conditions normales, le Pi n'est pas un facteur limitant de l'intestin, la production de CT et TCP ne devrait donc pas être affectée (Pratt *et al.*, 2010).

À l'inverse chez *P. aeruginosa*, la carence en phosphate s'accompagne d'une

augmentation de la virulence de cette bactérie opportuniste (Bains *et al.*, 2012; Rico-Jimenez *et al.*, 2016). En effet, la production de la toxine pyocyanine est augmentée et dépendante de l'activation de PhoB. Comme pour CT et TCP de chez *V. cholerae*, la régulation de PhoB n'est pas directe mais augmente l'expression du gène *rhlR* qui stimule à son tour l'expression du gène codant pour la pyocyanine (Jensen *et al.*, 2006). Il a été noté qu'après une opération chirurgicale, la concentration en Pi de l'intestin avait tendance à diminuer fortement jusqu'à atteindre des niveaux suffisants pour déclencher l'expression de facteurs de virulence de *P. aeruginosa*. Ainsi, l'administration postopératoire de Pi permettrait de contenir la colonisation des agents pathogènes (Long *et al.*, 2008). Aussi, l'hypophosphatémie sévère lors de septicémie est devenue un facteur prédictif de la mortalité (Shor *et al.*, 2006).

L'augmentation de la virulence induite par une carence en Pi a également été observée chez *B. anthracis* (Aggarwal *et al.*, 2015). Chez *B. anthracis* la diminution de la concentration en Pi induit le système à deux composants PhoPR. Il a été montré que le régulateur PhoP participe à la pathogénicité de la bactérie et pourrait donc constituer une cible potentielle contre l'anthrax (Aggarwal *et al.*, 2017).

La production de la capsule est un facteur de virulence important dans la pathogénicité de *Streptococcus pneumoniae*. La perte de la capsule entraîne la perte de la virulence de cette bactérie pathogène (Stollerman and Dale, 2008). Une étude a montré que *S. pneumoniae* doit maintenir un transport élevé de Pi pour assurer la synthèse de sa capsule (Zheng *et al.*, 2016). Ce résultat relie directement l'induction du régulon Pho à la virulence de cette bactérie pathogène.

Chez les *E. coli* pathogènes extraintestinaux (ExPEC), l'expression constitutive du régulon Pho mène à une diminution de la virulence (Crepin *et al.*, 2012; Daigle *et al.*, 1995; Lamarche and Harel, 2010). En effet, chez les souches de sérotypes O115 et O78, il a été montré à partir de mutants Δ*pst* respectifs que l'activation du régulon Pho menait *in vivo* à une atténuation de la virulence et de la capacité à causer des lésions extra-intestinales (Lamarche *et al.*, 2005; Ngeleka *et al.*, 1992). Chez la souche UPEC CFT073 (souche de référence UPEC), il a été montré que l'activation de PhoB, diminuait la production du fimbriae de type 1 et réduisait la colonisation de la vessie chez les souris (Crepin et al., 2012).

Chez les *E. coli* pathogènes de l'intestin (InPEC), le régulon Pho est impliqué dans la modulation de la virulence des EPEC et des EHEC. Chez les EPEC, la délétion du système Pst s'accompagne par une diminution de l'adhésion aux cellules épithéliales. Chez les EHEC, l'activation de PhoB module directement l'expression des gènes du LEE ainsi que des protéines sécrétées par le SST3 (Chekabab *et al.*, 2014). De plus, dans des conditions de carence en Pi, il a été montré *in vitro* que la production de la toxine Stx2 par la souche EHEC O157:H7 EDL933 augmente. Aussi, PhoB est capable de fixer *in vitro* la région promotrice des gènes du LEE et de Stx (Chekabab *et al.*, 2014). Une augmentation de la production des facteurs de virulence par les EHEC O157:H7 dans des conditions pauvres en phosphate pourrait leur donner un avantage sélectif à ce sérotype dans les environnements aquatiques pauvres en éléments nutritifs (Chekabab *et al.*, 2012). L'analyse transcriptomique montre qu'en plus de moduler l'expression de certains facteurs de virulence, l'activation de PhoB en réponse à la carence en Pi permet aussi d'induire un remodelage du métabolisme général essentiel à la survie des EHEC. Il semble que PhoB pourrait aussi moduler l'expression de nombreux gènes associés à la formation de biofilm permettant ainsi aux EHEC O157:H7 d'augmenter leur persistance dans l'environnement.

II.3.2.3 Le régulon Pho et la formation de biofilm

Chez certaines bactéries l'activation du régulon Pho est associée à une augmentation ou à une diminution de la formation de biofilm. Par exemple, il a été montré que PhoB pouvait jouer un rôle sur la concentration intracellulaire en di-guanosine monophosphate cyclique (di-GMP-c), un second messager connu pour son effet sur les biofilms (Haddad *et al.*, 2009; Pratt *et al.*, 2009). Une augmentation due la concentration en di-GMP-c intracellulaire permet la transition vers le mode de vie biofilm (Römling *et al.*, 2013). La synthèse et la dégradation du di-GMP-c sont assurées respectivement par les diguanylates cyclases (DGC) et les phosphodiesterases (PDE). En se liant à des domaines spécifiques de molécules régulatrices, le di-GMP-c contrôle l'expression de gènes en rapport avec le biofilm (Schirmer and Jenal, 2009).

Plusieurs études ont décrit l'effet du Pi sur la formation de biofilm chez *Pseudomonas*. Chez *P. aeruginosa*, l'activation du régulon Pho inhibe la formation de biofilm. Il a été montré que cette inhibition était en partie due à la modulation de la concentration en di-GMP-c à la suite

de l'activation d'une PDE. Cependant dans la souche PA14, cette inhibition est indépendante de la disponibilité de phosphate inorganique alors que chez la souche PAO1, l'inhibition de la formation de biofilm en condition faible en Pi ne semble pas due à l'activation du régulon Pho. En effet en absence de PhoB, le phénotype de formation de biofilm n'est pas modifié (Haddad *et al.*, 2009). Ces résultats montrent que le régulon Pho et la concentration en phosphate peuvent influencer indépendamment la formation de biofilm de *P. aeruginosa*. Monds *et al.* ont rapporté que chez *P. fluorescens*, l'activation de PhoB induit l'expression d'une PDE (RapA), qui abaisse la concentration en c-di-GMP. L'activation de RapA inhibe la sécrétion de la protéine d'adhésion LapA menant à une réduction de la formation de biofilm de *P. fluorescens*. Il a aussi été montré que le régulon Pho était impliqué dans la diminution de la formation de biofilm de *P. aureofaciens* (Monds *et al.*, 2001). Ces études ont mis en évidence le rôle de régulateur du Pi sur la formation de biofilm. Chez *P. aeruginosa* il a aussi été montré que PstS, la protéine qui lie le Pi extracellulaire, jouait un rôle dans la formation de biofilm. Un mutant Δ*pstS* a une formation de biofilm diminuée par rapport à la souche sauvage. De manière intéressante la fonction de PstS dans la formation de biofilm est indépendante de la prise en charge du phosphate de PstS. Elle dépend d'une extension de 15 résidus en N-terminal formant une boucle dont la présence est requise pour que la formation de biofilm soit optimale. Cette boucle n'est pas nécessaire pour activer le régulon Pho (Neznansky *et al.*, 2014).

Chez *V. cholerae*, l'opéron *acgAB* qui code pour une PDE (AcgA) et pour une DGC (AcgB) est indirectement induit par PhoB. Cette surexpression s'accompagne d'une augmentation de la motilité et une diminution de la formation de biofilm. Il semble que, dans les cas de faible Pi, l'activité PDE de AcgA ait priorité sur l'activité DGC de AcgB, ce qui mène à une diminution de la concentration en di-GMP-c (Pratt *et al.*, 2009).

L'effet du phosphate sur la formation de biofilm a été aussi montré chez les bactéries Gram+. Il a été montré que chez *B. anthracis* la formation de biofilm est inhibée dans un milieu pauvre en Pi (Aggarwal *et al.*, 2015).

En revanche, chez *Agrobacterium tumefaciens*, il a été montré que PhoB activait la formation de biofilm dans des conditions pauvres en Pi. Ce phénotype d'augmentation a été relié à des modifications de la surface de la bactérie, sans toutefois pouvoir identifier les

protéines responsables de ces changements (Danhorn *et al.*, 2004).

Chez *E. coli*, le rôle de PhoB dans la formation de biofilm dans des conditions de carence en phosphate n'a pas été étudié. Il a tout de même été montré chez *E. coli* K-12 qu'en phase stationnaire dans un milieu très riche en Pi, l'accumulation de polyPi inhibait la formation de biofilm. Cette inhibition est due à la suractivation de PhoBR qui est phosphorylé à cause du surplus de phosphate dans le milieu (Grillo-Puertas *et al.*, 2016). Dans ces conditions, PhoBR suractivé participe au maintien de polyPi dans la cellule, ce qui inhibe la formation de biofilm.

Contexte de recherche et objectifs du projet

Les STEC, et parmi eux les EHEC O157:H7, peuvent être à l'origine de toxi-infections alimentaires collectives induisant des colites hémorragiques et des SHU parfois mortels. Dans la nature le réservoir principal des STEC est le tractus intestinal des bovins. Excrétés dans les fèces, les STEC se propagent dans l'environnement en contaminant les produits issus de l'élevage bovin (viande, purins, lait, cuir). Une fois dans l'environnement les STEC adaptent leur style de vie pour pouvoir y survivre entre autres en formant des biofilms. Pour cela, les systèmes de régulation de l'expression des gènes sont essentiels et permettent aux bactéries de s'adapter au milieu. Ces systèmes de régulation de l'expression des gènes sont le plus souvent codés par des gènes conservés qui participent aussi au métabolisme bactérien, à la physiologie, à la virulence et à la réponse aux changements de l'environnement. Chez les STEC, la formation de biofilm complique le contrôle de la contamination dans les chaînes de production alimentaire. De plus, la formation de biofilms par les souches non-O157 est moins bien caractérisée que chez les souches O157. De plus, les bactéries formant des biofilms ont des caractéristiques différentes des bactéries planctoniques, de nouveaux outils et de nouvelles approches pour la prévention, le traitement et le diagnostic de ces bactéries pathogènes sont requis pour améliorer la sécurité alimentaire.

Problématique

Les facteurs permettant aux STEC de survivre dans l'environnement sous forme de biofilm sont peu connus et il est important de mieux les identifier et de mieux les caractériser.

Le rôle du régulateur PhoB et les facteurs impliqués dans la formation de biofilm de la souche EHEC O157:H7, EDL933 lors d'une carence en phosphate ne sont pas connus.

Hypothèse

L'hypothèse de ce travail de thèse est que la formation de biofilm contribue à la survie des STEC dans l'environnement. Pour cela, la bactérie perçoit et répond à son environnement en induisant l'expression de gènes codant pour des facteurs d'adhésion.

Objectifs

Pour tester cette hypothèse, nous avons défini deux objectifs généraux :

1 Évaluation et caractérisation des biofilms formés par une collection d'isolats STEC associés à des cas cliniques humain et de sérotype O157 et non-O157 dans des conditions proches de celles retrouvées dans l'environnement (Articles de recherches 1 et annexes 1).

a. Criblage de la formation de biofilm d'une collection de souches de STEC associées à des cas cliniques humains.
b. Recherche de facteurs associés à la production de biofilm.
   - Phénotypique : production de curli, cellulose, fimbriae de type 1.
   - Génotypique : recherche de gènes codant pour des fimbriae et des autotransporteurs.
c. Caractérisation de la matrice par marquages des constituants de la matrice, traitements enzymatiques et traitements aux désinfectants.

2 Étudier le rôle du régulateur PhoB dans la formation de biofilm de la souche O157:H7 EDL933 lors de carence en phosphate et identifier les membres du régulon Pho impliqués (Articles de recherches 2 et 3).

a. Evaluer la formation de biofilm de la souche O157:H7 EDL933 dans un milieu pauvre en phosphate (activation physiologique de PhoB) et du mutant Δ*pst* dans un milieu riche en phosphate (activation constitutive de PhoB).
b. Recherche de gènes codant pour des facteurs importants pour la formation de biofilm :
   - Criblage d'une banque de mutants à partir du mutant Δ*pst*.
   - Analyse de résultats de transcriptomique.
c. Vérification du contrôle de l'expression de ces gènes par PhoB (recherche de boîte Pho) et leur implication dans la formation de biofilm (création de mutants).

III. Section III- Caractérisation des biofilms formés par les STEC

III.1 Article de recherche 1: Le potentiel de formation de biofilm des isolats de *Escherichia coli* producteurs de Shiga-toxines associés avec des infections humaines.

Philippe Vogeleer, Yannick D.N. Tremblay, Grégory Jubelin, Mario Jacques and Josée Harel

Objectif de l'article: Les objectifs de cet article étaient de caractériser la formation de biofilms d'une collection de souches STEC regroupant les sérotypes les plus importants en santé humaine (O157 et non-O157), et d'identifier les facteurs qui contribuent à la formation de biofilm.

Contribution de l'étudiant : En tant que premier auteur de cet article, j'ai effectué la totalité des expérimentations, analysé l'ensemble des résultats et écrit le manuscrit. Pour ce papier Yannick DN Tremblay m'a aidé à la réflexion et à l'organisation de mes résultats. J'ai également coordonné et assemblé les corrections de mes collaborateurs et soumis le manuscrit au journal « Applied and Environmental Microbiology ».

Article publié dans le journal « Applied and Environmental Microbiology », Décembre 2015

Article de recherche 1: Biofilm-Forming Abilities of Shiga Toxin-Producing *Escherichia coli* Isolates Associated with Human Infections.

Running title: Environmental persistence of STEC

Philippe Vogeleer[1], Yannick D.N. Tremblay[1], Grégory Jubelin[2], Mario Jacques[1] and Josée Harel[1]*

[1] Groupe de Recherche sur les Maladies Infectieuses du Porc, Centre de Recherche d'Infectiologie Porcine et Avicole, Département de pathologie et microbiologie, Faculté de médecine vétérinaire, Université de Montréal, C. P. 5000, St-Hyacinthe, Québec, Canada J2S 7C6

[2] INRA, UR454 Unité de Microbiologie, Saint-Genès-Champanelle, France.

*Corresponding author:

Josée Harel,

Université de Montréal,

Faculté de médecine vétérinaire,

3200 Sicotte,

St-Hyacinthe, QC, J2S 7C6, Canada.

josee.harel@umontreal.ca

ABSTRACT

Forming biofilms may be a survival strategy of Shiga toxin-producing *Escherichia coli* to enable it to persist in the environment and the food industry. Here, we evaluate and characterize the biofilm-forming ability of 39 isolates of Shiga toxin-producing *Escherichia coli* isolates recovered from human infection and belonging to seropathotypes A, B, or C. The presence and/or production of biofilm factors such as curli, cellulose, autotransporter, and fimbriae were investigated. The polymeric matrix of these biofilms was analyzed by confocal microscopy and by enzymatic digestion. Cell viability and matrix integrity were examined after sanitizer treatments. Isolates of the seropathotype A (O157:H7 and O157:NM), which have the highest relative incidence of human infection, had a greater ability to form biofilms than isolates of seropathotype B or C. Seropathotype A isolates were unique in their ability to produce cellulose and poly-*N*-acetylglucosamine. The integrity of the biofilms was dependent on proteins. Two autotransporter genes, *ehaB* and *espP*, and two fimbrial genes, *z1538* and *lpf2*, were identified as potential genetic determinants for biofilm formation. Interestingly, the ability of several isolates from seropathotype A to form biofilms was associated with their ability to agglutinate yeast in a mannose-independent manner. We consider this an unidentified biofilm-associated factor produced by those isolates. Treatment with sanitizers reduced the viability of Shiga toxin-producing *Escherichia coli* but did not completely remove the biofilm matrix. Overall, our data indicate that biofilm formation could contribute to the persistence of Shiga toxin-producing *Escherichia coli* and specifically seropathotype A isolates in the environment.

INTRODUCTION

Shiga toxin-producing *Escherichia coli* (STEC) strains, including enterohemorrhagic *E. coli* (EHEC), are food-borne and waterborne human enteric pathogens responsible for infections. They are associated with important public health concerns in developed countries. Symptoms associated with STEC infections range from abdominal cramps and bloody diarrhea to postinfectious complications, such as hemolytic-uremic syndrome (HUS). HUS, a life-threatening complication of STEC infections, is a consequence of Shiga toxin production. According to the Public Health Agency of Canada (PHAC), more than 30,000 cases of STEC infections occur each year in Canada (1). Environmentally, the main reservoir for STEC is cattle. Transmission of STEC to humans typically is associated with the consumption of contaminated food such as undercooked beef, fresh produce, unpasteurized milk, or contaminated drinking water (2), but these pathogens also can be transmitted from person to person or via direct contact with animals or their feces.

The 2003 Karmali seropathotype model classifies STEC into seropathotypes based on their reported incidence in human disease, outbreaks, and/or association with the development of severe symptoms in humans (3). Serotypes frequently responsible for hemorrhagic colitis (HC) and HUS, O157:H7 and O157:NM, are assigned to seropathotype A. Seropathotype B strains are associated with outbreaks and HUS, but less commonly than those of seropathotype A, and they include serotypes O26:H11, O103:H2, O111:NM, O121:H19, O45:H2, and O145:NM. These serotypes belong to six serogroups (O26, O45, O103, O111, O121, and O145) that have been described by the CDC as the cause of most non-O157 STEC infections and are known as the “Big six”(4). Seropathotype C serotypes are associated with sporadic HUS cases but no epidemics. The serotypes in group C are O91:H21, O104:H21, O113:H21, O5:NM, O121:NM, and O165:H25. Seropathotype D serotypes are associated with diarrhea but not with outbreaks or HUS cases. Seropathotype E serotypes include STEC serotypes with no reported implication in human infection (3).

Biofilms are multicellular communities of bacteria that attach to abiotic or biotic surfaces and produce an extracellular polymeric matrix (5). The biofilm-forming ability of STEC has been investigated under different conditions, using different STEC isolates representing different

serotypes and origins (6,–8). Biofilm formation by STEC may be regarded as a survival strategy for this bacterium (9,–12). Indeed, bacteria within a biofilm are protected against several stresses, such as a nutrient-limited environment and sanitizers (13). This biofilm-mediated protection against sanitizers impedes contamination control, especially in food-processing plants (7). This allows biofilms to increase their survival and persistence in hostile environments such as water, a nutrient-limited environment, and food-processing plants, an environment where sanitizers are applied (11, 13, 14). In general, studies concerning STEC biofilms highlighted that their formation is heterogeneous and mostly dependent on the strains and the conditions used (7). However, there is limited information about the composition of the STEC biofilm matrix. Moreover, non-O157 isolates continue to gain importance as pathogens of concern (15). Their biofilm-forming abilities were shown to be different from those of O157 isolates (8). This gives importance to characterizing STEC biofilms and to understanding how these bacteria travel through the food supply chain from preharvest to consumer goods. The production of many adhesins has been associated with biofilm formation. Fimbriae such as type 1 fimbriae, curli, long polar fimbriae, and F9 fimbriae have been hypothesized to be required largely during the attachment step (16). The maturation step of STEC biofilm is thought to involve mostly autotransporters such as EhaA, EhaB, Agn43, Cah, and EspP (8, 17–20) and exopolysaccharides such as poly-*N*-acetylglucosamine (PGA), cellulose, and colanic acid (21). We hypothesize that its ability to form biofilms contributes to STEC persistence and that this consequently could influence their incidence. Therefore, the aim of this study was to evaluate and characterize the biofilm-forming ability of STEC isolates recovered from human infection that represent the most important seropathotypes. Furthermore, we investigated the putative link between adhesins or surface molecules/structures and biofilm formation.

We also characterized the composition of matrix and tolerance to sanitizers of the strongest biofilm formers.

MATERIALS AND METHODS

STEC isolates, storage, and culture conditions.

The collection of 39 STEC isolates associated with human infections that represent 14 different serotypes used in this study are described in Table 1 (3, 22,–25). French isolates were provided

by Christine Martin (INRA Clermont-Ferrand Theix), and North American isolates were provided by Mohamed Karmali from the Laboratory for Food-Borne Zoonoses of the Public Health Agency of Canada. Isolates were stored at −80°C in lysogeny broth (LB) containing 15% (vol/vol) glycerol. Each test was performed in triplicate and in three separate experiments. For each experiment, STEC isolates first were streaked onto LB agar and incubated overnight at 37°C.

Static biofilm formation assay.

The biofilm formation assay was performed as previously described (26). Briefly, overnight cultures at 37°C in LB media were diluted (1:100) in 5 ml of M9 medium with glucose (0.4%, wt/vol) and minerals (1.16 mM $MgSO_4$, 2 μM $FeCl_3$, 8 μM $CaCl_2$, and 16 μM $MnCl_2$) and incubated for 24 h at 37°C. These cultures were diluted (1:100) in M9 medium supplemented with glucose and minerals and were inoculated in triplicates into the microtiter plates (Costar 3370; Corning, NY). For all biofilm assays, the biofilm-positive STEC strain EDL 933 (26) and the biofilm-negative STEC isolate BJH-21 were used as positive and negative biofilm controls, respectively. Moreover, wells filled with sterile media were used as the blank value. After a 24-h incubation at 30°C, unattached cells were removed by washing three times with phosphate-buffered saline (PBS; 1.76 mM KH_2PO_4, 10 mM Na_2HPO_4, 137 mM NaCl, 2.7 mM KCl, pH 7.4). Plates were dried at 37°C for 15 min, and biofilms were stained with crystal violet (0.1% [wt/vol]) for 2 min. The crystal violet solution was removed, and the biofilms were washed three times with PBS and then dried at 37°C for 15 min. The stain was released with 150 μl of 80% (vol/vol) ethanol and 20% (vol/vol) acetone. Biofilms were quantified by measuring the absorbance at 595 nm with a microplate reader (Powerwave; BioTek Instruments, Winooski, VT). According to their absorbance, isolates were categorized as strong ($A_{595} > 0.6$), medium ($0.6 > A_{595} > 0.3$), and weak ($0.3 > A_{595} > 0.1$) biofilm formers or as non-biofilm formers ($A_{595} < 0.1$).

Biofilms in the BioFlux flowthrough device.

Growth of biofilms in the BioFlux 200 device (Fluxion Biosciences, South San Francisco, CA) was performed as described before (26). Briefly, *E. coli* cultures were prepared as described

above, and 1 ml from the 24-h culture was pelleted and resuspended in fresh prewarmed (30°C) M9 medium with glucose (0.4%, wt/vol) to an optical density at 600 nm (OD_{600}) of ~1. The microfluidic channels then were inoculated and the plate was incubated for 2 h at 30°C to allow bacteria to bind to the surface. Fresh M9 medium with glucose (0.4%, wt/vol) was added to the input reservoir, and the flow of fresh medium then was initiated at 1.0 dyne/cm^2 for 5 h, followed by a decrease of the flow to 0.5 dyne/cm^2 for an additional 17 h. Once the incubation was completed, biofilms were washed by injecting PBS, stained by injecting crystal violet, and washed by injecting PBS from the input reservoir for 20 min at 0.5 dyne/cm^2. Images of BioFlux biofilms were obtained using an inverted fluorescence microscope (Olympus CKX41; Markham, ON, Canada), a digital camera (Retiga EX; Q Imaging Surrey, BC, Canada), and the software provided with the BioFlux 200 device. Images of biofilms and cell attachment obtained from three independent replicates were analyzed using ImageJ (National Institutes of Health, Bethesda, MD). The thresholds of the 16-bit greyscale images were adjusted to fit the bacterial clusters, and these modified images were analyzed using the "Analyze Particles" function. The percentage of area covered represents the surface of the picture covered by the biofilms or the adhered cells.

CR and calcofluor phenotype assays.

Congo red (CR) or calcofluor white (CF) assays were performed as described previously (27). Briefly, 2 µl of an overnight LB culture grown at 37°C was spotted onto M9 agar supplemented with 0.4% glucose and minerals containing 0.004% (vol/vol) CR and 0.002% (vol/vol) brilliant blue or containing 0.02% (vol/vol) CF (F-3543; Sigma) and 1 mM HEPES. Once the drops were dry, the plates were incubated for 24 h or 48 h at 30°C or 37°C. The binding of CR was evaluated based on the color of the colony (red or pink colonies were considered positive and white colonies were considered negative), and binding of CF was evaluated by the emission of fluorescence by colonies exposed to a UVA light (400 to 315 nm). Statistical analysis was performed by using a Mann-Whitney test.

PCR detection of autotransporter and fimbria-encoding genes.

The presence of autotransporter and fimbria-encoding genes was detected by PCR on bacterial

lysates using primers described in the supplemental material (see Table S1). The primers were designed on conserved regions of genes based on alignment analysis of homologous genes. Two sets of primers were used to detect autotransporter-encoding genes *ehaA*, *ehaB*, *ehaC*, *ehaD*, and *ehaG*. The first set of primers amplified the passenger-encoding domain sequence (named *eha*$^{\alpha}$) where nucleotide divergences have been described. The other set of primers amplified the translocation-encoding domain sequence (named *eha*$^{\beta}$), which is highly conserved (8, 18, 28).

Detection of type 1 fimbriae.

The capacity of bacterial isolates to express a D-mannose-binding phenotype was measured by the ability to agglutinate *Saccharomyces cerevisiae* cells as described previously (29). Briefly, the 24-h M9 cultures prepared as described above were diluted (1:100) in 20 ml M9-0.4% glucose and incubated at 30°C without agitation for 24 h. An initial suspension of approximately 2×10^{11} CFU/ml in PBS was diluted by 2-fold serial dilution in a microtiter plate (Corning Costar no. 2797), and an equal volume of a commercial yeast suspension in PBS (final concentration, 1.5% [wt/vol]) was added to each well. After 30 min of incubation at 4°C, yeast agglutination was monitored visually by agglutination and precipitation of cells. The agglutination titer was established as the lowest bacterial dilution at which agglutination was observed. If α-D-mannopyranose (5% [wt/vol]) (Sigma) inhibited agglutination, yeast agglutination was considered to be due to type 1 fimbriae.

CLSM.

Biofilms were prepared as described above, and after 24 h of incubation at 30°C, biofilms were washed and stained with FilmTracer FM1-43 Green biofilm cell stain (Molecular Probes, Eugene, OR) according to the manufacturer's instructions as described previously (30). To determine the composition of the biofilm matrix, biofilms were stained with wheat germ agglutinin (WGA; Oregon Green 488; binds to *N*-acetyl-D-glucosamine and N-acetylneuraminic acid residues; Molecular Probes), FilmTracer SYPRO Ruby biofilm matrix stain (labels most classes of proteins; Molecular Probes), calcofluor white [binds to (1-3)-β- and (1-4)-β-D-glucopyranoside; Sigma], or BOBO-3 iodide (stains extracellular DNA; Molecular Probes) according to the manufacturer's instructions. After a 30-min incubation at room temperature

protected from light, the fluorescent marker solution was removed, biofilms were washed with water, and the wells were filled with 100 µl of water or PBS for WGA-stained biofilms. Stained biofilms were visualized by confocal laser scanning microscopy (CLSM; FV1000 IX81; Olympus, Markham, ON, Canada), and images were acquired using FluoView software (Olympus).

Biofilm dispersion assay.

Enzymatic dispersion of established biofilms was performed as described previously (31, 32). Briefly, biofilms were grown as described above, and after 24 h of incubation, 37.5 µl of solution containing DNase I (100 µg/ml in 150 mM NaCl, 1 mM $CaCl_2$), dispersin B (20 µg/ml in PBS; Kane Biotech Inc., Winnipeg, MB, Canada), cellulase (100 µg/ml in 50 mM sodium citrate, pH 5.0), or proteinase K (100 µg/ml in 50 mM Tris-HCl, pH 7.5, 1 mM $CaCl_2$) was added directly to the biofilms. Control wells were treated with 37.5 µl of the buffer without enzymes. Wells were treated for 1 h at 37°C, and biofilms were washed, stained, and quantified as described above.

Sanitizer treatments.

Five sanitizers commonly used on the farm and in food-processing industries were used to test the ability of STEC biofilm cells and matrix to survive sanitizer treatments. The sanitizers were Virkon, a peroxide compound; Aseptol 2000, a quaternary ammonium chloride-based sanitizer; bleach, a chlorine compound; and hydrogen peroxide (H_2O_2; Sigma) and ethanol. Sanitizers were diluted with sterile distilled water to concentrations that did not require rinsing after their use as indicated by the manufacturer. Biofilms were formed as described above, and after 24 h of incubation at 30°C, media were removed and wells were filled with 200 µl of PBS (nontreated control) or sanitizers. Five different sanitizers were used and prepared as follows. A bleach solution containing 200 ppm of sodium hypochlorite; a 1% (vol/vol) Aseptol 2000 solution (Laboratoire Meriel, Pleumeleuc, France) containing 0.127% glutaraldehyde and quaternary ammonium compounds, including 0.014% (vol/vol) dodecyl dimethyl ammonium chloride, 0.06% (vol/vol) benzalkonium chloride, and 0.007% (vol/vol) alkyl dimethyl ethyl benzyl ammonium chloride; a 1% (wt/vol) Virkon solution (Vetoquinol, Lavaltrie, QC, Canada)

containing 0.214% (wt/wt) potassium monopersulfate; a 5% (vol/vol) H_2O_2 solution (Sigma); or a 70% (vol/vol) ethanol solution. After 10 min of incubation at 25°C, wells were washed three times with 200 µl of neutralizing broth (Difco Laboratories). To evaluate the viability of STEC cells after the sanitation treatments, cells were harvested by scraping the surface with sterile pipette tips and rinsing the well with 200 µl of PBS. Bacterial cells were pooled from four replicate wells that received the same sanitization treatment. The volume of PBS was adjusted to 1 ml, vigorously vortexed, serially diluted in fresh PBS, and plated onto LB agar. The plates were incubated overnight at 37°C, and colonies on the plates then were counted to determine the number of STEC cells present. In addition to CFU, the metabolic activity of the treated biofilms also was evaluated using the CellTiter-Blue reagent (Promega Corporation) as described previously (33). CellTiter-Blue reagent is a resazurin solution that is reduced by viable cells into resorufin, which emits fluorescence. Briefly, treated biofilms were incubated at 37°C in LB containing 40 µl of CellTiter-Blue reagent. After 3 h of incubation, the level of fluorescence (excitation wavelength [λ_{ex}], 570 nm; emission wavelength, [λ_{em}], 600 nm) was measured using a microplate reader. The percentage of remaining metabolic activity allowed us to evaluate the number of surviving bacteria. Percent resazurin reduction was calculated using the following formula: (experimental well absorbance − negative-control absorbance)/positive-control absorbance × 100. To evaluate if the biofilm matrix was removed, crystal violet was added to sanitizer-treated biofilms as described for the biofilm formation assay.

Statistical analysis.

Statistical analyses were performed using GraphPad Prism, version 4.02 (GraphPad Software, San Diego, CA). The results for static biofilms at the serogroup level and the results for enzymatic digestion were analyzed using a nonparametric one-way analysis of variance (ANOVA) with Dunn's multiple-comparison posttest. A Mann-Whitney test with two-tailed distribution was performed to compare biofilm formation and seropathotype, the ability to bind CR and CF, or the presence of autotransporter and fimbria-encoding genes.

RESULTS

Seropathotype A isolates (O157:H7) have greater capacity to form biofilms.

STEC biofilm production was characterized using the previously determined static and dynamic conditions (26). STEC organisms were grown in M9 supplemented with 0.4% glucose medium in polystyrene microplates incubated at 30°C for 24 h, and biofilms were evaluated by crystal violet staining. Biofilm formation was tested after 24 h, 48 h, and 72 h of incubation. The 24 h time point was selected because the OD values of crystal violet staining were the highest at this time and had decreased after 48 h (data not shown). The capacity of isolates to form biofilms under static conditions was highly variable (OD of 0.08 for the lowest, OD of 1.8 for the highest). Depending on their capacity, isolates were classified as strong ($A_{595} > 0.6$), medium ($0.6 > A_{595} > 0.3$), or weak ($0.3 > A_{595} > 0.1$) biofilm formers or as non-biofilm formers ($A_{595} < 0.1$). Of the 39 isolates, 14 (35.9%) formed a strong biofilm, 13 (33.3%) formed a medium biofilm, 11 (28.2%) formed a weak biofilm, and 1 isolate of serotype O145:NM (2.5%) was not able to form biofilm (Fig. 1A). Interestingly, we noticed that under static conditions, the majority of seropathotype A isolates formed significantly stronger biofilms ($P < 0.01$) than isolates of other seropathotypes (Fig. 1B). At the serogroup level, isolates of serogroups O157 and O121 were strong biofilm formers, while O45 and O26 isolates were weak biofilm formers (Fig. 1A). When biofilms were grown under dynamic conditions, the capacity for STEC isolates to form biofilms was characterized by the coverage area. Under these conditions, 64.1% of STEC isolates were able to cover more than 50% of the area (Table 1). Under dynamic conditions, the majority (66.7%) of seropathotype A isolates formed strong biofilm covering more than 65% of the area. In addition, most isolates from serogroups O157 and O121 that formed strong biofilms under static conditions also were able to cover 69% and 89% of the area, respectively, under dynamic conditions. Similar observations were made for isolates from serogroup O45 that formed weak biofilms under static conditions and cover only 36% of the area in microfluidics. However, biofilms formed by O145:NM isolates were able to cover 92% of the area under dynamic conditions, whereas their biofilms were weak or absent when grown statically (Fig. 1A).

Production of curli and cellulose among STEC isolates is heterogeneous.

The occurrence of curli and cellulose or cellulose-like extracellular material production was analyzed. We grew STEC isolates at 30°C and 37°C for 24 h and 48 h on minimal agar plates containing Congo red dye (CR), indicative of curli and cellulose production, as well as on plates containing calcofluor white (CF), a fluorochrome that binds to polysaccharides with β-1,3 and β-1,4 linkages, such as cellulose, chitin, and succinoglycans (27). CR binding was a common characteristic in STEC isolates, since 37/39 (94.8%) of the tested isolates turned red on CR agar plates under at least one of the tested conditions (minimal medium; 30°C or 37°C; 24 h or 48 h) (see Table S2 in the supplemental material). The ability to bind CF was less frequent than that of CR (15/39; 38.5%), but the number of CF-positive isolates was more significant at 30°C (12/39; 30.7%) than at 37°C (9/39; 23.1%) (see Table S2). However, these CR and CF phenotypes do not strictly correlate with the capacity to form a biofilm under our experimental conditions (see Fig. S1).

Seropathotype A isolates (O157:H7) aggregate to yeast in a mannose-independent manner.

Among STEC isolates, 17 non-O157 isolates produced type 1 fimbriae, as they were able to agglutinate yeast in a mannose-dependent manner (Fig. 2A); no correlation between biofilm formation and production of type 1 fimbriae was observed (Fig. 2B). Interestingly, 7 seropathotype A (O157) isolates were able to agglutinate yeast in a mannose-independent manner (Fig. 2A), and this agglutination phenotype correlated with biofilm formation ($r^2 = 0.7$) (Fig. 2B).

Association between the presence of fimbrial and autotransporter genes and biofilm formation.

The presence of genes coding for factors that are putatively involved in STEC biofilm formation (8, 18, 34,–36) was examined by PCR using primers designed in conserved regions based on sequence alignment (see Table S1 in the supplemental material). We observed an association between the presence of fimbrial genes *z1538* and *lpf2* and autotransporter gene *ehaB*$^{\beta}$ or *espP*and biofilm formation (Fig. 3). As revealed by crystal violet staining, *z1538*-positive isolates and *lpf2*-positive isolates formed significantly ($P < 0.01$ and $P < 0.001$, respectively)

more biofilms than *z1538*-negative or *lpf2*-negative isolates (Fig. 3A and B). For genes *ehaA*, *ehaB*, *ehaC*, *ehaD*, and *ehaG*, we used primers designed to amplify the variable passenger-encoding domain, named α, and the more conserved translocating-encoding domain, named β. Interestingly, the β domain sequence, $ehaB^{\beta}$, was detected in most isolates (38/39), while the α passenger domain sequence, $ehaB^{\alpha}$, was detected only in O157:H7, O157:NM, and O121:H19 isolates (see Table S3). Furthermore, $ehaB^{\alpha}$-positive isolates formed significantly more ($P < 0.001$) biofilms than $ehaB^{\alpha}$-negative ones (Fig. 3C). This suggests that the passenger-encoding domain of the gene for EhaB in STEC plays a role in biofilm formation. Moreover, *espP*-positive isolates formed significantly ($P < 0.05$) more biofilms than *espP*-negative isolates (Fig. 3D). These data indicate that isolates with genes *z1538*, *lpf2*, $ehaB^{\beta}$, and/or *espP* were able to form significantly more biofilms than isolates without those genes.

STEC biofilm characterization.

Confocal laser scanning microscopy (CLSM) using different fluorescent probes was performed with 15 high-biofilm-producing isolates (9 seropathotype A [O157], 5 seropathotype B, and 1 seropathotype C). The four isolates shown in Fig. 4 were selected to represent results obtained for the other 11 isolates. The data obtained with FM1-43, a membrane stain, highlighted the morphological heterogeneity of STEC biofilms (Fig. 4). In general, protein and DNA, stained with SYPRO Ruby and BOBO-3, respectively, were weakly detected. Polysaccharides were observed only in biofilms produced by seropathotype A (O157:H7/O157:NM) isolates. Among the 9 seropathotype A (O157:H7/O157:NM) isolates, 7 were stained with WGA, suggesting the presence of PGA or at least the presence of *N*-acetyl-D-glucosamine and N-acetylneuraminic acid residues in the biofilm matrix. Finally, cellulose was detected in the biofilm matrix of 2 isolates of seropathotype A (Fig. 4). The biofilms also were digested with enzymes to further characterize the composition of the matrix. Among the 15 selected isolates, 11 isolates were significantly sensitive to the proteinase K treatment (Fig. 5A). Two O121:H19 isolates were sensitive to cellulase treatment (Fig. 5C). Isolates were not affected by DNase I (Fig. 5B). Although PGA was observed in some isolates by CLSM, no isolates were affected by dispersin B treatments (Fig. 5D). This suggested that proteins and, in some isolates, cellulose play a larger role than extracellular DNA or PGA in STEC biofilm integrity.

Efficacy of sanitizers on STEC biofilms.

To determine the influence of biofilms on STEC sensitivity toward sanitizers commonly used to decontaminate farm or food production surfaces, four types of disinfectant, chlorine (200 ppm bleach), quaternary ammonium compound (1% [vol/vol] Aseptol 2000), alcohol (70% [vol/vol] ethanol), and peroxide compounds (1% [vol/vol] Virkon and 5% [vol/vol] H_2O_2) were applied on 10 STEC isolates selected based on their capacity to form strong biofilms (5 seropathotype A, 4 seropathotype B, and 1 seropathotype C). The impact of sanitizers on STEC biofilm was determined by enumerating viable cells and, with the resazurin-based CellTiter-Blue solution, was used to measure the metabolic activity of cells remaining after the treatment. After a 10-min exposure, the five sanitizers decreased the number of viable cells by 99.2 to 99.7% and the metabolic activity was reduced by 97.9 to 98.9%. There was no significant difference between seropathotypes or isolates (Table 2). Moreover, a protective effect of biofilm was observed, since planktonic cells were more sensitive than biofilm cells to sanitizer treatments (data not shown). None of the sanitizers were able to totally remove STEC biofilm matrix, as evaluated by crystal violet (Table 2). Bleach (43% or 22% of remaining matrix) was the most effective sanitizer, followed by H_2O_2 (76% of remaining matrix) and ethanol (91% or 85% of remaining matrix). Aseptol 2000 was not able to remove the matrix of any seropathotype biofilms, and Virkon only affects seropathotype B biofilm matrix. In brief, sanitizers effectively reduce the viability of STEC cells within biofilms but are not able to completely remove the biofilm matrix (Table 2).

DISCUSSION

Biofilm-forming abilities of STEC isolates recovered from humans.

STEC, an important food-borne and waterborne pathogen, and STEC isolates of different origins (cattle, water, food, and human) have been shown to be able to form biofilms (6-8). Biofilms are thought to increase STEC survival and persistence in hostile environments such as water- or food-processing plants (37). Therefore, we hypothesized that biofilms could be involved in the transmission of STEC from the environment to humans. Consequently, for this

study, we selected STEC isolates associated with human infections. Biofilm formation of 39 STEC isolates belonging to seropathotypes A, B, and C was investigated. As shown in other studies, biofilm formation on polystyrene surfaces appeared to be a strain-dependent phenomenon (7, 8, 38, 39). An association between STEC serotypes and biofilm-forming abilities was suggested (40); however, in other studies this was not observed (7, 8). In our study, because of the low number of isolates per serotype, this association could not be determined.

As previously observed, static or dynamic conditions used to form biofilms can influence the biofilm-forming capacity of isolates (26). This is especially observed for O145 isolates that formed stronger biofilms under dynamic conditions than under static conditions. Under static conditions, metabolic waste and dispersing signals can accumulate, and this may negatively affect the biofilm-forming ability. Moreover, biofilm architecture can dramatically change when biofilms are grown under dynamic conditions (41, 42) and could explain the difference in the biofilm-forming abilities of some STEC isolates (Table 1). Nevertheless, this difference was not observed for all STEC isolates, which indicates that the mechanism behind STEC biofilm formation is heterogeneous. Using the seropathotype classification, we found that under static conditions, seropathotype A isolates formed significantly stronger biofilms than those of seropathotypes B and C (Fig. 1B), and that under dynamic conditions the majority of seropathotype A isolates were able to form strong biofilms. This biofilm-forming capacity of seropathotype A isolates could contribute to their persistence in the environment and influence their high relative incidence and their frequent involvement in outbreaks (3). It is reasonable to assume that an STEC strain coexists with several other STEC isolates as well as with other bacterial species (43,–47). Therefore, mixed STEC biofilms should be investigated in future work.

Factors potentially involved in STEC biofilm formation.

Biofilm formation has been shown to be mediated by bacterial surface structures that are regulated by environmental conditions. Here, we show that the production of curli as measured with Congo red binding was dependent on the isolates and growth conditions despite all STEC strains carrying the curli gene *csgA* (7). CF results indicative of curli and/or cellulose production also were variable and are similar to those of other studies (7, 8, 48). While curli or cellulose

production in some STEC isolates was shown to be associated with biofilm formation (6, 8, 34, 49,–51), these were shown to be nonessential for biofilm formation (7). In our study, no correlation was found between Congo red or calcofluor-positive isolates and biofilm formation or seropathotype (see Fig. S1 in supplemental material). This highlights a high variability in the mechanisms regulating the production of factors associated with biofilm formation and suggests that STEC strains adapt differently to various environments.

Although all isolates were PCR positive for type 1 fimbriae (see Table S3 in supplemental material), only seropathotype B and C isolates produced type 1 fimbriae. It has been shown that strains of seropathotype A isolates are unable to express type 1 fimbriae due to a 16-bp deletion in the regulatory switch region of *fimA* (52,–54). Interestingly, 7 seropathotype A isolates were able to agglutinate yeast in a mannose-independent manner and were able to autoagglutinate (Fig. 2A and data not shown). This phenotype correlated with biofilm formation ($r^2 = 0.70$) for those 7 isolates, suggesting that the production of this unidentified factor could contribute to biofilm formation (Fig. 2B).

Fimbriae and autotransporters are adhesion factors associated with biofilm formation in STEC (55). Fimbria-encoding genes *z1538* and *lpf2*, the passenger domain of the autotransporter gene *ehaB*, and the autotransporter gene *espP* are present in isolates producing significantly more biofilms (Fig. 3). As previously observed, all seropathotype A isolates were positive for *z1538*, a gene present in the seropathotype A-specific genomic O island 47 (56) while absent from other isolates. Given that seropathotype A isolates (*z1538* positive) formed significantly more biofilm than seropathotype B and C isolates (*z1538*-negative isolates) (Fig. 3A), it is possible that fimbrial adhesin encoded by O island 47 play a role in biofilm formation. To support this, Low *et al.* observed that *z1538* fimbrial gene cluster expression was increased under conditions similar to those used for biofilm formation (35). In addition, isolates positive for *lpf2* formed significantly more biofilm than *lpf2*-negative isolates (Fig. 3B). This suggests a biofilm formation role for the long polar fimbria of Lpf2. Expression of *lpf2* in *E. coli* O157:H7 has been shown to be increased under conditions similar to those used for biofilm formation (57) and when grown at 28°C rather than at 37°C (35). Lpf2 has been suggested to contribute to STEC adhesion (58). The precise role of both the *z1538* gene cluster and *lpf2* during biofilm

formation needs to be confirmed. The α passenger domain of *ehaB* was detected in isolates that formed strong biofilms at significant levels, such as those belonging to O157:H7, O157:NM, and O121:H19 serotypes (Fig. 3C). *ehaB* of reference strain EDL 933 (O157:H7) was shown to be involved in biofilm formation when overexpressed in *E. coli* K-12 (17). Therefore, it is possible that these EhaB variants found in O157:H7 and O121:H19 contribute to the establishment of biofilm. The plasmid-encoding gene *espP* was detected in most STEC isolates (Fig. 3D). Using an *espP* mutant, this gene already was shown to be associated with biofilm formation in O157:H7 (19). Seropathotype A isolates are equipped with fimbrial and autotransporter genes that could contribute to their biofilm capacity and their adaptation to different environments. Moreover, *lpf2*, *ehaB*, and *espP* also were found in the genome of environmental STEC strains, suggesting that those genes contribute to the STEC environmental lifestyle (59).

STEC biofilm matrix composition.

Biofilm matrix compositions of *E. coli* isolates were shown to be highly heterogeneous (20, 60, 61). The use of CLSM and fluorescent probes showed the presence of PGA and cellulose in the biofilm of seropathotype A isolates that are strong biofilm producers (Fig. 4). These were shown to be important in the development and architecture of biofilms in *E. coli* (20). To our knowledge, this is the first description of the matrix composition of STEC biofilms. Furthermore, a previous study showed that O157:H7 mutants lacking genes encoding PGA or cellulose synthesis were unable to adhere to alfalfa sprouts (21). Therefore, it is possible that our biofilm conditions stimulated the production of cellulose and PGA in seropathotype A isolates but not in seropathotype B and C isolates. Genome sequence database and PCR results indicate that O26:H11, O103:H2, O111:NM, O111H:8, O121:H19, and O157:H26 isolates are negative for *pgaA*, coding for PGA export from the periplasm, while it is present in seropathotype A isolates (data not shown) (62). This could explain why seropathotype A isolates have a greater potential to form biofilm than others. Alternatively, some other polysaccharide structure could be produced in seropathotype B and C isolates (63, 64). Nevertheless, biofilms were resistant to dispersin B treatment that targets PGA, but they were sensitive to a proteinase K treatment (Fig. 5). These findings suggest that proteins play an important role in biofilm

integrity, while PGA seems to be less necessary for biofilm integrity. Previous studies suggested that in *E. coli*, proteins such as adhesins (fimbriae and curli) and autotransporters participate in the structure of the biofilm by establishing cell-surface, cell-cell, and cell-matrix interactions (18, 34, 50, 65), while polysaccharides may have a protective role (66).

Sanitizer treatments.

Food-processing and farm environments provide a variety of conditions that might favor the formation of biofilm (67). Standard cleaning and sanitizing practices are used to reduce sources of microbial contamination on their products. As previously described, strong attachment of biofilms on surfaces may affect the efficiency of sanitizers and protect bacteria against sanitation protocols that are used to reduce contamination (7, 68, 69). In the present study, we examined if sanitizers commonly used in good sanitation practices were effective at both reducing STEC viability in biofilms and eliminating the biofilm matrix. Although sanitizer treatments were effective at reducing significantly the viability and the metabolism of STEC in biofilms, the biofilm matrix either remained or was partly removed depending on the sanitizer (Table 2). These results agree with previous reports (6, 7, 68, 69). Moreover, no significant differences in viability or metabolic activity were seen between seropathotypes or isolates (7). Additionally, matrix composition, such as the presence of cellulose or PGA, had no protective effect on the cells. Sanitizers cannot completely remove biofilm matrix on food-processing surfaces left after a sanitation protocol, which could lead to a faster recolonization of the surface (70). Interestingly, some sanitizers, such as bleach or H_2O_2, were more effective at removing the biofilm matrix of STEC. Our biofilm study is restricted to specific conditions and represents to some degree biofilm formation on food-processing equipment design and surface materials; nevertheless, our results are indicative of biofilm characteristics of STEC that caused human infections. Thus, STEC biofilm formation is a potential hazard in food hygiene and may become a source of cross-contamination in farm and food-processing environments. Because detached biofilms may serve as a continuous contamination source, prevention, removal, and inactivation of STEC biofilms are critical for improving hygiene and contamination control and enhancing food safety.

Conclusions.

We show that STEC isolates recovered from human infections formed biofilms in a seropathotype-dependent manner. Specifically, seropathotype A isolates clustering as serotypes O157:H7 and O157:NM, with the highest relative incidence and frequently involved in outbreaks, had a greater ability to form biofilms than seropathotype B or C isolates. Seropathotype A isolates were the only ones able to produce cellulose and PGA. Additionally, biofilm integrity was dependent on proteins, but they were not overly abundant in the biofilm matrix. Furthermore, two autotransporters, EhaB and EspP, and two fimbriae, one encoded by genes found on genomic O island 47 and Lpf2, were identified as potential genetic determinants for biofilm formation. Interestingly, some seropathotype A isolates were able to agglutinate yeast in a mannose-independent manner. This phenotype correlated with biofilm formation, suggesting that an unidentified biofilm-associated factor is produced by seropathotype A isolates. Treatment with sanitizers reduced STEC viability but did not completely remove the biofilm matrix. Overall, our data indicate that biofilm formation could contribute to the persistence of seropathotype A isolates in the environment and to the transmission and, consequently, the high incidence of serotype O157:H7 and O157:NM infections.

ACKNOWLEDGMENTS

We thank M. A. Karmali, K. Ziebell, and R. P. Johnson at the Laboratory for Food-Borne Zoonoses of the Public Health Agency of Canada for supplying North American STEC isolates and C. Martin from INRA Clermont-Ferrand Theix for supplying French STEC isolates. We are grateful to Judith Kashul for editing the manuscript. We thank Frederic Berthiaume for his help with confocal laser scanning microscopy assays.

FOOTNOTES

Supplemental material for this article may be found at http://dx.doi.org/10.1128/AEM.02983-15.

REFERENCES

1. Thomas MK, Murray R, Flockhart L, Pintar K, Pollari F, Fazil A, Nesbitt A, Marshall B. 2013. Estimates of the burden of foodborne illness in Canada for 30 specified pathogens and unspecified agents, circa 2006. Foodborne Pathog Dis 10:639–648. doi:10.1089/fpd.2012.1389.

2. Ferens WA, Hovde CJ. 2011. *Escherichia coli* O157:H7: animal reservoir and sources of human infection. Foodborne Pathog Dis 8:465–487. doi:10.1089/fpd.2010.0673.

3. Karmali MA, Mascarenhas M, Shen S, Ziebell K, Johnson S, Reid-Smith R, Isaac-Renton J, Clark C, Rahn K, Kaper JB. 2003. Association of genomic O island 122 of *Escherichia coli* EDL933 with verocytotoxin-producing *Escherichia coli* seropathotypes that are linked to epidemic and/or serious disease. J Clin Microbiol 41:4930–4940. doi:10.1128/JCM.41.11.4930-4940.2003.

4. Brooks JT, Sowers EG, Wells JG, Greene KD, Griffin PM, Hoekstra RM, Strockbine NA. 2005. Non-O157 Shiga toxin-producing *Escherichia coli* infections in the United States, 1983–2002. J Infect Dis 192:1422–1429. doi:10.1086/466536.

5. Costerton W, Veeh R, Shirtliff M, Pasmore M, Post C, Ehrlich G. 2003. The application of biofilm science to the study and control of chronic bacterial infections. J Clin Invest 112:1466–1477. doi:10.1172/JCI20365.

6. Park YJ, Chen J. 2015. Control of the biofilms formed by curli- and cellulose-expressing Shiga toxin-producing *Escherichia coli* using treatments with organic acids and commercial sanitizers. J Food Prot 78:990–995. doi:10.4315/0362-028X.JFP-14-382.

7. Wang R, Bono JL, Kalchayanand N, Shackelford S, Harhay DM. 2012. Biofilm formation by Shiga toxin-producing *Escherichia coli* O157:H7 and non-O157 strains and their tolerance to sanitizers commonly used in the food processing environment. J Food Prot 75:1418–1428. doi:10.4315/0362-028X.JFP-11-427.

8. Biscola FT, Abe CM, Guth BE. 2011. Determination of adhesin gene sequences in, and biofilm formation by, O157 and non-O157 Shiga toxin-producing *Escherichia coli* strains isolated from different sources. Appl Environ Microbiol 77:2201–2208. doi:10.1128/AEM.01920-10.

9. Villegas NA, Baronetti J, Albesa I, Polifroni R, Parma A, Etcheverria A, Becerra M, Padola N, Paraje M. 2013. Relevance of biofilms in the pathogenesis of Shiga toxin-producing *Escherichia coli* infection. ScientificWorldJournal 2013:607258. doi:10.1155/2013/607258.

10. Ryu JH, Kim H, Beuchat LR. 2004. Attachment and biofilm formation by *Escherichia coli* O157:H7 on stainless steel as influenced by exopolysaccharide production, nutrient availability, and temperature. J Food Prot 67:2123–2131.

11. Ryu JH, Beuchat LR. 2005. Biofilm formation by *Escherichia coli* O157:H7 on stainless steel: effect of exopolysaccharide and curli production on its resistance to chlorine. Appl Environ Microbiol 71:247–254. doi:10.1128/AEM.71.1.247-254.2005.

12. Santos Mendonça RC, Morelli AMF, Pereira JAM, de Carvalho MM, de Souza NL. 2012.Prediction of *Escherichia coli* O157:H7 adhesion and potential to form biofilm under experimental conditions. Food Control 23:389–396. doi:10.1016/j.foodcont.2011.08.004.

13. Marouani-Gadri N, Augier G, Carpentier B. 2009. Characterization of bacterial strains isolated from a beef-processing plant following cleaning and disinfection—influence of isolated strains on biofilm formation by Sakai and EDL 933 *Escherichia coli* O157:H7. Int J Food Microbiol 133:62–67. doi:10.1016/j.ijfoodmicro.2009.04.028.

14. Reisner A, Krogfelt KA, Klein BM, Zechner EL, Molin S. 2006. In vitro biofilm formation of commensal and pathogenic *Escherichia coli* strains: impact of environmental and genetic factors. J Bacteriol 188:3572–3581. doi:10.1128/JB.188.10.3572-3581.2006.

15. Crim SM, Griffin PM, Tauxe R, Marder EP, Gilliss D, Cronquist AB, Cartter M, Tobin-D'Angelo M, Blythe D, Smith K, Lathrop S, Zansky S, Cieslak PR, Dunn J, Holt KG, Wolpert B, Henao OL. 2015. Preliminary incidence and trends of infection with pathogens transmitted commonly through food-foodborne diseases active surveillance network, 10 U.S. sites, 2006-

2014. MMWR Morb Mortal Wkly Rep 64:495–499.

16. Beloin C, Valle J, Latour-Lambert P, Faure P, Kzreminski M, Balestrino D, Haagensen JA, Molin S, Prensier G, Arbeille B, Ghigo JM. 2004. Global impact of mature biofilm lifestyle on *Escherichia coli* K-12 gene expression. Mol Microbiol 51:659–674. doi:10.1046/j.1365-2958.2003.03865.x.

17. Wells TJ, McNeilly TN, Totsika M, Mahajan A, Gally DL, Schembri MA. 2009. The *Escherichia coli* O157:H7 EhaB autotransporter protein binds to laminin and collagen I and induces a serum IgA response in O157:H7 challenged cattle. Environ Microbiol 11:1803–1814. doi:10.1111/j.1462-2920.2009.01905.x.

18. Wells TJ, Sherlock O, Rivas L, Mahajan A, Beatson SA, Torpdahl M, Webb RI, Allsopp LP, Gobius KS, Gally DL, Schembri MA. 2008. EhaA is a novel autotransporter protein of enterohemorrhagic *Escherichia coli* O157:H7 that contributes to adhesion and biofilm formation. Environ Microbiol 10:589–604. doi:10.1111/j.1462-2920.2007.01479.x.

19. Puttamreddy S, Cornick NA, Minion FC. 2010. Genome-wide transposon mutagenesis reveals a role for pO157 genes in biofilm development in *Escherichia coli* O157:H7 EDL933. Infect Immun 78:2377–2384. doi:10.1128/IAI.00156-10.

20. Beloin C, Roux A, Ghigo JM. 2008. *Escherichia coli* biofilms. Curr Top Microbiol Immunol322:249–289.

21. Matthysse AG, Deora R, Mishra M, Torres AG. 2008. Polysaccharides cellulose, poly-beta-1,6-*N*-acetyl-d-glucosamine, and colanic acid are required for optimal binding of *Escherichia coli* O157:H7 strains to alfalfa sprouts and K-12 strains to plastic but not for binding to epithelial cells. Appl Environ Microbiol 74:2384–2390. doi:10.1128/AEM.01854-07.

22. Perna NT, Plunkett G III, Burland V, Mau B, Glasner JD, Rose DJ, Mayhew GF, Evans PS, Gregor J, Kirkpatrick HA, Posfai G, Hackett J, Klink S, Boutin A, Shao Y, Miller L, Grotbeck EJ, Davis NW, Lim A, Dimalanta ET, Potamousis KD, Apodaca J, Anantharaman TS, Lin J, Yen G, Schwartz DC, Welch RA, Blattner FR. 2001. Genome sequence of enterohaemorrhagic *Escherichia coli* O157:H7. Nature 409:529–533. doi:10.1038/35054089.

23. Michino H, Araki K, Minami S, Takaya S, Sakai N, Miyazaki M, Ono A, Yanagawa H. 1999. Massive outbreak of *Escherichia coli* O157:H7 infection in schoolchildren in Sakai City, Japan, associated with consumption of white radish sprouts. Am J Epidemiol 150:787–796. doi:10.1093/oxfordjournals.aje.a010082.

24. Griffin PM, Ostroff SM, Tauxe RV, Greene KD, Wells JG, Lewis JH, Blake PA. 1988.Illnesses associated with *Escherichia coli* O157:H7 infections. A broad clinical spectrum. Ann Intern Med 109:705–712. doi:10.7326/0003-4819-109-9-705.

25. Pradel N, Bertin Y, Martin C, Livrelli V. 2008. Molecular analysis of Shiga toxin-producing *Escherichia coli* strains isolated from hemolytic-uremic syndrome patients and dairy samples in France. Appl Environ Microbiol 74:2118–2128. doi:10.1128/aem.02688-07.

26. Tremblay YD, Vogeleer P, Jacques M, Harel J. 2015. High-throughput microfluidic method to study biofilm formation and host-pathogen interactions in pathogenic *Escherichia coli*. Appl Environ Microbiol 81:2827–2840. doi:10.1128/AEM.04208-14.

27. Da Re S, Ghigo JM. 2006. A CsgD-independent pathway for cellulose production and biofilm formation in *Escherichia coli*. J Bacteriol 188:3073–3087. doi:10.1128/JB.188.8.3073-3087.2006.

28. Totsika M, Wells TJ, Beloin C, Valle J, Allsopp LP, King NP, Ghigo JM, Schembri MA. 2012. Molecular characterization of the EhaG and UpaG trimeric autotransporter proteins from pathogenic *Escherichia coli*. Appl Environ Microbiol 78:2179–2189. doi:10.1128/AEM.06680-11.

29. Crepin S, Houle S, Charbonneau ME, Mourez M, Harel J, Dozois CM. 2012. Decreased expression of type 1 fimbriae by a *pst* mutant of uropathogenic *Escherichia coli* reduces urinary tract infection. Infect Immun 80:2802–2815. doi:10.1128/IAI.00162-12.

30. Bello-Orti B, Deslandes V, Tremblay YD, Labrie J, Howell KJ, Tucker AW, Maskell DJ, Aragon V, Jacques M. 2014. Biofilm formation by virulent and non-virulent strains of *Haemophilus parasuis*. Vet Res 45:104. doi:10.1186/s13567-014-0104-9.

31. Tremblay YD, Lamarche D, Chever P, Haine D, Messier S, Jacques M. 2013. Characterization of the ability of coagulase-negative staphylococci isolated from the milk of Canadian farms to form biofilms. J Dairy Sci 96:234–246. doi:10.3168/jds.2012-5795.

32. Orgaz B, Kives J, Pedregosa AM, Monistrol IF, Laborda F, SanJosé C. 2006. Bacterial biofilm removal using fungal enzymes. Enzyme Microb Technol 40:51–56. doi:10.1016/j.enzmictec.2005.10.037.

33. Tremblay YD, Caron V, Blondeau A, Messier S, Jacques M. 2014. Biofilm formation by coagulase-negative staphylococci: impact on the efficacy of antimicrobials and disinfectants commonly used on dairy farms. Vet Microbiol 172:511–518. doi:10.1016/j.vetmic.2014.06.007.

34. Cookson AL, Cooley WA, Woodward MJ. 2002. The role of type 1 and curli fimbriae of Shiga toxin-producing *Escherichia coli* in adherence to abiotic surfaces. Int J Med Microbiol292:195–205. doi:10.1078/1438-4221-00203.

35. Low AS, Holden N, Rosser T, Roe AJ, Constantinidou C, Hobman JL, Smith DG, Low JC, Gally DL. 2006. Analysis of fimbrial gene clusters and their expression in enterohaemorrhagic *Escherichia coli* O157:H7. Environ Microbiol 8:1033–1047. doi:10.1111/j.1462-2920.2006.00995.x.

36. Paton AW, Srimanote P, Woodrow MC, Paton JC. 2001. Characterization of Saa, a novel autoagglutinating adhesin produced by locus of enterocyte effacement-negative Shiga-toxigenic *Escherichia coli* strains that are virulent for humans. Infect Immun 69:6999–7009. doi:10.1128/IAI.69.11.6999-7009.2001.

37. Vogeleer P, Tremblay YD, Mafu AA, Jacques M, Harel J. 2014. Life on the outside: role of biofilms in environmental persistence of Shiga-toxin producing *Escherichia coli*. Front Microbiol 5:317. doi:10.3389/fmicb.2014.00317.

38. Alvarez-Ordonez A, Alvseike O, Omer MK, Heir E, Axelsson L, Holck A, Prieto M. 2013. Heterogeneity in resistance to food-related stresses and biofilm formation ability among verocytotoxigenic *Escherichia coli* strains. Int J Food Microbiol 161:220–230. doi:10.1016/j.ijfoodmicro.2012.12.008.

39. Dourou D, Beauchamp CS, Yoon Y, Geornaras I, Belk KE, Smith GC, Nychas GJ, Sofos JN. 2011. Attachment and biofilm formation by *Escherichia coli* O157:H7 at different temperatures, on various food-contact surfaces encountered in beef processing. Int J Food Microbiol 149:262–268. doi:10.1016/j.ijfoodmicro.2011.07.004.

40. Nesse LL, Sekse C, Berg K, Johannesen KC, Solheim H, Vestby LK, Urdahl AM. 2013.Potentially pathogenic *Escherichia coli* can produce biofilm under conditions relevant for the food production chain. Appl Environ Microbiol doi:10.1128/AEM.03331-1.

41. Purevdorj B, Costerton JW, Stoodley P. 2002. Influence of hydrodynamics and cell signaling on the structure and behavior of *Pseudomonas aeruginosa* biofilms. Appl Environ Microbiol68:4457–4464. doi:10.1128/AEM.68.9.4457-4464.2002.

42. Vejborg RM, Klemm P. 2009. Cellular chain formation in *Escherichia coli* biofilms. Microbiology 155:1407–1417. doi:10.1099/mic.0.026419-0.

43. Carter MQ, Xue K, Brandl MT, Liu F, Wu L, Louie JW, Mandrell RE, Zhou J. 2012.Functional metagenomics of *Escherichia coli* O157:H7 interactions with spinach indigenous microorganisms during biofilm formation. PLoS One 7:e44186. doi:10.1371/journal.pone.0044186.

44. Liu NT, Nou X, Bauchan GR, Murphy C, Lefcourt AM, Shelton DR, Lo YM. 2015. Effects of environmental parameters on the dual-species biofilms formed by *Escherichia coli* O157:H7 and *Ralstonia insidiosa*, a strong biofilm producer isolated from a fresh-cut produce processing plant. J Food Prot 78:121–127. doi:10.4315/0362-028X.JFP-14-302.

45. Liu NT, Nou X, Lefcourt AM, Shelton DR, Lo YM. 2014. Dual-species biofilm formation by *Escherichia coli* O157:H7 and environmental bacteria isolated from fresh-cut processing facilities. Int J Food Microbiol 171:15–20. doi:10.1016/j.ijfoodmicro.2013.11.007.

46. Wang R, Kalchayanand N, Bono JL. 2015. Sequence of colonization determines the composition of mixed biofilms by *Escherichia coli* O157:H7 and O111:H8 strains. J Food Prot78:1554–1559. doi:10.4315/0362-028X.JFP-15-009.

47. Wang R, Kalchayanand N, Bono JL, Schmidt JW, Bosilevac JM. 2012. Dual-serotype biofilm formation by Shiga toxin-producing *Escherichia coli* O157:H7 and O26:H11 strains. Appl Environ Microbiol 78:6341–6344. doi:10.1128/aem.01137-12.

48. Uhlich GA, Chen CY, Cottrell BJ, Nguyen LH. 2014. Growth media and temperature effects on biofilm formation by serotype O157:H7 and non-O157 Shiga toxin-producing *Escherichia coli*. FEMS Microbiol Lett 354:133–141. doi:10.1111/1574-6968.12439.

49. Ryu JH, Kim H, Frank JF, Beuchat LR. 2004. Attachment and biofilm formation on stainless steel by *Escherichia coli* O157:H7 as affected by curli production. Lett Appl Microbiol39:359–362. doi:10.1111/j.1472-765X.2004.01591.x.

50. Uhlich GA, Cooke PH, Solomon EB. 2006. Analyses of the red-dry-rough phenotype of an *Escherichia coli* O157:H7 strain and its role in biofilm formation and resistance to antibacterial agents. Appl Environ Microbiol 72:2564–2572. doi:10.1128/AEM.72.4.2564-2572.2006.

51. Lee JH, Kim YG, Cho MH, Wood TK, Lee J. 2011. Transcriptomic analysis for genetic mechanisms of the factors related to biofilm formation in *Escherichia coli* O157:H7. Curr Microbiol 62:1321–1330. doi:10.1007/s00284-010-9862-4.

52. Enami M, Nakasone N, Honma Y, Kakinohana S, Kudaka J, Iwanaga M. 1999. Expression of type I pili is abolished in verotoxin-producing *Escherichia coli* O157. FEMS Microbiol Lett179:467–472. doi:10.1111/j.1574-6968.1999.tb08764.x.

53. Roe AJ, Currie C, Smith DG, Gally DL. 2001. Analysis of type 1 fimbriae expression in verotoxigenic *Escherichia coli*: a comparison between serotypes O157 and O26. Microbiology147:145–152. doi:10.1099/00221287-147-1-145.

54. Li B, Koch WH, Cebula TA. 1997. Detection and characterization of the *fimA* gene of *Escherichia coli* O157:H7. Mol Cell Probes 11:397–406. doi:10.1006/mcpr.1997.0132.[ ]

55. McWilliams BD, Torres AG. 2015. Enterohemorrhagic *Escherichia coli* adhesins, p 157–174. *In* Sperandio V, Hovde C. (ed), Enterohemorrhagic *Escherichia coli* and other Shiga toxin-producing *E. coli*. ASM Press, Washington, DC. doi:10.1128/microbiolspec.EHEC-0003-2013.

56. Shen S, Mascarenhas M, Morgan R, Rahn K, Karmali MA. 2005. Identification of four fimbria-encoding genomic islands that are highly specific for verocytotoxin-producing *Escherichia coli* serotype O157 strains. J Clin Microbiol 43:3840–3850. doi:10.1128/JCM.43.8.3840-3850.2005.

57. Torres AG, Milflores-Flores L, Garcia-Gallegos JG, Patel SD, Best A, La Ragione RM, Martinez-Laguna Y, Woodward MJ. 2007. Environmental regulation and colonization attributes of the long polar fimbriae (LPF) of *Escherichia coli* O157:H7. Int J Med Microbiol 297:177–185. doi:10.1016/j.ijmm.2007.01.005.

58. Newton HJ, Sloan J, Bennett-Wood V, Adams LM, Robins-Browne RM, Hartland EL. 2004.Contribution of long polar fimbriae to the virulence of rabbit-specific enteropathogenic *Escherichia coli*. Infect Immun 72:1230–1239. doi:10.1128/IAI.72.3.1230-1239.2004.

59. Balière C, Rincé A, Blanco J, Dahbi G, Harel J, Vogeleer P, Giard J-C, Mariani-Kurdjian P, Gourmelon M. 2015. Prevalence and characterization of Shiga toxin-producing and enteropathogenic *Escherichia coli* in shellfish-harvesting areas and their watersheds. Front Microbiol 6:1356. doi:10.3389/fmicb.2015.01356.

60. Sutherland IW. 2001. The biofilm matrix—an immobilized but dynamic microbial environment. Trends Microbiol 9:222–227. doi:10.1016/S0966-842X(01)02012-1.

61. Hung C, Zhou Y, Pinkner JS, Dodson KW, Crowley JR, Heuser J, Chapman MR, Hadjifrangiskou M, Henderson JP, Hultgren SJ. 2013. *Escherichia coli* biofilms have an organized and complex extracellular matrix structure. mBio 4:e00645-13. doi:10.1128/mBio.00645-13.

62. Itoh Y, Rice JD, Goller C, Pannuri A, Taylor J, Meisner J, Beveridge TJ, Preston JF III, Romeo T. 2008. Roles of *pgaABCD* genes in synthesis, modification, and export of the *Escherichia coli* biofilm adhesin poly-beta-1,6-*N*-acetyl-d-glucosamine. J Bacteriol 190:3670–3680. doi:10.1128/JB.01920-07.

63. Danese PN, Pratt LA, Kolter R. 2000. Exopolysaccharide production is required for development of *Escherichia coli* K-12 biofilm architecture. J Bacteriol 182:3593–3596.

doi:10.1128/JB.182.12.3593-3596.2000.

64. Prigent-Combaret C, Prensier G, Le Thi TT, Vidal O, Lejeune P, Dorel C. 2000.Developmental pathway for biofilm formation in curli-producing *Escherichia coli* strains: role of flagella, curli and colanic acid. Environ Microbiol 2:450–464. doi:10.1046/j.1462-2920.2000.00128.x.

65. Valle J, Mabbett AN, Ulett GC, Toledo-Arana A, Wecker K, Totsika M, Schembri MA, Ghigo JM, Beloin C. 2008. UpaG, a new member of the trimeric autotransporter family of adhesins in uropathogenic *Escherichia coli*. J Bacteriol 190:4147–4161. doi:10.1128/JB.00122-08.

66. Yeh JY, Chen J. 2004. Production of slime polysaccharide by EHEC and STEC as well as the influence of culture conditions on slime production in *Escherichia coli* O157:H7. Lett Appl Microbiol 38:488–492. doi:10.1111/j.1472-765X.2004.01523.x.

67. Giaouris E, Heir E, Hebraud M, Chorianopoulos N, Langsrud S, Moretro T, Habimana O, Desvaux M, Renier S, Nychas GJ. 2013. Attachment and biofilm formation by foodborne bacteria in meat processing environments: causes, implications, role of bacterial interactions and control by alternative novel methods. Meat Sci 97:298–309. doi:10.1016/j.meatsci.2013.05.023.

68. Fouladkhah A, Geornaras I, Sofos JN. 2013. Biofilm formation of O157 and non-O157 Shiga toxin-producing *Escherichia coli* and multidrug-resistant and susceptible Salmonella typhimurium and Newport and their inactivation by sanitizers. J Food Sci 78:M880–M886. doi:10.1111/1750-3841.12123.

69. Marouani-Gadri N, Firmesse O, Chassaing D, Sandris-Nielsen D, Arneborg N, Carpentier B. 2010. Potential of *Escherichia coli* O157:H7 to persist and form viable but non-culturable cells on a food-contact surface subjected to cycles of soiling and chemical treatment. Int J Food Microbiol 144:96–103. doi:10.1016/j.ijfoodmicro.2010.09.002.

70. Larsen P, Olesen BH, Nielsen PH, Nielsen JL. 2008. Quantification of lipids and protein in thin biofilms by fluorescence staining. Biofouling 24:241–250.

doi:10.1080/08927010802040255.

TABLES

Tableau 1. List of STEC isolates used in this study.

[a] PHAC, Public Health Agency of Canada

Serotypes	Name	Seropathotype	References/Source
O157:H7			
	EDL933	A	(58)
	Sakai	A	(59)
	86 - 24	A	(60)
	AJH-4	A	(3)
	AJH-5	A	(3)
	AJH-6	A	(3)
	AJH-7	A	(3)
	AJH-8	A	(3)
	AJH-9	A	(3)
	AJH-10	A	(3)
	AJH-11	A	(61)
	AJH-12	A	(61)
	AJH-13	A	(61)
	AJH-14	A	(61)
O157:NM			
	AJH-15	A	(3)
O157:H26			
	CJH-1	C	(61)
O26:H11			
	BJH-1	B	(3)
	BJH-2	B	(3)
	BJH-3	B	(3)
	BJH-4	B	PHAC[a]
O45:H2			
	BJH-5	B	PHAC[a]
	BJH-6	B	PHAC[a]
	BJH-7	B	PHAC[a]
	BJH-8	B	PHAC[a]
O103:H2			
	BJH-9	B	(61)
O111:H8			
	BJH-10	B	PHAC[a]
	BJH-11	B	PHAC[a]

O111:NM			
	BJH-12	B	(3)
	BJH-13	B	(3)
	BJH-14	B	(3)
O121:H19			
	BJH-15	B	PHAC[a]
	BJH-16	B	PHAC[a]
	BJH-17	B	PHAC[a]
	BJH-18	B	(3)
O145:H25			
	CJH-2	C	PHAC[a]
O145:NM			
	BJH-19	B	PHAC[a]
	BJH-20	B	PHAC[a]
	BJH-21	B	PHAC[a]
O113:H21			
	CJH-3	C	(3)

Tableau 2. Bacterial survival and matrix remaining of seropathotypes A or seropathotypes B-C. [a]Averages of 3 independent biological replicates and percentage of remaining fluorescence (λ_{ex} 570 nm; λ_{em} 600nm) or absorbance (595 nm) compared to the control PBS treatment. [b]QAC means quaternary ammonium chloride.

Seropathotypes	Percentage of viability/ remaining matrix	Chlorine[a]	QAC[a.b]	Peroxide compounds[a]		Alcohol[a]
		Bleach (200 ppm)	Aseptol 2000 (1%)	Virkon (1%)	H_2O_2 (5%)	Ethanol (70%)
A (5)	Viability	0.8 (±0.7)	1.2 (±0.7)	0.4 (±0.1)	0.7 (±0.4)	2.4 (±0.9)
	Remaining matrix	53 (±14)	100 (±0)	100 (±2)	72 (±16)	92 (±10)
B-C (5)	Viability	1.7 (±0.6)	2.1 (±1.1)	1.9 (±1.1)	1.7 (±0.8)	2.8 (±0.9)
	Remaining matrix	22 (±8)	100 (±3)	65 (±9)	56 (±16)	71 (±17)

FIGURES

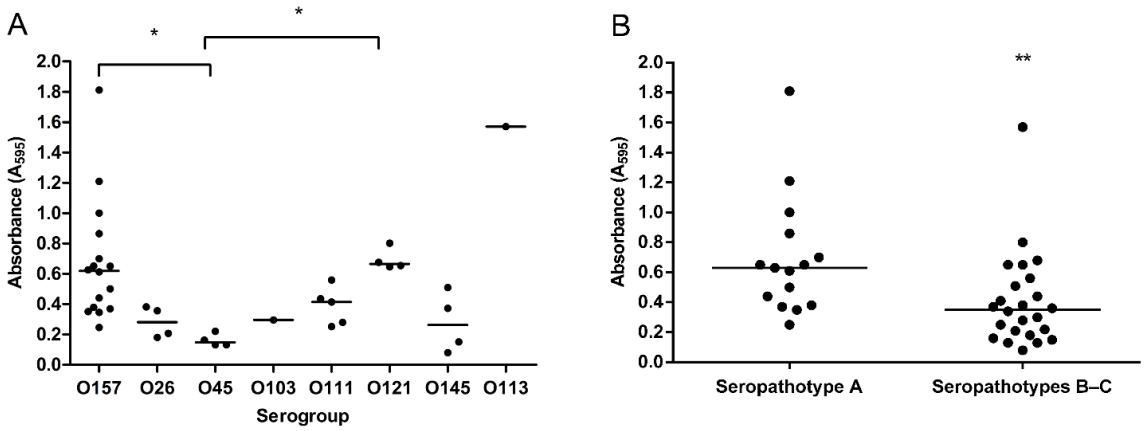

Figure 1. Biofilm formation by STEC isolates grouped by serotypes (A) and by seropathotypes (B). Biofilms were formed in M9 medium plus glucose (0.4% wt/vol) under static conditions in microtiter plates at 30°C and stained with crystal violet. The absorbance at 595 nm was measured. Results are the average for at least 3 biological replicates. The horizontal bars represent the median. Statistical analysis was performed by using a nonparametric one-way ANOVA with a Dunn's multiple-comparison post-test (A) and a t-test for seropathotype comparison (B). *: $P<0.05$ **: $P<0.01$.

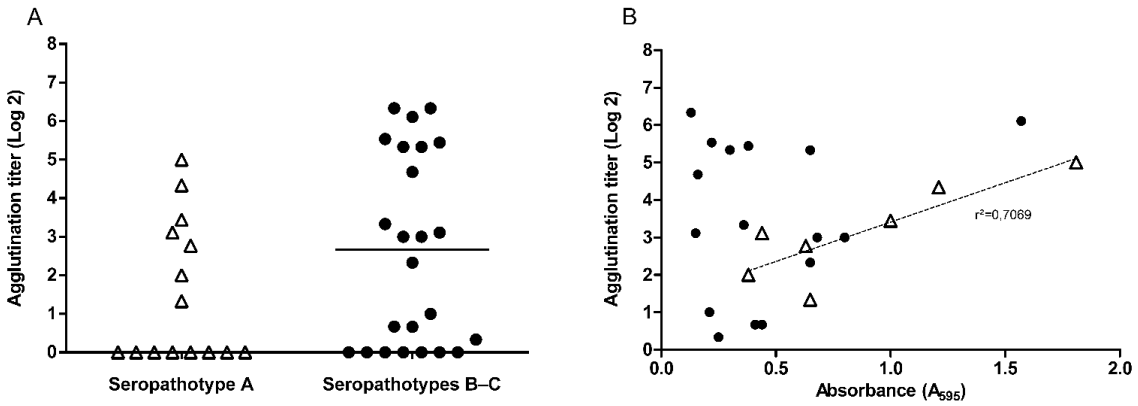

Figure 2. Yeast agglutination of seropathotype A and seropathotype B or C isolates (A) and mannose dependent and independent yeast agglutination in function of biofilm formation (B). Yeast agglutination was determined with 24-h static culture of isolates grown in M9 supplemented with 0.4% glucose. (A) Seropathotype A isolates are represented by filled or open triangles and seropathotype B–C are represented by solid dots. Some seropathotype A and seropathotypes B–C isolates were unable to agglutinate to yeast. The horizontal bars represent the median. (B) A linear regression analysis was made between the yeast agglutination titer and the amount of biofilm formed in static conditions. There was no correlation between mannose-dependent agglutination titer (indicative of type 1 fimbriae production) and biofilm formation (correlation coefficient (r2= 0.01)) represented by solid dots, whereas there was a correlation between mannose-independent agglutination isolates represented by open triangles and biofilm formation (r2= 0.70) represented by open triangles. Results are the average for at least 3 biological replicates.

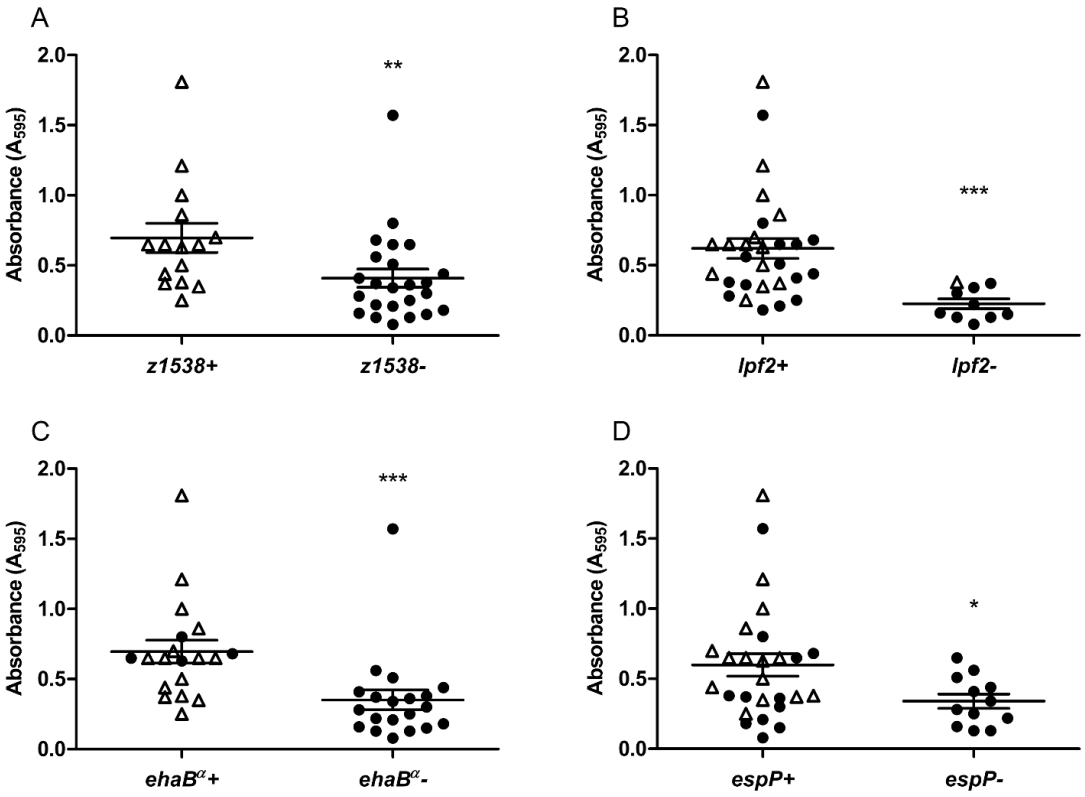

Figure 3. Biofilm formation and presence of fimbrial genes: *z1538* (A); *lpf2* (B); and autotransporter genes *ehaB*β (C) and *espP* (D). Open triangles represent seropathotype A isolates and solid dots represent seropathotype B–C isolates. The longer horizontal bars represent the mean and the shorter error bars represent the standard error of the mean. Statistical analysis was performed by using a Mann-Whitney test with two-tailed distribution. *: P<0.05; **: P<0.01; ***: P<0.001.

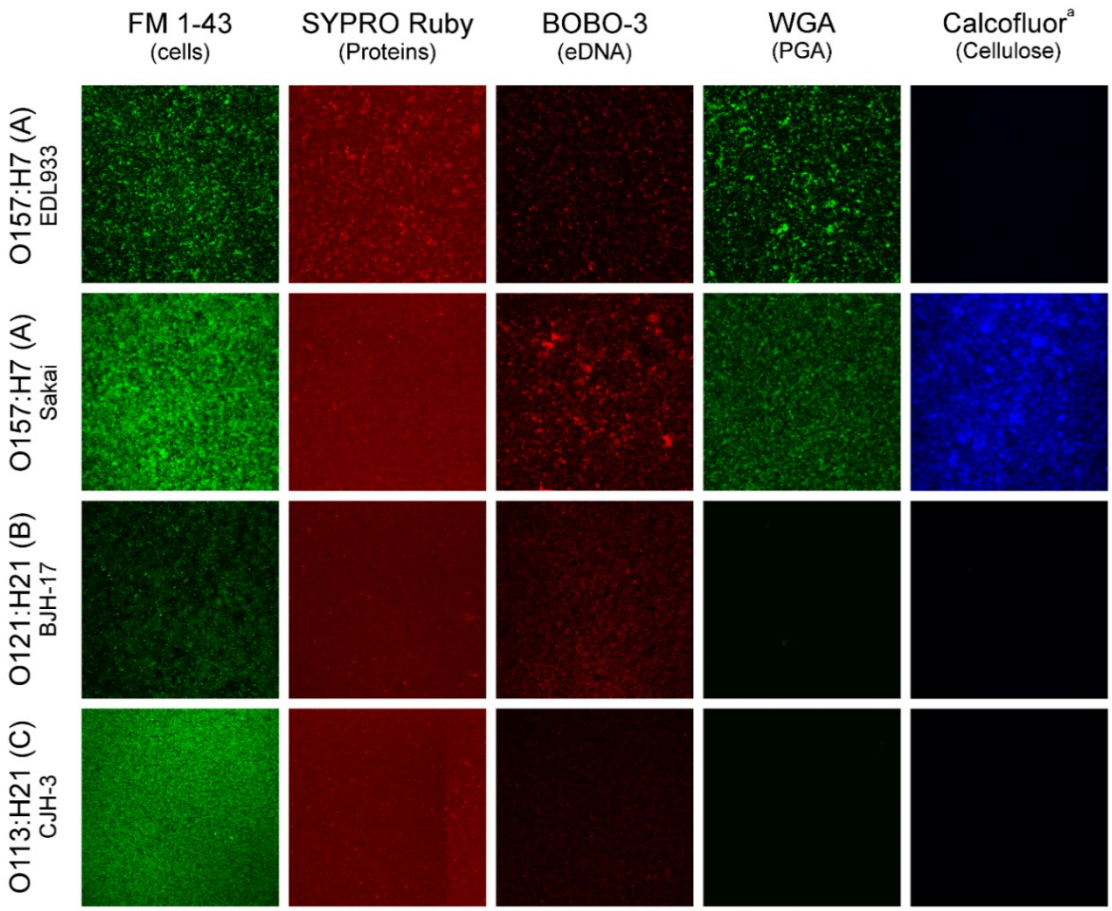

Figure 4. Images of 4 STEC biofilms obtained by CLSM. Biofilms were formed under static conditions in wells of microtiter plates and stained with FilmTracer™ FM 1–43, SYPRO Ruby, BOBO-3, wheat-germ agglutinin (WGA)-Oregon green 488 and calcofluor. The four isolates shown in figure 4 were selected to represent results obtain for the others 11 isolates.A field-of-view representative of 3 biological replicates is show for each isolate.

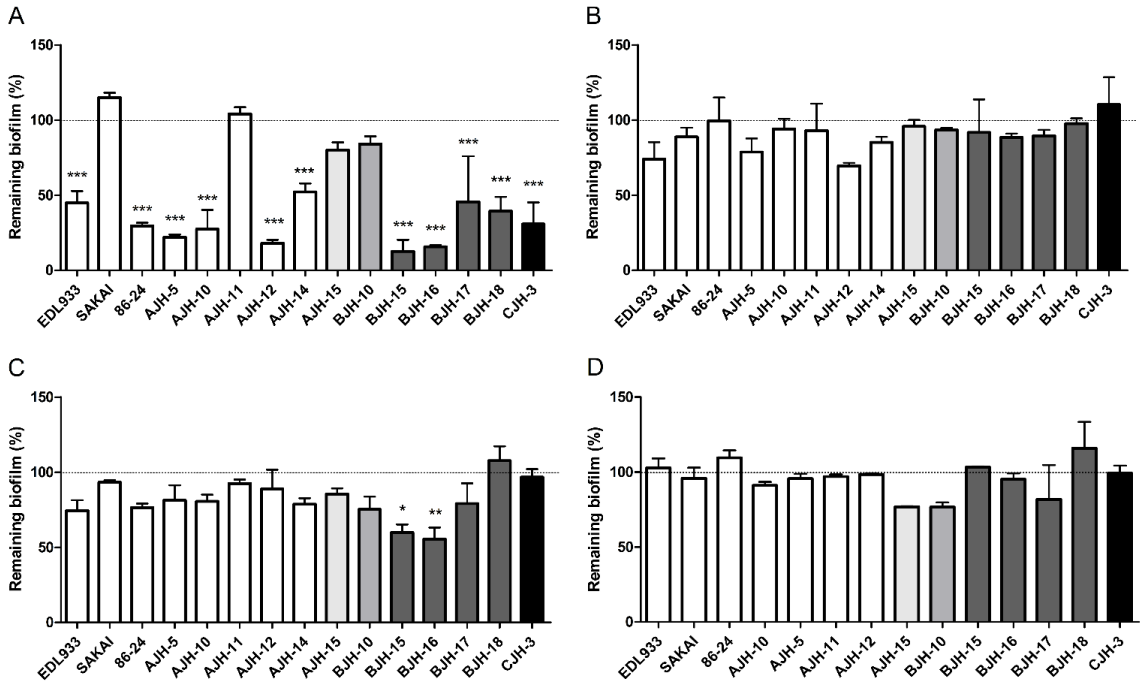

Figure 5. Effect of enzymatic treatments on STEC biofilms. Dispersion of STEC biofilms formed under static conditions in microtiter plates by proteinase K (A), DNase I (B), cellulose (C), and dispersin B (D). Results are the average for at least 3 biological replicates. The horizontal bars represent the mean and the shorter error bars represent the standard error of the mean. Statistical analysis was performed by using a nonparametric one-way ANOVA with a Dunn's multiple-comparison post test.*: $P<0.05$; **: $P<0.01$; ***: $P<0.001$.

SUPPLEMENTAL DATA

Tableau S1. Primers used in this study

	Primers name	Gene (name)	Primer sequence 5' → 3'	References
Autotransporter	*ehaA*$^{\alpha}$-F	z0402 (*ehaA*)	ATATCGGCTAAAGTGGAACAGG TCC	(18)
	ehaA$^{\alpha}$-R		CCTAACGCTAACTCAGAGTTGG TGC	This study
	ehaA$^{\alpha}$-F		GACGGGTGAGCAGAAACAAAC C	(18)
	ehaA$^{\alpha}$-R		ATCCAGGTAACCTGTGCTTGCG	(18)
	ehaB$^{\alpha}$-F	z0469 (*ehaB*)	AGTGCATGACTACTGATTGTGC TG	(18)
	ehaB$^{\alpha}$-R		CACATTAAACAAACCGCTCTGG	(18)
	ehaB$^{\beta}$-F		CCGTTGTTCTGCAACAGATGG	(18)
	ehaB$^{\beta}$-R		TCACCGTTCACATCGTTATCG	(18)
	ehaC$^{\alpha}$-F	yfaL (*ehaC*)	ATGAATGTCGGCGA(T/C)ACGC	(18)
	ehaC$^{\alpha}$-R		AGCGTACCGGA(G/A)GCGATTT G	(18)
	ehaC$^{\beta}$-F		ATGGTCAGACGCTGAATTTACG	(18)
	ehaC$^{\beta}$-R		TCCCTTTCTGCCACGCCACG	(18)
	ehaD$^{\alpha}$-F	ypjA (*ehaD*)	CACAACCATAAATGGTGGTCG	(18)
	ehaD$^{\alpha}$-R		TCTTTCTCAACAACCTGCCG	(18)
	ehaD$^{\beta}$-F		ATTCTCTGGGCGGCTATGCC	(18)
	ehaD$^{\beta}$-R		TTCCACGGGGATTCCACACC	(18)
	ehaG$^{\alpha}$-F	z5029 (*ehaG*)	GTGGAATGTTGTCGTCGTTTGG G	This study
	ehaG$^{\alpha}$-R		CTCTCGACTGGCTACCATTA	This study
	ehaG$^{\beta}$-F		AATACCCAGAGCATTACTAACC TG	(24)
	ehaG$^{\beta}$-R		TTGGGTCTACAAATTACAAGGT	(24)
	saa-F	LH0174 (saa)	CGTGATGAACAGGCTATTGC	(32)
	saa-R		ATGGACATGCCTGTGGCAAC	(32)
	espP-F	L7020 (e*spP*)	AAACAGCAGGCACTTGAACG	(62)
	espP-R		GGAGTCGTCAGTCAGTAGAT	(62)
	yejO-F	z3449 (*yejO*)	CTAACACTCCACAATCCGTC	This study
	yejO-R		CGCAAATTACCCCTTCAACC	This study
	Primers name	**Gene (name)**	**Primer sequence 5' → 3'**	**References**

Fimbriae	*loc1-F*	z0024	CTGGTCTCATTCTGGTCA	This study
	loc1-R		GGATGTCGATCAAGGAAC	This study
	loc2-F	z0152 (*yadN O157)*	AAAAGCACTTCTCGCAGC	This study
	loc2-R		GGCTGTTCGGTGCTTTAA	This study
	loc2b-F	ECO26_0144 (yadN nonO157)	TTGCTGTTTGGTCTGCGA	This study
	loc2b-R		CAGTGGTCTGGTTGTTGA	This study
	loc3-F	*z0686* (*sfmA*)	GCGGTACAATTCACTTTGAAGG	(31)
	loc3-R		CATTTGCTTGCCCTGCTGATGC	(31)
	loc4-F	*z0872* (*ybgD*)	TGTTCCATCCAGGCAAAG	This study
	loc4-R		GTGAAGTTATTGAAGCACC	This study
	loc5-F	*z1286* (*ycbQ*)	CTGTGGTATGTGCAACGTCC	(31)
	loc5-R		CCCCGTAGCGATATAATCAAC	(31)
	loc6-F	*z1538*	CCTACAGTCACTTTTCAGGG	(31)
	Loc6-R		GATTAATTAGAGGTAGCTCAGG	(31)
	loc7-F	*z2206*	CCAGTATTTTTCCATTACGC	This study
	loc7-R		CCGGTGGAGTTGTCATAA	This study
	loc8-F	*z1676* to *z1677* (*csgA-CsgC*)	CAGGTGTTGTTCCTCAGT	This study
	loc8-R		AAAGTGCCGCAAGGAGTAA	This study
	loc9-F	*z3277* (*yehB*)	TACCGAAGGTGATTGTGC	This study
	loc9-R		GATGCTTATGTCAATGGGC	This study
	Loc10-F	*z3601*	CTGCTTCGCTTTGCCTTT	This study
	Loc10-R		CTGGAAGTTGATATGGGTG	This study
	Loc11-F	*z4498* (*yraH*)	CTTTTCGCAGGTAATGCCG	(31)
	Loc11-R		TTAACGACAGCGTCTGCTTC	This study
	loc12-F	*z4968*	GTAACCRACGCGGGTATCAA	This study
	loc12-R		GCAGCAGGATTACTGGAA	This study

Tableau S2. Quantification of biofilm formation by STEC isolates in microtiter plates and in the microfluidic device. [a] Values are average (standard errors) of at least three independent replicates. [b] Absorbance read at 595nm after crystal violet staining. c % of area covered by the biofilm or cells.

Serotypes	Name	Seropathotype	Static biofilm[a,b]	Dynamic biofilm[a,c]
O157:H7				
	EDL933	A	0.86 (±0.29)	12 (±0.6)
	Sakai	A	1.81 (±0.48)	35 (±2)
	86 - 24	A	0.63 (±0.06)	**88 (±2)**
	AJH-4	A	0.25 (±0.11)	**90 (±1)**
	AJH-5	A	0.65 (±0.19)	**76 (±12)**
	AJH-6	A	0.38 (±0.06)	**67 (±6)**
	AJH-7	A	0.44 (±0.11)	**78(±2)**
	AJH-8	A	0.50 (±0.31)	**82 (±2)**
	AJH-9	A	0.31 (±0.06)	**97 (±2)**
	AJH-10	A	0.65 (±0.18)	**76 (±3)**
	AJH-11	A	1.21 (±0.39)	28 (±4)
	AJH-12	A	0.61 (±0.06)	**80 (±9)**
	AJH-13	A	0.37 (±0.02)	24 (±5)
	AJH-14	A	0.70 (±0.15)	**97 (±1)**
O157:NM				
	AJH-15	A	1.00 (±0.17)	23 (±5)
O157:H26				
	CJH-1	C	0.34 (±0.16)	**99 (±0.3)**
O26:H11				
	BJH-1	B	0.18 (±0.06)	**86 (±4)**
	BJH-2	B	0.35 (±0.07)	**65 (±33)**
	BJH-3	B	0.38 (±0.13)	9 (±2)
	BJH-4	B	0.21 (±0.067)	44 (±3)
O45:H2				
	BJH-5	B	0.22 (±0.04)	44 (±3)
	BJH-6	B	0.13 (±0.05)	27 (±3)
	BJH-7	B	0.13 (±0.03)	31 (±1)
	BJH-8	B	0.16 (±0.04)	43 (±1)
O103:H2				
	BJH-9	B	0.30 (±0.13)	37 (±5)
O111:H8				
	BJH-10	B	0.61 (±0.3)	**67 (±6)**
	BJH-11	B	0.25 (±0.1)	53 (±6)

O111:NM				
	BJH-12	B	0.43 (±0.25)	11 (±1)
	BJH-13	B	0.41 (±0.11)	**61 (±2)**
	BJH-14	B	0.28 (±0.09)	19 (±1)
O121:H19				
	BJH-15	B	0.68 (±0.31)	**93 (±3)**
	BJH-16	B	0.65 (±0.30)	**92 (±10)**
	BJH-17	B	0.65 (±0.19)	**75 (±4)**
	BJH-18	B	0.80 (±0.30)	**87 (±4)**
O145:H25				
	CJH-2	C	0.37 (±0.12)	**82 (±2)**
O145:NM				
	BJH-19	B	0.15 (±0.12)	**99 (±1)**
	BJH-20	B	0.51 (±0.30)	**96 (±1)**
	BJH-21	B	0.08 (±0.09)	**82 (±4)**
O113:H21				
	CJH-3	C	1.57 (±0.32)	**84 (±4)**

Tableau S3. Number of STEC colonies positive for Congo red or calcofluor staining classified by séropathotypes. [a] Results are average for 3 independent biological replicates. [b] Number in parentheses indicates number of isolates.

Seropathotype [b]	M9-Congo Red[a]					M9-Calcofluor[a]				
	30°C		37°C		All conditions	30°C		37°C		All conditions
	24 h	48 h	24 h	48 h		24 h	48 h	24 h	48 h	
A (15)	0	9	7	15	15	0	2	0	1	3
B (21)	5	12	10	19	19	2	9	7	8	11
C (3)	0	3	1	2	3	0	1	0	0	1
Total (39)	5	24	18	36	37	2	12	7	9	15

Tableau S4. Serotype distribution of autotransporter and fimbrial genes among STEC strains.

Serotype	No of strains	No. of strains positive by PCR for autotranpsorters genes:												
		ehaA $^{\alpha}$	*ehaA* $^{\beta}$	*ehaB* $^{\alpha}$	*ehaB* $^{\beta}$	*ehaC* $^{\alpha}$	*ehaC* $^{\beta}$	*ehaD* $^{\alpha}$	*ehaD* $^{\beta}$	*ehaG* $^{\alpha}$	*ehaG* $^{\beta}$	*saa*	*espP*	*yejO*
O157:H7 (A)	14	14	14	14	14	14	14	14	14	14	14	0	14	14
O157:NM (A)	1	1	1	1	1	1	1	0	1	0	1	0	1	1
O157:H26 (C)	1	0	0	0	1	1	1	1	1	1	0	0	0	1
O26:H11 (B)	4	4	4	0	4	4	4	0	0	4	4	0	4	4
O45:H2 (B)	4	4	4	0	4	4	4	0	0	4	4	0	0	4
O103:H2 (B)	1	1	1	0	1	1	1	1	1	1	1	0	1	1
O111:H8 (B)	1	1	1	0	0	1	1	0	0	1	1	0	0	1
O111:NM (B)	4	4	4	0	4	4	4	0	0	4	4	0	0	4
O121:H19 (B)	4	4	4	4	4	4	4	0	0	4	4	0	3	3
O145:H25 (C)	1	1	1	0	1	1	1	1	0	1	1	0	1	1
O145:NM (B)	3	3	3	0	3	3	3	1	0	3	3	0	2	2
O113:H21 (C)	1	1	1	0	1	1	1	0	0	1	1	1	1	0
Total	**39**	38	38	19	38	39	39	15	17	38	38	1	27	36

		No. of strains positive by PCR for fimbrial genes:													
		z0024	*yadN*	*sfmA*	*ybgD*	*ycbQ*	*z1538*	*z2206*	*sgA-csgC*	*yehB*	*z3601*	*yraH*	*z4968*	*z5122-z5*	*fim*
O157:H7 (A)	14	14	14	14	14	14	14	13	14	14	14	14	14	13	14
O157:NM (A)	1	1	1	1	1	1	1	1	1	1	1	1	1	1	1
O157:H26 (C)	1	0	1	1	1	1	0	1	1	1	1	1	1	0	1
O26:H11 (B)	4	0	4	4	4	4	0	3	4	4	4	4	4	4	4
O45:H2 (B)	4	0	4	4	4	4	0	4	4	2	4	4	4	0	4
O103:H2 (B)	1	0	1	1	1	1	0	1	1	1	1	1	1	0	1
O111:H8 (B)	1	0	1	1	1	1	0	1	1	0	1	1	1	1	1
O111:NM (B)	4	0	4	4	4	4	0	4	4	4	4	4	4	4	4
O121:H19 (B)	4	0	4	4	4	4	0	4	4	0	4	4	4	4	4
O145:H25 (C)	1	1	1	1	1	1	0	1	1	1	1	1	1	0	1
O145:NM (B)	3	2	3	3	3	2	0	3	3	3	3	2	2	1	3
O113:H21 (C)	1	0	1	1	1	1	0	1	1	0	1	1	0	1	1
Total	**39**	18	39	39	39	38	15	37	39	31	39	38	37	29	39

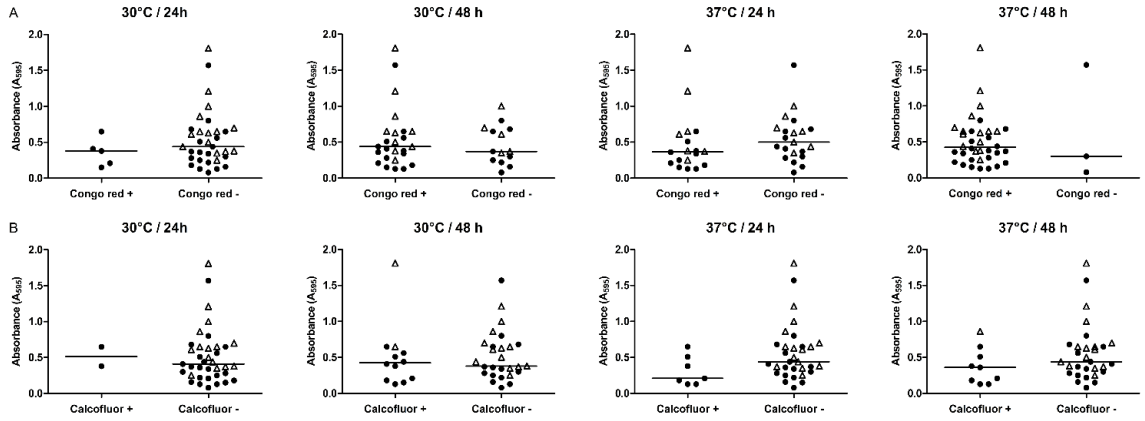

Figure S1. Biofilm formation and Congo red (A) or calcofluor white staining (B). The ability to bind CR on M9-CR agar (A) or CF on M9-CF agar (B) after 24 h or 48 h of incubation at 30°C or 37°C was not correlated neither with the 24 h biofilm formed in M9 plus glucose (0.4% wt/vol) in microtiter plates at 30°C, nor with seropathotypes. Open triangles represent seropathotype A isolates and filled dots represents seropathotypes B–C isolates. Results are the average for 3 independent biological replicates. The horizontal bars represent the median. Statistical analysis was performed by using a Mann Whitney test with two-tailed distribution.

IV. Section IV - Étude du rôle du régulon Pho dans la formation de biofilm des *Escherichia coli* O157 :H7

IV.1 Article de recherche 2: *Escherichia coli* O157:H7 répond à la carence en phosphate en modifiant les molécules de LPS impliquées dans la formation de biofilm

Philippe Vogeleer, Antony T. Vincent, Samuel M. Chekabab, Steve J. Charette, Alexey Novikov, Martine Caroff, Francis Beaudry, Mario Jacques, Josée Harel

Objectif de l'article : Les objectifs de cet article étaient d'étudier l'effet de la carence en phosphate sur la formation de biofilm de *E. coli* O157:H7 et d'identifier les facteurs qui contribue à la formation de biofilm et potentiellement régulés par le régulateur PhoB.

Contribution de l'étudiant : En tant que premier auteur de cet article, j'ai effectué la quasi totalité des expérimentations, analysé l'ensemble des résultats et écrit le manuscrit. Le traitement des résultats de séquençage a été fait par le Dr. Antony T. Vincent et la préparation des échantillons pour la puce de microarray a été faite par le Dr. Samuel M. Chekabab. L'analyse par spectromètre de masse des molécules de LPS a été réalisée par la compagnie LPS-Biosciences. Pour ce papier, Jean-Félix Sicard m'a aidé pour le criblage de la banque de mutant. J'ai également coordonné et assemblé les corrections de mes collaborateurs et soumis le manuscrit au journal « Journal of Bacteriology ». Cet article est également disponible en preprint sur le site bioRxiv (https://www.biorxiv.org/content/10.1101/536201v1) et porte le doi suivant : doi.org/10.1101/536201.

Escherichia coli O157:H7 responds to phosphate starvation by modifying LPS involved in biofilm formation

Philippe Vogeleer[a], Antony T. Vincent[b], Samuel M. Chekabab[c], Steve J. Charette[b], Alexey Novikov[d], Martine Caroff[d], Francis Beaudry[e], Mario Jacques[f], Josée Harel[a]#

[a]Groupe de Recherche sur les Maladies Infectieuses en Production Animale, Centre de Recherche en Infectiologie Porcine et Avicole, Faculté de médecine vétérinaire, Université de Montréal, Saint-Hyacinthe, QC, Canada.

[b]Institut de biologie intégrative et des systèmes, Faculté des sciences et de génie, Université Laval, Québec, QC, Canada.

[c] Food and Bioproduct Sciences, College of Agriculture and Bioresources, University of Saskatchewan, Saskatoon, SK, Canada

[d]LPS-BioSciences, Campus d'Orsay, Université Paris-Saclay, Orsay, France.

[e]Groupe de Recherche en Pharmacologie Animale du Québec, Département de Biomédecine Vétérinaire, Faculté de Médecine Vétérinaire, Université de Montréal, Saint-Hyacinthe, QC, Canada.

[f]Op+Lait, Regroupement de recherche pour un lait de qualité optimale, Faculté de Médecine Vétérinaire, Université de Montréal, Saint-Hyacinthe, QC, Canada.

Running Head: EHEC Biofilm formation upon phosphate starvation

#Address of correspondence : Josée Harel, Faculté de médecine vétérinaire, Université de Montréal, 3200 Sicotte, Saint-Hyacinthe, Québec, Canada J2S 2M2. Tel.: 450-773-8521 (ext. 8233); Fax: 450-778-8108; E-mail: josee.harel@umontreal.ca

ABSTRACT

In open environments such as water, enterohemorrhagic *Escherichia coli* O157:H7 responds to inorganic phosphate (Pi) starvation by inducing the Pho regulon controlled by PhoB. The phosphate-specific transport (Pst) system is the high-affinity Pi transporter. In the Δ*pst* mutant, PhoB is constitutively activated and regulates the expression of genes from the Pho regulon. In *E. coli* O157:H7, the Δ*pst* mutant, biofilm, and autoagglutination were increased. In the Δ*pst* Δ*phoB* mutant, biofilm and autoagglutination were similar to the wild-type strain, suggesting that PhoB is involved. We investigated the relationship between PhoB activation and enhanced biofilm formation by screening a transposon mutant library derived from Δ*pst* mutant for decreased autoagglutination and biofilms mutants. Lipopolysaccharide (LPS) genes involved in the synthesis of the LPS core were identified. Transcriptomic studies indicate the influence of Pi-starvation and *pst* mutation on LPS biosynthetic gene expression. LPS analysis indicated that the O-antigen was deficient in the Δ*pst* mutant. Interestingly, *waaH*, encoding a glycosyltransferase associated with LPS modifications in *E. coli* K-12, was highly expressed in the Δ*pst* mutant of *E. coli* O157:H7. Deletion of *waaH* from the Δ*pst* mutant and from the wild-type strain grown in Pi-starvation conditions decreased the biofilm formation but without affecting LPS. Our findings suggest that LPS core is involved in the autoagglutination and biofilm phenotypes of the Δ*pst* mutant and that WaaH plays a role in biofilm in response to Pi-starvation. This study highlights the importance of Pi-starvation in biofilm formation of *E. coli* O157:H7, which may affect its transmission and persistence.

IMPORTANCE Enterohemorrhagic *Escherichia coli* O157:H7 is a human pathogen responsible for bloody diarrhea that can lead sometimes to renal failure and even death. In the environment, O157:H7 can survive for prolonged periods of time under nutrient-deprived conditions. Biofilms are thought to participate in this environmental lifestyle. Previous reports have shown that the availability of extracellular inorganic phosphate (Pi) affected bacterial biofilm formation; however, nothing was known about O157:H7 biofilm formation. Our results show that O157:H7 membrane undergoes modifications upon PhoB activation leading to increased biofilm formation. A mutation in the Pst system results in the disruption of O-antigen production and this could influence the biofilm composition. This demonstrates how the *E. coli*

O157:H7 adapts to Pi starvation increasing its ability to occupy different ecological niches.

Keyword: EHEC, biofilm, phosphate, LPS, Pho regulon

INTRODUCTION

The human enteric pathogen Enterohemorrhagic *E. coli* O157:H7 (EHEC) is responsible for severe collective food-borne infections. Introducing and then consuming contaminated food into production chains contaminates humans. Cattle, the most important reservoir of pathogenic EHEC, are the main agents of its dissemination into the environment (1). Although fully equipped to infect and colonize the host's intestine, *E. coli* O157:H7 must also be able to respond to changing environmental conditions and to adapt its metabolism to nutrient availability (2).

Phosphorus, one of the most important elements for bacterial growth and survival is 3% of the total dry weight of bacterial cells and the fifth main element after carbon (50%), oxygen (20%), nitrogen (14%), and hydrogen (8%) (3, 4). At the cellular level, phosphorus is in its ionic form called phosphate (PO_4^{3-}) and inorganic phosphate (Pi) is the preferred phosphate source (5). Phosphate is found in many different components of the cell including cell membrane (phospholipids), nucleic acids (the backbone of DNA or RNA), proteins, and complex sugars (e.g. lipopolysaccharides [LPS]). It is also involved in signal transduction (phosphotransfer) and energy production (ATP) (6). Due to its importance for bacteria, phosphate homeostasis is tightly regulated by the two-component regulatory system PhoBR, in which PhoR is a histidine kinase and PhoB is the response regulator controlling expression of genes belonging to the Pho regulon. When the extracellular Pi concentration is high (Pi>4μM), PhoB is inactive and phosphate (Pho) regulon is at the basal expression level, avoiding the use of more complex forms of phosphate. With some environmental changes like nutrient availability and age of culture; and extracellular Pi concentration decreases (below 4 μM) PhoB is activated and regulates the expression of Pho regulon gene leading to changes in phosphate metabolism and transport. Under phosphate-limiting conditions, phosphate transport is controlled by the Pst system encoded by *pstSCAB-phoU* operon belonging to the Pho regulon (6). Any deletion of the *pstSCAB-phoU* operon constitutively activates PhoB leading to constitutive expression of the Pho regulon that results in mimicking phosphate-starvation conditions (7).

In addition to being involved in phosphate homeostasis, the Pho regulon has been connected to bacterial virulence and biofilm formation in several species including *Pseudomonas aeruginosa*, *P. aureofaciens*, *P. fluorescens*, *Agrobacterium tumefaciens*, *Vibrio*

cholerae, *Bacillus anthracis*, and *Cronobacter sakazakii* (8−15). Recent studies established that *E. coli* O157:H7 strains are able to form biofilms in different environments such as food surfaces, processing plants, and water (16, 17). Although EHEC biofilm formation appears to be strain-dependent, low-temperature conditions favor its formation (18, 19). Stress conditions including nutrient starvation or low oxygen influence biofilm formation by altering the oxidative stress leading to increased release of Shiga-toxin linking pathogenicity, biofilm formation, and stress (20).

In this study, we hypothesized that in EHEC, activation of the regulator PhoB controls the expression of genes that are involved in biofilm formation. Therefore, we investigated biofilm formation of EHEC under phosphate-starvation conditions. By screening a mutant library for decreased ability to agglutinate and to form a biofilm, genes in LPS biosynthetic pathways were over-represented. Further analysis revealed that LPS from the Δ*pst* mutant is lacking O-antigen repeats and that its core oligosaccharide was necessary for biofilm formation and agglutination. The glycosyltransferase coding gene *waaH* contributes to Pho regulated biofilm formation. This study highlighted the importance of phosphate-starvation conditions in EHEC biofilm formation that may impact its persistence.

RESULTS

Pi limitation promotes biofilm lifestyle of *E. coli* O157:H7. To investigate the effect of Pi starvation on *E. coli* O157:H7 biofilm formation, strain EDL933 was cultivated in high Pi (1.32 mM) or low Pi (1 μM) media in static conditions at 30°C. In low Pi conditions, the relative biofilm formation of EDL933 was 6.15 higher than in high Pi (Fig. 1A). This shows that in low Pi conditions *E. coli* O157:H7 biofilm lifestyle favor being in a biofilm over a planktonic lifestyle like floating as single cells in water (Fig. S1). In previous work, we established that under low Pi conditions, PhoB was activated (21). This allows us to suggest that PhoB could regulate the expression of genes that are related to biofilm formation.

Deletion of *pst* increases biofilm formation and autoagglutination. To further investigate the contribution of the Pho regulon in biofilm formation and autoagglutination, we used a series of mutants in which the Pho regulon is constitutively activated (Δ*pst* mutant) or Pho regulon is not activated (Δ*phoB* single mutant and Δ*phoB* Δ*pst* double mutant) (Table 1). The Pho regulon activation status of mutants was confirmed by measuring alkaline phosphatase reporter activity (Fig. S2).

The relative biofilm formation and the autoagglutination phenotype of Δ*pst* mutant in M9 conditions were significantly increased compared to EDL933 (Fig. 1B and 1C). Low biofilm level was restored to wild-type status in a *pst*-complemented strain. Single deletion of *phoB* appeared to have no impact on either biofilm formation or on autoagglutination. However, the double-deletion mutant, Δ*phoB* Δ*pst*, demonstrated low ability to form a biofilm (Fig. 1B). These results correlated with the Pho regulon activation (Fig. S2). Consequently, the activation of PhoB is required to enhance agglutination and biofilm formation of a Δ*pst* mutant.

The Δ*pst* mutant biofilm contains N-acetylglucosamine (GlcNAc). The higher biofilm formation of the Δ*pst* mutant was observed by confocal laser scanning microscopy (CLSM) with the FM1-43 stain confirming the crystal violet data (Fig. 2A). Moreover, while the Δ*pst* mutant appeared to form a much denser biofilm compared to EDL933, *pst*-complemented strains and a Δ*pst* Δ*phoB* mutant, had no difference in biofilm thickness (Fig. 2A). Also, while planktonic growth was almost abolished in low Pi conditions (Fig. S1B), biofilm density and thickness were similar to high Pi conditions (Fig. 2B). This last point

highlighted that in low Pi conditions, biofilm lifestyle is favored over planktonic lifestyle. By using fluorophores that stained proteins (Sypro), cellulose (Calcofluor), or N-acetylglucosamine (GlcNAc) residues (WGA), biofilm was characterized. Protein and cellulose were not detected in any biofilm matrices (data not shown). Interestingly, GlcNAc residues were detected in biofilm matrix formed by the Δ*pst* mutant and were absent in those formed by EDL933 and Δ*pst* + *pst*-complemented strain. Notably, GlcNAc residues were also detected in the Δ*pst ΔphoB* double-mutant matrix, indicating that this characteristic of the matrix is not due to PhoB activation. The absence of GlcNAc in the biofilm matrix of wild type strain grown in low Pi conditions (Fig. 2B) was also confirmed. Taken together, CLSM results confirmed that the Δ*pst* mutant formed denser biofilm than the wild type and that GlcNAc residues were contained in its matrix.

Identification of putative Pho regulon members involved biofilm formation. To identify Pho regulon members involved in enhanced biofilm and agglutination phenotypes of Δ*pst* mutant, a mini-Tn*10* transposon mutant library was generated from the Δ*pst* mutant. A total of 5118 mini-Tn*10* Cm^R mutants were screened for their reduced ability to autoagglutinate. From a total of 122 mutants displaying an autoagglutination phenotype different from Δ*pst* mutant, 93 (1.8% of the library) showed reduced ability to form a biofilm. Using high-throughput sequencing, 88 transposon insertion sites were identified (Table S2). Targeted genes were regrouped by categories of orthologous groups (COG) (Fig. 3). While the majority of genes had unknown functions, a high proportion of mutations associated with decreased biofilm formation was located in genes affecting the membrane and cell wall biosynthesis including genes of the LPS R3 core synthesis (*waa* locus).

Transposon insertion sites of several mutants are in LPS core synthesis genes. Five independent insertions that resulted in the loss of biofilm formation were identified in *waaC*, *waaE*, *waaF*, *waaG*, and *waaQ* from the LPS core oligosaccharide biosynthesis (*waa*) locus (Fig. 4A–C). In *E. coli* O157, the majority of enzymes required for core oligosaccharide assembly are encoded by genes within the chromosomal *waa* locus (22). The mutation sites were in genes *waaE* (also named *hldE),* involved in the synthesis of the heptose precursor (23); in genes *waaF* and *waaC* (encoding by the *rfaD-waaFCL* operon) that are responsible for the

addition of heptose I and II on the LPS core; and in genes *waaQ* and *waaG* (encoding by the *waaQGP* operon) involved in the addition of Heptose III and glucose I on the LPS core (Fig. 4A and 4B and Table S2). This result strongly suggests that LPS core synthesis is important for autoagglutination and biofilm formation of the Δ*pst* mutant. Moreover, the biofilm matrices of those Tn*10* mutants were negative for WGA staining (Fig. 4D), suggesting that an intact inner and outer LPS core structure is necessary for biofilm formation and that the detection of GlcNAc on the biofilm matrix is linked to the LPS structure of Δ*pst* mutant.

Concomitantly our transcriptomic studies supported the influence of *pst* mutation and Pi starvation on the LPS biosynthetic pathway. Many genes involved in lipid A, core and O-unit biosynthesis and export were downregulated in both the Δ*pst* mutant and during Pi starvation conditions (Table 2), suggesting that LPS synthesis could also be under the direct or indirect control of PhoB. *In silico* analysis identified putative Pho boxes in proximity to genes and/or operons involved in the different steps of LPS biosynthesis (Table 2) suggesting that genes involved in LPS synthesis could also be under the direct or indirect control of PhoB.

O-antigen is absent from LPS of the Δ*pst* mutant. The LPS pattern of planktonic and biofilm cells of the Δ*pst* mutant were analyzed by SDS-PAGE. The LPS molecules of *E. coli* O157:H7 comprise a R3 type core oligosaccharide (core OS) linked to the hydrophobic lipid A molecule, and are substituted by the long chain O157 antigenic polysaccharide (22). The SDS-PAGE LPS profile was examined to determine whether the *pst* mutation is accompanied by major changes to the LPS structure. LPS preparations were isolated either from cells grown in LB, or from biofilm, and planktonic cells grown in M9. Strain EDL933 and its Δ*pst* mutant differed mainly in the absence of O-specific chains in the mutant. Some differences were also observed for the stained molecular species migrating to the lower region of the gel corresponding to signals in the lower mass region of the MALDI mass spectrum. These are short chain LPS for EDL933 consisting of the lipid A and the core OS, together with the same plus one, two, or three additional repeats of O-units. The electrophoretic profiles of this LPS lower mass region was different in the Δ*pst* mutant. In this case, the core plus lipid A region is present and similar to that observed for the EDL933 strain, i.e. represented by a double band. At the same time, the bands corresponding to additional O-units are absent, and a weak additional band is present, migrating slightly less than the lipid A plus core (Fig. 5A). In the EDL933 LPS

preparation, the upper signal of the double band is very weak. These structural features are identified by MALDI-MS analysis and will be discussed in details in the MALDI-MS section.

Using Western blot analysis with anti-O157 monoclonal antibodies, O157 LPS-specific regular banding pattern was observed in EDL933, however band intensity was very weak in the Δ*pst* mutant (Fig. 5B). Thus, the Δ*pst* mutant predominantly produces rough type LPS species.

To further investigate LPS structure modifications, we used MALDI-TOF mass spectrometry to analyze the LPS extracts of EDL933 and the Δ*pst* mutant grown in LB medium ; and from biofilm and planktonic cells grown in M9 minimal medium (Fig. 6). We first analyzed the LPS polysaccharide or oligosaccharide moieties, isolated by mild acid hydrolysis. The studied *m/z* range corresponded to the low molecular weight species that were observed in the low mass-region of the SDS-PAGE (Fig. 5A). The negative-ion MALDI mass-spectra of the PS moieties of LPS isolated from different culture conditions of the EDL933 and those from cultures of the Δ*pst* mutant are presented in Figure 6. For better clarity, we set the upper limit of the presented *m/z* range at 2800u, which corresponds to the core plus one repeating O-chain unit. However, molecular ions containing up to three O-chain units were clearly detected for the wild-type strain. In the *m/z* region 1700-2100 of all the spectra presented in Figure 6, peaks corresponding to $[M-H]^-$ molecular ions of the core oligosaccharide were observed and will be further detailed. In the 2500-2800 region of all spectra of the EDL933 strain, the same pattern of peaks was observed shifted at 699 mass units. This shift corresponds to the mass of one repeating O-chain unit of *E. coli* O157 LPS O antigen, consisting of -GalNAc-PerNAc-Fuc-Glc- (24). As mentioned above, and in accordance to the SDS-PAGE data, we observed for the wild-type strain, molecular ion peaks corresponding to the addition of one, two and three repeating O-chain units (data not shown). The lack of an O-chain in the Δ*pst* mutant was confirmed by the absence of peaks corresponding to one or two O units (+ 699 u). Instead, for each culture condition, we observed a group of peaks shifted at plus 365 mass units relative to the peaks of the core oligosaccharide molecular species. This group of peaks could correspond to the weak additional band observed in SDS-PAGE for the mutant LPS. The mass of 365u of this additional structural element could be interpreted in different ways, e.g. a disaccharide unit containing a hexose (Hex) plus N-acetyl-hexose (HexNAc) or Hex plus pyrophosphoryl-ethanolamine (PPEA).

Core oligosaccharide structures varied as a function of culture conditions in a similar way for both strains. LPS core structures corresponded to R3 core type and were found in LPS from both EDL933 and the Δ*pst* mutant. On the basis of the characterized core structure (22), after hydrolysis, a major peak at 1868 m/z present in all six spectra (Figure 6) corresponds to the core region including a structure with 1 molecule of Kdo (the second Kdo is released during hydrolysis); 3 heptose (Hep); 4 Hex; and 2 HexNAc. For both strains grown in LB conditions, the major peaks appear at *m/z* 1868, 1948 and 1991. According to Kaniuk and collaborators, the last two peaks correspond respectively to addition of one phosphate (P) or one phosphoryl-ethanolamine (PEA) (22). A minor peak at *m/z* 1825 can be interpreted by the absence of an Ac group on one of the branched GlcN. All these peaks are also observed in spectra corresponding to the M9 cultures of both strains, however they are relatively small. Under these conditions two peaks at *m/z* 1906 and 2029 become major ones for both strains and can be interpreted by addition of P and PEA to the molecular species at *m/z* 1825 lacking one Ac. Such variability has previously been reported (22).

Lipid A structures are different between WT and mutant strains, and further modified according to culture conditions. The negative-ion mass-spectra of lipid A isolated from the EDL933 wild-type strain and the Δ*pst* mutant are presented in Figure 7A. They correspond to the WT and mutant grown under three different culture conditions, i.e. LB culture, M9 planktonic culture, and M9 biofilm culture. Peaks of three major molecular species were observed at *m/z:* 1797.4, 1920.5 and 2035.8, corresponding respectively to the non-modified *E. coli* classical hexa-acyl molecular species, the hexa-acyl molecular species with one phosphate group being substituted with a PEA residue, and a hepta-acyl molecular species with palmitoylation at the secondary C-2 position. The structures of this well-known molecular species are presented in Figure 7B. While the non-modified hexa-acyl molecular species is equally observed in all six mass spectra, the modified ones are differentially represented according to the different strains, and under different culture conditions.

Our data suggest that the substitution of the phosphate group with PEA is strongly increased when the wild-type strain is grown in minimal medium (M9) compared to growth in rich medium (LB). This is not the case for the Δ*pst* mutant for which the presence of the PEA substituted molecular species seems to be independent of growth conditions. It is also somewhat

intermediate between the two extreme levels observed for the EDL933 strain, i.e. higher than in the EDL933 LB culture and lower in both EDL933 M9 cultures.

As for the palmitoylated molecular species, these components are nearly absent in EDL933 LB and M9 planktonic cultures, as well as in the Δ*pst* mutant grown in LB. For EDL933, palmitoylated species are limited but detectable under M9 biofilm conditions. For the Δ*pst* mutant, palmitoylated species are reduced under M9 planktonic conditions, and considerably increased under M9 biofilm conditions. These observations suggest that lipid A palmitoylation in both strains is favored in the biofilm state. This is in line with our earlier findings (25). For the Δ*pst* mutant, the lipid A palmitoylation might be somewhat higher than for the wild-type strain in minimal medium (M9), since it is observed even in the M9 planktonic culture, while it is strongly inhibited in the rich medium (LB) for both strains.

The regulator PhoB is not involved in the absence of O-antigen. To assess the role of the regulator PhoB in the absence of O-antigen production in the Δ*pst* mutant, LPS from the Δ*pst* Δ*phoB* mutant and from wild-type EDL933 cells grown in low Pi conditions were analyzed by Western blot (Fig. 5B). While the Δ*pst* Δ*phoB* mutant was deficient in O-antigen, EDL933 made an O-chain antigen when grown in low Pi conditions. Moreover, PhoB complementation of the Δ*pst* Δ*phoB* mutant did not restore O-antigen (Fig. 5B). These results suggest that the absence of O-antigen is not under PhoB control and is specific to the *pst* mutation. (Fig 1A and 5B).

***waaH* encoding a glycosyltransferase contributes to biofilm formation.** While most of the genes involved in the biosynthesis and export of LPS were all downregulated, the gene *waaH* encoding for a predicted glycosyltransferase was strikingly upregulated in the Δ*pst* mutant (+45.9) and in low Pi conditions (+80.3) (Table 2). Klein *et al.* showed that *waaH* was responsible of the addition of glucuronic acid (GlcUA) on the third heptose of LPS R2 type core in *E. coli* K-12 strain but not for the R3 type core of O157 LPS (26−28) (Fig. 6). No modification corresponding to the GlcUA mass (176 u) was observed in the Δ*pst* mutant by MALDI-TOF analysis (Fig. 6). No difference in LPS patterns between Δ*waaH* single and Δ*pst* Δ*waaH* double mutant was observed by SDS-PAGE or Western blot (Fig. 8A and Fig. S7). Interestingly, biofilm formation was significantly reduced in the Δ*pst* Δ*waaH* double mutant (Fig. 8B), and in

the Δ*waaH* single mutant in low Pi conditions (Fig. 8C). However, the deletion of *waaH* did not affect the autoagglutination phenotype (data not shown). Thus, WaaH plays a role in biofilm formation in a Pho-dependant manner. Pho box consensus sequences were identified *in silico* in the promoter region of *waaH* of *E. coli* O157:H7 EDL933; and EMSA results showed PhoB dose-dependent shifts of the probes designed from the promoter region of *waaH* of EDL933 (Fig. S6A). Finally, Pho-regulated WaaH plays a role in *E. coli* O157:H7 biofilm formation in response to Pi-starvation and in the Δ*pst* mutant and is not associated with GlcUA addition to O157 LPS.

DISCUSSION

PhoB favors biofilm formation. In this study, we show that activation of the transcriptional regulator PhoB promotes biofilm formation in phosphate-starvation conditions and in the *pst* mutant where PhoB is derepressed. Activation of PhoB has been shown to affect biofilm formation in different bacterial species (8, 9, 11, 12, 14, 15, 29). Upon depletion of phosphate, the plant pathogen *A. tumefaciens* was shown to increase its biofilm formation. This was linked to the higher production of the unipolar polysaccharide adhesin (30). In pathogenic *E. coli*, phosphate limitation was shown to affect adhesion of enteropathogenic *E. coli* (31) and to increase virulence (21). In view of these results, we suggest that PhoB activation through phosphate starvation could have positive or negative effects on biofilm formation depending on species or even pathotype.

LPS are important for biofilm formation. Our study emphasizes the importance of LPS in biofilm formation and autoagglutination phenotypes of the Δ*pst* mutant as revealed by insertion mutants in genes involved in the core LPS biosynthesis. LPS are surface phosphorylated lipoglycans present in the outer leaflet of the outer membrane of Gram-negative bacteria (32). The LPS of *E. coli* O157:H7 is a tripartite molecule consisting of the hydrophobic anchor lipid A, the core OS, which is divided into the inner and outer core regions, and the O157-antigen polysaccharide (32, 33).

Within the collection of biofilm autoagglutination Tn*10* mutants generated from the Δ*pst* mutant, the transposon was inserted in genes within the *waa* locus that encode for enzymes mediating stepwise assembly of the LPS inner and outer core oligosaccharides (32) (Fig. 4). It

has already been reported that Tn*5* insertion mutants in genes involved in core LPS synthesis or in O157 antigen synthesis, showed a reduced biofilm phenotype (34). An association between inactivation of LPS core synthesis genes and a decrease of biofilm formation was also observed in uropathogenic *E. coli* and *E. coli* K-12 (35). The biofilm negative mutants here have an altered LPS sugar composition and exhibit the deep rough pattern of LPS. A study conducted by Nakao and collaborators revealed that the *hldE* and *waaC* mutants involved in core OS biosynthesis exhibited a deep-rough LPS phenotype and increased biofilm formation (23).

LPS of the Δ*pst* mutant are structurally different compared to the wild-type strain. The LPS structure of the Δ*pst* mutant is modified compared to its wild-type *E. coli* O157:H7. Mass spectrometry results confirmed that LPS of the Δ*pst* mutant are structurally different compared to EDL933 and culture conditions were shown to contribute to structural variability. The following major features were observed: 1) the absence of O-antigen in the mutant and the presence of an additional structure corresponding to 365.4u; 2) non-acetylation of the core lateral GlcN is increased in M9 conditions for both strains; 3) PEA substitution of the lipid A phosphate groups is culture dependent for the wild-type strain and not culture dependent for the mutant; 4) lipid A palmitoylation is increased under biofilm conditions for both strains. Therefore, the Δ*pst* mutant produces rough-type LPS. Interestingly, the O157 antigen is absent upon activation of PagP, an outer membrane enzyme responsible of lipid A palmitoylation (36). Moreover, it was shown that biofilm-associated lipid A palmitoylation is a general feature of Enterobacteriaceae and this was associated with PagP activation in *E. coli* mature biofilm (25). Interruption of the O-antigen in the Δ*per* mutant of *E. coli* O157:H7 has previously been associated with increased autoagglutination (37) and increased adherence to HeLa cells (38). This is in accordance with the autoagglutination phenotype of the Δ*pst* mutant. The addition of elements to core structures, blocking the addition of the O-chain has already been described in *Bordetella* species (39, 40).

Notably, the Δ*pst* Δ*phoB* mutant that lacked the O-antigen LPS chain showed a low biofilm forming phenotype similar to the wild-type strain EDL933 but did not decrease in autoagglutination (Fig. 1B). Moreover, O-antigen was present in EDL933 grown in low Pi conditions. This suggests that the absence of O-antigen is independent of PhoB activation and could be associated with autoagglutination. The absence of the O-antigen might facilitate

autoagglutination of the bacteria by exposing surface molecules involved in the enhanced phenomenon.

Confocal microscopy analyses of Δ*pst* mutant biofilm revealed that its biofilm matrix contained GlcNAc residues. But, these residues were absent in the biofilm matrices of all mutants with transposon inserted in genes involved in LPS biosynthesis (Fig. 2 and Fig. 4). This suggests that detection of GlcNAc in the biofilm matrix was linked to the LPS structure of the Δ*pst* mutant (Fig. 4). In *E. coli* O157:H7, the R3 core type LPS contains two molecules of GlcNAc (22): one linked to the heptose III from the inner core by *wabB* and the other linked to the galactose molecules from the outer core by an unknown protein (22). In addition, deletion of the *pga* operon responsible for poly-N- acetylglucosamine production in mutant Δ*pst* (double mutant Δ*pst* Δ*pgaABCD)* did not influence the biofilm phenotype nor GlcNAc production (Fig. S5). This discards the contribution of poly-N-acetylglucosamine production to the GlcNAc composition of the Δ*pst* mutant biofilm matrix. Although non-acetylation of the core lateral GlcN is increased when cells are grown in M9 medium for both strains (Fig. 6), we propose that detection of GlcNAc in the biofilm matrix could be due to the absence of O157 molecules allowing the core LPS to be more exposed at the surface.

Nutrient-limitation stress during low phosphate availability, activates the Pho and general stress regulons that elicit specific and non-specific responses, respectively (41). Under Pi-starvation conditions the LPS biosynthesis, export genes, and O-antigen biosynthesis genes were differentially expressed in *E. coli* O157:H7 and in the Δ*pst* mutant. We demonstrated that PhoB activation was not related to the absence of O-antigen. In addition, several putative Pho boxes were found upstream of operons and genes that are involved in LPS biosynthesis and export (Table 2). To deal with the stress of phosphate starvation, bacteria rely on different mechanisms to optimize the acquisition and bioavailability of phosphate and to maintain essential biochemical reactions. In this context, modifications of cell wall components such as LPS structures are part of the reorganization of the bacterial cell. Klein and collaborators showed that PhoB can regulate LPS heterogeneity (26, 42). In our study, major structural variations were observed in LPS structures in the Δ*pst* mutant. In addition to the absence of O-antigen and the presence of an additional structure corresponding to 365.4u, the Δ*pst* mutant exhibited a constitutive PEA substitution of the lipid A phosphate groups (Fig. 7). We previously found that lipid A and fatty acid composition are modified in the Δ*pst* mutant of avian pathogenic *E. coli*

(43, 44).

WaaH is a glycosyltransferase involved in biofilm formation. We also show here that the *waaH* (*yibD)* gene under PhoB control contributes to biofilm formation during phosphate starvation of wild-type strain EDL933 and the Δ*pst* mutant. Its expression was strongly induced in both *E. coli* O157:H7 grown in phosphate-starvation conditions and in the Δ*pst* mutant (Table 2). Interestingly, WaaH does not participate in the autoagglutination phenotype observed in Δ*pst* mutants. WaaH has been shown to be responsible for the addition of GlcUA on the inner core LPS of *E. coli* K-12 under phosphate-starvation conditions and under the control of PhoB. GlcUA modification was also observed in *E. coli* B, R2 and R4 core types and in *Salmonella,* but not in *E. coli* O157:H7 R3 core (26). The addition of GlcUA on the LPS core type was not detected by mass spectroscopy in LPS extracted from either EDL933 or from the Δ*pst* mutant. In *E. coli* O157:H7, the R3 core type, heptose III of its R3 core is decorated with GlcNAc by the plasmid-encoded gene *wabB* (Fig. 3). This precludes the addition of GlcUA on Heptose III (22, 26). Although the activity of WaaH in *E. coli* O157:H7 remains unknown, WaaH belongs to the glycosyltransferase 2 family and is conserved across the Proteobacteria phylum. Interestingly, WaaH shares 34% similarity with the glycosyltransferase PgaC, responsible for PGA elongation by adding GlcNAc molecules (26, 45). Thus, WaaH contributes to biofilm formation upon phosphate starvation and PhoB induction, its mechanism remains to be deciphered, but WaaH could be an interesting target for controlling biofilm formation.

CONCLUSION

Various lines of evidence suggest that the Pho regulon and key factors involved in nutritional and other stress responses are interrelated. To survive adverse conditions that may play a role in its transmission, persistence, and virulence *E. coli* O157:H7 has developed strategies such as biofilm formation involving the Pho regulon.

MATERIALS AND METHODS

Bacterial strains. The effect of the Pho regulon on EHEC O157:H7 biofilm formation was investigated using strain EDL933 and its derivative mutants (listed in Table 1). The

EDL933 Δ*pst* and Δ*phoB* mutants were previously constructed (46). The Δ*waaH* mutant and Δ*pst*Δ*phoB* or Δ*pst*Δ*waaH* double mutants were generated by allelic exchange of *phoB* or *waaH* genes using a suicide vector in EDL933 wild-type strain or in the EDL933 Δ*pst* mutant as previously described (47) with some modifications. Using the primers listed in Table S1, a tetracycline resistance cassette from pACYC184 was amplified and flanked by PCR with the 500 bp sequence adjacent to *phoB* or *waaH*. Tetracycline was used to select the Δ*waaH* mutant, and Δ*pst* Δ*waaH,* or Δ*pst*Δ*phoB* double mutants. Deletion of the *pgaABCD* operon was generated in EDL933 Δ*pst* using the lambda Red recombinase system (48) by recombining a chloramphenicol cassette from pKD3 in the *pga* locus of EDL933 Δ*pst*. The deletion of *phoB*, Δ*pgaABCD*, and *waaH* were confirmed by PCR and sequencing. Complementation of *waaH* was performed using the pTrc99a expression plasmid. The *waaH* ORF was amplified from the genome of EDL933 using the primers containing BamHI and SacI site of digestion as listed in Table S1. *waaH* was then inserted into pTRC99a downstream of the isopropyl-β-D-thiogalactopyranoside (IPTG) inducible pTrc promoter. As complementation was observed without induction by IPTG, IPTG was not added to the media. LB cultures were made from one isolated colony at 37°C on LB agar containing antibiotics when required and incubated for 24 h at 37°C. Antibiotics were used at the following concentrations: 10 μg/ml tetracycline (Tc); 50 μg/ml ampicillin (Amp); 25 μg/ml chloramphenicol (Cm); and 50 μg/ml kanamycin (Km).

Static biofilm formation assay. Biofilm formation was investigated as described previously (49) with modifications. Overnight cultures at 37°C in LB media were diluted (1:100) in 5 ml of morpholine propanesulfonic acid (MOPS) minimal medium (Teknova) containing 0.2% (wt/vol) glycerol, thiamine (0.1 μg/mL), and 1.32 mM (MOPS high Pi) KH_2PO_4 or in M9 medium with 0.2% (wt/vol) glycerol and minerals (1.16 mM $MgSO_4$, 2 μM $FeCl_3$, 8 μM $CaCl_2$, and 16 μM $MnCl_2$) and incubated for 24 h at 37°C with antibiotics when required. Effect of high and low phosphate concentration on EDL933 biofilm formation was studied using MOPS culture dilution (1:100) either in MOPS with 1.32 mM (MOPS high Pi) KH_2PO_4 or 1 μM (MOPS low Pi) KH_2PO_4. Biofilm formation of EDL933 and its derivative mutants was studied using M9 medium dilutions (1:100) with 0.2% (wt/vol) glycerol and minerals (1.16 mM $MgSO_4$, 2 μM $FeCl_3$, 8 μM $CaCl_2$, and 16 μM $MnCl_2$) without use of antibiotics. These dilutions were inoculated in triplicate into microtiter plates (Costar® 3370;

Corning, NY, USA). After 24 h of incubation at 30°C, unattached cells were removed by washing three times with distilled water. Plates were dried at 37°C for 15 min and biofilms were stained with 0.1% (wt/vol) crystal violet for 2 min. The crystal violet solution was removed and biofilms were washed three times with distilled water and then dried at 37°C for 15 min. The stain was released with 150 µl of 80% (vol/vol) ethanol and 20% (vol/vol) acetone. The biofilms were quantified by measuring the absorbance at 595 nm with a microplate reader (Powerwave; BioTek Instruments, Winooski, VT, USA). Moreover, while biofilms were stained with crystal violet and measured with the A_{595}, growth of the planktonic part of the culture (unattached cells) was tracked with OD_{600}. Relative biofilm formation corresponds to A_{595}/OD_{600} (50). One-way ANOVA with Dunnett's multiple-comparison post hoc tests were performed to calculate *p*-values.

Autoagglutination assays. Autoagglutination was determined using an assay described by Bansal et al (51) with modifications. EDL933 and its isogenic mutant were cultivated in LB media at 37°C and diluted 1/100 in M9 and incubated at 30°C for 24 h without agitation. After incubation, 100 µl of the upper phase was taken 1 cm below the surface and the OD_{600} was measured (OD_{Agg}). Cultures were then mixed by vortex for 10 s and OD_{600} was measured again (OD_{tot}). The percentage of autoagglutination was calculated by using this formula: $[(OD_{tot}-OD_{Agg}) / OD_{tot}] \times 100$. One-way ANOVA with Dunnett's multiple-comparison post hoc test was performed to calculate *p*-values.

Confocal laser scanning microscopy. Stained biofilms were visualized by confocal laser scanning microscopy at 40X (CLSM; FV1000 IX81; Olympus, Markham, ON, Canada) as previously described (49).

Screening of a Tn*10* Δ*pst* mutant library. Km^R Cm^R independent mutants were screened for the loss of autoagglutination. This assay is based on the ability of the Δ*pst* mutant to autoagglutinate and to form a larger ring at the bottom of a 96-well round microtiter plate compared to wild type (Fig. 1 and Fig. S3). As autoagglutination phenotypes were similar in LB and M9, LB was chosen to facilitate manipulations. Each plate was filled with 150 µl of LB broth and filled with one colony of Δ*pst* mutant containing Tn*10* insertions. In each plate, EDL933 and Δ*pst* mutant were used as negative and positive controls of agglutination

phenotype respectively, and wells containing LB only was used as a blank. After 24 h of incubation at 30°C with agitation, the ring sizes were eyes checked and mutants that loose the ability to form large rings were evaluated two more times for autoagglutination. Those mutants were evaluated for their biofilm formation in M9 broth at 30°C for 24 h, as described above. Mutants that lost the ability to form biofilm similar to the Δ*pst* mutant were stored at -80°C for further analysis. In order to avoid mutants with growth defects, OD_{600} was measured for 24h of incubation at 30°C in M9 broth (Fig. S4).

Identification of mini-Tn*10* insertion sites. Mini-Tn*10* insertion sites of Δ*pst* biofilm negative mutants were identified by DNA sequencing. To extract DNA, each transposon mutant was cultivated separately in LB media and 1 ml of 7 to 10 clones belonging to the same phenotype group were pooled. Genomic DNA was extracted with Qiagen DNeasy blood and tissue kits and pooled at an equimolar concentration in order to prepare a total of three sequencing libraries using KAPA Hyper Prep kit. The libraries were then sequenced using an Illumina MiSeq apparatus at the Plateforme d'Analyses Génomiques of the Institut de Biologie Intégrative et des Systèmes (IBIS, Université Laval). The resulting sequencing reads were mapped on the extremities of the sequence of the Tn*10* transposon using bwa version 0.7.12-r1039 (52). The mapped reads were subsequently converted to fastq format with SAMtools version 0.1.19-44428cd (52) and the Tn*10* transposon sequence was filtered from the reads using cutadapt version 1.10 (53). The resulting filtered reads were mapped using bwa on the genomic sequence of *E. coli* O157:H7 EDL933 (GenBank: AE005174.2). The features about where the reads mapped were found using featureCounts (54), which is included in the package subread version 1.5.0-p3. The presence of the transposon in intergenic regions was investigated using Artemis version 16.0.0 (55). Finally, categories of orthologous groups were analyzed with eggNOG-mapper.

Microarray experiment. EDL933 and its isogenic Δ*pst* mutant were grown in high Pi MOPS 0.2% (wt/vol) glucose condition until the OD600 nm reached 0.6 (56). Samples equal to 5×10^8 CFU were taken from this mid-log phase and processed for transcriptome analysis. One µg of the fragmented and biotinylated cDNAs, were hybridized onto Affymetrix GeneChip® *E. coli*. The data were processed using the FlexArray® software; Robust Multi-array Average (RMA) normalization. The levels of transcription obtained from 3 biological replicates of each

experimental condition were compared using the EB (Wright & Simon) algorithm. The comparison was conducted between the Δ*pst* mutant and the wild-type strain with the differential expression conditions corresponding to a 2-fold change (FC) cut-off and *p*-value < 0.05. Validation of microarray results was achieved by comparing the expression of eleven genes by qRT-PCR. The 16S rRNA gene, *tus*, was included for normalization within samples.

***In silico* evaluation of Pho boxes.** The presence of putative Pho boxes upstream of biofilm-related genes was evaluated with a previously constructed Pho box matrix (21) and was based on 12 known Pho boxes with O157:H7 EDL933 sequences (57). Using MEME suite web site with the FIMO tools version 4.12.0 (http://meme-suite.org/tools/fimo), nucleotide sequences of LPS promoting regions were scanned to find putative motif sequences.

LPS extraction. To extract LPS from planktonic and biofilm cells of EDL933 and its isogenic mutants, each strain was diluted (1/100) and grown in 6 Petri dishes containing 20 ml of M9 media for 24 h at 30°C. Planktonic cells (20 ml) were kept for further analyses. The 6 biofilms were washed with 20 ml of PBS. PBS (1 ml) was added in each plate and biofilms were scratched from the surface with a cell scratcher. Biofilm and planktonic cells were pelleted by centrifugation at 4000 rpm for 15 min and suspended to an OD_{600nm} of 0.6. Then, 1.5 ml of suspension was pelleted in a 2 ml Eppendorf tube at 13.000 rpm for 3 min. The supernatant was discarded and the pellet was stored at -20°C before LPS extraction. LPS was extracted as previously described (58). Briefly, a defrosted pellet was suspended in 50 µl of SDS-buffer (4% β-mercaptoethanol (BME), 4% SDS, and 10% glycerol in 0.1 M Tris-HCl, pH 6.8) and boiled for 10 min. After cooling down, 5 µl of 10 mg/ml solution of DNase I in DNase buffer (150 mM NaCl and 1 mM CaCl2) and 5 µl of 10 mg/ml RNase A in sterile water was added to samples and incubated at 37°C for 30 min. After adding 5 µl of 20 mg/ml proteinase K in proteinase K buffer (50 mM Tris-HCl and 1 mM $CaCl_2$), samples were incubated at 60°C for 1 hour. Each sample was treated with phenol by adding 50 µl of ice-cold Tris-saturated phenol and by incubating at 65°C for 15 min. Phenol treated samples were mixed by vortex every 5 min. Samples were cooled to room temperature and 500 µl of diethyl ether were added and mixed by vortex for 10 s. Samples were centrifuged at 20,600 x g for 10 m and the bottom phase was carefully removed. Phenol treatments were repeated at least three times. Alternatively, for

MALDI-MS analyses, LPS were extracted as described in the MALDI-MS section.

SDS-PAGE and Western blot analysis. Prior to gel electrophoresis, 100 µl of 2X SDS-buffer containing bromophenol blue 0.002% (wt/vol) were added to the extracted sample. 10 µl of LPS extracted sample were separated by electrophoresis on 15% SDS-PAGE at 100 volts for 18 min (upper gel) and then 200 volts for 60 min (lower gel). LPS samples were visualized by using the gel silver staining procedure according to the instructions of the manufacturer (Biorad). Briefly, the gel was covered with a fixative solution (methanol 40% and acid acetic 10% (vol/vol)). After overnight incubation, the gel was covered with 10% (vol/vol) oxidizer for 5 min and then washed 6 to 7 times with water for 15 min. The gels were then exposed to 10% (vol/vol) silver reagent for 20 min. After a 30 s wash in water, gels were developed in 3.2% Developer solution (wt/vol). LPS were also visualized by Western blot. After electrophoresis, polyacrylamide gel was stabilized by covering it with 1X transfer buffer (25 mM Tris-base pH 8.2, 192 mM glycine and 20% (vol/vol) methanol) for 30 min. LPS were then transferred to nitrocellulose membranes (Biorad) at 14 volts. After overnight transfer, the nitrocellulose membrane was blocked in T-TBS with 1% skimmed milk for 1 h. The membrane was washed 3 times with T-TBS and incubated with 1/1000 solution of primary O157:H7 monoclonal antibody (LifeSpan BioSciences) for 1 h 40 min. The membrane was washed three times with T-TBS for 3 x 5 min and incubated for 1 h with 1/1000 solution of horseradish peroxidase (HRP)-conjugated goat anti-mouse IgG antibody (1:1000; Biorad) and washed 3 times with T-TBS and 1 time with TBS. The antigen-antibody reaction was analyzed by using Opti-4CN detection kit according to the instructions of the manufacturer (Biorad).

Mass spectrometry analyses. LPS were extracted from different growth cultures of the wild-type EDL933 strain and its Δ*pst* mutant. The LPS-BioSciences proprietary LPS extraction method (59) was applied to 10 mg quantities of lyophilized bacterial pellets issued from the six bacterial cultures under study, i.e. EDL933 and Δ*pst* LB, M9 planktonic and M9 biofilm cultures. The non-discrimination of molecular species by the extraction procedure were verified by comparison of SDS PAGE profiles of the extracted LPS with those obtained from corresponding non-fractioned bacterial lysates (60).

Polysaccharide (PS) and lipid A moieties of each LPS were analyzed separately by MALDI MS.

Prior to the analyses, crude LPS samples were cleaved under mild acid hydrolytic conditions established in (61). Hydrolysates were lyophilized, and lipid A and PS moieties were extracted subsequently, first with a chloroform-methanol-water mixture for the lipids A, and then with water for the corresponding PS.

Each lipid A and PS samples were mixed on the MALDI target with appropriate matrix solutions and let dry. Di-hydroxy-benzoic acid (DHB) was used as a matrix. For lipid A analysis, DHB was dissolved at 10 µg/µl in 0.1 M citric acid in a chloroform-methanol water mixture and for PS analysis in 0.1 M citric acid in water. Different analyte/matrix ratios were tested.

MALDI MS analyses were performed in linear the negative-ion mode on a Shimadzu AXIMA Performance mass-spectrometer. Negatively charged $[M-H]^-$ molecular ions were desorbed by a 337 nm N2 laser pulses and analyzed in the linear mode. 1000 laser shots were accumulated for each sample (61).

Data availability. Microarray data have been deposited in the Gene Expression Omnibus database https://www.ncbi.nlm.nih.gov/geo/query/acc.cgi?acc=GSE125488 under accession number GSE125488.

ACKNOWLEDGMENTS

We thank Dr. Yannick D.N. Tremblay for sharing his expertise and technical assistance and Frederic Berthiaume for his help with confocal laser scanning microscopy assays. We are grateful to Judith Kashul for editing the manuscript. This work was supported by grants from the Natural Sciences and Engineering Research Council of Canada (RGPIN SD-25120-09) to Josée Harel and Fonds de la recherche du Québec en nature et technologies to Josée Harel and Mario Jacques (FRQNT PT165375) and a scholarship to Philippe Vogeleer from FRQNT Québec Wallonie program (FRQNT Regroupements stratégiques 111946).

REFERENCES

1. Ferens WA, Hovde CJ. 2011. *Escherichia coli* O157:H7: animal reservoir and sources of human infection. Foodborne pathogens and disease 8:465-487.

https://doi.org/10.1089/fpd.2010.0673.

2. Gyles CL. 2007. Shiga toxin-producing *Escherichia coli*: an overview. J Anim Sci 85:E45-62. https://doi.org/10.2527/jas.2006-508.

3. Lodish H, Berk A, Matsudaira P, Kaiser CA, Krieger M, Scott MP, Zipursky L, Darnell J. 2000. Molecular Cell Biology, 4th Edition. New York: W. H. Freeman. https://www.ncbi.nlm.nih.gov/books/NBK21475/.

4. Fagerbakke KM, Heldal M, Norland S. 1996. Content of carbon, nitrogen, oxygen, sulfur and phosphorus in native aquatic and cultured bacteria. Aquatic Microbial Ecology 10:15-27. https://doi.org/10.3354/ame010015.

5. VanBogelen RA, Olson ER, Wanner BL, Neidhardt FC. 1996. Global analysis of proteins synthesized during phosphorus restriction in *Escherichia coli*. Journal of bacteriology 178:4344-4366. https://doi.org/10.1128/jb.178.15.4344-4366.1996.

6. Wanner BL. 1996. Signal transduction in the control of phosphate-regulated genes of *Escherichia coli*. Kidney Int 49:964-7. https://doi.org/10.1038/ki.1996.136.

7. Crepin S, Chekabab SM, Le Bihan G, Bertrand N, Dozois CM, Harel J. 2011. The Pho regulon and the pathogenesis of *Escherichia coli*. Vet Microbiol 153:82-8. https://doi.org/10.1016/j.vetmic.2011.05.043.

8. Monds RD, Silby MW, Mahanty HK. 2001. Expression of the Pho regulon negatively regulates biofilm formation by *Pseudomonas aureofaciens* PA147-2. Mol Microbiol 42:415-26. https://doi.org/10.1046/j.1365-2958.2001.02641.

9. Pratt JT, McDonough E, Camilli A. 2009. PhoB regulates motility, biofilms, and cyclic di-GMP in *Vibrio cholerae*. J Bacteriol 191:6632-42. https://doi.org/10.1128/JB.00708-09.

10. Aggarwal S, Somani VK, Bhatnagar R. 2015. Phosphate starvation enhances the pathogenesis of *Bacillus anthracis*. Int J Med Microbiol 305:523-31. https://doi.org/10.1016/j.ijmm.2015.06.001.

11. Monds RD, Newell PD, Gross RH, O'Toole GA. 2007. Phosphate-dependent modulation of c-di-GMP levels regulates *Pseudomonas fluorescens* Pf0-1 biofilm formation by controlling secretion of the adhesin LapA. Mol Microbiol 63:656-79. https://doi.org/10.1111/j.1365-2958.2006.05539.x.

12. Newell PD, Yoshioka S, Hvorecny KL, Monds RD, O'Toole GA. 2011. Systematic analysis of diguanylate cyclases that promote biofilm formation by *Pseudomonas fluorescens* Pf0-1. J Bacteriol 193:4685-98. https://doi.org/10.1128/JB.05483-11.

13. Liang X, Hu X, Wang X, Wang J, Fang Y, Li Y. 2017. Characterization of the phosphate-specific transport system in *Cronobacter sakazakii* BAA-894. J Appl Microbiol 123:710-723. https://doi.org/10.1111/jam.13524.

14. Danhorn T, Hentzer M, Givskov M, Parsek MR, Fuqua C. 2004. Phosphorus limitation enhances biofilm formation of the plant pathogen *Agrobacterium tumefaciens* through the PhoR-PhoB regulatory system. J Bacteriol 186:4492-501. https://doi.org/10.1128/JB.186.14.4492-4501.2004.

15. Haddad A, Jensen V, Becker T, Haussler S. 2009. The Pho regulon influences biofilm formation and type three secretion in *Pseudomonas aeruginosa*. Environ Microbiol Rep 1:488-94. https://doi.org/10.1111/j.1758-2229.2009.00049.x.

16. Van Houdt R, Michiels CW. 2010. Biofilm formation and the food industry, a focus on the bacterial outer surface. J Appl Microbiol 109:1117-31. https://doi.org/10.1111/j.1365-2672.2010.04756.x.

17. Vogeleer P, Tremblay YD, Mafu AA, Jacques M, Harel J. 2014. Life on the outside: role of biofilms in environmental persistence of Shiga-toxin producing *Escherichia coli*. Front Microbiol 5:317. https://doi.org/10.3389/fmicb.2014.00317.

18. Wang J, Stanford K, McAllister TA, Johnson RP, Chen J, Hou H, Zhang G, Niu YD. 2016. Biofilm Formation, Virulence Gene Profiles, and Antimicrobial Resistance of Nine Serogroups of Non-O157 Shiga Toxin-Producing *Escherichia coli*. Foodborne Pathog Dis 13:316-24. https://doi.org/10.1089/fpd.2015.2099.

19. Ryu JH, Kim H, Frank JF, Beuchat LR. 2004. Attachment and biofilm formation on stainless steel by *Escherichia coli* O157:H7 as affected by curli production. Lett Appl Microbiol 39:359-62. https://doi.org/10.1111/j.1472-765X.2004.01591.x.

20. Villegas NA, Baronetti J, Albesa I, Polifroni R, Parma A, Etcheverria A, Becerra M, Padola N, Paraje M. 2013. Relevance of biofilms in the pathogenesis of Shiga-toxin-producing *Escherichia coli* infection. ScientificWorldJournal 2013:607258. https://doi.org/10.1155/2013/607258.

21. Chekabab SM, Jubelin G, Dozois CM, Harel J. 2014. PhoB activates *Escherichia coli* O157:H7 virulence factors in response to inorganic phosphate limitation. PLoS One 9:e94285. https://doi.org/10.1371/journal.pone.0094285.

22. Kaniuk NA, Vinogradov E, Li J, Monteiro MA, Whitfield C. 2004. Chromosomal and plasmid-encoded enzymes are required for assembly of the R3-type core oligosaccharide in the lipopolysaccharide of *Escherichia coli* O157:H7. J Biol Chem 279:31237-50. https://doi.org/10.1074/jbc.M401879200.

23. Nakao R, Ramstedt M, Wai SN, Uhlin BE. 2012. Enhanced biofilm formation by *Escherichia coli* LPS mutants defective in Hep biosynthesis. PLoS One 7:e51241. https://doi.org/10.1371/journal.pone.0051241.

24. Perry MB, MacLean L, Griffith DW. 1986. Structure of the O-chain polysaccharide of the phenol-phase soluble lipopolysaccharide of *Escherichia coli* O:157:H7. Biochem Cell Biol 64:21-8. https://doi.org/10.1139/o86-004

25. Chalabaev S, Chauhan A, Novikov A, Iyer P, Szczesny M, Beloin C, Caroff M, Ghigo JM. 2014. Biofilms formed by gram-negative bacteria undergo increased lipid a palmitoylation, enhancing in vivo survival. MBio 5. https://doi.org/10.1128/mBio.01116-14.

26. Klein G, Muller-Loennies S, Lindner B, Kobylak N, Brade H, Raina S. 2013. Molecular and structural basis of inner core lipopolysaccharide alterations in *Escherichia coli*: incorporation of glucuronic acid and phosphoethanolamine in the heptose region. J Biol Chem 288:8111-27. https://doi.org/10.1074/jbc.M112.445981.

27. Yoshida Y, Sugiyama S, Oyamada T, Yokoyama K, Kim SK, Makino K. 2011. Identification of PhoB binding sites of the *yibD* and *ytfK* promoter regions in *Escherichia coli*. J Microbiol 49:285-9. https://doi.org/10.1007/s12275-011-0360-6.

28. Baek JH, Lee SY. 2006. Novel gene members in the Pho regulon of *Escherichia coli*. FEMS Microbiol Lett 264:104-9. https://doi.org/10.1111/j.1574-6968.2006.00440.x.

29. Sultan SZ, Silva AJ, Benitez JA. 2010. The PhoB regulatory system modulates biofilm formation and stress response in El Tor biotype *Vibrio cholerae*. FEMS Microbiol Lett 302:22-31. https://doi.org/10.1111/j.1574-6968.2009.01837.x.

30. Xu J, Kim J, Danhorn T, Merritt PM, Fuqua C. 2012. Phosphorus limitation increases attachment in *Agrobacterium tumefaciens* and reveals a conditional functional redundancy in adhesin biosynthesis. Res Microbiol 163:674-84. https://doi.org/10.1016/jresmic.2012.10.013.

31. Ferreira GM, Spira B. 2008. The pst operon of enteropathogenic *Escherichia coli* enhances bacterial adherence to epithelial cells. Microbiology 154:2025-36. https://doi.org/10.1099/mic.0.2008/016634-0.

32. Raetz CRH, Whitfield C. 2002. Lipopolysaccharide endotoxins. Annual Review of Biochemistry 71:635-700. https://doi.org/10.1146/annurev.biochem.71.110601.135414.

33. Kuo CJ, Chen JW, Chiu HC, Teng CH, Hsu TI, Lu PJ, Syu WJ, Wang ST, Chou TC, Chen CS. 2016. Mutation of the enterohemorrhagic *Escherichia coli* core LPS biosynthesis enzyme RfaD confers hypersusceptibility to host intestinal innate immunity *in vivo*. Front Cell Infect Microbiol 6:82. https://doi.org/10.3389/fcimb.2016.00082.

34. Puttamreddy S, Cornick NA, Minion FC. 2010. Genome-wide transposon mutagenesis reveals a role for pO157 genes in biofilm development in *Escherichia coli* O157:H7 EDL933. Infect Immun 78:2377-84. https://doi.org/10.1128/iai.00156-10.

35. Hadjifrangiskou M, Gu AP, Pinkner JS, Kostakioti M, Zhang EW, Greene SE, Hultgren SJ. 2012. Transposon mutagenesis identifies uropathogenic *Escherichia coli* biofilm factors. J Bacteriol 194:6195-205. https://doi.org/10.1128/JB.01012-12.

36. Smith AE, Kim SH, Liu F, Jia W, Vinogradov E, Gyles CL, Bishop RE. 2008. PagP activation in the outer membrane triggers R3 core oligosaccharide truncation in the cytoplasm of *Escherichia coli* O157:H7. J Biol Chem 283:4332-43. https://doi.org/10.1074/jbc.M708163200.

37. Sheng H, Lim JY, Watkins MK, Minnich SA, Hovde CJ. 2008. Characterization of an *Escherichia coli* O157:H7 O-antigen deletion mutant and effect of the deletion on bacterial persistence in the mouse intestine and colonization at the bovine terminal rectal mucosa. Appl Environ Microbiol 74:5015-22. https://doi.org/10.1128/AEM.00743-08.

38. Bilge SS, Vary JC, Jr., Dowell SF, Tarr PI. 1996. Role of the *Escherichia coli* O157:H7 O side chain in adherence and analysis of an *rfb* locus. Infect Immun 64:4795-801.

39. Novikov A, Marr N, Caroff M. 2018. A comparative study of the complete lipopolysaccharide structures and biosynthesis loci of *Bordetella avium*, *B. hinzii*, and *B. trematum*. Biochimie. https://doi.org/10.1016/j.biochi.2018.12.011.

40. Vinogradov E. 2007. The structure of the core-O-chain linkage region of the lipopolysaccharide from *Bordetella hinzii*. Carbohydr Res 342:638-42. https://doi.org/10.1016/j.carres.2006.10.025.

41. Prágai Z, Harwood CR. 2002. Regulatory interactions between the Pho and σB-dependent general stress regulons of *Bacillus subtilis*. Microbiology 148:1593-1602. https://doi.org/10.1099/00221287-148-5-1593.

42. Klein G, Lindner B, Brade H, Raina S. 2011. Molecular basis of lipopolysaccharide heterogeneity in *Escherichia coli*: envelope stress-responsive regulators control the incorporation of glycoforms with a third 3-deoxy-alpha-D-manno-oct-2-ulosonic acid and rhamnose. J Biol Chem 286:42787-807. https://doi.org/10.1074/jbc.M111.291799.

43. Lamarche MG, Kim SH, Crepin S, Mourez M, Bertrand N, Bishop RE, Dubreuil JD, Harel J. 2008. Modulation of hexa-acyl pyrophosphate lipid A population under *Escherichia coli* phosphate (Pho) regulon activation. J Bacteriol 190:5256-64. https://doi.org/10.1128/JB.01536-07.

44. Lamarche MG, Harel J. 2010. Membrane homeostasis requires intact pst in extraintestinal pathogenic *Escherichia coli*. Curr Microbiol 60:356-9. https://doi.org/10.1007/s00284-009-9549-x.

45. Wang X, Preston JF, 3rd, Romeo T. 2004. The *pgaABCD* locus of *Escherichia coli* promotes the synthesis of a polysaccharide adhesin required for biofilm formation. J Bacteriol 186:2724-34. https://doi.org/10.1128/JB.186.9.2724–2734.2004.

46. Chekabab SM, Daigle F, Charette SJ, Dozois CM, Harel J. 2012. Survival of enterohemorrhagic *Escherichia coli* in the presence of *Acanthamoeba castellanii* and its dependence on Pho regulon. Microbiologyopen 1:427-37. https://doi.org/10.1002/mbo3.40.

47. Le Bihan G, Sicard JF, Garneau P, Bernalier-Donadille A, Gobert AP, Garrivier A, Martin C, Hay AG, Beaudry F, Harel J, Jubelin G. 2017. The NAG Sensor NagC Regulates LEE Gene Expression and Contributes to Gut Colonization by *Escherichia coli* O157:H7. Front Cell Infect Microbiol 7:134. https://doi.org/10.3389/fcimb.2017.00134.

48. Datsenko KA, Wanner BL. 2000. One-step inactivation of chromosomal genes in *Escherichia coli* K-12 using PCR products. Proc Natl Acad Sci U S A 97:6640-5. https://doi.org/10.1073/pnas.120163297.

49. Vogeleer P, Tremblay YD, Jubelin G, Jacques M, Harel J. 2015. Biofilm-Forming Abilities of Shiga Toxin-Producing *Escherichia coli* Isolates Associated with Human Infections. Appl Environ Microbiol 82:1448-58. https://doi.org/10.1128/AEM.02983-15.

50. Sicard J-F, Vogeleer P, Le Bihan G, Rodriguez Olivera Y, Beaudry F, Jacques M, Harel J. 2018. N-Acetyl-glucosamine influences the biofilm formation of *Escherichia coli*. Gut Pathogens 10:26. https://doi.org/10.1186/s13099-018-0252-y.

51. Bansal T, Jesudhasan P, Pillai S, Wood TK, Jayaraman A. 2008. Temporal regulation of enterohemorrhagic *Escherichia coli* virulence mediated by autoinducer-2. Appl Microbiol Biotechnol 78:811-9. https://doi.org/10.1007/s00253-008-1359-8.

52. Li H, Durbin R. 2009. Fast and accurate short read alignment with Burrows-Wheeler

transform. Bioinformatics 25:1754-60. https://doi.org/10.1093/bioinformatics/btp324.

53. Martin M. 2011. Cutadapt removes adapter sequences from high-throughput sequencing reads. EMB net journal 17:10-12. https://doi.org/10.14806/ej.17.1.200.

54. Liao Y, Smyth GK, Shi W. 2014. featureCounts: an efficient general purpose program for assigning sequence reads to genomic features. Bioinformatics 30:923-30. https://doi.org/10.1093/bioinformatics/btt656.

55. Carver T, Harris SR, Berriman M, Parkhill J, McQuillan JA. 2012. Artemis: an integrated platform for visualization and analysis of high-throughput sequence-based experimental data. Bioinformatics 28:464-9. https://doi.org/10.1093/bioinformatics/btr703.

56. Lee J, Bansal T, Jayaraman A, Bentley WE, Wood TK. 2007. Enterohemorrhagic *Escherichia coli* biofilms are inhibited by 7-hydroxyindole and stimulated by isatin. Appl Environ Microbiol 73:4100-9. https://doi.org/10.1128/AEM.00360-07.

57. Yuan ZC, Zaheer R, Morton R, Finan TM. 2006. Genome prediction of PhoB regulated promoters in *Sinorhizobium meliloti* and twelve proteobacteria. Nucleic Acids Res 34:2686-97. https://doi.org/10.1093/nar/gkl365.

58. Davis MR, Jr., Goldberg JB. 2012. Purification and visualization of lipopolysaccharide from Gram-negative bacteria by hot aqueous-phenol extraction. J Vis Exp doi:10.3791/3916. https://doi.org/10.3791/3916.

59. Caroff M. 2004. Novel method for isolating endotoxins. patent WO2004062690A1.

60. Hitchcock PJ, Brown TM. 1983. Morphological heterogeneity among *Salmonella* lipopolysaccharide chemotypes in silver-stained polyacrylamide gels. J Bacteriol 154:269-77.

61. Novikov A, Breton A, Caroff M. 2017. Micromethods for Isolation and Structural Characterization of Lipid A, and Polysaccharide Regions of Bacterial Lipopolysaccharides. Methods Mol Biol 1600:167-186. https://doi.org/10.1007/978-1-4939-6958-6_16.

62. Strockbine NA, Marques LR, Newland JW, Smith HW, Holmes RK, O'Brien AD. 1986.

Two toxin-converting phages from *Escherichia coli* O157:H7 strain 933 encode antigenically distinct toxins with similar biologic activities. Infect Immun 53:135-40.

63. Kang HY, Srinivasan J, Curtiss R, 3rd. 2002. Immune responses to recombinant pneumococcal PspA antigen delivered by live attenuated *Salmonella enterica* serovar typhimurium vaccine. Infect Immun 70:1739-49. https://doi.org/10.1128/IAI.70.4.1739-1749.2002.

64. Amann E, Ochs B, Abel KJ. 1988. Tightly regulated tac promoter vectors useful for the expression of unfused and fused proteins in *Escherichia coli*. Gene 69:301-15. https://doi.org/10.1016/0378-1119(88)90440-4.

ILLUSTRATIONS AND TABLES

TABLES

Table 1. Strains and plasmids used in this study.

Strain/Plasmid	Relevant characteristics	Source reference
Strain		
EDL933	*E. coli* O157:H7; wild-type	(62)
Δ*pst*	EDL933 Δ*pst*::*aphA* (Km^R)	(46)
Δ*pst* + *Cpst*	EDL933 Δ*pst*::*aphA* + pACYC184-pst operon (Km^R, Cm^R)	(46)
Δ*phoB*	EDL933 Δ*phoB*::*aphA* (Km^R)	(46)
Δ*pst* Δ*phoB*	EDL933 Δ*pst*::*aphA*; ΔphoB::tet R (Km^R, tc^R)	This study
Δ*pst*Δ*phoB* + *CphoB*	EDL933 Δ*pst*::*aphA*; ΔphoB::tet R + pHSG575-phoBR (Km^R, tc^R, Cm^R)	This study
EDL933 + pwaaH	*E. coli* O157:H7; wild-type + p*waaH (*Ap^R*)*	This study
Δ*waaH*	EDL933; Δ*waaH*::Tet R (Tc^R)	This study
Δ*waaH* + *CwaaH*	EDL933; Δ*waaH*::Tet R + p*waaH* (Tc^R, Ap^R)	This study
Δ*pst* Δ*waaH*	EDL933; Δ*pst::Km* Δ*waaH::Tet R* (Km^R, Tc^R)	This study
Δ*pst* Δ*waaH* + *CwaaH*	EDL933; Δ*pst::Km* Δ*waaH::Tet R* + *pwaaH* (Km^R, tc^R, Ap^R)	This study
χ7213	SM10λpir ΔasdA4, Km^R	(63)
TG1α	K-12 JM101 Δ(*mcrB-hsdSM*)5(*rK–mK–*)	
Plasmid		
pMEG-375	*sacRB mobRP4 oriR6K* Cm^R, Ap^R	S. Tinge, Megan Health Inc
pAN92	pACYC184, *pst* operon	(63)
pHSG575-phoBR	pHSG575, *phoBR*+ Cm^R Km^R	(21)
pTrc99a	expression vector with IPTG inducible lacI promoter; Ap^R	(64)
pwaaH	pTrc99a::waaH; Ap^R	This study
pGEM®-T	Cloning vector	Promega

Table 2. Fold-change of gene expression related to LPS synthesis in the Δ*pst* mutant compared to EDL933.

[a] As a comparison, the microarray fold change of those genes in low Pi compared to high Pi obtained in a previous study are also presented (21). [b] Pho boxes are present upstream of the boldface gene.

Gene	Microarray		Function	Genomic context[b]
	Δ*pst*	Low Pi		
Lipid A synthesis				
lpxD	ND	-2,7	UDP-3-O-[3-hydroxymyristoyl] glucosamine N-acyltransferase	*hlpA-lpxD operon*
lpxT	ND	-2,0	Kdo_2-Lipid A phosphotransferase	*yeiR-lpxT operon*
lpxB	-2,7	-4,4	lipid-A-disaccharide synthase	*fabZ-lpxAB-rhnB-dnaE-accA operon*
Core synthesis				
waaC	ND	-2,7	ADP-heptose:LPS heptosyl transferase I	***rfaD**waaFC**L** operon*
waaF	ND	-2,4	ADP-heptose:LPS heptosyltransferase II	***rfaD**waaFC**L** operon*
waaP	ND	-2,1	LPS core heptose(I) kinase	*waa**Q**GPIYJD operon*
waaQ	-2,7	-2,9	LPS core heptosyltransferase	*waa**Q**GPIYJD operon*
waaL	ND	-2,8	O antigen ligase	***rfaD**waaFC**L** operon*
waaH	+45,9	+80,3	Unknown function in R3 core type	***waaH***
O antigen synthesis				
wzx	-2,9	ND	Putative O antigen transporter	*wbdNwzywbdO**wzx**perwbdPz3198**fcl**wbdQmanCmanB-wbdR operon*
fcI	ND	-2,2	GDP-L-fucose synthase	*wbdNwzywbdO**wzx**perwbdPz3198**fcl**wbdQmanCmanB-wbdR* operon
LPS export				
msbA	-2,2	-2,7	Lipid A export ATP-binding/permease protein	*ycaI**msbA**ycaHycaQ-ycaRkdsB*
lptB	ND	-2,8	LPS export system ATP-binding protein	*yrbGHIK-yhbN**G***
lptC	-2,1	ND	LPS export system protein	*yrbGHIK-yhbN**G***
lptA	-2,5	-2,7	LPS export system protein	*yrbGHIK-yhbN**G***
lptE	ND	-2,2	LPS-assembly lipoprotein	*leuS-lptE-holA-nadD-cobC*
lptD	-3,5	-3,6	LPS-assembly protein	**lptD**-SurA-pdxA-rsmA-apaG-apaH

FIGURES

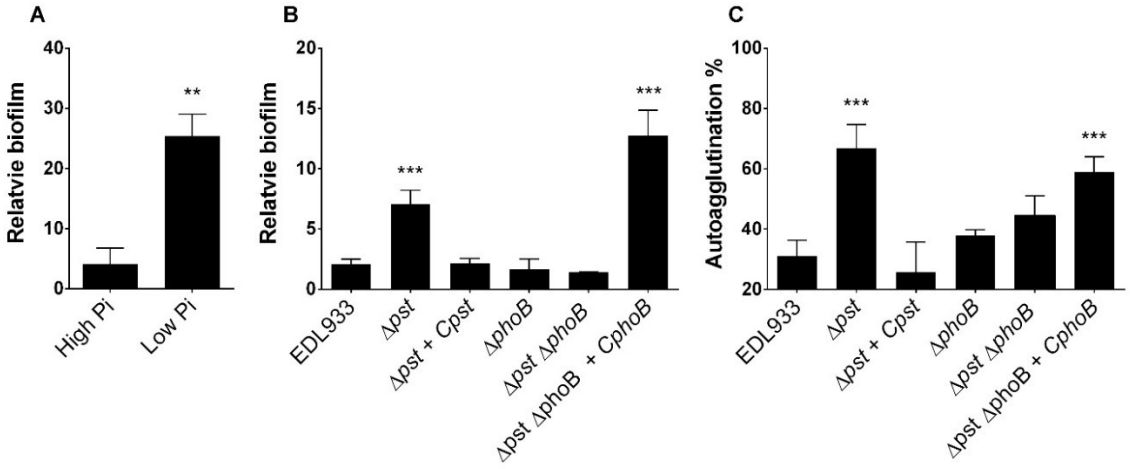

Figure 1. Biofilm and autoagglutination are increased when PhoB is activated. (A) Biofilm of EDL933 formed in MOPS medium containing either 1.32 mM (high Pi) or 1 µM (low Pi) of KH_2PO. (B) Biofilm formation of EDL933 and its isogenic mutants were formed in M9. The biofilms were evaluated under static conditions in microtiter plates at 30°C and stained with crystal violet. Relative biofilm formation corresponds to biofilm formation (A_{595})/planktonic growth (DO_{600}). (C) Autoagglutination was measured after 24 h of growth in M9. Results are averages from at least 3 biological replicates. Statistical analysis was performed using student's t-test (Fig 1A) or one-way ANOVA with Tukey's multiple comparison test (Fig 1B and 1C). ** *P<0.01; *** P<0.001.*

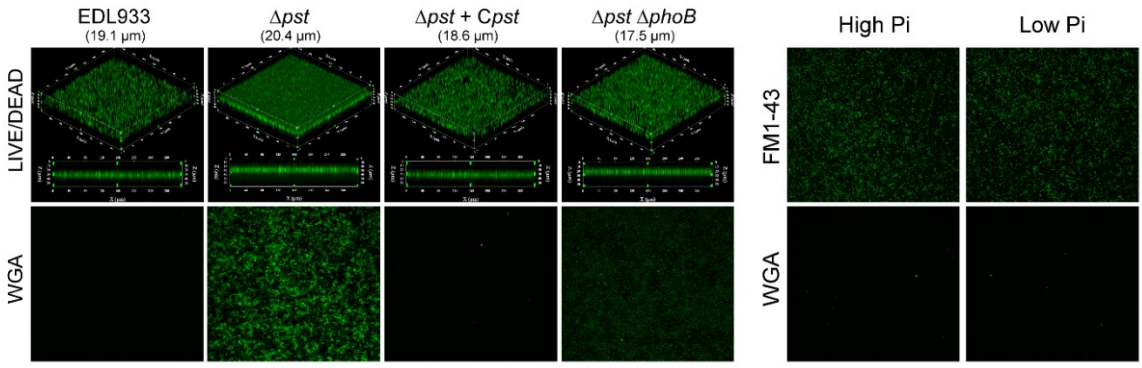

Figure 2. Δ*pst* mutant forms denser biofilm than wild type and exposes GlcNAC residues. Confocal laser scanning microscopy images of 24-h biofilms formed by EDL933 and its derivative mutants. (A) Projections of Z-stacks of biofilm stained with FM1-43 and photographs of biofilm stained with WGA. (B) Photos of EDL933 biofilms grown in MOPS high or low Pi, and stained with FM1-43 or WGA.

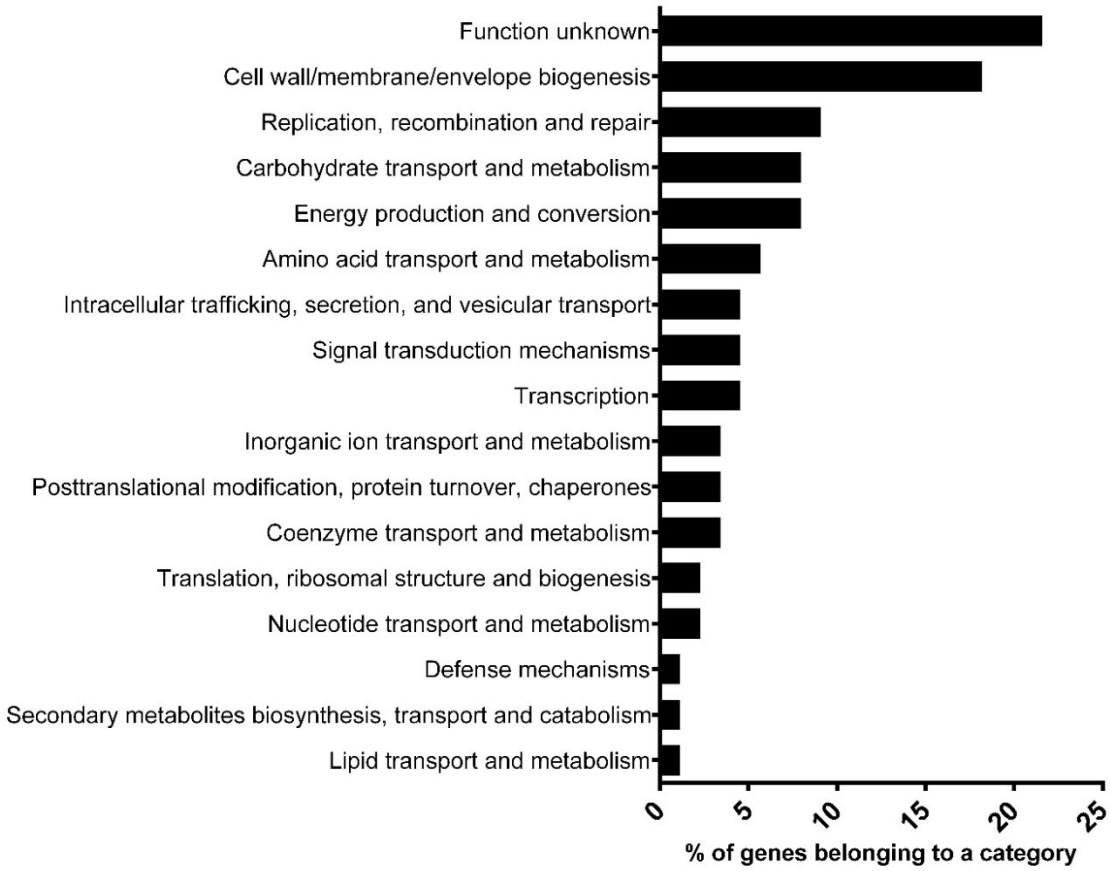

Figure 3. Biofilm and autoagglutination transposon mutants are mainly involved in cell wall synthesis. COG analysis with eggNOG-mapper revealed that transposons of autoagglutination and biofilm-negative mutants were inserted mainly in genes coding for cell wall synthesis and unknown function.

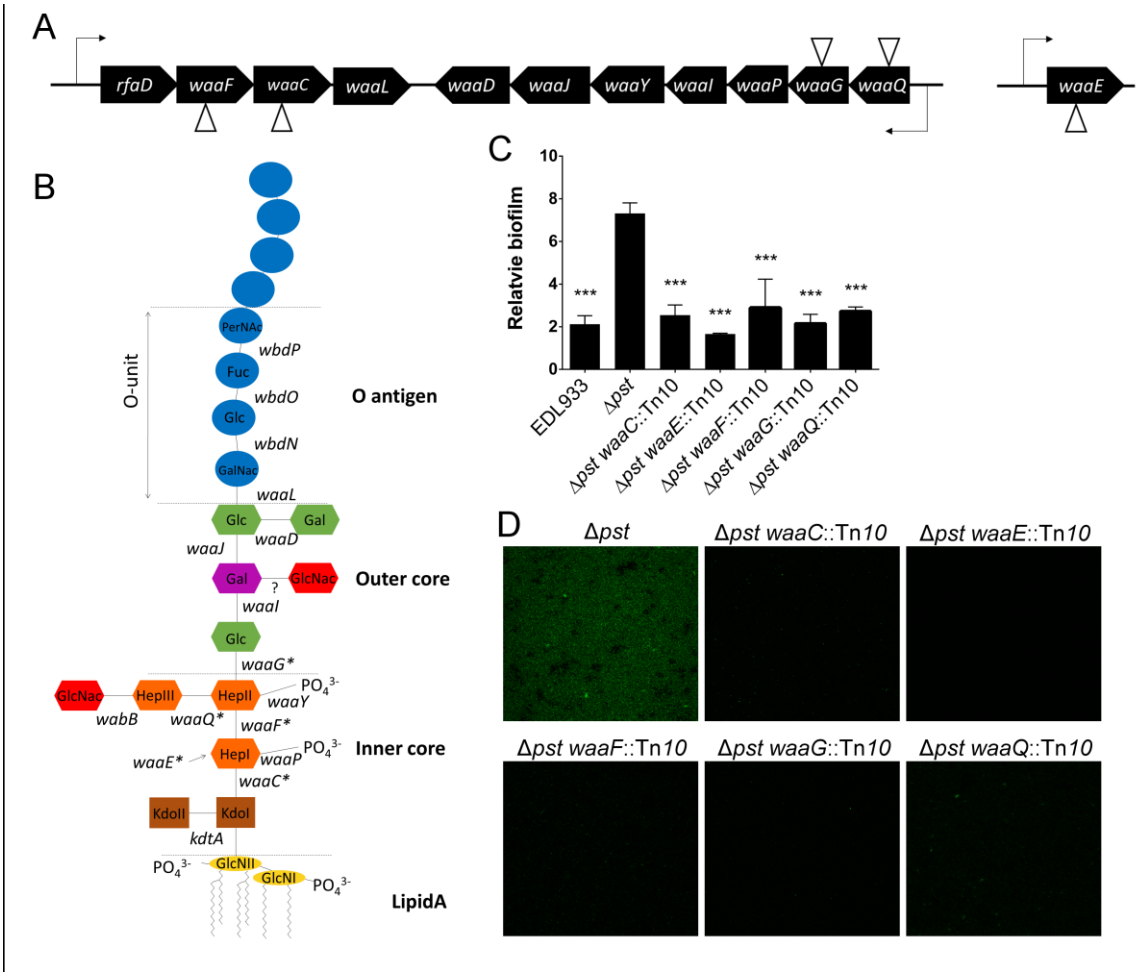

Figure 4. O157 LPS synthesis is important for biofilm formation by the Δ*pst* mutant. (A) Genetic organization of LPS core biosynthesis locus. Tn*10* insertion sites are indicated by triangles (B). Structure of O157 LPS structure. Genes with stars show genes where a transposon was inserted. Gene waaE is involved in the synthesis of ADP-L-glycero-β-D-manno-heptose, the heptose substrate for *waaC*, *waaF*, and *waaQ*. (C) Relative biofilm formation of Δ*pst*-derivative mutants with Tn*10* inserted in LPS synthesis genes in M9 at 30°C for 24 h. Relative biofilm formation corresponds to biofilm formation (A595)/planktonic growth (DO600). Results are averages from at least 3 biological replicates. Statistical analysis was performed using a one-way ANOVA with Tukey's multiple comparison post-test. Stars indicate significant results compared to Δ*pst* mutant *** $P < 0.001$. (D) Confocal laser scanning microscopy images of 24-h biofilms stained with WGA of EDL933, Δ*pst* mutant, and Δ*pst* derivative mutant with Tn10 inserted in LPS synthesis genes grown in M9 at 30°C for 24 h.

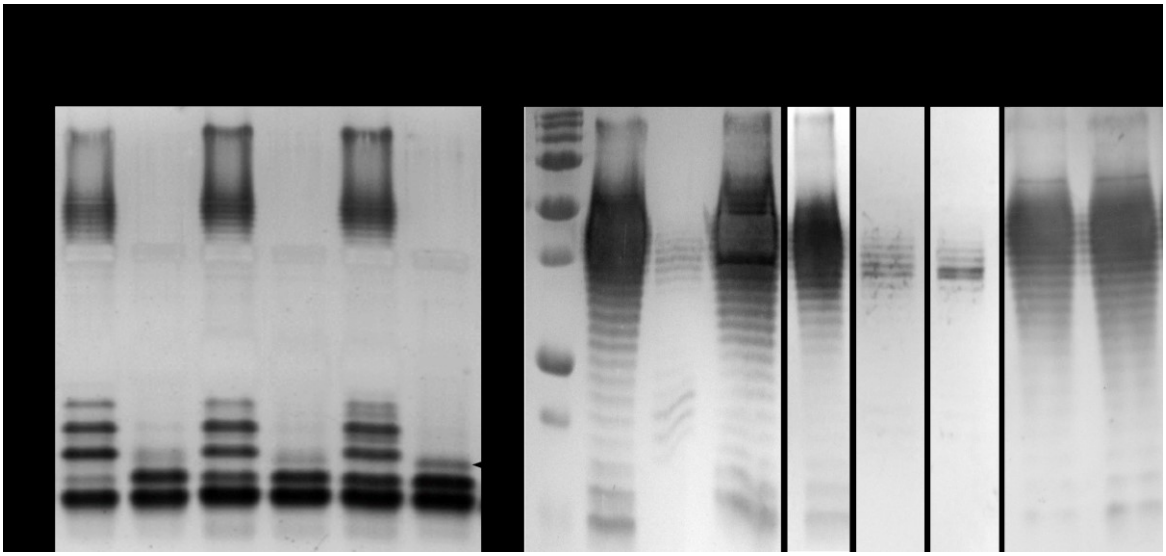

Figure 5. Deletion of *pst* leads to the absence of O157 LPS antigens. (A) LPS of EDL933 and the Δ*pst* mutant grown in LB and as planktonic or biofilm cells in M9 at 30°C were extracted, separated on 15% SDS-PAGE and then stained by silver stain. The black arrow shows the presence of an additional slower migrating band in Δ*pst* LPS extract that was absent in EDL933 LPS extract. (B) Western blot analysis of LPS extracts of EDL933 and its derivative mutants grown as biofilm cells in M9 at 30°C or of EDL933 grown as biofilm cells in MOPS high Pi or low Pi. LPS were revealed by using primary O157:H7 monoclonal antibody (1:1000) and a horseradish peroxidase-conjugated antibody (1:1000).

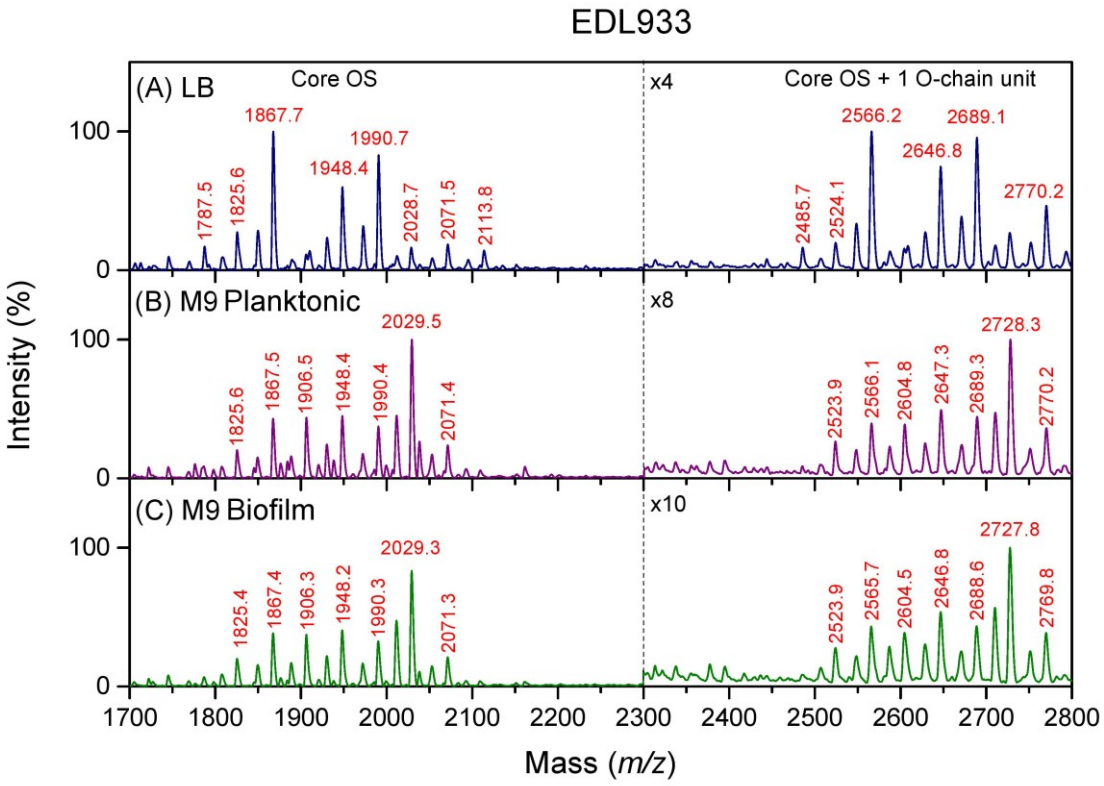
EDL933
(A) LB
Core OS
x4
Core OS + 1 O-chain unit
1867.7
1990.7
1948.4
1787.5
1825.6
2028.7
2071.5
2113.8
2566.2
2689.1
2646.8
2770.2
2485.7
2524.1
(B) M9 Planktonic
x8
2029.5
1825.6
1867.5
1906.5
1948.4
1990.4
2071.4
2728.3
2523.9
2566.1
2604.8
2647.3
2689.3
2770.2
(C) M9 Biofilm
x10
2029.3
1825.4
1867.4
1906.3
1948.2
1990.3
2071.3
2727.8
2523.9
2565.7
2604.5
2646.8
2688.6
2769.8
Intensity (%)
Mass (m/z)

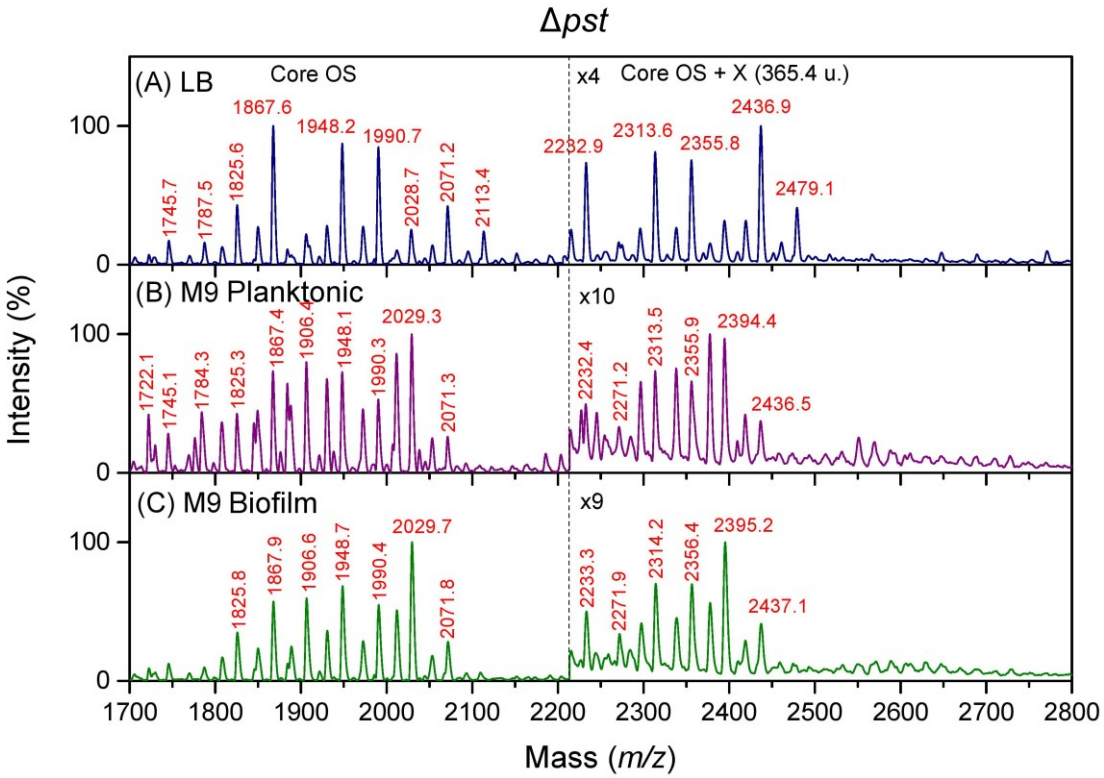
Δpst
(A) LB
Core OS
x4
Core OS + X (365.4 u.)
1867.6
1948.2
1990.7
1745.7
1787.5
1825.6
2028.7
2071.2
2113.4
2232.9
2313.6
2355.8
2436.9
2479.1
(B) M9 Planktonic
x10
2029.3
1722.1
1745.1
1784.3
1825.3
1867.4
1906.4
1948.1
1990.3
2071.3
2232.4
2271.2
2313.5
2355.9
2394.4
2436.5
(C) M9 Biofilm
x9
2029.7
1825.8
1867.9
1906.6
1948.7
1990.4
2071.8
2233.3
2271.9
2314.2
2356.4
2395.2
2437.1
Intensity (%)
Mass (m/z)

Figure 6. LPS of the Δ*pst* mutant are rough and lack O-antigen sugars. Mass spectroscopy analysis of LPS extracted from EDL933 (upper panel) and Δ*pst* mutant (bottom panel) grown in (A) LB or in M9 as planktonic (B) (M9 planktonic) or biofilm (C) (M9 biofilm) reveals the absence of the O chain from LPS of Δ*pst* mutant and presence of an additional peaks shifted at plus 365 mass units from the core peaks, and corresponding to a putative disaccharide. Moreover, this analysis suggests an increase of non-acetylated GlcN in the cores of both strains under M9 culture conditions. To better visualized the mass region between 2200 m/z and 2800 m/z for EDL933 and 2300 m/z and 2800 m/z for Δ*pst* mutant were zoomed-in. Core OS: core oligosaccharide; X: unknown structural element.

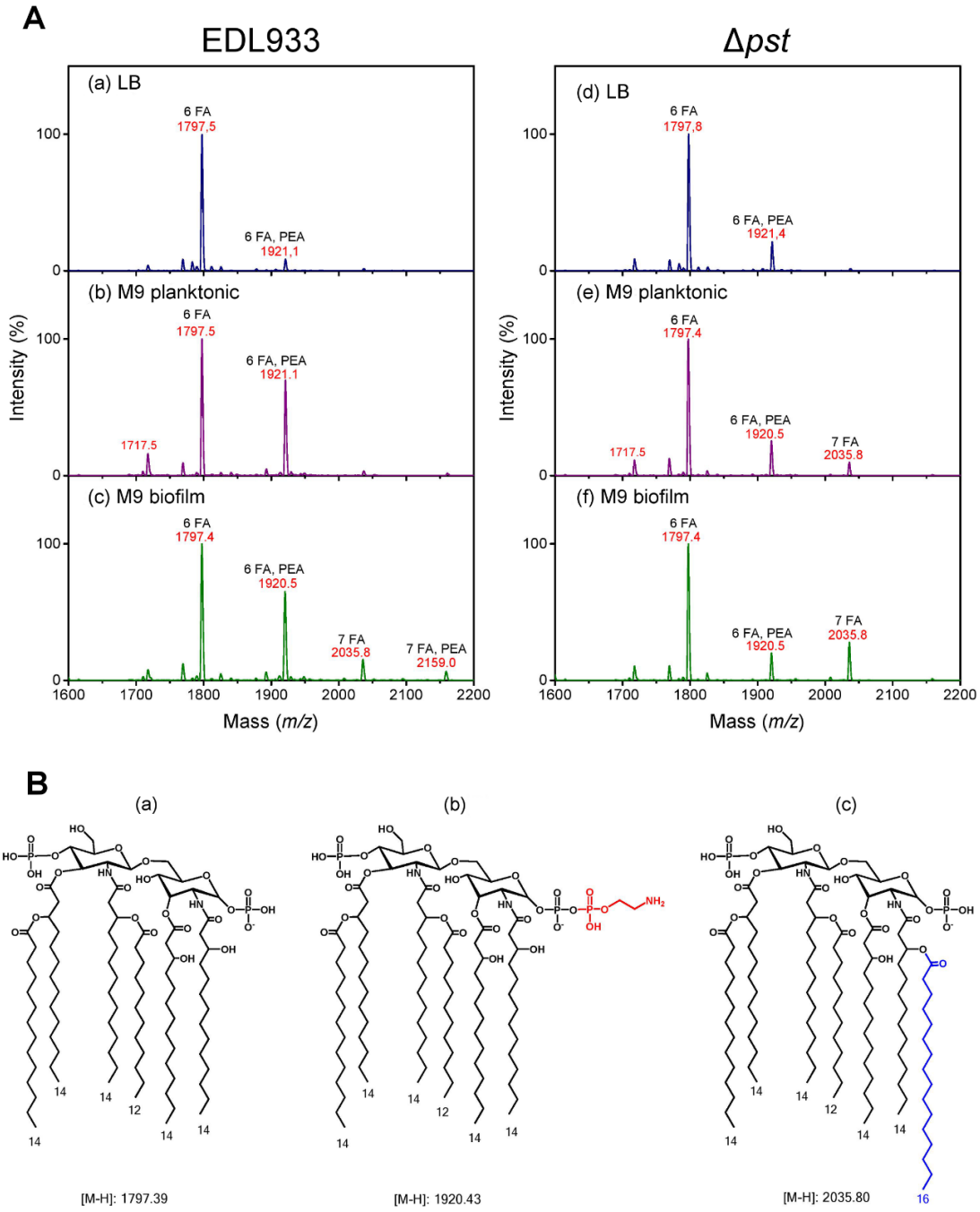

Figure 7. Lipid A structures are different between EDL933 and the Δ*pst* mutant, and differentially modified according to culture conditions. (A) Mass spectroscopy analysis of Lipid A from EDL933 (left panel) and Δ*pst* mutant (right panel) grown in (a and d) LB or in M9 as planktonic (b and e) (M9 planktonic) or biofilm (c and f) (M9 biofilm) reveals that PEA substitution is culture dependent for EDL933 and non-dependent for the Δ*pst* mutant. Moreover, palmitoylation is increased under biofilm conditions for both strains. (B) Structure representation of three major molecular species of lipid A corresponding to the hexa-acyl

molecular species (A), the hexa-acyl molecular species with one phosphate group being substituted with a PEA residue (B), and an hepta-acyl molecular species with palmitoylation at the secondary C-2 position (C). FA, fatty acid; PEA, phosphorylethanolamine.

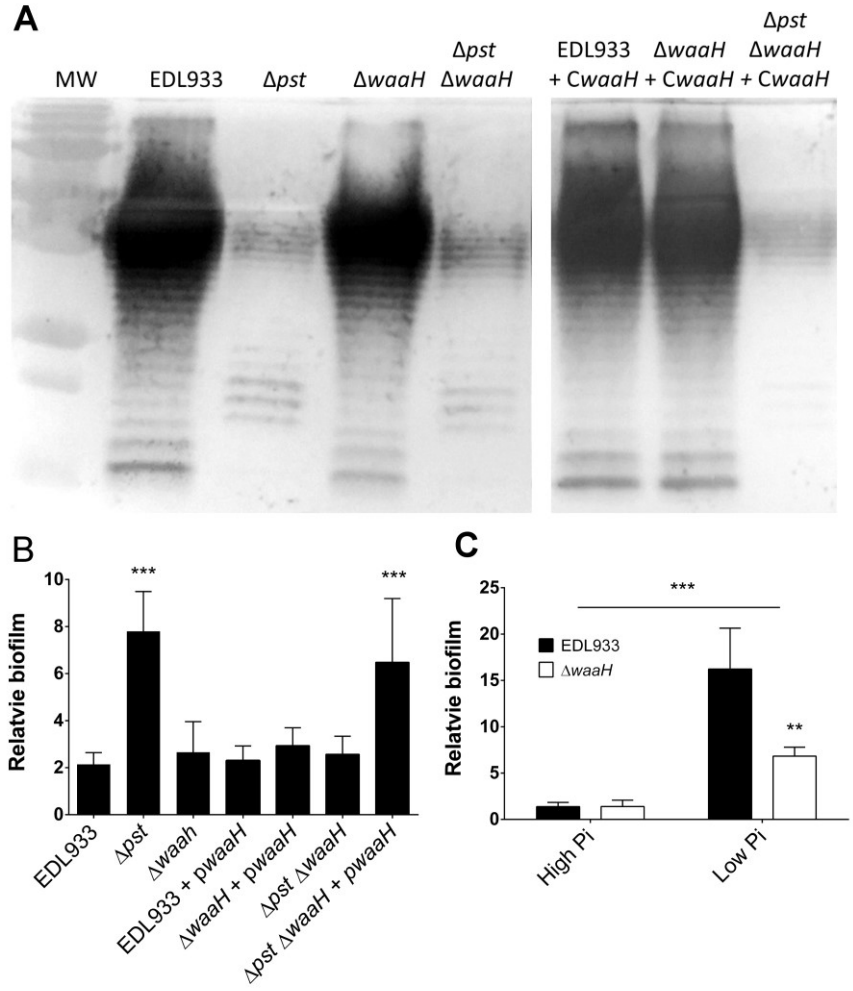

Figure 8. *waaH* plays a role in biofilm formation in response to Pi starvation but its function remains unknown. (A) Western blot of LPS extracts of EDL933 and its derivative mutants grown as biofilm cells in M9 at 30°C. (B) Relative biofilm formation of EDL933 and its derivative mutants cultured in M9 at 30°C for 24 h. Results are averages from at least 3 biological replicates. Relative biofilm formation corresponds to biofilm formation (A_{595})/planktonic growth (DO_{600}). Statistical analysis was performed using a one-way ANOVA with Tukey's multiple comparison post-test. Stars indicate significant results compared to Δ*pst* mutant *** $P < 0.001$. (C) Relative biofilm formation of EDL933 and Δ*waaH* grown in MOPS high Pi and low Pi at 30°C for 24 h. Results are averages from at least 3 biological replicates. Statistical analysis was performed using a two-way ANOVA with Bonferroni's multiple comparison post-test. ** $P = 0.0012$.

SUPPLEMENTAL MATERIAL

SUPPLEMENTAL METHODS

Alkaline phosphatase assay. Alkaline phosphatase was measured as described previously (40, 56). Briefly, 4 µg/ml of p-nitrophenyl phosphate was added to 500 µl of mid-log-phase (optical density at 600 nm [OD_{600}] of 0.6) culture cells permeabilized by 50 µl of 1% sodium dodecyl sulfate (SDS) and 50 µl of chloroform. Color development was monitored at 420 nm, and alkaline phosphatase activity was expressed in enzyme units per min, calculated as follows: $1{,}000 \times [OD_{420} \times (1.75 \times OD_{550})]/T$ (min) × V (ml) OD_{600}, where T stands for the length of reaction time and V stands for the culture cell volume.

Electrophoretic mobility shift assay (EMSA). EMSA were performed as described previously (Chekabab *et al.*, 2014). First, the probe corresponding to the promoter region of selected genes was amplified from EDL933 genome using primers listed in Table S1. The EMSA reaction mix consisted of 2.5, 5.0, 7.5, or 10.0 µM of $PhoB^{CA}$, 50 nM of 5′ 6-FAM probe, 0.1 mg/mL of calf thymus DNA, and 0.1 mg/mL of BSA in EMSA buffer (50 mM NaCl, 20 mM Tris, pH 7.4, 0.02% vol/vol sodium azide). Competitive EMSA assay was done with 50 nM of 6-FAM-labelled P*waaH* probe and unlabelled probes corresponding to P*waaH*. The ratio "cold probe/labelled probe" was 2/1. Positive and negative controls used probes corresponding to the PhoB promoter region or kanamycin promoter region. Reactions were incubated for 30 min at 25°C, and then loaded onto a 5% polyacrylamide gel (Biorad) running at 120 volts for 1 h in 1x TBE buffer. Fluorescent bands were visualized using the Fusion Suite imaging scanner.

Quantitative real time-PCR (qRT-PCR). To determine the relative copy number of copy transcripts under biofilm conditions, biofilms of ELD933, Δ*pst* mutant, Δ*pst* complemented, and Δ*pst phoB* double mutant were grown as described in the previous section in M9 supplemented with 0.2% glycerol. The only difference is that strains were inoculated in petri dishes to improve cell quantity and to facilitate harvesting. After 24 h of incubation in petri dishes, biofilms were washed 3 times with PBS and attached cells were harvested by using cell-scrapers (Sarstedt). RNA was extracted using Ribopure™-Bacteria Kit (Ambion) following the manufacturer's recommendations. cDNAs, standard curves, and quantitative PCR were performed as previously described (41). Results are presented as the ratios between the cDNA

copy number of the gene of interest, and the cDNA copy number of the housekeeping gene *tus*. One-way ANOVA with Dunnett's multiple-comparison post hoc test were performed to calculate *p*-values.

SUPPLEMENTAL TABLES

Table S1. List of primers used in this study.

Names	Sequence 5' to 3'	Use
AscI-phoB1-F	GGCGCGCCGTGGCGATGATGGGCAGAGG	Mutagenesis Δ*phoB*
Tet-phoB1-R	GACTTCAGGTGCTACATTTGGATTTGCCCTGTTGTAATAA	
Tet-phoB3-F	TTATTACAACAGGGCAAATCCAAATGTAGCACCTGAAGTC	Mutagenesis Δ*phoB*
Tet-phoB3-R	TTTAACAGCTGCTCGCGGCTCTCCGCAAGAATTGATTGGC	
Tet-PhoB2-F	GCCAATCAATTCTTGCGGAGAGCCGCGAGCAGCTGTTAAA	Mutagenesis Δ*phoB*
SacI-PhoB2-R	GAGCTCGTCATACTGCGATCCACCCA	
phoB-seq-F	CCAGCGTGCCAATATAAATG	Sequencing Δ*phoB*
phoB-seq-R	GCATCTGGTGTAAGCCGTAT	
Tet-waaH3-R	TCAGAGGTCGTCGGTAATTTCTCCGCAAGAATTGATTGGC	Mutagenesis Δ*waaH*
waaHcompBamHIF	CGGGATCCCGCGCTAGCGCAAATTAAAG	Mutagenesis Δ*waaH*
waaHcompSacIR	CGAGCTCGAGAGGTCGTCGGTAATTT	Mutagenesis Δ*waaH*
waaH EMSA 6FAM F	[FAM]TTTGCGTAATTAAAGATTCC	EMSA
waaH EMSA F	TTTGCGTAATTAAAGATTCC	EMSA
waaH EMSA R	GGGATTAACACGAAAAAGGG	EMSA
M-waaHFor	GTAATCAGGCGCTTATAC	Standard curve
M-waaHRev	CTCAACCGGTGTATTAAC	Standard curve
Q-waaHFor	GGCGGGTAATCTTAATATAG	qRT-PCR
Q-waaHRev	CATCATCAGGATATTGTCTG	qRT-PCR

Table S2. Mini-Tn*10* transposon autoagglutination- and biofilm-negative mutants of Δ*pst* mutant identified by high-throughput sequencing and classified by number of reads.

Locus tag	Gene ID	*e. coli*. bam	Predicted function
z1531	*Z1531*	46	Putative oxydoreductase
z4574	*arcB*	29	Aerobic respiration sensor-response protein; histidine protein kinase/phosphatase, sensor for arcA
Z3389	*yohI*	28	Putative regulator protein
Z5300	*rffH*	27	Glucose-1-phosphate thymidylyltransferase; synthesis of ECA
z5842	*fbp*	27	Fructose-bisphosphatase
z3270	*Z3270*	27	Uncharacterized protein
Z4931	*yhjA*	27	Putative cytochrome C peroxidase
z5433	*fdhE*	26	Affects formate dehydrogenase-N
z3016	*fliT*	25	Flagellar biosynthesis; repressor of class 3a and 3b operons (RflA activity)
z0275	*z0275*	25	Unknown function (Rhs Element Associated)
z5392	*dsbA*	24	Protein disulfide isomerase I, essential for cytochrome c synthesis and formate-dependent reduction
Z3789	*sseB*	24	Enhanced serine sensitivity
Z3891	*pheA*	24	Chorismate mutase / prephenate dehydratase
Z0941	*ybhI*	23	Putative membrane pump protein
Z1322	*yccA*	22	Putative carrier/transport protein
Z1744	*ycfM*	22	Outer membrane lipoprotein - activator of MrcB activity
z0335	*z0335*	22	Unknown protein encoded in prophage CP-933I
Z2417	*dbpA*	22	ATP-dependent RNA helicase
Z3257	*gatA*	21	Galactitol-specific enzyme IIA of phosphotransferase system
Z2195	*ydeK*	21	Hypothetical protein / predicted lipoprotein
Z5238	*atpI*	20	Membrane-bound ATP synthase, dispensable protein, affects expression of atpB
Z2904	*zwf*	20	Glucose-6-phosphate dehydrogenase
Z5412	*yihO*	19	Sulfoquinovose transporter / putative permease
Z2203	*z2203*	18	Putative fimbrial usher protein/predicted outer membrane export usher protein
Z5582	*purD*	18	Phosphoribosylglycinamide synthetase = GAR synthetase

Z4525	*pnp*	17	Polynucleotide phosphorylase; cytidylate kinase activity
Z5764	*yjeM*	17	Putative transport/ glutamate:GABA antiporter family
Z0153	*folK*	17	7, 8-dihydro-6-hydroxymethylpterin-pyrophosphokinase
Z1108	*ybjE*	17	L-lysine efflux transporter
Z6060	*Z6060*	17	Putative Q antiterminator encoded by prophage CP-933P
Z5297	*wecB*	16	UDP-N-acetyl glucosamine -2-epimerase; synthesis of ECA
Z2212	*yddA*	15	Putative transport protein, ABC superfamily - fused membrane component, ATP-binding component
Z3558	*ackA*	14	Acetate kinase
Z2611	*tus*	14	DNA-binding protein; inhibition of replication at Ter sites
ygfU	*ygfU*	14	Putative permease / urate:H+ symporter
Z0811	*yleB*	13	2-octaprenyl-3-methyl-6-methoxy-1,4-benzoquinone hydroxylase
Z5161	*z5161*	13	Unknown function No significant matches
Z2554	*yciF*	13	Putative structural proteins
Z2737	*nlpC*	13	Lipoprotein / NlpC-putative lipoprotein hydrolase
Z4199	*Z4199*	13	Unknown function
Z5792	*yjfM*	13	Hypothetical protein
Z4469	*tdcB*	12	Threonine dehydratase, catabolic
Z4851	*Z4851*	12	Unknown function
Z5038	*yibN*	12	Predicted rhodanese-related sulfurtransferase
Z5120	*escV*	11	Involved in type III secretion system biogenesis
Z5649	*qor*	11	Quinone oxidoreductase
Z5247	*yieN*	11	Regulatory ATPase RavA
Z4126	*Z4126*	11	Putative lipoprotein
Z3213	*cpsB*	10	Mannose-1-phosphate guanyltransferase, colanic acid synthesis
Z4378	*qseC*	10	Sensor protein QseC
Z5683	*yjcS*	10	Unknown function
Z1822	*Z1822*	10	Other or unknown (Phage or Prophage Related)
Z4405	*waaE*	10	Bifunctional heptose 7-phosphate kinase/heptose 1-phosphate adenyltransferase; LPS synthesis
Z4476	*yhaD*	10	Hypothetical protein / glycerate kinase I
Z3114	*Z3114*	10	Putative antiterminator Q homolog of prophage CP-933U

z4139	*recC*	9	Exonuclease V subunit gamma; Degradation of DNA
Z4499	*yraI*	9	Chaperone
Z4330	*Z4330*	9	Putative transposase
Z0381	*ykgC*	9	Predicted oxidoreductase with FAD/NAD(P)-binding domain and dimerization domain; hypochlorite stress response
Z0522	*yajO*	8	NAD(P)H-dependent xylose reductase
Z3129	*exoU*	8	Putative exodeoxyribonuclease VIII of prophage CP-933U
Z4139	*recC*	8	DNA helicase, ATP-dependent dsDNA/ssDNA exonuclease V subunit, ssDNA endonuclease
Z5849	*treC*	8	Trehalase 6-P hydrolase
Z1097	*Z1097*	8	Unknown function
Z1859	*phoP*	8	Transcriptional regulatory protein
Z5055	*waaG*	7	Glucosyltransferase I
Z5056	*waaQ*	7	Putative LPS biosynthesis enzyme
Z2722	*ydiF*	6	putative enzyme; Not classified
Z1324	*Z1324*	6	putative exodeoxyribonuclease VIII for cryptic prophage CP-933M
Z4967	*lpfC*	6	Putative fimbrial usher
Z5048	*waaC*	5	eptosyl transferase I
Z3948	*ypjA*	5	BC transporter ATP-binding protein
Z4127	*Z4127*	5	Hypothetical protein / cysteine sulfinate desulfinase
Z0156	*dksA*	4	naK suppressor protein; Transcription factor
Z3630	*emrK*	4	Multidrug resistance protein K
Z1817	*Z1817*	4	Unknown protein encoded by prophage CP-933N
Z1817	*Z1817*	4	Unknown protein encoded by prophage CP-933N
Z3792	*fdx*	3	carrier; Energy metabolism, carbon: Electron transport
Z1818	*Z1818*	3	Putative antirepressor protein encoded by prophage CP-933N
Z5259	*rrsC*	2	16S ribosomal RNA
Z5657	*uvrA*	2	Excinuclease ABC subunit A; repair system of DNA lesions.
Z3201	*wzx*	2	O antigen flippase Wzx
Z2761	*katE*	2	Catalase; hydroperoxidase HPII(III)
Z1215	*z1215*	2	Unknown / yfjQ / CP4-57 prophage; predicted protein
Z1655	*z1655*	2	Unknown

Z3576	*dedD*	1	Unknown function
Z5047	*waaF*	1	LPS heptosyltransferase
Z5585	*rrsE*	1	16S ribosomal RNA
Z5658	*ssb*	1	ssDNA-binding protein
Z5639	*ubiA*	1	4-hydroxybenzoate octaprenyltransferase
Z5717	*adiC*	1	Arginine:agmatin antiporter
Z0361	*ecpR*	1	Regulator of ECP operon
Z0521	*Z0521*	1	Unknown function
Z3017	*amyA*	1	Cytoplasmic alpha-amylase
Z4663	*yhdN*	1	Hypothetical protein
Z0269	*z0269*	1	Unknown function (Rhs Element Associated)

SUPPLEMENTAL FIGURES

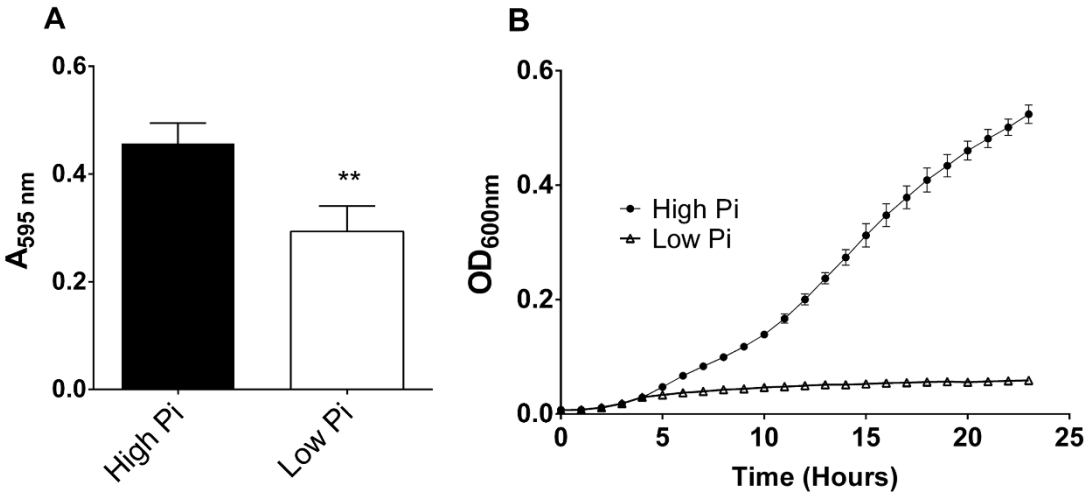

Figure S1. In low Pi conditions, EDL933 grows essentially as biofilm cells. (A) Absolute biofilm of EDL933 grown in MOPS high Pi and low Pi. (B) 24-h growth curve of EDL933 grown in MOPS high Pi (black point) and low Pi (white triangle). When stained with crystal violet and measured with an A595, absolute biofilm of EDL933 was 1.5 times higher in high Pi than in low Pi. However, when bacteria were cultivated in low Pi, cell density of the planktonic part was decreased 10 times in low Pi (DO600 0.05) compared to high Pi (DO600 0.5). In low Pi conditions it seems that the majority of bacteria grew as biofilms but not in the planktonic part. This observation is particularly obvious when the biofilm formation (A595) was corrected with the growth of the planktonic part (A595/OD600) (Fig. 1A). These results show that in low Pi conditions the *E. coli* O157:H7 biofilm lifestyle is favored over the planktonic lifestyle. Results are averages from at least 3 biological replicates. Statistical analysis was performed using a Student's t-test. * $P < 0.05$; ** $P < 0.01$.

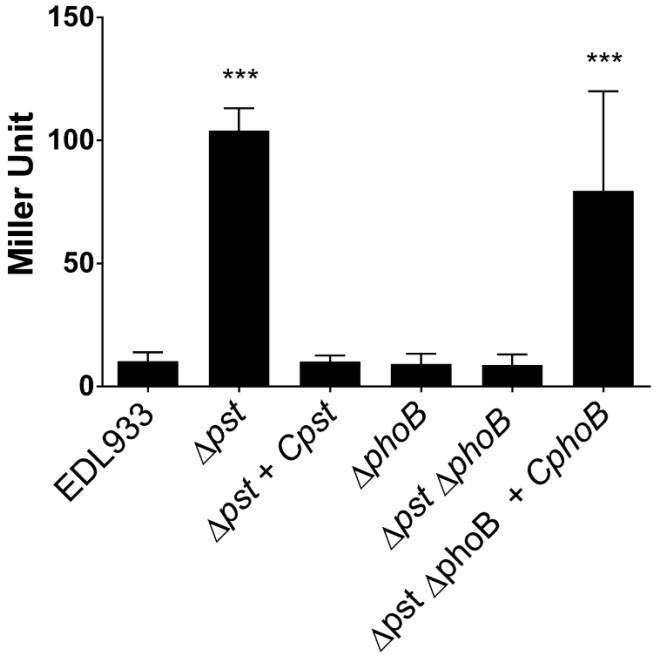

Figure S2. Activation status of the Pho regulon. Alkaline phosphatase activity of EDL933 and its derivative mutants was measured. PhoA activity (in Miller Units) of EDL933 and its derivative mutants were grown in M9 at 30°C for 24 h.

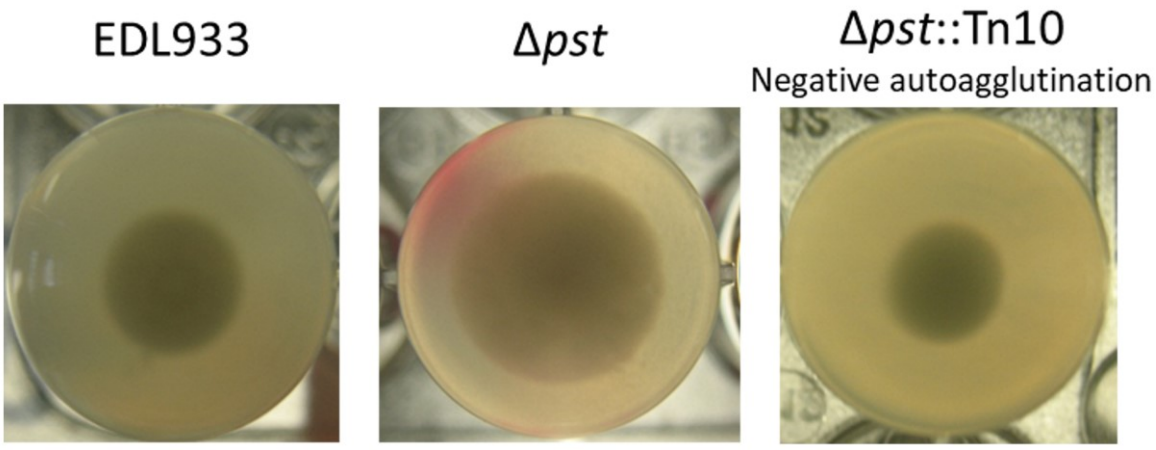

Figure S3. Phenotypes of autoagglutination observed for transposon mutant derived from Δ*pst* mutant. Autoagglutination phenotype of EDL933 and Δ*pst* mutant were used as negative and positive controls of autoagglutination phenotype. The transposon mutant derived from Δ*pst* mutant was scored as an autoagglutination negative phenotype when it exhibited a reduction of autoaggregate similar to EDL933.

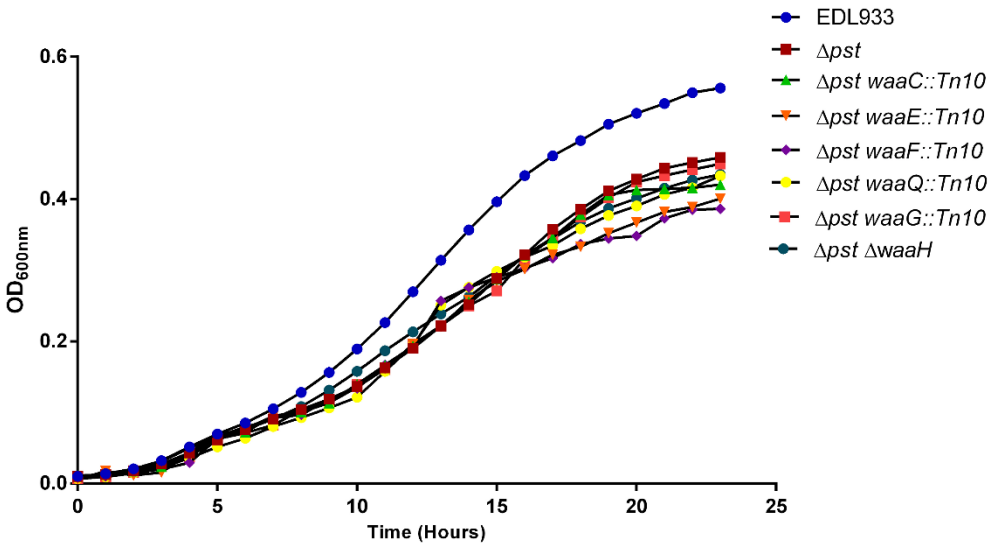

Figure S4. Growth curves of EDL933, Δ*pst* mutant, and Δ*pst* derivative mutants with Tn*10* inserted in core LPS genes (*waaC*, *waaE*, *waaF*, *waaQ*, *waaG*), and Δ*pst* Δ*waaH*. Bacteria isolates were grown in M9 medium with a mineral solution and glycerol 0.2% (vol/vol) at 30°C for 24 h.

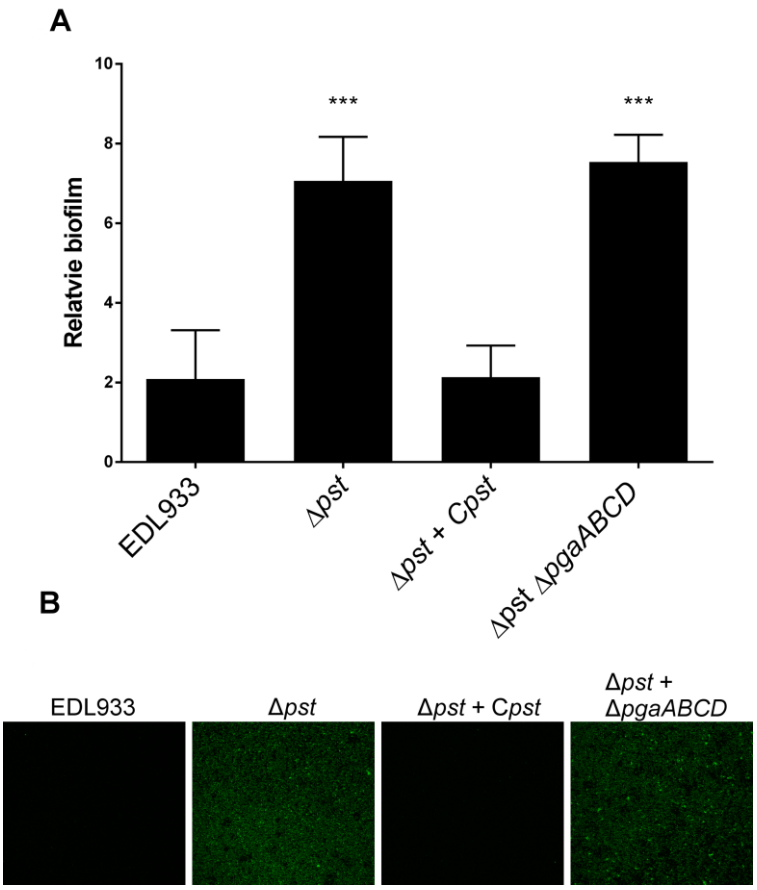

Figure S5. PGA production is not involved in biofilm formation of Δ*pst* mutant. (A). Relative biofilm formation of Δ*pst* ΔpgaABCD double mutant in M9 glycerol at 30 °C for 24 h. (B) Confocal laser scanning microscopy images of 24-h biofilms stained with WGA of EDL933, Δ*pst* mutant, Δ*pst* + C*pst*, and Δ*pst* pgaABCD grown in M9 supplemented by 0.2% glycerol at 30°C for 24 h. Results are averages from at least 3 biological replicates. Statistical analysis was performed using a one-way ANOVA with Tukey's multiple comparison post-test. * $P < 0.05$; ** $P < 0.01$; *** $P < 0.001$.

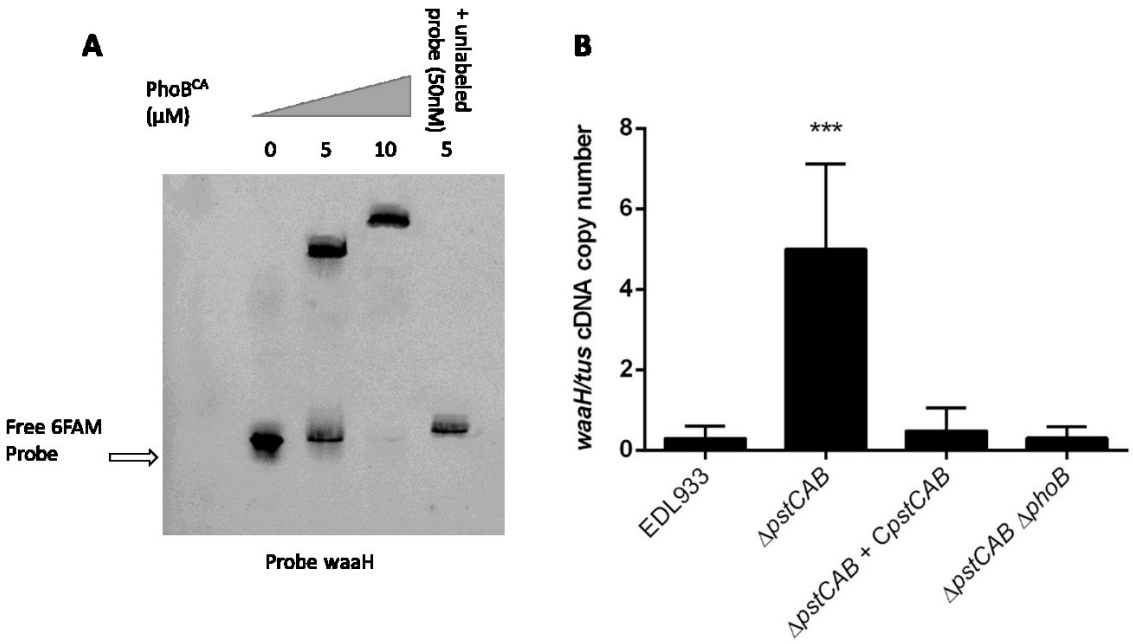

Figure S6 PhoB regulates *waaH* expression. (A) PhoB binds in vitro to *waaH* promoter regions. Increasing amounts of PhoBCA were used in the EMSA assay to shift the 6-FAM-labelled DNA probes amplified from *waaH* (−246 pb to +93 bp). (B) cDNA copy number of waaH compared to tus. cDNA was extracted from EDL933. DNA were synthesized from RNA extracted from biofilm cells of wild type, Δ*pst* mutant, Δ*pst* + *pst*-complemented, and Δ*pst* Δ*phoB* double mutant grown in M9 0.2% glycerol at 30°C for 24 h. Comparisons between cDNA wild type and its isogenic mutants were statistically analyzed by one-way ANOVA with Tukey's multiple comparison post-test. *** $P < 0.001$. Results are shown as the ratio copy number of gene transcripts/copy number of tus transcripts.

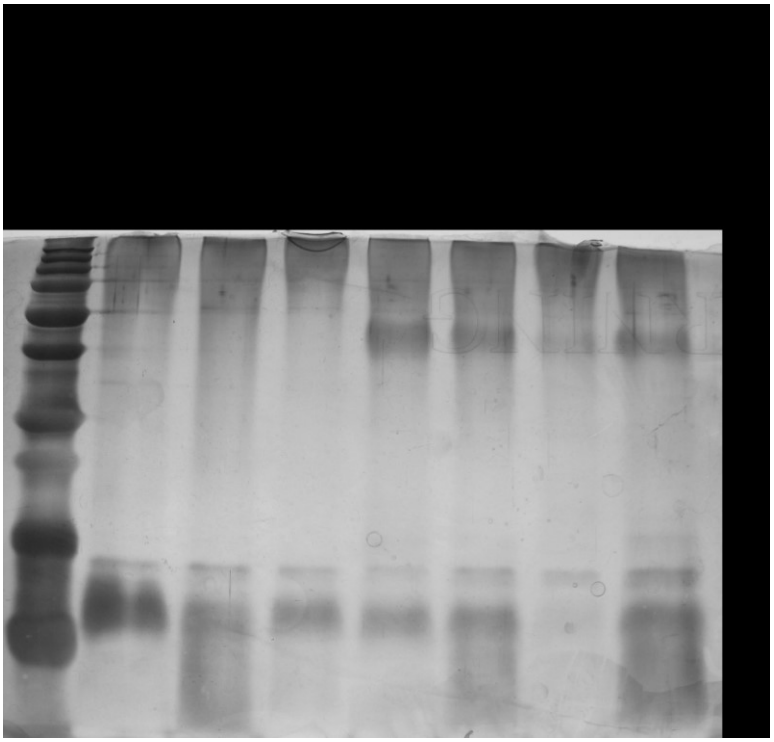

Figure S7. SDS-PAGE of LPS extracts of EDL933, Δ*pst* mutant, and Δ*waaH* mutant; and Δ*pst* Δ*waaH* double mutant, and complemented strains grown as biofilm cells in M9 at 30°C.

IV.2 Article de recherche 3: Lors de la carence en phosphate, l'autotransporteur tronqué YcgV est impliqué dans la formation de biofilm de O157:H7

Philippe Vogeleer, Mario Jacques and Josée Harel

Objectif de l'article : Les objectifs de cet article étaient de caractériser et d'identifier de nouveaux membres du régulon Pho et la carence en phosphate sur la formation de biofilm de *E. coli* O157:H7 afin d'identifier les facteurs qui contribuent à la formation de biofilm et potentiellement régulés par le régulateur PhoB.

Contribution de l'étudiant : En tant que premier auteur de cet article, j'ai effectué la totalité des expérimentations, analysé l'ensemble des résultats et écrit le manuscrit. J'ai également coordonné et assemblé les corrections de mes collaborateurs. Cet article sera soumis pour publication au journal « Journal of Bacteriology ».

Under phosphate starvation, the truncated autotransporter YcgV is involved in O157:H7 biofilm formation

Philippe Vogeleer[1], Mario Jacques[1,2] and Josée Harel[1]

[1]Groupe de Recherche sur les Maladies Infectieuses du Porc, Centre de Recherche en Infectiologie Porcine et Avicole, Faculté de médecine vétérinaire, Université de Montréal, St-Hyacinthe, Québec, Canada.

[2]Op+Lait, Regroupement de recherche pour un lait de qualité optimale, Faculté de Médecine Vétérinaire, Université de Montréal, Saint-Hyacinthe, QC, Canada.

#Address of correspondence: Josée Harel, Faculté de médecine vétérinaire, Université de Montréal, 3200 Sicotte, Saint-Hyacinthe, Québec, Canada J2S 2M2. Tel.: 450-773-8521 (ext. 8233); Fax: 450-778-8108; E-mail: josee.harel@umontreal.ca

ABSTRACT

In the environment enterohemorrhagic *Escherichia coli* (EHEC) O157:H7 respond to the phosphate starvation by inducing the Pho regulon controlled by PhoBR. The Pst (phosphate specific transport) system serves as a sensor of the extracellular inorganic phosphate (Pi) concentration. In isogenic Δ*pst* mutant of *E. coli* O157 EDL933 strain, the regulator PhoB was constitutively activated and expression of genes from the Pho regulon lead to an increase in biofilm formation. In a transcriptomic study, the gene $ycgV_{EDL933}$, encoding the AIDA-I type autotransporter YcgV, was identified among Pho regulated and biofilm related genes. Compared to others *E. coli* strains, most *E. coli* O157:H7 genomes encode a shorter version of YcgV that mainly consists of a functional passenger domain. We showed that truncated $YcgV_{EDL933}$ was Pho regulated and participated in biofilm formation of EDL933 upon phosphate starvation.

IMPORTANCE

EHEC O157:H7 are human pathogens responsible for foodborne and waterborne infections. The ability of O157:H7 strains to form biofilm is thought to participate to their survival in hostile environments. We have shown that upon extracellular inorganic phosphate (Pi) starvation, the activation of PhoB regulator favors the biofilm formation of O157:H7. We identified that in strain EDL933, PhoB controls the expression of a truncated autotransporter, $YcgV_{EDL933}$ that is involved in the biofilm formation. This illustrates how O157:H7 can adapt to nutritional stress such as phosphate starvation.

INTRODUCTION

Enterohemorrhagic *E. coli* (EHEC) O157:H7 are human pathogens responsible of severe collective food-borne and waterborne infections (1). EHEC O157:H7 possess many virulence factors, including Shiga toxins that contribute to cause disease in humans (2). In addition to play role in the pathogenesis, some virulence factors such as autotransporters and fimbriae are also involved in biofilm formation (3). EHEC O157:H7 strains have been shown to be able to form biofilm in different environments such as foods, processing plants and water (4-6). It was also reported that EHEC O157:H7 were best biofilm former in environmental conditions relating to stress such as low temperature, nutrient starvation or low oxygen (7-10). Moreover, many studies have described the potential role of biofilm to participate in the persistence of EHEC O157:H7 in the environment (11-13). In a previous study, we identified that EHEC O157:H7 was able to adapt and to survive in phosphate limiting environment (14).

Phosphate is one of the most important elements for bacteria and is found in many different cell components such as lipids, nucleic acids, proteins, complex sugars. Moreover, phosphate is also involved in signal transduction and energy production (15-16). Due to its importance for bacteria, phosphate homeostasis is tightly regulated by the two-component regulatory system PhoBR, in which PhoR is a histidine kinase and PhoB the response regulator controlling expression of genes belonging to the Pho regulon. When the extracellular phosphate concentration is high, PhoB is inactive and Pho regulon is at basal expression level. When extracellular phosphate concentration decreases (below 4 µM), PhoB is activated and regulates the expression of Pho regulon gene leading to changes in phosphate metabolism and transport (16). Under phosphate limiting condition, phosphate transport is controlled by the phosphate-specific transport (Pst) system encoded by *pstSCAB-phoU* operon belonging to the Pho regulon (17).

We previously reported that upon constitutive (Δ*pst* mutant) or physiological (phosphate starvation) activation of PhoB, EHEC O157:H7 increased its ability to form biofilm by modifying outer membrane composition including that of lipopolysaccharides (LPS) (Vogeleer *et al.*, 2019 submitted). The objective of this study was to identify new Pho regulon members involved in biofilm formation of EHEC O157:H7 strain EDL933. We found that PhoB is

regulating the expression of *ycgV*$_{EDL933}$ (*z1972*), encoding a truncated AIDA-I type autotransporter, and that the YcgV$_{EDL933}$ is involved in the increase of biofilm formation under phosphate starvation growth conditions.

RESULTS

Transcriptomic analysis revealed Pho regulon modulation of gene expression in biofilm

Transcriptomic analysis revealed that the AIDA-like autotransporter encoding gene *ycgV* (*z1972*) was upregulated more than 4 times in the Δ*pst* mutant grown in MOPS supplemented with phosphate (MOPS Pi+) (constitutive activation of PhoB) and in the EDL933 wild-type strain grown in MOPS depleted in Pi- (MOPS Pi-) (physiological activation of PhoB) (Vogeleer et al, 2019 submitted).

To confirm transcriptomic analyses, we performed RT-qPCR using cDNA extracted from biofilm cells. The expression level of *ycgV*$_{EDL933}$ was significantly increased by 8.7 times in the Δ*pst* mutant biofilm cells compared to wild-type and restored to a wild-type status in a *pst*-complemented strain and in the Δ*pst* Δ*phoB* mutant (Fig. 1A). The decrease expression of *ycgV* in the Δ*pst* Δ*phoB* mutant compared to the Δ*pst* mutant suggest that *ycgV* could be under the direct control of PhoB.

Activated PhoB binds the promoter region of *ycgV*

A putative Pho Box (with sequence [5'GTGTAATGTTTTTGTCAT3']) was identified at -256 bp upstream of the *ycgV* promoter region. To investigate whether PhoB directly binds to the *YcgV*$_{EDL933}$ promoter, EMSA experiments were performed using PhoB^{CA}, a constitutively active PhoB mutant that binds Pho regulon promoters in the absence of phosphorylation. EMSA results showed PhoB dependent shifts of the probe designed from *YcgV*$_{EDL933}$ and the control of PhoB promoter regions but not the negative control pKan promoter region (Fig. 1B). As expected, the addition of unlabelled probes (2:1) reduced the amount of shifted 6-FAM labelled probes. This data indicates that PhoB^{CA} can bind specifically to the *ycgV*$_{EDL933}$ promoter region *in vitro*.

In EDL933, *ycgV*$_{EDL933}$ encodes a truncated AIDA-I type autotransporter

The genetic region of EDL933 containing the $YcgV_{EDL933}$ encoding gene shares homology with *E. coli* K-12 but has a deletion of 3136 bp corresponding to the 3' coding sequence and a deletion of the *dhaR* gene encoding the regulator of the *dhaKLM* operon which encodes three subunits of the dihydroxyacetone (DHA) kinase upstream (Fig. 2A).

In *E. coli* K-12, the complete gene *ycgV* encodes a monomeric AIDA-I like autotransporter constituted of 955 amino acid and contains a N-terminal signal sequence, a functional passenger, a linker region and a C-terminal translocator domain (β domain). The gene $ycgV_{EDL933}$ encodes for a predicted protein of 547 aa that contains both a N-terminal signal peptide and a passenger domain that share 97.8 % identity with $YcgV_{MG1655}$ (Fig. 2B). To evaluate if $YcgV_{EDL933}$ is commonly found among O157:H7 strains, the protein sequence of $YcgV_{EDL933}$ was blasted against O157:H7 genome available on the NCBI web site. This deletion was detected in 56.3 % of O157:H7 strains (76/135) while the complete YcgV sequence is present in 17.8% of O157:H7 (24/135) strains and a shorter form of 386 aa in 21.5% of O157:H7 strains (29/135) (Fig. 2B).

$YcgV_{EDL933}$ participates in biofilm formation by strain EDL933

In low Pi growth conditions, while $ycgV_{EDL933}$ was upregulated, biofilm formation of strain EDL933 was increased (Fig 3A). This was also observed in the Δ*pst* mutant that mimics low phosphate conditions (PhoB constitutive activation). Interestingly, the Δ*pst* Δ*ycgV* mutant had a significantly reduced biofilm formation compared to the isogenic Δ*pst* mutant. Biofilm formation was restored to a Δ*pst* status when $ycgV_{EDL933}$ was complemented in the Δ*pst* Δ*ycgV* mutant (Fig. 3B). In low phosphate condition (MOPS Pi-), the ability of the Δ*ycgV* single mutant to form biofilm was reduced compared to EDL933. However, biofilm formation of Δ*ycgV* did not influence its biofilm ability when grown in Pi rich conditions (in M9 or in MOPS Pi+). The biofilm level was restored to a wild-type status in *ycgV*-complemented strain grown in MOPS Pi- (Fig. 3A). In addition, *ycgV* deletion or overexpression did not influence the autoagglutination ability of the strains (Fig. 3C). This indicates that $YcgV_{EDL933}$ does not contribute to autoagglutination ability of the Δ*pst* mutant. Taken together, these results show that $YcgV_{EDL933}$ is involved in the phosphate-dependant biofilm formation of strain EDL933.

$YcgV_{EDL933}$ is present in the outer membrane

To localise YcgV$_{EDL933}$ among subcellular fractions (periplasm, inner membrane, outer membrane) and supernatant, an anti-YcgV$_{EDL933}$ antibody was used for Western blot analyses. Two bands of approximately 60 and 65kDa, corresponding to the predicted molecular mass of YcgV$_{EDL933}$ (60kDa), were detected only in the outer membrane fraction of strains overexpressing *ycgV*$_{EDL933}$ (EDL933, Δ*ycgV* and Δ*pst* Δ*ycgV* harboring pTrc99A::*ycgV* in presence of IPTG 1mM) (Fig. 4). This result shows that YcgV$_{EDL933}$ can be found in the outer membrane of EDL933 and the isogenic mutant when overproduced.

DISCUSSION

YcgV$_{EDL933}$ is a Pho regulon member

Here we identified that in *E. coli* O157:H7 EDL933 strain, *ycgV*$_{EDL933}$ encodes for a truncated AIDA-I type autotransporter and that its expression is dependent on phosphate concentration conditions. YcgV belongs to the self-associating autotransporter (SAAT) family that is known to promote adhesion to epithelial cells, autoagglutination or biofilm formation (18-22). Wells and collaborators reported that the YcgV-encoding gene was found in the majority of commensal and DEC genomes but was truncated in 2 EHEC strains and absent in UPEC (18). Our analyses revealed that variant *ycgV*$_{EDL933}$ was common in most of O157:H7. It was proposed by Wells *et al.*, that *E. coli* pathotypes have different combination of autotransporter proteins that could have functions specific to their environment (18). In the same line we suggest that truncated YcgV$_{EDL933}$ could have a function in *E. coli* O157:H7 upon phosphate starvation.

Moreover, YcgV$_{EDL933}$ is involved in EDL933 O157:H7 biofilm formation upon Pi starvation. In *E. coli* K-12, the overexpressed YcgV was shown to increase adhesion and biofilm formation (23). An association between SAAT, autoagglutination and biofilm formation has been reported (18, 20-22). In 2008, Beloin *et al.*, have proposed that the importance of autotransporters such as YcgV could be revealed when the bacteria are under specific physiological conditions (25). In our study, the phosphate starvation condition revealed the contribution of YcgV$_{EDL933}$ to biofilm formation.

In this study, we have shown that expression of *ycgV*$_{EDL933}$ was increased in the Δ*pst* mutant of *E. coli* O157:H7 (constitutive activation PhoB) and upon Pi starvation (MOPS Pi-). Previous to

our study, upregulation of *ycgV* was also observed in a Δ*pst* mutant of avian pathogenic *E. coli* O78 strain χ7122 (26). Moreover, a putative Pho box was identified upstream of the $ycgV_{EDL933}$ and we have shown that $PhoB^{CA}$ directly interacts with the region upstream of $ycgV_{EDL933}$. In addition, this putative Pho box upstream of *ycgV* was also detected *in silico* in other *E. coli* strains including the K-12 strain MG1655 and APEC O78 strain χ7122. Thus, $YcgV_{EDL933}$ is under the control of the Pho regulon and plays a role in biofilm formation under specific phosphate stress condition.

Truncated $YcgV_{EDL933}$ consisting mainly in the passenger domain of SAAT plays a role in biofilm formation. Although, $YcgV_{EDL933}$ was detected in the outer membrane fraction when overexpressed, we ignore how $YcgV_{EDL933}$ that is missing the part of the linker and the translocator domain (β-domain) is present in the outer membrane. The SAAT are exported via the type V secretion pathway. The translocator domain (β-domain) of the autotransporter facilitates the translocation of the passenger across the outer membrane. However, other accessory factors such as the β-barrel assembly machinery (Bam) complex or periplasmic chaperone proteins were shown to play an important part in the translocation process to the cell surface (24-27). Also, two proteins, TamA and TamB that are part of the translocation and assembly module (TAM) were shown to be involved in the translocation of autotransporters in proteobacteria (28). Interestingly, *ycgV* was identified in a high-throughput screen of *E. coli* K-12 mutants deficient in cell envelope assembly (29), indicating a potential role of YcgV in the cell wall integrity. As *E. coli* O157:H7 membrane undergoes several modifications upon Pho regulon activation (30) (Vogeleer *et al.*, 2019 submitted), it is possible that in such conditions, $ycgV_{EDL933}$ could be inserted into the membrane and thereby contribute to biofilm formation. This would illustrate how pathogens such as O157:H7 are adapted to survive in different ecological niches.

MATERIALS AND METHODS

Bacterial strains and culture conditions. In this study, we used the strain EDL933 and its derived mutant (Table 1). Deletion of *ycgV* was achieved by allelic exchange using a suicide vector in EDL933 WT and/or the Δ*pst* mutant as previously described (31) with some modifications. Tetracycline resistance cassette from pACYC184 was amplified and flanked by

PCR with the 500 bp sequence adjacent to *ycgV*$_{EDL933}$ using the primers listed in Table 2. Tetracycline was used to select the Δ*ycgV* mutant and the Δ*pst* Δ*ycgV* double mutant. Deletion of Δ*ycgV* $_{EDL933}$ was confirmed by PCR and sequencing. Complementation of *ycgV*$_{EDL933}$ was performed using the pTrc99A expression plasmid. The *ycgV*$_{EDL933}$ ORF was amplified from the genome of EDL933 using the primers containing BamHI and SacI site of digestion (Table 2) and inserted into pTrc99A downstream of the isopropyl-β-D-thiogalactopyranoside (IPTG) inducible pTrc promoter. As complementation of biofilm phenotype was observed without induction by IPTG, IPTG was not added in the media. LB cultures were made from one isolated colony at 37°C on LB agar containing antibiotic when required and incubated for 24 h at 37°C with shaking. M9 minimal medium was prepared with 0.2% (w/v) glycerol and minerals (1.16 mM $MgSO_4$, 2 µM $FeCl_3$, 8 µM $CaCl_2$, and 16 µM $MnCl_2$). Morpholine propanesulfonic acid minimal medium (MOPS) (Teknova, Hollister, CA, USA) was prepared following the manufacturer instruction with 0.2% (w/v) glycerol, thiamine (0.1 µg/mL) and supplemented with either 1.32 mM KH_2PO_4 (MOPS Pi+) or 1 µM KH_2PO_4 (MOPS Pi-). When required antibiotics were used at the following concentrations: 10 µg/ml tetracycline (Tc), 50 µg/ml ampicillin (Amp), 25 µg/ml chloramphenicol (Cm) and 50 µg/ml kanamycin (Km).

***In silico* evaluation of Pho boxes.** Presence of putative Pho boxes upstream of biofilm related genes were evaluated with a previously constructed Pho box matrix (30). Pho box matrix was based on 12 known Pho boxes with O157:H7 EDL933 sequences identified by Yuan and colleagues (32). Using MEME suite web site with the FIMO tools version 4.12.0 (http://meme-suite.org/tools/fimo), nucleotide sequences of biofilm related gene promoting regions were scanned to find putative motif sequences with match *p*-value < 10^{-4}.

Quantitative real time PCR (qRT-PCR). To determine the relative copy number of *ycgV*$_{EDL933}$, the Δ*pst* mutant, the Δ*pst* + C*pst* mutant and the Δ*pst* Δ*phoB* double mutant were grown in M9 as described below for the static biofilm assay. The only difference is that strains were inoculated in petri dishes to improve cells quantity and to facilitate harvesting. After 24 h of incubation in petri dishes at 30°C, biofilms were washed 3 times with PBS and attached cells were harvested by using cell-scrapers (Sarstedt, Nümbrechet, Deutschland). RNAs was extracted from using Ribopure™-Bacteria Kit (Ambion, Carlsbad, CA, USA) by following the

manufacturer's recommendations. cDNAs, standard curves and quantitative PCR were performed as previously describe (31). Results are presented as the ratios between the cDNA copy number of the gene of interest and the cDNA copy number of the housekeeping gene *tus*. One-way ANOVA with Dunnett's multiple-comparison post hoc test were performed to calculate *p*-values.

Electrophoretic mobility shift assay (EMSA). EMSA were performed as previously described (30). First, probe corresponding to the promoter region of selected genes was amplified from EDL933 genome using primers listed in Table 2. The forward primer contained a 5′ 6-FAM fluorescein tag allowing detection on polyacrylamide gel using a chemiluminescence scanner. The EMSA reaction mix consisted of $PhoB^{CA}$ at the desired concentrations (2.5, 5.0, 7.5 or 10.0 µM), 50 nM final probe concentration, 0.1 mg/mL calf thymus DNA and 0.1 mg/mL BSA in EMSA buffer (50 mM NaCl, 20 mM Tris, pH 7.4, 0.02% v/v sodium azide). Competitive EMSA assay was done with 50 nM of 6-FAM labelled P*ycgV*$_{EDL933}$ probe and unlabelled probes corresponding to P*ycgV*$_{EDL933}$. The ratio "cold probe/labelled probe" was 2:1. Positive and negative controls were done using probes corresponding to PhoB promoter region or kanamycin promoter region. Reactions were incubated for 30 minutes at 25°C, and then loaded onto a 5% polyacrylamide gel (Biorad, Hercules, CA, USA) running at 120 V for 1h in 1x TBE buffer. Fluorescent bands were visualized using the Fusion Suite imaging scanner.

Static biofilm formation assay. Biofilm formation was investigated as previously described (33) with modifications. Overnight cultures at 37°C in LB were diluted (1:100) in MOPS Pi+ or in M9 and incubated at 37°C with antibiotic when required. After 24 h of incubation, culture was diluted (1:100) in M9 or in MOPS Pi+ or in MOPS Pi-. These dilutions were inoculated in triplicates into the microtiter plates Costar 3370 (Corning, NY, USA). After 24h of incubation at 30°C, unattached cells were removed by washing three times with distilled water. Plates were air dried at 37°C for 15 min and biofilms were stained with crystal violet (0.1% (w/v)) for 2 min. The crystal violet solution was removed, and biofilms were washed three times with distilled water and then air dried at 37°C for 15 min. The stain was released with 150 µl of 80% (v/v) ethanol and 20% (v/v) acetone. Biofilm were quantified by measuring the absorbance at 595 nm with a microplate reader (Powerwave; BioTek Instruments, Winooski, VT, USA).

Moreover, while biofilms were stained with CV and measured with the A_{595}, growth of the planktonic part of the culture (unattached cells) was tracked with OD_{600}. One-way ANOVA with Dunnett's multiple-comparison post hoc test were performed to calculate *p*-values.

Auto-agglutination assays. Auto-agglutination was determined using an assay described elsewhere (34). Briefly 24h M9 cultures of EDL933, and its isogenic mutant were diluted 1/100 in M9 and incubated at 30°C for 24h without agitation. After incubation, 100 µl of the upper phase was taken 1 cm below the surface and the OD600 was measured (OD_{Agg}). Cultures were then vortexed for 10 seconds and OD600 was measured again (OD_{tot}). Percentage of auto-agglutination was calculated by using this formula: $[(OD_{tot}-OD_{Agg}) / OD_{tot}] \times 100$. One-way ANOVA with Dunnett's multiple-comparison post hoc test were performed to calculate *p*-values.

Preparation of membrane fraction. Subcellular fractionation was performed as previously described (35). Briefly, bacteria were grown as described in biofilm section. Cultures were normalized at the same OD600nm and centrifuged at 3.700 g for 15 min. A volume of 9 ml of supernatants were collected, filtered through a 0.2 µm filter and then precipitated with 10% trichloroacetic acid at 4°C overnight. Once precipitated, supernatants were centrifuged at 3.700 x g for 45 min, resuspended in 200 µl of Tris base 1M. Pellets were resuspended in 1 ml of 10 mM Tris-HCl pH 8.0, 0.75 mM sucrose. Lysozyme (0.4 mg/ml) and EDTA pH 8 (10 mM final) were added and the sample was kept on ice for 30 min. Samples were centrifuged and while the pellets were resuspended in Tris-buffered saline (TBS, 50 mM Tris-HCl pH 8, 150 mM NaCl) containing proteases inhibitor cOmplete mini™ (Roche, Bâle, Switzerland). After sonication, the lysates were centrifuged at 21.000 x *g* for 30 min. The supernatant containing the cytoplasm fraction, were kept on ice to further analyses. To solubilize the inner membrane, the pellets were resuspended in 1 ml of TBS containing 1% Triton X-100. After 30 min of incubation on ice, the samples were centrifuged at 21.000 × *g* for 30 min. The pellets, corresponding to the outer membrane, were resuspended in TBS. Fractions were then separated by SDS-PAGE and $YcgV_{EDL933}$ was visualized by immunoblotting as describe below.

SDS-PAGE and Western blot. Fraction samples were diluted in twice-concentrated SDS-PAGE loading buffer containing β-mercaptoethanol and denatured by heating at 100 °C for 10

min. The samples were then separated by SDS-PAGE on 10% acrylamide gels. The gels were stained with Coomassie Blue or transferred to nitrocellulose membranes (Biorad, Hercules, CA, USA) at 100 volts. After 1 h of transfer, the nitrocellulose membrane was blocked in T-TBS with 1% skimmed milk for 1 h. The membrane was washed 3 times with T-TBS and incubated with 1:5000 solution of primary polyclonal antibody raised against $YcgV_{EDL933}$ peptide (GenScript, Piscataway, NJ, USA) for 1 h. The membrane was washed three times with T-TBS for 3 x 5 min and incubated for 1 h with 1:1000 solution of horseradish peroxidase (HRP)-conjugated goat anti-rabbit IgG antibody (1:1000; Biorad, Hercules, CA, USA) and washed 3 times with T-TBS and then 1 time with TBS. The antigen-antibody reaction was analyzed by using Opti-4CN detection kit according to the instructions of the manufacturer (Biorad, Hercules, CA, USA).

Acknowledgments

We are grateful to Frederic Berthiaume for technical assistance. This work was supported by grants from the Natural Sciences and Engineering Research Council of Canada (RGPIN SD-25120-09) to Josée Harel and Fonds de la recherche du Québec en nature et technologies to Josée Harel and Mario Jacques (FRQNT PT165375) and a scholarship to Philippe Vogeleer from FRQNT Québec Wallonie program (FRQNT Regroupements stratégiques 111946).

REFERENCES

1. Croxen MA, Finlay BB. 2010. Molecular mechanisms of *Escherichia coli* pathogenicity. Nat Rev Microbiol 8:26-38. https://doi.org/10.1038/nrmicro2265.

2. Paton AW, Paton JC. 1998. Detection and characterization of Shiga toxigenic *Escherichia coli* by using multiplex PCR assays for *stx1*, *stx2*, *eaeA*, enterohemorrhagic *E. coli hlyA*, rfb_{O111}, and rfb_{O157}. J Clin Microbiol 36:598-602.

3. Vogeleer P, Tremblay YD, Mafu AA, Jacques M, Harel J. 2014. Life on the outside: role of biofilms in environmental persistence of Shiga-toxin producing *Escherichia coli*. Front

Microbiol 5:317. https://doi.org/10.3389/fmicb.2014.00317.

4. Donlan RM, Costerton JW. 2002. Biofilms: survival mechanisms of clinically relevant microorganisms. Clin Microbiol Rev 15:167-93. https://doi.org/10.1128/CMR.15.2.167-193.2002.

5. Ryu JH, Beuchat LR. 2005. Biofilm formation by *Escherichia coli* O157:H7 on stainless steel: effect of exopolysaccharide and Curli production on its resistance to chlorine. Appl Environ Microbiol 71:247-54. https://doi.org/10.1128/AEM.71.1.247-254.2005.

6. Ryu JH, Kim H, Frank JF, Beuchat LR. 2004. Attachment and biofilm formation on stainless steel by *Escherichia coli* O157:H7 as affected by curli production. Lett Appl Microbiol 39:359-62. https://doi.org/10.1111/j.1472-765X.2004.01591.x.

7. Prigent-Combaret C, Vidal O, Dorel C, Lejeune P. 1999. Abiotic surface sensing and biofilm-dependent regulation of gene expression in *Escherichia coli*. J Bacteriol 181:5993-6002.

8. Ryu JH, Kim H, Beuchat LR. 2004. Attachment and biofilm formation by *Escherichia coli* O157:H7 on stainless steel as influenced by exopolysaccharide production, nutrient availability, and temperature. J Food Prot 67:2123-31. https://doi.org/10.4315/0362-028X-67.10.2123.

9. Vital M, Hammes F, Egli T. 2012. Competition of *Escherichia coli* O157 with a drinking water bacterial community at low nutrient concentrations. Water Res 46:6279-90. https://doi.org/10.1016/j.watres.2012.08.043.

10. Villegas NA, Baronetti J, Albesa I, Polifroni R, Parma A, Etcheverria A, Becerra M, Padola N, Paraje M. 2013. Relevance of biofilms in the pathogenesis of Shiga-toxin-producing *Escherichia coli* infection. ScientificWorldJournal 2013:607258. https://doi.org/10.1155/2013/607258.

11. Van Houdt R, Michiels CW. 2010. Biofilm formation and the food industry, a focus on the bacterial outer surface. J Appl Microbiol 109:1117-31. https://doi.org/10.1111/j.1365-

2672.2010.04756.x.

12. Visvalingam J, Ells TC, Yang X. 2017. Impact of persistent and nonpersistent generic *Escherichia coli* and *Salmonella sp*. recovered from a beef packing plant on biofilm formation by *E. coli* O157. J Appl Microbiol 123:1512-1521. https://doi.org/10.1111/jam.13591.

13. Segura A., Auffret P., Bibbal D., Bertoni M., Durand A., Jubelin G., Kérourédan M., Brugère H., Bertin Y., E. F. 2018. Factors Involved in the Persistence of a Shiga Toxin-Producing *Escherichia coli* O157:H7 Strain in Bovine Feces and Gastro-Intestinal Content. Frontiers in Microbiology. https://doi.org/10.3389/fmicb.2018.00375.

14. Chekabab SM, Daigle F, Charette SJ, Dozois CM, Harel J. 2012. Survival of enterohemorrhagic *Escherichia coli* in the presence of *Acanthamoeba castellanii* and its dependence on Pho regulon. Microbiologyopen 1:427-37. https://doi.org/10.1002/mbo3.40.

15. VanBogelen RA, Olson ER, Wanner BL, Neidhardt FC. 1996. Global analysis of proteins synthesized during phosphorus restriction in *Escherichia coli*. J Bacteriol 178:4344-66.

16. Wanner BL. 1996. Signal transduction in the control of phosphate-regulated genes of *Escherichia coli*. Kidney Int 49:964-7. https://doi.org/10.1038/ki.1996.136.

17. Crepin S, Chekabab SM, Le Bihan G, Bertrand N, Dozois CM, Harel J. 2011. The Pho regulon and the pathogenesis of *Escherichia coli*. Vet Microbiol 153:82-8. https://doi.org/10.1016/j.vetmic.2011.05.043.

18. Wells TJ, Totsika M, Schembri MA. 2010. Autotransporters of *Escherichia coli*: a sequence-based characterization. Microbiology 156:2459-69. https://doi.org/10.1099/mic.0.039024-0.

19. Charbonneau ME, Janvore J, Mourez M. 2009. Autoprocessing of the *Escherichia coli* AIDA-I autotransporter: a new mechanism involving acidic residues in the junction region. J Biol Chem 284:17340-51. https://doi.org/10.1074/jbc.M109.010108.

20. Wells TJ, Sherlock O, Rivas L, Mahajan A, Beatson SA, Torpdahl M, Webb RI, Allsopp

LP, Gobius KS, Gally DL, Schembri MA. 2008. EhaA is a novel autotransporter protein of enterohemorrhagic *Escherichia coli* O157:H7 that contributes to adhesion and biofilm formation. Environ Microbiol 10:589-604. https://doi.org/10.1111/j.1462-2920.2007.01479.x.

21. Allsopp LP, Totsika M, Tree JJ, Ulett GC, Mabbett AN, Wells TJ, Kobe B, Beatson SA, Schembri MA. 2010. UpaH is a newly identified autotransporter protein that contributes to biofilm formation and bladder colonization by uropathogenic *Escherichia coli* CFT073. Infect Immun 78:1659-69. https://doi.org/10.1128/IAI.01010-09.

22. Martinez-Gil M, Goh KGK, Rackaityte E, Sakamoto C, Audrain B, Moriel DG, Totsika M, Ghigo JM, Schembri MA, Beloin C. 2017. YeeJ is an inverse autotransporter from *Escherichia coli* that binds to peptidoglycan and promotes biofilm formation. Sci Rep 7:11326. https://doi.org/10.1038/s41598-017-10902-0.

23. Roux A, Beloin C, Ghigo JM. 2005. Combined inactivation and expression strategy to study gene function under physiological conditions: application to identification of new *Escherichia coli* adhesins. J Bacteriol 187:1001-13. https://doi.org/10.1128/JB.187.3.1001-1013.2005.

24. Henderson IR, Navarro-Garcia F, Desvaux M, Fernandez RC, Ala'Aldeen D. 2004. Type V protein secretion pathway: the autotransporter story. Microbiol Mol Biol Rev 68:692-744. https://doi.org/10.1128/mmbr.68.4.692-744.2004.

25. Beloin C, Roux A, Ghigo JM. 2008. *Escherichia coli* biofilms. Curr Top Microbiol Immunol 322:249-89.

26. Crepin S, Lamarche MG, Garneau P, Seguin J, Proulx J, Dozois CM, Harel J. 2008. Genome-wide transcriptional response of an avian pathogenic *Escherichia coli* (APEC) *pst* mutant. BMC Genomics 9:568. https://doi.org/10.1186/1471-2164-9-568.

27. Vo JL, Martinez Ortiz GC, Subedi P, Keerthikumar S, Mathivanan S, Paxman JJ, Heras B. 2017. Autotransporter Adhesins in *Escherichia coli* Pathogenesis. Proteomics 17. https://doi.org/10.1002/pmic.201600431.

28. Selkrig J, Mosbahi K, Webb CT, Belousoff MJ, Perry AJ, Wells TJ, Morris F, Leyton DL, Totsika M, Phan MD, Celik N, Kelly M, Oates C, Hartland EL, Robins-Browne RM, Ramarathinam SH, Purcell AW, Schembri MA, Strugnell RA, Henderson IR, Walker D, Lithgow T. 2012. Discovery of an archetypal protein transport system in bacterial outer membranes. Nat Struct Mol Biol 19:506-10, S1. https://doi.org/10.1038/nsmb.2261.

29. Paradis-Bleau C, Kritikos G, Orlova K, Typas A, Bernhardt TG. 2014. A genome-wide screen for bacterial envelope biogenesis mutants identifies a novel factor involved in cell wall precursor metabolism. PLoS Genet 10:e1004056. https://doi.org/10.1371/journal.pgen.1004056.

30. Chekabab SM, Jubelin G, Dozois CM, Harel J. 2014. PhoB activates *Escherichia coli* O157:H7 virulence factors in response to inorganic phosphate limitation. PLoS One 9:e94285. https://doi.org/10.1371/journal.pone.0094285.

31. Le Bihan G, Sicard JF, Garneau P, Bernalier-Donadille A, Gobert AP, Garrivier A, Martin C, Hay AG, Beaudry F, Harel J, Jubelin G. 2017. The NAG Sensor NagC Regulates LEE Gene Expression and Contributes to Gut Colonization by *Escherichia coli* O157:H7. Front Cell Infect Microbiol 7:134. https://doi.org/10.3389/fcimb.2017.00134.

32. Yuan ZC, Zaheer R, Morton R, Finan TM. 2006. Genome prediction of PhoB regulated promoters in *Sinorhizobium meliloti* and twelve proteobacteria. Nucleic Acids Res 34:2686-97. https://doi.org/10.1093/nar/gkl365.

33. Vogeleer P, Tremblay YD, Jubelin G, Jacques M, Harel J. 2015. Biofilm-Forming Abilities of Shiga Toxin-Producing *Escherichia coli* Isolates Associated with Human Infections. Appl Environ Microbiol 82:1448-58. https://doi.org/10.1128/AEM.02983-15.

34. Bansal T, Jesudhasan P, Pillai S, Wood TK, Jayaraman A. 2008. Temporal regulation of enterohemorrhagic *Escherichia coli* virulence mediated by autoinducer-2. Appl Microbiol Biotechnol 78:811-9. https://doi.org/10.1007/s00253-008-1359-8.

35. Rutherford N, Charbonneau ME, Berthiaume F, Betton JM, Mourez M. 2006. The periplasmic folding of a cysteineless autotransporter passenger domain interferes with its outer

membrane translocation. J Bacteriol 188:4111-6. https://doi.org/10.1128/JB.01949-05.

36. Strockbine NA, Marques LR, Newland JW, Smith HW, Holmes RK, O'Brien AD. 1986. Two toxin-converting phages from *Escherichia coli* O157:H7 strain 933 encode antigenically distinct toxins with similar biologic activities. Infect Immun 53:135-40.

37. Kang HY, Srinivasan J, Curtiss R, 3rd. 2002. Immune responses to recombinant pneumococcal PspA antigen delivered by live attenuated *Salmonella enterica* serovar typhimurium vaccine. Infect Immun 70:1739-49. https://doi.org/10.1128/IAI.70.4.1739-1749.2002.

ILLUSTRATIONS AND TABLES

Table 1. Strains and plasmids used in this study.

Strain/Plasmid	Relevant characteristics	Source reference
Strain		
EDL933	*E. coli* O157:H7; wild-type	(36)
EDL933 + C*ycgV*	*E. coli* O157:H7; wild-type + pTrc99A::$ycgV_{EDL933}$ (tc^R)	This study
Δpst	EDL933 Δ*pstCAB*::*aphA* (km^R)	(14)
ΔycgV	EDL933 Δ$ycgV_{EDL933}$::*tetR* (tc^R)	This study
ΔycgV + C*ycgV*	EDL933 Δ$ycgV_{EDL933}$::*tetR* + pTrc99A::$ycgV_{EDL933}$ (tc^R, amp^R)	This study
Δpst ΔycgV	EDL933 Δ*pstCAB*::*aphA*; Δ$ycgV_{EDL933}$::*tetR* (km^R, tc^R)	This study
Δpst ΔycgV + CycgV	EDL933 Δ*pstCAB*::*aphA*; Δ$ycgV_{EDL933}$::*tetR* + pTrc99A-$ycgV_{EDL933}$ (km^R, tc^R, amp^R)	This study
χ7213	SM10λpir Δ*asdA4* (km^R)	(37)
Plasmid		
pMEG-375	*sacRB* mobRP4 oriR6K (cm^R, amp^R)	S. Tinge, Megan Health Inc
pACYC184::*pst*	pACYC184, *pst* operon (cm^R, tc^R)	(37)
pTrc99A::$ycgV_{EDL933}$	pTrc99A, $ycgV_{EDL933}$ (amp^R, tc^R)	This study
pGEM®-T	Cloning vector	Promega

Table 2. List of primers used in this study.

Names	Sequence 5' à 3'	Use
AscI-ycgV1-F	GGCGCGCCGATATAACCACAGTGCATCG	Mutagenesis of Δ*ycgV*
Tet-ycgV1-R	GACTTCAGGTGCTACATTTGTGTGGTACGTTCCATGTCTC	
Tet-ycgV2-F	GCCAATCAATTCTTGCGGAGCCTATATAGTACCCAGGCTA	Mutagenesis of Δ*ycgV*
SacI-ycgV2-R	GAGCTCAAGTCCCCGAATAACGTGAT	
Tet-ycgV3-F	GAGACATGGAACGTACCACACAAATGTAGCACCTGAAGTC	Mutagenesis of Δ*ycgV*
Tet-ycgV3-R	TAGCCTGGGTACTATATAGGCTCCGCAAGAATTGATTGGC	
ycgV-seq-F	TTGCATGGCGCATTCAAAGA	Sequencing of Δ*ycgV*
ycgV-seq-R	ATTGACCACGCTCCAATATG	
comp ycgV BamHI F	CGGGATCCGAGACATGGAACGTACCACA	Complementation
comp ycgV SacI R	CGAGCTCGTAGCCTGGGTACTATATAGG	Complementation
ycgV-M-F	GATACAGGAAGTCAATATGG	mRNA quantification
ycgV-M-R	AGACCACCGATATAAACAC	
ycgV-Q-F	CAATATCAACCTGGGTAATG	mRNA quantification
ycgV-Q-R	GTCATCGTTACTCTTAATGG	
ycgV EMSA 6FAM F	[FAM]GGGCAAAATCAGAAACACAG	EMSA
ycgV EMSA F	GGGCAAAATCAGAAACACAG	
ycgV EMSA R	CAAGCGAAAATCCCATAACT	
Km EMSA 6FAM F	[FAM]CGAAACGATCCTCATCCTGT	EMSA (negative control)
Km EMSA F	CGAAACGATCCTCATCCTGT	
Km EMSA R	AAAGGAAGCGGAACACGTAG	
PhoB EMSA 6FAM F	[FAM]TGCCAGTCTGAGGTGTGAAG	EMSA (positive control)
PhoB EMSA F	TGCCAGTCTGAGGTGTGAAG	
PhoB EMSA R	CAGAATACGTCTCGCCATGA	

Figures

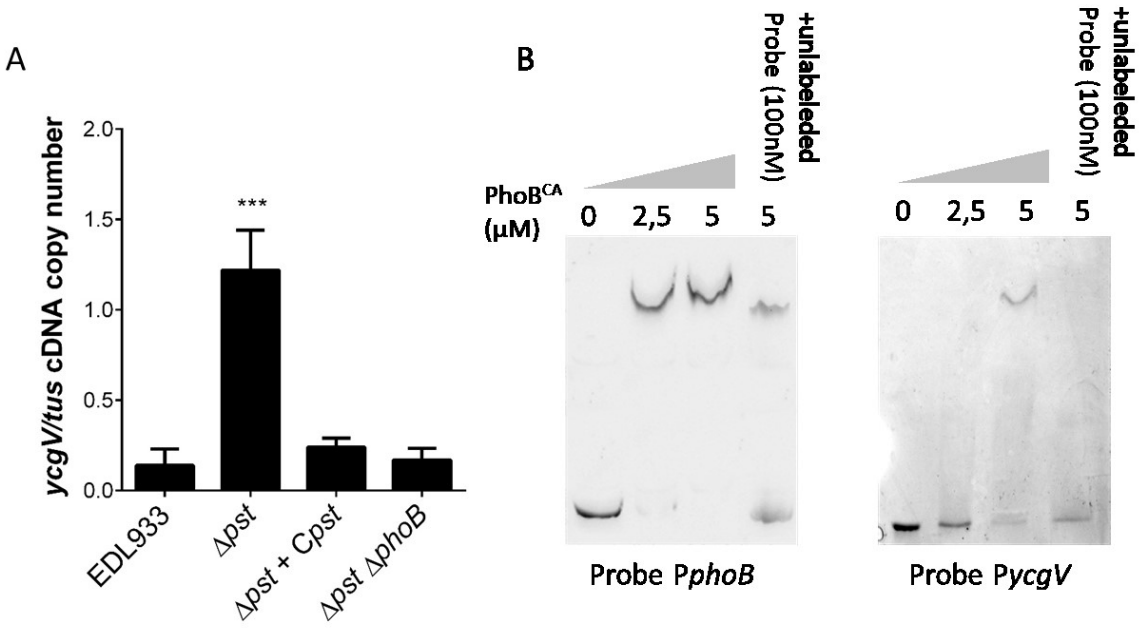

Figure 1. PhoB controls the expression of *ycgV*$_{EDL933}$ and binds to its promoter region. A. cDNA were synthetized from RNA extracted from biofilm cells of EDL933, Δ*pst* mutant, Δ*pst* + *pst*-complemented and Δ*pst* Δ*phoB* grown in M9 glycerol 0.2% for 24h at 30°C. Comparison between cDNA WT and its isogenic mutants were statistically analysed by one-way ANOVA with Tukey's multiple comparison post test. ***, $P < 0.001$. Results are shown as the ratio copy number of gene transcripts/copy number of *tus* transcripts. B. Increasing amounts (0, 2.5 µM or 5 µM) of PhoB^{CA} were used in the EMSA assay to shift the 6-FAM labelled DNA probes amplified from *phoB* (+2 to -218 bp) and *ycgV*$_{EDL933}$ (-141 to -344 bp) promoter regions.

A

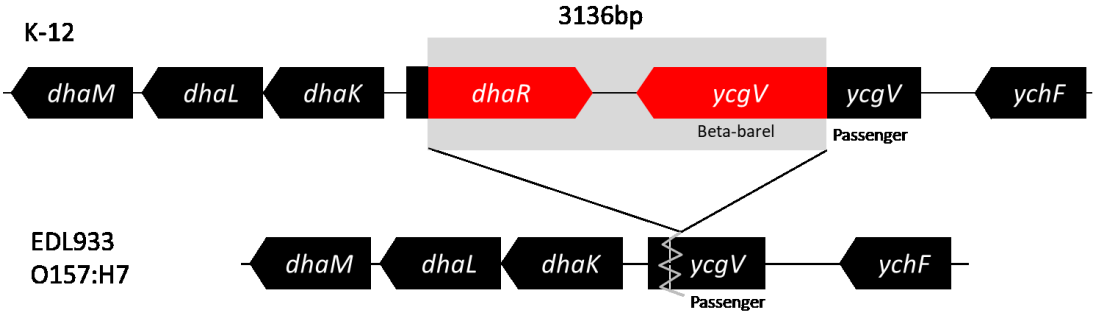

B

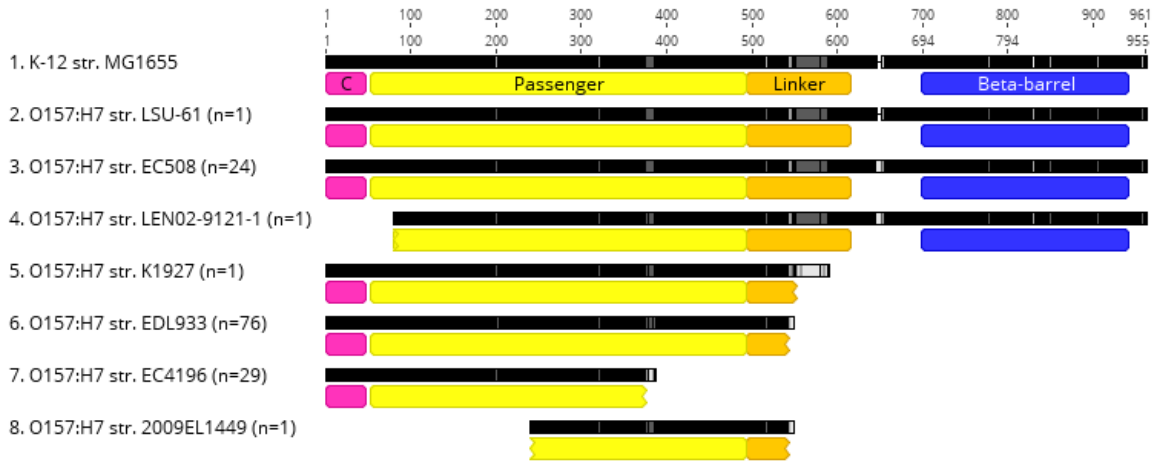

Figure 2. In most of O157:H7 strains, *ycgV* encodes a partial autotransporter. A. Comparison of the genomic context of *ycgV* of *E. coli* K-12 str. MG1655 (above sequence) and that of $ycgV_{EDL933}$ of *E. coli* O157:H7 str. EDL933 (Bottom). The sequence in red represents the 3136 bp deletion observed in for most of O157:H7 isolates. B. A total of 7 different YcgV variants were identified by BLAST comparing the YcgV of 135 O157:H7 strains. Those were mapped to YcgV of *E. coli* K-12 reference strain MG1655. YcgV sequences were obtained from the NCBI website (February 2019). The number of isolates with similar YcgV sequence is indicated by n=x. Indicated are the domains of the peptide signal (pink), the passenger (yellow), the linker (orange), the β-barrel (blue) as predicted using Interpro (https://www.ebi.ac.uk/interpro/protein/) website.

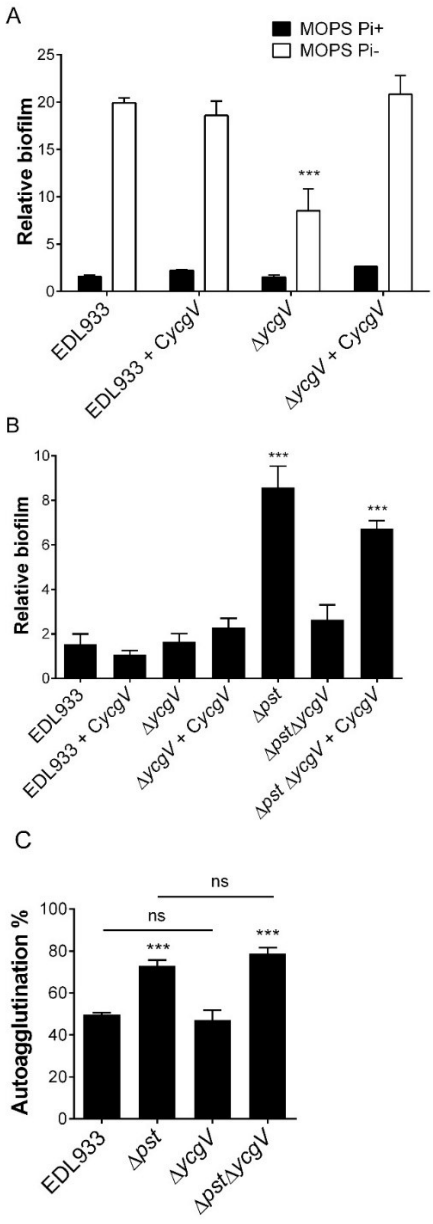

Figure 3. Partial autotransporter *ycgV*$_{EDL933}$ plays a role in biofilm formation of EDL 933 and of its isogenic Δ*pst* mutant. A. Relative biofilm formation of EDL933, Δ*ycgV* and *ycgV*-complemented strains grown in MOPS Pi+ (black bars) or in MOPS Pi- (white bars). Statistical analysis was performed B. Relative biofilm formation of EDL933, Δ*ycgV*, Δ*pst,* Δ*pst* Δ*ycgV* and ycg*V*-complemented strains grown in M9. C. Autoagglutination of EDL933, Δ*pst,* Δ*ycgV* and Δ*pst* Δ*ycgV* for 24 h in M9. Results are averages from at least 3 biological replicates. Statistical analysis was performed using a two-way ANOVA with Tukey's multiple comparison post-test (Fig 3A) or one-way ANOVA with Tukey's multiple comparison test (Fig 3B and 3C). *, $P < 0.05$; **, $P < 0.01$; ***, $P < 0.001$.

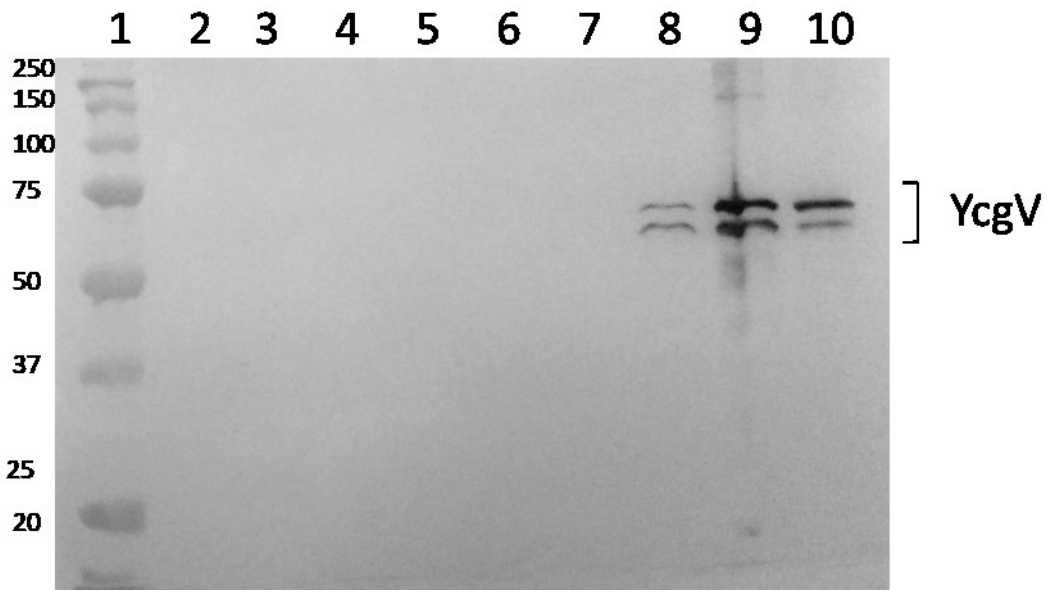

Figure 4. When *ycgV*$_{EDL933}$ is overexpressed, YcgV$_{EDL933}$ is localized in the outer membrane fraction. Two bands around 60 kDa were detected by Western blot of outer membrane fractions when *ycgV*$_{EDL933}$ was overexpressed in strains carrying pTrc99A::*ycgV*$_{EDL933}$ upon IPTG induction. 1. Molecular weight; 2. EDL933; 3. Δ*pst*; 4. Δ*ycgV*; 5. Δ*pst* Δ*ycgV*; 6. Δ*ycgV* + C*ycgV*; 7. Δ*pst* Δ*ycgV* + C*ycgV*; 8. EDL933 + C*ycgV*; 9. Δ*ycgV* + C*ycgV*; 10. Δ*pst* Δ*ycgV* +C*ycgV*. Lanes 2 to 7 correspond to outer membrane fraction of strains grown without IPTG induction and lanes 8 to 10 correspond to strains, grown with 1 mM IPTG induction.

V. Section V – Discussion générale

Ce projet de doctorat a consisté à caractériser le potentiel de formation des biofilms des souches STEC ainsi qu'à étudier l'impact de l'activation du régulon Pho sur la formation de biofilm d'une souche EHEC O157:H7. Les STEC sont des bactéries capables de s'adapter rapidement aux conditions changeantes de leurs environnements (le tractus intestinal des bovins, les fèces, l'eau, le sol, l'intestin humain). La capacité à former des biofilms dans des conditions environnementales hostiles permettrait d'augmenter la survie, la persistance et la transmission des STEC (Vogeleer *et al.*, 2014). Dans une première partie, nous avons donc voulu identifier quelles sont les caractéristiques des biofilms formés par les STEC (article 1). Dans une seconde partie, nous nous sommes intéressés à l'effet de la carence d'un nutriment, le phosphate, sur la formation de biofilm des EHEC O157:H7 (articles 2 et 3). Pris ensemble nos résultats montrent que les biofilms formés par les STEC sont divers à la fois en épaisseur, en structure et en composition et que grâce à des mécanismes de détection et de réponse aux signaux, les STEC et notamment les EHEC O157:H7, adoptent un mode de vie biofilm afin de survivre aux conditions hostiles de l'environnement. La formation de biofilm jouerait donc un rôle dans la transmission et la persistance des STEC dans l'environnement.

V.1 La formation de biofilm des STEC comme stratégie de survie dans l'environnement

V. 1.1 La formation de biofilm des STEC est hétérogène

Dans l'article de recherche 1, nous avons évalué le potentiel de formation de biofilm de 39 isolats de STEC tous associés à des cas d'infection chez l'humain et appartenant aux séropathotypes A, B ou C. Nous avons identifié que tous les isolats de notre collection étaient capables de former des biofilms. Précédemment à notre étude, il avait déjà été montré que les isolats STEC de différentes origines (bovins, eau, aliments et cliniques humaines) et de différents sérotypes étaient capables de former des biofilms (Biscola *et al.*, 2011; Park and Chen, 2015; Wang *et al.*, 2012a).

Par microscopie confocale, nous avons mis en évidence que pour une même condition de croissance, les biofilms formés par les isolats STEC variaient en termes de morphologie, de

structure et de composition. L'hétérogénéité de la matrice avait déjà été observée pour d'autres isolats de *E. coli* (Beloin *et al.*, 2008; Hung *et al.*, 2013). Alors que les protéines et l'ADN étaient faiblement détectés dans les biofilms STEC, nous avons pu mettre en évidence que la matrice des biofilms de certains isolats STEC était constituée de PGA ou de cellulose qui sont deux polysaccharides connus pour être importants pour le développement et l'architecture des biofilms chez *E. coli* (Beloin *et al.*, 2008). Nous avons également remarqué que même si les protéines n'étaient que faiblement détectées dans la matrice, elles jouaient un rôle important dans l'intégrité des biofilms formés par les STEC. La production de protéines telles que les autotransporteurs, le curli ou les fimbriae sont connues pour être impliqués dans la formation de biofilm des STEC et de *E. coli* en général (Cookson *et al.*, 2002; McWilliams and Torres, 2014; Shen *et al.*, 2005; Uhlich *et al.*, 2006; Valle *et al.*, 2008; Wells *et al.*, 2008). En ce sens, nous avons d'ailleurs pu mettre en évidence que quatre gènes codant pour des structures protéiques de surface étaient plus souvent présents chez les isolats STEC qui formaient significativement plus de biofilms. Parmi ces gènes figuraient deux gènes, *z1538* et *lpf2,* impliqués dans la production de fimbriae, et deux gènes, *ehaB* et *espP*, codant pour des autotransporteurs. Alors que le long fimbria polaire 2 et les autotransporteurs EhaB er EspP avaient déjà été associés au phénotype d'adhésion ou de formation de biofilm chez les STEC et chez *E. coli* en général (Newton et al., 2004; Puttamreddy, 2010; Wells et al., 2009b), les fimbriae associés au gène *z1538,* spécifique des souches de séropathotype A, porté sur l'îlot de pathogénicité OI-47, n'ont jamais été associés à la formation de biofilm. De manière intéressante, nous avons aussi identifié dans l'article 3 que la formation de biofilm des EHEC O157:H7 lors de carence en phosphate (article 3) était notamment due à la surexpression d'un gène codant pour un autotransporteur. Cette découverte est discutée plus loin (p. 231-234). Pris ensemble nos résultats suggèrent que les fimbriae et les autotransporteurs semblent jouer un rôle important dans la structure des biofilms formés par les STEC.

V.1.2 Des isolats adaptés pour former des biofilms à basse température

Au cours de cette thèse, nous avons aussi pu observer qu'en milieu minimal les souches STEC formaient plus de biofilm à basses températures (30°C) qu'à hautes températures (37°C). De précédentes études avaient montré que les STEC ont la capacité de former des biofilms à

basse température (Dourou *et al.*, 2011; Nesse *et al.*, 2014; Ryu *et al.*, 2004; Uhlich *et al.*, 2014). Dans notre cas, il est intéressant de noter que les isolats STEC isolés de patients malades avaient un meilleur potentiel de formation à basse température. Ceci suggère les STEC sont plus aptes à former un biofilm à l'extérieur de leur hôte. De plus, lors d'une étude en collaboration avec une équipe de l'Ifremer (Laboratoire Santé Environnement et Microbiologie, Unité Santé, Génétique et Microbiologie des Mollusques, Département Ressources Biologiques et Environnement, Ifremer Plouzané, France), nous avons également montré que les souches environnementales STEC et EPEC isolées de mollusques et de zones de cueillette de mollusques étaient capables de former de forts biofilms à de basse température (18°C). Certains sérotypes comme les souches de sérotype O26:H11, formaient d'ailleurs significativement plus de biofilm à 18°C qu'à 30°C (Annexe 2) (Baliere *et al.*, 2015). Des résultats préliminaires effectués au laboratoire ont permis de montrer que les souches EHEC O157:H7 EDL933 et Sakai étaient capables de former des biofilms à 4°C. Cependant la capacité de formation de biofilm à basse température ne semble pas être un facteur partagé par tous les phylogroupes et tous les pathotypes de *E. coli*. Par exemple, il a été constaté que les isolats de *E. coli* du phylogroupe B1 forment plus de biofilm à 37°C (Nielsen *et al.*, 2018). Lors de mon doctorat, j'ai aussi pu constater que les souches de pathotype AIEC formaient plus de biofilm à 37°C qu'à 30°C (Annexe 4) (Sicard *et al.*, 2018). Ceci suggère que pour les souches AIEC, la formation de biofilm jouerait un rôle plus important dans la colonisation du tractus gastrointetinale de l'hôte que dans la persitance dans l'environnement. Plusieurs études ont d'ailleurs montré la formation de biofilms pourrait jouer un rôle clé dans la colonisation bactérienne de l'intestin sain et dans les maladies intestinales (Annexe 3). Le paramètre de la température est donc à prendre en compte pour identifier dans quelle étape le processus de formation de biofilm est important. Pour détecter les changements de température, les bactéries utilisent des thermocapteurs comme les protéines, les lipides, l'ARN ou l'ADN. Ces thermocapteurs détectent les changements de température ambiante et adapte une réponse cellulaire adéquate. Il est connu que la température contrôle l'expression de facteurs de virulence des bactéries pathogènes (Lam *et al.*, 2014; Shapiro and Cowen, 2012). Chez d'autres espèces comme *S. aureus* et *P. aeruginosa*, les biofilms formés à 37°C sont plus importants que ceux formés à 25°C. En revanche, la température n'affectait pas la formation de biofilm de *Listeria monocytogenes* (Choi *et al.*, 2013). Ceci suggère que la température pourrait être un facteur de choix afin d'identifier dans

quel contexte le biofilm est important pour la bactérie étudiée. Donc, les STEC seraient capables de former des biofilms à des températures susceptibles d'être rencontrées dans l'environnement. Nous suggérons donc que la formation de biofilm des souches STEC serait donc majoritairement dépendante de la température. Pour aller plus loin, une étude à grande échelle testant la formation de biofilm de plusieurs souches *E. coli* de différents pathotypes, à différentes températures, pourrait être menée afin de vérifier cette hypothèse.

V.1.3 Les souches STEC de séropathotype A se distinguent

Plusieurs études ont évalué le potentiel de formation de biofilms des souches STEC de différents sérotypes. Quoiqu'une étude a pu montrer que les souches STEC de sérotype O103:H2 avait un plus grand potentiel de formation de biofilm par rapport aux souches de sérotype O26 :H11 et O103:H25, la majorité des études suggèrent que la formation de biofilm des souches STEC serait indépendante du sérotype (Biscola *et al.*, 2011; Nesse *et al.*, 2014; Wang *et al.*, 2012a). Dans notre étude, en raison du faible nombre d'isolats par sérotype, cette association n'a pu être déterminée. Cependant nous avons mis en évidence que les isolats de séropathotype A (O157:H7 et O157:NM) présentaient un meilleur potentiel de formation de biofilms que les isolats de séropathotypes B et C.

En plus de former des biofilms plus importants que les isolats STEC de séropathotypes B et C, les isolats de séropathotype A étaient les seules capables d'agglutiner la levure de manière mannose-indépendante. Ce phénotype était en corrélation avec la formation de biofilm et avec l'autoagglutination. Une étude actuellement menée par Yaindrys Rodriguez Olivera, (étudiante à la maitrise dans le laboratoire de Josée Harel) semble montrer que ce phénotype soit corrélé avec la production de curli par ces souches. De plus, les isolats de séropathotype A étaient les seuls à produire du PGA et de la cellulose. La production de ces polysaccharides ne semblait toutefois pas jouer de rôle ni dans l'intégrité du biofilm (comme montré par traitement enzymatique) ni dans la protection des cellules lors de traitements aux désinfectants. En effet, lors de traitement aux désinfectants, la viabilité et le métabolisme des cellules STEC dans les biofilms étaient significativement diminués. Cependant, les traitements aux désinfectants n'éliminaient pas ou peu la matrice des biofilms. Ces résultats, en accord avec de précédentes études (Fouladkhah *et al.*, 2013; Marouani-Gadri *et al.*, 2010; Park and Chen, 2015; Wang *et*

al., 2012a), montrent que les désinfectants ne peuvent pas éliminer complètement la matrice des biofilms. Ceci pourrait permettre une recolonisation plus rapide de la surface après un protocole de désinfection et augmenter le danger de contamination des usines de transformations alimentaires. Puisque nous avons montré que les protéines sont importantes pour la structure de la matrice et que les désinfectants sont efficaces pour réduire la viabilité des STEC, il serait donc intéressant de tester l'association désinfectant et protéase pour prévenir ou traiter de manière efficace les biofilms formés par les STEC.

En conclusion, parmi les isolats STEC cliniques, ceux du séropathotype A se démarquent des autres séropathotypes par leur aptitude à former des biofilms plus importants. Nos résultats montrent que la formation de biofilm dans l'environnement pourrait contribuer à la persistance des STEC et en particulier des sérotype O157:H7 et O157:NM, ce qui pourrait contribuer par conséquent à la forte incidence de ces sérotypes lors de toxi-infections alimentaires causées par les STEC.

V.1.4 La formation de biofilm est étroitement liée aux conditions de culture

Avant de commencer notre étude, nous avons déterminé quelles étaient les paramètres permettant une formation de biofilm optimale. Pour cela, les conditions de formation de biofilm ont été testées sur un petit groupe de souches pathogènes de *E. coli* de différents pathotypes, représentatifs de notre collection, et nous avons choisi les conditions qui permettaient une formation de biofilm optimale et avec la plus grande reproductibilité (surface, température, temps, quantité de bactéries au départ, milieu, source de carbone). Il est connu que la capacité de formation des biofilms d'une bactérie est dépendante des conditions du milieu dans lequel elle évolue (Choi *et al.*, 2013). Dans un premier temps, pour évaluer la formation de biofilms, les tests ont d'abord été effectués en conditions statiques en microplaque. Cette condition, facile et rapide permet de cribler un grand nombre de souches, mais présentent de nombreux défauts tels que l'accumulation de déchets, l'évaporation et le non renouvellement des nutriments (Tremblay et al., 2014; Tremblay et al., 2015), qui peuvent limiter la formation de biofilm.

Nous avons aussi mis au point et utilisé une technique de microfluidique pour étudier la formation de biofilms des *E. coli* pathogènes (Annexe 1) (Tremblay *et al.*, 2015). Nous avons

pu constater que certaines souches, qui formaient très peu de biofilm dans des conditions statiques, étaient en fait capables de former de forts biofilms dans des conditions dynamiques. Cette différence était particulièrement observée pour les isolats de sérotype O145:NM et O145:H25. Il a aussi été observé que dans des conditions dynamiques, l'architecture du biofilm formé par *E. coli* K-12 ou *P. aeruginosa* changeait dramatiquement par rapport à des conditions statiques (Purevdorj *et al.*, 2002; Vejborg and Klemm, 2009). Par exemple, nous avons pu identifier que le biofilm formé en condition dynamique par la souche AIEC LF82 avait une forme de champignon qui n'était pas observé en condition statique (Annexe 1) (Tremblay *et al.*, 2015). Ces changements peuvent s'expliquer par le fait qu'en condition dynamique, en plus de la présence de force de cisaillement exercée par le passage du flux, des facteurs néfastes pour la formation de biofilm tels que déchets métaboliques et les signaux de dispersion sont évacués. De plus des observations faites au laboratoire ont permis d'identifier qu'en présence de flux, certaines souches UPEC étaient capables de remonter à contrecourant et de contaminer le puits contenant le milieu de culture non-ensemencé. Il est intéressant de noter que ce phénomène n'a été observé que pour les souches UPEC qui sont connues pour leur capacité à coloniser le tractus urinaire. Pris ensemble nos résultats montrent à quel point la formation de biofilm bactérien des STEC et a fortiori de *E. coli,* est hétérogène et traduit la difficulté de classification des souches en fonction de leur potentiel de formation de biofilm.

De plus, si la formation de biofilm des STEC contribue à leur propagation dans l'environnement, il faut prendre en compte aussi que dans différents environnements ces souches STEC peuvent être en présence et évoluer avec des souches *E. coli* d'autres sérotypes ou d'autres espèces (Carter *et al.*, 2012; Liu *et al.*, 2015; Liu *et al.*, 2014; Wang *et al.*, 2015; Wang *et al.*, 2012b). Pour complètement caractériser le potentiel de formation de biofilm d'une souche, il faudrait donc idéalement évaluer son potentiel de formation de biofilm en présence d'espèces bactériennes issues du même environnement dans lequel la bactérie d'intérêt évolue.

V.2. La carence en Pi et l'induction du régulon Pho favorisent la formation de biofilm de *E. coli* O157:H7

Une variété de signaux extracellulaires, y compris les concentrations de nutriments (carbone, azote ou phosphate) et les conditions de croissance (pH, température, stress oxydatif ou stress osmotique) sont détectés par *E. coli* O157:H7. La détection et la réponse à diverses perturbations environnementales sont donc essentielles pour la survie de la bactérie dans l'environnement. En réponse aux stimuli environnementaux, l'activation des régulateurs de transcription modifie l'état physiologique et morphologique de la cellule permettant à la bactérie de s'adapter et de survivre. La privation de nutriments telle que la source de carbone est déjà considérée comme un signal pour favoriser la formation de biofilm de *E. coli* O157:H7 (Dewanti and Wong, 1995; Oh *et al.*, 2007; Ryu *et al.*, 2004).

V.2.1 Rôle de la carence en Pi sur la formation de biofilm

Le Pi est un élément essentiel pour la cellule bactérienne. Alors que la concentration en Pi est assez élevée (30 mM) dans la lumière intestinale d'un être humain en bonne santé, le Pi peut devenir limitant lorsque *E. coli* est en dehors de son hôte (Schurig-Briccio *et al.*, 2009). Ici nous nous sommes intéressés à l'effet de la carence en Pi sur la formation de biofilm de la souche EHEC O157:H7 EDL933. Précédemment à notre étude, le lien entre la carence en Pi et la formation de biofilm a déjà été rapporté chez d'autres espèces bactériennes, mais pas chez *E. coli*. Il avait déjà été établi que la concentration en Pi affectait la formation de biofilm de différentes espèces incluant des bactéries à Gram négatif telles que *V. cholera*e, *P. mirabilis, P. aeruginosa*, *P. fluorescens*, *P. aureofaciens* et *A. tumefaciens* et des bactéries à Gram positif telles que *Bacillus anthracis*. Chez *V. cholerae* et chez *P. fluorescens*, il a été montré que l'activation du régulateur PhoB jouait un rôle sur les concentrations intracellulaires en c-di-GMP, un second messager connu pour son effet sur les biofilms (Monds *et al.*, 2007; Pratt *et al.*, 2009). Chez *P. aeruginosa*, la limitation en Pi entraîne une augmentation de production de rhamnolipides qui sont des biosurfactants qui induisent la motilité et réduisent la formation de biofilm (Blus-Kadosh *et al.*, 2013). L'abolition du système Pst chez *P. mirabilis* (responsable d'ITU) entraîne un déficit de formation de biofilm dans un milieu à base d'urine humaine

(O'May *et al.*, 2009). Donc dans la plupart des cas, l'absence de Pi ou l'activation constitutive de PhoB due à la mutation du système Pst entraine une diminution de la formation du biofilm.

Dans notre étude, nous avons montré qu'en absence de Pi, EHEC O157:H7 EDL933 existait principalement sous forme de biofilm. Ceci avait également été observé chez un agent pathogène de plante, *A. tumefaciens*, pour lequel l'absence de Pi provoquait une plus grande production du polysaccharide d'adhésion unipolaire ce qui augmentait la formation de biofilm (Xu *et al.*, 2012). Il semble donc que dépendamment de l'espèce, voire peut-être même du pathotype d'une même espèce, l'activation du régulon Pho mène à une augmentation ou à une diminution de la formation de biofilm. Il est intéressant de noter que *A. tumefaciens* et *E. coli* O157 :H7, qui sont toutes deux des bactéries retrouvées dans l'environnement, s'adaptent à la carence en phosphate en augmentant leur formation de biofilm. Il est donc possible que la capacité à augmenter la formation de biofilm en conditions de carence en phosphate soit associée au mode de vie de la bactérie. Cependant ceci n'est pas observé chez *V. cholerae* qui est connu pour sa capacité de survie dans des milieux aquatiques dans lesquels la concentration de phosphate peut être faible (Pratt *et al.*, 2010). Toutefois, *V. cholerae* diffère de *A. tumefaciens* et de *E. coli* O157 :H7, car *V. cholerae* dispose de deux systèmes *pst* (Mudrak and Tamayo, 2012). La présence de deux systèmes *pst* pourrait permettre à *V. cholerae* une meilleure acquisition du phosphate par rapport à *A. tumefaciens* et *E. coli* O157:H7, limitant ainsi le risque de carence en phosphate. Pris ensemble, ces résultats suggèrent que la disponibilité en phosphate dans le milieu influence la formation de biofilm des bactéries.

V.2.2 Rôle du régulateur PhoB dans la formation de biofilm

Dans notre étude, nous avons pu mettre en évidence que l'augmentation de la formation de biofilm de la souche EHEC O157:H7 EDL933 en conditions de carence en phosphate était due à l'activation du régulateur PhoB. Pour cela nous avons utilisé un mutant isogène dérivé de la souche EDL933 Δ*pst*, dans lequel PhoB est constitutivement activée, qui mime donc des conditions de carence en Pi. Le mutant Δ*pst* produisait plus de biofilm. La suppression de *phoB* du mutant Δ*pst* menait à la formation d'un biofilm similaire au biofilm de la souche sauvage. Le régulateur PhoB est donc impliqué dans la formation de biofilm. Le rôle de PhoB dans la formation de biofilm a déjà été démontré chez d'autres espèces (Danhorn *et al.*, 2004; Haddad

et al., 2009; Monds *et al.*, 2007; Monds *et al.*, 2001; Newell *et al.*, 2011; Pratt *et al.*, 2009). Prises ensemble, ces observations nous permettent d'établir un lien entre la carence en Pi et la formation de biofilm chez *E. coli* O157:H7. Chez *E. coli* O157:H7, il a été montré que l'expression de PhoB pendant la formation de biofilm était augmentée (Bansal *et al.*, 2007). En revanche dans une autre étude, il a été montré chez un mutant Δ*rcsB* de la souche O157:H7 86-24, que l'expression de *phoB* était diminuée alors que la formation de biofilm était augmentée (Sharma *et al.*, 2017). Ce résultat suggère que dépendamment des conditions l'augmentation de l'expression de *phoB,* et de manière sous-jacente l'activation de PhoB, ne sont pas forcément requis pour activer la formation de biofilm. Ceci confirme l'existence de plusieurs voies d'activation de la formation de biofilm. De plus, il a aussi été montré que lorsque *E. coli* K-12 est cultivé dans un milieu très riche en Pi (40 mM), PhoB est activé pour assurer le stockage du Pi en polyPi. Lorsque PhoB est activé dans ces conditions, les auteurs ont observé une inhibition de la formation de biofilm (Grillo-Puertas *et al.*, 2016). Il serait possible que dépendamment des conditions d'activation, PhoB pourrait fonctionner comme un activateur ou un répresseur de la formation de biofilm de *E. coli*.

Chez d'autres espèces, telles que *P. fluorescens* et *V. cholerae*, l'activation de PhoB était associée à une modulation du niveau de c-di-GMP intracellulaire menant à la dispersion du biofilm (Monds *et al.*, 2007; Pratt *et al.*, 2009). Même si elle n'a pas été relié à la formation de biofilm, l'activation de PhoB a aussi été associée à la modulation du niveau de di-GMP-c intracellulaire chez la souche UPEC CFT073 (Crepin *et al.*, 2012; Crépin *et al.*, 2017). Il semble donc que dans certains cas le régulateur PhoB agisse sur les niveaux de di-GMP-c intracellulaires qui sont connus pour influencer la formation de biofilm chez *E. coli* et chez d'autres espèces (Beloin *et al.*, 2008).

Le régulateur PhoB peut aussi être activé par des mécanismes autres que la carence en Pi. En effet, il a été montré que certaines histidine kinases non spécifiques à PhoB pouvaient dans certains cas activer le régulateur PhoB. Parmi ces protéines figurent CreC, ArcB, KdpD, QseC, BasS et VanS (Fisher *et al.*, 1995; Haldimann *et al.*, 1998). Il a été proposé que l'activation non spécifique du régulon Pho participerait à l'émergence de sous-populations plus réactives, permettant une adaptation rapide à différents environnements (Zhou *et al.*, 2005).

PhoB pourrait donc contribuer à la régulation de la formation de biofilm dans des conditions autres que la carence en Pi. Pris ensemble, ces résultats indiquent que dépendamment ou indépendamment de la concentration en Pi, PhoB pourrait agir comme un régulateur de la formation de biofilm.

V.2.3 L'activation de PhoB réprime l'expression de nombreux composants de la surface de *E. coli* O157:H7.

Nos résultats de transcriptomique indiquent qu'une importante quantité de gènes codant pour des composants de la surface bactérienne ont une expression modulée chez le mutant Δ*pst* (activation constitutive de PhoB) ou lorsque la souche EDL933 est cultivée dans un milieu pauvre en phosphate (activation physiologique de PhoB) par rapport à la souche sauvage EDL933 cultivée dans un milieu riche en phosphate. Le fait que l'expression de nombreux gènes codant pour des composants de la surface bactérienne soit modulée suggère une possible restructuration de la paroi. L'analyse du profil transcriptomique a montré que chez le mutant Δ*pst,* plusieurs gènes tels que le « *Escherichia coli* common pilus » (ECP), le fimbriae F9, le PGA, le « *Escherichia coli* common antigen » (ECA), le LPS et l'acide colanique ainsi que certains gènes codant pour des protéines de l'enveloppe précédemment associées à la formation de biofilm (*btuB*, *proQ*, *mdoH*, *sdhCDAB* et *ybgC-tolQRAB*) étaient négativement régulés (Ebel *et al.*, 1997; Niba *et al.*, 2007; Otto *et al.*, 2001; Puttamreddy *et al.*, 2010). Ceci était également observé en réponse à une carence en Pi chez la souche sauvage. Une telle diminution de l'expression des gènes de surface pendant la formation de biofilm a déjà été observée dans une étude qui évaluait l'effet de l'urine sur la formation de biofilm de *E. coli* (Hancock and Klemm, 2007). De plus, il avait déjà été rapporté chez *E. coli* K-12 et chez des souches ExPEC et APEC que l'activation de PhoB affectait l'expression des gènes codant pour les composants membranaire comme le LPS, l'acide colanique, les protéines de la membrane externe et les lipides membranaires (Crepin *et al.*, 2008; Daigle *et al.*, 1995; Lamarche and Harel, 2010; Lamarche *et al.*, 2008; Ngeleka *et al.*, 1992; Yang *et al.*, 2012). Chez *Caulobacter crescentus*, il a été montré que la carence en Pi entrainait l'élongation du pédicule polaire (Gonin *et al.*, 2000). Ce phénotype a été relié à l'activation de la protéine PhoB et confirme l'implication de PhoB dans la restructuration membranaire lors de carence en phosphate. Il est intéressant de

noter que le phosphate est un composant majeur des phospholipides contenus dans la paroi cellulaire. Donc en absence de phosphate, les phospholipides membranaires ne sont pas renouvelés ce qui peut affecter la résistance de la paroi aux stress tels que le stress oxydatif et la pression osmotique, etc. On peut donc penser que lors de la carence en phosphate, PhoB contrôle la production des composants de surface afin d'assurer la résistance membranaire tout en économisant le phosphate. En ce sens, il a été montré que dans des conditions limitantes en phosphate, *Rhizobium meliloti* substitue les phospholipides membranaires par des lipides ne contenant pas de phosphore tels que le sulfoquinovosyle diacylglycérol, l'ornithine et le diacylglyceryle triméthylhomosérine. Dans cette étude, les auteurs ont démontré que la synthèse de diacylglycéryle-triméthylhomosérine était contrôlée par le régulateur PhoB (Geiger *et al.*, 1999). Donc dans des conditions de carence en phosphate, PhoB semble impliqué dans le réarrangement global des composants de surfaces. Nous suggérons que chez EHEC O157:H7 EDL933 ces réarrangements de la paroi participent à l'augmentation de la formation de biofilm lors de l'activation de PhoB.

V.2.4 PhoB contrôle l'expression de l'autotransporteur YcgV

Parmi les facteurs potentiellement régulés par PhoB et pouvant affecter la composition de la paroi, nous avons identifié que le gène *ycgV*, codant pour un autotransporteur du type AIDA-I, était surexprimé lorsque PhoB était activé. YcgV appartient à la famille des autotransporteurs auto-associés (SAAT), connue pour favoriser l'adhésion aux cellules épithéliales, l'autoagglutination ou la formation de biofilms (Allsopp *et al.*, 2010; Charbonneau *et al.*, 2009; Martinez-Gil *et al.*, 2017; Wells *et al.*, 2008; Wells *et al.*, 2010). Chez EDL933, le gène *ycgV* (nommé par la suite $ycgV_{EDL933}$) est présent sous forme tronqué par rapport à la copie présente chez *E. coli* K-12 (Wells *et al.*, 2010). Nos analyses ont révélé que ce variant $ycgV_{EDL933}$ était communément retrouvé chez les souches de sérotype O157:H7. Le gène $ycgV_{EDL933}$ code pour une protéine de 547 acides aminés (955 acides aminés chez *E. coli* K-12) qui correspond au domaine passager en N-terminal et à un fragment du domaine de liaison. Le domaine de translocation, normalement associé à la fonction de transport à travers la membrane externe est donc absent (Figure 1).

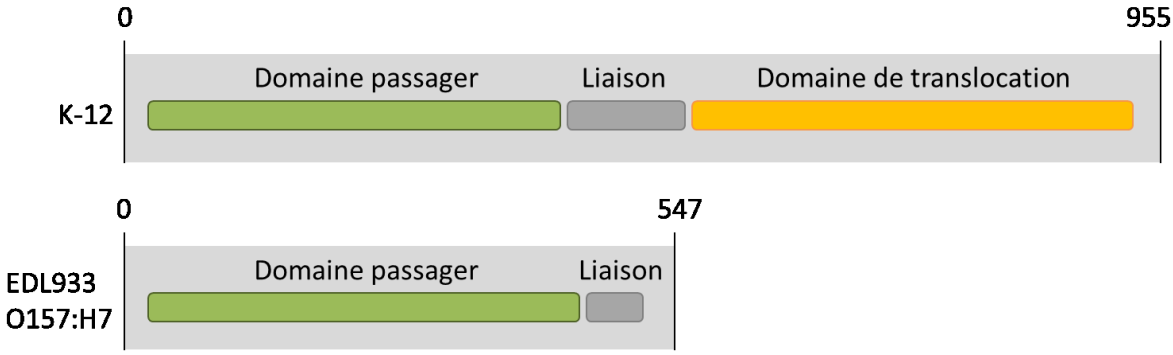

Figure 1. Organisation des domaines de l'autotransporteur YcgV de la souche *E. coli* K12 et de l'autotransporteur YcgV$_{EDL933}$ de la souche EHEC O157:H7 EDL933. Le domaine passager d'YcgV$_{EDL933}$ partage 97.8% d'identité avec le domaine passager de la souche *E. coli* K-12 mais ne dispose pas de domaine de translocation.

Toutefois nos résultats indiquent que *ycgV*$_{EDL933}$ tronqué est impliqué dans la formation de biofilm de O157:H7. Chez *E. coli* K-12 MG1655, il avait déjà été montré que la surexpression du gène *ycgV* codant pour la forme complète de YcgV entrainait une augmentation de l'adhésion et de la formation de biofilm. En revanche, la délétion de *ycgV* de la souche MG1655 n'avait pas d'effet sur la formation de biofilm. En 2008, il a été proposé que les autotransporteurs dont la suppression n'avait pas d'effet sur la formation de biofilm (i.e. YcgV) puissent être exprimés dans des conditions physiologiques particulières (Beloin *et al.*, 2008). Il est donc possible que nous ayons identifié la carence en Pi comme la condition physiologique particulière nécessaire à la production de YcgV$_{EDL933}$ puisque *ycgV*$_{EDL933}$ est surexprimé dans le mutant Δ*pst* et chez la souche sauvage en conditions de carence en Pi.

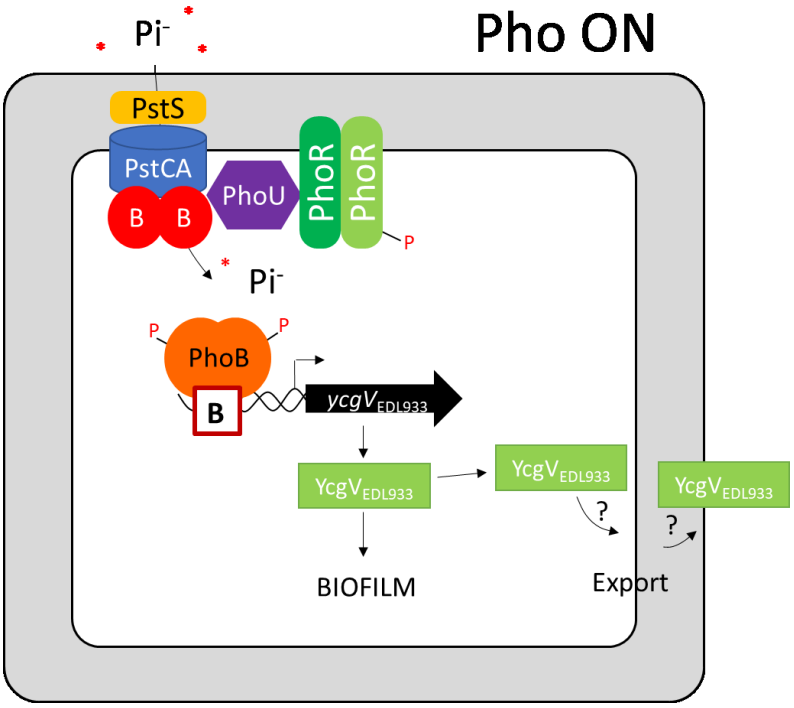

Figure 2. Modèle de la régulation de *ycgV*$_{EDL933}$ par PhoB. En condition de carence en Pi, le régulateur transcriptionnel PhoB est activé, il se lie à une région contenant une boîte Pho située en amont du gène *ycgV*$_{EDL933}$ et active l'expression de ce gène. La protéine YcgV$_{EDL933}$ est constituée d'un domaine passager de type AIDA-1 et participe à la formation de formation de biofilm de EDL933 dans des conditions de carence en Pi. YcgV$_{EDL933}$ peut être retrouvé dans la membrane externe mais son exposition sur la face externe ainsi que le mécanisme de translocation sont inconnus.

De plus, nous avons aussi mis en évidence que le gène *ycgV*$_{EDL933}$ était sous le contrôle direct de PhoB. En effet une boîte Pho a été identifiée en amont de *ycgV*$_{EDL933}$ et nous avons montré que lorsque PhoB est activé, il intérgissait directement avec la région promotrice de *ycgV*$_{EDL933}$. Cette boîte Pho située en amont de *ycgV* est également détectée *in silico* dans d'autres souches d' *E. coli*, telles que la souche *E. coli* K-12 MG1655 et la souche APEC O78 7122. Ceci suggère que *ycgV* puisse aussi être régulé par PhoB chez différentes souches de *E. coli*. Cependant cette régulation devra être déterminée dans une étude future. Ainsi, *ycgV*$_{EDL933}$ est sous le contrôle du régulon Pho et contribue à la formation de biofilm lorsque la concentration de phosphate est limitante (Figure 2).

Puisque YcgV$_{EDL933}$ joue un rôle dans la formation de biofilm lorsque PhoB est activé,

nous suggérons aussi que même s'il est tronqué, un autotransporteur partiel pourrait jouer un rôle dans l'adaptation de la bactérie dans son environnement (Figure 2). De plus, grâce à une analyse par Western blot, la présence de $YcgV_{EDL933a}$ a pu être détectée au niveau de la membrane externe lorsque celui-ci était surexprimé.

Le mécanisme d'export d'un autotransporteur ne contenant que le domaine passager tel que $YcgV_{EDL933}$ n'a pas été rapporté. Généralement, l'export des SAAT est assuré par la voie de sécrétion de type V. Le domaine de translocation de l'autotransporteur participe à la translocation de son domaine passager à travers la membrane externe. Cependant, il a été démontré que d'autres facteurs accessoires tels que le complexe Bam ou les protéines chaperonnes du périplasme jouent un rôle important dans le processus de translocation à la surface de la cellule (Henderson *et al.*, 2004; Vo *et al.*, 2017). En outre, deux protéines, TamA et TamB, faisant partie du module de translocation et d'assemblage, se sont révélées impliquées dans la translocation d'autotransporteurs de protéobactéries (Selkrig *et al.*, 2012). Plusieurs hypothèses sont envisagées pour expliquer la présence possible de $YcgV_{EDL933}$ dans la paroi bactérienne. Est-il possible qu'en absence du domaine de translocation, l'export de $YcgV_{EDL933}$ soit pris en charge par certains de ces systèmes? Ou bien est-il possible que l'export de $YcgV_{EDL933}$ se fasse grâce à un domaine de translocation fourni en *trans* ? Cependant l'effet *trans* n'a jamais été rapporté. En tenant compte du réarrangement membranaire induit par le signal de carence en Pi, le mécanisme d'export de $YcgV_{EDL933}$ devra donc être étudié dans une étude future.

De manière intéressante, *ycgV* a aussi été identifié dans un criblage à haut débit qui visait à sélectionner des mutants de *E. coli* K-12 déficients pour l'assemblage de l'enveloppe cellulaire (Paradis-Bleau et al., 2014). Ceci indique que YcgV pourrait jouer un rôle dans l'intégrité de la paroi cellulaire, tout du moins chez *E. coli* K-12. Comme la paroi de *E. coli* O157:H7 subit plusieurs modifications lors de l'activation du régulateur PhoB (Chekabab *et al.*, 2014) (article 2), il est possible que, dans de telles conditions, $YcgV_{EDL933}$ puisse participer à la restructuration de la membrane et contribuer à la formation de biofilm. Pris ensemble, ces résultats montrent que YcgV est impliqué dans la formation de biofilm lorsque le phosphate est limitant et suggèrent un rôle dans la modification de la paroi bactérienne. Ces observations illustrent la

façon dont les agents pathogènes tels que O157:H7 sont adaptés pour survivre dans différentes niches écologiques.

V.2.5 Le mutant Δ*pst* se distingue

Le mutant Δ*pst* contient du N-acétylglucosamine dans son biofilm

En plus de former des biofilms plus importants par rapport à la souche sauvage, la matrice du biofilm du mutant Δ*pst* contenait du N-acétylglucosamine (NAG) tel que visualisé par microscopie confocale et marquage avec une lectine fluorescente. La présence de NAG par O-glycosylation a déjà été reliée avec la formation de biofilm (Wang *et al.*, 2012c). Cependant la présence de NAG n'était pas suffisante pour expliquer l'augmentation de la formation de biofilm. En effet du NAG était également présent dans le biofilm moins important formé par le double mutant Δ*pst* Δ*phoB*. De plus, le fait que le NAG ne soit pas détecté dans la matrice du biofilm formé par EDL933 en condition limitante en Pi suggère que le régulateur PhoB n'est pas impliqué dans ce phénotype. Nous proposons que ce phénotype PhoB indépendant soit dû à l'effet de la délétion de *pst* qui mène non seulement à l'expression exacerbée de *phoB* mais aussi à l'expression de plusieurs régulateurs de stress (Crepin *et al.*, 2008).

Chez *E. coli*, plusieurs polysaccharides de surface peuvent contenir du NAG incluant le PGA, le ECA, le peptidoglycane et le LPS (Ali *et al.*, 2006; Meier-Dieter *et al.*, 1990; Vollmer and Bertsche, 2008; Wang *et al.*, 2004; Whitfield and Trent, 2014). Cependant l'expression de la plupart des gènes reliés à la production de ces polysaccharides était diminuée chez le mutant Δ*pst* par rapport à la souche sauvage. De plus, nous avons pu mettre en évidence que la présence de NAG dans le biofilm formé par le mutant Δ*pst* n'était pas associée à la production de PGA puisque la délétion de l'opéron *pgaABCD* du mutant Δ*pst* n'avait aucun impact ni sur la formation de biofilm ni sur la production de NAG. Par contre, l'expression de CsrC et de CsrB, deux petits ARN régulateurs impliqués dans la régulation post-traductionnelle de PGA et dans la formation de biofilm (Bak *et al.*, 2015), était augmentée dans le mutant Δ*pst*. Par conséquent, il est possible que CsrB et CsrC jouent un rôle dans la production de PGA (Wang *et al.*, 2005). Ceci demeure à être confirmé.

La détection de NAG dans la matrice du biofilm du mutant Δ*pst* pourrait donc être

expliquée soit par la glycosylation de protéines comme précédemment observé lorsque le protéome de *E. coli* K-12 était mis en contact avec du « wheat germ agglutinin » (WGA) (Wang *et al.*, 2012c), soit par l'exposition de résidus NAG des molécules de LPS ayant subi des modifications (tel que discuté plus loin p. 237). De toute évidence, la présence de NAG à la surface dans le biofilm souligne le fait que la paroi du mutant Δ*pst* a subi des modifications.

Le LPS contribue à la formation de biofilm du mutant Δ*pst*

Pour étudier les effets de la mutation *pst* sur la formation de biofilm, nous avons utilisé, en plus de l'étude transcriptomique, une approche de criblage d'une banque de mutants obtenue par transposition aléatoire dans le mutant Δ*pst*. La sélection de mutants dérivés du mutant Δ*pst* a été basée sur la diminution de l'autoagglutination et de la formation de biofilms (article 2). La majorité des sites dans lesquels le transposon était inséré, étaient des gènes impliqués dans la synthèse de la paroi bactérienne. Ces résultats coïncident avec nos conclusions tirées des résultats de transcriptomique : la paroi de *E. coli* O157:H7 est modifiée et joue un rôle clé dans le mécanisme d'augmentation de la formation de biofilm lors d'une carence en phosphate. Ceci suggère que la paroi du mutant Δ*pst* doit subir des modifications de composition et/ou de structure favorisant la formation de biofilm.

De manière intéressante, chez plusieurs de ces double mutants le transposon s'est inséré dans le locus *waa* responsable de la synthèse des enzymes nécessaires à l'assemblage du LPS (Raetz and Whitfield, 2002) (Figure 3). Comme décrit dans la revue de littérature, les LPS sont des lipoglycanes phosphorylés exposés à la surface et insérés dans le feuillet externe de la membrane externe des bactéries à Gram négatif (Raetz and Whitfield, 2002). Le LPS est une molécule tripartite constituée du lipide A hydrophobe ancré dans la membrane externe (endotoxine), d'un noyau oligosaccharidique central, qui est divisé en une région interne et une région externe, et du polysaccharide antigène O. Chez *E. coli* O157 :H7, cet antigène O est le O157 (Kuo *et al.*, 2016; Raetz and Whitfield, 2002). L'implication du LPS dans la formation de biofilm des souches *E. coli* incluant les EHEC O157:H7 a déjà été démontrée. Ainsi, il a été montré que les gènes impliqués dans la synthèse du noyau du LPS ou dans la synthèse de l'antigène O157 présentaient un phénotype de biofilm réduit (Puttamreddy *et al.*, 2010). Ceci a également été observé chez les UPEC et *E. coli* K-12 (Hadjifrangiskou *et al.*, 2012). Dans notre

étude, les mutants dérivés de Δ*pst* qui avaient une insertion du transposon dans les gènes de synthèse du noyau du LPS, produisant donc un LPS dont le noyau était tronqué, avaient tous des phénotypes diminués pour l'autoagglutination et la formation de biofilm. Nous avons aussi remarqué que chez ces mutants les biofilms ne contenaient pas de NAG. Nous suggérons donc que la détection de NAG dans le mutant Δ*pst* soit due à des modification de la molécule de LPS (Figure 4). Ces résultats montrent que la synthèse des noyaux LPS sont nécessaires pour assurer la formation de biofilm du mutant Δ*pst*.

Le LPS du mutant Δ*pst* est structurellement différent

Chez le mutant Δ*pst*, la structure du LPS est modifiée par rapport à la souche sauvage EHEC O157:H7 EDL933. Le mutant Δ*pst* produit de façon très majoritaire un LPS rugueux (rough), c'est-à-dire sans antigène O157 et a perdu sa spécificité antigénique liée à l'antigène O157. Ainsi, le LPS mutant Δ*pst* est principalement constitué du lipide A, enchâssé dans la membrane externe qui représente la partie proximale du LPS, le noyau, sa partie médiane, et n'a pas l'antigène O, sa partie distale « libre » dans le milieu extérieur. Il est intéressant de noter que l'interruption de la production de l'antigène O chez un mutant Δ*per* de *E. coli* O157:H7 a déjà été associée à une augmentation de l'autoagglutination (Sheng *et al.*, 2008). Ceci coïncide avec le phénotype d'autoagglutination observé chez le mutant Δ*pst*. En absence de la structure de chaînes latérales spécifique à l'antigène O les autres composantes de la membrane externe de la paroi bactérienne sont exposées, favorisant une interaction plus rapprochée entre les cellules. Ceci pourrait expliquer le phénotype d'autoagglutination observé chez les mutants déficients en antigène O. L'absence de l'antigène O157 pourrait également expliquer la détection de NAG dans la matrice des biofilms du mutant Δ*pst*. En effet deux molécules de NAG sont présentes dans le noyau du LPS de O157:H7 (Figure 3). En absence d'antigène O, le marqueur WGA révélait plus efficacement le NAG du LPS ainsi exposé. En ce sens, les mutants dérivés du mutant Δ*pst* avec le transposon inséré dans le locus *waa* étaient négatifs au NAG et produisaient un LPS dont le noyau était altéré (Figure 3).

L'absence de l'antigène O157 a déjà été observée lors de l'activation de PagP, une enzyme de la membrane externe responsable de la palmitoylation du lipide A (Smith *et al.*, 2008). De plus, il a été démontré que la palmitoylation associée à la formation de biofilm est

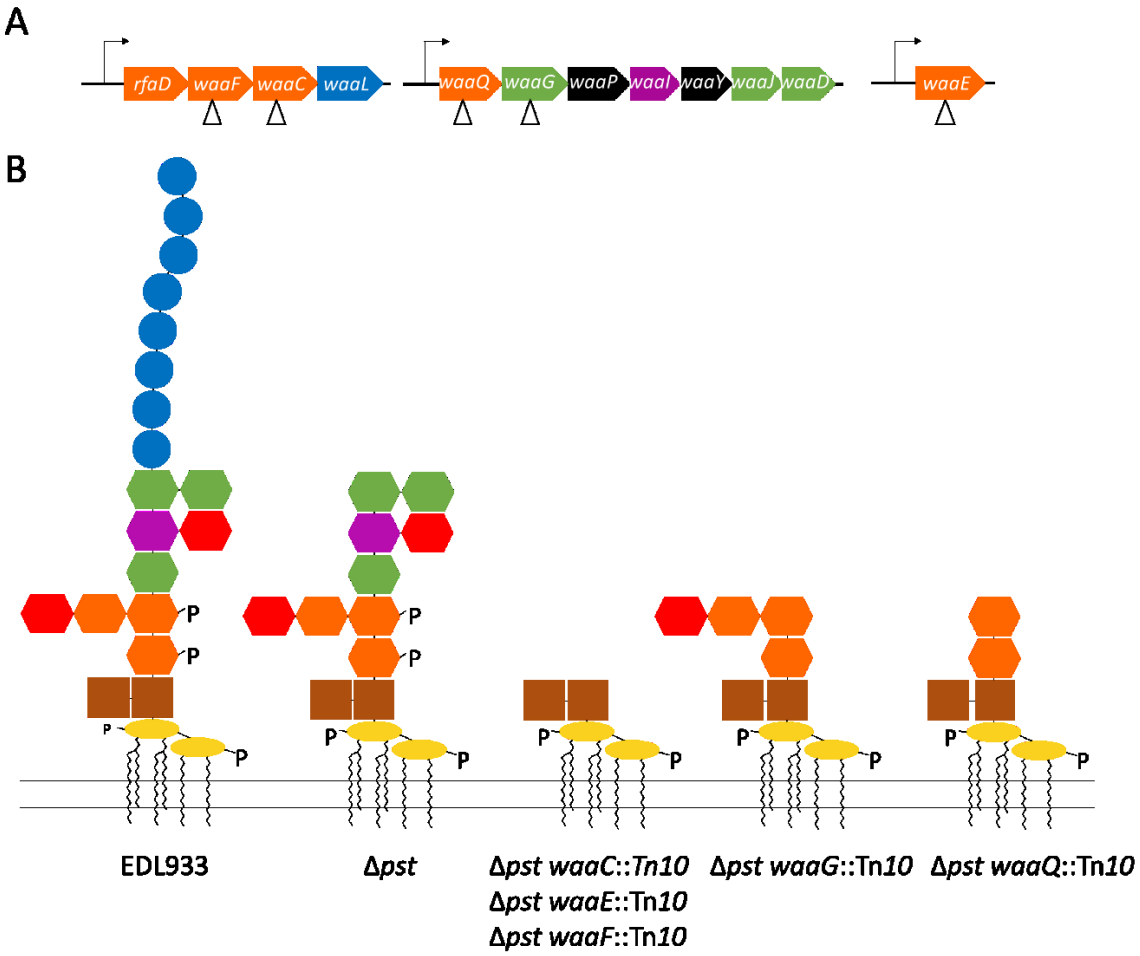

Figure 3. Représentations du locus *waa* et structure des molécules de LPS de EDL933, du mutant Δ*pst* et de ses différents mutants dérivés *waa*::Tn*10*. A. Organisation génétique du locus de biosynthèse du noyau du LPS. Les sites d'insertion du transposon Tn*10* sont indiquées par des triangles. La couleur du gène correspond à son implication dans la synthèse ou l'ajout des molécules de même couleur représenté sur le schéma du bas. B. Structure du LPS des O157:H7 (type R3). Jaune : lipide A ; Marron : KDO ; Orange : heptose ; Rouge : NAG ; Bleu : antigène-O ; Vert : glucose ; Noir : phosphate ; Violet :galactose.

une caractéristique générale des Entérobactéries (Smith *et al.*, 2008). Il a aussi été montré que la palmitoylation du lipide A par PagP était une modification observée dans les biofilms matures d'*E. coli* K-12 (Chalabaev *et al.*, 2014). Alors que PhoB a été identifié comme régulateur de l'expression de *pagP* chez *E. coli* K-12 (Yang *et al.*, 2012), nous avons observé que la palmitoylation du lipide A était augmentée à la fois chez la souche sauvage et chez le mutant Δ*pst* (PhoB activée) cultivés sous forme de biofilm. Ceci suggère que la palmitoylation du lipide

A, ne peut expliquer à elle seule l'absence d'antigène O et l'augmentation de la formation de biofilm du mutant Δ*pst*.

En revanche, nous avons détecté la présence d'une structure supplémentaire sur le LPS du mutant Δ*pst* qui est absente chez la souche sauvage EDL933 au niveau du noyau. Cette structure inconnue de 365.4 u pourrait soit correspondre à un disaccharide contenant un hexose et un N-acétyl-hexose (HexNAc) ou un hexose plus un pyrophosphoryl-éthanolamine (PPEA). Il est donc possible que les modifications des molécules de LPS, comme l'ajout du composé de 365.4 u, entrainent l'arrêt de la synthèse de l'antigène O chez le mutant Δ*pst*.

Le rôle de PhoB dans les modifications du LPS du mutant Δ*pst*

La production de l'antigène O157 ne semble pas sous le contrôle de PhoB puisque la présence de l'antigène O157 n'est pas restaurée chez le double mutant Δ*pst* Δ*phoB* et que la production d'antigène O157 ne semble pas affectée lorsque EDL933 est cultivée dans des conditions pauvres en Pi.

La présence de l'antigène O157 ne semble donc pas impliquée dans l'augmentation de la formation de biofilm du mutant Δ*pst.* Cependant l'absence d'antigène O157 pourrait tout de même être associée au phénotype d'autoagglutination. En effet le mutant Δ*pst* déficient en antigène O157 avait une meilleure capacité d'autoagglutination que la souche sauvage. L'absence d'antigène O157 faciliterait l'autoagglutination de la bactérie en favorisant l'exposition des molécules de surface impliquées dans le phénomène d'agrégation.

Cependant le régulateur PhoB pourrait tout de même jouer un rôle dans la régulation de la production de LPS. En effet, des travaux réalisés par Klein et ses collaborateurs ont montré que PhoB régule l'hétérogénéité des molécules de LPS (Klein *et al.*, 2011; Klein *et al.*, 2013). Sachant que la synthèse des molécules de LPS nécessite la consommation de phosphate, il peut être envisagé que lors d'une carence en phosphate, un mécanisme de régulation non identifié permettrait de réduire le coût métabolique de la synthèse de structures de surface tel que le LPS. Cette fonction pourrait être assuré par la protéine PhoB mais aussi par d'autres régulateurs de stress généraux connus pour être activés lorsque le phosphate est limitant (Pragai and Harwood, 2002) (Figure 4).

V.2.6 WaaH est une glycosyltransférase impliquée dans la formation de biofilm.

Nous avons également identifié que le gène *waaH* (*yibD*) est sous le contrôle de PhoB et contribue à la formation de biofilm chez le mutant Δ*pst* et lorsque la souche EDL933 est cultivée en absence de Pi. WaaH ne participait pas au phénotype d'autoagglutination observé chez le mutant Δ*pst*. Grâce aux résultats de transcriptomique, nous avons observé que l'expression de *waaH* était fortement induite à la fois dans EHEC O157:H7 EDL933 cultivé dans des conditions de carence en phosphate et dans le mutant Δ*pst*. Nous avons aussi montré que PhoB fixait une boîte Pho dans la région promotrice de *waaH*.

WaaH est une glycosyltransférase responsable de l'ajout de GlcUA sur l'heptose III du noyau interne des LPS de *E. coli* K-12 et dont l'expression du gène sous le contrôle de PhoB et est induite dans des conditions de carence en Pi (Baek and Lee, 2006; Klein *et al.*, 2013; Yoshida *et al.*, 2011). Une modification de GlcUA a été observée pour les noyaux internes de types B, K-12, R2 et R4 des LPS de *E. coli* et chez *Salmonella* mais pas celui de *E. coli* O157:H7 qui est de type R3 ni pour celui de type R1 (Klein *et al.*, 2013). Chez *E. coli* O157:H7, l'heptose III du noyau de type R3 est décoré avec du NAG par l'activité du gène *wabB* présent sur le plasmide pO157 (Kaniuk *et al.*, 2004; Klein *et al.*, 2013). Ceci pourrait empêcher l'ajout de GlcUA sur Heptose III par WaaH. Donc le rôle de WaaH chez les *E. coli* avec un LPS de type R1 et R3 est inconnu. Cependant, l'analyse du LPS par SDS-PAGE et par Western blot avec l'anticorps O157 du mutant Δ*waaH* et du double mutant Δ*pst* Δ*waaH*, permet de conclure que WaaH n'est pas responsable de l'absence d'antigène O. Il est intéressant de noter que WaaH partage 34% de similitude avec la glycosyltransférase PgaC, responsable de la polymérisation du PGA (Klein *et al.*, 2013; Wang *et al.*, 2004). Cependant, WaaH n'est pas non plus responsable de la présence de NAG dans le biofilm du mutant Δ*pst* (discuté p. 237), puisque du NAG était détecté dans le biofilm du double mutant Δ*pst* Δ*waaH*. Nous serions intéressés à examiner si WaaH a une fonction de modification du LPS telle que l'ajout dans le LPS du mutant Δ*pst* d'une forme associée au pic de 365.4 u détecté par spectrométrie de masse. Cette possible modification sera vérifiée bientôt par analyse par spectrométrie de masse du LPS extrait du double mutant Δ*pst* Δ*waaH*. En revanche si ce n'est pas le cas, il est aussi envisageable que WaaH soit responsable

de la glycosylation d'autres composés intervenant dans la structure membranaire tel que des protéines ou des lipides. En effet, nous savons que WaaH appartient à la famille des glycosyltransférases 2 et est conservé dans le phylum des protéobactéries (Klein *et al.*, 2013; Wang *et al.*, 2004). Ainsi, lors d'une carence en phosphate et de l'induction de PhoB, WaaH contribue à la formation de biofilm. Même si son mécanisme reste à découvrir, WaaH pourrait être une cible intéressante pour contrôler la formation de biofilm (Figure 4).

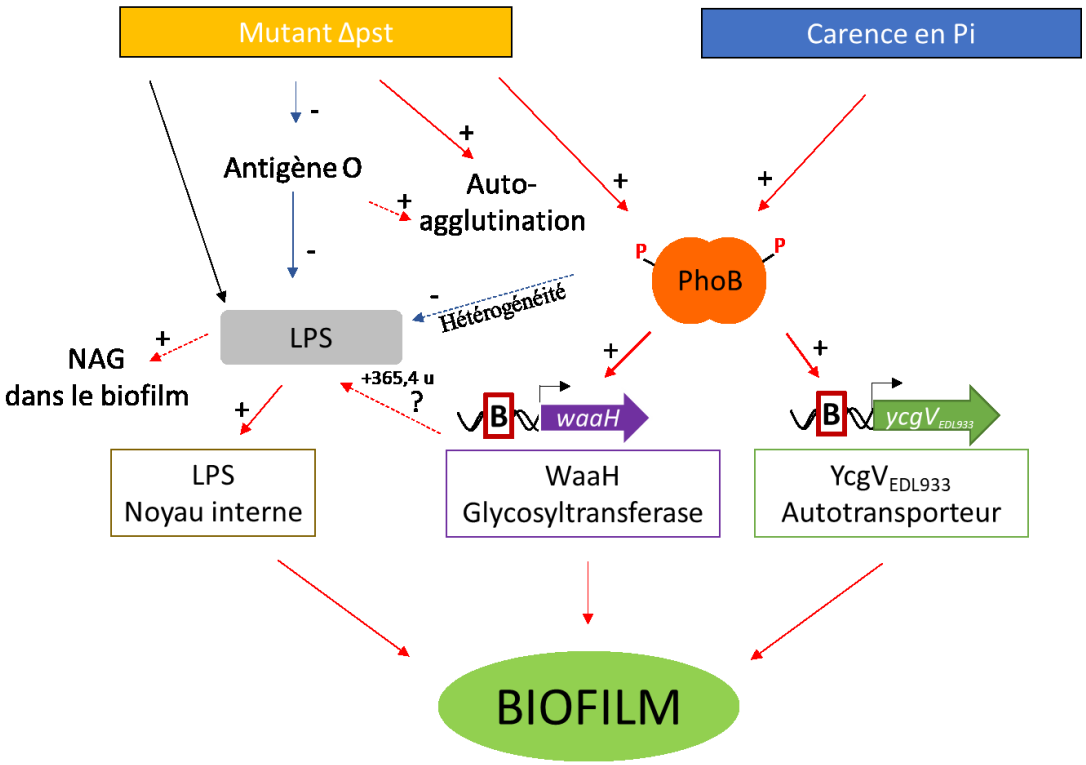

Figure 4. Modèle représentant les modifications impliquées dans la formation de biofilm de O157:H7 du mutant Δ*pst* et lors de carence en Pi. Les flèches continues indiquent les liens existants entre les différents facteurs. Les flèches discontinues indiquent les liens plus hypothétiques. Une flèche rouge indique l'activation et une flèche bleue, la répression.

- PhoB active l'expression de *waaH* et *ycgV*$_{EDL933}$ codant respectivement pour une glycosyltransférase et un autotransporteur. Ceux-ci sont impliqués dans la formation de biofilm lors de carence en Pi et du mutant Δ*pst*. La régulation de *waaH* et *ycgV*$_{EDL933}$ par PhoB qui se lierait à une région contenant des séquences de liaison de PhoB (boîtes Pho) en amont de ces deux gènes (B).
- Le noyau interne du LPS est important pour la formation de biofilm du mutant Δ*pst* et est modifié. Une délétion du système Pst entraine des modifications de la structure de LPS qui sont i) l'absence de l'antigène O157 et ii) la présence d'un composé de 365,4 u sur le noyau du LPS. i) L'absence d'antigène O pourrait expliquer le phénotype augmenté d'autoagglutination et la présence de NAG dans la matrice du biofilm du mutant Δ*pst*. ii) La fonction inconnue de WaaH pourrait être l'ajout du composé de 365,4 u sur le noyau du LPS.
- Dans ce modèle, en condition de carence en Pi, l'activation de PhoB contrôle directement ou indirectement la baisse d'hétérogénéité des molécules de LPS afin d'économiser le Pi et optimiser sa biodisponibilité afin de maintenir des réactions biochimiques essentielles et une paroi stable.

V.2.7 Utilisation de composés contenant du phosphate pour éviter la formation de biofilm des STEC

Le but de cette étude est d'apporter des connaissances supplémentaires pour limiter au maximum la formation de biofilm par les STEC. Comme il a été proposé par Giaouris et ses collaborateurs, les usines de transformation agroalimentaires et les fermes sont des zones qui pourraient favoriser la formation de biofilms (Giaouris et al., 2014). Dans ces environnements, des pratiques standardisées de nettoyage et de désinfections sont appliquées pour réduire les sources potentielles de contamination microbienne. Cependant, comme décrit précédemment, les biofilms bactériens ont une sensibilité réduite aux désinfectants et permettent la persistance de bactéries résidentes dans les chaines de production. Dans notre premier article, nous avons d'ailleurs montré que les souches STEC de différents sérotypes, toléraient mieux les traitements aux désinfectants sous forme biofilm que sous forme planctonique (Vogeleer *et al.*, 2015). Ces résultats sont en accord avec des études antérieures (Fouladkhah *et al.*, 2013; Marouani-Gadri *et al.*, 2010; Park and Chen, 2015; Wang *et al.*, 2012a). De plus, même si une diminution de la viabilité des cellules était constatée lors de ces traitements, la matrice du biofilm restait fixée à la surface. Ceci pourrait permettre une recolonisation plus rapide de la surface (Larsen *et al.*, 2008). Par conséquent, la mise au point de stratégies alternatives de lutte contre les infections associées aux biofilms est nécessaire. Dans le chapitre consacré à l'étude de la carence en phosphate sur la formation de biofilm, nous montrons qu'en carence en phosphate, *E. coli* O157:H7 forme plus de biofilm. Une solution envisageable pour lutter contre la formation de biofilm des souches STEC, tout du moins des souches *E. coli* O157:H7, serait l'utilisation de surface recouverte d'ions phosphate. De telles procédures existent et sont possibles sur différentes surfaces telles que le verre ou l'acier inoxydable. Des études portant sur la qualité de l'eau ont montré que la présence de phosphate modifiait la charge de la surface ce qui entrainait une diminution de la fixation bactérienne (Appenzeller *et al.*, 2002; Wang *et al.*, 2011). Sachant que nous avons montré que le phosphate a aussi un effet d'un point de vu métabolique sur la formation de biofilm de *E. coli* O157:H7, il serait intéressant d'étudier l'impact de la présence de surface recouverte d'ions phosphate sur la persistance de *E. coli* O157:H7 dans l'industrie agroalimentaire. De plus, il existe aussi des surfaces en verre dans lesquelles la silice traditionnelle est remplacée par du phosphate. Ces verres de phosphate

permettent d'introduire de manière plus stable que dans le verre traditionnel, des ions antibactériens tels que les ions argent (Ag^{+}) ou cuivre ($Cu2^{+}$) (Abou Neel *et al.*, 2009). Il a déjà été montré que de telles surfaces avaient des effets antibactériens contre *P. aeruginosa* et *S. aureus* sous forme planctonique et sous forme biofilm (Ahmed *et al.*, 2006b; Valappil *et al.*, 2008).

VI. Section VI – Conclusions

Dans ce projet de doctorat, nous avons établi les conclusions et perspectives suivantes :

Axe 1. Évaluation et caractérisation des biofilms formés par une collection d'isolats STEC associés à des cas cliniques humain et de sérotype O157 et non-O157 dans des conditions proches de celles retrouvées dans l'environnement.

- Nous avons montré que dans les conditions testées (24 h, M9, 30°C, surface en polystyrène, en condition statique ou dynamique), la capacité des STEC à former des biofilms est variable.

- Nous avons montré que la formation de biofilms des isolats STEC est favorisée par des températures inférieures à 37°C et lorsque les nutriments sont limités. Ceci suggère que le biofilm joue un rôle lorsque la bactérie est à l'extérieur de son hôte.

- Nous avons identifié que les isolats du séropathotype A (O157:H7 et O157:NM), qui ont l'incidence relative la plus élevée dans les infections aux STEC chez l'humain, ont un meilleur potentiel de formation de biofilm par rapport aux d'isolats cliniques du séropathotype B ou C. En effet, ils forment significativement plus de biofilms, leur matrice est la seule à contenir de la cellulose et du PGA et la formation de biofilm de plusieurs isolats du séropathotype A est associée à leur capacité unique à agglutiner la levure de manière mannose-indépendante.

- Nous avons identifié que parmi les isolats STEC testés, deux gènes codant pour des autotransporteurs *ehaB* et *espP*, et deux gènes fimbriaires, *z1538* et *lpf2*, sont plus fréquemment retrouvés chez les isolats qui forment le plus de biofilm.

- Nous avons montré par traitement enzymatique, que les protéines jouent un rôle important dans l'intégrité du biofilm des STEC.

- Le traitement avec des désinfectants réduit considérablement la viabilité des STEC mais n'élimine pas complètement la matrice du biofilm.

Perspectives Axe 1:

Ces découvertes sur les biofilms formés par les STEC, en condition environnementale, offrent plusieurs perspectives intéressantes :

- Au niveau épidémiologique, il serait intéressant d'analyser la formation de biofilm d'un plus grand nombre de souches STEC afin de vérifier l'association qui pourrait exister entre le potentiel de formation de biofilm et la haute fréquence d'implication dans les épidémies des souches de séropathotype A.

- Au niveau des chaînes de production, il serait intéressant de tester l'utilisation de produit à base de protéase lors des opérations de nettoyage pour assurer l'élimination de la matrice des biofilms formés par les STEC. De plus, il serait également pertinent de tester l'association de désinfectants avec protéase pour à la fois tuer les cellules STEC et éliminer la matrice. Ceci diminuerait le risque de recontamination.

- En diagnostique, les gènes *ehaB*, *espP*, *z1538* et *lpf2*, pourraient constituer des déterminants génétiques potentiels pour la formation de biofilm.

Axe 2 : Étudier le rôle du régulateur PhoB dans la formation de biofilm de la souche O157:H7 EDL933 lors de carence en Pi **et identifier les membres du régulon Pho impliqués (Article de recherche 2 et 3).**

- Nous avons clairement démontré le rôle du régulateur PhoB dans la formation de biofilm de la souche O157:H7 EDL933 à la fois lors de carence en Pi et dans le mutant Δ*pst*.

- Lorsque PhoB est activé, la paroi bactérienne de la souche O157:H7 EDL933 subit d'importantes modifications qui favorisent l'autoagglutination et la formation de biofilm.

- Nos résultats mettent en évidence que lors du stress généré par la carence en Pi ou par l'activation de PhoB, des mécanismes sont activés pour assurer la modification de la

composition de la paroi bactérienne, incluant les LPS, qui mènent à l'augmentation du potentiel de formation de biofilm.

- Nous avons identifié que PhoB induisait l'expression du gène *waaH* qui code pour une glycosyltransférase. Chez *E. coli* K-12 WaaH est impliquée dans la modification du LPS (Klein et al., 2013). Nous avons démontré que WaaH contribue à la formation de biofilm chez le mutant Δ*pst* et lorsque la souche O157:H7 EDL933 est cultivée en carence en Pi.

- Chez le mutant Δ*pst*, nous avons identifié que les molécules de LPS sont modifiées et sont impliquées dans la formation de biofilm de ce mutant. En revanche les molécules de LPS ne semblent pas modifiées en conditions de carence en Pi.

- Nous avons démontré que chez la souche O157:H7 EDL933, PhoB active l'expression du gène *ycgV* qui code pour un autotransporteur tronqué et que YcgV contribue à la formation de biofilm chez le mutant Δ*pst* et lorsque la souche O157:H7 EDL933 est cultivée en carence en Pi.

Perspectives Axe 2 :

Grâce aux connaissances acquises lors de cette études, nous pensons que plusieurs points pourraient être explorés :

- Evaluer l'impact de la carence en Pi sur la formation de biofilm d'autres souches STEC de sérotype O157 et non-O157 ainsi qu'examiner si l'activation du régulon Pho chez d'autres souches STEC induit des modifications similaires au niveau de la paroi. Ceci permettrait de vérifier si ces mécanismes résultant de l'activation du régulon Pho, sont généralisés parmi les STEC ou souches spécifiques.

- Après avoir validé nos résultats sur différentes souches STEC, il serait intéressant de tester si l'utilisation de surfaces industrielles recouvertes d'ions phosphate diminuerait le potentiel de formation de biofilm des STEC.

- Aucune étude ne rapporte la participation d'un autotransporteur tronqué dans la formation de biofilm. Du point de vue de la recherche fondamentale, il serait intéressant d'identifier le mécanisme par lequel cette protéine participe à la formation du biofilm. Il serait également pertinent de mener une étude génomique plus poussée afin de savoir si les autotransporteurs tronqués sont répandus.

- En perspective de la découverte du rôle de WaaH dans la formation de biofilm lors de carence en Pi, il serait intéressant de connaître sa fonction. Ceci pourrait être mené par une étude enzymologique pour identifier son substrat.

VII. Section VII – Bibliographie

Abou Neel, E.A., Pickup, D.M., Valappil, S.P., Newport, R.J., Knowles, J.C., 2009. Bioactive functional materials: a perspective on phosphate-based glasses. J Mater Chem. 19, 690-701.

Abu-Ali, G.S., Ouellette, L.M., Henderson, S.T., Lacher, D.W., Riordan, J.T., Whittam, T.S., Manning, S.D., 2010. Increased adherence and expression of virulence genes in a lineage of *Escherichia coli* O157:H7 commonly associated with human infections. PloS one. 5, e10167.

Aggarwal, S., Somani, V.K., Bhatnagar, R., 2015. Phosphate starvation enhances the pathogenesis of *Bacillus anthracis*. Int J Med Microbiol. 305, 523-531.

Aggarwal, S., Somani, V.K., Gupta, V., Kaur, J., Singh, D., Grover, A., Bhatnagar, R., 2017. Functional characterization of PhoPR two component system and its implication in regulating phosphate homeostasis in *Bacillus anthracis*. Biochim Biophys Acta. 1861, 2956-2970.

Ahmed, A., Li, J., Shiloach, Y., Robbins, J.B., Szu, S.C., 2006a. Safety and immunogenicity of *Escherichia coli* O157 O-specific polysaccharide conjugate vaccine in 2-5-year-old children. J Infect Dis. 193, 515-521.

Ahmed, I., Ready, D., Wilson, M., Knowles, J.C., 2006b. Antimicrobial effect of silver-doped phosphate-based glasses. J Biomed Mater Res A. 79, 618-626.

Ake, J.A., Jelacic, S., Ciol, M.A., Watkins, S.L., Murray, K.F., Christie, D.L., Klein, E.J., Tarr, P.I., 2005. Relative nephroprotection during *Escherichia coli* O157:H7 infections: association with intravenous volume expansion. Pediatrics. 115, e673-680.

Albi, T., Serrano, A., 2016. Inorganic polyphosphate in the microbial world. Emerging roles for a multifaceted biopolymer. World J Microb Biot. 32, 27.

Ali, T., Weintraub, A., Widmalm, G., 2006. Structural determination of the O-antigenic polysaccharide from the Shiga toxin-producing *Escherichia coli* O171. Carbohydr Res. 341, 1878-1883.

Allsopp, L.P., Totsika, M., Tree, J.J., Ulett, G.C., Mabbett, A.N., Wells, T.J., Kobe, B., Beatson, S.A., Schembri, M.A., 2010. UpaH is a newly identified autotransporter protein that contributes to biofilm formation and bladder colonization by uropathogenic *Escherichia coli* CFT073. Infect Immun. 78, 1659-1669.

Ambudkar, S.V., Anantharam, V., Maloney, P.C., 1990. UhpT, the sugar phosphate antiporter of *Escherichia coli*, functions as a monomer. J Biol Chem. 265, 12287-12292.

Appenzeller, B.M., Duval, Y.B., Thomas, F., Block, J.C., 2002. Influence of phosphate on

bacterial adhesion onto iron oxyhydroxide in drinking water. Environ Sci Technol. 36, 646-652.

Asadulghani, M., Ogura, Y., Ooka, T., Itoh, T., Sawaguchi, A., Iguchi, A., Nakayama, K., Hayashi, T., 2009. The defective prophage pool of *Escherichia coli* O157: prophage-prophage interactions potentiate horizontal transfer of virulence determinants. PLoS Pathog. 5, e1000408.

Bachhawat, P., Swapna, G.V., Montelione, G.T., Stock, A.M., 2005. Mechanism of activation for transcription factor PhoB suggested by different modes of dimerization in the inactive and active states. Structure. 13, 1353-1363.

Baek, J.H., Lee, S.Y., 2006. Novel gene members in the Pho regulon of *Escherichia coli*. FEMS Microbiol Lett. 264, 104-109.

Bains, M., Fernandez, L., Hancock, R.E., 2012. Phosphate starvation promotes swarming motility and cytotoxicity of *Pseudomonas aeruginosa*. Appl Environ Microbiol. 78, 6762-6768.

Bak, G., Lee, J., Suk, S., Kim, D., Young Lee, J., Kim, K.S., Choi, B.S., Lee, Y., 2015. Identification of novel sRNAs involved in biofilm formation, motility, and fimbriae formation in *Escherichia coli*. Sci Rep. 5, 15287.

Baliere, C., Rince, A., Blanco, J., Dahbi, G., Harel, J., Vogeleer, P., Giard, J.C., Mariani-Kurkdjian, P., Gourmelon, M., 2015. Prevalence and Characterization of Shiga Toxin-Producing and Enteropathogenic *Escherichia coli* in Shellfish-Harvesting Areas and Their Watersheds. Front Microbiol. 6, 1356.

Bansal, T., Englert, D., Lee, J., Hegde, M., Wood, T.K., Jayaraman, A., 2007. Differential effects of epinephrine, norepinephrine, and indole on *Escherichia coli* O157:H7 chemotaxis, colonization, and gene expression. Infect Immun. 75, 4597-4607.

Baruch, K., Gur-Arie, L., Nadler, C., Koby, S., Yerushalmi, G., Ben-Neriah, Y., Yogev, O., Shaulian, E., Guttman, C., Zarivach, R., Rosenshine, I., 2011. Metalloprotease type III effectors that specifically cleave JNK and NF-kappaB. EMBO J. 30, 221-231.

Beis, K., 2015. Structural basis for the mechanism of ABC transporters. Biochem Soc Trans. 43, 889-893.

Beloin, C., Roux, A., Ghigo, J.M., 2008. *Escherichia coli* biofilms. Curr Top Microbiol Immunol. 322, 249-289.

Berry, E.D., Wells, J.E., 2010. *Escherichia coli* O157:H7: recent advances in research on occurrence, transmission, and control in cattle and the production environment. Adv Food

Nutr Res. 60, 67-117.

Berry, E.D., Wells, J.E., Varel, V.H., Hales, K.E., Kalchayanand, N., 2017. Persistence of *Escherichia coli* O157:H7 and Total *Escherichia coli* in Feces and Feedlot Surface Manure from Cattle Fed Diets with and without Corn or Sorghum Wet Distillers Grains with Solubles. J Food Prot. 80, 1317-1327.

Binks, S., Regan, K., Richenberg, J., Chevassut, T., 2012. Microbes without frontiers: severe haemolytic-uraemic syndrome due to *E. coli* O104:H4. BMJ case reports. 2012.

Biscola, F.T., Abe, C.M., Guth, B.E., 2011. Determination of adhesin gene sequences in, and biofilm formation by, O157 and non-O157 Shiga toxin-producing *Escherichia coli* strains isolated from different sources. Appl Environ Microbiol. 77, 2201-2208.

Bitzan, M., Poole, R., Mehran, M., Sicard, E., Brockus, C., Thuning-Roberson, C., Riviere, M., 2009. Safety and pharmacokinetics of chimeric anti-Shiga toxin 1 and anti-Shiga toxin 2 monoclonal antibodies in healthy volunteers. Antimicrob Agents Chemother. 53, 3081-3087.

Blanco, A.G., Canals, A., Coll, M., 2012. PhoB transcriptional activator binds hierarchically to Pho box promoters. Biol Chem. 393, 1165-1171.

Blanco, A.G., Sola, M., Gomis-Ruth, F.X., Coll, M., 2002. Tandem DNA recognition by PhoB, a two-component signal transduction transcriptional activator. Structure. 10, 701-713.

Blus-Kadosh, I., Zilka, A., Yerushalmi, G., Banin, E., 2013. The effect of *pstS* and *phoB* on quorum sensing and swarming motility in *Pseudomonas aeruginosa*. PloS one. 8, e74444.

Boerlin, P., McEwen, S.A., Boerlin-Petzold, F., Wilson, J.B., Johnson, R.P., Gyles, C.L., 1999. Associations between virulence factors of Shiga toxin-producing *Escherichia coli* and disease in humans. J Clin Microbiol. 37, 497-503.

Bono, J.L., Keen, J.E., Clawson, M.L., Durso, L.M., Heaton, M.P., Laegreid, W.W., 2007. Association of *Escherichia coli* O157:H7 tir polymorphisms with human infection. BMC infectious diseases. 7, 98.

Bottger, P., Pedersen, L., 2005. Evolutionary and experimental analyses of inorganic phosphate transporter PiT family reveals two related signature sequences harboring highly conserved aspartic acids critical for sodium-dependent phosphate transport function of human PiT2. FEBS J. 272, 3060-3074.

Bottger, P., Pedersen, L., 2011. Mapping of the minimal inorganic phosphate transporting unit of human PiT2 suggests a structure universal to PiT-related proteins from all kingdoms of life. BMC Biochem. 12, 21.

Brunder, W., Khan, A.S., Hacker, J., Karch, H., 2001. Novel type of fimbriae encoded by the large plasmid of sorbitol-fermenting enterohemorrhagic *Escherichia coli* O157:H(-). Infect Immun. 69, 4447-4457.

Brunder, W., Schmidt, H., Frosch, M., Karch, H., 1999. The large plasmids of Shiga-toxin-producing *Escherichia coli* (STEC) are highly variable genetic elements. Microbiology. 145 (Pt 5), 1005-1014.

Brunder, W., Schmidt, H., Karch, H., 1996. KatP, a novel catalase-peroxidase encoded by the large plasmid of enterohaemorrhagic *Escherichia coli* O157:H7. Microbiology. 142 (Pt 11), 3305-3315.

Brunder, W., Schmidt, H., Karch, H., 1997. EspP, a novel extracellular serine protease of enterohaemorrhagic *Escherichia coli* O157:H7 cleaves human coagulation factor V. Mol Microbiol. 24, 767-778.

Brussow, H., Canchaya, C., Hardt, W.D., 2004. Phages and the evolution of bacterial pathogens: from genomic rearrangements to lysogenic conversion. Microbiol Mol Biol Rev. 68, 560-602, table of contents.

Butler, B.A., Thomson, D.U., Nagaraja, T.G., Loneragan, G.H., Reinhardt, C.D., 2012. A Commercially Available SRP Vaccine Reduces Prevalence of *E. coli* O157:H7 in Feces of Beef Cattle Under Commercial Feedlot Conditions Meat Food Saf.

Cadona, J.S., Bustamante, A.V., Gonzalez, J., Sanso, A.M., 2018. Erratum: Jimena Soledad Cadona, et al.; Pathogenicity Islands Distribution in Non-O157 Shiga Toxin-Producing *Escherichia coli* (STEC). Genes 2018, 9, 81.

Campellone, K.G., Robbins, D., Leong, J.M., 2004. EspFU is a translocated EHEC effector that interacts with Tir and N-WASP and promotes Nck-independent actin assembly. Dev Cell. 7, 217-228.

Canada, G.o. 2015. National Enteric Surveillance Program Annual Summary 2013: Public Health Agency of Canada, Canada, C.P.H.A.o., ed.

Canals, A., Blanco, A.G., Coll, M., 2012. sigma70 and PhoB activator: getting a better grip. Transcription. 3, 160-164.

Capra, E.J., Laub, M.T., 2012. Evolution of two-component signal transduction systems. Annual review of microbiology. 66, 325-347.

Carmany, D.O., Hollingsworth, K., McCleary, W.R., 2003. Genetic and biochemical studies of phosphatase activity of PhoR. J Bacteriol. 185, 1112-1115.

Carter, M.Q., Xue, K., Brandl, M.T., Liu, F., Wu, L., Louie, J.W., Mandrell, R.E., Zhou, J.,

2012. Functional metagenomics of *Escherichia coli* O157:H7 interactions with spinach indigenous microorganisms during biofilm formation. PloS one. 7, e44186.

Centers for Disease Control and Prevention A, G.U.D.o.H.a.H.S., 2014. FoodNet 2014 Surveillance Report Diseases NCfEaZI, editor.

Chalabaev, S., Chauhan, A., Novikov, A., Iyer, P., Szczesny, M., Beloin, C., Caroff, M., Ghigo, J.M., 2014. Biofilms formed by gram-negative bacteria undergo increased lipid a palmitoylation, enhancing in vivo survival. MBio. 5.

Characklis, W.G., 1973. Attached microbial growths-II. Frictional resistance due to microbial slimes. Water Res. 7, 1249-1258.

Charbonneau, M.E., Janvore, J., Mourez, M., 2009. Autoprocessing of the *Escherichia coli* AIDA-I autotransporter: a new mechanism involving acidic residues in the junction region. J Biol Chem. 284, 17340-17351.

Chekabab, S.M., Daigle, F., Charette, S.J., Dozois, C.M., Harel, J., 2012. Survival of enterohemorrhagic *Escherichia coli* in the presence of *Acanthamoeba castellanii* and its dependence on Pho regulon. MicrobiologyOpen. 1, 427-437.

Chekabab, S.M., Jubelin, G., Dozois, C.M., Harel, J., 2014. PhoB activates *Escherichia coli* O157:H7 virulence factors in response to inorganic phosphate limitation. PloS one. 9, e94285.

Choi, N.-Y., Kim, B.-R., Bae, Y.-M., Lee, S.-Y., 2013. Biofilm formation, attachment, and cell hydrophobicity of foodborne pathogens under varied environmental conditions. J Korean Soc Appl Bi. 56, 207-220.

Chui, L., Christianson, S., Alexander, Arseneau, V., Bekal, S., Berenger, B., Chen, Y., Davidson, R., Farrell, D.J., German, G.J., Gilbert, L., Hoang, L.M.N., Johnson, R.P., MacKeen, A., Maki, A., Nadon, C., Nickerson, E., Peralta, A., Radons Arneso, S.M., Yu, Y., Ziebell, K. 2018. Recommandations du Réseau des laboratoires de santé publique du Canada (RLSPC) pour la détection en laboratoire d'*Escherichia coli* producteurs de Shiga-toxines (O157 et non-O157). In Relevé des maladies transmissibles au Canada, Canada, G.d., ed., 268-272.

Colello, R., Velez, M.V., Gonzalez, J., Montero, D.A., Bustamante, A.V., Del Canto, F., Etcheverria, A.I., Vidal, R., Padola, N.L., 2018. First report of the distribution of Locus of Adhesion and Autoaggregation (LAA) pathogenicity island in LEE-negative Shiga toxin-producing *Escherichia coli* isolates from Argentina. Microb Pathog. 123, 259-263.

Cookson, A.L., Cooley, W.A., Woodward, M.J., 2002. The role of type 1 and curli fimbriae of Shiga toxin-producing *Escherichia coli* in adherence to abiotic surfaces. Int J Med

Microbiol. 292, 195-205.

Coombes, B.K., Wickham, M.E., Mascarenhas, M., Gruenheid, S., Finlay, B.B., Karmali, M.A., 2008. Molecular analysis as an aid to assess the public health risk of non-O157 Shiga toxin-producing *Escherichia coli* strains. Appl Environ Microbiol. 74, 2153-2160.

Corogeanu, D., Willmes, R., Wolke, M., Plum, G., Utermohlen, O., Kronke, M., 2012. Therapeutic concentrations of antibiotics inhibit Shiga toxin release from enterohemorrhagic *E. coli* O104:H4 from the 2011 German outbreak. BMC Microbiol. 12, 160.

Costerton, J.W., Geesey, G.G., Cheng, K.J., 1978. How bacteria stick. Sci Am. 238, 86-95.

Cox, G.B., Webb, D., Godovac-Zimmermann, J., Rosenberg, H., 1988. Arg-220 of the PstA protein is required for phosphate transport through the phosphate-specific transport system in *Escherichia coli* but not for alkaline phosphatase repression. J Bacteriol. 170, 2283-2286.

Cox, G.B., Webb, D., Rosenberg, H., 1989. Specific amino acid residues in both the PstB and PstC proteins are required for phosphate transport by the *Escherichia coli* Pst system. J Bacteriol. 171, 1531-1534.

Crane, J.K., McNamara, B.P., Donnenberg, M.S., 2001. Role of EspF in host cell death induced by enteropathogenic *Escherichia coli*. Cell Microbiol. 3, 197-211.

Crepin, S., Houle, S., Charbonneau, M.E., Mourez, M., Harel, J., Dozois, C.M., 2012. Decreased expression of type 1 fimbriae by a *pst* mutant of uropathogenic *Escherichia coli* reduces urinary tract infection. Infect Immun. 80, 2802-2815.

Crepin, S., Lamarche, M.G., Garneau, P., Seguin, J., Proulx, J., Dozois, C.M., Harel, J., 2008. Genome-wide transcriptional response of an avian pathogenic *Escherichia coli* (APEC) *pst* mutant. BMC genomics. 9, 568.

Crepin, S., Porcheron, G., Houle, S., Harel, J., Dozois, C.M., 2017. Altered Regulation of the Diguanylate Cyclase YaiC Reduces Production of Type 1 Fimbriae in a Pst Mutant of Uropathogenic *Escherichia coli* CFT073. J Bacteriol. 199, e00168-00117.

Croxen, M.A., Finlay, B.B., 2010. Molecular mechanisms of *Escherichia coli* pathogenicity. Nature reviews. Microbiology. 8, 26-38.

Dahan, S., Wiles, S., La Ragione, R.M., Best, A., Woodward, M.J., Stevens, M.P., Shaw, R.K., Chong, Y., Knutton, S., Phillips, A., Frankel, G., 2005. EspJ is a prophage-carried type III effector protein of attaching and effacing pathogens that modulates infection dynamics. Infect Immun. 73, 679-686.

Daigle, F., Fairbrother, J.M., Harel, J., 1995. Identification of a mutation in the *pst-phoU* operon that reduces pathogenicity of an *Escherichia coli* strain causing septicemia in pigs. Infect Immun. 63, 4924-4927.

Danhorn, T., Hentzer, M., Givskov, M., Parsek, M.R., Fuqua, C., 2004. Phosphorus limitation enhances biofilm formation of the plant pathogen *Agrobacterium tumefaciens* through the PhoR-PhoB regulatory system. J Bacteriol. 186, 4492-4501.

Daram, P., Brunner, S., Rausch, C., Steiner, C., Amrhein, N., Bucher, M., 1999. Pht2;1 encodes a low-affinity phosphate transporter from *Arabidopsis*. Plant Cell. 11, 2153-2166.

Davidson, A.L., Dassa, E., Orelle, C., Chen, J., 2008. Structure, function, and evolution of bacterial ATP-binding cassette systems. Microbiol Mol Biol Rev. 72, 317-364, table of contents.

Dewanti, R., Wong, A.C., 1995. Influence of culture conditions on biofilm formation by *Escherichia coli* O157:H7. Int J Food Microbiol. 26, 147-164.

Dick, C.F., Dos-Santos, A.L., Meyer-Fernandes, J.R., 2014. Inorganic phosphate uptake in unicellular eukaryotes. Biochim Biophys Acta. 1840, 2123-2127.

Dinh, A., Anathasayanan, A., Rubin, L.M., 2015. Safe and effective use of eculizumab in the treatment of severe Shiga toxin *Escherichia coli*-associated hemolytic uremic syndrome. Am J Health Syst Pharm. 72, 117-120.

Donohue-Rolfe, A., Keusch, G.T., 1983. Shigella dysenteriae 1 cytotoxin: periplasmic protein releasable by polymyxin B and osmotic shock. Infect Immun. 39, 270-274.

Doughty, S., Sloan, J., Bennett-Wood, V., Robertson, M., Robins-Browne, R.M., Hartland, E.L., 2002. Identification of a novel fimbrial gene cluster related to long polar fimbriae in locus of enterocyte effacement-negative strains of enterohemorrhagic *Escherichia coli*. Infect Immun. 70, 6761-6769.

Dourou, D., Beauchamp, C.S., Yoon, Y., Geornaras, I., Belk, K.E., Smith, G.C., Nychas, G.J., Sofos, J.N., 2011. Attachment and biofilm formation by *Escherichia coli* O157:H7 at different temperatures, on various food-contact surfaces encountered in beef processing. Int J Food Microbiol. 149, 262-268.

Ebel, W., Vaughn, G.J., Peters, H.K., 3rd, Trempy, J.E., 1997. Inactivation of *mdoH* leads to increased expression of colanic acid capsular polysaccharide in *Escherichia coli*. J Bacteriol. 179, 6858-6861.

Echtenkamp, F., Deng, W., Wickham, M.E., Vazquez, A., Puente, J.L., Thanabalasuriar, A., Gruenheid, S., Finlay, B.B., Hardwidge, P.R., 2008. Characterization of the NleF effector

protein from attaching and effacing bacterial pathogens. FEMS Microbiol Lett. 281, 98-107.

Elder, J., Nightingale, K. 2013. Tracking of pathogens via virulence factors: Shiga toxin-producing *Escherichia coli* in cattle and potential risks for human disease, In: Adv Microb Food Saf. 227-259.

Elvin, C.M., Hardy, C.M., Rosenberg, H., 1985. Pi exchange mediated by the GlpT-dependent sn-glycerol-3-phosphate transport system in *Escherichia coli*. J Bacteriol. 161, 1054-1058.

Eppens, E.F., Saint, N., Van Gelder, P., van Boxtel, R., Tommassen, J., 1997. Role of the constriction loop in the gating of outer membrane porin PhoE of *Escherichia coli*. FEBS Lett. 415, 317-320.

Etcheverria, A.I., Padola, N.L., 2013. Shiga toxin-producing *Escherichia coli*: factors involved in virulence and cattle colonization. Virulence. 4, 366-372.

Etzkorn, M., Kneuper, H., Dunnwald, P., Vijayan, V., Kramer, J., Griesinger, C., Becker, S., Unden, G., Baldus, M., 2008. Plasticity of the PAS domain and a potential role for signal transduction in the histidine kinase DcuS. Nat Struct Mol Biol. 15, 1031-1039.

Fadlallah, S.M., Rahal, E.A., Sabra, A., Kissoyan, K.A., Matar, G.M., 2015. Effect of rifampicin and gentamicin on Shiga toxin 2 expression level and the SOS response in *Escherichia coli* O104:H4. Foodborne Pathog Dis. 12, 47-55.

Feng, P., Lampel, K.A., Karch, H., Whittam, T.S., 1998. Genotypic and phenotypic changes in the emergence of *Escherichia coli* O157:H7. J Infect Dis. 177, 1750-1753.

Ferens, W.A., Hovde, C.J., 2011. *Escherichia coli* O157:H7: animal reservoir and sources of human infection. Foodborne Pathog Dis. 8, 465-487.

Fingermann, M., Avila, L., De Marco, M.B., Vazquez, L., Di Biase, D.N., Muller, A.V., Lescano, M., Dokmetjian, J.C., Fernandez Castillo, S., Perez Quinoy, J.L., 2018. OMV-based vaccine formulations against Shiga toxin producing *Escherichia coli* strains are both protective in mice and immunogenic in calves. Hum Vaccin Immunother. 14, 2208-2213.

Fisher, S.L., Jiang, W., Wanner, B.L., Walsh, C.T., 1995. Cross-talk between the histidine protein kinase VanS and the response regulator PhoB. Characterization and identification of a VanS domain that inhibits activation of PhoB. J Biol Chem. 270, 23143-23149.

Flemming, H.C., Wingender, J., 2010. The biofilm matrix. Nature reviews. Microbiology. 8, 623-633.

Fouladkhah, A., Geornaras, I., Sofos, J.N., 2013. Biofilm formation of O157 and non-O157

Shiga toxin-producing *Escherichia coli* and multidrug-resistant and susceptible Salmonella typhimurium and newport and their inactivation by sanitizers. J Food Sci. 78, M880-886.

Frank, C., Werber, D., Cramer, J.P., Askar, M., Faber, M., an der Heiden, M., Bernard, H., Fruth, A., Prager, R., Spode, A., Wadl, M., Zoufaly, A., Jordan, S., Kemper, M.J., Follin, P., Muller, L., King, L.A., Rosner, B., Buchholz, U., Stark, K., Krause, G., Team, H.U.S.I., 2011. Epidemic profile of Shiga-toxin-producing *Escherichia coli* O104:H4 outbreak in Germany. N Engl J Med. 365, 1771-1780.

Frankel, G., Phillips, A.D., Trabulsi, L.R., Knutton, S., Dougan, G., Matthews, S., 2001. Intimin and the host cell--is it bound to end in Tir(s)? Trends Microbiol. 9, 214-218.

Fratamico, P.M., Yan, X., Caprioli, A., Esposito, G., Needleman, D.S., Pepe, T., Tozzoli, R., Cortesi, M.L., Morabito, S., 2011. The complete DNA sequence and analysis of the virulence plasmid and of five additional plasmids carried by Shiga toxin-producing *Escherichia coli* O26:H11 strain H30. Int J Med Microbiol. 301, 192-203.

Frenzen, P.D., Drake, A., Angulo, F.J., Emerging Infections Program FoodNet Working, G., 2005. Economic cost of illness due to *Escherichia coli* O157 infections in the United States. J Food Prot. 68, 2623-2630.

Fukushima, H., Hashizume, T., Morita, Y., Tanaka, J., Azuma, K., Mizumoto, Y., Kaneno, M., Matsuura, M., Konma, K., Kitani, T., 1999. Clinical experiences in Sakai City Hospital during the massive outbreak of enterohemorrhagic *Escherichia coli* O157 infections in Sakai City, 1996. Pediatr Int. 41, 213-217.

Galperin, M.Y., 2010. Diversity of structure and function of response regulator output domains. Curr Opin Microbiol. 13, 150-159.

Gao, R., Stock, A.M., 2009. Biological insights from structures of two-component proteins. Annual review of microbiology. 63, 133-154.

Gardner, S.G., Johns, K.D., Tanner, R., McCleary, W.R., 2014. The PhoU protein from *Escherichia coli* interacts with PhoR, PstB, and metals to form a phosphate-signaling complex at the membrane. J Bacteriol. 196, 1741-1752.

Garmendia, J., Phillips, A.D., Carlier, M.F., Chong, Y., Schuller, S., Marches, O., Dahan, S., Oswald, E., Shaw, R.K., Knutton, S., Frankel, G., 2004. TccP is an enterohaemorrhagic *Escherichia coli* O157:H7 type III effector protein that couples Tir to the actin-cytoskeleton. Cell Microbiol. 6, 1167-1183.

Geerdes-Fenge, H.F., Lobermann, M., Nurnberg, M., Fritzsche, C., Koball, S., Henschel, J., Hohn, R., Schober, H.C., Mitzner, S., Podbielski, A., Reisinger, E.C., 2013. Ciprofloxacin

reduces the risk of hemolytic uremic syndrome in patients with *Escherichia coli* O104:H4-associated diarrhea. Infection. 41, 669-673.

Geiger, O., Rohrs, V., Weissenmayer, B., Finan, T.M., Thomas-Oates, J.E., 1999. The regulator gene *phoB* mediates phosphate stress-controlled synthesis of the membrane lipid diacylglyceryl-N,N,N-trimethylhomoserine in *Rhizobium* (*Sinorhizobium*) *meliloti*. Mol Microbiol. 32, 63-73.

Giaouris, E., Heir, E., Hebraud, M., Chorianopoulos, N., Langsrud, S., Moretro, T., Habimana, O., Desvaux, M., Renier, S., Nychas, G.J., 2014. Attachment and biofilm formation by foodborne bacteria in meat processing environments: causes, implications, role of bacterial interactions and control by alternative novel methods. Meat science. 97, 298-309.

Gonin, M., Quardokus, E.M., O'Donnol, D., Maddock, J., Brun, Y.V., 2000. Regulation of stalk elongation by phosphate in *Caulobacter crescentus*. J Bacteriol. 182, 337-347.

Grif, K., Dierich, M.P., Karch, H., Allerberger, F., 1998. Strain-specific differences in the amount of Shiga toxin released from enterohemorrhagic *Escherichia coli* O157 following exposure to subinhibitory concentrations of antimicrobial agents. Eur J Clin Microbiol Infect Dis. 17, 761-766.

Griffin, P.M., Tauxe, R.V., 1991. The epidemiology of infections caused by *Escherichia coli* O157:H7, other enterohemorrhagic *E. coli*, and the associated hemolytic uremic syndrome. Epidemiol Rev. 13, 60-98.

Grillo-Puertas, M., Rintoul, M.R., Rapisarda, V.A., 2016. PhoB activation in non-limiting phosphate condition by the maintenance of high polyphosphate levels in the stationary phase inhibits biofilm formation in *Escherichia coli*. Microbiology. 162, 1000-1008.

Gruenheid, S., Sekirov, I., Thomas, N.A., Deng, W., O'Donnell, P., Goode, D., Li, Y., Frey, E.A., Brown, N.F., Metalnikov, P., Pawson, T., Ashman, K., Finlay, B.B., 2004. Identification and characterization of NleA, a non-LEE-encoded type III translocated virulence factor of enterohaemorrhagic *Escherichia coli* O157:H7. Mol Microbiol. 51, 1233-1249.

Gyles, C.L., 2007. Shiga toxin-producing *Escherichia coli*: an overview. J Animal Sci. 85, E45-62.

Haddad, A., Jensen, V., Becker, T., Haussler, S., 2009. The Pho regulon influences biofilm formation and type three secretion in *Pseudomonas aeruginosa*. Environmental microbiology reports. 1, 488-494.

Hadjifrangiskou, M., Gu, A.P., Pinkner, J.S., Kostakioti, M., Zhang, E.W., Greene, S.E.,

Hultgren, S.J., 2012. Transposon mutagenesis identifies uropathogenic *Escherichia coli* biofilm factors. J Bacteriol. 194, 6195-6205.

Haldimann, A., Daniels, L.L., Wanner, B.L., 1998. Use of new methods for construction of tightly regulated arabinose and rhamnose promoter fusions in studies of the *Escherichia coli* phosphate regulon. J Bacteriol. 180, 1277-1286.

Hancock, V., Klemm, P., 2007. Global gene expression profiling of asymptomatic bacteriuria *Escherichia coli* during biofilm growth in human urine. Infect Immun. 75, 966-976.

Harris, R.M., Webb, D.C., Howitt, S.M., Cox, G.B., 2001. Characterization of PitA and PitB from *Escherichia coli*. J Bacteriol. 183, 5008-5014.

Hayashi, T., Makino, K., Ohnishi, M., Kurokawa, K., Ishii, K., Yokoyama, K., Han, C.G., Ohtsubo, E., Nakayama, K., Murata, T., Tanaka, M., Tobe, T., Iida, T., Takami, H., Honda, T., Sasakawa, C., Ogasawara, N., Yasunaga, T., Kuhara, S., Shiba, T., Hattori, M., Shinagawa, H., 2001. Complete genome sequence of enterohemorrhagic *Escherichia coli* O157:H7 and genomic comparison with a laboratory strain K-12. DNA Res. 8, 11-22.

Hemrajani, C., Berger, C.N., Robinson, K.S., Marches, O., Mousnier, A., Frankel, G., 2010. NleH effectors interact with Bax inhibitor-1 to block apoptosis during enteropathogenic *Escherichia coli* infection. Proc Natl Acad Sci USA. 107, 3129-3134.

Henderson, I.R., Navarro-Garcia, F., Desvaux, M., Fernandez, R.C., Ala'Aldeen, D., 2004. Type V protein secretion pathway: the autotransporter story. Microbiol Mol Biol Rev. 68, 692-744.

Herold, S., Paton, J.C., Paton, A.W., 2009. Sab, a novel autotransporter of locus of enterocyte effacement-negative shiga-toxigenic *Escherichia coli* O113:H21, contributes to adherence and biofilm formation. Infect Immun. 77, 3234-3243.

Hoey, D.E., Currie, C., Else, R.W., Nutikka, A., Lingwood, C.A., Gally, D.L., Smith, D.G., 2002. Expression of receptors for verotoxin 1 from *Escherichia coli* O157 on bovine intestinal epithelium. J Med Microbiol. 51, 143-149.

Hoffer, S.M., Schoondermark, P., van Veen, H.W., Tommassen, J., 2001. Activation by gene amplification of *pitB*, encoding a third phosphate transporter of *Escherichia coli* K-12. J Bacteriol. 183, 4659-4663.

Hoffer, S.M., Tommassen, J., 2001. The phosphate-binding protein of *Escherichia coli* is not essential for P(i)-regulated expression of the pho regulon. J Bacteriol. 183, 5768-5771.

Hoffman, M.A., Menge, C., Casey, T.A., Laegreid, W., Bosworth, B.T., Dean-Nystrom, E.A., 2006. Bovine immune response to shiga-toxigenic *Escherichia coli* O157:H7. Clin

Vaccine Immunol. 13, 1322-1327.

Holgersson, J., Jovall, P.A., Breimer, M.E., 1991. Glycosphingolipids of human large intestine: detailed structural characterization with special reference to blood group compounds and bacterial receptor structures. J Biochem. 110, 120-131.

Hsieh, Y.J., Wanner, B.L., 2010. Global regulation by the seven-component Pi signaling system. Curr Opin Microbiol. 13, 198-203.

Hung, C., Zhou, Y., Pinkner, J.S., Dodson, K.W., Crowley, J.R., Heuser, J., Chapman, M.R., Hadjifrangiskou, M., Henderson, J.P., Hultgren, S.J., 2013. *Escherichia coli* Biofilms Have an Organized and Complex Extracellular Matrix Structure. MBio. 4, e00645-00613.

Ichinohe, N., Ohara-Nemoto, Y., Nemoto, T.K., Kimura, S., Ichinohe, S., 2009. Effects of fosfomycin on Shiga toxin-producing *Escherichia coli*: quantification of copy numbers of Shiga toxin-encoding genes and their expression levels using real-time PCR. J Med Microbiol. 58, 971-973.

Ikeda, K., Ida, O., Kimoto, K., Takatorige, T., Nakanishi, N., Tatara, K., 1999. Effect of early fosfomycin treatment on prevention of hemolytic uremic syndrome accompanying *Escherichia coli* O157:H7 infection. Clin Nephrol. 52, 357-362.

Jacewicz, M.S., Acheson, D.W., Binion, D.G., West, G.A., Lincicome, L.L., Fiocchi, C., Keusch, G.T., 1999. Responses of human intestinal microvascular endothelial cells to Shiga toxins 1 and 2 and pathogenesis of hemorrhagic colitis. Infect Immun. 67, 1439-1444.

Jacques, M., Aragon, V., Tremblay, Y.D., 2010. Biofilm formation in bacterial pathogens of veterinary importance. Animal health research reviews / Conference of Research Workers in Animal Diseases. 11, 97-121.

Jensen, V., Lons, D., Zaoui, C., Bredenbruch, F., Meissner, A., Dieterich, G., Munch, R., Haussler, S., 2006. RhlR expression in *Pseudomonas aeruginosa* is modulated by the *Pseudomonas* quinolone signal via PhoB-dependent and -independent pathways. J Bacteriol. 188, 8601-8606.

Jones, H.C., Roth, I.L., Sanders, W.M., 3rd, 1969. Electron microscopic study of a slime layer. J Bacteriol. 99, 316-325.

Ju, W., Shen, J., Toro, M., Zhao, S., Meng, J., 2013. Distribution of pathogenicity islands OI-122, OI-43/48, and OI-57 and a high-pathogenicity island in Shiga toxin-producing *Escherichia coli*. Appl Environ Microbiol. 79, 3406-3412.

Kaniuk, N.A., Vinogradov, E., Li, J., Monteiro, M.A., Whitfield, C., 2004. Chromosomal and

plasmid-encoded enzymes are required for assembly of the R3-type core oligosaccharide in the lipopolysaccharide of *Escherichia coli* O157:H7. J Biol Chem. 279, 31237-31250.

Kaper, J.B., Nataro, J.P., Mobley, H.L., 2004. Pathogenic *Escherichia coli*. Nature reviews. Microbiology. 2, 123-140.

Karmali, M.A., 2017. Emerging Public Health Challenges of Shiga Toxin-Producing *Escherichia coli* Related to Changes in the Pathogen, the Population, and the Environment. Clin Infect Dis. 64, 371-376.

Karmali, M.A., Mascarenhas, M., Shen, S., Ziebell, K., Johnson, S., Reid-Smith, R., Isaac-Renton, J., Clark, C., Rahn, K., Kaper, J.B., 2003. Association of genomic O island 122 of *Escherichia coli* EDL 933 with verocytotoxin-producing *Escherichia coli* seropathotypes that are linked to epidemic and/or serious disease. J Clin Microbiol. 41, 4930-4940.

Kielstein, J.T., Beutel, G., Fleig, S., Steinhoff, J., Meyer, T.N., Hafer, C., Kuhlmann, U., Bramstedt, J., Panzer, U., Vischedyk, M., Busch, V., Ries, W., Mitzner, S., Mees, S., Stracke, S., Nurnberger, J., Gerke, P., Wiesner, M., Sucke, B., Abu-Tair, M., Kribben, A., Klause, N., Schindler, R., Merkel, F., Schnatter, S., Dorresteijn, E.M., Samuelsson, O., Brunkhorst, R., Collaborators of the, D.S.-H.U.S.r., 2012. Best supportive care and therapeutic plasma exchange with or without eculizumab in Shiga-toxin-producing *E. coli* O104:H4 induced haemolytic-uraemic syndrome: an analysis of the German STEC-HUS registry. Nephrol Dial Transplant. 27, 3807-3815.

Kim, M., Ogawa, M., Fujita, Y., Yoshikawa, Y., Nagai, T., Koyama, T., Nagai, S., Lange, A., Fassler, R., Sasakawa, C., 2009. Bacteria hijack integrin-linked kinase to stabilize focal adhesions and block cell detachment. Nature. 459, 578-582.

Kimura, S., Makino, K., Shinagawa, H., Amemura, M., Nakata, A., 1989. Regulation of the phosphate regulon of *Escherichia coli*: characterization of the promoter of the *pstS* gene. Mol Gen Genet. 215, 374-380.

Kjell Magne Fagerbakke, M.H., Svein Norland 1966. Content of carbon, nitrogen, oxygen, sulfur and phosphorus in native aquatic and cultured bacteria. Aquat microb ecol. 10, 15-27.

Klapproth, J.M., Scaletsky, I.C., McNamara, B.P., Lai, L.C., Malstrom, C., James, S.P., Donnenberg, M.S., 2000. A large toxin from pathogenic *Escherichia coli* strains that inhibits lymphocyte activation. Infect Immun. 68, 2148-2155.

Klein, G., Lindner, B., Brade, H., Raina, S., 2011. Molecular basis of lipopolysaccharide heterogeneity in *Escherichia coli*: envelope stress-responsive regulators control the incorporation of glycoforms with a third 3-deoxy-alpha-D-manno-oct-2-ulosonic acid and

rhamnose. J Biol Chem. 286, 42787-42807.

Klein, G., Muller-Loennies, S., Lindner, B., Kobylak, N., Brade, H., Raina, S., 2013. Molecular and structural basis of inner core lipopolysaccharide alterations in *Escherichia coli*: incorporation of glucuronic acid and phosphoethanolamine in the heptose region. J Biol Chem. 288, 8111-8127.

Knutton, S., Rosenshine, I., Pallen, M.J., Nisan, I., Neves, B.C., Bain, C., Wolff, C., Dougan, G., Frankel, G., 1998. A novel EspA-associated surface organelle of enteropathogenic *Escherichia coli* involved in protein translocation into epithelial cells. EMBO J. 17, 2166-2176.

Konadu, E.Y., Parke, J.C., Jr., Tran, H.T., Bryla, D.A., Robbins, J.B., Szu, S.C., 1998. Investigational vaccine for *Escherichia coli* O157: phase 1 study of O157 O-specific polysaccharide-*Pseudomonas aeruginosa* recombinant exoprotein A conjugates in adults. J Infect Dis. 177, 383-387.

Konczy, P., Ziebell, K., Mascarenhas, M., Choi, A., Michaud, C., Kropinski, A.M., Whittam, T.S., Wickham, M., Finlay, B., Karmali, M.A., 2008. Genomic O island 122, locus for enterocyte effacement, and the evolution of virulent verocytotoxin-producing *Escherichia coli*. J Bacteriol. 190, 5832-5840.

Konowalchuk, J., Speirs, J.I., Stavric, S., 1977. Vero response to a cytotoxin of *Escherichia coli*. Infect Immun. 18, 775-779.

Kuo, C.J., Chen, J.W., Chiu, H.C., Teng, C.H., Hsu, T.I., Lu, P.J., Syu, W.J., Wang, S.T., Chou, T.C., Chen, C.S., 2016. Mutation of the Enterohemorrhagic *Escherichia coli* Core LPS Biosynthesis Enzyme RfaD Confers Hypersusceptibility to Host Intestinal Innate Immunity In vivo. Front Cell Infect Microbiol. 6, 82.

Lam, O., Wheeler, J., Tang, C.M., 2014. Thermal control of virulence factors in bacteria: a hot topic. Virulence. 5, 852-862.

Lamarche, M.G., Dozois, C.M., Daigle, F., Caza, M., Curtiss, R., 3rd, Dubreuil, J.D., Harel, J., 2005. Inactivation of the *pst* system reduces the virulence of an avian pathogenic *Escherichia coli* O78 strain. Infect Immun. 73, 4138-4145.

Lamarche, M.G., Harel, J., 2010. Membrane homeostasis requires intact pst in extraintestinal pathogenic *Escherichia coli*. Curr Microbiol. 60, 356-359.

Lamarche, M.G., Kim, S.H., Crepin, S., Mourez, M., Bertrand, N., Bishop, R.E., Dubreuil, J.D., Harel, J., 2008. Modulation of hexa-acyl pyrophosphate lipid A population under *Escherichia coli* phosphate (Pho) regulon activation. J Bacteriol. 190, 5256-5264.

Lapeyraque, A.L., Malina, M., Fremeaux-Bacchi, V., Boppel, T., Kirschfink, M., Oualha, M., Proulx, F., Clermont, M.J., Le Deist, F., Niaudet, P., Schaefer, F., 2011. Eculizumab in severe Shiga-toxin-associated HUS. N Engl J Med. 364, 2561-2563.

Larsen, P., Olesen, B.H., Nielsen, P.H., Nielsen, J.L., 2008. Quantification of lipids and protein in thin biofilms by fluorescence staining. Biofouling. 24, 241-250.

Lee, 2011a. Transcriptomic Analysis for Genetic Mechanisms of the Factors. Curr Microbiol.

Lemon, K.P., Earl, A.M., Vlamakis, H.C., Aguilar, C., Kolter, R., 2008. Biofilm development with an emphasis on *Bacillus subtilis*. Curr Top Microbiol Immunol. 322, 1-16.

Leyton, D.L., Sloan, J., Hill, R.E., Doughty, S., Hartland, E.L., 2003. Transfer region of pO113 from enterohemorrhagic *Escherichia coli:* similarity with R64 and identification of a novel plasmid-encoded autotransporter, EpeA. Infect Immun. 71, 6307-6319.

Lim, J.Y., La, H.J., Sheng, H., Forney, L.J., Hovde, C.J., 2010a. Influence of plasmid pO157 on *Escherichia coli* O157:H7 Sakai biofilm formation. Appl Environ Microbiol. 76, 963-966.

Lim, J.Y., Yoon, J., Hovde, C.J., 2010b. A brief overview of *Escherichia coli* O157:H7 and its plasmid O157. J Microbiol Biotechn. 20, 5-14.

Liu, N.T., Nou, X., Bauchan, G.R., Murphy, C., Lefcourt, A.M., Shelton, D.R., Lo, Y.M., 2015. Effects of environmental parameters on the dual-species biofilms formed by *Escherichia coli* O157:H7 and *Ralstonia insidiosa*, a strong biofilm producer isolated from a fresh-cut produce processing plant. J Food Prot. 78, 121-127.

Liu, N.T., Nou, X., Lefcourt, A.M., Shelton, D.R., Lo, Y.M., 2014. Dual-species biofilm formation by *Escherichia coli* O157:H7 and environmental bacteria isolated from fresh-cut processing facilities. Int J Food Microbiol. 171, 15-20.

Long, J., Zaborina, O., Holbrook, C., Zaborin, A., Alverdy, J., 2008. Depletion of intestinal phosphate after operative injury activates the virulence of *P. aeruginosa* causing lethal gut-derived sepsis. Surgery. 144, 189-197.

Mahfoud, R., Manis, A., Binnington, B., Ackerley, C., Lingwood, C.A., 2010. A major fraction of glycosphingolipids in model and cellular cholesterol-containing membranes is undetectable by their binding proteins. J Biol Chem. 285, 36049-36059.

Majowicz, S.E., Scallan, E., Jones-Bitton, A., Sargeant, J.M., Stapleton, J., Angulo, F.J., Yeung, D.H., Kirk, M.D., 2014. Global incidence of human Shiga toxin-producing *Escherichia coli* infections and deaths: a systematic review and knowledge synthesis. Foodborne Pathog Dis. 11, 447-455.

Makino, K., Amemura, M., Kim, S.K., Nakata, A., Shinagawa, H., 1993. Role of the sigma 70

subunit of RNA polymerase in transcriptional activation by activator protein PhoB in *Escherichia coli*. Genes Dev. 7, 149-160.

Makino, K., Shinagawa, H., Amemura, M., Kawamoto, T., Yamada, M., Nakata, A., 1989. Signal transduction in the phosphate regulon of *Escherichia coli* involves phosphotransfer between PhoR and PhoB proteins. J Mol Biol. 210, 551-559.

Makino, K., Shinagawa, H., Amemura, M., Kimura, S., Nakata, A., Ishihama, A., 1988. Regulation of the phosphate regulon of *Escherichia coli.* Activation of pstS transcription by PhoB protein in vitro. J Mol Biol. 203, 85-95.

Makino, K., Shinagawa, H., Amemura, M., Nakata, A., 1986. Nucleotide sequence of the *phoB* gene, the positive regulatory gene for the phosphate regulon of *Escherichia coli* K-12. J Mol Biol. 190, 37-44.

Maloney, P.C., 1983. Relationship between phosphorylation potential and electrochemical H+ gradient during glycolysis in *Streptococcus lactis*. J Bacteriol. 153, 1461-1470.

Malyukova, I., Murray, K.F., Zhu, C., Boedeker, E., Kane, A., Patterson, K., Peterson, J.R., Donowitz, M., Kovbasnjuk, O., 2009. Macropinocytosis in Shiga toxin 1 uptake by human intestinal epithelial cells and transcellular transcytosis. Am J Physiol-Gastr L. 296, G78-92.

Manning, S.D., Motiwala, A.S., Springman, A.C., Qi, W., Lacher, D.W., Ouellette, L.M., Mladonicky, J.M., Somsel, P., Rudrik, J.T., Dietrich, S.E., Zhang, W., Swaminathan, B., Alland, D., Whittam, T.S., 2008. Variation in virulence among clades of *Escherichia coli* O157:H7 associated with disease outbreaks. Proc Natl Acad Sci USA. 105, 4868-4873.

Marches, O., Covarelli, V., Dahan, S., Cougoule, C., Bhatta, P., Frankel, G., Caron, E., 2008. EspJ of enteropathogenic and enterohaemorrhagic *Escherichia coli* inhibits opsono-phagocytosis. Cell Microbiol. 10, 1104-1115.

Marches, O., Ledger, T.N., Boury, M., Ohara, M., Tu, X., Goffaux, F., Mainil, J., Rosenshine, I., Sugai, M., De Rycke, J., Oswald, E., 2003. Enteropathogenic and enterohaemorrhagic *Escherichia coli* deliver a novel effector called Cif, which blocks cell cycle G2/M transition. Mol Microbiol. 50, 1553-1567.

Marouani-Gadri, N., Firmesse, O., Chassaing, D., Sandris-Nielsen, D., Arneborg, N., Carpentier, B., 2010. Potential of *Escherichia coli* O157:H7 to persist and form viable but non-culturable cells on a food-contact surface subjected to cycles of soiling and chemical treatment. Int J Food Microbiol. 144, 96-103.

Martinez-Gil, M., Goh, K.G.K., Rackaityte, E., Sakamoto, C., Audrain, B., Moriel, D.G., Totsika, M., Ghigo, J.M., Schembri, M.A., Beloin, C., 2017. YeeJ is an inverse

autotransporter from *Escherichia coli* that binds to peptidoglycan and promotes biofilm formation. Sci Rep. 7, 11326.

Martorelli, L., Garimano, N., Fiorentino, G.A., Vilte, D.A., Garbaccio, S.G., Barth, S.A., Menge, C., Ibarra, C., Palermo, M.S., Cataldi, A., 2018. Efficacy of a recombinant Intimin, EspB and Shiga toxin 2B vaccine in calves experimentally challenged with *Escherichia coli* O157:H7. Vaccine. 36, 3949-3959.

Mason, P.W., Carbone, D.P., Cushman, R.A., Waggoner, A.S., 1981. The importance of inorganic phosphate in regulation of energy metabolism of *Streptococcus lactis*. J Biol Chem. 256, 1861-1866.

McCleary, W.R., 1996. The activation of PhoB by acetylphosphate. Mol Microbiol. 20, 1155-1163.

McCleary, W.R., 2017. Molecular Mechanisms of Phosphate Homeostasis in *Escherichia coli.* IntechOpen. Samie, A. (ed.) *Escherichia coli*, chap. 17.

McKee, M.L., Melton-Celsa, A.R., Moxley, R.A., Francis, D.H., O'Brien, A.D., 1995. Enterohemorrhagic *Escherichia coli* O157:H7 requires intimin to colonize the gnotobiotic pig intestine and to adhere to HEp-2 cells. Infect Immun. 63, 3739-3744.

McNamara, B.P., Koutsouris, A., O'Connell, C.B., Nougayrede, J.P., Donnenberg, M.S., Hecht, G., 2001. Translocated EspF protein from enteropathogenic *Escherichia coli* disrupts host intestinal barrier function. J Clin Invest. 107, 621-629.

McWilliams, B.D., Torres, A.G., 2014. Enterohemorrhagic *Escherichia coli* Adhesins. Microbiol Spectr. 2.

Meier-Dieter, U., Starman, R., Barr, K., Mayer, H., Rick, P.D., 1990. Biosynthesis of enterobacterial common antigen in *Escherichia coli*. Biochemical characterization of Tn10 insertion mutants defective in enterobacterial common antigen synthesis. J Biol Chem. 265, 13490-13497.

Melton-Celsa, A.R., 2014. Shiga Toxin (Stx) Classification, Structure, and Function. Microbiol Spectr. 2, EHEC-0024-2013.

Melton-Celsa, A.R., Carvalho, H.M., Thuning-Roberson, C., O'Brien, A.D., 2015. Protective efficacy and pharmacokinetics of human/mouse chimeric anti-Stx1 and anti-Stx2 antibodies in mice. Clin Vaccine Immunol. 22, 448-455.

Melton-Celsa, A.R., O'Brien, A.D., 2014. New Therapeutic Developments against Shiga Toxin-Producing *Escherichia coli*. Microbiol Spectr. 2.

Menge, C., Blessenohl, M., Eisenberg, T., Stamm, I., Baljer, G., 2004a. Bovine ileal

intraepithelial lymphocytes represent target cells for Shiga toxin 1 from *Escherichia coli*. Infect Immun. 72, 1896-1905.

Menge, C., Stamm, I., Van Diemen, P.M., Sopp, P., Baljer, G., Wallis, T.S., Stevens, M.P., 2004b. Phenotypic and functional characterization of intraepithelial lymphocytes in a bovine ligated intestinal loop model of enterohaemorrhagic *Escherichia coli* infection. J Med Microbiol. 53, 573-579.

Menge, C., Wieler, L.H., Schlapp, T., Baljer, G., 1999. Shiga toxin 1 from *Escherichia coli* blocks activation and proliferation of bovine lymphocyte subpopulations *in vitro*. Infect Immun. 67, 2209-2217.

Menne, J., Nitschke, M., Stingele, R., Abu-Tair, M., Beneke, J., Bramstedt, J., Bremer, J.P., Brunkhorst, R., Busch, V., Dengler, R., Deuschl, G., Fellermann, K., Fickenscher, H., Gerigk, C., Goettsche, A., Greeve, J., Hafer, C., Hagenmuller, F., Haller, H., Herget-Rosenthal, S., Hertenstein, B., Hofmann, C., Lang, M., Kielstein, J.T., Klostermeier, U.C., Knobloch, J., Kuehbacher, M., Kunzendorf, U., Lehnert, H., Manns, M.P., Menne, T.F., Meyer, T.N., Michael, C., Munte, T., Neumann-Grutzeck, C., Nuernberger, J., Pavenstaedt, H., Ramazan, L., Renders, L., Repenthin, J., Ries, W., Rohr, A., Rump, L.C., Samuelsson, O., Sayk, F., Schmidt, B.M., Schnatter, S., Schocklmann, H., Schreiber, S., von Seydewitz, C.U., Steinhoff, J., Stracke, S., Suerbaum, S., van de Loo, A., Vischedyk, M., Weissenborn, K., Wellhoner, P., Wiesner, M., Zeissig, S., Buning, J., Schiffer, M., Kuehbacher, T., consortium, E.-H., 2012. Validation of treatment strategies for enterohaemorrhagic *Escherichia coli* O104:H4 induced haemolytic uraemic syndrome: case-control study. BMJ. 345, e4565.

Michino, H., Araki, K., Minami, S., Takaya, S., Sakai, N., Miyazaki, M., Ono, A., Yanagawa, H., 1999. Massive outbreak of *Escherichia coli* O157:H7 infection in schoolchildren in Sakai City, Japan, associated with consumption of white radish sprouts. Am J Epidemiol. 150, 787-796.

Miller, S.I., Kukral, A.M., Mekalanos, J.J., 1989. A two-component regulatory system (*phoP phoQ*) controls *Salmonella typhimurium* virulence. Proc Natl Acad Sci U S A. 86, 5054-5058.

Monds, R.D., Newell, P.D., Gross, R.H., O'Toole, G.A., 2007. Phosphate-dependent modulation of c-di-GMP levels regulates *Pseudomonas fluorescens* Pf0-1 biofilm formation by controlling secretion of the adhesin LapA. Mol Microbiol. 63, 656-679.

Monds, R.D., Silby, M.W., Mahanty, H.K., 2001. Expression of the Pho regulon negatively regulates biofilm formation by *Pseudomonas aureofaciens* PA147-2. Mol Microbiol. 42, 415-426.

Montero, D.A., Velasco, J., Del Canto, F., Puente, J.L., Padola, N.L., Rasko, D.A., Farfan, M.,

Salazar, J.C., Vidal, R., 2017. Locus of Adhesion and Autoaggregation (LAA), a pathogenicity island present in emerging Shiga Toxin-producing *Escherichia coli* strains. Sci Rep. 7, 7011.

Motomura, K., Hirota, R., Ohnaka, N., Okada, M., Ikeda, T., Morohoshi, T., Ohtake, H., Kuroda, A., 2011. Overproduction of YjbB reduces the level of polyphosphate in *Escherichia coli*: a hypothetical role of YjbB in phosphate export and polyphosphate accumulation. FEMS Microbiol Lett. 320, 25-32.

Moussay, E., Stamm, I., Taubert, A., Baljer, G., Menge, C., 2006. *Escherichia coli* Shiga toxin 1 enhances il-4 transcripts in bovine ileal intraepithelial lymphocytes. Vet Immunol Immunopathol. 113, 367-382.

Mudrak, B., Tamayo, R., 2012. The *Vibrio cholerae* Pst2 phosphate transport system is upregulated in biofilms and contributes to biofilm-induced hyperinfectivity. Infect Immun. 80, 1794-1802.

Nadler, C., Baruch, K., Kobi, S., Mills, E., Haviv, G., Farago, M., Alkalay, I., Bartfeld, S., Meyer, T.F., Ben-Neriah, Y., Rosenshine, I., 2010. The type III secretion effector NleE inhibits NF-kappaB activation. PLoS Pathog. 6, e1000743.

Nassar, F.J., Rahal, E.A., Sabra, A., Matar, G.M., 2013. Effects of subinhibitory concentrations of antimicrobial agents on *Escherichia coli* O157:H7 Shiga toxin release and role of the SOS response. Foodborne Pathog Dis. 10, 805-812.

Nataro, J.P., Kaper, J.B., 1998. Diarrheagenic *Escherichia coli*. Clin Microbiol Rev. 11, 142-201.

National Association of State Public Health Veterinarians, I., Centers for Disease, C., Prevention, Council of, S., Territorial, E., American Veterinary Medical, A., 2007. Compendium of measures to prevent disease associated with animals in public settings, 2007: National Association of State Public Health Veterinarians, Inc. (NASPHV). MMWR. Recommendations and reports : Morbidity and mortality weekly report. Recommendations and reports / Centers for Disease Control. 56, 1-14.

Naylor, S.W., Roe, A.J., Nart, P., Spears, K., Smith, D.G., Low, J.C., Gally, D.L., 2005. *Escherichia coli* O157:H7 forms attaching and effacing lesions at the terminal rectum of cattle and colonization requires the LEE4 operon. Microbiology. 151, 2773-2781.

Nesse, L.L., Sekse, C., Berg, K., Johannesen, K.C., Solheim, H., Vestby, L.K., Urdahl, A.M., 2014. Potentially pathogenic *Escherichia coli* can form a biofilm under conditions relevant to the food production chain. Appl Environ Microbiol. 80, 2042-2049.

Newell, P.D., Yoshioka, S., Hvorecny, K.L., Monds, R.D., O'Toole, G.A., 2011. Systematic

analysis of diguanylate cyclases that promote biofilm formation by *Pseudomonas fluorescens* Pf0-1. J Bacteriol. 193, 4685-4698.

Newton, H.J., Pearson, J.S., Badea, L., Kelly, M., Lucas, M., Holloway, G., Wagstaff, K.M., Dunstone, M.A., Sloan, J., Whisstock, J.C., Kaper, J.B., Robins-Browne, R.M., Jans, D.A., Frankel, G., Phillips, A.D., Coulson, B.S., Hartland, E.L., 2010. The type III effectors NleE and NleB from enteropathogenic *E. coli* and OspZ from *Shigella* block nuclear translocation of NF-kappaB p65. PLoS Pathog. 6, e1000898.

Newton, H.J., Sloan, J., Bennett-Wood, V., Adams, L.M., Robins-Browne, R.M., Hartland, E.L., 2004. Contribution of long polar fimbriae to the virulence of rabbit-specific enteropathogenic *Escherichia coli*. Infect Immun. 72, 1230-1239.

Neznansky, A., Blus-Kadosh, I., Yerushalmi, G., Banin, E., Opatowsky, Y., 2014. The *Pseudomonas aeruginosa* phosphate transport protein PstS plays a phosphate-independent role in biofilm formation. FASEB journal: official publication of the Federation of American Societies for Experimental Biology. 28, 5223-5233.

Ngeleka, M., Harel, J., Jacques, M., Fairbrother, J.M., 1992. Characterization of a polysaccharide capsular antigen of septicemic *Escherichia coli* O115:K "V165" :F165 and evaluation of its role in pathogenicity. Infect Immun. 60, 5048-5056.

Niba, E.T., Naka, Y., Nagase, M., Mori, H., Kitakawa, M., 2007. A genome-wide approach to identify the genes involved in biofilm formation in *E. coli*. DNA Res. 14, 237-246.

Nicholls, L., Grant, T.H., Robins-Browne, R.M., 2000. Identification of a novel genetic locus that is required for in vitro adhesion of a clinical isolate of enterohaemorrhagic *Escherichia coli* to epithelial cells. Mol Microbiol. 35, 275-288.

Nielsen, D.W., Klimavicz, J.S., Cavender, T., Wannemuehler, Y., Barbieri, N.L., Nolan, L.K., Logue, C.M., 2018. The Impact of Media, Phylogenetic Classification, and *E. coli* Pathotypes on Biofilm Formation in Extraintestinal and Commensal *E. coli* From Humans and Animals. Front Microbiol. 9, 902.

Nitschke, M., Sayk, F., Hartel, C., Roseland, R.T., Hauswaldt, S., Steinhoff, J., Fellermann, K., Derad, I., Wellhoner, P., Buning, J., Tiemer, B., Katalinic, A., Rupp, J., Lehnert, H., Solbach, W., Knobloch, J.K., 2012. Association between azithromycin therapy and duration of bacterial shedding among patients with Shiga toxin-producing enteroaggregative *Escherichia coli* O104:H4. Jama. 307, 1046-1052.

O'Brien, A.D., LaVeck, G.D., Thompson, M.R., Formal, S.B., 1982. Production of Shigella dysenteriae type 1-like cytotoxin by *Escherichia coli*. J Infect Dis. 146, 763-769.

O'Brien, A.D., Melton, A.R., Schmitt, C.K., McKee, M.L., Batts, M.L., Griffin, D.E., 1993.

Profile of *Escherichia coli* O157:H7 pathogen responsible for hamburger-borne outbreak of hemorrhagic colitis and hemolytic uremic syndrome in Washington. J Clin Microbiol. 31, 2799-2801.

O'May, G.A., Jacobsen, S.M., Longwell, M., Stoodley, P., Mobley, H.L., Shirtliff, M.E., 2009. The high-affinity phosphate transporter Pst in *Proteus mirabilis* HI4320 and its importance in biofilm formation. Microbiology. 155, 1523-1535.

O'Reilly, K.M., Low, J.C., Denwood, M.J., Gally, D.L., Evans, J., Gunn, G.J., Mellor, D.J., Reid, S.W., Matthews, L., 2010. Associations between the presence of virulence determinants and the epidemiology and ecology of zoonotic *Escherichia coli*. Appl Environ Microbiol. 76, 8110-8116.

O'Ryan, M., Vidal, R., del Canto, F., Carlos Salazar, J., Montero, D., 2015. Vaccines for viral and bacterial pathogens causing acute gastroenteritis: Part II: Vaccines for *Shigella*, *Salmonella*, enterotoxigenic *E. coli* (ETEC) enterohemorragic *E. coli* (EHEC) and *Campylobacter jejuni*. Hum Vaccin Immunother. 11, 601-619.

Oh, Y.J., Jo, W., Yang, Y., Park, S., 2007. Influence of culture conditions on *Escherichia coli* O157:H7 biofilm formation by atomic force microscopy. Ultramicroscopy. 107, 869-874.

Ohnishi, M., Kurokawa, K., Hayashi, T., 2001. Diversification of *Escherichia coli* genomes: are bacteriophages the major contributors? Trends Microbiol. 9, 481-485.

Otto, K., Norbeck, J., Larsson, T., Karlsson, K.A., Hermansson, M., 2001. Adhesion of type 1-fimbriated *Escherichia coli* to abiotic surfaces leads to altered composition of outer membrane proteins. J Bacteriol. 183, 2445-2453.

Paradis-Bleau, C., Kritikos, G., Orlova, K., Typas, A., Bernhardt, T.G., 2014. A genome-wide screen for bacterial envelope biogenesis mutants identifies a novel factor involved in cell wall precursor metabolism. PLoS genetics. 10, e1004056.

Park, Y.J., Chen, J., 2015. Control of the Biofilms Formed by Curli- and Cellulose-Expressing Shiga Toxin-Producing *Escherichia coli* Using Treatments with Organic Acids and Commercial Sanitizers. J Food Prot. 78, 990-995.

Paton, A.W., Paton, J.C., 1998. Detection and characterization of Shiga toxigenic *Escherichia coli* by using multiplex PCR assays for *stx1*, *stx2*, *eaeA*, enterohemorrhagic *E. coli hlyA*, *rfb*O111, and *rfb*O157. J Clin Microbiol. 36, 598-602.

Paton, A.W., Srimanote, P., Talbot, U.M., Wang, H., Paton, J.C., 2004. A new family of potent AB(5) cytotoxins produced by Shiga toxigenic *Escherichia coli*. J Exp Med. 200, 35-46.

Paton, A.W., Srimanote, P., Woodrow, M.C., Paton, J.C., 2001. Characterization of Saa, a novel

autoagglutinating adhesin produced by locus of enterocyte effacement-negative Shiga-toxigenic *Escherichia coli* strains that are virulent for humans. Infect Immun. 69, 6999-7009.

Patzer, S.I., Hantke, K., 1998. The ZnuABC high-affinity zinc uptake system and its regulator Zur in *Escherichia coli*. Mol Microbiol. 28, 1199-1210.

Pearson, J.S., Riedmaier, P., Marches, O., Frankel, G., Hartland, E.L., 2011. A type III effector protease NleC from enteropathogenic *Escherichia coli* targets NF-kappaB for degradation. Mol Microbiol. 80, 219-230.

Perna, N.T., Plunkett, G., 3rd, Burland, V., Mau, B., Glasner, J.D., Rose, D.J., Mayhew, G.F., Evans, P.S., Gregor, J., Kirkpatrick, H.A., Posfai, G., Hackett, J., Klink, S., Boutin, A., Shao, Y., Miller, L., Grotbeck, E.J., Davis, N.W., Lim, A., Dimalanta, E.T., Potamousis, K.D., Apodaca, J., Anantharaman, T.S., Lin, J., Yen, G., Schwartz, D.C., Welch, R.A., Blattner, F.R., 2001. Genome sequence of enterohaemorrhagic *Escherichia coli* O157:H7. Nature. 409, 529-533.

Peterson, C.N., Mandel, M.J., Silhavy, T.J., 2005. *Escherichia coli* starvation diets: essential nutrients weigh in distinctly. J Bacteriol. 187, 7549-7553.

Philpott, D.J., Ackerley, C.A., Kiliaan, A.J., Karmali, M.A., Perdue, M.H., Sherman, P.M., 1997. Translocation of verotoxin-1 across T84 monolayers: mechanism of bacterial toxin penetration of epithelium. Am J Physiol. 273, G1349-1358.

Pinyon, R.A., Paton, J.C., Paton, A.W., Botten, J.A., Morona, R., 2004. Refinement of a therapeutic Shiga toxin-binding probiotic for human trials. J Infect Dis. 189, 1547-1555.

Piscatelli, H., Kotkar, S.A., McBee, M.E., Muthupalani, S., Schauer, D.B., Mandrell, R.E., Leong, J.M., Zhou, D., 2011. The EHEC type III effector NleL is an E3 ubiquitin ligase that modulates pedestal formation. PloS one. 6, e19331.

Poirier, K., Faucher, S.P., Beland, M., Brousseau, R., Gannon, V., Martin, C., Harel, J., Daigle, F., 2008. *Escherichia coli* O157:H7 survives within human macrophages: global gene expression profile and involvement of the Shiga toxins. Infect Immun. 76, 4814-4822.

Pragai, Z., Harwood, C.R., 2002. Regulatory interactions between the Pho and sigma(B)-dependent general stress regulons of *Bacillus subtilis*. Microbiology. 148, 1593-1602.

Pratt, J.T., Ismail, A.M., Camilli, A., 2010. PhoB regulates both environmental and virulence gene expression in *Vibrio cholerae*. Mol Microbiol. 77, 1595-1605.

Pratt, J.T., McDonough, E., Camilli, A., 2009. PhoB regulates motility, biofilms, and cyclic di-GMP in *Vibrio cholerae*. J Bacteriol. 191, 6632-6642.

Pruimboom-Brees, I.M., Morgan, T.W., Ackermann, M.R., Nystrom, E.D., Samuel, J.E., Cornick, N.A., Moon, H.W., 2000. Cattle lack vascular receptors for *Escherichia coli* O157:H7 Shiga toxins. Proc Natl Acad Sci U S A. 97, 10325-10329.

Purevdorj, B., Costerton, J.W., Stoodley, P., 2002. Influence of hydrodynamics and cell signaling on the structure and behavior of *Pseudomonas aeruginosa* biofilms. Appl Environ Microbiol. 68, 4457-4464.

Puttamreddy, S., Cornick, N.A., Minion, F.C., 2010. Genome-wide transposon mutagenesis reveals a role for pO157 genes in biofilm development in *Escherichia coli* O157:H7 EDL933. Infect Immun. 78, 2377-2384.

Qadri, S.M., Kayali, S., 1998. Enterohemorrhagic *Escherichia coli.* A dangerous food-borne pathogen. Postgrad Med. 103, 179-180, 185-177.

Raetz, C.R., Whitfield, C., 2002. Lipopolysaccharide endotoxins. Annu Rev Biochem. 71, 635-700.

Rahal, E.A., Fadlallah, S.M., Nassar, F.J., Kazzi, N., Matar, G.M., 2015. Approaches to treatment of emerging Shiga toxin-producing *Escherichia coli* infections highlighting the O104:H4 serotype. Front Cell Infect Microbiol. 5, 24.

Rangel, J.M., Sparling, P.H., Crowe, C., Griffin, P.M., Swerdlow, D.L., 2005. Epidemiology of *Escherichia coli* O157:H7 outbreaks, United States, 1982-2002. Emerg Infect Dis. 11, 603-609.

Rao, N.N., Liu, S., Kornberg, A., 1998. Inorganic polyphosphate in *Escherichia coli*: the phosphate regulon and the stringent response. J Bacteriol. 180, 2186-2193.

Rao, N.N., Roberts, M.F., Torriani, A., Yashphe, J., 1993. Effect of *glpT* and *glpD* mutations on expression of the *phoA* gene in *Escherichia coli*. J Bacteriol. 175, 74-79.

Rao, N.N., Wang, E., Yashphe, J., Torriani, A., 1986. Nucleotide pool in pho regulon mutants and alkaline phosphatase synthesis in *Escherichia coli*. J Bacteriol. 166, 205-211.

Rendon, M.A., Saldana, Z., Erdem, A.L., Monteiro-Neto, V., Vazquez, A., Kaper, J.B., Puente, J.L., Giron, J.A., 2007. Commensal and pathogenic *Escherichia coli* use a common pilus adherence factor for epithelial cell colonization. Proc Natl Acad Sci U S A. 104, 10637-10642.

Renwick, S.A., Wilson, J.B., Clarke, R.C., Lior, H., Borczyk, A.A., Spika, J., Rahn, K., McFadden, K., Brouwer, A., Copps, A., et al., 1993. Evidence of direct transmission of *Escherichia coli* O157:H7 infection between calves and a human. J Infect Dis. 168, 792-793.

Rice, C.D., Pollard, J.E., Lewis, Z.T., McCleary, W.R., 2009. Employment of a promoter-swapping technique shows that PhoU modulates the activity of the PstSCAB2 ABC transporter in *Escherichia coli*. Appl Environ Microbiol. 75, 573-582.

Richards, J.J., Melander, C., 2009. Controlling bacterial biofilms. Chembiochem. 10, 2287-2294.

Rico-Jimenez, M., Reyes-Darias, J.A., Ortega, A., Diez Pena, A.I., Morel, B., Krell, T., 2016. Two different mechanisms mediate chemotaxis to inorganic phosphate in *Pseudomonas aeruginosa*. Sci Rep. 6, 28967.

Robinson, C.M., Sinclair, J.F., Smith, M.J., O'Brien, A.D., 2006. Shiga toxin of enterohemorrhagic *Escherichia coli type* O157:H7 promotes intestinal colonization. Proc Natl Acad Sci U S A. 103, 9667-9672.

Römling, U., Galperin, M.Y., Gomelsky, M., 2013. Cyclic di-GMP: the First 25 Years of a Universal Bacterial Second Messenger. Microbiol Mol Biol Rev. 77, 1-52.

Ryu, J.H., Kim, H., Beuchat, L.R., 2004. Attachment and biofilm formation by *Escherichia coli* O157:H7 on stainless steel as influenced by exopolysaccharide production, nutrient availability, and temperature. J Food Prot. 67, 2123-2131.

Saier, M.H., Jr., Reddy, V.S., Tsu, B.V., Ahmed, M.S., Li, C., Moreno-Hagelsieb, G., 2016. The Transporter Classification Database (TCDB): recent advances. Nucleic Acids Res. 44, D372-379.

Santos-Beneit, F., 2015. The Pho regulon: a huge regulatory network in bacteria. Front Microbiol. 6, 402.

Santos, M.F., New, R.R., Andrade, G.R., Ozaki, C.Y., Sant'Anna, O.A., Mendonca-Previato, L., Trabulsi, L.R., Domingos, M.O., 2010. Lipopolysaccharide as an antigen target for the formulation of a universal vaccine against *Escherichia coli* O111 strains. Clin Vaccine Immunol. 17, 1772-1780.

Sargeant, J.M., Amezcua, M.R., Rajic, A., Waddell, L., 2007. Pre-harvest interventions to reduce the shedding of *E. coli* O157 in the faeces of weaned domestic ruminants: a systematic review. Zoonoses Public Hlth. 54, 260-277.

Scheutz, F., Nielsen, E.M., Frimodt-Moller, J., Boisen, N., Morabito, S., Tozzoli, R., Nataro, J.P., Caprioli, A., 2011. Characteristics of the enteroaggregative Shiga toxin/verotoxin-producing *Escherichia coli* O104:H4 strain causing the outbreak of haemolytic uraemic syndrome in Germany, May to June 2011. Euro Surveill. 16.

Schirmer, T., Jenal, U., 2009. Structural and mechanistic determinants of c-di-GMP signalling.

Nature reviews. Microbiology. 7, 724-735.

Schmidt, H., Hensel, M., 2004. Pathogenicity islands in bacterial pathogenesis. Clin Microbiol Rev. 17, 14-56.

Schmidt, H., Karch, H., Beutin, L., 1994. The large-sized plasmids of enterohemorrhagic *Escherichia coli* O157 strains encode hemolysins which are presumably members of the *E. coli* alpha-hemolysin family. FEMS Microbiol Lett. 117, 189-196.

Schmidt, N., Barth, S.A., Frahm, J., Meyer, U., Danicke, S., Geue, L., Menge, C., 2018. Decreased STEC shedding by cattle following passive and active vaccination based on recombinant *Escherichia coli* Shiga toxoids. Vet Res. 49, 28.

Schuller, S., Frankel, G., Phillips, A.D., 2004. Interaction of Shiga toxin from *Escherichia coli* with human intestinal epithelial cell lines and explants: Stx2 induces epithelial damage in organ culture. Cell Microbiol. 6, 289-301.

Schurig-Briccio, L.A., Farias, R.N., Rintoul, M.R., Rapisarda, V.A., 2009. Phosphate-enhanced stationary-phase fitness of *Escherichia coli* is related to inorganic polyphosphate level. J Bacteriol. 191, 4478-4481.

Selkrig, J., Mosbahi, K., Webb, C.T., Belousoff, M.J., Perry, A.J., Wells, T.J., Morris, F., Leyton, D.L., Totsika, M., Phan, M.D., Celik, N., Kelly, M., Oates, C., Hartland, E.L., Robins-Browne, R.M., Ramarathinam, S.H., Purcell, A.W., Schembri, M.A., Strugnell, R.A., Henderson, I.R., Walker, D., Lithgow, T., 2012. Discovery of an archetypal protein transport system in bacterial outer membranes. Nat Struct Mol Biol. 19, 506-510, S501.

Shames, S.R., Deng, W., Guttman, J.A., de Hoog, C.L., Li, Y., Hardwidge, P.R., Sham, H.P., Vallance, B.A., Foster, L.J., Finlay, B.B., 2010. The pathogenic *E. coli* type III effector EspZ interacts with host CD98 and facilitates host cell prosurvival signalling. Cell Microbiol. 12, 1322-1339.

Shane, A.L., Mody, R.K., Crump, J.A., Tarr, P.I., Steiner, T.S., Kotloff, K., Langley, J.M., Wanke, C., Warren, C.A., Cheng, A.C., Cantey, J., Pickering, L.K., 2017. 2017 Infectious Diseases Society of America Clinical Practice Guidelines for the Diagnosis and Management of Infectious Diarrhea. Clin Infect Dis. 65, 1963-1973.

Shapiro, R.S., Cowen, L.E., 2012. Thermal control of microbial development and virulence: molecular mechanisms of microbial temperature sensing. MBio. 3, e00238-00212.

Sharma, V.K., Bayles, D.O., Alt, D.P., Looft, T., Brunelle, B.W., Stasko, J.A., 2017. Disruption of *rcsB* by a duplicated sequence in a curli-producing *Escherichia coli* O157:H7 results in differential gene expression in relation to biofilm formation, stress responses and metabolism. BMC Microbiol. 17, 56.

Shen, N., Zhou, Y., 2016. Enhanced biological phosphorus removal with different carbon sources. Applied microbiology and biotechnology. 100, 4735-4745.

Shen, S., Mascarenhas, M., Morgan, R., Rahn, K., Karmali, M.A., 2005. Identification of four fimbria-encoding genomic islands that are highly specific for verocytotoxin-producing *Escherichia coli* serotype O157 strains. J Clin Microbiol. 43, 3840-3850.

Sheng, H., Lim, J.Y., Watkins, M.K., Minnich, S.A., Hovde, C.J., 2008. Characterization of an *Escherichia coli* O157:H7 O-antigen deletion mutant and effect of the deletion on bacterial persistence in the mouse intestine and colonization at the bovine terminal rectal mucosa. Appl Environ Microbiol. 74, 5015-5022.

Shimizu, T., Ohta, Y., Noda, M., 2009. Shiga toxin 2 is specifically released from bacterial cells by two different mechanisms. Infect Immun. 77, 2813-2823.

Shor, R., Halabe, A., Rishver, S., Tilis, Y., Matas, Z., Fux, A., Boaz, M., Weinstein, J., 2006. Severe hypophosphatemia in sepsis as a mortality predictor. Annals of clinical and laboratory science. 36, 67-72.

Shukla, R., Slack, R., George, A., Cheasty, T., Rowe, B., Scutter, J., 1995. *Escherichia coli* O157 infection associated with a farm visitor centre. Communicable disease report. CDR review. 5, R86-90.

Shulman, R.G., Brown, T.R., Ugurbil, K., Ogawa, S., Cohen, S.M., den Hollander, J.A., 1979. Cellular applications of 31P and 13C nuclear magnetic resonance. Science. 205, 160-166.

Sicard, J.F., Vogeleer, P., Le Bihan, G., Rodriguez Olivera, Y., Beaudry, F., Jacques, M., Harel, J., 2018. N-Acetyl-glucosamine influences the biofilm formation of *Escherichia coli*. Gut Pathog. 10, 26.

Smith, A.E., Kim, S.H., Liu, F., Jia, W., Vinogradov, E., Gyles, C.L., Bishop, R.E., 2008. PagP activation in the outer membrane triggers R3 core oligosaccharide truncation in the cytoplasm of *Escherichia coli* O157:H7. J Biol Chem. 283, 4332-4343.

Smith, D.R., Moxley, R.A., Peterson, R.E., Klopfenstein, T.J., Erickson, G.E., Bretschneider, G., Berberov, E.M., Clowser, S., 2009. A two-dose regimen of a vaccine against type III secreted proteins reduced *Escherichia coli* O157:H7 colonization of the terminal rectum in beef cattle in commercial feedlots. Foodborne Pathog Dis. 6, 155-161.

Spira, B., Aguena, M., de Castro Oliveira, J.V., Yagil, E., 2010. Alternative promoters in the pst operon of *Escherichia coli*. Mol Genet Genomics. 284, 489-498.

Stamm, I., Wuhrer, M., Geyer, R., Baljer, G., Menge, C., 2002. Bovine lymphocytes express functional receptors for *Escherichia coli* Shiga toxin 1. Microb Pathog. 33, 251-264.

Steed, P.M., Wanner, B.L., 1993. Use of the rep technique for allele replacement to construct mutants with deletions of the *pstSCAB-phoU* operon: evidence of a new role for the PhoU protein in the phosphate regulon. J Bacteriol. 175, 6797-6809.

Stevens, M.P., Roe, A.J., Vlisidou, I., van Diemen, P.M., La Ragione, R.M., Best, A., Woodward, M.J., Gally, D.L., Wallis, T.S., 2004. Mutation of *toxB* and a truncated version of the *efa-1* gene in *Escherichia coli* O157:H7 influences the expression and secretion of locus of enterocyte effacement-encoded proteins but not intestinal colonization in calves or sheep. Infect Immun. 72, 5402-5411.

Stock, A.M., Robinson, V.L., Goudreau, P.N., 2000. Two-component signal transduction. Annu Rev Biochem. 69, 183-215.

Stollerman, G.H., Dale, J.B., 2008. The importance of the group a streptococcus capsule in the pathogenesis of human infections: a historical perspective. Clin Infect Dis. 46, 1038-1045.

Stoodley, P., Sauer, K., Davies, D.G., Costerton, J.W., 2002. Biofilms as complex differentiated communities. Annual review of microbiology. 56, 187-209.

Strachan, N.J., Doyle, M.P., Kasuga, F., Rotariu, O., Ogden, I.D., 2005. Dose response modelling of *Escherichia coli* O157 incorporating data from foodborne and environmental outbreaks. Int J Food Microbiol. 103, 35-47.

Strockbine, N.A., Marques, L.R., Newland, J.W., Smith, H.W., Holmes, R.K., O'Brien, A.D., 1986. Two toxin-converting phages from *Escherichia coli* O157:H7 strain 933 encode antigenically distinct toxins with similar biologic activities. Infect Immun. 53, 135-140.

Sung, L.M., Jackson, M.P., O'Brien, A.D., Holmes, R.K., 1990. Transcription of the Shiga-like toxin type II and Shiga-like toxin type II variant operons of *Escherichia coli*. J Bacteriol. 172, 6386-6395.

Surin, B.P., Rosenberg, H., Cox, G.B., 1985. Phosphate-specific transport system of *Escherichia coli*: nucleotide sequence and gene-polypeptide relationships. J Bacteriol. 161, 189-198.

Tarr, 2005. Shiga-toxin-producing *Escherichia coli* and haemolytic uraemic syndrome. Lancet.

Tarr, P.I., Bilge, S.S., Vary, J.C., Jr., Jelacic, S., Habeeb, R.L., Ward, T.R., Baylor, M.R., Besser, T.E., 2000. Iha: a novel *Escherichia coli* O157:H7 adherence-conferring molecule encoded on a recently acquired chromosomal island of conserved structure. Infect Immun. 68, 1400-1407.

Tatsuno, I., Horie, M., Abe, H., Miki, T., Makino, K., Shinagawa, H., Taguchi, H., Kamiya, S., Hayashi, T., Sasakawa, C., 2001. *toxB* gene on pO157 of enterohemorrhagic *Escherichia coli* O157:H7 is required for full epithelial cell adherence phenotype. Infect Immun. 69,

6660-6669.

Teunis, P., Takumi, K., Shinagawa, K., 2004. Dose response for infection by *Escherichia coli* O157:H7 from outbreak data. Risk Anal. 24, 401-407.

Thanabalasuriar, A., Koutsouris, A., Weflen, A., Mimee, M., Hecht, G., Gruenheid, S., 2010. The bacterial virulence factor NleA is required for the disruption of intestinal tight junctions by enteropathogenic *Escherichia coli*. Cell Microbiol. 12, 31-41.

Thomson, D.U., Loneragan, G.H., Thornton, A.B., Lechtenberg, K.F., Emery, D.A., Burkhardt, D.T., Nagaraja, T.G., 2009. Use of a siderophore receptor and porin proteins-based vaccine to control the burden of *Escherichia coli* O157:H7 in feedlot cattle. Foodborne Pathog Dis. 6, 871-877.

Toma, C., Martinez Espinosa, E., Song, T., Miliwebsky, E., Chinen, I., Iyoda, S., Iwanaga, M., Rivas, M., 2004. Distribution of putative adhesins in different seropathotypes of Shiga toxin-producing *Escherichia coli*. J Clin Microbiol. 42, 4937-4946.

Torres, A.G., Giron, J.A., Perna, N.T., Burland, V., Blattner, F.R., Avelino-Flores, F., Kaper, J.B., 2002. Identification and characterization of *lpfABCC'DE*, a fimbrial operon of enterohemorrhagic *Escherichia coli* O157:H7. Infect Immun. 70, 5416-5427.

Torriani, A., 1960. Influence of inorganic phosphate in the formation of phosphatases by *Escherichia coli*. Biochim Biophys Acta. 38, 460-469.

Tremblay, Y.D., Hathroubi, S., Jacques, M., 2014. Bacterial biofilms: their importance in animal health and public health. Can J Vet Res. 78, 110-116.

Tremblay, Y.D., Vogeleer, P., Jacques, M., Harel, J., 2015. High-throughput microfluidic method to study biofilm formation and host-pathogen interactions in pathogenic *Escherichia coli*. Appl Environ Microbiol. 81, 2827-2840.

Uhlich, G.A., Chen, C.Y., Cottrell, B.J., Nguyen, L.H., 2014. Growth media and temperature effects on biofilm formation by serotype O157:H7 and non-O157 Shiga toxin-producing *Escherichia coli*. FEMS Microbiol Lett. 354, 133-141.

Uhlich, G.A., Cooke, P.H., Solomon, E.B., 2006. Analyses of the red-dry-rough phenotype of an *Escherichia coli* O157:H7 strain and its role in biofilm formation and resistance to antibacterial agents. Appl Environ Microbiol. 72, 2564-2572.

Ullrich, S., Bremer, P., Neumann-Grutzeck, C., Otto, H., Ruther, C., von Seydewitz, C.U., Meyer, G.P., Ahmadi-Simab, K., Rother, J., Hogan, B., Schwenk, W., Fischbach, R., Caselitz, J., Puttfarcken, J., Huggett, S., Tiedeken, P., Pober, J., Kirkiles-Smith, N.C., Hagenmuller, F., 2013. Symptoms and clinical course of EHEC O104 infection in

hospitalized patients: a prospective single center study. PloS one. 8, e55278.

USDA 2017. FSIS Compliance Guideline for Minimizing the Risk of Shiga Toxinroducing *Escherichia coli* (STEC) and *Salmonella* in Beef (including Veal) Slaughter Operations 2017, USDA, ed.

Valappil, S.P., Knowles, J.C., Wilson, M., 2008. Effect of silver-doped phosphate-based glasses on bacterial biofilm growth. Appl Environ Microbiol. 74, 5228-5230.

Valle, J., Mabbett, A.N., Ulett, G.C., Toledo-Arana, A., Wecker, K., Totsika, M., Schembri, M.A., Ghigo, J.M., Beloin, C., 2008. UpaG, a new member of the trimeric autotransporter family of adhesins in uropathogenic *Escherichia coli*. J Bacteriol. 190, 4147-4161.

van Veen, H.W., Abee, T., Kortstee, G.J., Konings, W.N., Zehnder, A.J., 1994. Translocation of metal phosphate via the phosphate inorganic transport system of *Escherichia coli*. Biochemistry. 33, 1766-1770.

VanBogelen, R.A., Olson, E.R., Wanner, B.L., Neidhardt, F.C., 1996. Global analysis of proteins synthesized during phosphorus restriction in *Escherichia coli*. J Bacteriol. 178, 4344-4366.

Vejborg, R.M., Klemm, P., 2009. Cellular chain formation in *Escherichia coli* biofilms. Microbiology. 155, 1407-1417.

Vlisidou, I., Marches, O., Dziva, F., Mundy, R., Frankel, G., Stevens, M.P., 2006. Identification and characterization of EspK, a type III secreted effector protein of enterohaemorrhagic *Escherichia coli* O157:H7. FEMS Microbiol Lett. 263, 32-40.

Vo, J.L., Martinez Ortiz, G.C., Subedi, P., Keerthikumar, S., Mathivanan, S., Paxman, J.J., Heras, B., 2017. Autotransporter Adhesins in *Escherichia coli* Pathogenesis. Proteomics. 17.

Vogeleer, P., Tremblay, Y.D., Mafu, A.A., Jacques, M., Harel, J., 2014. Life on the outside: role of biofilms in environmental persistence of Shiga-toxin producing *Escherichia coli*. Front Microbiol. 5, 317.

Vogeleer, P., Tremblay, Y.D.N., Jubelin, G., Jacques, M., Harel, J., 2015. Biofilm-Forming Abilities of Shiga Toxin-Producing *Escherichia coli* Isolates Associated with Human Infections. Appl Environ Microbiol. 82, 1448-1458.

Vollmer, W., Bertsche, U., 2008. Murein (peptidoglycan) structure, architecture and biosynthesis in *Escherichia coli*. Biochim Biophys Acta. 1778, 1714-1734.

Vossenkamper, A., Marches, O., Fairclough, P.D., Warnes, G., Stagg, A.J., Lindsay, J.O., Evans, P.C., Luong le, A., Croft, N.M., Naik, S., Frankel, G., MacDonald, T.T., 2010.

Inhibition of NF-kappaB signaling in human dendritic cells by the enteropathogenic *Escherichia coli* effector protein NleE. J Immunol. 185, 4118-4127.

Vuppada, R.K., Hansen, C.R., Strickland, K.A.P., Kelly, K.M., McCleary, W.R., 2018. Phosphate signaling through alternate conformations of the PstSCAB phosphate transporter. BMC Microbiol. 18, 8.

Wagner, P.L., Acheson, D.W., Waldor, M.K., 2001. Human neutrophils and their products induce Shiga toxin production by enterohemorrhagic *Escherichia coli*. Infect Immun. 69, 1934-1937.

Wang, L., Xu, S., Li, J., 2011. Effects of phosphate on the transport of *Escherichia coli* O157:H7 in saturated quartz sand. Environ Sci Technol. 45, 9566-9573.

Wang, R., Bono, J.L., Kalchayanand, N., Shackelford, S., Harhay, D.M., 2012a. Biofilm formation by Shiga toxin-producing *Escherichia coli* O157:H7 and Non-O157 strains and their tolerance to sanitizers commonly used in the food processing environment. J Food Prot. 75, 1418-1428.

Wang, R., Kalchayanand, N., Bono, J.L., 2015. Sequence of Colonization Determines the Composition of Mixed Biofilms by *Escherichia coli* O157:H7 and O111:H8 Strains. J Food Prot. 78, 1554-1559.

Wang, R., Kalchayanand, N., Bono, J.L., Schmidt, J.W., Bosilevac, J.M., 2012b. Dual-serotype biofilm formation by shiga toxin-producing *Escherichia coli* O157:H7 and O26:H11 strains. Appl Environ Microbiol. 78, 6341-6344.

Wang, X., Dubey, A.K., Suzuki, K., Baker, C.S., Babitzke, P., Romeo, T., 2005. CsrA post-transcriptionally represses *pgaABCD*, responsible for synthesis of a biofilm polysaccharide adhesin of *Escherichia coli*. Mol Microbiol. 56, 1648-1663.

Wang, X., Preston, J.F., 3rd, Romeo, T., 2004. The *pgaABCD* locus of *Escherichia coli* promotes the synthesis of a polysaccharide adhesin required for biofilm formation. J Bacteriol. 186, 2724-2734.

Wang, Z.X., Deng, R.P., Jiang, H.W., Guo, S.J., Le, H.Y., Zhao, X.D., Chen, C.S., Zhang, J.B., Tao, S.C., 2012c. Global identification of prokaryotic glycoproteins based on an *Escherichia coli* proteome microarray. PloS one. 7, e49080.

Wanner, B.L., 1996. Phosphorous assimilation and control of the phosphate regulonWashington, D.C.: ASM Press.

Wells, J.E., Shackelford, S.D., Berry, E.D., Kalchayanand, N., Guerini, M.N., Varel, V.H., Arthur, T.M., Bosilevac, J.M., Freetly, H.C., Wheeler, T.L., Ferrell, C.L., Koohmaraie,

M., 2009a. Prevalence and level of *Escherichia coli* O157:H7 in feces and on hides of feedlot steers fed diets with or without wet distillers grains with solubles. J Food Prot. 72, 1624-1633.

Wells, T.J., McNeilly, T.N., Totsika, M., Mahajan, A., Gally, D.L., Schembri, M.A., 2009b. The *Escherichia coli* O157:H7 EhaB autotransporter protein binds to laminin and collagen I and induces a serum IgA response in O157:H7 challenged cattle. Environ microbiol. 11, 1803-1814.

Wells, T.J., Sherlock, O., Rivas, L., Mahajan, A., Beatson, S.A., Torpdahl, M., Webb, R.I., Allsopp, L.P., Gobius, K.S., Gally, D.L., Schembri, M.A., 2008. EhaA is a novel autotransporter protein of enterohemorrhagic *Escherichia coli* O157:H7 that contributes to adhesion and biofilm formation. Environ microbiol. 10, 589-604.

Wells, T.J., Totsika, M., Schembri, M.A., 2010. Autotransporters of *Escherichia coli*: a sequence-based characterization. Microbiology. 156, 2459-2469.

Whitfield, C., Trent, M.S., 2014. Biosynthesis and export of bacterial lipopolysaccharides. Annu Rev Biochem. 83, 99-128.

Wilkens, S., 2015. Structure and mechanism of ABC transporters. F1000Prime Rep. 7, 14.

Willsky, G.R., Malamy, M.H., 1980. Characterization of two genetically separable inorganic phosphate transport systems in *Escherichia coli*. J Bacteriol. 144, 356-365.

Wilson, J., Spika, J., Clarke, R., McEwen, S., Johnson, R., Rahn, K., Renwick, S., Karmali, M., Lior, H., Alves, D., Gyles, C., Sandhu, K., 1998. Verocytotoxigenic *Escherichia coli* infection in dairy farm families. Can Commun Dis Rep. 24, 17-20.

Wu, B., Skarina, T., Yee, A., Jobin, M.C., Dileo, R., Semesi, A., Fares, C., Lemak, A., Coombes, B.K., Arrowsmith, C.H., Singer, A.U., Savchenko, A., 2010. NleG Type 3 effectors from enterohaemorrhagic *Escherichia coli* are U-Box E3 ubiquitin ligases. PLoS Pathog. 6, e1000960.

Xavier, K.B., Kossmann, M., Santos, H., Boos, W., 1995. Kinetic analysis by in vivo 31P nuclear magnetic resonance of internal Pi during the uptake of sn-glycerol-3-phosphate by the pho regulon-dependent Ugp system and the glp regulon-dependent GlpT system. J Bacteriol. 177, 699-704.

Xicohtencatl-Cortes, J., Monteiro-Neto, V., Ledesma, M.A., Jordan, D.M., Francetic, O., Kaper, J.B., Puente, J.L., Giron, J.A., 2007. Intestinal adherence associated with type IV pili of enterohemorrhagic *Escherichia coli* O157:H7. J Clin Invest. 117, 3519-3529.

Xu, J., Kim, J., Danhorn, T., Merritt, P.M., Fuqua, C., 2012. Phosphorus limitation increases

attachment in *Agrobacterium tumefaciens* and reveals a conditional functional redundancy in adhesin biosynthesis. Res Microbiol. 163, 674-684.

Yang, C., Huang, T.W., Wen, S.Y., Chang, C.Y., Tsai, S.F., Wu, W.F., Chang, C.H., 2012. Genome-wide PhoB binding and gene expression profiles reveal the hierarchical gene regulatory network of phosphate starvation in *Escherichia coli*. PloS one. 7, e47314.

Yoshida, Y., Sugiyama, S., Oyamada, T., Yokoyama, K., Kim, S.K., Makino, K., 2011. Identification of PhoB binding sites of the *yibD* and *ytfK* promoter regions in *Escherichia coli*. J Microbiol. 49, 285-289.

Yoshida, Y., Sugiyama, S., Oyamada, T., Yokoyama, K., Makino, K., 2012. Novel members of the phosphate regulon in *Escherichia coli* O157:H7 identified using a whole-genome shotgun approach. Gene. 502, 27-35.

Yuan, Z.C., Zaheer, R., Morton, R., Finan, T.M., 2006. Genome prediction of PhoB regulated promoters in *Sinorhizobium meliloti* and twelve proteobacteria. Nucleic Acids Res. 34, 2686-2697.

Zheng, J.J., Sinha, D., Wayne, K.J., Winkler, M.E., 2016. Physiological Roles of the Dual Phosphate Transporter Systems in Low and High Phosphate Conditions and in Capsule Maintenance of *Streptococcus pneumoniae* D39. Front Cell Infect Microbiol. 6, 63.

Zhou, L., Grégori, G., Blackman Jennifer, M., Robinson, J.P., Wanner Barry, L. 2005. Stochastic activation of the response regulator PhoB by noncognate histidine kinases. In J Integr Bioinf, 10.

Zobell, C.E., 1943. The Effect of Solid Surfaces upon Bacterial Activity. J Bacteriol. 46, 39-56.

Zumbrun, S.D., Hanson, L., Sinclair, J.F., Freedy, J., Melton-Celsa, A.R., Rodriguez-Canales, J., Hanson, J.C., O'Brien, A.D., 2010. Human intestinal tissue and cultured colonic cells contain globotriaosylceramide synthase mRNA and the alternate Shiga toxin receptor globotetraosylceramide. Infect Immun. 78, 4488-4499.

Zumbrun, S.D., Melton-Celsa, A.R., Smith, M.A., Gilbreath, J.J., Merrell, D.S., O'Brien, A.D., 2013. Dietary choice affects Shiga toxin-producing *Escherichia coli* (STEC) O157:H7 colonization and disease. Proc Natl Acad Sci USA. 110, E2126-2133.

Annexes

Annexe 1: High-throughput microfluidic method to study biofilm formation and host-pathogen interactions in pathogenic *Escherichia coli*

En tant que deuxième auteur de cet article, j'ai réalisé plusieurs des expériences de formation de biofilms que ce soit en conditions statiques et en conditions dynamique sur surface abiotique (verre ou plastique) et biotique (cellule eucaryote). J'ai aussi contribué à la rédaction de l'article avant soumission. J'ai également assuré la totalité des expériences exigées lors de la révision de l'article. Cet article a été publié en 2015 dans le journal « Applied and Environmental Microbiology ».

AEM
Journals.ASM.org

High-Throughput Microfluidic Method To Study Biofilm Formation and Host-Pathogen Interactions in Pathogenic *Escherichia coli*

Yannick D. N. Tremblay, Philippe Vogeleer, Mario Jacques, Josée Harel

D partement de Pathologie et Microbiologie, Groupe de Recherche sur les Maladies Infectieuses du Porc, Centre de Recherche en Infectiologie Porcine et Avicole, Facult de M decine V t rinaire, Universit de Montr al, St-Hyacinthe, Qu bec, Canada

Biofilm formation and host-pathogen interactions are frequently studied using multiwell plates; however, these closed systems lack shear force, which is present at several sites in the host, such as the intestinal and urinary tracts. Recently, microfluidic systems that incorporate shear force and very small volumes have been developed to provide cell biology models that resemble *in vivo* conditions. Therefore, the objective of this study was to determine if the BioFlux 200 microfluidic system could be used to study host-pathogen interactions and biofilm formation by pathogenic *Escherichia coli*. Strains of various pathotypes were selected to establish the growth conditions for the formation of biofilms in the BioFlux 200 system on abiotic (glass) or biotic (eukaryotic-cell) surfaces. Biofilm formation on glass was observed for the majority of strains when they were grown in M9 medium at 30°C but not in RPMI medium at 37°C. In contrast, HRT-18 cell monolayers enhanced binding and, in most cases, biofilm formation by pathogenic *E. coli* in RPMI medium at 37°C. As a proof of principle, the biofilm-forming ability of a diffusely adherent *E. coli* mutant strain lacking AIDA-I, a known mediator of attachment, was assessed in our models. In contrast to the parental strain, which formed a strong biofilm, the mutant formed a thin biofilm on glass or isolated clusters on HRT-18 monolayers. In conclusion, we describe a microfluidic method for high-throughput screening that could be used to identify novel factors involved in *E. coli* biofilm formation and host-pathogen interactions under shear force.

Biofilms are defined as bacterial communities encased in a self-produced polymeric matrix that is attached to a surface (1). The ability to form a biofilm is virtually a universal trait of bacteria and other microorganisms. Growth as a biofilm offers protection against hostile environments, the immune response, and bactericidal concentrations of antibiotics or disinfectants (1). Biofilms have frequently been studied using the 96-microtiter plate model because it is a platform that requires small volumes and is suited for high-throughput screening (1). The major flaws of the microtiter model are that it is a closed system and does not incorporate shear force. It is generally accepted that biofilms will develop in the presence of shear force in the environment (1). The MBEC assay, formerly known as the Calgary Biofilm Device, was developed to incorporate shear force into high-throughput screens (2); however, this model is a closed system. In a closed system, dispersing signals and metabolic waste accumulate, and nutrients become depleted. These events are not always favorable for biofilm studies and may lead to the rapid dispersal of the biofilm before it is quantified.

Open systems, which have both a continuous flow of fresh medium and shear force, have been developed and are frequently used in the laboratory (1). These include the drip-flow reactor, flow cells, perfused biofilm fermenters, the CDC biofilm reactor, the rotating-disc reactor, the modified Robbins device, and the annular reactor (reviewed in reference 3). Some disadvantages of these systems are that they often require large volumes, are prone to contamination, and are not suited for high-throughput screens. In an effort to combine small volumes, high-throughput ability, and shear force in an open system, researchers have proposed the use of microfluidic models to study biofilms (4–7). Some models have yet to demonstrate their high-throughput potential (5, 7), while others require the system to be fabricated in the laboratory, which may not be feasible for all biofilm researchers (4-7). The platform proposed by Benoit et al. (4) has high-throughput capability and uses a specialized instrument, the BioFlux device, that is commercially available. One plate model contains 24 channels (6 mm long, 350 μm wide, 70 μm high) connecting 48 wells, and the BioFlux system can control four plates simultaneously. This system allows for the study of 96 independent biofilms in an experiment. Additionally, two different shear force settings per plate can be tested simultaneously. Furthermore, 50 μl is the minimum volume required for seeding or coating, and wells can contain as much as 1.25 ml of liquid, resulting in 11 to 20 h of continuous flow without replenishment at commonly used flow rates (4). The BioFlux device has also been used for the study of dental plaque biofilms (8) and for real-time monitoring of promoter activity during biofilm formation by *Staphylococcus aureus* (9).

The BioFlux device was initially developed to provide a cell biology model that resembles *in vivo* conditions. Currently, host-pathogen interactions are often studied using cell line monolayers cultured in flasks or on tissue culture plates. As with microtiter plates used in biofilm formation assays, these dishes are closed systems, which often leads to the accumulation of bacterial prod-

Received 24 December 2014 **Accepted** 6 February 2015
Accepted manuscript posted online 13 February 2015
Citation Tremblay YDN, Vogeleer P, Jacques M, Harel J. 2015. High-throughput microfluidic method to study biofilm formation and host-pathogen interactions in pathogenic *Escherichia coli*. Appl Environ Microbiol 81:2827–2840. doi:10.1128/AEM.04208-14.
Editor: H. L. Drake
Address correspondence to Jos e Harel, josee.harel@umontreal.ca.
Supplemental material for this article may be found at http://dx.doi.org/10.1128/AEM.04208-14.

doi:10.1128/AEM.04208-14

TABLE 1 List of strains and plasmid used in this study

Species, *E. coli* pathotype, or plasmid	Strain identification	Origin or description	Ampicillin concn (μg/ml)[a]	Source or reference
Bacteria				
Commensal *E. coli* K-12	MG1655	Human	NA	31
	MG1655 mCherry	MG1655 expressing mCherry	100	This study
Intestinal *E. coli* (InPEC)				
Adherent invasive (AIEC)	LF82	Human	NA	32
Enterohemorrhagic (EHEC)	EDL933	Human	NA	33
	Sakai	Human	NA	34
	EDL933 mCherry	EDL933 expressing mCherry	200	This study
	Sakai mCherry	Sakai expressing mCherry	200	This study
Enteropathogenic (EPEC)	E2348/69	Human	NA	35
	E2348/69 mCherry	E2348/69 expressing mCherry	200	This study
Atypical EPEC (aEPEC)	ECL1001	Pig	NA	36
	ECL1001 mCherry	ECL1001 expressing mCherry	200	This study
Diffusely adherent (DAEC)	2787	Human	NA	37
	2787 mCherry	2787 expressing mCherry	200	This study
	2787 Δ*aidA*	Human	NA	38
	2787 Δ*aidA* mCherry	2787 Δ*aidA* expressing mCherry	200	This study
Enteroaggregative (EAEC)	17.2	Human	NA	39
	17.2 mCherry	17.2 expressing mCherry	400	This study
Citrobacter rodentium	DBS100	Mouse	400	40
	DBS100 mCherry	*C. rodentium* expressing mCherry		This study
Extraintestinal *E. coli* (ExPEC)				
Septicemic (SEPEC)	31A	Human	NA	41
	31A mCherry	31A expressing mCherry	400	This study
Uropathogenic (UPEC)	CFT073	Human	NA	42
	CFT073 mCherry	CFT073 expressing mCherry	200	This study
	J96	Human	NA	43
	F11	Human	NA	44
	536	Human	NA	45
Avian pathogenic (APEC)	χ7122	Poultry	NA	46
Plasmid, pmCherry		pUC-based plasmid encoding mCherry		Clontech

[a] NA, not applicable.

ucts, such as metabolites and toxins, that are cytotoxic. Furthermore, there is a lack of shear force in these models, and shear force is present at several sites in the host, such as the intestinal and urinary tracts (10). To overcome these limitations, several open systems have been proposed (10–13), but most systems still share some of the limitations described above (11, 12). Therefore, the BioFlux device would provide a new high-throughput tool for the study of host-pathogen interactions under conditions that resemble *in vivo* conditions.

Escherichia coli is a Gram-negative bacterium that can be part of the normal intestinal microbiota of animals and humans but can also be a pathogen of veterinary and human health importance (14). Pathogenic *E. coli* strains are typically divided into two major groups based on their infection sites: intestinal/diarrheagenic pathogenic *E. coli* (InPEC) and extraintestinal pathogenic *E. coli* (ExPEC). Among ExPEC strains, uropathogenic *E. coli* (UPEC) infects the urinary tract, whereas neonatal meningitis-associated *E. coli* (NMEC) infects the meninges. For InPEC strains associated with diarrheal infections, several pathotypes have been well characterized, including enteropathogenic *E. coli* (EPEC), enterotoxigenic *E. coli* (ETEC), enterohemorrhagic *E. coli* (EHEC), enteroaggregative *E. coli* (EAEC), enteroinvasive *E. coli* (EIEC), diffusely adherent *E. coli* (DAEC), and adherent-invasive *E. coli* (AIEC) (14). Given their diverse genetic makeups, which are responsible for diverse infectious processes, pathogenic *E. coli* strains are good models with which to test the potential of the BioFlux system as a tool for the study of host-pathogen interactions. Furthermore, biofilm formation in the BioFlux system by pathogenic *E. coli* has yet to be fully investigated.

In this study, we describe the conditions required to grow biofilms of different *E. coli* pathotypes and monolayers of HRT-18 cells in the BioFlux system. Additionally, we present a new application for the BioFlux system, which describes the development of microcolonies or biofilms in real time by pathogenic *E. coli* on an HRT-18 monolayer in the presence of shear force. This new tool provides an improved platform for the study of host interactions with pathogenic *E. coli*.

MATERIALS AND METHODS

Bacterial strains and growth conditions. The bacterial strains used in this study are described in Table 1. Bacteria were routinely cultured on lysogeny broth (LB) agar (1% [wt/vol] tryptone, 0.5% [wt/vol] yeast extract, 1% [wt/vol] NaCl, 1.5% [wt/vol] agar) or in LB. To introduce pmCherry (Clontech, Mountain View, CA) into the desired bacterial strains, bacteria were transformed by electroporation as described elsewhere (15), and positive transformants were selected on LB agar with the appropriate ampicillin concentration (Table 1).

Biofilms in microtiter plates. The assay of biofilm formation in microtiter plates was adapted from the work of Wu et al. (16) and is sum-

FIG 1 Flow chart of the protocol used to grow biofilms in microtiter and BioFlux plates and to investigate host-pathogen interactions using the BioFlux 200 system.

marized in Fig. 1. Briefly, colonies of *E. coli* from LB agar were resuspended in 5 ml of fresh LB and were incubated at 37°C with shaking (180 rpm) for 16 h. These cultures were then diluted (1:100) in 5 ml of M9 medium with glucose (0.4%, wt/vol) and minerals (1.16 mM $MgSO_4$, 2 μM $FeCl_3$, 8 μM $CaCl_2$, and 16 μM $MnCl_2$) and were incubated at 37°C with shaking (180 rpm) for 24 h. Dilutions (1:100 in M9 medium with glucose and minerals or Roswell Park Memorial Institute [RPMI] medium [Gibco, Burlington, ON, Canada] supplemented with 10% fetal bovine serum [Gibco]) of these cultures were deposited in triplicate in the wells of 96-well microtiter plates (150 μl; Costar 3370; Corning, Corning, NY, USA) or in the Lab-Tek chamber slide system (300 μl; Nunc 177402; Thermo Scientific, Ottawa, ON, Canada). The plates and the Lab-Tek chambers were incubated for 24 h at 30°C and 37°C, respectively. The liquid medium was then removed using a multichannel pipette, and unattached cells were removed by washing three times with phosphate-buffered saline (PBS) (1.76 mM KH_2PO_4, 10 mM Na_2HPO_4, 137 mM NaCl, 2.7 mM KCl [pH 7.4]). Plates were dried at 37°C for 15 min, and the biofilms were stained with crystal violet (0.1%, wt/vol) for 2 min at room temperature. The crystal violet solution was removed, and the biofilms were washed three times with distilled water and were then dried at 37°C for 15 min. The stain was then released with 70% (vol/vol) ethanol, and the amount of released stain was quantified by measuring the absorbance at 590 nm with a microplate reader (PowerWave; Bio-Tek Instruments, Winooski, VT, USA).

Biofilms in the BioFlux flowthrough device. The method for growing biofilms in the BioFlux 200 device (Fluxion Biosciences, South San Francisco, CA, USA) was adapted from the work of Benoit et al. (4) and from the manufacturer's recommendations; the protocol is summarized in

Fig. 1. Briefly, colonies of *E. coli* on LB agar were resuspended in 5 ml of fresh LB and were incubated at 37°C with shaking (180 rpm) for 16 h. These cultures were then diluted (1:100) in 5 ml of M9 medium with glucose (0.4%, wt/vol) and were incubated at 37°C with shaking (180 rpm) for 24 h. A 1-ml volume was transferred to a 1.5-ml Eppendorf tube, and the bacteria were collected by centrifugation (14,000 × *g*, 2 min). The pellets were resuspended in fresh prewarmed (30°C) M9 medium with glucose (0.4%, wt/vol) or fresh prewarmed (37°C) RPMI medium with fetal bovine serum to an optical density at 600 nm (OD_{600}) of ≈1. The microfluidic channels were wetted with prewarmed (30°C) M9 medium with glucose (0.4%, wt/vol) and were inoculated by injecting the bacterial suspension into the output reservoir for 20 s at 0.5 dyne/cm^2. The microfluidic plate was incubated for 2 h at 30°C to allow bacteria to bind to the surface. Fresh prewarmed (30°C) M9 medium with glucose (0.4%, wt/vol) was added to the input reservoir, and the flow of fresh medium was initiated at 1.0 dyne/cm^2 for 5 h. The spent medium was then removed from the output reservoir; fresh prewarmed (30°C) medium was added to the input reservoir; and the flow was lowered to 0.5 dyne/cm^2 for an additional 17 h. Once the incubation was completed, biofilms were washed by injecting PBS from the input reservoir for 20 min at 0.5 dyne/cm^2, stained by injecting crystal violet or FM1-43 dye (Life Technologies, Inc., Burlington, ON, Canada) from the input reservoir for 20 min, and washed by injecting PBS from the input reservoir for 20 min at 0.5 dyne/cm^2. Images of crystal violet-stained BioFlux biofilms were obtained using an inverted fluorescence microscope equipped with a 40× objective (CKX41; Olympus, Markham, ON, Canada), a digital camera (Retiga EX; QImaging, Surrey, BC, Canada), and the software provided with the BioFlux 200 device. The FM1-43-stained biofilms were visualized with a confocal microscope with a 40× objective (FV1000 IX81; Olympus, Markham, ON, Canada). The fluorophore was excited (λ_{em}, 488 nm) and detected (λ_{em}, 525 nm ± 25 nm) as recommended by the manufacturer. The laser was set between 666 V and 795 V with a 1% gain, which minimized saturation and autofluorescence, as determined with nonstained samples. The images were acquired using FluoView software (Olympus).

Enzymatic treatment of preformed biofilms. Biofilms were prepared either in a microtiter plate or in the BioFlux device as described above. For the microtiter plate biofilms, enzymatic treatments were performed as described previously (17). Briefly, enzyme solutions (proteinase K [500 μg/ml] in 50 mM Tris-HCl [pH 7.5], 1 mM $CaCl_2$, or DNase I [500 μg/ml] in 150 mM NaCl, 1 mM $CaCl_2$) were added to the wells and were incubated at 37°C for 1 h. The biofilms were then washed, stained, and quantified as described above.

For the BioFlux biofilms, fresh and spent media were removed from the wells, and an enzyme solution (proteinase K [125 μg/ml] or DNase I [125 μg/ml] in M9 medium) or fresh medium (untreated control) was added to the input wells. The solutions were injected into the channel for 1 h at 0.5 dyne/cm^2. The biofilms were then washed with PBS and were stained as described above. Images of the biofilms were captured as described above.

Cell culture. The HRT-18 cell line, a human colorectal adenocarcinoma cell line, was grown in RPMI medium supplemented with 10% fetal bovine serum (Gibco), 1% penicillin-streptomycin (100×; Gibco), and 1% amphotericin B (Fungizone; 250 μg/ml; Gibco). The HEp-2 cell line, derived from human larynx carcinoma, and the SJPL cell line, of monkey origin (18), were grown in Dulbecco's modified Eagle medium (DMEM) supplemented with 10% fetal bovine serum (Gibco), 1% penicillin-streptomycin (100×; Gibco), and 1% amphotericin B (250 μg/ml; Gibco). Cells were grown in T175 flasks (Sarstedt, Nümbrecht, Germany) at 37°C under an atmosphere enriched with 5% CO_2.

Growth of cell lines in the BioFlux flowthrough device. The method for growing cell lines in the BioFlux 200 device (Fluxion Biosciences) was adapted from the manufacturer's recommendations. The microfluidic channels were wetted with prewarmed (37°C) RPMI medium or DMEM, and HEp-2, SJPL, or HRT-18 cells at a concentration of 5×10^6, 5×10^6, or 2×10^7 per ml, respectively, were injected from the output reservoir into the channel for 30 s at 0.5 dyne/cm^2. The microfluidic plate was incubated for 4 to 8 h, 16 to 24 h, or 8 to 16 h at 37°C under an atmosphere enriched with 5% CO_2 to allow the SJPL, HEp-2, or HRT-18 cells, respectively, to attach to the surface. Once the cells were attached, 1.2 ml or 0.3 ml of fresh prewarmed (37°C) RPMI medium or DMEM supplemented with fetal bovine serum was added to the input or output reservoir, respectively. This created a flow between the input and output reservoirs equivalent to gravity (gravity flow), which was required for optimal growth of the monolayer. The cells were incubated at 37°C under an atmosphere enriched with 5% CO_2 for approximately 48 to 72 h, until the cells reached 95% to 100% confluence in the channel.

Adhesion of pathogenic *E. coli* to HRT-18 cells in the BioFlux flowthrough device. An overview of the protocol is shown in Fig. 1. Colonies of *E. coli* strains carrying pmCherry on LB agar with ampicillin (concentrations listed in Table 1) were resuspended in 5 ml M9 medium with glucose (0.4%, wt/vol) and ampicillin (concentrations listed in Table 1) and were incubated at 37°C with shaking (180 rpm) for 24 h. A 250-μl volume was transferred to a 1.5-ml Eppendorf tube, and the bacteria were collected by centrifugation (14,000 × *g*, 2 min). The pellets were resuspended in fresh prewarmed (37°C) complete RPMI medium or DMEM supplemented with fetal calf serum to an OD_{600} of ≈0.5. The microfluidic channels containing the 95% to 100% confluent cell monolayers were inoculated by injecting the bacterial suspension from the output reservoir for 20 s at 0.5 dyne/cm^2. The microfluidic plate was incubated for 1.5 h at 37°C to allow the bacteria to bind to the cells. Fresh prewarmed (37°C) complete RPMI medium or DMEM supplemented with fetal calf serum was added to the input reservoir, and the flow of fresh medium was initiated at 0.5 dyne/cm^2 for 16 h. Once the incubation was completed, weakly attached or unattached bacteria were removed by injecting PBS from the input reservoir for 20 min at 0.5 dyne/cm^2, and eukaryotic cells and attached bacteria were fixed by injecting the fixing solution (50% [vol/vol] methanol, 50% [vol/vol] acetone) from the input reservoir for 20 min at 0.5 dyne/cm^2 and were washed by injecting PBS from the input reservoir for 20 min at 0.5 dyne/cm^2. Cells and bacteria were stained with 4′,6-diamidino-2-phenylindole (DAPI; Life Technologies) by injecting the dye from the input reservoir for 20 min at 0.5 dyne/cm^2, and excess dye was removed by injecting PBS from the input reservoir for 20 min at 0.5 dyne/cm^2. The plate was then observed with a confocal microscope equipped with a 20× objective (Olympus FV1000 IX81). The fluorophores were excited (λ_{ex}, 405 nm for DAPI or 543 nm for mCherry) and detected (λ_{em}, 450 nm ± 25 nm for DAPI or 605 nm ± 100 nm for mCherry) as recommended by the manufacturers. The laser was set between 404 and 458 V with a 1% gain for DAPI and between 672 and 830 V with a 54% gain for mCherry. These settings minimized saturation and autofluorescence, as determined with nonstained samples. Images were acquired using FluoView software (Olympus).

To measure the viability of the cell lines, weakly attached or unattached bacteria were washed by injecting Dulbecco's PBS (DPBS; Gibco) from the input reservoir for 20 min at 0.5 dyne/cm^2, stained with trypan blue (0.4% solution; Life Technologies, Inc.) for 20 min at 0.5 dyne/cm^2, and washed by injecting DPBS from the input reservoir for 20 min at 0.5 dyne/cm^2. Cells stained with trypan blue in the channel were counted using an inverted fluorescence microscope equipped with a 20× objective (Olympus CKX41).

The growth of the bacteria was also monitored by taking a picture every 10 min using an inverted fluorescence microscope equipped with a 10× objective (Olympus CKX41), a digital camera (Retiga EX; QImaging), and the software provided with the BioFlux 200 device. Pictures were assembled to create a time lapse video using the software provided with the BioFlux 200 device.

Image analysis. Images of biofilms and cell attachment were analyzed using ImageJ (National Institutes of Health, Bethesda, MD, USA). The 16-bit grayscale images were adjusted with the threshold function to fit the bacterial structure and were analyzed using the "Analyze Particles" function.

Confocal images were analyzed using Image-Pro software (version 9.0; Media Cybernetics, Inc., Bethesda, MD, USA) as described previously (19). Briefly, a 3-dimensional (3D) image of cell attachment for each strain was generated using a minimum of 15 image layers, and the Z-distance was kept within the same range between samples. An isoimage was then created from the reconstructed 3D image. This isoimage was used to measure the volume and height of the bacterial cluster. Biomass was calculated by dividing the total volume by the surface area of the field of view.

Statistical analysis. The results for the static biofilms were analyzed using two-way analysis of variance (ANOVA) followed by a Bonferroni *post hoc* comparison using GraphPad Prism, version 4.02 (GraphPad Software, San Diego, CA, USA). The results of the enzymatic digestions and the comparisons of the DAEC 2787 parental and mutant strains were analyzed using a Mann-Whitney U test with two-tailed distribution.

RESULTS

Static biofilms. We first sought to establish if strains belonging to different *E. coli* pathotypes had the ability to form biofilms under similar conditions. Combinations of two abiotic surfaces (polystyrene versus glass) and growth conditions (M9 medium with 0.4% [wt/vol] glucose versus RPMI medium with fetal bovine serum) were tested. Only atypical EPEC (aEPEC) ECL1001 was unable to form a biofilm (OD_{590}, ≤0.110) under any of the conditions tested (Fig. 2A). AIEC LF82 formed biofilms that yielded similar OD_{590} values regardless of the growth condition and surface. For most strains, there was no significant difference between the surfaces tested; however, on a glass surface with M9 medium with 0.4% (wt/vol) glucose, EHEC Sakai formed more biofilm, whereas UPEC CFT073 formed less biofilm, than on a polystyrene surface (Fig. 2). M9 medium with 0.4% (wt/vol) glucose significantly increased biofilm formation over that with RPMI medium with fetal bovine serum for EHEC Sakai and the ExPEC strains, with the exception of avian-pathogenic *E. coli* (APEC) strain χ7122. Although there was no significant difference between M9 medium with 0.4% (wt/vol) glucose and RPMI medium with fetal bovine serum for the other strains, the average level of biofilm formation in RPMI medium with fetal bovine serum was never above an OD_{590} of 0.3, except for AIEC LF82 (Fig. 2). Furthermore, microscopy images of the biofilms indicated that most strains formed no or limited biofilms with RPMI medium compared to biofilm formation with M9 medium with 0.4% (wt/vol) glucose (see Fig. S1 in the supplemental material). Therefore, M9 medium with 0.4% (wt/vol) glucose at 30°C is the growth condition that supports consistent formation of biofilms regardless of the surface.

In M9 medium with 0.4% (wt/vol) glucose at 30°C on microtiter plates, the *E. coli* K-12 strain MG1655 had a moderate (0.400 ≤OD_{590} ≤1.000) ability to form biofilms. EPEC E2348/69, AIEC LF82, and EAEC 17.2 had weak (0.110 ≤OD_{590} ≤0.400) to moderate biofilm-forming ability, whereas EHEC EDL933, EHEC Sakai, and *Citrobacter rodentium* DBS100 had a moderate to strong (OD_{590}, ≥1.000) ability to form biofilms (Fig. 2). Among ExPEC strains, the four UPEC isolates and septicemic *E. coli* (SEPEC) 31A were strong biofilm formers, whereas APEC χ7122 was a moderate biofilm former (Fig. 2).

BioFlux biofilms. Given that most pathotypes formed biofilms at 30°C in M9 medium with 0.4% (wt/vol) glucose, it was decided that these conditions would be used to optimize the microfluidic assay. The variable parameters were first tested with EHEC strains EDL933 and Sakai, and these parameters included the inoculum density (OD_{600}, 0.125, 0.25, 0.5, or 1.0), the incubation time for the initial adhesion (1, 2, or 4 h), and the shear force (0.5 to 2.0 dynes/cm^2) during biofilm formation. The minimum inoculum density that yielded a biofilm was an OD_{600} of 0.5, but an OD_{600} of 1.0 gave more consistent results and therefore was selected for further testing. The best incubation time for the initial adhesion was 2 h, because a 1-h adhesion time gave inconsistent results and a 4-h adhesion time often resulted in overgrowth 12 h after the flow was initiated. This overgrowth blocked the channel or contaminated the input reservoir. The two EHEC strains were able to form biofilms with a shear force as high as 1.0 dyne/cm^2. Unfortunately, the input reservoir was sometimes contaminated when the shear force was set to the lower setting. Both strains are motile, and it was hypothesized that these strains could travel upstream in

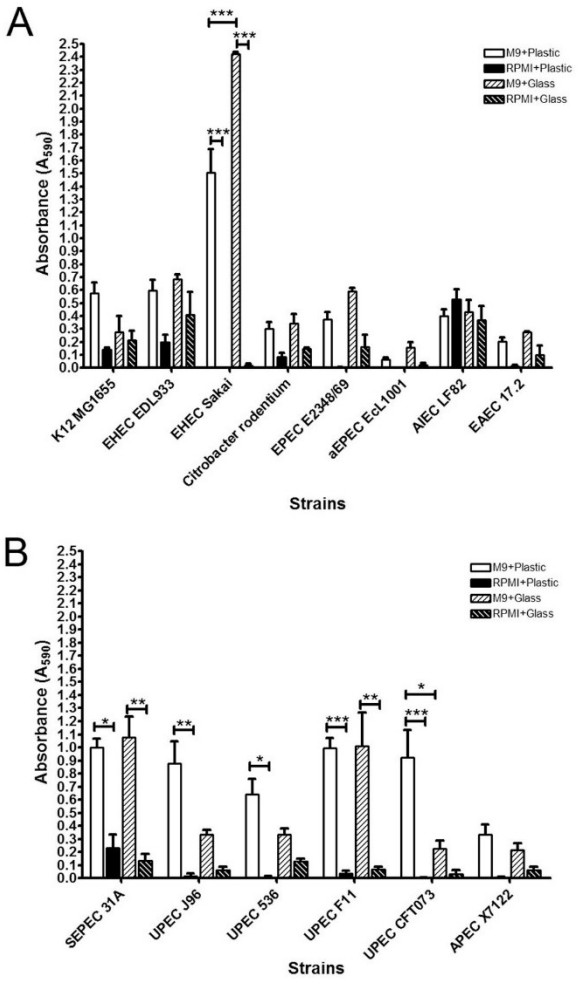

FIG 2 Biofilm formation by representative strains of different pathotypes on polystyrene (microtiter plate) or glass (Lab-Tek chambers). InPEC (A) or ExPEC (B) biofilms were formed in M9 medium plus glucose (0.4%, wt/vol) at 30°C or in RPMI medium at 37°C for 24 h and were stained with crystal violet, and the absorbance at 590 nm was measured. Results are averages for at least 3 biological replicates. Error bars represent standard error. *, $P < 0.05$; **, $P < 0.01$; ***, $P < 0.001$.

the presence of shear force. Upstream motility has been observed for *E. coli* previously (20). In an effort to fix this problem, the shear force was set to 1.0 dyne/cm^2 for the first 5 h and was then decreased to 0.5 dyne/cm^2. Biofilm formation was more consistent, and the input reservoir was never contaminated, with these settings. Surprisingly, this appeared to stimulate biofilm formation. Overall, it was decided that biofilm formation would be tested using an initial inoculum at an OD_{600} of 1.0, with 2 h of incubation for the initial attachment, and with the shear force set at 1.0 dyne/cm^2 for the first 5 h, followed by a decrease to 0.5 dyne/cm^2 for the next 17 h. This final protocol is summarized in Fig. 1. Once the protocol was optimized, biofilm formation was tested at 37°C in RPMI medium with 10% fetal bovine serum. Although initial adhesion was observed, the majority of the strains were not able to remain attached and form a biofilm; only UPEC J96 was able to form a biofilm (see Fig. S2 in the supplemental material).

Quantification of BioFlux biofilms. Benoit et al. (4) used green fluorescent protein (GFP) and a plate reader to quantify the effects of antibiotics on biofilms; however, we could not use a plate reader, because *E. coli* poorly expressed the mCherry fluorescent protein in M9 medium at 30°C (data not shown). Quantification of CFU is difficult, because the output well containing the planktonic cells will often contaminate the samples during sample collection. Additionally, larger volumes were required to release crystal violet from the strong biofilm formers, which diluted the stain, in some cases, below the detection level of the microplate reader. Furthermore, releasing the stain did not allow for differentiation between weak and moderate biofilms. Therefore, stain release was not sensitive enough for appropriate analysis. Thus, image analysis of the field of view provided the best option for quantifying biofilm formation.

The "Analyze Particles" function of ImageJ allows the measurement of biofilm structures such as microcolonies or single cells (average particle size), the number of structures measured (number of particles), and the percentage of the area covered by these structures (Table 2). Furthermore, 3D reconstruction of confocal images allows for the measurement of biomass and maximum height (Table 2). Overall, these measurements can help classify strains based on their ability to form biofilms. For example, a weak biofilm former (e.g., EHEC EDL933, EHEC Sakai, aEPEC ECL1001, and *C. rodentium* DBS100) has >1,000 particles of 10 to 30 pixels that occupy less than 50% of the field of view (Fig. 3 and Table 2). These strains also have biomass that is less than 5 $\mu m^3/\mu m^2$. On the other hand, strong biofilm formers (e.g., K-12 MG1655, APEC χ7122, EPEC E2348/69, UPEC 536, UPEC F11, and UPEC J96) had fewer particles (<200) that were larger (>500 pixels) and covered >70% of the field of view (Fig. 3 and 4 and Table 2). Their biomasses were also greater than 6 $\mu m^3/\mu m^2$. The only strain that fell between the two categories was AIEC LF82. Its biofilms covered a large part of the surface and formed few but large particles; however, its biomass was smaller than 5 $\mu m^3/\mu m^2$. This lower biomass was mostly due to the fact that AIEC LF82 formed mushroom-shaped biofilms, defined by a large projection sitting on a stalk. This was not observed for the other strains. Biomass could not be measured for EAEC 17.2 and SEPEC 31A, because both strains frequently formed structures that reduced the flow of the medium inside the channel after 20 h of growth with continuous flow (Fig. 3 and 4). This blockage did not allow for effective penetration of the fluorescent dye and thus did not allow for confocal microscopy analysis.

All strains tested were able to remain attached under shear force in the BioFlux system, and this did not always correlate with their abilities to form biofilms in microtiter plates (Fig. 2, 3, and 4). For example, EHEC EDL933, EHEC Sakai, *C. rodentium* DBS100, and UPEC CFT073 were considered to be moderate to strong biofilm formers in microtiter plates but formed small, thin biofilms in the BioFlux system. Conversely, K-12 MG1655, APEC χ7122, AIEC LF82, EPEC E2348/69, and EAEC 17.2 were weak to moderate biofilm formers in microtiter plates but appeared to thrive in the BioFlux system, where they formed strong, structured biofilms. On the other hand, SEPEC 31A and the UPEC strains, except for CFT073, were strong biofilm formers in microtiter plates and formed strong biofilms in the BioFlux system, whereas the aEPEC strain did not form biofilms in microtiter plates and formed a thin biofilm-like structure in the BioFlux system.

Enzymatic treatment. Enzymatic treatments are often used to characterize the composition of the biofilm matrix. Thus, we first treated the biofilms formed in microtiter plates in order to identify strains that were sensitive to DNase or proteinase K. Strains were selected based on their abilities to form moderate to strong biofilms in both microtiter and BioFlux 200 plates. Therefore, the K-12 strain MG1655, EPEC E2348/69, AIEC LF82, SEPEC 31A, and the four UPEC isolates were used for our test in the microtiter plate assay (Fig. 2 and 3 and Table 2). In this assay, all biofilms, except for AIEC LF82 biofilms, were significantly sensitive to proteinase K treatment (Fig. 5A), and all isolates were resistant to DNase treatment (Fig. 5B).

E. coli K-12 MG1655, EPEC E2348/69, and AIEC LF82 were selected for further tests in the BioFlux 200 system to ensure that the enzymatic treatment assay could be used with the microfluidic system. As with the microtiter plate assay, the biofilms of K-12 MG1655 and EPEC E2348/69 were significantly sensitive to proteinase K treatment and resistant to DNase digestion (Fig. 5C and Table 2). Biofilms of AIEC LF82 was resistant to proteinase K digestion and DNase treatment (Fig. 5C and Table 2). Therefore, enzymatic treatment can be used to characterize the matrix composition of biofilms formed using the BioFlux 200 system.

Adhesion of pathogenic *E. coli* to HRT-18 monolayers. To determine the seeding concentrations for cell lines, cells at a concentration of 5×10^5, 1×10^6, 5×10^6, 1×10^7, 5×10^7, or 1×10^8 per ml were injected into the channel. Cells were first grown without flow for as long as 72 h. The cells never reached confluence, and most appeared to be dead or unhealthy (data not shown). To improve cell viability and confluence, cells at the concentrations given above were injected and were then incubated without any flow for 4 h, 8 h, 16 h, or 24 h in order to measure the time required for initial attachment. Gravity flow, which is achieved by adding 1.2 ml of medium to the input well and 0.3 ml of medium to the output well, was then initiated, and cells were monitored for as long as 96 h. The minimum incubation times for the initial attachment of SJPL, HRT-18, and HEp-2 cells were 4, 8, and 16 h, respectively. When the incubation time was too short, the cells detached as soon as the flow was initiated. Incubations for longer than 24 h without flow resulted in cell death and the inability to develop a confluent monolayer. SJPL and HEp-2 cells at concentrations between 1×10^6 and 5×10^6 per ml and HRT-18 cells at concentrations between 1×10^7 and 5×10^7 per ml were able to reach 95% to 100% confluence between 36 h and 96 h. A larger number of HRT-18 cells were required for seeding, because they are smaller than SJPL or HEp-2 cells. Seeding the wells with 10-

TABLE 2 Quantification of biofilm formation and cell attachment of *E. coli* pathotypes using a microfluidic system[a]

Assay, strain, and treatment	No. of particles	Avg particle size (pixels)[b]	% of area covered	Biomass ($\mu m^3/\mu m^2$)[c]	Height (μm)
Biofilm formation					
EHEC EDL933	1,828 (±250)	10.5 (±5)	18 (±5)	3.88 (±1.06)	31 (±3)
EHEC Sakai	1,430 (±127)	30.0 (±7.4)	41 (±12)	2.64 (±0.86)	35 (±4)
C. rodentium DBS100	1,517 (±148)	21.5 (±8.3)	31 (±6)	2.06 (±0.42)	23 (±5
AIEC LF82	14 (±7)	7,132.1 (±258.9)	95 (±14)	2.44 (±1.85)	37 (±5)
EPEC	123 (±22)	623.7 (±250.6)	73 (±17)	8.43 (±1.23)	38 (±3)
aEPEC ECL1001	2,644 (±311)	13.0 (±4.8)	33 (±9)	3.05 (±0.65)	22 (±6)
K-12 MG1655	45 (±8)	1,967.4 (±127.2)	84 (±15)	7.85 (±0.92)	27 (±4)
EAEC 17.2	23 (±6)	3,876.7 (±289.6)	85 (±17)	ND[d]	ND[d]
SEPEC 31A	144 (±24)	541.4 (±114.9)	74 (±8)	ND[d]	ND[d]
APEC	14 (±4)	7,148.6 (±356.8)	95 (±6)	8.08 (±1.04)	26 (±2)
UPEC 536	97 (±17)	917.1 (±95.8)	85 (±13)	10.39 (±0.76)	31 (±4)
UPEC F11	78 (±13)	1,120.9 (±108.3)	83 (±12)	17.28 (3.02)	50 (±7)
UPEC CFT073	1,100 (±206)	45.9 (±35.1)	36 (±21)	2.54 (±1.56)	22(±14)
UPEC J96	12 (±5)	8,197.8 (±312.9)	93 (±7)	9.53 (±1.03)	29 (±4)
Enzymatic treatment					
K-12 MG1655					
Control	102 (±21)	575.3 (±148.2)	70 (±8)	NA[e]	NA
Proteinase K	383(±25)	30.6 (±14.9)	14 (±3)	NA	NA
DNase	124 (±19)	405.4 (±74.9)	64 (±9)	NA	NA
EPEC					
Control	285 (±34)	165.9 (±30.8)	58 (±16)	NA	NA
Proteinase K	331 (±14)	22.8 (±11.6)	9 (±2)	NA	NA
DNase	198 (±11)	247.9 (±21.6)	64 (±14)	NA	NA
AIEC LF82					
Control	100 (±5)	580.7 (±210.6)	71 (±17)	NA	NA
Proteinase K	385 (±37)	83.3 (±34.5)	39 (±11)	NA	NA
DNase	178 (±16)	270.8 (±97.3)	61 (±10)	NA	NA
Cell attachment					
Negative control	5 (±3)	1.4 (±0.5)	0.07 (±0.05)	ND[f]	ND[f]
K12 MG1655	41 (±10)	2.9 (±0.6)	1 (±0.6)	ND[f]	ND[f]
EHEC EDL933	200 (±16)	6.5 (±0.9)	13 (±2)	2.17 (±0.31)	25 (±2)
EHEC Sakai	61 (±11)	39.4 (±5.6)	24 (±4)	1.99 (±0.21)	20 (±1)
C. rodentium DBS100	32 (±5)	230.7 (±50.9)	73 (±9)	1.36 (±0.12)	8 (±1)
EPEC	78 (±19)	64.7 (±14.3)	48 (±5)	3.18 (±0.32)	28 (±3)
aEPEC ECL1001	111 (±23)	11.1 (±3.8)	12 (±2)	0.31 (±0.09)	19 (±2)
EAEC 17.2	70 (±9)	48.6 (±6.5)	34 (±5)	5.23 (±0.83)	33 (±4)
SEPEC 31A	276 (±31)	7.0 (±1.2)	19 (±2)	1.82 (±0.43)	39 (±3)
UPEC CFT073	83 (±16)	11.3 (±1.6)	9 (±3)	0.25 (±0.07)	13 (±2)

[a] Values are averages (standard errors) for 3 independent biological replicates.
[b] Two pixels are approximately equivalent to 1 bacterial cell.
[c] ND, not determined; NA, not applicable.
[d] The microfluidic channel was blocked and did not allow effective penetration of the dye.
[e] NA, images were not captured with a confocal microscope.
[f] The absence of fluorescence in the mCherry channel did not allow for the detection of measureable biofilms.

fold fewer cells than the optimal seeding concentration resulted in a maximum of 50% confluence. Conversely, when wells were seeded with 10-fold more cells than the optimal seeding concentration, cells and debris blocked the microfluidic channels. Furthermore, HEp-2 cells occasionally grew as stacks that blocked the channel and, as a result, did not always reach 95% to 100% confluence (see Fig. S3 in the supplemental material). These cells were not used for any of our assays because of the inconsistent results. Overall, it was decided that HRT-18 cells would be seeded at an initial inoculum of 5×10^7 per ml, incubated for 8 h to 16 h for the initial attachment, and grown with a gravity flow until the cells reached 95% to 100% confluence. SJPL cells were seeded at 5×10^6 per ml and were incubated for 4 h to 8 h for the initial attachment; they were able to reach 95% to 100% confluence after 36 h (see Fig. S3). Using these parameters, cell monolayers were subjected to different shear forces (0.5 to 1.0 dyne/cm^2) for as long as 48 h. The monolayers were able to remain attached with shear forces as high as 1.0 dyne/cm^2 for 48 h. Furthermore, 30 (±15) HRT-18 cells in the channel, which contained $\sim 5 \times 10^5$ cells, were stained with trypan blue, indicating that >99% of the cells had intact membranes (see Table S1 in the supplemental material). Additionally, cell death can be assessed by looking at the integrity of the monolayer, because dead cells will usually detach and be removed by the flow of medium.

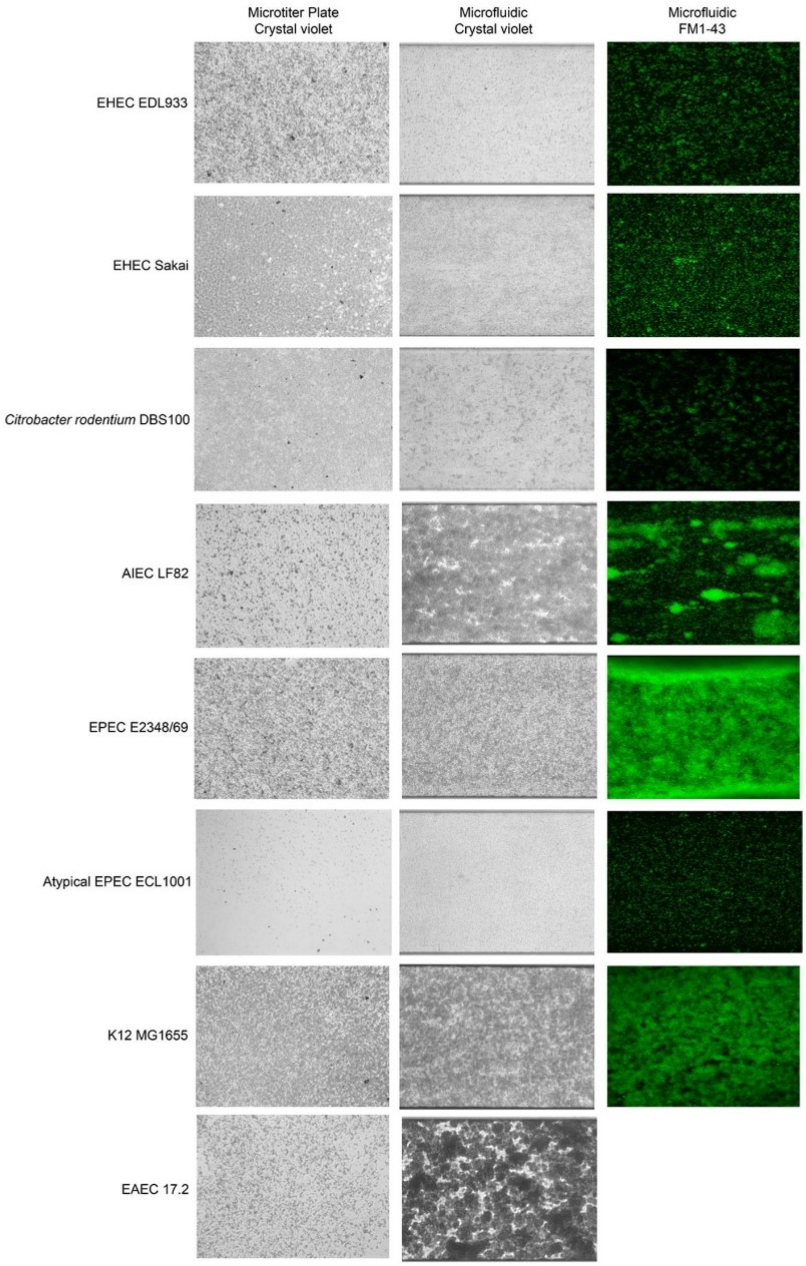

FIG 3 Biofilm formation by representative InPEC strains in the presence of shear force in a microfluidic system. Biofilms were formed in M9 medium plus glucose (0.4%, wt/vol) at 30°C in the presence of shear force (1.0 dyne/cm^2 for 5 h, followed by 0.5 dyne/cm^2 for 17 h) and were stained with crystal violet or FM1-43. Biofilms formed in a microtiter plate are shown for reference purposes. A field of view representative of 3 biological replicates is shown for each strain, and images were captured using either an inverted microscope and a digital camera (crystal violet-stained biofilms) or a confocal microscope (FM1-43-stained biofilms). The fluorescent image for EAEC 17.2 is missing because the microfluidic channel was blocked and did not allow for effective penetration of the dye.

In contrast to its behavior under biofilm growth conditions (M9 medium and 30°C), *E. coli* readily produced mCherry in RPMI medium at 37°C, allowing the use of strains carrying pmCherry for microscopy analysis. Initial tests with HRT-18 or SJPL monolayers were then performed with EHEC EDL933 carrying the pmCherry plasmid. Different inoculum densities (OD_{600}, 0.125, 0.25, 0.5, or 1.0) were tested to establish the optimal conditions, but shear force was fixed at 0.5 dyne/cm^2. It was also noted that the medium acidified, as indicated by a change in the color of the medium, within 1.5 h. Therefore, an incubation time of 1.5 h for the early

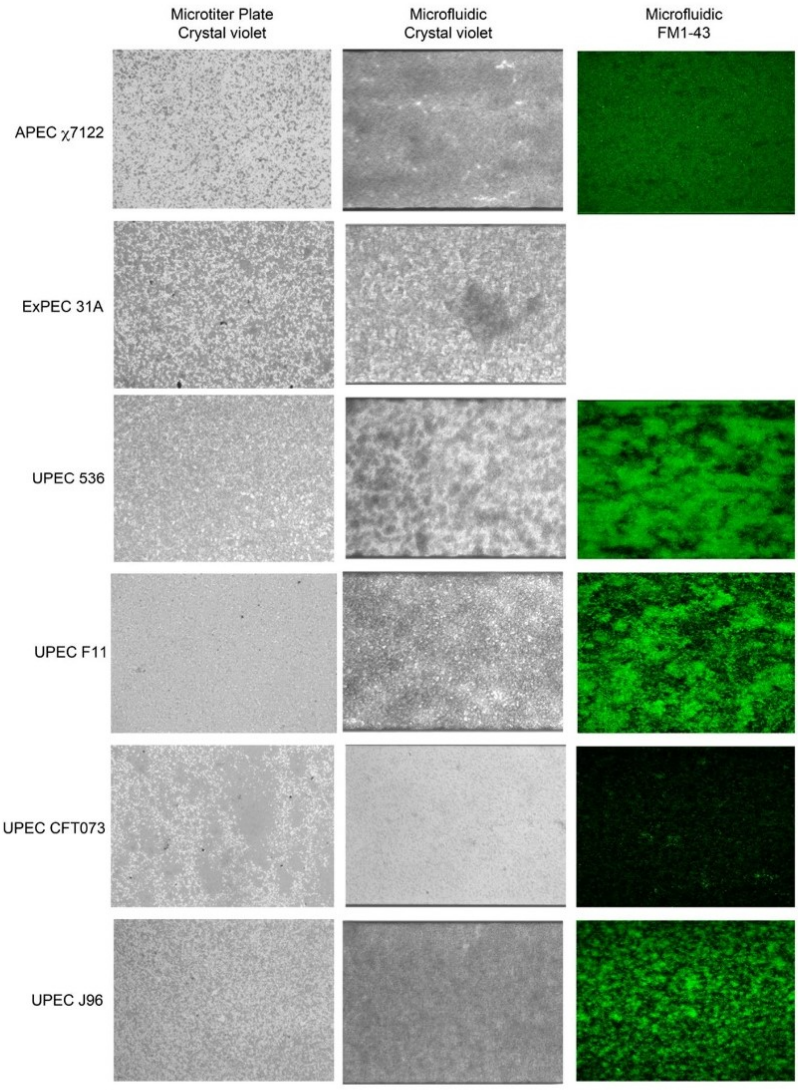

FIG 4 Biofilm formation by representative ExPEC strains in the presence of shear force in a microfluidic system. Biofilms were formed in M9 medium plus glucose (0.4%, wt/vol) at 30°C in the presence of shear force (1.0 dyne/cm^2 for 5 h, followed by 0.5 dyne/cm^2 for 17 h) and were stained with crystal violet or FM1-43. Biofilms formed in a microtiter plate are shown for reference purposes. A field of view representative of 3 biological replicates is shown for each strain, and images were captured using either an inverted microscope and a digital camera (crystal violet-stained biofilms) or a confocal microscope (FM1-43-stained biofilms). The fluorescent image for ExPEC 31A is missing because the microfluidic channel was blocked and did not allow for effective penetration of the dye.

adhesion of *E. coli* to HRT-18 monolayers was selected instead of the 2 h used in the BioFlux biofilm assay. Tests were also performed with monolayers at 100% and 50% confluence. EHEC EDL933 was not able to attach to or remain on SJPL monolayers in the presence of shear force; therefore, SJPL monolayers were not used for further tests. At 50% confluence, EHEC EDL933 bound specifically to HRT-18 monolayers and did not attach to the glass surface (see Fig. S4 in the supplemental material). At 100% confluence, after 17 h, EHEC EDL933 was attached to cell monolayers and was able to form microcolonies (Fig. 6). The best initial inoculum density was an OD_{600} of 0.5; at lower densities (OD_{600}, 0.125 or 0.25), very few cells were observed, and at an OD_{600} of 1.0, the channel was blocked after 12 h (see Video S1 in the supplemental material). At higher densities, the growth of EHEC EDL933 on HRT-18 monolayers could be monitored visually in real time using phase-contrast microscopy, which confirmed the presence of bacteria in the growth chamber (see Video S1). On average, 120 (±21) cells incubated with EHEC EDL933 were stained with trypan blue (approximately 4 times more cells than those incubated with the negative control and stained with trypan blue) (see Table S1 in the supplemental material). However, more than 99% of the cells within the monolayer had intact membranes. Further-

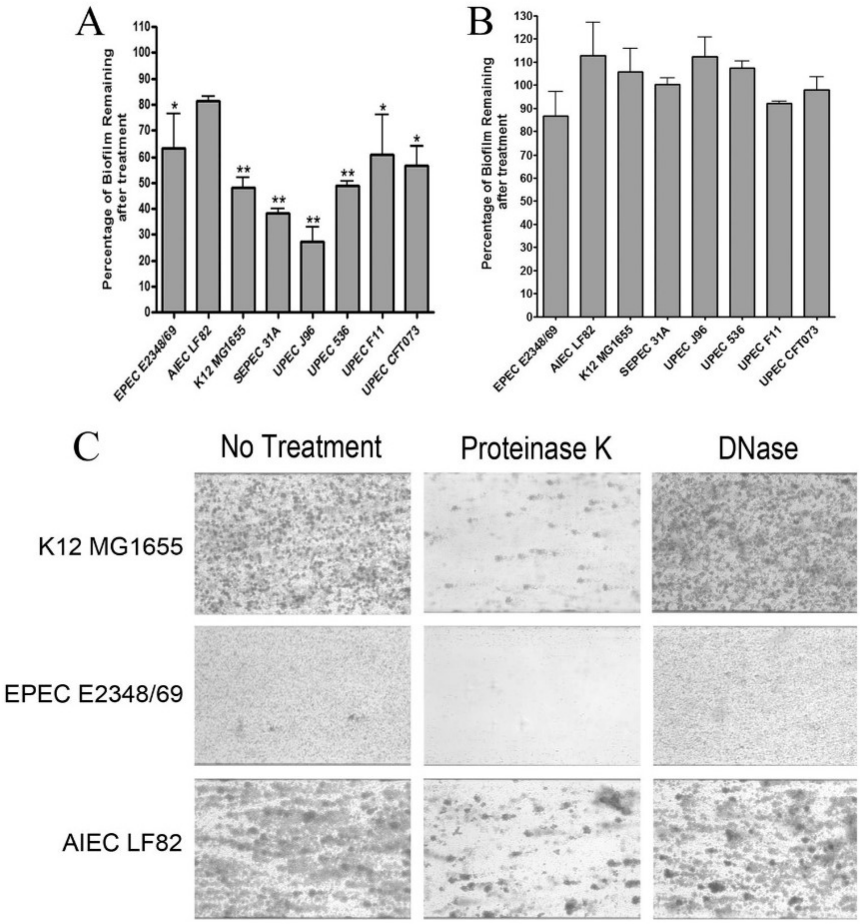

FIG 5 Enzymatic treatment of preformed biofilms of selected pathotypes. (A and B) Biofilms formed in microtiter plates were treated with protease (A) or DNase (B) for 1 h. Absorbance was read at 590 nm. Results are averages for 3 independent biological replicates; error bars represent standard error. *, $P < 0.05$; **, $P < 0.01$. (C) Biofilms formed in the BioFlux 200 system were also treated with protease or DNase for 1 h. The remaining biofilms were then stained with crystal violet. A field of view representative of 3 independent replicates is shown for each test. Images were captured using an inverted microscope and a digital camera.

more, the monolayer remained intact, indicating that attachment and growth of EHEC EDL933 did not cause detachment of the HRT-18 monolayer.

To see if this assay could be used for strains belonging to other pathotypes, representative strains were selected based on their biofilm-forming abilities and were transformed with pmCherry. UPEC J96 was not selected, because it was able to form a biofilm in the BioFlux system when grown in RPMI medium (see Fig. S2 in the supplemental material). The introduction of pmCherry into the strains did not affect their biofilm-forming ability in the microtiter plate assay in M9 medium with 0.4% (wt/vol) glucose. The next step was to ensure that the pathogenic *E. coli* strains did not form biofilms under the conditions used to grow the HRT-18 monolayer (37°C in RPMI medium). This was important in order to ensure that the *E. coli* strains specifically bound the cells and not the glass of the BioFlux plate. The same parameters described for the BioFlux biofilm assay were used, except that instead of being grown in M9 medium at 30°C, the bacteria were grown in RPMI medium at 37°C. As observed above, none of the strains stayed attached to the glass surface in the absence of cells under the conditions used to grow the HRT-18 cell monolayer. Except for the K-12 strain MG1655, all strains were able to bind to HRT-18 monolayers, and most strains were able to form some aggregates. The abilities of some strains to grow on HRT-18 monolayers were similar to their abilities to form biofilms in the BioFlux system. For example, EPEC E2348/69, a strong BioFlux biofilm former, had the best ability to attach to the cell monolayer and form a biofilm-like structure, whereas aEPEC ECL1001, a weak BioFlux biofilm former, only bound and formed small aggregates (Fig. 6). This finding is also supported by image analysis; EPEC E2348/69 had fewer particles (78 particles) but larger aggregates (64 pixels), with a biomass of 3.18 $\mu m^3/\mu m^2$ covering 48% of the surface, whereas aEPEC ECL1001 had more particles (111 particles) but smaller aggregates (11 pixels), with a biomass of 0.31 $\mu m^3/\mu m^2$ covering 12% of the surface (Table 2). Furthermore, both EHEC EDL933 and EHEC Sakai were able to form microcolonies on HRT-18 monolayers, but EHEC Sakai formed larger particles (6.5 versus 39 pixels) and more numerous microcolonies (13% versus

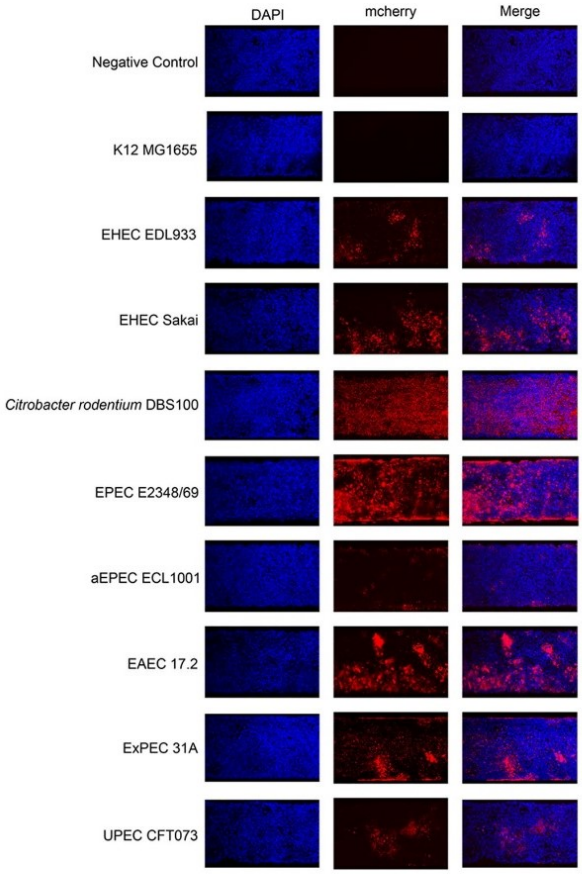

FIG 6 Attachment and growth of representative strains of different pathotypes on HRT-18 monolayers in the presence of shear force in a microfluidic system. Strains were incubated for 1.5 h in the presence of a preformed cell monolayer to allow initial attachment; they were then subjected to shear force (0.5 dyne/cm^2) for 16 h. Cells and bacteria were then washed, fixed, and stained with DAPI. The attachment and growth of bacteria on HRT-18 monolayers were observed with a confocal microscope by exciting and detecting the fluorophore (DAPI or mCherry). A field of view representative of 3 independent replicates for each strain is shown.

24% surface coverage) than EHEC EDL933, as observed with their BioFlux biofilms (Fig. 3 and 6 and Table 2). However, these differences did not result in significant differences in biomass between the two EHEC strains (Table 2). Additionally, *C. rodentium* DBS100, an EHEC surrogate and a natural mouse pathogen, could only attach and did not form any large aggregates or microcolonies (Fig. 6). It also formed a thinner layer (up to 8 μm thick) with a smaller biomass (1.36 μm^3/μm^2) than most strains, for which cluster heights ranged from 13 to 39 μm (Table 2). In contrast to their BioFlux biofilm formation, EAEC 17.2, SEPEC 31A, and UPEC CFT073 did not form extensive biofilm structures on HRT-18 monolayers (Fig. 3, 4, and 6). EAEC 17.2 formed large, tall microcolonies (as high as 33 μm) that had the largest biomass (5.23 μm^3/μm^2) of the strains, whereas SEPEC 31A and UPEC CFT073 only formed scattered aggregates and had some of the smallest biomasses (Fig. 6 and Table 2). However, the SEPEC 31A strain formed the tallest microcolonies, measuring as much as 39 μm (Table 2).

Cell death was assessed by trypan blue staining, and the number of trypan blue-positive cells per channel ranged from 105 to 1,044 for infected cells (see Table S1 in the supplemental material). The number of trypan blue-positive cells was pathotype dependent, and the standard deviation between biological replicates was less than 22 cells. EAEC 17.2 had the greatest number of trypan blue-positive cells (see Table S1). Cell death was also assessed by ensuring that the HRT-18 monolayers remained intact and that no gaps were present. Except for those infected with EAEC 17.2, the monolayers remained intact during infection. With EAEC 17.2, small gaps appeared after 17 h of incubation, suggesting that cells had died and detached from the substrate and had been carried out of the channel by the flow of medium.

As observed with EHEC EDL933, the SEPEC 31A, EAEC 17.2, EPEC E2348/69, aEPEC ECL1001, and EHEC Sakai strains were able to attach to, and form microcolonies on, HRT-18 monolayers when confluence was less than 90% (data not shown). Again, none of the strains attached to the glass surface of the BioFlux plate, confirming that the attachment was specific for the HRT-18 monolayers. On the other hand, *C. rodentium* DS100 and UPEC CFT073 required the cell monolayer to be at 95% to 100% confluence for any attachment to be observable.

Evaluation of the effect of a deletion of the *aidA* gene, which encodes a protein involved in adhesion and biofilm formation. One of the purposes of developing our application was to provide a high-throughput platform for the testing and screening of mutants. As a proof of concept, we selected an *aidA* deletion mutant of diffusely adherent *E. coli* (DAEC) strain 2787, because the autotransporter adhesin AIDA-I plays a role in biofilm formation, and deletion of *aidA* results in decreased cell adhesion (21). DAEC 2787 and DAEC 2787 Δ*aidA* were first tested in the microtiter plate assay. There was a significant decrease ($P < 0.01$) in biofilm formation by the Δ*aidA* strain (Fig. 7A). The parental strain is a weak biofilm former, and based on our biofilm threshold (A_{595}, ≥0.110), the Δ*aidA* strain did not form a biofilm (Fig. 7A). The biofilm-forming ability of the Δ*aidA* strain was then assessed in our BioFlux biofilm assay. Again, there was a significant decrease ($P < 0.01$) in biofilm formation by the Δ*aidA* strain (Fig. 7B and Table 3). Although the Δ*aidA* strain remained attached to the glass surface and formed a thin layer of biofilm, the parental strain formed a stronger biofilm than the mutant, with a larger biomass (Fig. 7B and Table 3). This finding was further supported by image analysis, which indicated that the parental strain covered more surface and formed larger structures than the Δ*aidA* strain (Table 3). These results indicate that the parameters of our BioFlux biofilm assay can be used to screen biofilm mutants.

Both strains were then transformed with pmCherry, and these transformants were used in our BioFlux cell adhesion assay. In the presence of shear force, the parental strain remained attached and was able to grow and form a biofilm (Fig. 7C). The Δ*aidA* strain was able to remain attached to the monolayers, but it was able to form only small microcolonies (Fig. 7C). The biomass of the structure formed by the Δ*aidA* strain was significantly smaller ($P < 0.01$) than that of the parental strain (Table 3). Furthermore, the mutant formed smaller particles and covered less surface than the parental strain but formed taller clusters (Table 3). Again, these results indicate that the cell adhesion assay in the BioFlux system can be used to screen mutants that have decreased cell

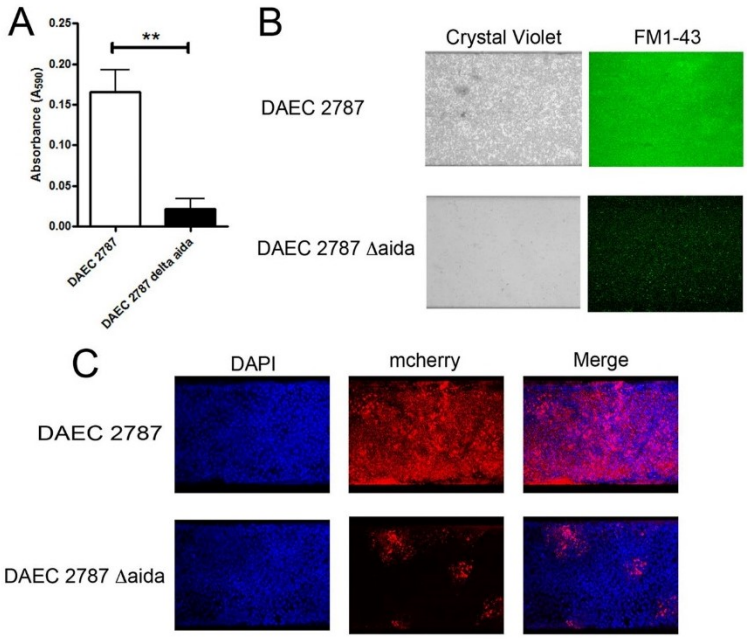

FIG 7 Decreased biofilm formation and cell attachment by a DAEC Δ*aidA* strain. Biofilm formation by a DAEC Δ*aidA* mutant and its parental strain was evaluated in microtiter plates (A) or in the BioFlux system on an abiotic (B) or a biotic (C) surface. For microtiter plates, absorbance was measured at 590 nm, and results are averages for 3 independent biological replicates; error bars represent standard error. **, $P < 0.01$.

adhesion. Furthermore, there was no difference in cell death as assessed by trypan blue staining. A total of 39 (±14) cells infected with the parental strain and 45 (±5) cells infected with the Δ*aidA* strain were stained with trypan blue (see Table S1 in the supplemental material).

DISCUSSION

Biofilm formation and host-pathogen interactions are often studied in systems that do not incorporate physiologically relevant conditions, such as shear force created by the flow of bodily fluids. For example, shear force can range from 4 to 50 dynes/cm^2 in blood vessels (22) and from 4 to 35 dynes/cm^2 in the intestinal epithelium during peristalsis (23), while it can be less than 1 dyne/cm^2 *in utero* (24) and between the brush border microvilli of epithelial cells (25). Furthermore, it is very difficult to culture eukaryotic cells in the presence of bacteria for the extended periods that would allow biofilm formation. Microfluidic systems could provide a means to overcome the limitations of commonly used models. The BioFlux device was developed to provide models that resemble *in vivo* conditions and allows for the formation of biofilms on both biotic and abiotic surfaces in the presence of shear force. Using pathogenic *E. coli* strains as model bacteria and the human colorectal adenocarcinoma cell line HRT-18, we demonstrate that the BioFlux 200 system can be used to study biofilm formation on biotic and abiotic surfaces in the presence of shear force. Furthermore, our model allows host-pathogen interactions to be studied over long periods without significant cell death.

Interestingly, pathogenic *E. coli* strains did not form biofilms on the glass surface of the BioFlux plate when cell line growth conditions were used (37°C in RPMI medium); they required the presence of an HRT-18 monolayer to form biofilm-like structures. However, pathogenic *E. coli* strains were able to form biofilms on a glass surface at a lower temperature (30°C) and in minimal medium (M9 medium with glucose). These differences could provide

TABLE 3 Quantification of biofilm formation and cell attachment by DAEC 2787 and DAEC 2787 Δ*aidA* using a microfluidic system[a]

Assay and strain	No. of particles	Avg particle size (pixels)[b]	% of area covered	Biomass (μm^3/μm^2)	Height (μm)
Biofilm formation					
DAEC 2787	43 (±11)	835.3 (±142.4)	75 (±8)	7.60 (±1.21)	20 (±2)
DAEC 2787 Δ*aidA*	617 (±97)	6.4 (±1.3)	9 (±3)	2.49 (±0.89)	24 (±3)
Cell attachment					
DAEC 2787	92 (±31)	404.0 (±44.3)	80 (±11)	3.84 (±1.11)	11 (±2)
DAEC 2787 Δ*aidA*	288 (±77)	29.1 (±13.3)	18 (±5)	0.59 (±0.18)	23 (±4)

[a] Values are averages (standard errors) for 3 independent biological replicates.
[b] Two pixels are approximately equivalent to 1 bacterial cell.

a good basis for investigating factors associated with biofilms under environmental conditions (e.g., on the surfaces found in food-processing plants) or in the context of host-pathogen interactions (by use of cell monolayers). Furthermore, we demonstrated that our model could distinguish between a parental strain that formed strong biofilms and an isogenic mutant that failed to form an extensive biofilm on either a biotic or an abiotic surface. This would permit the use of the high-throughput capability of the system to screen for mutants so as to identify novel factors involved in host-pathogen interactions.

In addition to screening mutants so as to identify new factors, our model could be used to revisit mutants of known virulence factors. For example, EPEC E2348/69 formed strong biofilms, whereas aEPEC ECL1001 formed weak biofilms. One of the major differences between EPEC and aEPEC is the absence of the bundle-forming pili (BFP) in aEPEC (26). BFP are located on the large EPEC adherence factor (EAF) plasmid, and this plasmid and the BFP have been associated with increased efficiency of attaching and effacing (A/E) lesions (27). Furthermore, BFP have been associated with biofilm formation on abiotic surfaces by the EPEC reference strain in the absence or presence of shear force (26). Therefore, it would be interesting to investigate the role of BFP during attachment and biofilm formation on HRT-18 monolayers using our model. Other fimbriae of interest would be the aggregative adherence fimbriae (AAF) of EAEC. AAF have been implicated in biofilm formation (28), and biofilm formation by EAEC 17.2 in the BioFlux device was enhanced over that in the microtiter plate assay. Shear force has been shown to enhance binding by the type 1 fimbriae of certain *E. coli* strains (29), and it would interesting to see if this is also the case for AAF.

Like EPEC and aEPEC, EHEC and *C. rodentium* are pathogens that cause A/E lesions (14, 30). These are associated with a type III secretion system (T3SS) that secretes the bacterial receptor Tir into the host cells and allows intimate attachment of the bacteria via the adhesin intimin (14). Therefore, future investigations could focus on the role of intimate attachment during the formation of biofilms on HRT-18 monolayers under shear force. Furthermore, the expression and injection of effectors could potentially be monitored in real time to further assess the role of the T3SS during attachment and infection.

Our model is also a potential tool for screening compounds and probiotic bacteria that effectively inhibit biofilm formation by pathogenic *E. coli* on mammalian cells. Furthermore, cell lines of diverse origins (different organs or different animal species) could be grown in our model. We were able to grow the SJPL cell line, which is of monkey origin, and the HEp-2 cell line, which is derived from human larynx carcinoma, as monolayers using conditions similar to those described for HRT-18 cells (data not shown). However, not every cell line grew consistently well in the BioFlux plate (HEp-2 cells), and EHEC strains demonstrated a certain specificity toward human cells; they were not able to attach to, or remain on, SJPL cells in the presence of shear force.

In conclusion, we established the conditions required to grow biofilms of different *E. coli* pathotypes on HRT-18 monolayers in the BioFlux system. Furthermore, we developed a BioFlux protocol (Fig. 1) that allows for the development of microcolonies or biofilms by pathogenic *E. coli* on HRT-18 monolayers in the presence of shear force. This new tool will likely help investigators study the interactions of pathogenic *E. coli* strains with their hosts in a model that could reflect certain *in vivo* conditions.

ACKNOWLEDGMENTS

This research was supported by a Team grant from the Fonds de Recherche du Québec, Nature et Technologies (FRQ-NT PT165375), to J.H. and M.J. and by discovery grants from the Natural Sciences and Engineering Research Council of Canada to J.H. and M.J. P.V. is also a recipient of a scholarship from the CRIPA (FRQNT Regroupements stratégiques 111946).

We thank Michael Mourez for generously providing the Δ*aidA* strain and Samantha Gruenheid for providing *Citrobacter rodentium* DBS100. Jenny-Lee Thomassin is also acknowledged for proofreading the manuscript.

REFERENCES

1. **Jacques M, Aragon V, Tremblay YDN.** 2010. Biofilm formation in bacterial pathogens of veterinary importance. Anim Health Res Rev **11:**97–121. http://dx.doi.org/10.1017/S1466252310000149.
2. **Ceri H, Olson ME, Stremick C, Read RR, Morck D, Buret A.** 1999. The Calgary Biofilm Device: new technology for rapid determination of antibiotic susceptibilities of bacterial biofilms. J Clin Microbiol **37:**1771–1776.
3. **McBain AJ.** 2009. In vitro biofilm models: an overview. Adv Appl Microbiol **69:**99–132. http://dx.doi.org/10.1016/S0065-2164(09)69004-3.
4. **Benoit MR, Conant CG, Ionescu-Zanetti C, Schwartz M, Matin A.** 2010. New device for high-throughput viability screening of flow biofilms. Appl Environ Microbiol **76:**4136–4142. http://dx.doi.org/10.1128/AEM.03065-09.
5. **Kim KP, Kim YG, Choi CH, Kim HE, Lee SH, Chang WS, Lee CS.** 2010. In situ monitoring of antibiotic susceptibility of bacterial biofilms in a microfluidic device. Lab Chip **10:**3296–3299. http://dx.doi.org/10.1039/c0lc00154f.
6. **Kim J, Hegde M, Kim SH, Wood TK, Jayaraman A.** 2012. A microfluidic device for high throughput bacterial biofilm studies. Lab Chip **12:**1157–1163. http://dx.doi.org/10.1039/c2lc20800h.
7. **Lee JH, Kaplan JB, Lee WY.** 2008. Microfluidic devices for studying growth and detachment of *Staphylococcus epidermidis* biofilms. Biomed Microdevices **10:**489–498. http://dx.doi.org/10.1007/s10544-007-9157-0.
8. **Nance WC, Dowd SE, Samarian D, Chludzinski J, Delli J, Battista J, Rickard AH.** 2013. A high-throughput microfluidic dental plaque biofilm system to visualize and quantify the effect of antimicrobials. J Antimicrob Chemother **68:**2550–2560. http://dx.doi.org/10.1093/jac/dkt211.
9. **Moormeier DE, Endres JL, Mann EE, Sadykov MR, Horswill AR, Rice KC, Fey PD, Bayles KW.** 2013. Use of microfluidic technology to analyze gene expression during *Staphylococcus aureus* biofilm formation reveals distinct physiological niches. Appl Environ Microbiol **79:**3413–3424. http://dx.doi.org/10.1128/AEM.00395-13.
10. **Soyer M, Duménil G.** 2011. Introducing shear stress in the study of bacterial adhesion. J Vis Exp **55:**e3241. http://dx.doi.org/10.3791/3241.
11. **Kim J, Hegde M, Jayaraman A.** 2010. Co-culture of epithelial cells and bacteria for investigating host-pathogen interactions. Lab Chip **10:**43–50. http://dx.doi.org/10.1039/b911367c.
12. **Kim J, Hegde M, Jayaraman A.** 2010. Microfluidic co-culture of epithelial cells and bacteria for investigating soluble signal-mediated interactions. J Vis Exp **38:**1749. http://dx.doi.org/10.3791/1749.
13. **Soyer M, Duménil G.** 2012. A laminar-flow chamber assay for measuring bacterial adhesion under shear stress. Methods Mol Biol **799:**185–195. http://dx.doi.org/10.1007/978-1-61779-346-2_12.
14. **Croxen MA, Finlay BB.** 2010. Molecular mechanisms of *Escherichia coli* pathogenicity. Nat Rev Microbiol **8:**26–38. http://dx.doi.org/10.1038/nrmicro2265.
15. **Sambrook J, Fritsch EF, Maniatis T.** 1989. Molecular cloning: a laboratory manual, 2nd ed. Cold Spring Harbor Laboratory Press, Cold Spring Harbor, NY.
16. **Wu C, Labrie J, Tremblay YDN, Haine D, Mourez M, Jacques M.** 2013. Zinc as an agent for the prevention of biofilm formation by pathogenic bacteria. J Appl Microbiol **115:**30–40. http://dx.doi.org/10.1111/jam.12197.
17. **Tremblay YDN, Lamarche D, Chever P, Haine D, Messier S, Jacques M.** 2013. Characterization of the ability of coagulase-negative staphylococci isolated from the milk of Canadian farms to form biofilms. J Dairy Sci **96:**234–246. http://dx.doi.org/10.3168/jds.2012-5795.
18. **Silversides DW, Music N, Jacques M, Gagnon CA, Webby R.** 2010. Investigation of the species origin of the St. Jude porcine lung epithelial

cell line (SJPL) made available to researchers. J Virol **84:**5454–5455. http://dx.doi.org/10.1128/JVI.00042-10.

19. **Tremblay YDN, Deslandes V, Jacques M.** 2013. *Actinobacillus pleuropneumoniae* genes expression in biofilms cultured under static conditions and in a drip-flow apparatus. BMC Genomics **14:**364. http://dx.doi.org/10.1186/1471-2164-14-364.
20. **Kaya T, Koser H.** 2012. Direct upstream motility in *Escherichia coli*. Biophys J **102:**1514–1523. http://dx.doi.org/10.1016/j.bpj.2012.03.001.
21. **Charbonneau ME, Mourez M.** 2007. Functional organization of the autotransporter adhesin involved in diffuse adherence. J Bacteriol **189:**9020–9029. http://dx.doi.org/10.1128/JB.01238-07.
22. **Davies PF.** 1995. Flow-mediated endothelial mechanotransduction. Physiol Rev **75:**519–560.
23. **Jeffrey B, Udaykumar HS, Schulze KS.** 2003. Flow fields generated by peristaltic reflex in isolated guinea pig ileum: impact of contraction depth and shoulders. Am J Physiol Gastrointest Liver Physiol **285:**G907–G918. http://dx.doi.org/10.1152/ajpgi.00062.2003.
24. **Stock UA, Vacanti JP.** 2001. Cardiovascular physiology during fetal development and implications for tissue engineering. Tissue Eng **7:**1–7. http://dx.doi.org/10.1089/107632701300003241.
25. **Guo P, Weinstein AM, Weinbaum S.** 2000. A hydrodynamic mechanosensory hypothesis for brush border microvilli. Am J Physiol Renal Physiol **279:**F698–F712.
26. **Trabulsi LR, Keller R, Tardelli Gomes TA.** 2002. Typical and atypical enteropathogenic *Escherichia coli*. Emerg Infect Dis **8:**508–513. http://dx.doi.org/10.3201/eid0805.010385.
27. **Moreira CG, Palmer K, Whiteley M, Sircili MP, Trabulsi LR, Castro AF, Sperandio V.** 2006. Bundle-forming pili and EspA are involved in biofilm formation by enteropathogenic *Escherichia coli*. J Bacteriol **188:**3952–3961. http://dx.doi.org/10.1128/JB.00177-06.
28. **Sheikh J, Hicks S, Dall'Agnol M, Phillips AD, Nataro JP.** 2001. Roles for Fis and YafK in biofilm formation by enteroaggregative *Escherichia coli*. Mol Microbiol **41:**983–997. http://dx.doi.org/10.1046/j.1365-2958.2001.02512.x.
29. **Thomas WE, Trintchina E, Forero M, Vogel V, Sokurenko EV.** 2002. Bacterial adhesion to target cells enhanced by shear force. Cell **109:**913–923. http://dx.doi.org/10.1016/S0092-8674(02)00796-1.
30. **Mundy R, Girard F, FitzGerald AJ, Frankel G.** 2006. Comparison of colonization dynamics and pathology of mice infected with enteropathogenic *Escherichia coli*, enterohaemorrhagic *E. coli* and *Citrobacter rodentium*. FEMS Microbiol Lett **265:**126–132. http://dx.doi.org/10.1111/j.1574-6968.2006.00481.x.
31. **Blattner FR, Plunkett G, III, Bloch CA, Perna NT, Burland V, Riley M, Collado-Vides J, Glasner JD, Rode CK, Mayhew GF, Gregor J, Davis NW, Kirkpatrick HA, Goeden MA, Rose DJ, Mau B, Shao Y.** 1997. The complete genome sequence of *Escherichia coli* K-12. Science **277:**1453–1462. http://dx.doi.org/10.1126/science.277.5331.1453.
32. **Darfeuille-Michaud A, Boudeau J, Bulois P, Neut C, Glasser AL, Barnich N, Bringer MA, Swidsinski A, Beaugerie L, Colombel JF.** 2004. High prevalence of adherent-invasive *Escherichia coli* associated with ileal mucosa in Crohn's disease. Gastroenterology **127:**412–421. http://dx.doi.org/10.1053/j.gastro.2004.04.061.
33. **Perna NT, Plunkett G, III, Burland V, Mau B, Glasner JD, Rose DJ, Mayhew GF, Evans PS, Gregor J, Kirkpatrick HA, Pósfai G, Hackett J, Klink S, Boutin A, Shao Y, Miller L, Grotbeck EJ, Davis NW, Lim A, Dimalanta ET, Potamousis KD, Apodaca J, Anantharaman TS, Lin J, Yen G, Schwartz DC, Welch RA, Blattner FR.** 2001. Genome sequence of enterohaemorrhagic *Escherichia coli* O157:H7. Nature **409:**529–533. http://dx.doi.org/10.1038/35054089.
34. **Hayashi T, Makino K, Ohnishi M, Kurokawa K, Ishii K, Yokoyama K, Han CG, Ohtsubo E, Nakayama K, Murata T, Tanaka M, Tobe T, Iida T, Takami H, Honda T, Sasakawa C, Ogasawara N, Yasunaga T, Kuhara S, Shiba T, Hattori M, Shinagawa H.** 2001. Complete genome sequence of enterohemorrhagic *Escherichia coli* O157:H7 and genomic comparison with a laboratory strain K-12. DNA Res **8:**11–22. http://dx.doi.org/10.1093/dnares/8.1.11.
35. **Elliott SJ, Wainwright LA, McDaniel TK, Jarvis KG, Deng YK, Lai LC, McNamara BP, Donnenberg MS, Kaper JB.** 1998. The complete sequence of the locus of enterocyte effacement (LEE) from enteropathogenic *Escherichia coli* E2348/69. Mol Microbiol **28:**1–4.
36. **Zhu C, Harel J, Jacques M, Desautels C, Donnenberg MS, Beaudry M, Fairbrother JM.** 1994. Virulence properties and attaching-effacing activity of *Escherichia coli* O45 from swine postweaning diarrhea. Infect Immun **62:**4153–4159.
37. **Benz I, Schmidt MA.** 1992. AIDA-I, the adhesin involved in diffuse adherence of the diarrhoeagenic *Escherichia coli* strain 2787 (O126:H27), is synthesized via a precursor molecule. Mol Microbiol **6:**1539–1546. http://dx.doi.org/10.1111/j.1365-2958.1992.tb00875.x.
38. **Charbonneau MÈ, Côté JP, Haurat MF, Reiz B, Crépin S, Berthiaume F, Dozois CM, Feldman MF, Mourez M.** 2012. A structural motif is the recognition site for a new family of bacterial protein O-glycosyltransferases. Mol Microbiol **83:**894–907. http://dx.doi.org/10.1111/j.1365-2958.2012.07973.x.
39. **Rich C, Favre-Bonte S, Sapena F, Joly B, Forestier C.** 1999. Characterization of enteroaggregative *Escherichia coli* isolates. FEMS Microbiol Lett **173:**55–61. http://dx.doi.org/10.1111/j.1574-6968.1999.tb13484.x.
40. **Schauer DB, Falkow S.** 1993. Attaching and effacing locus of a *Citrobacter freundii* biotype that causes transmissible murine colonic hyperplasia. Infect Immun **61:**2486–2492.
41. **Bertin Y, Martin C, Girardeau JP, Pohl P, Contrepois M.** 1998. Association of genes encoding P fimbriae, CS31A antigen and EAST 1 toxin among CNF1-producing *Escherichia coli* strains from cattle with septicemia and diarrhea. FEMS Microbiol Lett **162:**235–239. http://dx.doi.org/10.1111/j.1574-6968.1998.tb13004.x.
42. **Welch RA, Burland V, Plunkett G, III, Redford P, Roesch P, Rasko D, Buckles EL, Liou SR, Boutin A, Hackett J, Stroud D, Mayhew GF, Rose DJ, Zhou S, Schwartz DC, Perna NT, Mobley HL, Donnenberg MS, Blattner FR.** 2002. Extensive mosaic structure revealed by the complete genome sequence of uropathogenic *Escherichia coli*. Proc Natl Acad Sci U S A **99:**17020–17024. http://dx.doi.org/10.1073/pnas.252529799.
43. **Blum G, Falbo V, Caprioli A, Hacker J.** 1995. Gene clusters encoding the cytotoxic necrotizing factor type 1, Prs-fimbriae and alpha-hemolysin form the pathogenicity island II of the uropathogenic *Escherichia coli* strain J96. FEMS Microbiol Lett **126:**189–195. http://dx.doi.org/10.1111/j.1574-6968.1995.tb07415.x.
44. **Stapleton A, Moseley S, Stamm WE.** 1991. Urovirulence determinants in *Escherichia coli* isolates causing first-episode and recurrent cystitis in women. J Infect Dis **163:**773–779. http://dx.doi.org/10.1093/infdis/163.4.773.
45. **Hacker J, Knapp S, Goebel W.** 1983. Spontaneous deletions and flanking regions of the chromosomally inherited hemolysin determinant of an *Escherichia coli* O6 strain. J Bacteriol **154:**1145–1152.
46. **Provence DL, Curtiss R, III.** 1992. Role of *crl* in avian pathogenic *Escherichia coli*: a knockout mutation of *crl* does not affect hemagglutination activity, fibronectin binding, or curli production. Infect Immun **60:**4460–4467.

Annexe 2: Prevalence and characterization of Shiga-toxin-producing and enteropathogenic *Escherichia coli* in shellfish-harvesting areas and their watersheds

Pour cet article, j'ai conçu, réaliser et analyser les expériences de formation de biofilm. J'ai également rédigé les sections qui concernent la formation de biofilm. Cet article a été publié en 2015 dans le journal « Frontiers in microbiology ».

frontiers in Microbiology

ORIGINAL RESEARCH
published: 01 December 2015
doi: 10.3389/fmicb.2015.01356

Prevalence and Characterization of Shiga Toxin-Producing and Enteropathogenic *Escherichia coli* in Shellfish-Harvesting Areas and Their Watersheds

*Charlotte Balière[1], Alain Rincé[2], Jorge Blanco[3], Ghizlane Dahbi[3], Josée Harel[4], Philippe Vogeleer[4], Jean-Christophe Giard[5], Patricia Mariani-Kurkdjian[6,7,8] and Michèle Gourmelon[1]**

[1] Laboratoire Santé Environnement et Microbiologie, Unité Santé, Génétique et Microbiologie des Mollusques, Département Ressources Biologiques et Environnement, Ifremer, Plouzané, France, [2] U2RM EA4655 Stress/Virulence, Normandie-Université, University of Caen Normandy, Caen, France, [3] Departamento de Microbioloxía e Parasitoloxía, Facultade de Veterinaria, Universidade de Santiago de Compostela, Lugo, Spain, [4] Groupe de Recherche sur les Maladies Infectieuses du Porc, Département de Pathologie et Microbiologie, Faculté de Médecine Vétérinaire, Centre de Recherche d'Infectiologie Porcine et Avicole, Université de Montréal, Saint-Hyacinthe, QC, Canada, [5] U2RM EA4655 Antibio-Résistance, Normandie-Université, University of Caen Normandy, Caen, France, [6] Service de Microbiologie, CNR Associé Escherichia coli, AP-HP, Hôpital Robert-Debré, Paris, France, [7] Infection, Antimicrobials, Modelling, Evolution, UMR 1137, INSERM, Paris, France, [8] Infection, Antimicrobials, Modelling, Evolution, UMR 1137, Université Paris Diderot – Sorbonne Paris Cité, Paris, France*

OPEN ACCESS

Edited by:
Anton F. Post, University of Rhode Island, USA

Reviewed by:
Erin Katherine Lipp, University of Georgia, USA
Dale Leavitt, Roger Williams University, USA

***Correspondence:**
Michèle Gourmelon
michele.gourmelon@ifremer.fr

Specialty section:
This article was submitted to Aquatic Microbiology, a section of the journal Frontiers in Microbiology

Received: *14 August 2015*
Accepted: *16 November 2015*
Published: *01 December 2015*

Citation:
Balière C, Rincé A, Blanco J, Dahbi G, Harel J, Vogeleer P, Giard J-C, Mariani-Kurkdjian P and Gourmelon M (2015) Prevalence and Characterization of Shiga Toxin-Producing and Enteropathogenic Escherichia coli in Shellfish-Harvesting Areas and Their Watersheds. Front. Microbiol. 6:1356. doi: 10.3389/fmicb.2015.01356

During a 2-years study, the presence of Shiga-toxin producing *Escherichia coli* (STEC) and enteropathogenic *E. coli* (EPEC) was investigated in shellfish ($n = 238$), seawater ($n = 12$), and surface sediment ($n = 39$) collected from three French coastal shellfish-harvesting areas and freshwaters ($n = 216$) in their watersheds. PCR detection of Shiga toxin- (*stx1/stx2*) and intimin- (*eae*) genes following enrichment from these samples revealed the presence of least one of the *stx* genes in 30.3% of shellfish batches, 85.9% of freshwater, 41.7% of seawater, and 28.2% of sediment samples, while the *eae* gene was observed in 74.8, 100, 100, and 43.6% of shellfish batches, freshwater, seawater, and sediment samples, respectively. Twenty-eight STEC and 89 EPEC strains were isolated and analyzed in order to determine their serotype, phylogroup, and genetic relatedness and to evaluate the presence of the *saa* and *ehxA* genes encoding the STEC autoagglutinating adhesin and the enterohemolysin A, respectively. Finally, the ability to form biofilms and antimicrobial susceptibility were investigated for a selection of strains. Eighteen serotypes were identified among the STEC isolates and 57 among the EPEC isolates. A high diversity was observed within these strains, as 79 different PFGE patterns and 48 distinguishable sequence types were identified. Strains were found to belong mainly to phylogroups B1 and B2 and virulence was observed to be low as more than 85% of the strains possessed only *stx1*, *stx2,* or *eae* genes. One STEC and several EPEC strains belonged to three of the five highly pathogenic serogroups (i.e., O26, O103, and O145). The subset of strains tested for their capacity to form biofilms was mainly strongly to moderately adherent and

more strains formed a strong biofilm at 18 than at 30°C. Finally, more than 85% of analyzed strains were found to be sensitive to the 16 tested antibiotics. These data suggest the low risk of human infection by STEC if shellfish from these shellfish-harvesting areas were consumed.

Keywords: STEC, EPEC, shellfish, water, MLST, PFGE, biofilms

INTRODUCTION

The microbiological quality of coastal environments can be impacted by urban and agricultural fecal wastes from watersheds. Moreover, shellfish can accumulate and concentrate pathogenic micro-organisms, such as *Salmonella,* pathogenic *Escherichia coli* (*E. coli*) and noroviruses present in surrounding waters by their filter-feeding activities (Potasman et al., 2002). This can lead to closures or downgrading of shellfish-harvesting areas and to outbreaks of food poisoning through consumption of contaminated shellfish (Iwamoto et al., 2010).

Enumeration of *E. coli,* a fecal bacterial indicator, is the standard way to assess the level of fecal microorganisms in water and shellfish and indirectly, to estimate the associated potential risk to human health from all waterborne enteric pathogens (e.g., through classification of bathing areas and shellfish-harvesting areas; Anonymous, 2004). However, in addition to being a fecal indicator and a commensal bacterium, *E. coli* includes strains that can be pathogenic to humans. These can cause diarrhea and extra-intestinal diseases after acquiring virulence genes by genetic mobile elements such as bacteriophages, pathogenicity islands, and plasmids (Touchon et al., 2009). Pathogenic *E. coli* are distributed into diarrheagenic *E. coli* pathotypes including enterotoxigenic *E. coli* (ETEC), *Shigella*/enteroinvasive *E. coli* (EIEC), enteroaggregative *E. coli* (EAEC), diffusely adherent *E. coli* (DAEC), enteropathogenic *E. coli* (EPEC), Shiga toxin-producing *E. coli* (STEC; for review, Croxen et al., 2013) and into extra-intestinal *E. coli* pathotypes (Russo and Johnson, 2000).

Escherichia coli occurrence in seafood is considered a sanitary case and may represent a risk to the consumers if related to diarrheagenic *E. coli* (for review, Costa, 2013).

The study presented here focuses on EPEC (one of the main causes of diarrhea in infants) and STEC (an emerging zoonotic pathogen).

Enteropathogenic *E. coli* is an important cause of infantile watery diarrhea, which is more frequently encountered in low-income countries than in the industrialized world (Nataro and Kaper, 1998). They are known to create distinctive lesions on the surface of intestinal epithelial cells, called attaching and effacing (A/E) lesions. This property is encoded by genes, including *eae*, grouped together in a pathogenicity island referred to the 'locus of enterocyte effacement' (LEE; Paton and Paton, 1998). EPEC is transmitted from host to host via the fecal-oral route through contaminated surfaces, waters and food and human carriers. Humans, including symptomatic and asymptomatic children and asymptomatic adults, are the most likely source (Levine and Edelman, 1984). Animals, such as cattle and wildlife species, have been found to be additional sources (Singh et al., 2015). Twelve O serogroups have been recognized as EPEC by the World Health Organization: O26, O55, O86, O111, O114, O119, O125, O126, O127, O128, O142, and O158 (WHO, 1987).

Shiga-toxin producing *Escherichia coli* are responsible for the mucoid-bloody diarrhea that can progress to hemolytic uremic-syndrome (HUS), especially in children. One of the most important pathogenicity factors produced by STEC strains is the Shiga toxin (Stx), encoded by a lambdoid bacteriophage (O'Brien et al., 1984). Shiga toxins can be divided into two types, Stx1 (almost identical to Shiga toxin produced by *Shigella dysenteriae* type 1) and Stx2, encoded by *stx1* and *stx2* genes, respectively (Scheutz et al., 2012). In addition, the STEC strains are often able to produce the A/E lesions as a result of the presence of the LEE pathogenicity island, as in EPEC. This subset of STEC strains is also known as enterohemorrhagic *E. coli* (EHEC; McDaniel et al., 1995). Instead of this LEE pathogenicity island, they can also possess the auto-agglutinating adhesin factor designated Saa (STEC autoagglutinating adhesin; Paton et al., 2001). Adhesion to the intestinal mucosa is an essential step in the infection cycle of *E. coli*, which contributes to pathogenesis in humans. Other factors are involved in the virulence of STEC but also of EPEC, such as enterohemolysin A, encoded by the *ehxA* gene and associated with cytotoxic effects on endothelial cells that may contribute to the development of HUS (Jiang et al., 2015). STEC infections have been reported following the ingestion of contaminated food or water, after bathing in contaminated waters or contact with animals (for review, Croxen et al., 2013). The principal reservoir of STEC is the digestive tract of animals, particularly of cattle that are healthy carriers (Bibbal et al., 2015). Other animals, such as sheep, goats, swine, birds, and other wild animals, as well as humans, can also harbor STEC (Mora et al., 2012; Chandran and Mazumder, 2013).

Most human illness is caused by the serotype STEC O157:H7 (Paton and Paton, 1998). However, it is becoming evident that non-O157 isolates belonging to the serogroups O26, O45, O91, O103, O111, O113, O121, O145 also cause significant human illness (Mellmann et al., 2009; USDA, 2011). In Europe, O157:H7 and the four serotypes: O26:H11, O103:H2, O111:H8, and O145:H28 are the most widely implicated in human STEC infections, constituting the five highly pathogenic serotypes (EFSA, 2013).

Shiga-toxin producing *Escherichia coli* and EPEC contamination of the environment may occur through the spreading of livestock manure, animal waste on pastures, via wastewaters from slaughterhouses or from treatment plant effluents and by wildlife (Muniesa et al., 2006; Singh et al., 2015).

In such environments, STEC and EPEC strains are exposed to various stresses, such as low temperature or nutrient depletion and the ability to form biofilm could be an advantage to increase persistence (Vogeleer et al., 2014).

To date, very few studies have focused on the detection and isolation of pathogenic *E. coli* belonging to the STEC and EPEC pathovars in coastal environments (Gourmelon et al., 2006; Bennani et al., 2011). The aim of the study presented here was to detect and characterize STEC and EPEC strains from French shellfish-harvesting areas and their upstream watershed in order to assess the diversity of these pathogenic *E. coli* potentially present in this type of hostile environment. For this purpose, during a 2-years study, shellfish batches, freshwater, seawater, and surface sediment samples from three selected shellfish-harvesting areas and their upstream watersheds, the location of intensive livestock activities (cattle, swine, poultry, and/or sheep), were analyzed monthly to evaluate the presence of STEC and EPEC strains.

MATERIALS AND METHODS

Sampling Locations and Sample Description

Shellfish, water, and surface sediment samples were collected from three shellfish-harvesting sites on the French coast of within the Eastern English Channel and their watersheds. One of these sites, located in Brittany (site 1), corresponded to a 121 km^2 watershed, characterized by intensive livestock farming (cattle, swine, and poultry), with a human population of about 9,000 inhabitants. The two others were situated in Normandy; site 2 was characterized by a 1,000 km^2 catchment, with large livestock farming (cattle, sheep, swine, and poultry) and about 40,000 inhabitants, while the second site (site 3) corresponded to a 50 km^2 watersheds with large livestock farming (cattle, sheep, and swine) and about 7,000 inhabitants. These two latter watersheds are geographically closer together than the Brittany site (location of the sites Supplementary Figure S1). The three shellfish-harvesting areas are classified as category B for oysters (*Crassostrea gigas*) and mussels (*Mytilus edulis*) and as category C for common cockles (*Cerastoderma edule*) according to European regulation (European Directive 91/492/EEC; Anonymous, 2004). Shellfish from category B shellfish-harvesting areas must be depurated before being sold and shellfish from category C areas must be relayed at least 2 months prior to sale for consumption. Shellfish [oyster, mussel, and common cockle batches (site 1, $n = 120$; site 2, $n = 72$; and site 3, $n = 46$)] and freshwater samples from nine sampling sites upstream of shellfish-harvesting areas (site 1, $n = 96$; site 2, $n = 72$; site 3, $n = 48$) were collected monthly from February 2013 to January 2015, whereas surface sediment samples (site 1, $n = 13$; site 2, $n = 13$; site 3, $n = 13$) were collected from February 2013 to January 2014 and seawater samples (site 1, $n = 12$) from February 2014 to January 2015.

Isolation of STEC and EPEC Strains

Samples were transported in insulated cooler boxes to the laboratory and analyzed within 24 h. After opening, total shellfish flesh, including shellfish flesh and intravalvular liquid, were homogenized in a commercial blender (Waring Products Division, Torrington, CT, USA) for 60 s at high speed. Twenty-five grams of homogenized total shellfish flesh were inoculated into 225 ml of buffered peptone water (BPW). For surface sediments, 10 g were introduced into the same volume of BPW. For water samples, 1 L was filtered using 0.45 μm cellulose membranes (Pall Gelman GN-6 Metricel; Pall Corporation, St Germain-en-Laye, France) and the filter was placed in 225 ml of BPW. Incubation was performed at 37°C for 24 h.

Shiga-toxin producing *Escherichia coli* and EPEC strains were isolated from the environmental samples using three additional protocols. The first one, described by Balière et al. (2015), involves application of the ISO/TS-13136 method, which focuses on isolation of strains belonging to the five highly pathogenic serotypes and was applied to samples collected from February 2013 to February 2014. The two other protocols involve the isolation of STEC and EPEC with or without an enrichment step and independently from the serotype. These were applied to samples collected from February 2013 to January 2015.

For the protocol with an enrichment step (described in Balière et al., 2015), DNA was extracted from 500 μL of each BPW enrichment broth using NucliSENS Nucleic Acid Extraction Reagents for miniMAG (BioMérieux, Marcy l'Etoile, France), according to the manufacturer's instructions. The *stx* and *eae* genes were detected by real-time PCR (Agilent MX3000P, Waldbronn, Germany), using primers and probes published previously (Nielsen and Andersen, 2003; Perelle et al., 2007), according to the ISO/TS-13136: 2012 technical specification, with slight modifications concerning the PCR cycles [denaturation for 10 s at 95°C, primer annealing for 5 s at 55°C, and extension for 25 s at 60°C (45 cycles)]. BPW broths identified positive for *stx* and *eae* were screened for STEC and EPEC isolates by streaking 1 μL of these broths onto Tryptone-Bile-X-glucuronide agar (TBX; AES chemunex, Bruz, France) and onto chromID^{TM} agar (BioMérieux), followed by incubation at 44°C for 24 h.

The final protocol to be used involves the screening of *E. coli* isolated directly from the water and shellfish samples without an enrichment step. For this protocol, 1, 10, and 100 ml of water were filtered through 0.45 μm cellulose membranes and the filters were placed onto TBX agar. For shellfish, 10 g of blended total shellfish flesh were distributed onto five empty and sterile plates with overlay super-cooled TBX agar. All TBX plates were incubated at 44°C for 24 h. Presumptive STEC and EPEC isolates were confirmed by real-time PCRs targeting *stx1*, *stx2*, and *eae* genes, as described above after a DNA extraction of each isolate by boiling at 100°C, for 15 min.

The STEC and EPEC isolates were characterized using several protocols as described below.

Serotyping

The serotypes of the STEC and EPEC strains were characterized using the serotyping method by agglutination, as described by Blanco et al. (2003).

More precisely, determination of O and H antigens was carried out by agglutination as previously described (Guinée et al., 1981), employing all available O (O1-O185) and

H (H1-H56) antisera. All antisera were absorbed with the corresponding cross-reacting antigens to remove the non-specific agglutinins. The O and H antisera were produced in the Laboratorio de Referencia de *E. coli* (USC, Lugo, Spain). Isolates that did not react with O antisera were considered as non-typeable (ONT) and those non-motile were HNM.

Detection of Enterohemolysin and Adhesin

The presence of e*hxA* (encoding enterohemolysin A) and *saa* (encoding STEC autoagglutining adhesin) genes in these isolates was investigated by conventional PCR using primers previously described by Paton and Paton (2002).

Phylogenetic Group

Isolates were classified into the four main *E. coli* phylogenetic groups (A, B1, B2, or D) using a conventional triplex PCR method based on the detection of two genes, *chuA*, required for heme transport in enterohemorrhagic O157:H7 *E. coli, yjaA*, initially identified in the recent complete genome sequence of *E. coli* K-12, for which the function is unknown, and of an anonymous DNA fragment designated TSPE4.C2 using primers described previously by Clermont et al. (2000).

Pulsed-field Gel Electrophoresis

The genetic relatedness of the isolates was studied by the pulsed-field gel electrophoresis method (PFGE) according to Bidet et al. (2005). Isolated strains were inoculated in nutrient broth containing 1.3% NaCl (Bio-Rad, Marnes-la-coquette, France) and incubated at 37°C for 24 h. Bacterial DNA was extracted from 400 µl of the enrichment broth using the CHEF Bacterial Genomic DNA Plug Kit (Bio-Rad) according to the manufacturer's recommendations. Bacterial DNA was digested for between 16 and 20 h at 37°C with the restriction endonuclease *XbaI* (Roche Diagnostic, Meylan, France) according to the manufacturer's recommendations. Each electrophoresis was performed using a lambda ladder molecular mass marker (Bio-Rad) for the normalization of gel images. The migration was performed on a 1% agarose gel using the CHEF-DRIII apparatus (Bio-Rad) at 6 V cm^{-1} for 27 h, with pulse times varying linearly between two and 49 s. The bacterial DNA restriction patterns were analyzed using the Bionumerics software 7.5 (Applied Maths, Kortrijk, Belgium). The similarity of PFGE profiles was compared and a dendrogram was created using the band-based Dice unweighted-pair group method, using average linkages (UPGMA), based on 1% position tolerance and 0% position optimization. Branch quality was evaluated using Cophenetic correlation. PFGE patterns were considered clonally related when they had a similarity coefficient higher than 80%.

Multilocus Sequencing Typing

The genetic relatedness of the isolates was also studied using the multilocus sequencing typing method (MLST). Fragments of seven housekeeping genes, i.e., *adk* (adenylate kinase), *fumC* (fumarate hydratase), *gyrB* (DNA gyrase), *icd* (isocitrate/isopropylmalate dehydrogenase), *mdh* (malate dehydrogenase), *purA* (adenylosuccinate dehydrogenase), and *recA* (ATP/GTP binding motif) were amplified and sequenced using suitable primers (Wirth et al., 2006) with minor modifications for the *recA* primers (recAR 5′-TCG-TCG-AAA-TCT-ACG-GAC-CGG-A-3′; recAF1 5′-ACC-TTT-GTA-GCT-GTA-CCA-CG-3′). The PCR cycle included denaturation for 60 s at 95°C, primer annealing for 60 s at 56°C (for *adk*, *purA*, *recA*, and *icd*), at 65°C (for *mdh* and *gyrB*), or at 68°C (for *fumC*), and extension for 60 s at 72°C (35 cycles) in MJ Research PTC-200 (DNA Engine, Waltham, MA, USA). Sequencing was performed in both directions with the fluorescent dye terminator Sanger method on ABI3730 (Applied Biosystem) by Eurofins Genomics (Ebersberg, Germany). The alleles and sequence types (ST) were assigned in accordance with the *E. coli* MLST database (http://mlst.warwick.ac.uk/mlst/dbs/Ecoli).

Static Biofilm Formation Assay

A biofilm formation assay was performed as previously described by Tremblay et al. (2015). In addition to the incubation temperature of 30°C, the ability to form biofilms was also tested at 18°C, in order to reproduce marine temperate environmental conditions (Moldoveanu, 2012). Briefly, overnight cultures at 37°C in LB media were diluted (1:100) in 5 ml of M9 medium with glucose (0.4% wt/vol) and minerals (1.16 mM $MgSO_4$, 2 µM $FeCl_3$, 8 µM $CaCl_2$, and 16 µM $MnCl_2$) and incubated for 24 h at 37°C. These cultures were diluted (1:100) in M9 medium supplemented with glucose and minerals and were inoculated in triplicate into microtitre plates (Costar 3370; Corning, NY, USA). After 24 h of incubation at 18 or 30°C, unattached cells were removed by washing three times with phosphate-buffered saline (PBS). Plates were dried at 37°C for 15 min and biofilms were stained with crystal violet (0.1% wt/vol) for 2 min. After removal of crystal violet solution, the biofilms were washed three times with PBS and dried at 37°C for 15 min. The biofilm stain was dissolved with 150 µl of 80% (vol/vol) ethanol and 20% (vol/vol) acetone and biofilms were quantified by measuring the absorbance at 590 nm (OD_{590}) with a microplate reader (Powerwave; BioTek Instruments, Winooski, VT, USA). The results for the static biofilms formed at 18 and 30°C were compared using two-way analysis of variance (ANOVA) followed by a Bonferroni *post hoc* comparison using GraphPad Prism, version 4.02 (GraphPad Software, San Diego, CA, USA). Strains were divided into three groups based on the OD_{590} of bacterial biofilm: strong ($A_{590} > 0.6$), medium ($0.6 \geq A_{590} \geq 0.3$) and weak or none ($A_{590} < 0.3$).

Antibiotic Resistance

Antimicrobial susceptibility testing based on the disk diffusion method was performed on a selection of STEC and EPEC isolates. Sixteen antibiotics were tested: Tobramycin (10 µg), Fosfomycin (50 µg), Cefalotin (30 µg), Imipenem (10 µg), Tigecyclin (15 µg), Gentamycin (15 µg), Cefotaxim (30 µg), Cefoxitin (30 µg), Doxycyclin (30 µg), Ciprofloxacin (5 µg), Augmentin (20 µg

amoxicilin; 10 μg clavulanic acid), Ticarcillin (75 μg), Bactrim (1.25 μg trimethoprim; 23.75 μg sulfamethoxazol), Nalidixic acid (30 μg), Amikacin (30 μg), Amoxicillin (25 μg) on Mueller-Hinton medium (AES chemunex, Bruz, France). Plates were incubated at 37°C for 24 h.

Environmental Data and Statistical Analysis

Rainfall data (2-days cumulative rainfall before sampling date) were provided by the meteorological stations from Meteo France at Pleurtuit (site 1) and at Coutances (sites 2 and 3). The water temperature was measured manually at each sampling. The data on temperature and precipitation were categorized into three groups whose boundaries were defined so that they are likely to categorize the data significantly for the studied sites and they allow to have in each category a number of sample consistent with a reliable statistical analysis. Comparisons of STEC and EPEC prevalence between the type of samples, the site, the season, the temperature and the precipitation were analyzed by the chi-square test. A p-value of <0.05 was considered statistically significant.

RESULTS

Detection and Isolation of STEC and EPEC Strains

The *stx* gene was detected in 30.3, 85.9, 41.7, and 28.2% of shellfish, freshwater, seawater and surface sediment enrichment broths, respectively (**Table 1**). The *eae* gene was detected in 74.8, 100, 100, and 43.6% of shellfish, freshwater, seawater, and surface sediment enrichment broths, respectively (**Table 1**). STEC were isolated from 5.0% of the 238 shellfish, 5.6% of the 216 freshwater, 8.3% of the 12 seawater, and 2.6% of the 39 surface sediment samples analyzed, whereas EPEC were isolated from 8.0, 21.3, and 33.3% of the shellfish, freshwater, and seawater samples, respectively. No EPEC were isolated from surface sediments (**Table 2**). A total of 57 STEC and 117 EPEC isolates were obtained from these samples. However, as 29 STEC and 28 EPEC had identical serotypes, PFGE and MLST patterns, virulence gene profiles, and phylogroups to other isolates cultivated from the same samples, they were considered to be replicates and not retained. The remaining 28 STEC and 89 EPEC isolates represented 0.2 and 0.7% of the total *E. coli* (n = 12,016), respectively (**Table 3**).

TABLE 2 | Isolation of STEC and EPEC as regard to sample parameters.

Sample parameter	No. of samples	No. of samples with at least one STEC isolate (%)[a]	No. of samples with at least one EPEC isolate (%)[a]
Type			
Shellfish	238	12 (5.0)	19 (8.0)
Freshwater	216	12 (5.6)	46 (21.3)
Seawater	12	1 (8.3)	4 (33.3)
Superficial sediment	39	1 (2.6)	0
χ^2 test		$p = 0.845$	$p = 3.09\ 10^{-5}$
Site			
Site 1	241	10 (4.1)	34 (14.1)
Site 2	157	7 (4.5)	20 (12.7)
Site 3	107	9 (8.4)	15 (14.0)
χ^2 test		$p = 0.244$	$p = 0.931$
Season			
Fall	146	4 (2.7)	11 (7.5)
Summer	126	17 (13.5)	22 (17.5)
Autumn	124	3 (2.4)	24 (19.4)
Winter	109	2 (1.8)	12 (11.0)
χ^2 test		$p = 4.44\ 10^{-5}$	$p = 0.0314$
Temperature (°C)			
0–<10	172	5 (2.9)	15 (8.7)
10–<15	189	14 (7.4)	29 (15.3)
15–>15	144	7 (4.9)	25 (17.4)
χ^2 test		$p = 0.167$	$p = 0.086$
Precipitation (mm)[b]			
0–<1	253	17 (6.7)	30 (11.9)
1–<10	144	5 (3.5)	21 (14.6)
10–>10	108	4 (3.7)	18 (16.7)
χ^2 test		$p = 0.296$	$p = 0.495$
Total	505	26 (5.1)	69 (13.7)

[a]*Percentage calculated based on the total of no. samples for each type of sample.*
[b]*Precipitation: 2-days cumulative rainfall before sampling date.*

Shiga-toxin producing *Escherichia coli* strains represented 0.2, 0.2, and 0.3%, of the isolated *E. coli* from sites 1–3, respectively. EPEC strains represented 0.8, 0.6, and 0.7% of the isolated *E. coli* from sites 1–3, respectively (**Table 3**).

For the three sites, the majority of STEC strains derived from freshwater samples (50, 57.1, and 44.4% of samples from sites 1–3, respectively) and from shellfish batches (41.7, 42.9, and 44.4% in the sites 1–3, respectively; **Table 3**). Only two STEC strains were isolated from seawater and surface sediment samples from sites

TABLE 1 | Prevalence of *stx* and *eae* genes in shellfish, freshwater, seawater, and superficial sediment enrichment broths.

Type of sample	No. of samples	No. of *stx*-positive broth (%)[a]	No. of *eae*-positive broth (%)[a]	No. of *stx*- and *eae*-positive broth (%)[a]
Shellfish	238	72 (30.3)	178 (74.8)	64 (26.9)
Freshwater	216	196 (85.9)	216 (100)	196 (85.9)
Seawater	12	5 (41.7)	12 (100)	5 (41.7)
Superficial sediment	39	11 (28.2)	17 (43.6)	8 (20.5)
Total	505	284 (56.2)	423 (83.7)	273 (54.1)

[a]*Percentage calculated based on the total of no. samples for each type of sample.*

TABLE 3 | Number of STEC and EPEC strains isolated from shellfish, freshwater, seawater, and superficial sediment samples collected in the three shellfish-harvesting areas and their watersheds, as regard to the total number of *E. coli* isolates.

Type of sample	Total (%)[a]	Shellfish (%)	Freshwater (%)	Seawater (%)	Superficial sediment (%)
Site 1					
No. *E. coli* isolates	5,676	1,343	3,410	225	30
No. STEC strains	12 (0.2)	5 (41.7)[b]	6 (50.0)[b]	1 (8.3)[b]	0
No. EPEC strains	47 (0.8)	8 (17.4)[b]	35 (76.1)[b]	4 (8.5)[b]	0
Site 2					
No. *E. coli* isolates	3,682	757	2,925	nd[c]	4
No. STEC strains	7 (0.2)	3 (42.9)[b]	4 (57.1)[b]	nd	0
No. EPEC strains	23 (0.6)	10 (43.5)[b]	13 (56.5)[b]	nd	0
Site 3					
No. *E. coli* isolates	2,658	678	2,036	nd	83
No. STEC strains	9 (0.3)	4 (44.4)[b]	4 (44.4)[b]	nd	1 (11.1)[b]
No. EPEC strains	19 (0.7)	5 (26.3)[b]	14 (73.7)[b]	nd	0
Total of the three sites					
No. *E. coli* isolates	12,016	2,778	8,371	225	117
No. STEC strains	28 (0.2)	12 (42.9)[b]	14 (50.0)[b]	1 (3.6)[b]	1 (3.6)[b]
No. EPEC strains	89 (0.7)	23 (25.8)[b]	62 (69.7)[b]	4 (4.5)[b]	0

[a]*Percentage calculated based on the total of no. E. coli isolates from each sites.* [b]*Percentage calculated based on the total of no. STEC or EPEC strains isolated from the three sites.* [c]*nd: non-determined.*

1 and 3, respectively. The majority of EPEC strains derived from the freshwater samples (76.1, 56.5, and 73.7% of samples from sites 1–3, respectively) and the remaining EPEC derived from shellfish batches (17.4, 43.5, and 26.3%, respectively) and seawater samples (8.5% only in the site 1; **Table 3**).

Nearly one third of the STEC strains were obtained from samples collected in May 2013 (32.1%, 9/28), whereas the EPEC strains were mostly obtained from samples collected in November 2013 (21.3%, 19/89) and August 2014 (12.4%, 11/89; **Table 4**). The entire sample set demonstrated a seasonal effect with potential pathogenic *E. coli* as STEC strains were significantly more frequently isolated in Summer and EPEC strains in Summer and Autumn ($p < 0.05$; **Table 2**). However, no correlation between the prevalence of both STEC and EPEC and pluviometry nor temperature was observed (**Table 2**).

Virulence Gene Profiles

By considering the presence of a single virulence gene or a combination of the four virulence genes investigated (i.e., *stx, eae, ehxA,* and *saa*) in the 117 STEC or EPEC strains, eight virulence gene profiles were found. The most frequent profile presented the *eae* gene only (70.1% of the strains) followed by the profile presenting the *stx2* gene only (11.1%) and the profile presenting the *stx1* gene only (7.7%). Seven strains (6.0%) were shown to possess the *eae* and *ehxA* genes. The *stx1-stx2-ehxA-saa* profile was found in three strains and three other virulence gene profiles were observed only once, i.e., the *stx1-eae-ehxA*, the *stx1-stx2-saa*, and the *stx2-ehxA-saa* profiles (**Table 4**).

Seven STEC strains carrying *stx1*, three carrying *stx2*, and two carrying both *stx1* and *stx2* genes were isolated from the site 1 whereas three STEC strains harboring the *stx1* gene, 11 the *stx2* gene, and two presenting both *stx1* and *stx2* genes were recovered from sites 2 and 3.

Phylogroups

The STEC strains ($n = 28$) were mainly distributed among the phylogroups A, B1, and D (39.3, 35.7, 21.4%, respectively). Only one strain belonged to phylogroup B2. The EPEC strains ($n = 89$) belonged to all the phylogroups; the strains from phylogroup B1 and B2 (38.2 and 38.2%, respectively) being more prevalent than those from phylogroups A and D (18.0 and 5.7%, respectively; **Table 5**). More precisely, at site 1, the STEC strains were mainly divided between phylogroups B1 and D. At sites 2 and 3, the STEC strains were divided between phylogroups A and B1. At sites 1–3, the EPEC strains belonged to all the investigated phylogroups, with a majority belonging to phylogroups B1 and B2.

Serotyping

The 117 (STEC or EPEC) strains selected in this study belonged to 44 O antigens and 24 H antigens and presented 75 distinguishable serotypes (**Table 4**). Among all strains, 13 strains were non-typable (NT) for the O antigen [ONT:H2 ($n = 1$), ONT:H31 ($n = 1$), ONT:H34 ($n = 1$), ONT:H6 ($n = 6$), ONT:H8 ($n = 2$), ONT:H10 ($n = 1$), ONT:H11 ($n = 1$)] and 24 strains were uncharacterized for the H antigen (HNM: non-motile or HNT: non-typable).Two strains were non-typable for either antigens (ONT:HNT).

Eighteen different serotypes (O:H) were identified among the STEC strains. Only one STEC belonging to one of the five highly pathogenic serotypes was isolated: an O26:H11 $stx1^{+}$, eae^{+}, and $ehxA^{+}$ strain, from a mussel batch. One strain from serotype O91:H21 and carrying *stx1*, *stx2*, *ehxA,* and *saa* genes was also identified among the STEC strains. The most detected serotype among the STEC strains was the O100:HNM ($n = 9$). Fifteen additional serotypes (O149:H31/HNM, O154:H31/HNM, O130:H11, O15:H16, O185:H28, O2:H32, O28:H1, O63:H11, O76:H19, O8:H12, O88:H25, ONT:H10, and ONT:H11) were

TABLE 4 | Characteristics of STEC and EPEC strains isolated from the three French shellfish-harvesting sites from the Eastern English Channel coastal area and their watersheds.

Serotype (no. of isolate)	Virulence gene (no. of isolate)	Sample origin (no. of isolate)	Sampling site (no. of isolate)	Sampling month-year	Precipitation (mm)
STEC					
O100:HNM (9)	*stx2*	SFm(1), SFc(1),	2	May-13	0.1
		FW(1), SFo(1), SFm(1)	3	May-13	0.1
		SFm(1), S(1)	3	June-13	6.1
		SFm	2	March-14	0.1
		SFo	3	June-14	0
O15:H16(1)	*stx2*	SFm	1	June-13	0.2
O2:H32(1)	*stx2*	SW	1	February-14	0
O8:H19(2)	*stx2*	FW	3	June-14	0
		FW	3	July-14	1.4
O149:H1(1)	*stx1*	FW	1	April-13	1.6
O149:HNM(1)	*stx1*	FW	1	April-13	1.6
O154:H31(2)	*stx1*	SFo(1), FW(1)	1	May-13	0.1
O154:HNM(1)	*stx1*	SFm	1	November-14	15.4
O28: H1(1)	*stx1*	SFc	1	March-14	0.1
O76:H19(1)	*stx1*	FW	2	August-14	26.0
O88:H25(1)	*stx1*	FW	2	September-14	0.4
ONT:H10(1)	*stx1*	FW	2	April-14	0.3
O26:H11(1)	*stx1+eae+ehxA*	SFm	1	November-13	15.4
O63:H6(1)	*stx2+ehxA+saa*	FW	1	November-14	24.0
ONT:H11(1)	*stx1+stx2+saa*	FW	1	May-13	1.8
O185:H28(1)	*stx1+stx2+ehxA+saa*	FW	2	Apr-13	1.6
O130:H11(1)	*stx1+stx2+ehxA+saa*	FW	1	December-13	0
O91:H21(1)	*stx1+stx2+ehxA+saa*	FW	3	May-13	1.8
EPEC					
O103:H25(1)	*eae*	FW	3	March-14	0.1
O103:HNM(1)	*eae*	FW	1	February-14	0
O108:H21(3)	*eae*	FW	3	November-13	0.1
		SFc	2	January-14	6.5
		FW	3	July-14	1.4
O113:H6(4)	*eae*	SFm(1), SFc(1)	1	November-13	15.4
		FW	3	November-13	0.1
		SFo	3	August-14	26
O116:H20(1)	*eae*	FW	1	November-13	15.4
O125:H6(2)	*eae*	FW	1	November-13	15.4
		FW	2	September-14	0.4
O128:H2(1)	*eae*	FW	2	November-13	0
O137:H6(2)	*eae*	FW	1	August-13	1.0
		FW	3	January-15	2.3
O145:H34(1)	*eae*	FW	1	July-14	6.5
O146:H21(1)	*eae*	SFm	3	August-14	26.0
O146:H6(1)	*eae*	SFc	2	September-14	0.4
O15:H2(2)	*eae*	FW	3	August-14	26.0
		SFm	2	January-15	2.3
O153:H21(1)	*eae*	FW	1	January-14	7.2
O157:H16(1)	*eae*	FW	1	July-14	6.5
O159:H7(1)	*eae*	FW	1	November-14	24.0
O167:H3(1)	*eae*	FW	1	August-13	2.8
O179:H31(2)	*eae*	FW	1	January-14	7.2
		FW	3	June-14	0
O2:H45(1)	*eae*	FW	2	December-13	0
O20:HNT(1)	*eae*	SW	1	April-14	0

(Continued)

TABLE 4 | Continued

Serotype (no. of isolate)	Virulence gene (no. of isolate)	Sample origin (no. of isolate)	Sampling site (no. of isolate)	Sampling month-year	Precipitation (mm)
O23:H8(2)	*eae*	FW	2	August-13	0.7
		SFc	2	August-14	26.0
O25:H2(1)	*eae*	FW	1	September-14	0
O28:H16(1)	*eae*	SFm	1	November-13	15.4
O29:H19(1)	*eae*	FW	2	October-13	22.8
O33:H6(1)	*eae*	FW	1	February-14	0
O39:HNM(1)	*eae*	FW	1	January-14	7.2
O40:HNM(1)	*eae*	FW	1	February-14	0
O42:H37(1)	*eae*	FW	3	March-13	0
O5:H40(1)	*eae*	SFm	2	February-13	0.8
O51:HNM(1)	*eae*	FW	2	October-13	22.8
O63:H6(4)	*eae*	FW	1	November-13	15.4
		FW	2	November-13	0.1
		FW	1	January-14	7.2
		FW	3	October-14	0.5
O63:HNM(1)	*eae*	FW	3	October-14	0.5
O71:H49(2)	*eae*	SFm(1), SFc(1)	1	October-13	0.4
O71:HNM(1)	*eae*	FW	1	August-14	1.0
O8:H14(1)	*eae*	FW	1	November-13	15.4
O85:H31(1)	*eae*	FW	1	October-14	8.3
O85:HNM(1)	*eae*	FW	1	August-14	1.0
O86:H31(1)	*eae*	SFc	2	August-14	26.0
O88:H25(1)	*eae*	SFm	3	September-14	0.4
O88:H8(1)	*eae*	SFo	3	August-14	26.0
O9:HNM(1)	*eae*	FW	2	November-13	0.1
O91:H10(1)	*eae*	SFc	1	July-14	6.5
O98:H56(1)	*eae*	FW	1	December-14	0
O98:H8(1)	*eae*	SFm	1	November-13	15.4
O98:HNM(2)	*eae*	SW	1	February-14	0
		FW	1	March-14	0
O98:HNT(1)	*eae*	FW	1	December-14	0
ONT:H2(1)	*eae*	FW	1	August-13	2.8
ONT:H31(1)	*eae*	FW	1	October-14	8.3
ONT:H34(1)	*eae*	FW	3	December-14	10.6
ONT:H6(6)	*eae*	FW	1	September-13	1.0
		FW	1	August-14	1.0
		FW	3	September-14	0.4
		FW	3	October-14	0.5
		SFm	2	December-14	0
		SW	1	December-14	10.6
ONT:H8(2)	*eae*	FW	1	April-14	0
		FW	1	August-14	1
ONT:HNT(2)	*eae*	SW	1	November-14	24.0
		FW	3	October-14	10.6
O28:HNM(1)	*eae+ehxA*	FW	1	June-14	0.2
O145:H28(2)	*eae+ehxA*	SFm(1), SFc(1)	2	June-13	6.1
O177:H11(1)	*eae+ehxA*	FW	2	July-14	1.4
O26:H11(6)	*eae(5), eae+ehxA(1)*	FW	2	August-13	0.7
		FW(3), SFm(1), SFc(1)	1	November-13	15.4
O103:H2(3)	*eae(2), eae+ehxA(1)*	FW	2	February-13	0.8
		FW	2	June-13	6.1
		FW	1	November-13	15.4
O153:H2(3)	*eae(2), eae+ehxA(2)*	SFm(1), FW(1)	2 (1), 3 (1)	March-14	0.1
		SFc	2	July-14	1.4

NT, non-typable; NM, non-motile. Sample origin: SF: shellfish, o: oyster, m: mussel, c: cockle, FW: freshwater, SW: seawater, S: superficial sediment. ( ): number of strain and when it is not specified the no. of strain is one. (1) Brittany site, (2) first Normandy site, and (3) second Normandy site. Precipitation: 2-days cumulative rainfall before sampling date.

TABLE 5 | Distribution of phylogroup A, B1, B2, and D among STEC and EPEC strains isolated in the three French shellfish-harvesting sites from the Eastern English Channel coastal area and their watersheds.

Phylogroup	Total	A (%)	B1 (%)	B2 (%)	D (%)
Site 1					
No. STEC strains (%)[a]	12	2 (16.7)	4 (33.3)	0	6 (50.0)
No. EPEC strains (%)[b]	47	13 (27.7)	13 (27.7)	19 (40.4)	2 (4.4)
Site 2					
No. STEC strains (%)[a]	7	3 (42.9)	3 (42.9)	1 (14.2)	0
No. EPEC strains (%)[b]	23	2 (8.7)	13 (56.5)	5 (21.7)	3 (13.0)
Site 3					
No. STEC strains (%)[a]	9	6 (66.7)	3 (33.3)	0	0
No. EPEC strains (%)[b]	19	1 (5.3)	8 (42.1)	10 (52.6)	0
Total of the three sites					
No. STEC strains (%)[c]	28	11 (39.3)	10 (35.7)	1 (3.6)	6 (21.4)
No. EPEC strains (%)[c]	89	16 (18.0)	34 (38.2)	34 (38.2)	5 (5.7)

[a]*Percentage calculated based on the total no. of STEC strains isolated from each site.* [b]*Percentage calculated based on the total no. of EPEC strains isolated from each site.* [c]*Percentage calculated based on the total no. of STEC and EPEC strains isolated from the three sites.*

identified within the STEC strains and contained one or two individual isolates each.

Fifty-seven serotypes were identified among the EPEC strains. Eleven strains belonged to the highly pathogenic serotypes: O26:H11 ($n = 6$), O103:H2 ($n = 3$), and O145:H28 ($n = 2$). The remaining EPEC strains belong to a large diversity of serotypes listed in **Table 4**.

It should be noted that some serotypes were isolated at different months and in different types of samples. For example, the nine strains of serotype O100:HNM *stx2*$^+$ were isolated from seven shellfish batches ($n = 7$; oyster, mussel, and common cockle batches), from one freshwater ($n = 1$) and from one surface sediment sample ($n = 1$). Three O154:H31 *stx1*$^+$ and their immotile form were isolated from two shellfish batches ($n = 2$; oyster and mussel batches) and from one freshwater sample ($n = 1$). The EPEC serotypes, O108:H21 ($n = 3$), O113:H6 ($n = 4$), O15:H2 ($n = 2$), O153:H2 ($n = 3$), O23:H8 ($n = 2$), O26:H11 ($n = 6$), and O71:H49/HNM ($n = 3$) were all isolated from shellfish batches and also from freshwater samples (**Table 4**).

The same serotypes were sometimes isolated from geographically independent sites. For example, serotypes O103:H2, O125:H6, and O26:H11 were isolated from sites 1 and 2 and serotypes O113:H6, O137:H6, and O179:H31 from sites 1 and 3. Finally, the O63:H6 and ONT:H6 serotypes were isolated from all the three sites (**Table 4**).

PFGE and MLST Profiles

The genetic relatedness of 26 STEC and 79 EPEC strains was investigated by PFGE and MLST analysis (Supplementary Figure S2). Seventy-nine distinguishable PFGE patterns (PT) and 46 distinguishable sequence types (STs) were obtained. Seven other STs (seven strains, one STEC and six EPEC) were obtained but have not as yet been described. These results demonstrate a high level of genetic diversity among the strains isolated. The highest diversity was observed for the EPEC strains, which represented 8.1% of the PTs identified (64/79) and 71.7% of the STs (33/46).

The STEC serotype O100:HNM ($n = 9$) presented identical PT (D) and ST (ST933; **Figure 1A**) despite of their three specificities: isolated (a) from oyster, mussel, and common cockle batches, freshwater, and superficial sediment samples, (b) from the sites 2 and 3, (c) during the sampling campaigns of May 2013, June 2013, March 2014, and June 2014. With regards to the major serotypes (**Figure 1B**), the six EPEC O26:H11 strains presented three additional PTs (i.e., L, BV, and AL) and two STs (i.e., ST29 and ST48) isolated from mussel and common cockle batches and freshwater samples. One of those belonging to the ST29 was isolated from the same mussel batch from which the STEC O26:H11 belonging to the ST21 was isolated. A unique PT (I) was observed for the two EPEC O145:H28 (ST not yet described), isolated from mussel and common cockle batches and sampled during the same campaign (June 2013). Both O103:H2 isolated during two different months (i.e., June 2013 and November 2013) had distinguishable PTs (i.e., M and N) and STs (i.e., ST1146 and ST343). Additionally, identical PTs and STs were found among the other STEC and EPEC strains isolated from different types of sample (i.e., shellfish vs. freshwater) or between shellfish batches (i.e., mussel vs. common cockle) and between freshwater samples, often from samples taken from the same sites on the same date (e.g., O153:H2, O108:H21 serotypes; Supplementary Figure S2).

Biofilm Formation

Biofilm formation by a subset of 13 EPEC and nine STEC strains was evaluated at 18 and 30°C on plastic surface. At both temperatures, strains varied in their ability to form biofilm (OD590 = 0.03 for the lowest, OD590 = 1.9 for the highest). In general, a large number of strains were strongly to moderately adherent and more strains formed a biofilm at 18 than at 30°C (**Figure 2**). Indeed, 11 of the 22 strains formed strong biofilms [serotypes O2:H32, O149:H1, ONT:H11, O91:H21, O185:H28, O26:H11 ($n = 2$), O145:H28 ($n = 1$), O103:H2 ($n = 3$)], six formed medium biofilms [serotypes O26:H11 ($n = 3$), O145:H28 ($n = 2$) and O125:H6] and five formed weak biofilms or no biofilm at all [serotypes O100:HNM, O154:H31, O15:H16, and O26:H11 ($n = 2$)]. At 30°C, 11 strains formed strong biofilms [serotypes O2:H32, O149:H1, ONT:H11, O91:H21, O185:H28, O145:H28 ($n = 3$), O103:H2 ($n = 2$) and O125:H6] but

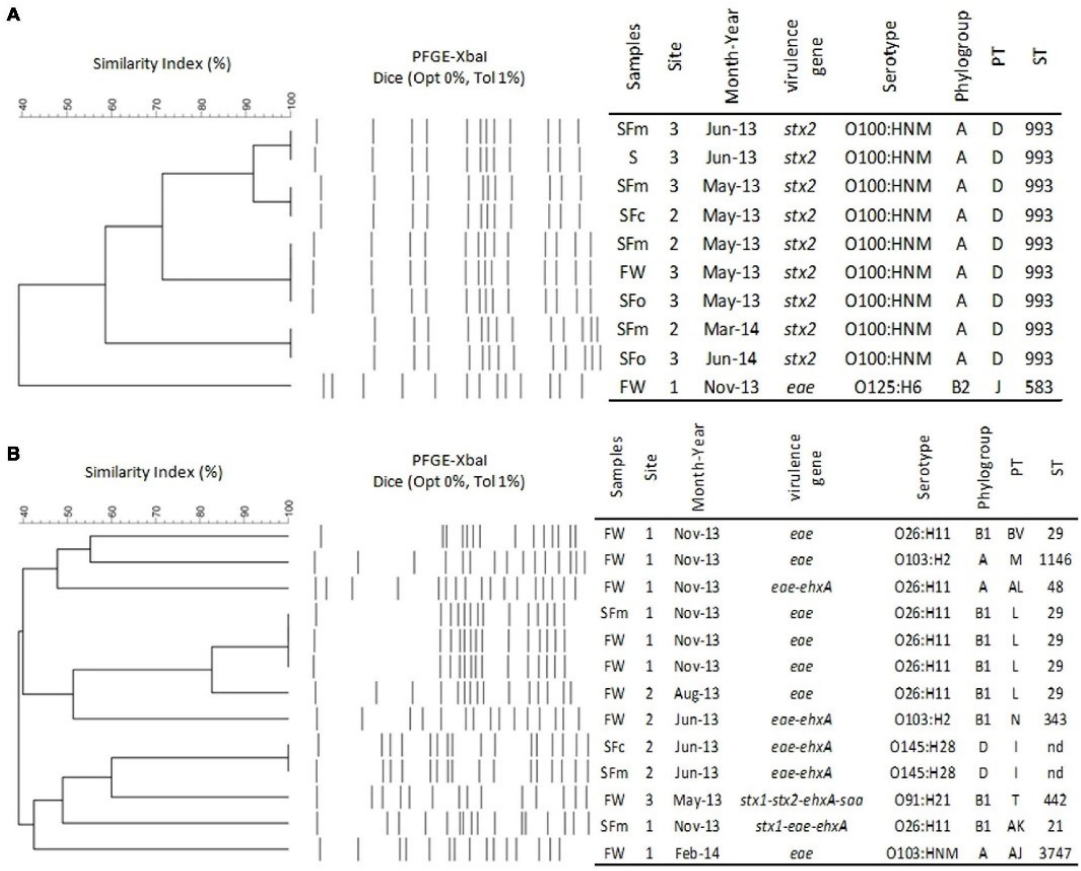

Samples	Site	Month-Year	virulence gene	Serotype	Phylogroup	PT	ST
SFm	3	Jun-13	*stx2*	O100:HNM	A	D	993
S	3	Jun-13	*stx2*	O100:HNM	A	D	993
SFm	3	May-13	*stx2*	O100:HNM	A	D	993
SFc	2	May-13	*stx2*	O100:HNM	A	D	993
SFm	2	May-13	*stx2*	O100:HNM	A	D	993
FW	3	May-13	*stx2*	O100:HNM	A	D	993
SFo	3	May-13	*stx2*	O100:HNM	A	D	993
SFm	2	Mar-14	*stx2*	O100:HNM	A	D	993
SFo	3	Jun-14	*stx2*	O100:HNM	A	D	993
FW	1	Nov-13	*eae*	O125:H6	B2	J	583

Samples	Site	Month-Year	virulence gene	Serotype	Phylogroup	PT	ST
FW	1	Nov-13	*eae*	O26:H11	B1	BV	29
FW	1	Nov-13	*eae*	O103:H2	A	M	1146
FW	1	Nov-13	*eae-ehxA*	O26:H11	A	AL	48
SFm	1	Nov-13	*eae*	O26:H11	B1	L	29
FW	1	Nov-13	*eae*	O26:H11	B1	L	29
FW	1	Nov-13	*eae*	O26:H11	B1	L	29
FW	2	Aug-13	*eae*	O26:H11	B1	L	29
FW	2	Jun-13	*eae-ehxA*	O103:H2	B1	N	343
SFc	2	Jun-13	*eae-ehxA*	O145:H28	D	I	nd
SFm	2	Jun-13	*eae-ehxA*	O145:H28	D	I	nd
FW	3	May-13	*stx1-stx2-ehxA-saa*	O91:H21	B1	T	442
SFm	1	Nov-13	*stx1-eae-ehxA*	O26:H11	B1	AK	21
FW	1	Feb-14	*eae*	O103:HNM	A	AJ	3747

FIGURE 1 | Focused dendograms of *XbaI* PFGE patterns (PTs), characteristics and Sequence Types (STs) of 9 STEC O100:HNM (A) and the 13 major serotypes (B) isolated from freshwater (FW), shellfish (SF) [oyster (o), mussel (m), or cockle (c)] and superficial sediment (S), from the Brittany site (1) and the two Normandy sites (2 and 3). The similarity of PFGE profiles was compared and dendogram was created with the Bionumerics software 7.5 (Applied Maths, Belgium), using the band-based Dice unweighted-pair group method, using average linkages (UPGMA), based on 1% position tolerance. NT: non-typable, NM: non-motile, nd: not determined.

fewer ($n = 2$) were able to form a medium biofilm (O26:H11 and O145:H28) and nine formed a weak biofilm [serotypes O100:HNM, O15:H16, O154:H31, O26:H11 ($n = 6$); **Figure 2**]. Interestingly, all O26:H11 strains formed significantly (Mann–Whitney test) more biofilm ($p < 0.05$) at 18°C than at 30°C.

Antibiotic Resistance

Antimicrobial susceptibility testing based on the disk diffusion method was performed on 38 EPEC strains and on all STEC strains ($n = 28$). Most of the analyzed STEC and EPEC strains [i.e., 85.7% (24/28) and 73.7% (28/38), respectively] were sensitive toward all 16 used antibiotics. Only four STEC strains were resistant to one antibiotic (i.e., Doxycyclin). With regard to EPEC, 7.9% (3/38) of strains [i.e., serotypes O63:H6, O71:H49, and O98:H8] were resistant to one antibiotic (i.e., Doxycyclin or Imipenem) and 13.2% (5/38) of strains were resistant to two antibiotics (i.e., Cefotaxim/Cefoxitin, O63:H6 or Doxycyclin/Bactrim, O26:H11 or Ticarcillin/Amoxicillin, O26:H11, $n = 3$). One of the O26:H11 serotype was resistant to three antibiotics (i.e., Gentamycin/Ticarcillin/Amoxicillin). Finally, the O2:H45 serotype ($n = 1$) was resistant to four antibiotics (i.e., Cefalotin/Imipenem/Cefotaxim/Cefoxitin).

DISCUSSION

To our knowledge, this study is the first to focus on the detection and characterization of environmental STEC and EPEC strains from shellfish-harvesting areas and their upstream watershed. Overall, among the environmental samples analyzed ($n = 505$), very few STEC (0.2%, $n = 28$) or EPEC (0.7%, $n = 89$) strains were obtained from the *E. coli* that were isolated ($n = 12{,}016$) and in comparison with the number of shellfish, water or surface sediment samples that were found to be positive for *stx* and

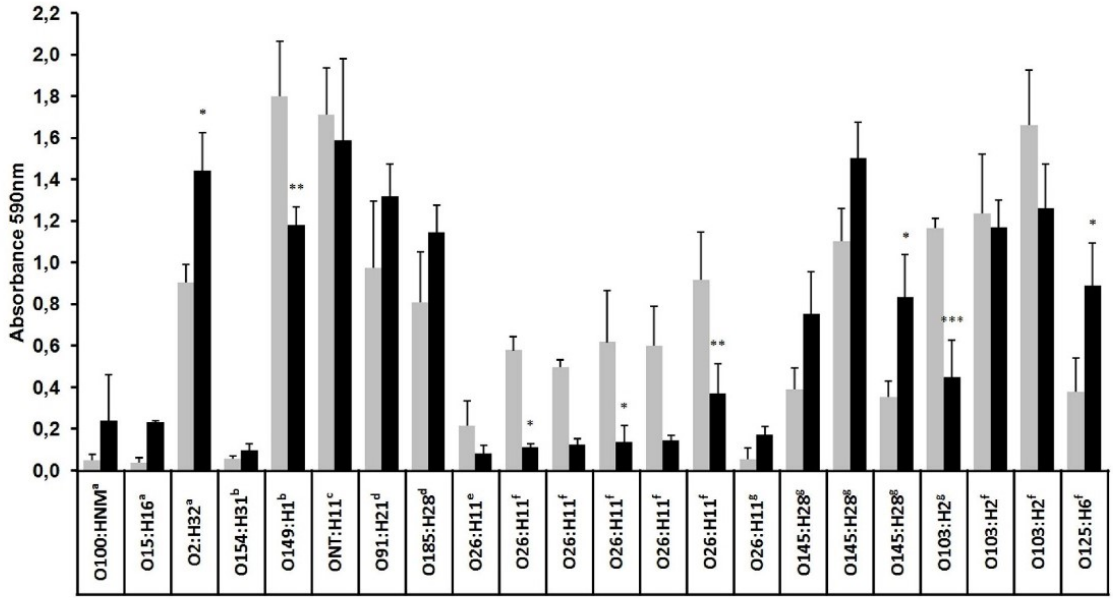

FIGURE 2 | Biofilm formation by EPEC and STEC strains at low and high temperatures. Biofilms were formed on polystyrene in M9 medium supplemented with glucose (0.4% wt/vol) at 18°C (gray bars) or 30°C (dark bars) for 24 h and were stained with crystal violet, and the absorbance at 590 nm was measured. The results are the average of at least three biological replicates and the error bar represent the standard error. The results for the static biofilms formed at 18 and 30°C were compared using two-way analysis of variance (ANOVA) followed by a Bonferroni *post hoc* comparison. $^{*}p < 0.05$; $^{**}p < 0.01$; $^{***}p < 0.001$. [a]*stx2*$^{+}$, [b]*stx1*$^{+}$, [c]*stx1*$^{+}$-*stx2*$^{+}$, [d]*stx1*$^{+}$-*stx2*$^{+}$-*ehxA*$^{+}$-*saa*$^{+}$, [e]*stx1*$^{+}$-*eae*$^{+}$, [f]*eae*$^{+}$, [g]*eae*$^{+}$-*ehxA*$^{+}$.

eae genes (54.1%, 273/505). The higher proportion of EPEC than STEC strains isolated from these environmental samples is in agreement with the results obtained in previous studies (Hamilton et al., 2010; Chandran and Mazumder, 2015). For example, only 3.6% EPEC and no STEC were detected among the 24,493 *E. coli* isolated from seawater collected in Santa Catalina Island, CA, USA (Hamilton et al., 2010). Conversely, more STEC strains (6.2%) than EPEC strains (1.8%) were isolated from water samples from the Yeongsan river basin in South Korea ($n = 3{,}480$ *E. coli*; Jang et al., 2014). The low level of isolation of STEC or EPEC vs. the high frequency of detection of genetic markers in the analyzed samples has also been observed in various studies focusing on cattle feces, food, and samples from the environment (Miyagi et al., 2001; Bai et al., 2015; Bibbal et al., 2015). The low level of isolation of STEC vs. the high detection of *stx* genes in the environmental samples could be explained by the presence of free *stx*-encoding bacteriophages in the environment (Martinez-Castillo et al., 2013) and the presence of viable but non-culturable or dead bacteria as a result of the stressful conditions (sunlight, salinity, oligotrophy, predation, etc.) in riverine and especially coastal environments (Gourmelon et al., 1997, for review Rozen and Belkin, 2001). The difficulties of isolating these bacteria from environmental samples containing a significant background flora could also contribute to this low recovery of strains (Pradel et al., 2000; Gourmelon et al., 2006).

The strains isolated in coastal areas of Brittany (site 1) and Normandy (sites 2 and 3) present a high diversity of serotypes as has been previously reported for environmental samples in California or Spain (García-Aljaro et al., 2005; Cooley et al., 2014). A subset of the serotypes isolated in the present study was previously isolated from humans, animals, or the environment. Serotypes such as O8:H14, O26:H11, O76:H19, O91:H21, O103:H2/HNM, O145:H28, and O154:H31 have previously been associated with human infections (Beutin and Fach, 2014). In addition, STEC serotypes O130:H11 and O154:HNM were detected in healthy cattle and waters (Hornitzky et al., 2002), the serotype O157:H16 in dogs, humans, and in the environment (Feng et al., 2012), and the serotype O149:H1 in shellfish (Gourmelon et al., 2006). The STEC O100:HNM was previously detected in swine fecal samples, wild boar feces, and drinking water contaminated by waste water (García-Aljaro et al., 2005; Lienemann et al., 2011; Mora et al., 2012).

In addition, a high genetic diversity among the 105 genotyped strains was observed, with 79 PFGE patterns and 46 distinguishable sequence types in agreement with the high genetic diversity observed by PFGE in other studies for STEC and EPEC strains (Bibbal et al., 2015; Singh et al., 2015). In this study, PFGE was found to be more discriminatory than MLST as previously described for bacteria such as *Salmonella* isolated in Californian coastal waters (Walters et al., 2013). For example, seven strains belonging to ST10 (seven different serotypes) were further discriminated into seven distinct PTs (S, AG, AH, AW, X, G, and Y). The identification of numerous PTs and STs highlights the potential presence of different strains in a same sample and

the presence of genetic diversity between strains belonging to the same serotype (e.g., *E. coli* O26:H11 ST21 and ST29 in the same mussel batch).

The non-detection of *E. coli* from the O157:H7 serotype in the shellfish, water and surface sediment samples investigated (from February 2013 to February 2014 ($n = 282$, Balière et al., 2015) is in agreement with the low detection or absence of *E. coli* O157 in shellfish and environmental water previously observed (Miyagi et al., 2001; Manna et al., 2008).

Several EPEC strains belonging to the highly pathogenic serogroups (i.e., O26, O103, and O145) were also isolated from some of the shellfish batches or freshwater samples that were analyzed. The STEC O26:H11 ST21 found in a mussel batch was shown to be implicated in STEC infections and has been detected in cattle in Europe (Zweifel et al., 2013).

The EPEC O26:H11 ST29 isolated in this study can be strains with no previous contact with *stx*-bacteriophages or bacteria that have lost the *stx*-bacteriophage either during their passage from their original source to water or shellfish or during their isolation steps. The presence of these bacteria in coastal environments could present a risk to human health as these EPEC could be lysogenized by *stx1*- or *stx2*-converting bacteriophages, which are present in the same environment and could become STEC of the highly pathogenic serotypes. In fact, Bielaszewska et al. (2007) demonstrated that STEC O26 strains can lose their *stx*-bacteriophages and become EPEC O26, and conversely EPEC O26 can be lysogenized by *stx1*- or *stx2*-bacteriophages and become STEC O26. Even if the conversion of strains was found to occur in the digestive tract of different animals (Toth et al., 2003) and in various food matrices (Imamovic et al., 2009), the environment could also provide the conditions for conversion of strains. However, the potential conversion of *E. coli* strains in the environment still needs to be evaluated in more details (Dumke et al., 2006). Interestingly, Solheim et al. (2013) have demonstrated the conversion of an *E. coli* strain (serotype O103:H25) by bacteriophages in a biofilm at 37°C, but also at 20°C.

In addition, another STEC strain isolated in a freshwater sample could present a potential human risk. Indeed, an O91:H21 *E. coli* was found to belong to ST442, a sequence type that had previously been isolated from adult patients in Germany with symptoms that ranged from diarrhea to hemolytic uremic syndrome (Mellmann et al., 2009).

The majority of strains isolated in this study would present low virulence as most of the isolated strains (87.2%) possessed only one of the five virulence genes (*stx1, stx2, eae, ehxA,* or *saa)*; i.e., 70.1% of the strains carried the *eae* gene, 7.7% *stx1* and 11.1% *stx2*). The STEC O26:H11 was the only STEC isolate to carry the *eae* gene. These results are in agreement with previous studies describing STEC strains isolated from the environment (García-Aljaro et al., 2005) with the exception of the analysis of water samples from a Californian central coast agricultural region where Cooley et al. (2014) showed that the majority of STEC strains isolated contained *stx1*, *stx2,* and *eae* genes. The low level of isolation of STEC strains carrying the *saa* gene encoding another adherence factor, the STEC autoagglutinating adhesion, or the gene *ehxA* encoding enterohemolysin A was in agreement with the results obtained from water samples in Spain by García-Aljaro et al. (2005).

Most of the STEC strains in this study were classified into the A, B1, and D phylogroups. Phylogroups A and B1 were also the main phylogroups of environmental STEC strains isolated by García-Aljaro et al. (2005) in Spain. In the Yeongsan river basin of South Korea, STEC strains isolated belonged mainly to phylogroup D and to a lesser extent to phylogroups A, B1, and B2 (Jang et al., 2014). In Brittany and Normandy, overall, the EPEC strains belonged mainly to phylogroups B1 and B2 and to a lesser extent to A and D. EPEC strains isolated from water samples in South Korea belonged mainly to the B2 phylogroups (Jang et al., 2014). The frequent isolation of *E. coli* from B1 phylogroup in the present study is in agreement with recent data showing that environmentally persistent *E. coli* belong mainly to the B1 phylogroup (Berthe et al., 2013).

Phenotypic differences in the ability to form biofilms among tested strains underline the genetic diversity of STEC or EPEC strains. Our study demonstrates that more than half of the tested strains (17/22) were able to form biofilms on polystyrene at 18 or 30°C, and most of these strains were able to form strong biofilm at 18°C, a temperature close to marine environment condition. A similar result had been observed previously when *E. coli* K12 biofilm was grown at low temperature (White-Ziegler et al., 2008). It has been shown that low temperatures (<30°C) promote the expression of genes associated with biofilm development, including genes involved in curli (*csgA* and *mlrA*) or cellulose (*yaiC*) production (Olsen et al., 1989; Arnqvist et al., 1992; White-Ziegler et al., 2008). Interestingly, although O26:H11 strains formed weaker biofilms than other strains, they formed significantly stronger biofilms at 18°C than at 30°C. Also, all but one O26:H11 strains were negative for *pgaA*, a gene coding for the export of poly-*N*-acetyl-D-glucosamine (PGA) that promotes biofilm formation (Itoh et al., 2008; data not shown). In addition, *pgaA* sequence is also absent in the sequenced genomes of STEC O26 strains available in GenBank. In conclusion, the ability of strains to form a biofilm might contribute to their persistence in coastal environments.

This study highlights the presence of a specific geographic distribution of some of the STEC and EPEC serotypes and a persistence of some of these serotypes in the coastal environments from Brittany and Normandy investigated in this study. The isolation of the serotype O100:HNM positive for *stx2* (PT D and ST993), at different dates (over a period of 1 year), in shellfish, waters and surface sediments from both sites in Normandy (sites 2 and 3), but its absence in Brittany (site 1), highlights potential specific contamination sources in these region and the higher persistence of some of these specific strains. This had previously been shown in water samples from California for O157 strains isolated up to 19 months apart by Cooley et al. (2014). The various livestock breeding in the three watersheds, i.e., mainly swine, poultry and bovine in Brittany and sheep, bovine and swine in Normandy, could explain differences in strain detection at specific sites. A potential explanation of the frequent isolation of the STEC O100:HNM is the high carriage of this *E. coli* strain in the animals in the upstream watersheds. Bibbal et al. (2015) have identified farms harboring STEC bovine carriers, highlighting the

fact that STEC of a given serotype could be carried by several animals belonging to the same farm. A probable prediction of the presence of these STEC strains in the coastal environment is their re-introduction to the water and consequently to shellfish from animal reservoirs, which enables persistence at high titer for months (Cooley et al., 2014). Another explanation could be that they are present in surface sediments in which a better persistence could occur and then they are re-introduced to the water and then filtered and accumulated by shellfish. The evaluation of the persistence of STEC and EPEC (especially those isolated several times in this study, i.e., *E. coli* O100 and *E. coli* O26) in freshwaters and seawaters and in shellfish needs to be studied to better understand their frequent detection in such shellfish-harvesting areas. Several studies have been carried out to evaluate the persistence of STEC in water or superficial sediments and these have shown that some *E. coli* strains are able to persist in the environment for periods of a few days to several months (Fremaux et al., 2010) and that the persistence could be variable according to the serotypes (Ma et al., 2014).

This study critically evaluated the nature of STEC and EPEC strains present in coastal environments. Knowledge of strains circulating in the environment is crucial to the investigation of potential new STEC serotypes and their human health risk. These results confirm that the environment is a reservoir for these strains. The presence of both EPEC strains and *stx*-converting bacteriophages in the same samples could lead to new pathogenic *E. coli*.

The risk of a human infection by STEC caused by shellfish consumption seems to be limited for two reasons. First, a depuration step or relaying step has to be performed before shellfish from category B and C areas, respectively, reach market. Secondly, STEC were present in only a few samples and the majority of STEC strains lacked genes associated with high human virulence, such as *eae,* and few of the STEC isolated in this study have previously been shown to be involved in human infections.

ACKNOWLEDGMENTS

This work was funded by the European Regional Development Fund Interreg IVA Programme, as part of the collaborative project RiskManche. The thesis of CB was supported by a grant from Ifremer and the Agence de l'Eau Loire-Bretagne. We thank Clémence Balière from the University of Caen and Céline Courroux from Hôpital Robert-Debré, for their participation in the sampling and technical assistance and Dominique Hervio-Heath (Ifremer) and Huw Taylor (University of Brighton, UK) for their critical review of the manuscript. Work in the LREC-USC-laboratory was financed by the grant CN2012/303 from Consellería de Cultura, Educación e Ordenación Universitaria (Xunta de Galicia) and The European Regional Development Fund, ERDF).

SUPPLEMENTARY MATERIAL

The Supplementary Material for this article can be found online at: http://journal.frontiersin.org/article/10.3389/fmicb.2015.01356

REFERENCES

Anonymous (2004). Regulation (EC) No 854/2004 of the European parliament and of the council of 29 April 2004 laying down specific rules for the organisation of official controls on products of animal origin intended for human consumption. *Official J. Euro. Union* L139, 83–127.

Arnqvist, A., Olsen, A., Pfeifer, J., Russell, D. G., and Normark, S. (1992). The Crl protein activates cryptic genes for curli formation and fibronectin binding in *Escherichia coli* HB101. *Mol. Microbiol.* 6, 2443–2452. doi: 10.1111/j.1365-2958.1992.tb01420.x

Bai, X., Wang, H., Xin, Y., Wei, R., Tang, X., Zhao, A., et al. (2015). Prevalence and characteristics of Shiga toxin-producing *Escherichia coli* isolated from retail raw meats in China. *Int. J. Food Microbiol.* 200, 31–38. doi: 10.1016/j.ijfoodmicro.2015.01.018

Balière, C., Rincé, A., Thevenot, D., and Gourmelon, M. (2015). Successful detection of pathogenic Shiga-toxin-producing *Escherichia coli* in shellfish, environmental waters and sediment using the ISO/TS-13136 method. *Lett. Appl. Microbiol.* 60, 315–320. doi: 10.1111/lam.12386

Bennani, M., Badri, S., Baibai, T., Oubrim, N., Hassar, M., Cohen, N., et al. (2011). First detection of Shiga toxin-producing *Escherichia coli* in shellfish and coastal environments of Morocco. *Appl. Biochem. Biotechnol.* 165, 290–299. doi: 10.1007/s12010-011-9251-x

Berthe, T., Ratajczak, M., Clermont, O., Denamur, E., and Petit, F. (2013). Evidence for coexistence of distinct *Escherichia coli* populations in various aquatic environments and their survival in estuary water. *Appl. Environ. Microbiol.* 79, 4684–4693. doi: 10.1128/AEM.00698-13

Beutin, L., and Fach, P. (2014). Detection of Shiga toxin-producing *Escherichia coli* from nonhuman sources and strain typing. *Microbiol. Spectr.* 2, EHEC–0001–2013. doi: 10.1128/microbiolspec.EHEC-0001-2013

Bibbal, D., Loukiadis, E., Kerouredan, M., Ferre, F., Dilasser, F., de Garam, C. P., et al. (2015). Prevalence of carriage of Shiga toxin-producing *Escherichia coli* serotypes O157:H7, O26:H11, O103:H2, O111:H8, and O145:H28 among slaughtered adult cattle in France. *Appl. Environ. Microbiol.* 81, 1397–1405. doi: 10.1128/aem.03315-14

Bidet, P., Mariani-Kurkdjian, P., Grimont, F., Brahimi, N., Courroux, C., Grimont, P., et al. (2005). Characterization of *Escherichia coli* O157:H7 isolates causing haemolytic uraemic syndrome in France. *J. Med. Microbiol.* 54, 71–75. doi: 10.1099/jmm.0.45841-0

Bielaszewska, M., Prager, R., Köck, R., Mellmann, A., Zhang, W., Tschäpe, H., et al. (2007). Shiga toxin gene loss and transfer in vitro and in vivo during enterohemorrhagic *Escherichia coli* O26 infection in humans. *Appl. Environ. Microbiol.* 73, 3144–3150. doi: 10.1128/AEM.02937-06

Blanco, M., Blanco, J. E., Mora, A., Rey, J., Alonso, J. M., Hermoso, M., et al. (2003). Serotypes, virulence genes, and intimin types of Shiga toxin (verotoxin)-producing *Escherichia coli* isolates from healthy sheep in Spain. *J. Clin. Microbiol.* 41, 1351–1356. doi: 10.1128/JCM.41.4.1351-1356.2003

Chandran, A., and Mazumder, A. (2013). Prevalence of diarrhea-associated virulence genes and genetic diversity in *Escherichia coli* isolates from fecal material of various animal hosts. *Appl. Environ. Microbiol.* 79, 7371–7380. doi: 10.1128/AEM.02653-13

Chandran, A., and Mazumder, A. (2015). Pathogenic potential, genetic diversity, and population structure of *Escherichia coli* strains isolated from a forest-dominated watershed (Comox Lake) in British Columbia, Canada. *Appl. Environ. Microbiol.* 81, 1779–1789. doi: 10.1128/aem.03738-14

Clermont, O., Bonacorsi, S., and Bingen, E. (2000). Rapid and simple determination of the *Escherichia coli* phylogenetic group. *Appl. Environ. Microbiol.* 66, 4555–4558. doi: 10.1128/AEM.66.10.4555-4558.2000

Cooley, M. B., Quiñones, B., Oryang, D., Mandrell, R. E., and Gorski, L. (2014). Prevalence of shiga toxin producing *Escherichia coli*, *Salmonella enterica*,

and *Listeria monocytogenes* at public access watershed sites in a California Central Coast agricultural region. *Front. Cell. Infect. Microbiol.* 4:30. doi: 10.3389/fcimb.2014.00030

Costa, R. A. (2013). *Escherichia coli* in seafood: a brief overview. *Adv. Biosci. Biotechnol.* 4, 450–454. doi: 10.4236/abb.2013.43A060

Croxen, M. A., Law, R. J., Scholz, R., Keeney, K. M., Wlodarska, M., and Finlay, B. B. (2013). Recent advances in understanding enteric pathogenic *Escherichia coli*. *Clin. Microbiol. Rev.* 26, 822–880. doi: 10.1128/CMR.00022-13

Dumke, R., Schröter-Bobsin, U., Jacobs, E., and Röske, I. (2006). Detection of phages carrying the Shiga toxin 1 and 2 genes in waste water and river water samples. *Lett. Appl. Microbiol.* 42, 48–53. doi: 10.1111/j.1472-765X.2005.01809.x

EFSA (2013). EFSA Panel on Biological Hazards (BIOHAZ); scientific opinion on VTEC-seropathotype and scientific criteria regarding pathogenicity assessment. *EFSA J.* 11, 3138. doi: 10.2903/j.efsa.2013.3138

Feng, P. C. H., Keys, C., Lacher, D. W., Beutin, L., Bentancor, A., Heuvelink, A., et al. (2012). Clonal relations of atypical enteropathogenic *Escherichia coli* O157:H16 strains isolated from various sources from several countries. *FEMS Microbiol. Lett.* 337, 126–131. doi: 10.1111/1574-6968.12017

Fremaux, B., Prigent-Combaret, C., Beutin, L., Gleizal, A., Trevisan, D., Quetin, P., et al. (2010). Survival and spread of Shiga toxin-producing *Escherichia coli* in alpine pasture grasslands. *J. Appl. Microbiol.* 108, 1332–1343. doi: 10.1111/j.1365-2672.2009.04527.x

García-Aljaro, C., Muniesa, M., Blanco, J. E., Blanco, M., Blanco, J., Jofre, J., et al. (2005). Characterization of Shiga toxin-producing *Escherichia coli* isolated from aquatic environments. *FEMS Microbiol. Lett.* 246, 55–65. doi: 10.1016/j.femsle.2005.03.038

Gourmelon, M., Montet, M., Lozach, S., Le Mennec, C., Pommepuy, M., Beutin, L., et al. (2006). First isolation of Shiga toxin 1d producing *Escherichia coli* variant strains in shellfish from coastal areas in France. *J. Appl. Microbiol.* 100, 85–97. doi: 10.1111/j.1365-2672.2005.02753.x

Gourmelon, M., Touati, D., Pommepuy, M., and Cormier, M. (1997). Survival of *Escherichia coli* exposed to visible light in seawater: analysis of rpoS-dependent effects. *Can. J. Microbiol.* 43, 1036–1043. doi: 10.1139/m97-148

Guinée, P. A. M., Jansen, H. W., Wadstrom, T., and Sellwood, R. (1981). "*Escherichia coli* associated with neonatal diarrhoea in piglets and calves," in *Laboratory Diagnosis in Neonatal Calf and Pig Diarrhoea: Current Topics in Veterinary and Animal Science*, Vol. 13, eds P. W. De Leeww and P. A. M. Guinée (Hague: Martinus Nijhoff), 126–162.

Hamilton, M. J., Hadi, A. Z., Griffith, J. F., Ishii, S., and Sadowsky, M. J. (2010). Large scale analysis of virulence genes in *Escherichia coli* strains isolated from Avalon Bay, CA. *Water Res.* 44, 5463–5473. doi: 10.1016/j.watres.2010.06.058

Hornitzky, M. A., Vanselow, B. A., Walker, K., Bettelheim, K. A., Corney, B., Gill, P., et al. (2002). Virulence properties and serotypes of Shiga toxin-producing *Escherichia coli* from healthy Australian cattle. *Appl. Environ. Microbiol.* 68, 6439–6445. doi: 10.1128/AEM.68.12.6439-6445.2002

Imamovic, L., Jofre, J., Schmidt, H., Serra-Moreno, R., and Muniesa, M. (2009). Phage-mediated Shiga toxin 2 gene transfer in food and water. *Appl. Environ. Microbiol.* 75, 1764–1768. doi: 10.1128/AEM.02273-08

Itoh, Y., Rice, J. D., Goller, C., Pannuri, A., Taylor, J., Meisner, J., et al. (2008). Roles of pgaABCD genes in synthesis, modification, and export of the *Escherichia coli* biofilm adhesin poly-beta-1,6-N-acetyl-D-glucosamine. *J. Bacteriol.* 190, 3670–3680. doi: 10.1128/JB.01920-07

Iwamoto, M., Ayers, T., Mahon, B. E., and Swerdlow, D. L. (2010). Epidemiology of seafood-associated infections in the United States. *Clin. Microbiol. Rev.* 23, 399–411. doi: 10.1128/CMR.00059-09

Jang, J., Di, D. Y., Lee, A., Unno, T., Sadowsky, M. J., and Hur, H. G. (2014). Seasonal and genotypic changes in *Escherichia coli* phylogenetic groups in the Yeongsan River basin of South Korea. *PLoS ONE* 9:e100585. doi: 10.1371/journal.pone.0100585

Jiang, C., An, T., Wang, S., Wang, G., Si, W., Tu, Y., et al. (2015). Role of the ehxA gene from *Escherichia coli* serotype O82 in hemolysis, biofilm formation, and in vivo virulence. *Can. J. Microbiol.* 61, 335–341. doi: 10.1139/cjm-2014-0824

Levine, M. M., and Edelman, R. (1984). Enteropathogenic *Escherichia coli* of classic serotypes associated with infant diarrhea: epidemiology and pathogenesis. *Epidemiol. Rev.* 6, 31–51.

Lienemann, T., Pitkanen, T., Antikainen, J., Molsa, E., Miettinen, I., Haukka, K., et al. (2011). Shiga Toxin-Producing *Escherichia coli* O100:H-: stx(2e) in Drinking Water Contaminated by Waste Water in Finland. *Curr. Microbiol.* 62, 1239–1244. doi: 10.1007/s00284-010-9832-x

Ma, J., Ibekwe, A. M., Crowley, D. E., and Yang, C.-H. (2014). Persistence of *Escherichia coli* O157 and non-O157 strains in agricultural soils. *Sci. Total Environ.* 490, 822–829. doi: 10.1016/j.scitotenv.2014.05.069

Manna, S. K., Das, R., and Manna, C. (2008). Microbiological quality of finfish and shellfish with special reference to Shiga toxin-producing *Escherichia coli* O157. *J. Food. Sci.* 73, M283–M286. doi: 10.1111/j.1750-3841.2008.00815.x

Martinez-Castillo, A., Quirós, P., Navarro, F., Miró, E., and Muniesa, M. (2013). Shiga toxin 2-encoding bacteriophages in human fecal samples from healthy individuals. *Appl. Environ. Microbiol.* 79, 4862–4868. doi: 10.1128/AEM.01158-13

McDaniel, T. K., Jarvis, K. G., Donnenberg, M. S., and Kaper, J. B. (1995). A genetic locus of enterocyte effacement conserved among diverse enterobacterial pathogens. *Proc. Natl. Acad. Sci. U.S.A.* 92, 1664–1668. doi: 10.1073/pnas.92.5.1664

Mellmann, A., Fruth, A., Friedrich, A. W., Wieler, L. H., Harmsen, D., Werber, D., et al. (2009). Phylogeny and disease association of Shiga toxin-producing *Escherichia coli* O91. *Emerg. Infect. Dis.* 15, 1474–1477. doi: 10.3201/eid1509.090161

Miyagi, K., Omura, K., Ogawa, A., Hanafusa, M., Nakano, Y., Morimatsu, S., et al. (2001). Survival of Shiga toxin-producing *Escherichia coli* O157 in marine water and frequent detection of the Shiga toxin gene in marine water samples from an estuary port. *Epidemiol. Infect.* 126, 129–133.

Moldoveanu, A. M. (2012). Environmental factors influences on bacterial biofilms formation. *Ann. RSCB* XVII, 118–126.

Mora, A., López, C., Dhabi, G., López-Beceiro, A. M., Fidalgo, L. E., Díaz, E. A., et al. (2012). Seropathotypes, phylogroups, *Stx* subtypes, and intimin types of wildlife-carried, Shiga toxin-producing *Escherichia coli* strains with the same characteristics as human-pathogenic isolates. *Appl. Environ. Microbiol.* 78, 2578–2585. doi: 10.1128/AEM.07520-11

Muniesa, M., Jofre, J., García-Aljaro, C., and Blanch, A. R. (2006). Occurrence of *Escherichia coli* O157:H7 and other enterohemorrhagic *Escherichia coli* in the environment. *Environ. Sci. Technol.* 40, 7141–7149. doi: 10.1021/es060927k

Nataro, J. P., and Kaper, J. B. (1998). Diarrheagenic *Escherichia coli*. *Clin. Microbiol. Rev.* 11, 142–201.

Nielsen, E. M., and Andersen, M. T. (2003). Detection and characterization of verocytotoxin-producing *Escherichia coli* by automated 5' nuclease PCR assay. *J. Clin. Microbiol.* 41, 2884–2893. doi: 10.1128/JCM.41.7.2884-2893.2003

O'Brien, A. D., Newland, J. W., Miller, S. F., Holmes, R. K., Smith, H. W., and Formal, S. B. (1984). Shiga-like toxin-converting phages from *Escherichia coli* strains that cause hemorrhagic colitis or infantile diarrhea. *Science* 226, 694–696. doi: 10.1126/science.6387911

Olsen, A., Jonsson, A., and Normark, S. (1989). Fibronectin binding mediated by a novel class of surface organelles on *Escherichia coli*. *Nature* 338, 652–655. doi: 10.1038/338652a0

Paton, A. W., and Paton, J. C. (2002). Direct detection and characterization of Shiga toxigenic *Escherichia coli* by Multiplex PCR for stx1, stx2, eae, ehxA, and saa. *J. Clin. Microbiol.* 40, 271–274. doi: 10.1128/JCM.40.1.271-274.2002

Paton, A. W., Srimanote, P., Woodrow, M. C., and Paton, J. C. (2001). Characterization of saa, a novel autoagglutinating adhesin produced by locus of enterocyte effacement-negative shiga-toxigenic *Escherichia coli* strains that are virulent for humans. *Infect. Immun.* 69, 6999–7009. doi: 10.1128/IAI.69.11.6999-7009.2001

Paton, J. C., and Paton, A. W. (1998). Pathogenesis and diagnosis of Shiga toxin-producing *Escherichia coli* infections. *Clin. Microbiol. Rev.* 11, 450–479.

Perelle, S., Dilasser, F., Grout, J., and Fach, P. (2007). Screening food raw materials for the presence of the world's most frequent clinical cases of Shiga toxin-encoding *Escherichia coli* O26, O103, O111, O145 and O157. *Int. J. Food Microbiol.* 113, 284–288. doi: 10.1016/j.ijfoodmicro.2006.08.014

Potasman, I., Paz, A., and Odeh, M. (2002). Infectious outbreaks associated with bivalve shellfish consumption: a worldwide perspective. *Clin. Infect. Dis.* 35, 921–928. doi: 10.1086/342330

Pradel, N., Livrelli, V., Champs, C. D., Palcoux, J.-B., Reynaud, A., Scheutz, F., et al. (2000). Prevalence and characterization of Shiga toxin-producing *Escherichia coli* isolated from cattle, food, and children during a one-year prospective study in France. *J. Clin. Microbiol.* 38, 1023–1031.

Rozen, Y., and Belkin, S. (2001). Survival of enteric bacteria in seawater. *FEMS Microbiol. Rev.* 25, 513–529. doi: 10.1111/j.1574-6976.2001.tb00589.x

Russo, T. A., and Johnson, J. R. (2000). Proposal for a new inclusive designation for extraintestinal pathogenic isolates of *Escherichia coli*: ExPEC. *J. Infect. Dis.* 181, 1753–1754. doi: 10.1086/315418

Scheutz, F., Teel, L. D., Beutin, L., Piérard, D., Buvens, G., Karch, H., et al. (2012). Multicenter evaluation of a sequence-based protocol for subtyping Shiga toxins and standardizing Stx nomenclature. *J. Clin. Microbiol.* 50, 2951–2963. doi: 10.1128/JCM.00860-12

Singh, P., Sha, Q., Lacher, D. W., Del Valle, J., Mosci, R. E., Moore, J. A., et al. (2015). Characterization of enteropathogenic and Shiga toxin-producing *Escherichia coli* in cattle and deer in a shared agroecosystem. *Front. Cell. Infect. Microbiol.* 5:29. doi: 10.3389/fcimb.2015.00029

Solheim, H. T., Sekse, C., Urdahl, A. M., Wasteson, Y., and Nesse, L. L. (2013). Biofilm as an environment for dissemination of stx genes by transduction. *Appl. Environ. Microbiol.* 79, 896–900. doi: 10.1128/AEM.03512-12

Toth, I., Schmidt, H., Dow, M., Malik, A., Oswald, E., and Nagy, B. (2003). Transduction of porcine enteropathogenic *Escherichia coli* with a derivative of a shiga toxin 2-encoding bacteriophage in a porcine ligated ileal loop system. *Appl. Environ. Microbiol.* 69, 7242–7247. doi: 10.1128/AEM.69.12.7242-7247.2003

Touchon, M., Hoede, C., Tenaillon, O., Barbe, V., Baeriswyl, S., Bidet, P., et al. (2009). Organised genome dynamics in the *Escherichia coli* species results in highly diverse adaptive paths. *PLoS Genet.* 5:e1000344. doi: 10.1371/journal.pgen.1000344

Tremblay, Y. D., Vogeleer, P., Jacques, M., and Harel, J. (2015). High-throughput microfluidic method to study biofilm formation and host-pathogen interactions in pathogenic *Escherichia coli*. *Appl. Environ. Microbiol.* 81, 2827–2840. doi: 10.1128/AEM.04208-14

Usda Food Safety and Inspection Service (2011). *Risk Profile for Pathogenic Non-O157 Shiga Toxin-Producing Escherichia coli (non-O157STEC)*. USDA Food Safety and Inspection Service, Washington, DC. Available at: http://www.fsis.usda.gov/pdf/non_o157_stec_risk_profile.pdf

Vogeleer, P., Tremblay, Y. D., Mafu, A. A., Jacques, M., and Harel, J. (2014). Life on the outside: role of biofilms in environmental persistence of Shiga-toxin producing *Escherichia coli*. *Front. Microbiol.* 5:317. doi: 10.3389/fmicb.2014.00317

Walters, S. P., González-Escalona, N., Son, I., Melka, D. C., Sassoubre, L. M., and Boehm, A. B. (2013). *Salmonella enterica* diversity in central Californian coastal waterways. *Appl. Environ. Microbiol.* 19, 4199–4209. doi: 10.1128/AEM.00930-13

White-Ziegler, C. A., Um, S., Perez, N. M., Berns, A. L., Malhowski, A. J., and Young, S. (2008). Low temperature (23 degrees C) increases expression of biofilm-, cold-shock- and RpoS-dependent genes in *Escherichia coli* K-12. *Microbiology* 154, 148–166. doi: 10.1099/mic.0.2007/012021-0

WHO (1987). *Program for Control of Diarrhoeal Diseases. Manual for Laboratory Investigation of Acute Enteric Infections*. Geneva: World Health Organization.

Wirth, T., Falush, D., Lan, R., Colles, F., Mensa, P., Wieler, L. H., et al. (2006). Sex and virulence in *Escherichia coli*: an evolutionary perspective. *Mol. Microbiol.* 60, 1136–1151. doi: 10.1111/j.1365-2958.2006.05172.x

Zweifel, C., Cernela, N., and Stephan, R. (2013). Detection of the emerging Shiga toxin-producing *Escherichia coli* O26:H11/H- sequence type 29 (ST29) clone in human patients and healthy cattle in Switzerland. *Appl. Environ. Microbiol.* 79, 5411–5413. doi: 10.1128/AEM.01728-13

Conflict of Interest Statement: The authors declare that the research was conducted in the absence of any commercial or financial relationships that could be construed as a potential conflict of interest.

Annexe 3: Interactions of intestinal bacteria with components of the intestinal mucus

En tant que troisième auteur de cet article de revue, j'ai rédigé le paragraphe concernant l'interaction entre la formation de biofilm bactérien et le mucus. J'ai également apporté mes commentaires sur l'ensemble de la revue avant soumission. Cet revue a été publié en 2018 dans le journal « Frontiers in Cellular and Infection Microbiology ».

frontiers in Cellular and Infection Microbiology

REVIEW
published: 05 September 2017
doi: 10.3389/fcimb.2017.00387

Interactions of Intestinal Bacteria with Components of the Intestinal Mucus

*Jean-Félix Sicard[1], Guillaume Le Bihan[1], Philippe Vogeleer[1], Mario Jacques[2] and Josée Harel[1]**

[1] *Centre de Recherche en Infectiologie Porcine et Aviaire, Faculté de Médecine Vétérinaire, Université de Montréal, Saint-Hyacinthe, QC, Canada,* [2] *Regroupement de Recherche Pour un Lait de Qualité Optimale (Op+Lait), Faculté de Médecine Vétérinaire, Université de Montréal, Saint-Hyacinthe, QC, Canada*

The human gut is colonized by a variety of large amounts of microbes that are collectively called intestinal microbiota. Most of these microbial residents will grow within the mucus layer that overlies the gut epithelium and will act as the first line of defense against both commensal and invading microbes. This mucus is essentially formed by mucins, a family of highly glycosylated protein that are secreted by specialize cells in the gut. In this Review, we examine how commensal members of the microbiota and pathogenic bacteria use mucus to their advantage to promote their growth, develop biofilms and colonize the intestine. We also discuss how mucus-derived components act as nutrient and chemical cues for adaptation and pathogenesis of bacteria and how bacteria can influence the composition of the mucus layer.

Keywords: mucus, commensals, pathogens, biofilm, microbiota, microflora, goblet cells

OPEN ACCESS

Edited by:
Pascale Alard,
University of Louisville, United States

Reviewed by:
Valerio Iebba,
Sapienza Università di Roma, Italy
Bruce Vallance,
University of British Columbia, Canada

****Correspondence:***
Josée Harel
josee.harel@umontreal.ca

Received: *02 May 2017*
Accepted: *18 August 2017*
Published: *05 September 2017*

Citation:
Sicard J-F, Le Bihan G, Vogeleer P, Jacques M and Harel J (2017) Interactions of Intestinal Bacteria with Components of the Intestinal Mucus. Front. Cell. Infect. Microbiol. 7:387. doi: 10.3389/fcimb.2017.00387

INTRODUCTION

The gastrointestinal tract harbors a complex bacterial community called the intestinal microbiota that, in healthy conditions, maintains a commensal relationship with our body. Various mechanisms are used by the host to keep intestinal homeostasis and to prevent aberrant immune responses directed against the microbiota. One of these is the production of a mucus layer that covers the epithelial cells of the gut. This mucus is synthesized and secreted by host goblet cells and form an integral structural component of the mammal intestine. Its major function is to protect the intestinal epithelium from damage caused by food and digestive secretions (Deplancke and Gaskins, 2001). The mucus layer provides a niche for bacterial colonization because it contains attachment sites and is also a carbon source (Harel et al., 1993). Effectively, the mucus is a direct source of carbohydrates that are released in the lumen. Therefore, several bacterial species of the microbiota can use mucus glycan as a carbon source (Ouwerkerk et al., 2013). An alteration in glycan availability modifies the composition of the microbiota (Martens et al., 2008). The mucus layer also prevents pathogens from reaching and persisting on the intestinal epithelial surfaces and thereby is a major component of innate immunity. It is constantly renewed and acts as a trap for commensal residents, but also for pathogens, preventing their access to the epithelia (Johansson et al., 2008; Bertin et al., 2013). Although its composition and thickness vary along the gut, the mucus layer is mainly

Abbreviations: MLG, Mucus gel layer; A/E, Attaching and effacing; NAG, *N*-acetyl-D-glucosamine; NANA, *N*-acetylneuraminic acid; EHEC, Enterohemorrhagic *E. coli;* MUB, Mucus-binding proteins; LAB, Lactic acid bacteria; HBGA, Histoblood group antigen; SIgA, Secretory IgA; AIEC, Adherent invasive *E. coli;* LPB, LPS-binding protein; TLR, Toll-like receptor; VPI, *Vibrio* pathogenicity island.

formed of glycoproteins containing different glycans; nonspecific antimicrobial molecules, such as antimicrobial peptides (AMP); secreted antibodies targeting specific microbial antigens; and other intestinal proteins (McGuckin et al., 2011; Antoni et al., 2014). Interaction with the mucus layer is important for the colonization of gut commensals as well as some pathogens that have evolved to adhere to mucus and exploit it (Juge, 2012). Some pathogens also use mucus components as a cue to modulate the expression of virulence genes and thereby adapt to the host environment. In this Review, we describe the interactions between bacteria and components of the human mucus layer: their use as carbon sources, adhesion sites and their genetic adaptation (**Figure 1**).

THE GASTROINTESTINAL MUCUS

Mucus Composition

The intestinal mucus is composed mainly of mucins that are complex agglomerates of structural glycoproteins with specific O-linked glycans (O-glycans) produced by specialized cells of the host called goblet cells (Forstner, 1995). Mucins can either be secreted and form a gel, or be produced as membrane-bound glycoproteins that are part of the epithelial glycocalyx (Johansson et al., 2008, 2011; Jonckheere et al., 2013; Nilsson et al., 2014). These glycoproteins share a common structure made of tandem repeated amino acids rich in proline, threonine and serine and are call PTS domains. These sequences of amino acid provide sites for the covalent attachment of the polysaccharides and are widely *O*-glycosylated (Moran et al., 2011). Four different types of polysaccharide core structures are commonly found in mucin glycoproteins. These cores are formed by a combination of three polysaccharides, galactose, N-acetyl-galactosamine and N-acetyl-glucosamine (Larsson et al., 2009; Juge, 2012). Different chains of glycan will be attached to the core. The terminal monosaccharide is usually a fucose or a sialic acid (Larsson et al., 2009; Juge, 2012). Oligosaccharide chains are also sulfated, especially in colonic regions (Rho et al., 2005). The mucin proteins MUC1, MUC5AC, and MUC6 mainly form the mucus layer in the stomach, whereas MUC2 is the most abundant mucin in the small intestine and the colon (Johansson et al., 2009; Moran et al., 2011). The thickness of the mucus layer varies through the gut. The colon, which harbors the highest density of microorganisms, is covered by the thickest mucus layer (Gum et al., 1994). It is composed of an inner layer that is dense and firmly attached to the epithelium and an outer loose layer that is exposed to bacterial proteolytic activity. The numerous O-glycans of the outer layer can serve as adhesion sites and as nutrients for bacteria while the inner layer is less permissive to bacterial penetration in healthy individuals (Johansson et al., 2008, 2011). Most bacterial residents are present in the outer mucus layer and the competition for survival in this niche shapes the composition of the microbiota. The differential resource utilization of bacterial species participates to the establishment of distinct communities that includes non-mucolytic bacteria (Li et al., 2015).

Role of the Mucus Layer

The mucus barrier has an important role in regulating the severity of infectious diseases. It provides protection against many intestinal pathogens, including *Yersinia enterocolitica*, *Shigella flexneri*, *Salmonella*, and *Citrobacter rodentium* (Mantle and Rombough, 1993; Bergstrom et al., 2010; Arike and Hansson, 2016). MUC2 (Mouse, Muc2) plays a crucial role

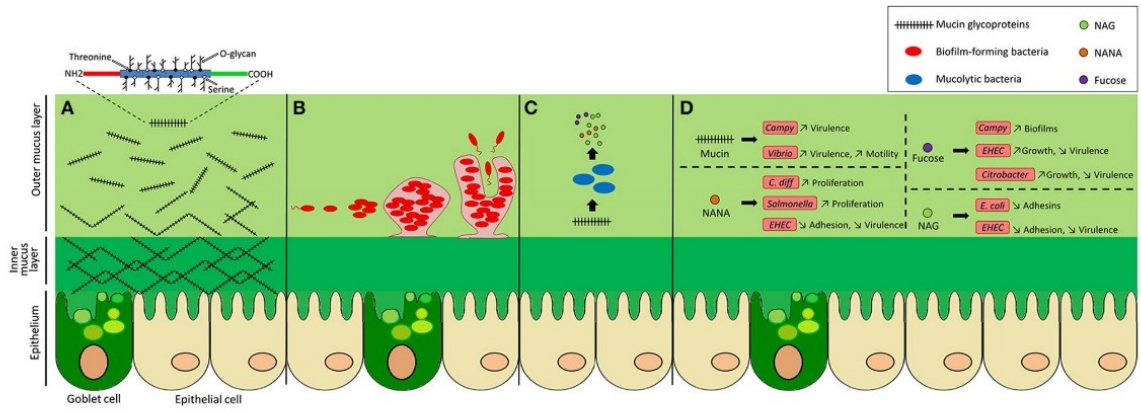

FIGURE 1 | Bacterial activities in the colonic mucus layer environment. The colonic epithelium is covered by a mucus gel layer formed of glycoproteins called mucins. **(A)** Mucins consist of a protein core and a high number of O-linked glycans. They are secreted by goblet cells and are assembled into a net-like structure that forms a dense inner layer, firmly attached to cells, that does not allow bacteria to penetrate. Further from the epithelium, the outer layer becomes loose and permissive, providing a niche for intestinal bacteria. **(B)** Mucus oligosaccharides can act as adhesion sites for bacteria, facilitating their colonization. Some bacteria are able to form microcolonies and biofilms. **(C)** Bacteria with mucolytic activity can release monosaccharides from mucin O-glycans and metabolize them. These sugars can also be utilized by nearby bacteria. **(D)** Mucus components can influence the behavior of pathogenic bacteria by increasing or decreasing their virulence expression, adhesion, motility, proliferation, or growth.

during infection. Using *Muc2*-deficient mice, it was shown that the glycoprotein is critical in controlling *Salmonella* infection (Zarepour et al., 2013). Moreover, *Muc2*$^{-/-}$ mice revealed higher susceptibility to attaching and effacing (A/E) *Citrobacter rodentium* infections (Bergstrom et al., 2010).

An alteration of mucosal integrity is generally associated with health problems, such as inflammatory bowel diseases, including ulcerative colitis and Crohn's disease (Trabucchi et al., 1986; Hanski et al., 1999). During ulcerative colitis, alteration of mucus integrity results in a thinner mucus layer due to goblet cell depletion (Pullan et al., 1994) and a reduced O-glycosylation and sulfation of mucins (Raouf et al., 1992; Larsson et al., 2011). During Crohn's disease, the mucus layer is essentially continuous and comparable to healthy mucosa (Strugala et al., 2008) although there is evidence of abnormal expression and glycosylation of the mucin (Buisine et al., 2001; Moehle et al., 2006; Dorofeyev et al., 2013). These changes in the mucosal environment could also be linked to dysbiosis, an abnormal change in the composition of the intestinal microbiota due to Crohn's disease. Once impaired, the mucus barrier becomes permeable to bacteria that are able to access the epithelium and therefore cause inflammation (Antoni et al., 2014; Johansson et al., 2014), which is why the integrity of the mucus layer is critical for the upkeep of a homeostatic relationship between the intestinal microbiota and its host.

MUCIN AS A GROWTH SUBSTRATE

Mucin proteins are highly glycosylated and therefore constitute a carbon and energy source for intestinal microbiota. A key nutritional aspect of the mucus layer for gut bacteria is its high polysaccharide content with up to 80% of the mucin biomass being composed of mostly O-linked glycans (Johansson et al., 2009, 2011; Marcobal et al., 2013).

Mucolytic Bacteria

A distinct subset of intestinal bacteria possesses the enzymatic activity, such as glycosidases, necessary for the degradation of mucin oligosaccharides, which can be further metabolized by resident microbiota (Koropatkin et al., 2012; Ouwerkerk et al., 2013). Indeed, various anaerobic bacteria species of gut microbiota, such as *Akkermansia muciniphila* (Derrien et al., 2004; Png et al., 2010), *Bacteroides thetaiotaomicron* (Xu et al., 2003; Sonnenburg et al., 2005), *Bifidobacterium bifidum* (Crociani et al., 1994; Png et al., 2010; Garrido et al., 2011), *Bacteroides fragilis* (Macfarlane and Gibson, 1991; Swidsinski et al., 2005a; Huang et al., 2011), *Ruminococcus gnavus* (Png et al., 2010; Crost et al., 2013), and *Ruminococcus torques* (Hoskins et al., 1985; Png et al., 2010) are now known as mucin-degrading specialists. These bacteria will use their specific enzymatic activities to release monosaccharides attached to the mucin glycoproteins. Some mucolytic bacteria, such as *B. thetaiotaomicron,* that possess an important variety of glycosidases, are better suited for the utilization of a wide range of glycans (Xu et al., 2003; Marcobal et al., 2013). To complete the degradation of mucins, a combination of enzymatic activity of several mucolytic bacteria is needed (Derrien et al., 2010; Marcobal et al., 2013). Therefore, MUC2 glycans act as nutritional sources for bacteria that can utilize the mucus-derived sugars, but lack the enzymes necessary for cleaving sugar linkages (Johansson et al., 2015; Arike and Hansson, 2016). Commonly, several bacteria collaborate in a community and it has been shown that the sulfatase activity of some commensal bacteria on sulfomucin allows glycosidases to access and act on mucins (Rho et al., 2005). Released saccharides, such as *N*-acetyl-D-glucosamine (GlcNAc also called NAG), *N*-acetylgalactosamine (GalNAc), galactose, fucose and sialic acid (*N*-acetylneuraminic acid also called NANA) can then be used by the degrader itself or by other resident bacteria (Bjursell et al., 2006; Martens et al., 2008; Sonnenburg et al., 2010). As example, commensal *E. coli* that are limited to growth on mono- or disaccharides, are unable to degrade the complex polysaccharides that constitute mucin (Hoskins et al., 1985) and therefore use such carbohydrate sources (Chang et al., 2004; Png et al., 2010; Bertin et al., 2013). Another example is vancomycin-resistant *Enterococcus* that can grow on mucin pre-digested with extracts from human stools, but not on purified mucin. This suggests that *Enterococcus* can benefit of the microbiota activity on mucin and uses released mucus-derived products (Pultz et al., 2006). In this way, mucolytic bacteria make mucus O-glycan derived products also available for other bacterial residents.

Use of Mucus-Derived Nutrients by Pathogens

Intestinal pathogens have developed strategies to compete with commensal microflora for nutrients, such as carbohydrates and these strategies have been reviewed in Conway and Cohen (2015), Vogt et al. (2015), and Baumler and Sperandio (2016). Pathogenic and commensal *E. coli* strains displayed considerable catabolic diversity when colonizing streptomycin-treated mice, indicating that nutrient availability can influence their colonization success and their niche adaptation (Maltby et al., 2013). For example, pathogenic *E. coli* such as enterohemorrhagic *E. coli* (EHEC) strain EDL933 efficiently utilizes some mucus-derived monosaccharides. This can provide competitive growth compared to that of commensal *E. coli* (Fabich et al., 2008). Moreover, the metabolic flexibility of some pathogenic strains to use both glycolytic and gluconeogenic nutrients may be advantageous (Bertin et al., 2013). The pathogen *Vibrio cholerae*'s preferential use of mucus-derived monosaccharides, such as GlcNAc and sialic acid confers an advantage in the infant mouse model of infection (Almagro-Moreno et al., 2015). *C. jejuni* also possess the ability to metabolize fucose. Its growth is enhanced in culture medium supplemented with it (Alemka et al., 2012). In addition, antibiotic treatment also perturbs the microbiota and therefore affects the availability of mucin carbohydrates. The concentration of free fucose and sialic acid reaching high levels during antibiotic treatment facilitates expansion of pathogens such as *Salmonella enterica* serotype Typhimurium and *Clostridium difficile* (Ng et al., 2013). In addition, *Salmonella* serotype Typhimurium is known both to bind glycoprotein containing sialic acids (Vimal et al., 2000) and to have the ability to release the carbohydrate using its sialidase (Hoyer et al.,

1992). Thereby, to colonize specific niches, many pathogens have evolved in a way to use mucus-derived sugars as a carbon source.

BACTERIAL ADHESION TO MUCINS

Mucins proteins are highly glycosylated. Their O-glycans are used as ligands for bacterial adhesins (Juge, 2012). It can be speculated that adhesion to mucins may initiate colonization of the intestine. The carbohydrate structures on mucins can provide initial attachment site to bacteria including specialized pathogens and could facilitate the invasion of epithelial cells (Derrien et al., 2010). As example, pathogenic microorganisms, such as *Campylobacter* and enterotoxinogenic *E. coli* (ETEC) are known to adhere to the glycoprotein MUC1 that is present in human breast milk. This interferes with colonization of these pathogens in the infant GI tract (Martin-Sosa et al., 2002; Ruiz-Palacios et al., 2003). Although no specific mucus-adherent microflora was identified (van der Waaij et al., 2005), there are evidence that bacteria can bind directly to mucins by expressing specific proteins, pili, fimbriae and flagella (**Table 1**).

Interactions between Mucin and Surface Proteins

To adhere to mucus, commensal and pathogenic bacteria use different strategies. First, they can produce proteins that specifically bind the mucus. Mucus-binding proteins (MUB) are cell-surface proteins mainly described in lactic acid bacteria (LAB) (Boekhorst et al., 2006), especially in *Lactobacillus reuteri* (Roos and Jonsson, 2002; MacKenzie et al., 2009). MUB contain domains that are similar to the model mucin-binding protein (MucBP) from the Pfam database (Boekhorst et al., 2006). The MucBP domain is found in a variety of bacterial proteins that are known for their capacity to adhere to mucus (Juge, 2012). MUB also share structural and functional homology with pathogenic Gram-positive adhesins that have specificity to sialylated mucin glycans (Etzold et al., 2014). For example, some surface proteins of *Listeria monocytogenes* contain a MucBP domain similar to those found in *Lactobacillus*, allowing them to adhere to mucin (Bierne et al., 2007; Mariscotti et al., 2014). The causative agent of cholera, *V. cholerae*, can also bind to mucin using surface protein called GbpA (chitin-binding protein) that binds specifically to N-acetyl D-glucosamine residues of intestinal mucins (Bhowmick et al., 2008). In addition, *C. jejuni* is well-known for its ability to interact with different human histoblood group antigens (HBGAs) expressed in mucosa (Naughton et al., 2013). The major outer membrane protein (MOMP) of *C. jejuni* is involved in these interactions (Mahdavi et al., 2014). This way, *C. jejuni* can interact with intestinal mucin MUC2 in the intestine (Tu et al., 2008). Furthermore, *Bifidobacterium* spp. is also known for its specific adhesion to mucus. For example, in a *B. bifidum* mucin-binding assay, the expression of an extracellular transaldolase correlated with a positive

TABLE 1 | Bacterial adhesion to mucin components.

Bacteria		Adhesin	Mucin glycoprotein	Mucin component	References
COMMENSAL BACTERIA					
Bacteroides fragilis					Huang et al., 2011
Bifidobacterium bifidum		Extracellular transaldolase			Marcobal et al., 2013
Bifidobacterium longum subsp. *infantis*		Family 1 of solute binding proteins		Mucin oligosaccharides	Garrido et al., 2011
Escherichia coli Nissle 1917		Flagellum			Troge et al., 2012
Lactic acid bacteria		MUB			Boekhorst et al., 2006
		Pili			Kankainen et al., 2009; Le et al., 2013
PATHOGENS					
Campylobacter jejuni		Carbohydrate-lectin, FlaA, MOMP	MUC2		Tu et al., 2008; Naughton et al., 2013; Mahdavi et al., 2014
Clostridium difficile		FliC		Cecal mucus	Tasteyre et al., 2001
		FliD			
Escherichia coli	UPEC CFT073	F9 fimbriae		Galβ1-3GlcNAc structures	Wurpel et al., 2014
	EPEC E2348/69	H6 flagella	MUC2	Mucin-type core 2 O-glycan	Erdem et al., 2007; Ye et al., 2015
	EHEC EDL933	H7 flagella	MUC2	Mucin-type core 2 O-glycan	Erdem et al., 2007; Ye et al., 2015
Listeria monocytogenes		LPXTG-internalin proteins (MucBP) LmiA			Bierne et al., 2007; Mariscotti et al., 2014
Salmonellae enterica serotype Typhimurium		Fimbrial adhesin (std operon)		Alpha1-2 fucosylated receptor(s)	Chessa et al., 2009
Vibrio cholerae		Vibrio polysaccharide (VPS)			Liu et al., 2015
		Chitin-binding protein (GbpA)		N-acetyl D-glucosamine	Bhowmick et al., 2008

mucin-binding phenotype (Gonzalez-Rodriguez et al., 2012). *B. longum* subsp. *infantis* is another species that binds specifically to mucin using family-1 solute binding proteins (Kankainen et al., 2009). Interestingly, a study using gnotobiotic mice colonized by *B. fragilis* and *E. coli* revealed that the commensal bacterium *B. fragilis* was found in the mucus layer while *E. coli* was only found in the lumen. Further analysis showed that *B. fragilis* specifically binds to highly purified mucins. This indicated that a direct bond with intestinal mucus could be a mechanism used by *B. fragilis* for gut colonization (Huang et al., 2011).

Interactions between Mucin and Pili/Fimbriae

In addition to produce specific mucus binding proteins, some bacteria can also use cell-surface appendix, such as pili or fimbriae to bind the mucus. For example, production of pili by LAB was shown to be implicated in mucus-binding activity (Douillard et al., 2013) and moreover, the SpaC pilus protein of *L. rhamnosus* GG was shown to strongly binds the human mucins (Kankainen et al., 2009). An *in vitro* study using mucus-secreting HT29-MTX intestinal epithelial cell model showed that the adhesion of *Salmonellae enterica* serotype Typhimurium to mucus-secreting intestinal epithelial cells was higher than in non- and low-mucus producing cells (Gagnon et al., 2013). Moreover, virulent strains seem to bind more efficiently to mucus than avirulent strains and the binding that preferentially targets the neutral mucin is mannose-dependant (Vimal et al., 2000). As with some uropathogenic *E. coli* (Wurpel et al., 2014), the adhesion of *S. enterica* serotype Typhimurium could be the result of interaction between fimbrial adhesin and mucin glycans, more specifically terminal fucose residues (Chessa et al., 2009). The *E. coli* K88 (F4) fimbriae is also able to bind mucus from the small intestines of 35-day-old piglets with a specificity to the glycolipid galactosylceramide (Blomberg et al., 1993). Hence, pili and fimbriae are involved in specific adhesion to mucus.

Interactions between Mucin and Flagella

Many enteric bacteria also produce flagellum. In addition to their role in motility, flagella are also involved in adhesion. As example, the *E. coli* probiotic strain Nissle 1917 was shown to be able to interact, via its flagella, with human and porcine mucus but not with murine mucus. Furthermore, the mucus component gluconate has been identified as one receptor for the adhesion of these flagella (Troge et al., 2012). Other studies have revealed the role of the flagella for the binding of mucin glycoproteins by *C. difficile* (Tasteyre et al., 2001) and pathogenic *E. coli* (Erdem et al., 2007). Indeed, a mutation of the flagellum element *fliC* prevents the adhesion of EPEC and EHEC to mucins (Erdem et al., 2007). More recently, the flagella of EPEC (O127:H6) and EHEC (O157:H7) were shown to adhere to mucin-type core 2 O-glycan in MUC2. *C. jejuni* is another pathogen that uses its flagella to bind mucin. It was showed that the major flagella subunit protein (FlaA) is also involved in the adhesion to HBGA in the mucus. Therefore, flagella can be used in attachment strategies by gut residents.

BACTERIAL BIOFILM AND MUCUS

There are more mucus-associated bacteria in the proximal region of the colon than in distal colonic sites. Among the complex microbial communities within the gut, some are believed to form mucosal biofilm, that is a complex and self-produced polymeric matrix where microorganisms can attach to each other and be attached to the mucosal surface (de Vos, 2015). The rapid growth of the intestinal mucus and the lack of effective preservation techniques complicated the study investigating biofilms in healthy individuals (Bollinger et al., 2007; de Vos, 2015). However, biofilms were observed in artificial mucin gels that simulate the proximal and distal colon (Macfarlane et al., 2005), and also by electron microscopy in uninflamed proximal large bowel of mice (Swidsinski et al., 2005a), rat, baboon, and humans (Palestrant et al., 2004). Some evidence, such as the rates of plasmids transfer and the expression of colonization factors by gut bacteria, plead for the presence of biofilms in the gut (Macfarlane et al., 1997; Licht et al., 1999; Hooper and Gordon, 2001). In addition, components of the mucus layer, such as secretory IgA (SIgA) and mucins are likely to play a role in biofilm formation as they have been shown to modulate biofilm production *in vitro* (Bollinger et al., 2003, 2006; Slizova et al., 2015). Moreover, adherence of bacteria to mucin proteins could lead to growth of microcolonies that could further develop into biofilms (Kleessen and Blaut, 2007). Biofilms could also be formed on the surface of intestinal or gastric epithelia and interact with the secreted or membrane-bound mucins.

Alteration of the mucus layer occurs in cases of inflammatory bowel diseases (Bodger et al., 2006; Baumgart et al., 2007; Sheng et al., 2012). The increased presence of *B. fragilis* group and *Enterobacteriaceae* and their ability to form biofilms could play a role in these diseases (Swidsinski et al., 2005b, 2009). Within the *Enterobacteriaceae* family, the adherent-invasive *E. coli* (AIEC) strains associated with Crohn's disease (Masseret et al., 2001; Darfeuille-Michaud et al., 2004; Eaves-Pyles et al., 2008; Martinez-Medina et al., 2009a), are shown to be higher biofilm producers than non-AIEC strains (Martinez-Medina et al., 2009b). As with inflammatory bowel diseases, impaired mucin production is related to colorectal cancer (Weiss et al., 1996; Kim and Ho, 2010) that is also linked to the presence of bacterial biofilms (Dejea et al., 2014). Altogether, these studies show that biofilms could play a key role in bacterial colonization of the healthy gut and in intestinal diseases.

ROLE OF MUCIN COMPONENTS IN MODULATION OF BACTERIAL VIRULENCE

In addition to acting as a carbon source or as receptors, mucin glycoprotein can influence the expression of different genes implicated in colonization and pathogenicity (Vogt et al., 2015). As example, MUC2 in the mucus layer can play a modulatory role in the pathogenesis of pathogens. Indeed, the ability of *S. enterica* serotype Typhimurium to cause cecal pathology in muc2$^{-/-}$ mice is more dependent on its *invA* gene, coding a *Salmonella* inner membrane protein component of the SPI-1 type

3 secretion system, than it is in wild-type mice (Zarepour et al., 2013). *C. jejuni* can also utilize mucin proteins as a signal to modulate the expression of its virulence factors. Many virulence genes of this pathogen are upregulated in the presence of MUC2 glycoprotein (Tu et al., 2008). Another example is the ability of *V. cholerae* to downregulate the expression of *vps*, coding for its polysaccharide, in response to mucosal signaling and inversely promoting motility in the mucus (Liu et al., 2015). Mucin also activates the two-component sensor histidine kinase ChiS in *V. cholera*. ChiS is the regulator of the chitinases and the chitin utilization pathway, but also plays a role in the virulence of the bacteria since the mutant strain is hypovirulent (Chourashi et al., 2016). Released monosaccharides from mucin O-glycans degradation can also act as a chemical cue to help pathogens to sense their environment and adapt accordingly. As such, sialic acid and GlcNAc are signals that regulate type 1 fimbriae gene expression and curli activity in *E. coli* (Barnhart et al., 2006; Konopka, 2012). GlcNAc and sialic acid also play roles in the virulence of EHEC. In aerobic condition, these mucin-derived sugars inhibit EHEC adhesion to epithelial cells. These amino sugars also repress the expression of genes of the locus of enterocyte effacement (LEE) via the transcriptional regulator NagC involved in the regulation of NAG catabolism (Le Bihan et al., 2017). In contrast, as the sole carbon sources under microaerobic conditions, sialic acid and NAG were shown to stimulate the production of EspB, an effector of the LEE (Carlson-Banning and Sperandio, 2016). EHEC and *C. rodentium* also sense fucose by a two-component system FusKR. It represses the expression of virulence genes while promoting growth (Pacheco et al., 2012; Keeney and Finlay, 2013). Moreover, it was also shown that fucose influences chemotaxis and biofilm formation of *C. jejuni* that are important during infection (Dwivedi et al., 2016). Thus, mucus and its derived sugars can play a role in the expression of virulence genes by pathogens.

MODULATION OF MUCIN COMPOSITION BY BACTERIA

Microbial molecular exchange with the host influences mucin composition. Several bacterial effectors can modulate the expression of mucin by mucus-producing cells (**Table 2**). Studies

TABLE 2 | Effects of bacterial effectors on mucin.

Bacteria		Effector	Target	Effect on mucin	References
Campylobacter jejuni			Distal colonic biopsies	Increased expression of MUC1	Linden et al., 2008
Clostridium difficile			Distal colonic biopsies	Increased expression of MUC1	Linden et al., 2008
		ToxA	HT-29 cells	Decrease of mucin exocytosis	Kelly et al., 1994; Branka et al., 1997
E. coli	EAEC	Secreted protein Pic	Hog gastric, bovine sub-maxillary and crude mouse large intestine mucin	Mucinase activity / Degradation	Henderson et al., 1999; Harrington et al., 2009
			Goblet cells	Secretagogue activity/Hypersecretion	Navarro-Garcia et al., 2010
	ETEC	Secreted EatA	Purified MUC2	Degradation of MUC2	Kumar et al., 2014
	AIEC (LF82)		T84 cells	Diminished expression of MUC2 and MUC5A	Elatrech et al., 2015
	EHEC (O157:H7)	Adhesion	HT-29 cells	Increased expression of MUC2	Xue et al., 2014
Lacto-bacillus	*plantarum* 299v		HT-29 cells	Increased MUC2 secretion	Mack et al., 1999
	rhamnosus GG		HT-29 cells	Increased MUC2 secretion	Mack et al., 1999
	casei GG		Caco-2 cells	Increased MUC2 secretion	Mattar et al., 2002
Listeria monocytogenes		Listeriolysin O (LLO)	HT29-MTX cells	Increased transcription of MUC3, MUC4 and MUC12 Increased secretion of MUC5A	Coconnier et al., 1998; Lievin-Le Moal et al., 2002, 2005
Salmonella St Paul			Distal colonic biopsies	Increased expression of MUC1	Linden et al., 2008
Shigella flexneri		SST3	Mucin-producing polarized human intestinal epithelial cells	Alteration of glycosylation/ Increased permeability	Sperandio et al., 2013
		Secreted protein Pic	Hog gastric, bovine sub-maxillary, crude mouse large-intestine mucin	Mucinase activity / Degradation	Henderson et al., 1999; Harrington et al., 2009
			Goblet cells	Secretagogue activity / Hypersecretion	Navarro-Garcia et al., 2010
Vibrio cholerae		Toxin CT	Goblet cells	Increased mucin secretion	Lencer et al., 1990; Epple et al., 1997
		Secreted TagA	LS174T goblet cell surface mucin	Cleaves mucin glycoproteins	Szabady et al., 2011
Yersinia enterocolitica		Virulence Plasmid	Rabbit small intestinal mucin	Degradation/Solubilisation	Mantle and Rombough, 1993

using germ-free rats revealed that the presence of microflora through the gastro intestinal tract has a strong and positive influence on the thickness and composition of the mucin (Szentkuti et al., 1990; Enss et al., 1992; Sharma et al., 1995). Different probiotic agents, such as *Lactobacillus* species, can stimulate the production of MUC2 and thereby the secretion of mucin in the intestine, improving pathogen resistance (Mack et al., 1999; Mattar et al., 2002; Caballero-Franco et al., 2007). Other commensal bacteria, such as *B. thetaiotaomicron* can increase the differentiation of goblet cells and their mucus-related gene expression (Wrzosek et al., 2013). Moreover, bacterial fermentation products, such as short-chain fatty acids (SCFAs) like butyrate and propionate enhance the production of MUC2 by the goblet cell in the gut (Barcelo et al., 2000; Burger-van Paassen et al., 2009). This could explain the therapeutic effect of butyrate in colitis where the mucin layer is altered (Finnie et al., 1995). Therefore, commensal residents are important in the maintenance of the mucus layer integrity.

Modulation of Mucin by Pathogens

Pathogens have also adapted mechanisms to modulate mucin secretion to enhance pathogenesis by acting on the mucin-secreting cells, altering or inhibiting mucin production (**Table 2**). One of them is *S. flexneri* that alters the mucus layer through a type III secretion system-dependent manner. This pathogen will act on different elements, such as gene expression, mucin glycosylation and secretion, leading to a less effective mucus barrier (Sperandio et al., 2013). *C. difficile* produces a toxin, ToxA that is responsible for barrier dysfunction and causes severe inflammatory enteritis. ToxA also decreases the mucin exocytosis of colonic mucus-producing cells (Kelly et al., 1994; Branka et al., 1997). The recognition of bacterial components by these cells can also lead to an increased production and secretion of mucin in order to harm the present pathogen. As example, the adhesion of the EHEC O157:H7 to human colon cells HT-29 leads to an increased expression of MUC2 (Xue et al., 2014). Moreover, the cholera toxin of *V. cholerae* and lysteriolysin O of *L. monocytogenes* enhance the secretion of mucin by goblet cells and HT29-MTX cells, respectively (Lencer et al., 1990; Epple et al., 1997; Coconnier et al., 1998; Lievin-Le Moal et al., 2002, 2005). Surprisingly, the Pic protein secreted by *S. flexneri* and enteroaggregative *E. coli* (Henderson et al., 1999; Harrington et al., 2009) is known for its mucolytic activity, but is also a potent mucus secretagogue that induced hypersecretion of mucus by goblet cells (Navarro-Garcia et al., 2010). These studies show how pathogens can affect the behavior of mucus-producing cells in their advantage.

Mucin Degradation by Pathogens

Pathogens also developed specific mechanisms to subvert and penetrate the mucus barrier. Some bacteria can directly act on the mucin through a mucinase activity. During enterotoxigenic *E. coli* infections, the autotransporter A (EatA) is involve in mucin degradation and this participate to the delivery of *E. coli* toxins to the cell surface (Kumar et al., 2014). Another example is the adherent and invasive *E. coli* strain LF82, associated with Crohn's disease. LF82 possesses a protease called Vat-AIEC that is implicated in the degradation of mucins and therefore decreases mucus viscosity (Gibold et al., 2016). The Pic autotransporter found in enteroaggregative *E. coli* and *Shigella flexneri* can also degrade various glycoproteins including mucins (Henderson et al., 1999; Harrington et al., 2009). Moreover, the plasmid-bearing *Yersinia enterocolitica*, which contain mucin-degrading enzyme(s), will increase the permeability of the mucus gel layer, allowing the bacteria to move more easily through the mucin (Mantle and Rombough, 1993). *V. cholerae* also produces a secreted protease called TagA that is encoded by the *Vibrio* pathogenicity island (VPI). TagA specifically cleaves mucin glycoproteins and may directly modify host cell surface molecules during *V. cholerae* infection (Szabady et al., 2011). Therefore, to facilitate their infection process, pathogens can directly modify the mucus.

Inflammation and Mucins

Pathogens associated molecular patterns, such as lipopolysaccharide (LPS) and peptidoglycan are also known to stimulate mucin production (Petersson et al., 2011). This stimulation can occur directly on secreting cells, but also be through proinflammatory cytokine production. Recognition of LPS by LPS-binding protein (LBP), CD14, and TLR4 (Toll-Like Receptor) leads to a strong pro-inflammatory response in mammalian cells. LPS has been shown to induce mucin gene expression by binding to TLR4 and LBP (Dohrman et al., 1998; Smirnova et al., 2003). LPS and flagellin from Gram-negative bacteria as well as lipoteichoic acid, a component of the cell wall of Gram-positive bacteria, induce mucin upregulation through the Ras pathway (McNamara and Basbaum, 2001; Theodoropoulos and Carraway, 2007). LPS also increases the production of IL-8 by goblet cells, which leads to secretion of mucin (Smirnova et al., 2003). In addition, pro-inflammatory cytokine IL-6 and TNF-α increase secretion of MUC2, MUC5A, MUC5B, and MUC6 by the intestinal cell line *LS180* despite a reduced glycosylation (Enss et al., 2000). Inflammation could be one of the aspects affecting the integrity of the mucus layer in inflammatory bowel diseases. Furthermore, the AIEC strain LF82 is able to alter the expression of the mucin gene and IL-8 of colonic cells T84 that could also lead to a defective mucus layer (Elatrech et al., 2015). Thus, pathogens can also alter the mucus production indirectly, through inflammation.

CONCLUSION

Intestinal bacteria have adapted to colonize the mucus layer by adhering to intestinal mucus components, using mucus-derived nutrients and sensing chemical cues for adaptation. In many ways, pathogenic bacteria have used these strategies for successful infection. There has been growing recognition of the important role played by the mucus barrier and microbiota and their interaction with the pathogens in regulating the severity of infectious diseases. But, the precise mechanisms by which enteric bacterial pathogens interact with mucus components in combination with the microbiota activity are being investigated. As the mucus layer acts as a first line of defense against enteric bacteria, further investigations are needed to understand the interactions between pathogens, microbiota and the mucus layer, in order to develop efficient therapeutic strategies. Identifying

and characterizing specific mucin signal(s) and corresponding regulatory adaptation and virulence responses could contribute to the development of new anti-infective strategies. In doing so, other weapons could be added to the arsenal against intestinal pathogens.

AUTHOR CONTRIBUTIONS

All authors listed have made a substantial, direct and intellectual contribution to the work, and approved it for publication. The manuscript was written by J-FS and JH and was duly revised by GLB, PV and MJ.

ACKNOWLEDGMENTS

We thank Judith Kashul for editing the manuscript. This research was supported by a Team grant from the Fonds de Recherche du Québec, Nature et Technologies (FRQNT PT165375), to JH and MJ and by the Discovery grant program of the Natural Sciences and Engineering Research Council of Canada (RGPIN-2015-05373 to JH and RGPIN-2016-04203 to MJ). J-FS is a recipient of a scholarship from the NSERC Collaborative Research and Training Experience Program in Milk Quality; and PV is a recipient of a scholarship from the FRQNT Québec Wallonie program.

REFERENCES

Alemka, A., Corcionivoschi, N., and Bourke, B. (2012). Defense and adaptation: the complex inter-relationship between *Campylobacter jejuni* and mucus. *Front. Cell Infect. Microbiol.* 2:15. doi: 10.3389/fcimb.2012.00015

Almagro-Moreno, S., Pruss, K., and Taylor, R. K. (2015). Intestinal colonization dynamics of *Vibrio cholerae*. *PLoS Pathog.* 11:e1004787. doi: 10.1371/journal.ppat.1004787

Antoni, L., Nuding, S., Wehkamp, J., and Stange, E. F. (2014). Intestinal barrier in inflammatory bowel disease. *World J. Gastroenterol.* 20, 1165–1179. doi: 10.3748/wjg.v20.i5.1165

Arike, L., and Hansson, G. C. (2016). The densely o-glycosylated MUC2 mucin protects the intestine and provides food for the commensal bacteria. *J. Mol. Biol.* 428, 3221–3229. doi: 10.1016/j.jmb.2016.02.010

Barcelo, A., Claustre, J., Moro, F., Chayvialle, J. A., Cuber, J. C., and Plaisancie, P. (2000). Mucin secretion is modulated by luminal factors in the isolated vascularly perfused rat colon. *Gut* 46, 218–224. doi: 10.1136/gut.46.2.218

Barnhart, M. M., Lynem, J., and Chapman, M. R. (2006). GlcNAc-6P levels modulate the expression of Curli fibers by *Escherichia coli*. *J. Bacteriol.* 188, 5212–5219. doi: 10.1128/JB.00234-06

Baumgart, M., Dogan, B., Rishniw, M., Weitzman, G., Bosworth, B., Yantiss, R., et al. (2007). Culture independent analysis of ileal mucosa reveals a selective increase in invasive *Escherichia coli* of novel phylogeny relative to depletion of *Clostridiales* in Crohn's disease involving the ileum. *ISME J.* 1, 403–418. doi: 10.1038/ismej.2007.52

Baumler, A. J., and Sperandio, V. (2016). Interactions between the microbiota and pathogenic bacteria in the gut. *Nature* 535, 85–93. doi: 10.1038/nature18849

Bergstrom, K. S., Kissoon-Singh, V., Gibson, D. L., Ma, C., Montero, M., Sham, H. P., et al. (2010). MUC2 protects against lethal infectious colitis by disassociating pathogenic and commensal bacteria from the colonic mucosa. *PLoS Pathog.* 6:e1000902. doi: 10.1371/journal.ppat.1000902

Bertin, Y., Chaucheyras-Durand, F., Robbe-Masselot, C., Durand, A., de la Foye, A., Harel, J., et al. (2013). Carbohydrate utilization by enterohaemorrhagic *Escherichia coli* O157:H7 in bovine intestinal content. *Environ. Microbiol.* 15, 610–622. doi: 10.1111/1462-2920.12019

Bhowmick, R., Ghosal, A., Das, B., Koley, H., Saha, D. R., Ganguly, S., et al. (2008). Intestinal adherence of *Vibrio cholerae* involves a coordinated interaction between colonization factor GbpA and mucin. *Infect. Immun.* 76, 4968–4977. doi: 10.1128/IAI.01615-07

Bierne, H., Sabet, C., Personnic, N., and Cossart, P. (2007). Internalins: a complex family of leucine-rich repeat-containing proteins in *Listeria* monocytogenes. *Microbes Infect.* 9, 1156–1166. doi: 10.1016/j.micinf.2007.05.003

Bjursell, M. K., Martens, E. C., and Gordon, J. I. (2006). Functional genomic and metabolic studies of the adaptations of a prominent adult human gut symbiont, *Bacteroides thetaiotaomicron*, to the suckling period. *J. Biol. Chem.* 281, 36269–36279. doi: 10.1074/jbc.M606509200

Blomberg, L., Krivan, H. C., Cohen, P. S., and Conway, P. L. (1993). Piglet ileal mucus contains protein and glycolipid (galactosylceramide) receptors specific for *Escherichia coli* K88 fimbriae. *Infect. Immun.* 61, 2526–2531.

Bodger, K., Halfvarson, J., Dodson, A. R., Campbell, F., Wilson, S., Lee, R., et al. (2006). Altered colonic glycoprotein expression in unaffected monozygotic twins of inflammatory bowel disease patients. *Gut* 55, 973–977. doi: 10.1136/gut.2005.086413

Boekhorst, J., Helmer, Q., Kleerebezem, M., and Siezen, R. J. (2006). Comparative analysis of proteins with a mucus-binding domain found exclusively in lactic acid bacteria. *Microbiology* 152(Pt 1), 273–280. doi: 10.1099/mic.0.28415-0

Bollinger, R. R., Barbas, A. S., Bush, E. L., Lin, S. S., and Parker, W. (2007). Biofilms in the normal human large bowel: fact rather than fiction. *Gut* 56, 1481–1482.

Bollinger, R. R., Everett, M. L., Palestrant, D., Love, S. D., Lin, S. S., and Parker, W. (2003). Human secretory immunoglobulin A may contribute to biofilm formation in the gut. *Immunology* 109, 580–587. doi: 10.1046/j.1365-2567.2003.01700.x

Bollinger, R. R., Everett, M. L., Wahl, S. D., Lee, Y. H., Orndorff, P. E., and Parker, W. (2006). Secretory IgA and mucin-mediated biofilm formation by environmental strains of *Escherichia coli*: role of type 1 pili. *Mol. Immunol.* 43, 378–387. doi: 10.1016/j.molimm.2005.02.013

Branka, J. E., Vallette, G., Jarry, A., Bou-Hanna, C., Lemarre, P., Van, P. N., et al. (1997). Early functional effects of *Clostridium* difficile toxin A on human colonocytes. *Gastroenterology* 112, 1887–1894. doi: 10.1053/gast.1997.v112.pm9178681

Buisine, M. P., Desreumaux, P., Leteurtre, E., Copin, M. C., Colombel, J. F., Porchet, N., et al. (2001). Mucin gene expression in intestinal epithelial cells in Crohn's disease. *Gut* 49, 544–551. doi: 10.1136/gut.49.4.544

Burger-van Paassen, N., Vincent, A., Puiman, P. J., van der Sluis, M., Bouma, J., Boehm, G., et al. (2009). The regulation of intestinal mucin MUC2 expression by short-chain fatty acids: implications for epithelial protection. *Biochem. J.* 420, 211–219. doi: 10.1042/BJ20082222

Caballero-Franco, C., Keller, K., De Simone, C., and Chadee, K. (2007). The VSL#3 probiotic formula induces mucin 554 gene expression and secretion in colonic epithelial cells. *Am. J. Physiol. Gastrointest. Liver Physiol.* 292, G315–G322. doi: 10.1152/ajpgi.00265.2006

Carlson-Banning, K. M., and Sperandio, V. (2016). Catabolite and oxygen regulation of enterohemorrhagic *Escherichia coli* virulence. *MBio* 7:e01852-16. doi: 10.1128/mBio.01852-16

Chang, D. E., Smalley, D. J., Tucker, D. L., Leatham, M. P., Norris, W. E., Stevenson, S. J., et al. (2004). Carbon nutrition of *Escherichia coli* in the mouse intestine. *Proc. Natl. Acad. Sci. U.S.A.* 101, 7427–7432. doi: 10.1073/pnas.0307888101

Chessa, D., Winter, M. G., Jakomin, M., and Baumler, A. J. (2009). *Salmonella enterica* serotype Typhimurium Std fimbriae bind terminal α(1,2)fucose residues in the cecal mucosa. *Mol. Microbiol.* 71, 864–875. doi: 10.1111/j.1365-2958.2008.06566.x

Chourashi, R., Mondal, M., Sinha, R., Debnath, A., Das, S., Koley, H., et al. (2016). Role of a sensor histidine kinase ChiS of *Vibrio cholerae* in pathogenesis. *Int. J. Med. Microbiol.* 306, 657–665. doi: 10.1016/j.ijmm.2016.09.003

Coconnier, M. H., Dlissi, E., Robard, M., Laboisse, C. L., Gaillard, J. L., and Servin, A. L. (1998). *Listeria* monocytogenes stimulates mucus exocytosis in cultured human polarized mucosecreting intestinal cells through action of listeriolysin O. *Infect. Immun.* 66, 3673–3681.

Conway, T., and Cohen, P. S. (2015). Commensal and pathogenic *Escherichia coli* metabolism in the gut. *Microbiol. Spectr.* 3, 343–362. doi: 10.1128/microbiolspec.MBP-0006-2014

Crociani, F., Alessandrini, A., Mucci, M. M., and Biavati, B. (1994). Degradation of complex carbohydrates by *Bifidobacterium* spp. *Int. J. Food Microbiol.* 24, 199–210. doi: 10.1016/0168-1605(94)90119-8

Crost, E. H., Tailford, L. E., Le Gall, G., Fons, M., Henrissat, B., and Juge, N. (2013). Utilisation of mucin glycans by the human gut symbiont Ruminococcus gnavus is strain-dependent. *PLoS ONE* 8:e76341. doi: 10.1371/journal.pone.0076341

Darfeuille-Michaud, A., Boudeau, J., Bulois, P., Neut, C., Glasser, A. L., Barnich, N., et al. (2004). High prevalence of adherent-invasive *Escherichia coli* associated with ileal mucosa in Crohn's disease. *Gastroenterology* 127, 412–421. doi: 10.1053/j.gastro.2004.04.061

Dejea, C. M., Wick, E. C., Hechenbleikner, E. M., White, J. R., Mark Welch, J. L., Rossetti, B. J., et al. (2014). Microbiota organization is a distinct feature of proximal colorectal cancers. *Proc. Natl. Acad. Sci. U.S.A.* 111, 18321–18326. doi: 10.1073/pnas.1406199111

Deplancke, B., and Gaskins, H. R. (2001). Microbial modulation of innate defense: goblet cells and the intestinal mucus layer. *Am. J. Clin. Nutr.* 73, 1131s–1141s.

Derrien, M., van Passel, M. W., van de Bovenkamp, J. H., Schipper, R. G., de Vos, W. M., and Dekker, J. (2010). Mucin-bacterial interactions in the human oral cavity and digestive tract. *Gut Microbes* 1, 254–268. doi: 10.4161/gmic.1.4.12778

Derrien, M., Vaughan, E. E., Plugge, C. M., and de Vos, W. M. (2004). *Akkermansia muciniphila* gen. nov., sp. nov., a human intestinal mucin-degrading bacterium. *Int. J. Syst. Evol. Microbiol.* 54(Pt 5), 1469–1476. doi: 10.1099/ijs.0.02873-0

de Vos, W. M. (2015). Microbial biofilms and the human intestinal microbiome. *NPJ Biofilms Microbiomes* 1:15005. doi: 10.1038/npjbiofilms.2015.5

Dohrman, A., Miyata, S., Gallup, M., Li, J. D., Chapelin, C., Coste, A., et al. (1998). Mucin gene (MUC 2 and MUC 5AC) upregulation by Gram-positive and Gram-negative bacteria. *Biochim. Biophys. Acta* 1406, 251–259. doi: 10.1016/S0925-4439(98)00010-6

Dorofeyev, A. E., Vasilenko, I. V., Rassokhina, O. A., and Kondratiuk, R. B. (2013). Mucosal barrier in ulcerative colitis and Crohn's disease. *Gastroenterol. Res. Pract.* 2013:431231. doi: 10.1155/2013/431231

Douillard, F. P., Ribbera, A., Jarvinen, H. M., Kant, R., Pietila, T. E., Randazzo, C., et al. (2013). Comparative genomic and functional analysis of *Lactobacillus casei* and *Lactobacillus rhamnosus* strains marketed as probiotics. *Appl. Environ. Microbiol.* 79, 1923–1933. doi: 10.1128/AEM.03467-12

Dwivedi, R., Nothaft, H., Garber, J., Xin Kin, L., Stahl, M., Flint, A., et al. (2016). L-fucose influences chemotaxis and biofilm formation in *Campylobacter jejuni*. *Mol. Microbiol.* 101, 575–589. doi: 10.1111/mmi.13409

Eaves-Pyles, T., Allen, C. A., Taormina, J., Swidsinski, A., Tutt, C. B., Jezek, G. E., et al. (2008). *Escherichia coli* isolated from a Crohn's disease patient adheres, invades, and induces inflammatory responses in polarized intestinal epithelial cells. *Int. J. Med. Microbiol.* 298, 397–409. doi: 10.1016/j.ijmm.2007.05.011

Elatrech, I., Marzaioli, V., Boukemara, H., Bournier, O., Neut, C., Darfeuille-Michaud, A., et al. (2015). *Escherichia coli* LF82 differentially regulates ROS production and mucin expression in intestinal epithelial T84 cells: implication of NOX1. *Inflamm. Bowel Dis.* 21, 1018–1026. doi: 10.1097/MIB.0000000000000365

Enss, M. L., Cornberg, M., Wagner, S., Gebert, A., Henrichs, M., Eisenblatter, R., et al. (2000). Proinflammatory cytokines trigger MUC gene expression and mucin release in the intestinal cancer cell line LS180. *Inflamm. Res.* 49, 162–169. doi: 10.1007/s000110050576

Enss, M. L., Grosse-Siestrup, H., Schmidt-Wittig, U., and Gartner, K. (1992). Changes in colonic mucins of germfree rats in response to the introduction of a "normal" rat microbial flora. Rat colonic mucin. *J. Exp. Anim. Sci.* 35, 110–119.

Epple, H. J., Kreusel, K. M., Hanski, C., Schulzke, J. D., Riecken, E. O., and Fromm, M. (1997). Differential stimulation of intestinal mucin secretion by cholera toxin and carbachol. *Pflugers Arch.* 433, 638–647.

Erdem, A. L., Avelino, F., Xicohtencatl-Cortes, J., and Giron, J. A. (2007). Host protein binding and adhesive properties of H6 and H7 flagella of attaching and effacing *Escherichia coli*. *J. Bacteriol.* 189, 7426–7435. doi: 10.1128/JB.00464-07

Etzold, S., Kober, O. I., Mackenzie, D. A., Tailford, L. E., Gunning, A. P., Walshaw, J., et al. (2014). Structural basis for adaptation of lactobacilli to gastrointestinal mucus. *Environ. Microbiol.* 16, 888–903. doi: 10.1111/1462-2920.12377

Fabich, A. J., Jones, S. A., Chowdhury, F. Z., Cernosek, A., Anderson, A., Smalley, D., et al. (2008). Comparison of carbon nutrition for pathogenic and commensal *Escherichia coli* strains in the mouse intestine. *Infect. Immun.* 76, 1143–1152. doi: 10.1128/IAI.01386-07

Finnie, I. A., Dwarakanath, A. D., Taylor, B. A., and Rhodes, J. M. (1995). Colonic mucin synthesis is increased by sodium butyrate. *Gut* 36, 93–99.

Forstner, G. (1995). Signal transduction, packaging and secretion of mucins. *Annu. Rev. Physiol.* 57, 585–605.

Gagnon, M., Zihler Berner, A., Chervet, N., Chassard, C., and Lacroix, C. (2013). Comparison of the Caco-2, HT-29 and the mucus-secreting HT29-MTX intestinal cell models to investigate *Salmonella* adhesion and invasion. *J. Microbiol. Methods* 94, 274–279. doi: 10.1016/j.mimet.2013.06.027

Garrido, D., Kim, J. H., German, J. B., Raybould, H. E., and Mills, D. A. (2011). Oligosaccharide binding proteins from *Bifidobacterium longum* subsp. infantis reveal a preference for host glycans. *PLoS ONE* 6:e17315. doi: 10.1371/journal.pone.0017315

Gibold, L., Garenaux, E., Dalmasso, G., Gallucci, C., Cia, D., Mottet-Auselo, B., et al. (2016). The Vat-AIEC protease promotes crossing of the intestinal mucus layer by Crohn's disease-associated *Escherichia coli*. *Cell. Microbiol.* 18, 617–631. doi: 10.1111/cmi.12539

Gonzalez-Rodriguez, I., Sanchez, B., Ruiz, L., Turroni, F., Ventura, M., Ruas-Madiedo, P., et al. (2012). Role of extracellular transaldolase from *Bifidobacterium bifidum* in mucin adhesion and aggregation. *Appl. Environ. Microbiol.* 78, 3992–3998. doi: 10.1128/AEM.08024-11

Gum, J. R. Jr., Hicks, J. W., Toribara, N. W., Siddiki, B., and Kim, Y. S. (1994). Molecular cloning of human intestinal mucin (MUC2) cDNA. Identification of the amino terminus and overall sequence similarity to prepro-von Willebrand factor. *J. Biol. Chem.* 269, 2440–2446.

Hanski, C., Born, M., Foss, H. D., Marowski, B., Mansmann, U., Arasteh, K., et al. (1999). Defective post-transcriptional processing of MUC2 mucin in ulcerative colitis and in Crohn's disease increases detectability of the MUC2 protein core. *J. Pathol.* 188, 304–311.

Harel, J., Fairbrother, J., Forget, C., Desautels, C., and Moore, J. (1993). Virulence factors associated with F165-positive *Escherichia coli* strains isolated from piglets and calves. *Vet. Microbiol.* 38, 139–155.

Harrington, S. M., Sheikh, J., Henderson, I. R., Ruiz-Perez, F., Cohen, P. S., and Nataro, J. P. (2009). The pic protease of enteroaggregative *Escherichia coli* promotes intestinal colonization and growth in the presence of mucin. *Infect. Immun.* 77, 2465–2473. doi: 10.1128/IAI.01494-08

Henderson, I. R., Czeczulin, J., Eslava, C., Noriega, F., and Nataro, J. P. (1999). Characterization of pic, a secreted protease of *Shigella flexneri* and enteroaggregative *Escherichia coli*. *Infect. Immun.* 67, 5587–5596.

Hooper, L. V., and Gordon, J. I. (2001). Commensal host-bacterial relationships in the gut. *Science* 292, 1115–1118. doi: 10.1126/science.1058709

Hoskins, L. C., Agustines, M., McKee, W. B., Boulding, E. T., Kriaris, M., and Niedermeyer, G. (1985). Mucin degradation in human colon ecosystems. Isolation and properties of fecal strains that degrade ABH blood group antigens and oligosaccharides from mucin glycoproteins. *J. Clin. Invest.* 75, 944–953.

Hoyer, L. L., Hamilton, A. C., Steenbergen, S. M., and Vimr, E. R. (1992). Cloning, sequencing and distribution of the *Salmonella typhimurium* LT2 sialidase gene, nanH, provides evidence for interspecies gene transfer. *Mol. Microbiol.* 6, 873–884.

Huang, J. Y., Lee, S. M., and Mazmanian, S. K. (2011). The human commensal *Bacteroides fragilis* binds intestinal mucin. *Anaerobe* 17, 137–141. doi: 10.1016/j.anaerobe.2011.05.017

Johansson, M. E., Gustafsson, J. K., Holmen-Larsson, J., Jabbar, K. S., Xia, L., Xu, H., et al. (2014). Bacteria penetrate the normally impenetrable inner colon mucus layer in both murine colitis models and patients with ulcerative colitis. *Gut* 63, 281–291. doi: 10.1136/gutjnl-2012-303207

Johansson, M. E., Jakobsson, H. E., Holmen-Larsson, J., Schutte, A., Ermund, A., Rodriguez-Pineiro, A. M., et al. (2015). Normalization of host intestinal mucus layers requires long-term microbial colonization. *Cell Host Microbe* 18, 582–592. doi: 10.1016/j.chom.2015.10.007

Johansson, M. E., Larsson, J. M., and Hansson, G. C. (2011). The two mucus layers of colon are organized by the MUC2 mucin, whereas the outer layer is a legislator of host-microbial interactions. *Proc. Natl. Acad. Sci. U.S.A.* 108(Suppl. 1), 4659–4665. doi: 10.1073/pnas.1006451107

Johansson, M. E., Phillipson, M., Petersson, J., Velcich, A., Holm, L., and Hansson, G. C. (2008). The inner of the two Muc2 mucin-dependent mucus layers in colon is devoid of bacteria. *Proc. Natl. Acad. Sci. U.S.A.* 105, 15064–15069. doi: 10.1073/pnas.0803124105

Johansson, M. E., Thomsson, K. A., and Hansson, G. C. (2009). Proteomic analyses of the two mucus layers of the colon barrier reveal that their main component, the Muc2 mucin, is strongly bound to the Fcgbp protein. *J. Proteome Res.* 8, 3549–3557. doi: 10.1021/pr9002504

Jonckheere, N., Skrypek, N., Frenois, F., and Van Seuningen, I. (2013). Membrane-bound mucin modular domains: from structure to function. *Biochimie* 95, 1077–1086. doi: 10.1016/j.biochi.2012.11.005

Juge, N. (2012). Microbial adhesins to gastrointestinal mucus. *Trends Microbiol.* 20, 30–39. doi: 10.1016/j.tim.2011.10.001

Kankainen, M., Paulin, L., Tynkkynen, S., von Ossowski, I., Reunanen, J., Partanen, P., et al. (2009). Comparative genomic analysis of *Lactobacillus rhamnosus* GG reveals pili containing a human- mucus binding protein. *Proc. Natl. Acad. Sci. U.S.A.* 106, 17193–17198. doi: 10.1073/pnas.0908876106

Keeney, K. M., and Finlay, B. B. (2013). Microbiology: EHEC downregulates virulence in response to intestinal fucose. *Curr. Biol.* 23, R108–R110. doi: 10.1016/j.cub.2012.12.027

Kelly, C. P., Becker, S., Linevsky, J. K., Joshi, M. A., O'Keane, J. C., Dickey, B. F., et al. (1994). Neutrophil recruitment in *Clostridium* difficile toxin A enteritis in the rabbit. *J. Clin. Invest.* 93, 1257–1265. doi: 10.1172/JCI117080

Kim, Y. S., and Ho, S. B. (2010). Intestinal goblet cells and mucins in health and disease: recent insights and progress. *Curr. Gastroenterol. Rep.* 12, 319–330. doi: 10.1007/s11894-010-0131-2

Kleessen, B., and Blaut, M. (2007). Modulation of gut mucosal biofilms. *Br. J. Nutr.* 93, S35–S40. doi: 10.1079/BJN20041346

Konopka, J. B. (2012). N-acetylglucosamine (GlcNAc) functions in cell signaling. *Scientifica (Cairo)* 2012:489208. doi: 10.6064/2012/489208

Koropatkin, N. M., Cameron, E. A., and Martens, E. C. (2012). How glycan metabolism shapes the human gut microbiota. *Nat. Rev. Microbiol.* 10, 323–335. doi: 10.1038/nrmicro2746

Kumar, P., Luo, Q., Vickers, T. J., Sheikh, A., Lewis, W. G., and Fleckenstein, J. M. (2014). EatA, an immunogenic protective antigen of enterotoxigenic *Escherichia coli*, degrades intestinal mucin. *Infect. Immun.* 82, 500–508. doi: 10.1128/IAI.01078-13

Larsson, J. M., Karlsson, H., Crespo, J. G., Johansson, M. E., Eklund, L., Sjovall, H., et al. (2011). Altered O-glycosylation profile of MUC2 mucin occurs in active ulcerative colitis and is associated with increased inflammation. *Inflamm. Bowel Dis.* 17, 2299–2307. doi: 10.1002/ibd.21625

Larsson, J. M., Karlsson, H., Sjovall, H., and Hansson, G. C. (2009). A complex, but uniform O-glycosylation of the human MUC2 mucin from colonic biopsies analyzed by nanoLC/MSn. *Glycobiology* 19, 756–766. doi: 10.1093/glycob/cwp048

Le, D. T., Tran, T. L., Duviau, M. P., Meyrand, M., Guerardel, Y., Castelain, M., et al. (2013). Unraveling the role of surface mucus-binding protein and pili in muco-adhesion of *Lactococcus lactis*. *PLoS ONE* 8:e79850. doi: 10.1371/journal.pone.0079850

Le Bihan, G., Sicard, J. F., Garneau, P., Bernalier-Donadille, A., Gobert, A. P., Garrivier, A., et al. (2017). The NAG sensor NagC regulates LEE gene expression and contributes to gut colonization by *Escherichia coli* O157:H7. *Front. Cell. Infect. Microbiol.* 7:134. doi: 10.3389/fcimb.2017.00134

Lencer, W. I., Reinhart, F. D., and Neutra, M. R. (1990). Interaction of cholera toxin with cloned human goblet cells in monolayer culture. *Am. J. Physiol.* 258(1 Pt 1), G96–G102.

Li, H., Limenitakis, J. P., Fuhrer, T., Geuking, M. B., Lawson, M. A., Wyss, M., et al. (2015). The outer mucus layer hosts a distinct intestinal microbial niche. *Nat. Commun.* 6:8292. doi: 10.1038/ncomms9292

Licht, T. R., Christensen, B. B., Krogfelt, K. A., and Molin, S. (1999). Plasmid transfer in the animal intestine and other dynamic bacterial populations: the role of community structure and environment. *Microbiology* 145(Pt 9), 2615–2622. doi: 10.1099/00221287-145-9-2615

Lievin-Le Moal, V., Huet, G., Aubert, J. P., Bara, J., Forgue-Lafitte, M. E., Servin, A. L., et al. (2002). Activation of mucin exocytosis and upregulation of MUC genes in polarized human intestinal mucin-secreting cells by the thiol-activated exotoxin listeriolysin O. *Cell. Microbiol.* 4, 515–529. doi: 10.1046/j.1462-5822.2002.00210.x

Lievin-Le Moal, V., Servin, A. L., and Coconnier-Polter, M. H. (2005). The increase in mucin exocytosis and the upregulation of MUC genes encoding for membrane-bound mucins induced by the thiol-activated exotoxin listeriolysin O is a host cell defence response that inhibits the cell-entry of *Listeria monocytogenes*. *Cell. Microbiol.* 7, 1035–1048. doi: 10.1111/j.1462-5822.2005.00532.x

Linden, S. K., Florin, T. H., and McGuckin, M. A. (2008). Mucin dynamics in intestinal bacterial infection. *PLoS ONE* 3:e3952. doi: 10.1371/journal.pone.0003952

Liu, Z., Wang, Y., Liu, S., Sheng, Y., Rueggeberg, K. G., Wang, H. et al. (2015). *Vibrio cholerae* represses polysaccharide synthesis to promote motility in mucosa. *Infect. Immun.* 83, 1114–1121. doi: 10.1128/IAI.02841-14

Macfarlane, G. T., and Gibson, G. R. (1991). Formation of glycoprotein degrading enzymes by *Bacteroides fragilis*. *FEMS Microbiol. Lett.* 61, 289–293. doi: 10.1111/j.1574-6968.1991.tb04363.x

Macfarlane, S., McBain, A. J., and Macfarlane, G. T. (1997). Consequences of biofilm and sessile growth in the large intestine. *Adv. Dent. Res.* 11, 59–68. doi: 10.1177/08959374970110011801

Macfarlane, S., Woodmansey, E. J., and Macfarlane, G. T. (2005). Colonization of mucin by human intestinal bacteria and establishment of biofilm communities in a two-stage continuous culture system. *Appl. Environ. Microbiol.* 71, 7483–7492. doi: 10.1128/AEM.71.11.7483-7492.2005

Mack, D. R., Michail, S., Wei, S., McDougall, L., and Hollingsworth, M. A. (1999). Probiotics inhibit enteropathogenic *E. coli* adherence *in vitro* by inducing intestinal mucin gene expression. *Am. J. Physiol.* 276(4 Pt 1), G941–G950.

MacKenzie, D. A., Tailford, L. E., Hemmings, A. M., and Juge, N. (2009). Crystal structure of a mucus-binding protein repeat reveals an unexpected functional immunoglobulin binding activity. *J. Biol. Chem.* 284, 32444–32453. doi: 10.1074/jbc.M109.040907

Mahdavi, J., Pirinccioglu, N., Oldfield, N. J., Carlsohn, E., Stoof, J., Aslam, A., et al. (2014). A novel O-linked glycan modulates Campylobacter jejuni major outer membrane protein-mediated adhesion to human histo-blood group antigens and chicken colonization. *Open Biol.* 4:130202. doi: 10.1098/rsob.130202

Maltby, R., Leatham-Jensen, M. P., Gibson, T., Cohen, P. S., and Conway, T. (2013). Nutritional basis for colonization resistance by human commensal *Escherichia coli* strains HS and Nissle 1917 against *E. coli* O157:H7 in the mouse intestine. *PLoS ONE* 8:e53957. doi: 10.1371/journal.pone.0053957

Mantle, M., and Rombough, C. (1993). Growth in and breakdown of purified rabbit small intestinal mucin by *Yersinia enterocolitica*. *Infect. Immun.* 61, 4131–4138.

Marcobal, A., Southwick, A. M., Earle, K. A. and Sonnenburg, J. L. (2013). A refined palate: bacterial consumption of host glycans in the gut. *Glycobiology* 23, 1038–1046. doi: 10.1093/glycob/cwt040

Mariscotti, J. F., Quereda, J. J., Garcia-Del Portillo, F., and Pucciarelli, M. G. (2014). The *Listeria* monocytogenes LPXTG surface protein Lmo1413 is an invasin with capacity to bind mucin. *Int. J. Med. Microbiol.* 304, 393–404. doi: 10.1016/j.ijmm.2014.01.003

Martens, E. C., Chiang, H. C., and Gordon, J. I. (2008). Mucosal glycan foraging enhances fitness and transmission of a saccharolytic human gut bacterial symbiont. *Cell Host Microbe* 4, 447–457. doi: 10.1016/j.chom.2008.09.007

Martinez-Medina, M., Aldeguer, X., Lopez-Siles, M., Gonzalez-Huix, F., Lopez-Oliu, C., Dahbi, G., et al. (2009a). Molecular diversity of *Escherichia coli* in the human gut: new ecological evidence supporting the role of adherent-invasive *E. coli* (AIEC) in Crohn's disease. *Inflamm Bowel Dis.* 15, 872–882. doi: 10.1002/ibd.20860

Martinez-Medina, M., Naves, P., Blanco, J., Aldeguer, X., Blanco, J. E., Blanco, M., et al. (2009b). Biofilm formation as a novel phenotypic feature of adherent-invasive *Escherichia coli* (AIEC). *BMC Microbiol.* 9:202. doi: 10.1186/1471-2180-9-202

Martin-Sosa, S., Martin, M. J., and Hueso, P. (2002). The sialylated fraction of milk oligosaccharides is partially responsible for binding to enterotoxigenic and uropathogenic *Escherichia coli* human strains. *J. Nutr.* 132, 3067–3072.

Masseret, E., Boudeau, J., Colombel, J. F., Neut, C., Desreumaux, P., Joly, B., et al. (2001). Genetically related *Escherichia coli* strains associated with Crohn's disease. *Gut* 48, 320–325. doi: 10.1136/gut.48.3.320

Mattar, A. F., Teitelbaum, D. H., Drongowski, R. A., Yongyi, F., Harmon, C. M., and Coran, A. G. (2002). Probiotics up-regulate MUC-2 mucin gene expression in a Caco-2 cell-culture model. *Pediatr. Surg. Int.* 18, 586–590. doi: 10.1007/s00383-002-0855-7

McGuckin, M. A., Linden, S. K., Sutton, P., and Florin, T. H. (2011). Mucin dynamics and enteric pathogens. *Nat. Rev. Microbiol.* 9, 265–278. doi: 10.1038/nrmicro2538

McNamara, N., and Basbaum, C. (2001). Signaling networks controlling mucin production in response to Gram-positive and Gram-negative bacteria. *Glycoconj. J.* 18, 715–722. doi: 10.1023/A:1020875423678

Moehle, C., Ackermann, N., Langmann, T., Aslanidis, C., Kel, A., Kel-Margoulis, O., et al. (2006). Aberrant intestinal expression and allelic variants of mucin genes associated with inflammatory bowel disease. *J. Mol. Med.* 84, 1055–1066. doi: 10.1007/s00109-006-0100-2

Moran, A. P., Gupta, A., and Joshi, L. (2011). Sweet-talk: role of host glycosylation in bacterial pathogenesis of the gastrointestinal tract. *Gut* 60, 1412–1425. doi: 10.1136/gut.2010.212704

Naughton, J. A., Marino, K., Dolan, B., Reid, C., Gough, R., Gallagher, M. E., et al. (2013). Divergent mechanisms of interaction of *Helicobacter pylori* and *Campylobacter jejuni* with mucus and mucins. *Infect. Immun.* 81, 2838–2850. doi: 10.1128/IAI.00415-13

Navarro-Garcia, F., Gutierrez-Jimenez, J., Garcia-Tovar, C., Castro, L. A., Salazar-Gonzalez, H., and Cordova, V. (2010). Pic, an autotransporter protein secreted by different pathogens in the *Enterobacteriaceae* family, is a potent mucus secretagogue. *Infect. Immun.* 78, 4101–4109. doi: 10.1128/IAI.00523-10

Ng, K. M., Ferreyra, J. A., Higginbottom, S. K., Lynch, J. B., Kashyap, P. C., Gopinath, S., et al. (2013). Microbiota-liberated host sugars facilitate post-antibiotic expansion of enteric pathogens. *Nature* 502, 96–99. doi: 10.1038/nature12503

Nilsson, H. E., Ambort, D., Backstrom, M., Thomsson, E., Koeck, P. J., Hansson, G. C., et al. (2014). Intestinal MUC2 mucin supramolecular topology by packing and release resting on D3 domain assembly. *J. Mol. Biol.* 426, 2567–2579. doi: 10.1016/j.jmb.2014.04.027

Ouwerkerk, J. P., de Vos, W. M., and Belzer, C. (2013). Glycobiome: bacteria and mucus at the epithelial interface. *Best Pract. Res. Clin. Gastroenterol.* 27, 25–38. doi: 10.1016/j.bpg.2013.03.001

Pacheco, A. R., Curtis, M. M., Ritchie, J. M., Munera, D., Waldor, M. K., Moreira, C. G., et al. (2012). Fucose sensing regulates bacterial intestinal colonization. *Nature* 492, 113–117. doi: 10.1038/nature11623

Palestrant, D., Holzknecht, Z. E., Collins, B. H., Parker, W., Miller, S. E., and Bollinger, R. R. (2004). Microbial biofilms in the gut: visualization by electron microscopy and by acridine orange staining. *Ultrastruct. Pathol.* 28, 23–27. doi: 10.1080/01913120490275196

Petersson, J., Schreiber, O., Hansson, G. C., Gendler, S. J., Velcich, A., Lundberg, J. O., et al. (2011). Importance and regulation of the colonic mucus barrier in a mouse model of colitis. *Am. J. Physiol. Gastrointest. Liver Physiol.* 300, G327–G333. doi: 10.1152/ajpgi.00422.2010

Png, C. W., Linden, S. K., Gilshenan, K. S., Zoetendal, E. G., McSweeney, C. S., Sly, L. I., et al. (2010). Mucolytic bacteria with increased prevalence in IBD mucosa augment *in vitro* utilization of mucin by other bacteria. *Am. J. Gastroenterol.* 105, 2420–2428. doi: 10.1038/ajg.2010.281

Pullan, R. D., Thomas, G. A., Rhodes, M., Newcombe, R. G., Williams, G. T., Allen, A., et al. (1994). Thickness of adherent mucus gel on colonic mucosa in humans and its relevance to colitis. *Gut* 35, 353–359. doi: 10.1136/gut.35.3.353

Pultz, N. J., Hoskins, L. C., and Donskey, C. J. (2006). Vancomycin-resistant *Enterococci* may obtain nutritional support by scavenging carbohydrate fragments generated during mucin degradation by the anaerobic microbiota of the colon. *Microb. Drug Resist.* 12, 63–67. doi: 10.1089/mdr.2006.12.63

Raouf, A. H., Tsai, H. H., Parker, N., Hoffman, J., Walker, R. J., and Rhodes, J. M. (1992). Sulphation of colonic and rectal mucin in inflammatory bowel disease: reduced sulphation of rectal mucus in ulcerative colitis. *Clin. Sci.* 83, 623–626. doi: 10.1042/cs0830623

Rho, J. H., Wright, D. P., Christie, D. L., Clinch, K., Furneaux, R. H., and Roberton, A. M. (2005). A novel mechanism for desulfation of mucin: identification and cloning of a mucin-desulfating glycosidase (sulfoglycosidase) from Prevotella strain RS2. *J. Bacteriol.* 187, 1543–1551. doi: 10.1128/JB.187.5.1543-1551.2005

Roos, S., and Jonsson, H. (2002). A high-molecular-mass cell-surface protein from *Lactobacillus reuteri* 1063 adheres to mucus components. *Microbiology* 148(Pt 2), 433–442. doi: 10.1099/00221287-148-2-433

Ruiz-Palacios, G. M., Cervantes, L. E., Ramos, P., Chavez-Munguia, B., and Newburg, D. S. (2003). *Campylobacter jejuni* binds intestinal H(O) antigen (Fuc α1, 2Gal β1, 4GlcNAc), and fucosyloligosaccharides of human milk inhibit its binding and infection. *J. Biol. Chem.* 278, 14112–14120. doi: 10.1074/jbc.M207744200

Sharma, R., Schumacher, U., Ronaasen, V., and Coates, M. (1995). Rat intestinal mucosal responses to a microbial flora and different diets. *Gut* 36, 209–214. doi: 10.1136/gut.36.2.209

Sheng, Y. H., Hasnain, S. Z., Florin, T. H., and McGuckin, M. A. (2012). Mucins in inflammatory bowel diseases and colorectal cancer. *J. Gastroenterol. Hepatol.* 27, 28–38. doi: 10.1111/j.1440-1746.2011.06909.x

Slizova, M., Nemcova, R., Mad'ar, M., Hadryova, J., Gancarcikova, S., Popper, M., et al. (2015). Analysis of biofilm formation by intestinal *lactobacilli*. *Can. J. Microbiol.* 61, 437–446. doi: 10.1139/cjm-2015-0007

Smirnova, M. G., Guo, L., Birchall, J. P., and Pearson, J. P. (2003). LPS up-regulates mucin and cytokine mRNA expression and stimulates mucin and cytokine secretion in goblet cells. *Cell. Immunol.* 221, 42–49. doi: 10.1016/S0008-8749(03)00059-5

Sonnenburg, E. D., Zheng, H., Joglekar, P., Higginbottom, S. K., Firbank, S. J., Bolam, D. N., et al. (2010). Specificity of polysaccharide use in intestinal bacteroides species determines diet-induced microbiota alterations. *Cell* 141, 1241–1252. doi: 10.1016/j.cell.2010.05.005

Sonnenburg, J. L., Xu, J., Leip, D. D., Chen, C. H., Westover, B. P., Weatherford, J., et al. (2005). Glycan foraging *in vivo* by an intestine-adapted bacterial symbiont. *Science* 307, 1955–1959. doi: 10.1126/science.1109051

Sperandio, B., Fischer, N., Joncquel Chevalier-Curt, M., Rossez, Y., Roux, P., Robbe Masselot, C., et al. (2013). Virulent *Shigella flexneri* affects secretion, expression, and glycosylation of gel-forming mucins in mucus-producing cells. *Infect. Immun.* 81, 3632–3643. doi: 10.1128/IAI.00551-13

Strugala, V., Dettmar, P. W., and Pearson, J. P. (2008). Thickness and continuity of the adherent colonic mucus barrier in active and quiescent ulcerative colitis and Crohn's disease. *Int. J. Clin. Pract.* 62, 762–769. doi: 10.1111/j.1742-1241.2007.01665.x

Swidsinski, A., Loening-Baucke, V., and Herber, A. (2009). Mucosal flora in Crohn's disease and ulcerative colitis-an overview. *J. Physiol. Pharmacol.* 60(Suppl. 6), 61–71.

Swidsinski, A., Loening-Baucke, V., Lochs, H., and Hale, L. P. (2005a). Spatial organization of bacterial flora in normal and inflamed intestine: a fluorescence *in situ* hybridization study in mice. *World J. Gastroenterol.* 11, 1131–1140. doi: 10.3748/wjg.v11.i8.1131

Swidsinski, A., Weber, J., Loening-Baucke, V., Hale, L. P., and Lochs, H. (2005b). Spatial organization and composition of the mucosal flora in patients with inflammatory bowel disease. *J. Clin. Microbiol.* 43, 3380–3389. doi: 10.1128/JCM.43.7.3380-3389.2005

Szabady, R. L., Yanta, J. H., Halladin, D. K., Schofield, M. J., and Welch, R. A. (2011). TagA is a secreted protease of *Vibrio cholerae* that specifically cleaves mucin glycoproteins. *Microbiology* 157(Pt 2), 516–525. doi: 10.1099/mic.0.044529-0

Szentkuti, L., Riedesel, H., Enss, M. L., Gaertner, K., and Von Engelhardt, W. (1990). Pre-epithelial mucus layer in the colon of conventional and germ-free rats. *Histochem. J.* 22, 491–497. doi: 10.1007/BF01007234

Tasteyre, A., Barc, M. C., Collignon, A., Boureau, H., and Karjalainen, T. (2001). Role of FliC and FliD flagellar proteins of *Clostridium difficile* in adherence and gut colonization. *Infect. Immun.* 69, 7937–7940. doi: 10.1128/IAI.69.12.7937-7940.2001

Theodoropoulos, G., and Carraway, K. L. (2007). Molecular signaling in the regulation of mucins. *J. Cell. Biochem.* 102, 1103–1116. doi: 10.1002/jcb.21539

Trabucchi, E., Mukenge, S., Baratti, C., Colombo, R., Fregoni, F., and Montorsi, W. (1986). Differential diagnosis of Crohn's disease of the colon from ulcerative colitis: ultrastructure study with the scanning electron microscope. *Int. J. Tissue React.* 8, 79–84.

Troge, A., Scheppach, W., Schroeder, B. O., Rund, S. A., Heuner, K., Wehkamp, J., et al. (2012). More than a marine propeller–the flagellum of the probiotic *Escherichia coli* strain Nissle 1917 is the major adhesin mediating binding to human mucus. *Int. J. Med. Microbiol.* 302, 304–314. doi: 10.1016/j.ijmm.2012.09.004

Tu, Q. V., McGuckin, M. A., and Mendz, G. L. (2008). *Campylobacter jejuni* response to human mucin MUC2: modulation of colonization and pathogenicity determinants. *J. Med. Microbiol.* 57(Pt 7), 795–802. doi: 10.1099/jmm.0.47752-0

van der Waaij, L. A., Harmsen, H. J., Madjipour, M., Kroese, F. G., Zwiers, M., van Dullemen, H. M., et al. (2005). Bacterial population analysis of human colon and terminal ileum biopsies with 16S rRNA-based fluorescent probes: commensal bacteria live in suspension and have no direct contact with epithelial cells. *Inflamm. Bowel Dis.* 11, 865–871. doi: 10.1097/01.mib.0000179212.80778.d3

Vimal, D. B., Khullar, M., Gupta, S., and Ganguly, N. K. (2000). Intestinal mucins: the binding sites for *Salmonella typhimurium*. *Mol. Cell. Biochem.* 204, 107–117. doi: 10.1023/A:1007015312036

Vogt, S. L., Pena-Diaz, J., and Finlay, B. B. (2015). Chemical communication in the gut: effects of microbiota-generated metabolites on gastrointestinal bacterial pathogens. *Anaerobe* 34, 106–115. doi: 10.1016/j.anaerobe.2015.05.002

Weiss, A. A., Babyatsky, M. W., Ogata, S., Chen, A., and Itzkowitz, S. H. (1996). Expression of MUC2 and MUC3 mRNA in human normal, malignant, and inflammatory intestinal tissues. *J. Histochem. Cytochem.* 44, 1161–1166. doi: 10.1177/44.10.8813081

Wrzosek, L., Miquel, S., Noordine, M. L., Bouet, S., Joncquel Chevalier-Curt, M., Robert, V., et al. (2013). *Bacteroides thetaiotaomicron* and *Faecalibacterium prausnitzii* influence the production of mucus glycans and the development of goblet cells in the colonic epithelium of a gnotobiotic model rodent. *BMC Biol.* 11:61. doi: 10.1186/1741-7007-11-61

Wurpel, D. J., Totsika, M., Allsopp, L. P., Hartley-Tassell, L. E., Day, C. J., Peters, K. M., et al. (2014). F9 fimbriae of uropathogenic *Escherichia coli* are expressed at low temperature and recognise Galbeta1-3GlcNAc-containing glycans. *PLoS ONE* 9:e93177. doi: 10.1371/journal.pone.0093177

Xu, J., Bjursell, M. K., Himrod, J., Deng, S., Carmichael, L. K., Chiang, H. C., et al. (2003). A genomic view of the human-*Bacteroides thetaiotaomicron* symbiosis. *Science* 299, 2074–2076. doi: 10.1126/science.1080029

Xue, Y., Zhang, H., Wang, H., Hu, J., Du, M., and Zhu, M. J. (2014). Host inflammatory response inhibits *Escherichia coli* O157:H7 adhesion to gut epithelium through augmentation of mucin expression. *Infect. Immun.* 82, 1921–1930. doi: 10.1128/IAI.01589-13

Ye, J., Song, L., Liu, Y., Pan, Q., Zhong, X., Li, S., et al. (2015). Core 2 Mucin-Type O-Glycan is related to EPEC and EHEC O157:H7 adherence to human colon carcinoma HT-29 epithelial cells. *Dig. Dis. Sci.* 60, 1977–1990. doi: 10.1007/s10620-015-3548-5

Zarepour, M., Bhullar, K., Montero, M., Ma, C., Huang, T., Velcich, A., et al. (2013). The mucin Muc2 limits pathogen burdens and epithelial barrier dysfunction during *Salmonella enterica* serovar Typhimurium colitis. *Infect. Immun.* 81, 3672–3683. doi: 10.1128/IAI.00854-13

Conflict of Interest Statement: The authors declare that the research was conducted in the absence of any commercial or financial relationships that could be construed as a potential conflict of interest.

Annexe 4: N-Acetyl-glucosamine influences the biofilm formation of *Escherichia coli*

En tant que deuxième auteur de cet article, j'ai réalisé les expériences préliminaires qui ont mené à cette étude. J'ai aussi mis au point les conditions permettant la formation de biofilm des souches AIEC. J'ai également étroitement contribué à l'évolution de l'étude en proposant les tests de formation de biofilm en microfluidique avec ajout de NAG. J'ai également apporté mes commentaires et corrections sur l'ensemble de l'article avant soumission. Cet revue a été publié en 2018 dans le journal « Gut pathogens ».

Sicard *et al. Gut Pathog (2018) 10:26*
https://doi.org/10.1186/s13099-018-0252-y

Gut Pathogens

RESEARCH Open Access

N-Acetyl-glucosamine influences the biofilm formation of *Escherichia coli*

Jean-Félix Sicard[1], Philippe Vogeleer[1], Guillaume Le Bihan[1], Yaindrys Rodriguez Olivera[1], Francis Beaudry[1], Mario Jacques[2] and Josée Harel[1*]

Abstract

Background: The intestinal mucous layer is a physical barrier that limits the contact between bacteria and host epithelial cells. There is growing evidence that microbiota-produced metabolites can also be specifically sensed by gut pathogens as signals to induce or repress virulence genes. Many *E. coli*, including adherent and invasive (AIEC) strains, can form biofilm. This property can promote their intestinal colonization and resistance to immune mechanisms. We sought to evaluate the impact of mucus-derived sugars on biofilm formation of *E. coli*.

Results: We showed that the mucin sugar *N*-acetyl-glucosamine (NAG) can reduce biofilm formation of AIEC strain LF82. We demonstrated that the inactivation of the regulatory protein NagC, by addition of NAG or by mutation of *nagC* gene, reduced the biofilm formation of LF82 in static condition. Interestingly, real-time monitoring of biofilm formation of LF82 using microfluidic system showed that the mutation of *nagC* impairs the early process of biofilm development of LF82. Thus, NAG sensor NagC is involved in the early steps of biofilm formation of AIEC strain LF82 under both static and dynamic conditions. Its implication is partly due to the activation of type 1 fimbriae. NAG can also influence biofilm formation of other intestinal *E. coli* strains.

Conclusions: This study highlights how catabolism can be involved in biofilm formation of *E. coli*. Mucus-derived sugars can influence virulence properties of pathogenic *E. coli* and this study will help us better understand the mechanisms used to prevent colonization of the intestinal mucosa by pathogens.

Keywords: *Escherichia coli*, AIEC, Biofilms, Mucus, *N*-Acetyl-glucosamine

Background

Escherichia coli is a highly versatile bacterial species commonly found as part of the intestinal microbiota of warm-blooded animals. Most isolates are harmless but some have acquired virulence genes that allow them to cause numerous diseases within the gut (intestinal pathogenic *E. coli*, InPEC) or extra-intestinally (extra-intestinal pathogenic *E. coli*; ExPEC). Commensal *E. coli* colonize the large intestine in vertebrates and appear to reside inside the mucus layer without contacting the underlying epithelium [1]. In contrast, InPEC possess the ability to penetrate the mucus layer and colonize the mucosa causing disease such as diarrhea [2]. Adherent-invasive *E. coli* (AIEC) strains share many genetic and phenotypic features with ExPEC strains but are rather involved in inflammatory bowel disease (IBD), including Crohn's disease (CD) [3–5].

The mucus layer that covers the intestinal epithelium plays a critical role in gut homeostasis. The intestinal mucus contains mucins which are highly *O*-glycosylated proteins. Mucins play an important role in shaping the intestinal microbiota as an alteration of the glycan availability modifies the microbiota composition [6]. By producing specific glycosidases, several species of the gut microbiota release sugars from *O*-glycans into the intestinal lumen [7, 8]. Released mucus-derived sugars, including *N*-acetylglucosamine (NAG), *N*-acetylneuraminic acid (NANA), galactose, fucose, mannose and

*Correspondence: josee.harel@umontreal.ca
[1] Groupe de Recherche sur les Maladies Infectieuses en Production Animale, Centre de Recherche en Infectiologie Porcine et Avicole, Faculté de Médecine Vétérinaire, Université de Montréal, St-Hyacinthe, QC J2S 2M2, Canada
Full list of author information is available at the end of the article

N-acetylgalactosamine provide direct source of carbohydrates and promote the growth of commensal and pathogenic bacteria including *E. coli* [7–10]. In addition to their role as nutrients, some mucus-derived sugars can act as regulatory signals that influence bacterial colonization and adherence to intestinal cells [11–14]. Enterohemorrhagic *E. coli* (EHEC) uses fucose, NAG and NANA as signaling molecules to modulate its metabolism and regulate the expression of its virulence repertoire [12, 15]. We recently showed that the catabolism of NAG and NANA inhibits EHEC adhesion to epithelial cells through down-regulation of the locus of enterocytes effacement expression under NagC regulatory control [16].

Biofilms could play a key role in bacterial colonization of the healthy gut and in intestinal diseases. Mucin has been reported to be involved in biofilm formation by *E. coli* [17, 18], suggesting its potential role in modulating *E. coli* colonization in the intestinal tract. The ability of biofilm formation in vitro varies extensively among *E. coli* isolates [19] and many *E. coli* strains are believed to form biofilm in the intestinal tract [20]. As such, AIEC are known to be higher biofilm producers than non-AIEC strains [21]. The ability to form biofilm could be part of the etiology of IBD since an increased presence of biofilms formed by the *Bacteroides fragilis* group and the *Enterobacteriaceae* family has been observed in intestinal biopsy specimens of people affected with these diseases [22, 23].

Alteration of the gut mucosal integrity and of microbiota could also change the mucus-derived sugars availability. Our hypothesis is that in healthy conditions, the integrity of the intestinal mucus and the functions of gut microbiota prevent biofilm formation of pathogenic *E. coli*. We evaluated the influence of mucus-derived sugars on biofilm formation of AIEC reference strain LF82. We show that NAG can reduce biofilm formation of LF82 and that the transcriptional regulator of NAG catabolism, NagC appears to be involved in the early steps of its biofilm formation. We also showed that mucus-derived sugars can influence biofilm formation of different *E. coli* strains from other pathotypes.

Methods

Bacterial strains and growth conditions

Bacterial strains used in this study are listed in Table 1. Bacteria were routinely cultured on lysogeny broth (LB) agar [1% (wt/vol) tryptone, 0.5% (wt/vol) yeast extract, 1% (wt/vol) NaCl, 1.5% (wt/vol) agar] at 37 °C and single colonies were transferred in liquid LB. When required, the growth medium was supplemented with kanamycin (50 µg/ml) and/or chloramphenicol (25 µg/ml). A set of commensal and pathogenic *E. coli* that comprises AIEC strain LF82, EHEC strain EDL933, enteroagregative *E. coli* (EAEC) strain 17.2, laboratory *E. coli* (K-12) strain MG1655 as well as commensal murine *E. coli* strain NC101 were included in the biofilm studies.

Mutagenesis and complementation

The LF82Δ*nagC* mutant was constructed by allelic exchange using a suicide vector as described in our previous work [16]. Primers used for mutagenesis are listed in Additional file 1: Table S1. Briefly, the suicide vector

Table 1 List of strains and plasmids used in this study

Strains	Characteristics	Origin	Disease	References
LF82	Wild type AIEC O83:H1 AmpR	Human	Crohn's disease	[4]
LF82Δ*nagC*	LF82 Δ*nagC* AmpR KanR			This study
MG1655	Laboratory *E. coli* K-12	Human	Healthy	[47]
EDL933	Wild type EHEC O157:H7	Human	Diarrhea, HUS	[48]
17.2	Wild type EAEC	Human	Diarrhea	[49]
NC101	Wild type commensal (AIEC-like)	Mouse	Mouse colitis	[50]
χ7213	*thi-1 thr-1 leuB6 glnV44 fhuA21 lacY1 recA1 RP4-2-Tc*::Mu *λpir ΔasdA4 Δzhf-2*::Tn10			[51]
Plamids	**Characteristics**	**References**		
pGEM®-T	Cloning vector	Promega Corp., Madison, WI, USA		
pMEG-375	Suicide vector sacRB mobRP4 oriR6K; CmR ApR	Roy Curtiss III, Arizona State University, Tempe, AZ, USA		
p*ΔnagC*	pMEG-375 with Δ*nagC*:: Km^R	[16]		
pTrc99a	expression vector with IPTG inducible lacI promoter; ApR	[52]		
p*nagC*	pTrc99a with *nagC*	[16]		
p*nagC*-JFS	p*nagC* with Cm^R	This study		

pMEG-375 containing the kanamycin resistance cassette from pKD13 flanked with 500 pb sequences upstream and downstream of the *nagC* open reading frame was transformed in a diaminopimelic acid auxotrophic *E. coli* strain χ7213 (λpir and Δ*asdA4*). χ7213 was used as a donor to transfer the plasmid in *E. coli* strain LF82 by conjugation. Single crossover mutants were selected on LB agar without diaminopimelic acid, containing kanamycin. A second selection of double crossovers mutants was made using the *sacB* counter selection on LB agar without NaCl, containing 10% (wt/vol) of sucrose [24]. The mutation of *nagC* was confirmed by PCR and sequencing of an amplicon containing the region of interest. Complementation was performed using a derivative of the expression vector. The ORF of *nagC* was amplified in *E. coli* strain LF82 and inserted downstream of the pTrc promoter in the expression plasmid forming the p*nagC*. A resistance cassette of chloramphenicol was amplified from pACYC184 and inserted in p*nagC*, forming the p*nagC*-JFS.

Static biofilm assay

The assay of biofilm formation was done in 96-well microtiter plates as previously described [25]. Isolated colonies from LB agar were resuspended in fresh LB (5 ml) and incubated at 37 °C with shaking (180 rpm). Overnight cultures were diluted (1:100) in fresh medium; either LB, LB without salt (LBWS) or M9 medium with 0.4% glucose (wt/vol) and minerals (1.2 mM $MgSO_4$, 2 µM $FeCl_3$, 8 µM $CaCl_2$, and 16 µM $MnCl_2$). When required, the growth medium was supplemented with NAG, NANA or fucose (Sigma-Aldrich, St. Louis, MO, USA) at a concentration of 1 mM. A volume of 150 µl of these cultures was deposited in triplicate in the wells. Plates were incubated either at 30 or 37 °C for 24 h, without shaking. After incubation, total growth was measured at OD_{630} with a microplate reader (PowerWave; Bio-Tek Instruments, Winooski, VT, USA). Afterwards, the media were discarded, and each well washed three times with phosphate-buffered saline (PBS) to remove unattached cells. The biofilms were stained with crystal violet 0.1% (wt/vol) for 2 min at room temperature. The crystal violet solution was removed, and the biofilms washed six times with PBS. Finally, an 80% (vol/vol) ethanol and 20% (vol/vol) acetone solution was added to release the stain and the amount of biofilm quantified by measuring at OD_{595}. Specific biofilm formation (SBF) index was calculated [21, 26]. Results are the ratio of biofilm measured at OD_{595} over total growth measured at OD_{630}. To evaluate the effects of mucus-derived sugars addition on biofilm formation of different strains, one-way ANOVA with Dunnett's multiple comparison test was performed to calculate *P*-values. To evaluate the impact of the mutation of *nagC* on AIEC strain LF82, two-way ANOVA with Tukey's multiple comparison test was performed to calculate *P*-values $^{*}P<0.05$; $^{**}P<0.01$; $^{***}P<0.001$.

Flow-through biofilm assay (BioFlux device)

The biofilm formation assay in the BioFlux 200 device (Fluxion Biosciences, South San Francisco, CA, USA) was adapted from our previous work [25]. Biofilm formation occurs in the microfluidic channel of the device where fresh media constantly flow through causing a shear force that is similar to physiological condition [25]. *E. coli* strains were isolated on LB agar and resuspended in 5 ml of fresh LB medium. They were incubated overnight at 37 °C with shaking (180 rpm). A 0.5 ml volume of culture was transferred to a microtube and bacteria were collected by centrifugation (13,000*g*, 2 min). LB medium was used to resuspend the pellet to an $OD_{600} \approx 1$. Prewarmed LB ± NAG (1 mM) was injected in the microfluidic system to fill the channels. Bacteria were injected from the output reservoir for 30 s at 0.5 dyne/cm^2. The microfluidic plate was incubated at 30 °C for 2 h to allow the adhesion of bacteria on the surface of the channels. After adhesion, prewarmed LB ± NAG (1 mM) was added to the inlet wells and the microfluidic plate was connected to the BioFlux system. Temperature was adjusted to 30 °C and the flow was initiated at 1.0 dyne/cm^2. After 4 h, the used medium was removed from the outlet well and prewarmed fresh medium was added in the inlet well. Flow was then reduced at 0.5 dyne/cm^2 for the next 18 h. Images of the BioFlux biofilms were obtained with an inverted optic microscope equipped with a 40× objective (CKX41; Olympus, Markham, ON, Canada), a digital camera (Retiga EX; QImaging, Surrey, BC, Canada), and the software provided with the BioFlux 200 device. Images were treated using the software imageJ (National Institutes of Health, Bethesda, MD, USA) to quantify the amount of biofilm in the microfluidic channel. The 16-bit grayscale images were adjusted with the threshold function to include the bacterial structure before particle analysis. One-way ANOVA with Dunnett's multiple comparison test was performed to calculate *P*-values.

Detection of type 1 fimbriae

The capacity of LF82 and the *nagC* mutant to produce type 1 fimbriae was evaluated by the ability to agglutinate to *Saccharomyces cerevisiae* cells in a mannose-dependant way. As previously described [27], cultures were grown at 30 °C in 20 ml of LB for 24 h without shaking to enhance expression of type 1 fimbriae. NAG was added in the medium at a final concentration of 1 mM. The concentration of an initial suspension of approximately 2×10^{11} CFU/ml in PBS was reduced by twofold serial dilutions in microtiter plate (Corning,

2797). An equal volume of a commercial yeast suspension in PBS 3% (wt/vol) (Fleischmann's Active Dry) was added to each well. After 30 min of incubation at 4 °C, yeast agglutination was observable by precipitation of cells in the wells of the plate. The agglutination titer was recorded as the most diluted bacterial sample giving a positive aggregation reaction. Yeast agglutination was considered dependent of type 1 fimbriae if α-D-mannopyranose 5% (wt/vol) (Sigma-Aldrich) inhibited agglutination. One-way ANOVA with Dunnett's multiple comparison test was performed to calculate *P*-values.

Quantitative RT-PCR (qRT-PCR)

Bacteria were precultured as described in previous section. A dilution (1:100) was done in 40 ml of LB ± NAG (1 mM) and bacteria were incubated in polystyrene petri dish overnight at 30 °C. Biofilms were washed with PBS and recovered with a cell scraper. RNA was extracted from biofilm cells using Ambion® RiboPure™-Bacteria Kit (ThermoFisher Scientific, Burlington, ON, Canada), according to the manufacturer's recommendations. As described in [15], the absence of residual DNA in RNA samples was confirmed by PCR with primers targeting *rpoA*. Complementary DNA (cDNA) was synthetized from 10 µg of RNA, using a reverse transcriptase and random hexanucleotide primers. A standard curve was performed to determine the copy number of targeted transcript in 50 ng of cDNA. Primers used are listed in Additional file 1: Table S1. Results are presented as the ratios between the cDNA copy number of the gene of interest and the cDNA copy number of the housekeeping gene. One-way ANOVA with Dunnett's multiple comparison test was performed to calculate *P*-values.

Results

NAG reduces biofilm formation of AIEC strain LF82

We investigated the impact of mucus-derived sugars, including NAG, NANA and fucose, on biofilm formation of the AIEC reference strain LF82. LB culture medium was selected for optimal growth of biofilms in static condition. Upon the addition of 1 mM of NAG, the specific biofilm formation (SBF) index of LF82 was significantly lower ($P < 0.01$) than the SBF index of LF82 grown in LB alone. Addition of NANA and fucose in the medium did not influence the biofilm formation of the strain (Fig. 1). The three mucus-derived sugars did not affect the growth of the strain after 24 h (data not shown). A time course measurement of NAG consumption by LF82 grown in LB supplemented with 1 mM of NAG indicated that NAG was catabolized within 4 h (Additional file 2: Figure S1).

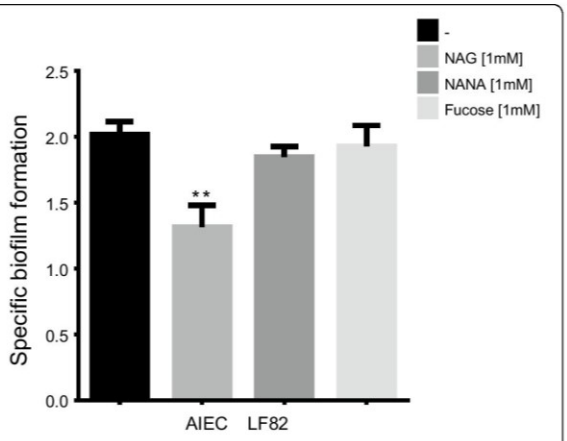

Fig. 1 Impact of mucus-derived sugars on specific biofilm formation of AIEC strain LF82. Biofilms of strain LF82 were formed in LB medium under static conditions at 30 °C. NAG, NANA or fucose were supplemented at a concentration of 1 mM. SBF values are the mean and standard error of at least 3 biological experiments. Statistical significance was calculated by one-way ANOVA with Dunnett's multiple comparison test $^{**}P < 0.01$

NAG reduces specific biofilm formation of LF82 by inactivating the transcriptional regulator NagC

The regulation of AIEC strain LF82 biofilm formation by NAG was further investigated. The activity of the regulator NagC is inactivated by the presence of NAG-6-P, a catabolic derivate of NAG. Therefore, a mutant strain in *nagC* gene was created. The SBF index of LF82Δ*nagC* mutant was significantly lower ($P < 0.05$) than the SBF index of the WT strain. This reduction of biofilm formation was similar to that observed upon the addition of NAG (Fig. 2). The wild-type phenotype was restored in the complemented strain expressing *nagC*. Interestingly, no additional repression was observed upon the addition of NAG in the Δ*nagC* mutant. This indicates that LF82 biofilm repression by NAG is NagC dependent.

NagC is involved in the first steps of biofilm formation of LF82 in presence of a shear force

To further investigate the role of NagC on biofilm formation of LF82, the dynamics of biofilm formation were monitored and visualized in real time using the BioFlux device (Fig. 3a). Real time imaging with LF82 clearly revealed the apparition of microcolonies 6 h after the initiation of the flow. These microcolonies grew overtime and the production of polymeric matrix became more apparent at 10 h. After 18 h, the channel was almost entirely covered with biofilm. At 24 h, mature biofilms were formed. The kinetics of biofilm formation of LF82Δ*nagC* was different from that of the WT LF82. In early time points, a reduced number of microcolonies

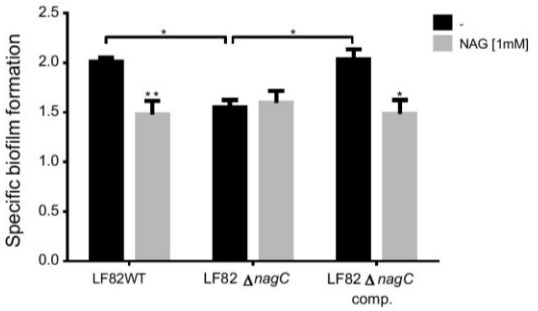

Fig. 2 NagC positively influences the biofilm formation of AIEC strain LF82. Biofilms of strain LF82, its isogenic mutant Δ*nagC* and complemented Δ*nagC* were formed in LB medium under static condition at 30 °C. NAG was supplemented at a concentration of 1 mM. SBF values are the mean and standard error of 4 biological replicates. Statistical analysis was calculated by two-way ANOVA with Tukey's multiple comparison test *$P<0.05$; **$P<0.01$

was observed in the mutant strain. Quantification results revealed a significant ($P<0.01$) decrease in biofilm coverage of the mutant strain when compared to the WT strain at 6, 8 and 10 h after the activation of the flow. At 16 and 18 h, the biofilm structure of LF82Δ*nagC* mutant was similar to that of the WT. Again, wild-type phenotype was restored in the complemented strain (Fig. 3a, b). This suggests that the *nagC* mutation impairs the first steps of biofilm formation of LF82 and involves surface adhesion and/or cell to cell interactions. In contrast to what we observed in static condition, supplementation of NAG did not affect biofilm formation in the microfluidic system.

The mutation of *nagC* impaired the production of type 1 fimbriae of LF82

To determine the role of type 1 pili in the NagC-dependent reduction of biofilm formation of LF82, the expression and the production of type 1 fimbriae were evaluated in the mutant strain. The expression of *fimA*, encoding the major structural subunit of type 1 fimbriae, was measured in grown biofilms (Fig. 4a). Results showed a significant ($P<0.01$) reduction of 3.5-fold of *fimA* transcription in the LF82Δ*nagC* strain when compared to WT strain (Fig. 4a). The expression of *fimA* was restored in the complemented strain. However, the effect of supplementation of NAG in medium on the expression of *fimA* was not statistically significant but slightly increased (Fig. 4a). The production of type 1 fimbriae was measured by mannose-sensitive agglutination to *S. cerevisiae* and was significantly lower ($P<0.01$) by 2 Log_2 in LF82Δ*nagC* mutant in comparison to WT strain (Fig. 4b). Type 1 pili production was restored in the complemented strain. Addition of NAG during growth did not affect the production of type 1 fimbriae. Interestingly, NAG is rapidly consumed within 4 h of bacterial growth in LB medium supplemented with NAG, as measured by mass spectrometry (Additional file 2). Thus, the repressive effect of NAG on type 1 fimbriae production might be transient. Addition of mannose was previously reported to reduce the biofilm of LF82 by interfering with type 1 fimbriae adhesion [40]. In presence of mannose, biofilm formation of LF82 was decreased in either LB or NAG supplemented medium indicating that type 1 fimbriae is involved in biofilm in these conditions (Additional file 3: Figure S2).Taken together these results show that expression and production of type 1 fimbriae are regulated by NagC in LF82. Type 1 fimbriae or other structures participating to LF82 biofilm might be influenced by NAG supplementation.

The impact of mucus-derived sugars on biofilm formation varies among *E. coli* strains

Biofilm formation of a set of distinct *E. coli* strains was tested in different culture media to determine optimal conditions. LB medium was used for strains 17.2 and MG1655, whereas LBWS and M9 with glucose were used as the optimized culture media for biofilm formation of strains NC101 and EDL933, respectively. The effect of addition of NAG, NANA or fucose on biofilm formation was evaluated in static condition. The influence of mucus-derived sugars was variable, strain-dependent and did not affect the growth of bacteria as measured with optical density (Additional file 4: Figure S3). Our data showed that the mean OD value of biofilm formed by murine strain NC101 was significantly decreased in the presence of the all three sugars ($P<0.01$). Supplementation of the medium with NAG ($P<0.01$) or NANA ($P<0.05$), significantly reduced biofilm formation of EHEC strain EDL933. A slight reduction was also observed upon the addition of NAG in EAEC strain 17.2 and K-12 strain MG1655 (Fig. 5).

Discussion

There is growing evidence that microbiota-produced metabolites can also be specifically sensed by pathogens as signals to induce or repress virulence genes [28]. We show that the mucin sugars NAG, NANA and fucose can reduce the biofilm formation of AIEC strain LF82 and other pathogenic *E. coli*. A recent study showed that fucose modulated biofilm formation of *Campylobacter jejuni* [29]. We observed that the influence of mucus-derived sugars on biofilm formation was strain-dependent, reflecting the high genetic diversity and the variability of metabolic patterns between *E. coli* strains [30, 31]. It is known that *E. coli* preference for

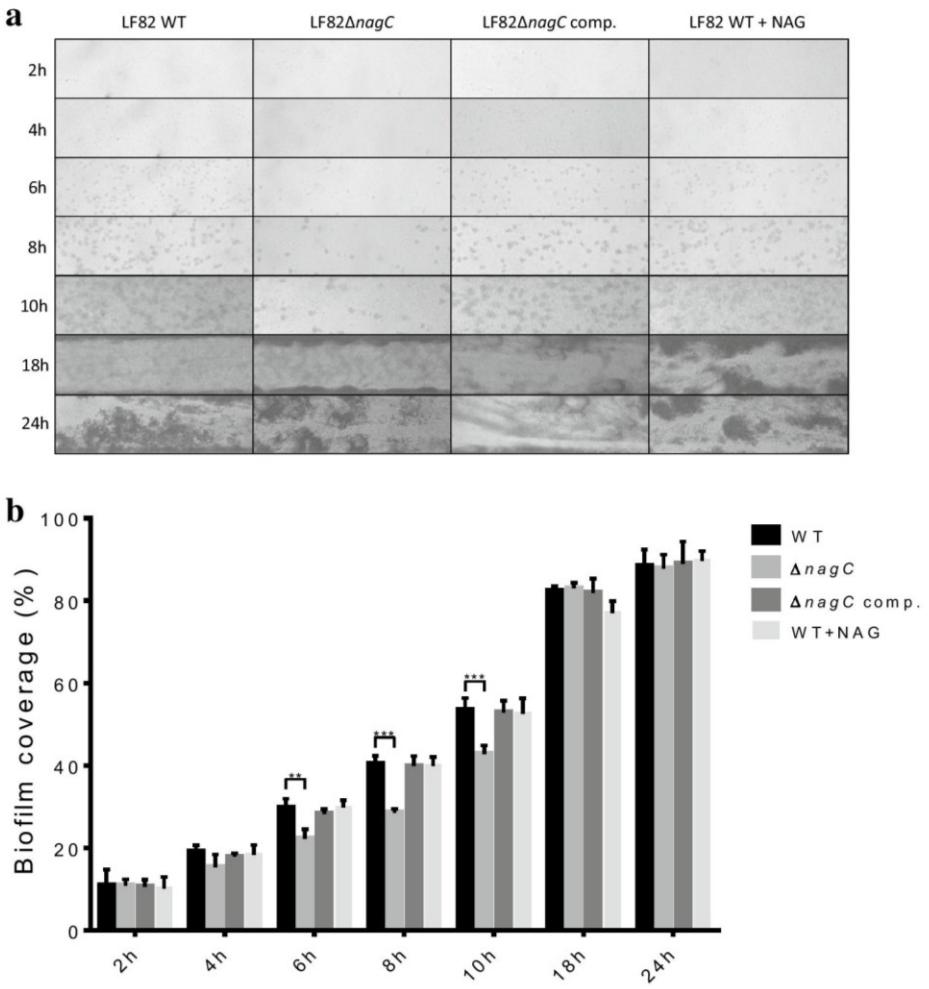

Fig. 3 The biofilm formation is delayed in *nagC* mutant of LF82 in a microfluidic system. **a** Biofilms of strain LF82, its isogenic mutant Δ*nagC* and complemented Δ*nagC* were formed in LB medium at 30 °C in the BioFlux 200 microfluidic system. NAG was supplemented at a concentration of 1 mM. A field of view representative of 3 independent replicates is shown for each test. Images were captured by phase contrast microcopy using a digital camera. **b** Quantification of biofilm formation was made using the "Analyze Particles" function of ImageJ and results show the percentage of the area covered by biofilm structures in images pictures. Statistical significance was calculated by one-way ANOVA with Dunnett's multiple comparison test ***P* 0.01; ****P* 0.001

mucus-derived sugars varies from one strain to another [10, 32, 33]. Interestingly, the repressor effect of NAG was common among the tested *E. coli* strains as NAG supplementation reduced biofilm formation of AIEC strain LF82, murine strain NC101, EHEC strain EDL933 and to a lower extent EAEC strain 17.2 and K-12 strain MG1655.

We demonstrated that the effect of NAG on biofilm formation of AIEC strain LF82 is NagC-dependent. NagC is a repressor of *nag* operon involved in catabolism of NAG in *E. coli* [34, 35]. The uptake of this sugar leads to the production of intracellular NAG-6-P that will inactivate the regulator NagC [36]. Our study shows that the inactivation of NagC, whether it is caused by the catabolism of NAG or by a mutation of *nagC*, is responsible for the decreased biofilm formation. Thus, NagC is a positive regulator of biofilm formation in LF82. Interestingly, NagC is also involved in the expression of the locus of enterocytes effacement virulence genes of EHEC as well as type 1 fimbriae of *E. coli* K-12 [13, 16, 36].

The real-time monitoring of LF82 biofilm formation using microfluidic system showed that early steps are impaired by the mutation of *nagC*. Biofilm formation initially required the attachment of the bacteria to

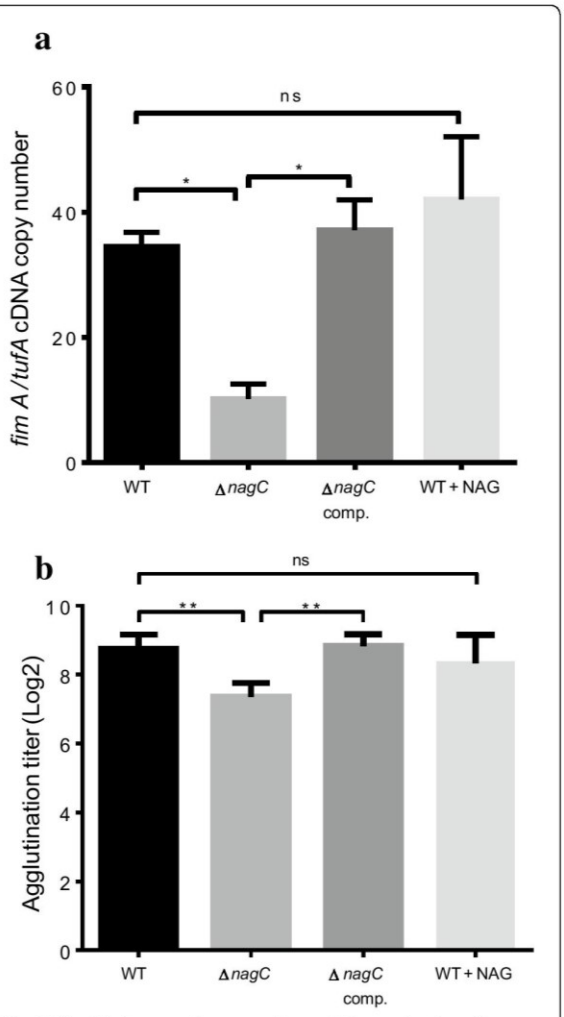

Fig. 4 NagC influences the expression and the production of type 1 fimbriae of LF82. **a** The expression of type 1 fimbriae subunit *fimA* was measured by qRT-PCR in LF82 WT strain, its Δ*nagC* derivative and the complemented mutant grown as biofilm in LB media. NAG was also supplemented at a concentration of 1 mM in media used for WT strain. Results are shown as the ratio of copy number of *fimA* transcript/copy numbers of *tufA* transcript. **b** Production of type 1 fimbriae was also evaluated for each strain by mannose specific agglutination to the yeast *S. cerevisiae*. LB medium was used in the experiments and NAG was supplemented at a concentration of 1 mM when needed. Results are the mean values and standard error of 3 biological experiments. Statistical analyzes were made using one-way ANOVA with Dunnett's multiple comparison test **P* 0.05; ***P* 0.01

a surface and the cell-to-cell adhesion that leads to the formation of microcolonies. Thus, during these steps, NagC might influence the expression of structures involved in early adhesion of bacteria. In contrast to the situation in static conditions, the biofilm in dynamic conditions was insensitive to the presence of NAG. It is possible that constant renewal of media in dynamic conditions influences NAG catabolism and thus NagC activity.

Type 1 fimbriae are key factors that facilitate adhesion to a surface and cell-to-cell aggregation during establishment of biofilm on abiotic surfaces [37, 38]. They also participate in biofilm formation and in the adhesion-and-invasion process in AIEC strains such as LF82 [21, 39, 40]. In the present study, we show that NagC activates the gene expression and the production of type 1 fimbriae of AIEC strain LF82. This is similar to the work showing NagC regulation on type 1 fimbriae in *E. coli* K-12 MG1655 [13]. Based on NagC consensus DNA binding site generated from known NagC binding sequences [13, 16, 41, 42], two different binding sites were found upstream of the promoter of *fimB* recombinase in LF82. FimB is involved in the OFF-to-ON switching of type 1 fimbriation and sequences found in LF82 were identical and in the same distance to those of *fimB* promoter in K-12 strain MG1655 [13] (Additional file 5: Figure S4). This indicates that NagC control on type 1 fimbriae could influence at least in part the biofilm formation of LF82. In contrast, NAG supplementation did not influence type 1 fimbriae production of LF82 strain. It is possible that NAG-dependant repression on type 1 fimbriae was transient because NAG is rapidly consumed by the strain). NAG might also influence other factors contributing to biofilm formation of LF82 as NAG was also shown to influence the production of curli in *E. coli* K-12 [11].

Dysbiosis that occurs during IBD can favor AIEC growth and probably biofilm formation [43]. As glycosylation of the mucin is defective in CD [44] and microbiota activity is modified, it is possible that the availability of mucin sugars will influence not only the metabolic activity but also the virulence behavior including the pathogens' ability of biofilm formation. Thus, factors that regulate biofilm formation could signal to repress expression of the type 1 fimbriae and other factors contributing to biofilm of LF82. By affecting the concentration of free NAG available in the digestive tract, gut bacterial species expressing *N*-acetylglucosaminidase [6] might therefore influence *E. coli* biofilm formation through a modulation of NagC activity. Interestingly, administration of glucosamine can reduce production of pro-inflammatory cytokines and therefore intestinal inflammation in murine model of IBD could influence the activity of the flora including AIEC and reduce their biofilm formation and colonization ability [45, 46].

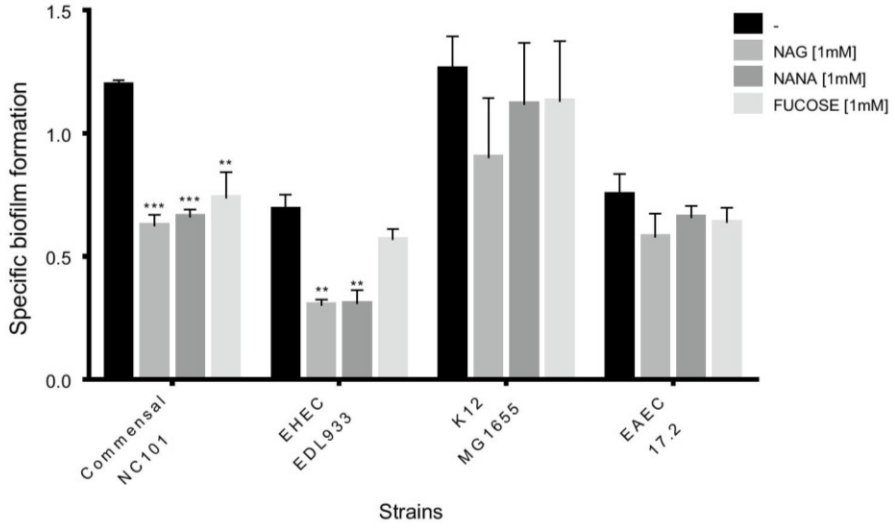

Fig. 5 Mucus-derived sugars can influence the specific biofilm formation of different strains of *E. coli*. Strain specific optimized conditions for biofilm formation were identified. LB was used for EAEC strain 17.2 and K-12 strain MG1655. LBWS was used for AIEC strain NC101 and M9 with glucose was used for EHEC strain EDL933. Biofilms were formed under static conditions at 30 °C except for strain EDL933 that was grown at 37 °C. NAG, NANA and fucose were supplemented at a concentration of 1 mM. SBF values are the mean and standard error of at least 3 biological experiments. Statistical analysis was made using one-way ANOVA with Dunnett's multiple comparison test **P* 0.05; ***P* 0.01; ****P* 0.001

Conclusion

In conclusion, the presence of mucin-derived sugars can influence biofilm formation of different *E. coli* strains. This study highlights that the diminution of biofilm formation of AIEC strain LF82 in the presence of NAG is NagC-dependent. Indeed, the NAG sensor NagC is involved in the early steps of biofilm formation of strain LF82 and its implication could be partly due to the control of type 1 fimbriae.

Additional files

Additional file 1: Table S1. List of primers used in this study.

Additional file 2: Figure S1. Monitoring of NAG consumption by LF82 WT, LF82Δ*nagC* and the complemented strain when grown under static condition. Concentration of NAG was measured by mass spectrometry.

Additional file 3: Figure S2. Specific biofilm formation of LF82 was evaluated in the presence or absence of mannose in either in LB or LB supplemented with NAG.

Additional file 4: Figure S3. The effect of the addition of mucus-derived sugars on growth of strains.

Additional file 5: Figure S4. NagC consensus DNA binding sites and nucleotide BLAST of LF82 and MG1655.

Abbreviations

AIEC: adherent and invasive *E. coli*; NAG: *N*-acetyl-glucosamine; InPEC: intestinal pathogenic *E. coli*; ExPEC: extra-intestinal pathogenic *E. coli*; IBD: inflammatory bowel disease; CD: Crohn's disease; NANA: *N*-acetylneuraminic acid; EHEC: enterohemorrhagic *E. coli*; LB: lysogeny broth; EAEC: enteroagregative *E. coli*; LBWS: LB without salt; PBS: phosphate-buffered saline; OD: optical density; SBF: specific biofilm formation; cDNA: complementary DNA.

Authors' contributions

The experiments were performed mainly by JFS with the help of PV. JFS and JH performed the data analysis. The study was designed by JH, JFS, GLB and PV. All authors read and approved the final manuscript.

Author details

[1] Groupe de Recherche sur les Maladies Infectieuses en Production Animale, Centre de Recherche en Infectiologie Porcine et Avicole, Faculté de Médecine Vétérinaire, Université de Montréal, St-Hyacinthe, QC J2S 2M2, Canada. [2] Regroupement de Recherche Pour un Lait de Qualité Optimale (Op+Lait), Faculté de Médecine Vétérinaire, Université de Montréal, Saint-Hyacinthe, QC J2S 2M2, Canada.

Acknowledgements

We thank Joan Pena and Yaindrys Rodriguez Olivera for their help with qRT-PCR assays. We also thank Jean-Charles Côté for proofreading the manuscript.

Competing interests

The authors declare that they have no competing interests.

Funding

This research was supported by a Team Grant from the Fonds de Recherche du Québec, Nature et Technologies (FRQNT PT165375), to JH, MJ and FB and by the Discovery grant program of the Natural Sciences and Engineering Research Council of Canada (RGPIN-2015-05373 to JH and RGPIN-2016-04203 to MJ). JFS is a recipient of a scholarship from the NSERC Collaborative Research and Training Experience Program in Milk Quality; and PV is a recipient of a scholarship from the FRQNT Québec Wallonie program.

Publisher's Note

Received: 3 April 2018 Accepted: 18 June 2018
Published online: 22 June 2018

References

1. Poulsen LK, Lan F, Kristensen CS, Hobolth P, Molin S, Krogfelt KA. Spatial distribution of *Escherichia coli* in the mouse large intestine inferred from rRNA in situ hybridization. Infect Immun. 1994;62(11):5191–4.
2. Torres AG, Zhou X, Kaper JB. Adherence of diarrheagenic *Escherichia coli* strains to epithelial cells. Infect Immun. 2005;73(1):18–29.
3. Darfeuille-Michaud A. Adherent-invasive *Escherichia coli*: a putative new *E. coli* pathotype associated with Crohn's disease. Int J Med Microbiol. 2002;292(3–4):185–93.
4. Darfeuille-Michaud A, Boudeau J, Bulois P, Neut C, Glasser AL, Barnich N, Bringer MA, Swidsinski A, Beaugerie L, Colombel JF. High prevalence of adherent-invasive *Escherichia coli* associated with ileal mucosa in Crohn's disease. Gastroenterology. 2004;127(2):412–21.
5. Martinez-Medina M, Garcia-Gil LJ. *Escherichia coli* in chronic inflammatory bowel diseases: an update on adherent invasive *Escherichia coli* pathogenicity. World J Gastrointest Pathophysiol. 2014;5(3):213–27.
6. Martens EC, Chiang HC, Gordon JI. Mucosal glycan foraging enhances fitness and transmission of a saccharolytic human gut bacterial symbiont. Cell Host Microbe. 2008;4(5):447–57.
7. Bertin Y, Chaucheyras-Durand F, Robbe-Masselot C, Durand A, de la Foye A, Harel J, Cohen PS, Conway T, Forano E, Martin C. Carbohydrate utilization by enterohaemorrhagic *Escherichia coli* O157:H7 in bovine intestinal content. Environ Microbiol. 2013;15(2):610–22.
8. Ng KM, Ferreyra JA, Higginbottom SK, Lynch JB, Kashyap PC, Gopinath S, Naidu N, Choudhury B, Weimer BC, Monack DM, et al. Microbiota-liberated host sugars facilitate post-antibiotic expansion of enteric pathogens. Nature. 2013;502(7469):96–9.
9. Conway T, Cohen PS. Commensal and pathogenic Escherichia coli metabolism in the gut. Microbiol Spectr. 2015. https://doi.org/10.1128/microbiolspec.MBP-0006-2014
10. Fabich AJ, Jones SA, Chowdhury FZ, Cernosek A, Anderson A, Smalley D, McHargue JW, Hightower GA, Smith JT, Autieri SM, et al. Comparison of carbon nutrition for pathogenic and commensal *Escherichia coli* strains in the mouse intestine. Infect Immun. 2008;76(3):1143–52.
11. Barnhart MM, Lynem J, Chapman MR. GlcNAc-6P levels modulate the expression of Curli fibers by *Escherichia coli*. J Bacteriol. 2006;188(14):5212–9.
12. Pacheco AR, Curtis MM, Ritchie JM, Munera D, Waldor MK, Moreira CG, Sperandio V. Fucose sensing regulates bacterial intestinal colonization. Nature. 2012;492(7427):113–7.
13. Sohanpal BK, El-Labany S, Lahooti M, Plumbridge JA, Blomfield IC. Integrated regulatory responses of fimB to *N*-acetylneuraminic (sialic) acid and GlcNAc in *Escherichia coli* K-12. Proc Natl Acad Sci USA. 2004;101(46):16322–7.
14. Vogt SL, Pena-Diaz J, Finlay BB. Chemical communication in the gut: effects of microbiota-generated metabolites on gastrointestinal bacterial pathogens. Anaerobe. 2015;34:106–15.
15. Le Bihan G, Jubelin G, Garneau P, Bernalier-Donadille A, Martin C, Beaudry F, Harel J. Transcriptome analysis of *Escherichia coli* O157:H7 grown in vitro in the sterile-filtrated cecal content of human gut microbiota associated rats reveals an adaptive expression of metabolic and virulence genes. Microbes Infect. 2015;17(1):23–33.
16. Le Bihan G, Sicard JF, Garneau P, Bernalier-Donadille A, Gobert AP, Garrivier A, Martin C, Hay AG, Beaudry F, Harel J, et al. The NAG sensor NagC regulates LEE gene expression and contributes to gut colonization by *Escherichia coli* O157:H7. Front Cell Infect Microbiol. 2017;7:134.
17. Bollinger RR, Barbas AS, Bush EL, Lin SS, Parker W. Biofilms in the normal human large bowel: fact rather than fiction. Gut. 2007;56(10):1481–2.
18. Bollinger RR, Everett ML, Wahl SD, Lee YH, Orndorff PE, Parker W. Secretory IgA and mucin-mediated biofilm formation by environmental strains of *Escherichia coli*: role of type 1 pili. Mol Immunol. 2006;43(4):378–87.
19. Reisner A, Krogfelt KA, Klein BM, Zechner EL, Molin S. In vitro biofilm formation of commensal and pathogenic *Escherichia coli* strains: impact of environmental and genetic factors. J Bacteriol. 2006;188(10):3572–81.
20. Rossi E, Cimdins A, Luthje P, Brauner A, Sjoling A, Landini P, Romling U. "It's a gut feeling"—*Escherichia coli* biofilm formation in the gastrointestinal tract environment. Crit Rev Microbiol. 2017;44:1–30.
21. Martinez-Medina M, Naves P, Blanco J, Aldeguer X, Blanco JE, Blanco M, Ponte C, Soriano F, Darfeuille-Michaud A, Garcia-Gil LJ. Biofilm formation as a novel phenotypic feature of adherent-invasive *Escherichia coli* (AIEC). BMC Microbiol. 2009;9:202.
22. Swidsinski A, Weber J, Loening-Baucke V, Hale LP, Lochs H. Spatial organization and composition of the mucosal flora in patients with inflammatory bowel disease. J Clin Microbiol. 2005;43(7):3380–9.
23. Swidsinski A, Loening-Baucke V, Herber A. Mucosal flora in Crohn's disease and ulcerative colitis—an overview. J Physiol Pharmacol. 2009;60(Suppl 6):61–71.
24. Kaniga K, Delor I, Cornelis GR. A wide-host-range suicide vector for improving reverse genetics in Gram-negative bacteria: inactivation of the blaA gene of *Yersinia enterocolitica*. Gene. 1991;109(1):137–41.
25. Tremblay YD, Vogeleer P, Jacques M, Harel J. High-throughput microfluidic method to study biofilm formation and host-pathogen interactions in pathogenic *Escherichia coli*. Appl Environ Microbiol. 2015;81(8):2827–40.
26. Naves P, del Prado G, Huelves L, Gracia M, Ruiz V, Blanco J, Rodriguez-Cerrato V, Ponte MC, Soriano F. Measurement of biofilm formation by clinical isolates of *Escherichia coli* is method-dependent. J Appl Microbiol. 2008;105(2):585–90.
27. Vogeleer P, Tremblay YD, Jubelin G, Jacques M, Harel J. Biofilm-forming abilities of shiga toxin-producing *Escherichia coli* isolates associated with human infections. Appl Environ Microbiol. 2015;82(5):1448–58.
28. Baumler AJ, Sperandio V. Interactions between the microbiota and pathogenic bacteria in the gut. Nature. 2016;535(7610):85–93.
29. Dwivedi R, Nothaft H, Garber J, Xin Kin L, Stahl M, Flint A, van Vliet AH, Stintzi A, Szymanski CM. L-Fucose influences chemotaxis and biofilm formation in *Campylobacter jejuni*. Mol Microbiol. 2016;101(4):575–89.
30. Baumler DJ, Peplinski RG, Reed JL, Glasner JD, Perna NT. The evolution of metabolic networks of *E. coli*. BMC Syst Biol. 2011;5:182.
31. Meador JP, Caldwell ME, Cohen PS, Conway T. *Escherichia coli* pathotypes occupy distinct niches in the mouse intestine. Infect Immun. 2014;82(5):1931–8.
32. Chang DE, Smalley DJ, Tucker DL, Leatham MP, Norris WE, Stevenson SJ, Anderson AB, Grissom JE, Laux DC, Cohen PS, et al. Carbon nutrition of *Escherichia coli* in the mouse intestine. Proc Natl Acad Sci USA. 2004;101(19):7427–32.
33. Maltby R, Leatham-Jensen MP, Gibson T, Cohen PS, Conway T. Nutritional basis for colonization resistance by human commensal *Escherichia coli* strains HS and Nissle 1917 against *E. coli* O157:H7 in the mouse intestine. PLoS ONE. 2013;8(1):e53957.
34. Plumbridge J, Kolb A. CAP and Nag repressor binding to the regulatory regions of the nagE-B and manX genes of *Escherichia coli*. J Mol Biol. 1991;217(4):661–79.
35. Plumbridge J, Kolb A. DNA loop formation between Nag repressor molecules bound to its two operator sites is necessary for repression of the nag regulon of *Escherichia coli* in vivo. Mol Microbiol. 1993;10(5):973–81.
36. El Qaidi S, Plumbridge J. Switching control of expression of ptsG from the Mlc regulon to the NagC regulon. J Bacteriol. 2008;190(13):4677–86.
37. Schembri MA, Christiansen G, Klemm P. FimH-mediated autoaggregation of *Escherichia coli*. Mol Microbiol. 2001;41(6):1419–30.
38. Pratt LA, Kolter R. Genetic analysis of *Escherichia coli* biofilm formation: roles of flagella, motility, chemotaxis and type I pili. Mol Microbiol. 1998;30(2):285–93.
39. Barnich N, Boudeau J, Claret L, Darfeuille-Michaud A. Regulatory and functional co-operation of flagella and type 1 pili in adhesive and invasive abilities of AIEC strain LF82 isolated from a patient with Crohn's disease. Mol Microbiol. 2003;48(3):781–94.
40. Nickerson KP, McDonald C. Crohn's disease-associated adherent-invasive *Escherichia coli* adhesion is enhanced by exposure to the ubiquitous dietary polysaccharide maltodextrin. PLoS ONE. 2012;7(12):e52132.
41. El Qaidi S, Allemand F, Oberto J, Plumbridge J. Repression of galP, the galactose transporter in *Escherichia coli*, requires the specific regulator of *N*-acetylglucosamine metabolism. Mol Microbiol. 2009;71(1):146–57.
42. Plumbridge J. Co-ordinated regulation of amino sugar biosynthesis and degradation: the NagC repressor acts as both an activator and a repressor for the transcription of the glmUS operon and requires two separated NagC binding sites. EMBO J. 1995;14(16):3958–65.

43. Agus A, Massier S, Darfeuille-Michaud A, Billard E, Barnich N. Understanding host-adherent-invasive *Escherichia coli* interaction in Crohn's disease: opening up new therapeutic strategies. Biomed Res Int. 2014;2014:567929.
44. Strugala V, Dettmar PW, Pearson JP. Thickness and continuity of the adherent colonic mucus barrier in active and quiescent ulcerative colitis and Crohn's disease. Int J Clin Pract. 2008;62(5):762–9.
45. Azuma K, Osaki T, Kurozumi S, Kiyose M, Tsuka T, Murahata Y, Imagawa T, Itoh N, Minami S, Sato K, et al. Anti-inflammatory effects of orally administered glucosamine oligomer in an experimental model of inflammatory bowel disease. Carbohydr Polym. 2015;115:448–56.
46. Bak YK, Lampe JW, Sung MK. Effects of dietary supplementation of glucosamine sulfate on intestinal inflammation in a mouse model of experimental colitis. J Gastroenterol Hepatol. 2014;29(5):957–63.
47. Blattner FR, Plunkett G 3rd, Bloch CA, Perna NT, Burland V, Riley M, Collado-Vides J, Glasner JD, Rode CK, Mayhew GF, et al. The complete genome sequence of *Escherichia coli* K-12. Science. 1997;277(5331):1453–62.
48. Perna NT, Plunkett G 3rd, Burland V, Mau B, Glasner JD, Rose DJ, Mayhew GF, Evans PS, Gregor J, Kirkpatrick HA, et al. Genome sequence of enterohaemorrhagic *Escherichia coli* O157:H7. Nature. 2001;409(6819):529–33.
49. Rich C, Favre-Bonte S, Sapena F, Joly B, Forestier C. Characterization of enteroaggregative *Escherichia coli* isolates. FEMS Microbiol Lett. 1999;173(1):55–61.
50. Kim SC, Tonkonogy SL, Albright CA, Tsang J, Balish EJ, Braun J, Huycke MM, Sartor RB. Variable phenotypes of enterocolitis in interleukin 10-deficient mice monoassociated with two different commensal bacteria. Gastroenterology. 2005;128(4):891–906.
51. Roland K, Curtiss R 3rd, Sizemore D. Construction and evaluation of a delta cya delta crp *Salmonella typhimurium* strain expressing avian pathogenic *Escherichia coli* O78 LPS as a vaccine to prevent airsacculitis in chickens. Avian Dis. 1999;43(3):429–41.
52. Amann E, Ochs B, Abel KJ. Tightly regulated tac promoter vectors useful for the expression of unfused and fused proteins in *Escherichia coli*. Gene. 1988;69(2):301–15.